MINISTERE DE LôALIMENTATION DE LôAGRICULTURE ET DE LA PECHE
MONTPELLIER SUPAGRO

Thèse

Délivré par Montpellier SupAgro pour obtenir le grade de Docteur

École doctorale: **SIBAGHE** – Systèmes Intégrés en Biologie, Agronomie, Géosciences, Hydrosciences, Environnement

Spécialité: **ESA** – Écosystèmes et Sciences Agronomiques

Laboratoire dôaccueil:

- UMR «Centre de Biologie pour la Gestion des Populations» - 755 avenue du Campus Agropolis, CS 30016 F-34988 Montferrier-sur-Lez Cedex, France

- UMR « Institut Sophia-Agrobiotech » - 400 route des Chappes, 06903 Sophia-Antipolis, France

Apports des marqueurs moléculaires à la systématique, biogéographie et écologie des espèces euro-méditerranéennes du genre *Eupelmus* - implications pour leur utilisation en lutte biologique

Présentée et soutenue publiquement par

Fadel AL KHATIB

Le 20 Novembre 2015

JURY

Gérard DELVARE, Chargé de Recherche, CBGP, Montpellier	**Co-directeur de thèse**
Anne LE-RALEC, Professeur, Agrocampus Ouest, Rennes	**Examinateur**
Andrew POLASZEK, Chercheur, Muséum d'Histoire Naturelle, Londres	**Rapporteur**
Nicolas RIS, Ingénieur de Recherche, INRA-PACA, Sophia-Antipolis	**Co-directeur de thèse**
Jean-François SILVAIN, Directeur de Recherche, IRD, Gif-sur-Yvette	**Rapporteur**
Marie-Stéphane TIXIER, Professeur, Montpellier SupAgro	**Examinateur**

RÉSUMÉ

Le genre *Eupelmus* Dalman (Chalcidoidea: Eupelmidae: Eupelminae) comprend des ecto-parasitoïdes s'attaquant essentiellement aux stades larvaires et nymphaux de divers insectes holométaboles. Jusqu'à présent, la systématique du genre *Eupelmus* restait mal résolue compte tenu des données limitées et restreintes à la morphologie et de l'absence de révisions taxonomiques récentes, fiables et globales. Dans ce contexte, de nombreuses questions se posent concernant (i) la pertinence de la classification infra-générique actuelle du genre *Eupelmus*; (ii) le statut taxonomique des certaines espèces décrites; (iii) la fiabilité des informations écologiques telles que la gamme d'hôtes et la distribution géographique et, donc, (iv) la compréhension des processus de spécialisation écologique et du rôle potentiel de certaines espèces d'*Eupelmus* comme auxiliaires de lutte biologique. Cette thèse a donc eu pour objectif d'aborder l'ensemble de ces questions en utilisant, à des fins de phylogénie et de taxonomie, une approche intégrative combinant des données moléculaires (ADN mitochondrial et nucléaire) et morphologiques.

Les résultats obtenus concernant les relations phylogénétiques infra-générique montrent que l'arrangement du genre *Eupelmus* en trois sous-genres (*Eupelmus*, *Episolindelia* et *Macroneura*), ne peut pas être retenu et que ce genre devrait etre subdivisé en une douzaine de groupes d'espèces. De plus, l'étude de la taxonomie de deux complexes (ensemble d'espèces morphologiquement proches), les complexes "*urozonus*" et "*vesicularis*", met globalement en évidence une diversité insoupçonnée dans la zone Euro-méditerranéenne et plus d'une dizaine d'espèces ont été découvertes et décrites comme de nouvelles espèces à l'occasion de ces travaux. D'une façon générale, les caractères morphologiques, les marqueurs nucléaires et les marqueurs mitochondriaux se sont révélés relativement concordants sauf au sein du complexe *vesicularis* qui présente une divergence plus marquée au niveau d'ADN mitochondrial.

Dans le cadre particulier du groupe *urozonus*, ce travail de thèse nous a également permis d'étudier l'évolution de la spécificité d'hôtes en lien avec une phylogénie moléculaire multi-locus relativement bien résolue et une estimation de la longueur d'ovipositeur, un caractère morphologique susceptible d'expliquer l'accès aux hôtes. D'une façon générale, les analyses comparatives révèlent que la spécificité d'hôtes n'est pas contrainte par la phylogénie. Nous observons ainsi des spectres d'hôtes très contrastés entre des espèces phylogénétiquement très

proches. De même, la longueur d'ovipositeur, qui semble un caractère très labile à cette échelle, ne semble pas déterminer le spectre d'hôtes. L'ensemble des résultats obtenus ont finalement été utilisées de façon à mieux comprendre le rôle potentiel de certaines espèces d'*Eupelmus* sur des insectes ravageurs, la mouche de l'olive *Bactrocera oleae* et le cynips du châtaignier *Dryocosmus kuriphilus*.

Mots clef: *Eupelmus*, marqueurs moléculaires, morphologie, phylogénie multi-locus, spécialisation écologique, systématique, taxonomie intégrative.

ABSTRACT

The genus *Eupelmus* Dalman (Chalcidoidea: Eupelmidae: Eupelminae) includes ecto-parasitoids attacking mostly pupal and larval stages of various holometabolous insects. So far, the systematics of *Eupelmus* remained poorly resolved due to limited data restricted to morphological information, and the absence of recent, reliable and comprehensive taxonomic revisions. In this context, many questions arise concerning (i) the relevance of the current sub-generic classification of *Eupelmus*; (ii) the taxonomic status of some described species; (iii) the reliability of ecological information such as host range and geographical distribution; and therefore, (iv) the understanding of the ecological processes/specialization and the potential role of certain species of *Eupelmus* as auxiliaries in biological control. This thesis has therefore aimed to address all of these questions by using, for the purposes of phylogeny and taxonomy, an integrative approach combining molecular (nuclear and mitochondrial DNA) and morphological data.

The results obtained concerning the sub-generic phylogenetic relationships show that the arrangement of *Eupelmus* into three subgenera (*Eupelmus*, *Episolindelia* and *Macroneura*), can not be retained and that this genus should be subdivided into a dozen species groups. In addition, the study of taxonomy of two complexes (sets of morphologically similar species), the complex "*urozonus*" and "*vesicularis*", highlights unsuspected diversity in the Euro-Mediterranean area and more than ten species have been discovered and described as new species during this work. Generally, the morphological characteristics, nuclear markers and mitochondrial markers have been relatively consistent except within the *vesicularis* complex which exhibits more marked divergence in the mitochondrial DNA.

In the particular case of the *urozonus* species group, this thesis work has also allowed us to study the evolution of host specificity in relation to a relatively well-resolved multi-locus molecular phylogeny and an estimate of the length of ovipositor, a morphological character that could explain the ability to parasitize protected hosts. In general, the comparative analyses show that the host specificity is not constrained by the phylogeny. We observe highly contrasting hosts ranges between closely phylogenetically related species. Similarly, the length of the ovipositor, which seems a very labile character at this scale, does not seem to determine the host range. All the results obtained have finally been used to better understand the potential role of some *Eupelmus* species on two insect pests, the fruit olive fly *Bactrocera oleae* and the chestnut gall wasp *Dryocosmus kuriphilus*.

Key words: Ecological specialization, *Eupelmus*, integrative taxonomy, molecular markers, morphology, multi-locus phylogeny, systematics.

REMERCIEMENTS

Je tiens à remercier en premier lieu le Dieu qui m'a accordé sa grâce et la patience pour réaliser cette étude.

J'adresse mes remerciements chaleureux à mes encadrants de thèse: M. **Gérard DELVARE** et M. **Nicolas RIS**, pour m'avoir accueilli dans leurs laboratoires, pour leur soutien constant tout au long de ces études, pour leur gentillesse et leur confiance pendant ces années de travail.

Je souhaite exprimer toute ma gratitude envers les membres du jury, Mme. **Anne LE-RALEC; M. Andrew POLASZEK; M. Jean-François SILVAIN; et Mme. Marie-Stéphane TIXIER** d'avoir accepté de juger ce travail.

Mes remerciements à mon gouvernement syrien qui m'a octroyé cette bourse d'étude afin que je puisse continuer mes études supérieures ici en France. Mes remerciements également au CIRAD et à l'INRA qui ont également participé au soutien financier de ma thèse.

Mes remerciements également à mon encadrant interne de thèse, M. **Mohamed QOJA NAHAL** d'avoir accepté de diriger mon travail et pour sa confiance pendant ces années de travail.

J'adresse mes remerciements aux gens avec qui j'ai pu valoriser scientifiquement les résultats de mon travail: M. **Lucian FUSU**; M. **Jean-Yves RASPLUS**; Mme. **Astrid CRUAUD**; et M. **Gary GIBSON**.

Je remercie particulièrement Mme. **Sylvie WAROT** et Mme. **Astrid CRUAUD** pour leurs aides et leurs conseils précieux concernant la biologie moléculaire et la phylogénie.

Je tiens à remercier M. **Edy SPAGNOL**; M. **Jean LECOMTE**; et Mme. **Laura LORU** ainsi que de nombreux autres collègues pour les échantillons fournis pour cette étude.

Je remercie tous les membres de l'Equipe «Recherche et Développement en Lutte biologique», plus particulièrement **Jean-claude MALAUSA**; **Nicolas BOROWIEC**; **Marcel THAON**; **Géraldine BOUT**; et **Alexandre BOUT** pour leurs aides et leurs conseils précieux. Je remercie également **Pascal GORY** pour le temps qu'il a passé avec moi concernant les démarches administratives et pour sa sympathie.

Je dédie ce travail à mes **parents**, sans qui je ne serais pas où j'en suis aujourd'hui; Merci à tous les membres de ma famille, qui m'ont toujours soutenu.

Finalement, je ne trouve pas les mots qu'il faut pour exprimer mes remerciements du fond de mon cœur à mon épouse Fatima et à mes deux enfants, Khawla et Abdul Moneim.

SOMMAIRE

1. INTRODUCTION

1.1. Préambule

L'objectif de ma venue en France était de me m'initier et familiariser aux techniques de la biologie moléculaire en systématique des insectes, car cette technologie, notamment le séquençage de l'ADN, ne constitue pas encore une pratique courante dans mon pays d'origine (la Syrie) en l'absence de chercheurs spécialistes de ce domaine scientifique.

Ma thèse s'inscrit donc dans le cadre d'une question d'actualité car les outils moléculaires attirent chaque jour davantage l'attention des entomologistes car elles ouvrent de nouveaux champs: accélération de la découverte de la biodiversité via la réalisation d'identifications fiables et précises; discrimination et description des nouvelles espèces basée sur une approche intégrative; meilleure appréhension de l'histoire évolutive via l'inférence des relations phylogénétiques résolues et robustes, etc.

Ce travail de thèse porte sur le genre *Eupelmus* Dalman (Hymenoptera: Eupelmidae: Eupelminae), qui renferme des parasitoïdes s'attaquant essentiellement aux stades larvaires et nymphaux de divers insectes holométaboles; il est par ailleurs le plus diversifié des genres de la sous-famille. Il m'a été proposé comme sujet de thèse une étude systématique du genre considérant: (i) qu'il renferme des espèces potentiellement utilisables en lutte biologique par conservation; (ii) que son étude phylogénétique était uniquement basée sur des données morphologiques avec la question de la pertinence de la classification sous-générique subséquente; (iii) l'absence de révisions taxonomiques récentes et utilisables pour la faune euro-méditerranéenne; (iv) la présence soupçonnée de complexes d'espèces morphologiquement similaires, avec un questionnement portant sur la délimitation des espèces décrites; et (v) les conséquences de cette situation sur la fiabilité des informations écologiques comme les spectres d'hôtes, la distribution géographique des espèces, etc.

Ce travail de thèse a donc eu pour objectif de répondre à plusieurs questions scientifiques se rapportant au genre *Eupelmus*, avec pour chacune d'entre elles une approche faisant largement appel aux données moléculaires: (i) relations phylogénétiques au sein du genre et implication pour la classification sous-générique; (ii) phylogénie multi-locus des espèces appartenant au groupe, *urozonus*, de loin le plus diversifié et qui renferme par ailleurs les auxiliaires susceptibles d'être utilisées dans les programmes de la lutte biologique par conservation; (iii) compréhension du rôle de la spécialisation trophique dans la spéciation écologique chez les

espèces du même groupe; (iv) études de complexes d'espèces appartenant aux groupes *urozonus* et *vesicularis*, dans une approche intégrative faisant appel aux données morphologiques et moléculaires.

1.2. Contexte disciplinaire: la phylogénie et la taxonomie

1.2.1. Taxonomie

1.2.1.1. Définition

Le terme **óótaxonomieôô** est issue de deux mots grecs: ''*taxis*'' signifiant l'arrangement ou la division et ''*nomos*'' signifiant la loi. Donc, la taxonomie est les "lois de l'arrangement ou la division" (Guerra-Garcĺa *et al.*, 2008; Enghoff, 2009). La taxonomie peut etre ainsi définie comme la discipline qui s'intéresse à identifier, décrire, classifier et nommer des groupes d'organismes vivant (espèces), existants ou éteints (Padial *et al.*, 2010). Un autre concept biologique associé est celui de **ñsystématiqueò** qui peut être définie comme la discipline biologique de la classification des groupes d'organismes (espèces) dans des séries hiérarchiques pour refléter leurs relations évolutives (Guerra-Garcĺa *et al.*, 2008). Comme indiqué par Schuh & Brower (2009) le terme de systématique a été utilisé comme un synonyme de taxonomie, ces discussions sémantiques ayant fait l'objet de controverses. Nous adopterons ici le point de vue de Padial *et al.*, (2010) qui considèrent que la taxonomie comporte la classification et fait partie de la systématique qui inclue également la phylogénie. Dans la pratique, les systématiciens étudient l'histoire évolutive des groupes des espèces mais n'ont pas forcément les connaissances nécessaires pour valider ou décrire des espèces tandis que les taxonomistes peuvent, dans certains cas, décrire de nouvelles espèces sans forcément recourir à des approches phylogénétiques (Wägele, 2005). Il est important de rappeler que, sans la taxonomie, personne ne serait certain de l'identité des organismes étudiés (Guerra-Garcĺa *et al.*, 2008). Comme le nom scientifique d'un organisme est une "étiquette fonctionnelle" à partir de laquelle n'importe quelle information concernant cet organisme peut être obtenue (Narendran, 2008), la taxonomie est une pierre essentielle pour un nombre des recherches utiles dont la biodiversité, la lutte contre des ravageurs, la conservation, la gestion des organismes de quarantaine, la santé publique, etc. (Narendran, 2008; Blaxter, 2004;

Rosen, 1986). Trois approches peuvent être distinguées en taxonomie: la taxonomie traditionnelle, la taxonomie moléculaire et la taxonomie intégrative.

1.2.1.2. La taxonomie traditionnelle, basée sur la morphologie

Cette approche repose sur l'utilisation des particularités externes, morphologiques ou phénotypiques (incluant des notions de couleur), des organismes afin de déterminer l'identité de ces organismes et délimiter les espèces (Narendran, 2008). Cette approche est à la base de la taxonomie et la description de la plupart des espèces est essentiellement effectuée jusqu'à maintenant sur ces critères (Padial *et al.*, 2010). La reconnaissance des organismes à partir des caractères morphologiques présente des avantages appréciés par la plupart des taxonomistes, en particulier la possibilité d'être applicable aux collections des spécimens conservées dans les musées ainsi qu'aux fossiles (Hillis, 1987). Par ailleurs, les caractères morphologiques servent à déterminer immédiatement l'identité des individus par simple inspection visuelle (Padial *et al.*, 2010).

Des inconvénients liés à cette méthode existent toutefois: (i) Echec pour délimiter des espèces appartenant aux complexes ou groupes possédant un grand niveau de la similarité morphologique (cas des espèces cryptiques) (Padial *et al.*, 2010; Gebiola *et al.,* 2012); (ii) Imprécision du diagnostic si des caractères présentant une plasticité phénotypique (influence de la plante-hôte ou de l'insecte hôte) sont utilisés (Gebiola *et al.,* 2012, Quicke, 1997; Delvare, 2005; Delvare *et al.*, 2014); (iii) Définition d'un caractère morphologique et interprétation de ces états qui relèvent parfois d'un jugement subjectif (Padial *et al.*, 2010); (v) Nécessité d'un grand nombre d'individus afin de démontrer la fixation d'un état d'un caractère morphologique (Wiens & Servedio, 2000). Par ailleurs, d'autres raisons pourraient être mentionnées pouvant limiter le recours à la morphologie pour identifier les organismes sous investigation, telles que la grave pénurie d'expertise pour un nombre important de groupes d'organismes; et le délai nécessaire pour obtenir l'identité d'un taxon à cause, notamment, de la nécessité de consulter des experts souvent distant (Tahseen, 2014).

1.2.1.3. La taxonomie moléculaire

1.2.1.3.1. Avantage et inconvénients de la taxonomie moléculaire

Compte tenu des limites précédemment décrites et de la nécessité de maintenir voire accélérer la découverte et la description de la diversité biologique (Guerra-GarcÍa *et al.*, 2008; Tahseen, 2014), l'utilisation de caractères moléculaires est apparue comme une alternative et/ou un complément intéressant. Les avantages liés à ces marqueurs moléculaires sont: (i) leur neutralité à l'influence de l'environnement et au stade du développement (Hillis, 1987; Bashasab *et al.*, 2006); (ii) leur utilité pour la délimitation des espèces qui ne possèdent pas de caractères morphologiques diagnostics ou qui présentent des espèces cryptiques (Hillis, 1987); (iii) la quantité d'informations disponible et sa diversité (ADN nucléaire, mitochondrial voire celui d'endosymbiotes associés) (Patwardhan *et al.*, 2014). Par contre, les marqueurs moléculaires ont des limites dans certains cas: (i) les méthodes moléculaires sont difficilement applicables sur des individus conservés à l'état sec ou sur des fossiles suite à la dégradation de l'ADN (Hoy, 2013); (ii) l'utilisation d'un nombre trop limité de marqueurs peut conduire à une discordance entre la structuration observée et la structuration réelle suite notamment à des processus d'hybridations inter-spécifiques (formation des individus hybrides comme un résultat d'un croisement entre au moins deux espèces proches), d'introgression (immigration via l'hybridation et le rétrocroisement de gènes d'une espèce vers le pool génétique d'une autre espèce génétiquement assez proche) ou de "incomplete lineage sorting" (retenu des polymorphismes ancestraux pour certain gènes au travers des événements de spéciation) (Rannala & Yang, 2008; Hoy, 2013) et (iii) pour les espèces rares, il peut encore exister un risque de dégrader la morphologie des spécimens-types lors de l'extraction d'ADN.

1.2.1.3.2. La démarche de ñBarcodingò

L'approche dite de "**barcodingò** (en anglais, "DNA Barcoding") est une technique basée sur l'utilisation de courtes régions standardisées du génome (appelées "barcodes") pour discriminer les taxa étudiés (Hebert *et al.*, 2003). Pour les animaux, la séquence d'ADN adoptée comme un barcode est une région d'environ 600-700pb du gène de la Cytochrome Oxydase I (*COI*) (Hebert *et al.*, 2003). Le "barcoding" est basé sur l'hypothèse que la variation génétique intra-spécifique de barcode est bien inférieure à la variation génétique inter-spécifique ("gap du barcoding"). Dans ce cas, les clusters génétiques mis en évidence peuvent être considérés comme des espèces indépendantes (Dasmahapatra & Mallet, 2006; Dasmahapatra *et al.*, 2010; Goldstein & DeSalle, 2010). Le barcoding d'ADN n'a pas l'objectif d'établir les relations phylogénétiques entre les taxons analysés ou de remplacer la taxonomie moléculaire mais plutôt de développer une méthode d'identification des espèces,

standardisée, rapide, moins chère et accessible pour des non-spécialistes afin de: (i) **assigner précisément les spécimens sous investigations aux espèces déjà décrites**; (ii) **favoriser la découverte et la description des nouvelles espèces**; et (iii) **faciliter la discrimination des espèces cryptiques** ou les complexes composés des espèces proches morphologiquement (Hebert *et al.*, 2003; Janzen *et al.*, 2005; Hebert *et al.*, 2004; Hajibabaei *et al.*, 2007; Frézal & Leblois, 2008; Goldstein & DeSalle, 2010).

Beaucoup d'études ont prouvé l'utilité et efficacité de cette approche d'identification dans des groupes de taxa difficiles ou mal connus (Hebert *et al.*, 2004; Janzen et al., 2005; Smith *et al.*, 2006; Pauls *et al.*, 2010). La démarche du barcoding a aussi permis **de faciliter lôassociation entre des individus ayant de différents stades de développement** (Ahrens *et al.*, 2007) **ou entre sexes**, pour les espèces présentant un dimorphisme sexuel important (Janzen *et al.*, 2005).

Malgré le succès incontestable de cette technique, plusieurs limites biologiques ou techniques sont évoquées incluant:

- **Présence des copies non-fonctionnelles** (appelées "numts = nuclear-mitochondrial DNA") du gène *COI* dans le noyau et qui conduisent à sur-estimer artificiellement la diversité au sein d'un taxon (Song *et al.*, 2008; Xiao *et al.*, 2010; Jordal & Kambestad, 2014).

- **Phénomène dôhétéroplasmie** qui se réfère à l'existence de plusieurs allèles de *COI* dans les cellules de l'individu (Magnacca & Brown, 2010; Berthier *et al.*, 2011). Ce phénomène pourrait empêcher d'obtenir directement sans clonage des séquences propres de *COI* et augmenter la variation intra-spécifique des séquences de taxon et donc conduire à des déterminations incorrectes (Rubinoff *et al.*, 2006).

- **Biais liés à la transmission maternelle.** Comme les gènes mitochondriaux sont hérités de la mère aux descendants, certains phénomènes peuvent conduire à des résultats peu fiables (Rubinoff *et al.*, 2006; Frézal & Leblois, 2008; Galtier *et al.*, 2009). Un de ces phénomènes est l'infection de certaines populations de la même espèce par différentes souche d'une bactérie endosymbiotique héritée maternellement comme *Wolbachia* pouvant entrainer la mort des mâles ou **lôincompatibilité cytoplasmique**, peut construire une source de la réduction de la diversité intra-spécifique au sein des séquences de *COI* car la sélection indirecte exécrée sur les souches de la bactérie conduit à fixer un haplotype unique de *COI* chez chuque population porteuse de cette bactérie. Par conséquent, le "gap du barcoding" est plus prononcé et cela favorise ainsi à construire des hypothèses des espèces cryptiques.

L'autre processus évolutif important qui nuit à la performance de l'ADN mitochondrial en tant que barcode est l'**introgression inter-spécifique**. En effet, ce phénomène homogénéise l'ADNmt d'espèces distinctes, réduisant la divergence inter-spécifique. Enfin, l'**isolement intra-spécifique** entre les populations à cause d'une faible mobilité, de spécificités différentes d'hôtes peuvent accélérer la divergence de l'ADNmt par rapport à la vitesse habituelle et conduire à sur-estimer le nombre d'espèces.

- **Diversité des taxa représentés** et, pour chacun d'eux, **étendue de la couverture géographique.** Ces deux paramètres peuvent en effet influencer la valeur du "gap du barcoding"et changer les conclusions. Plusieurs études ont mis en évidence l'influence de la taille d'échantillonnage sur l'estimation de la diversité intra- ou inter- et géographique (Meyer & Paulay, 2005; Bergsten *et al.*, 2012).

- **Taux de mutation trop faible** du gène *COI* et pas suffisant pour la différenciation des espèces sœurs récemment divergentes (Velzen *et al.,* 2012).

1.2.1.4. La taxonomie intégrative

Les caractères utilisés dans les études taxonomiques ne sont pas limités à la morphologie ou à l'ADN et d'autres types de caractères peuvent aussi être pris en compte: écologiques (spectre d'insectes hôtes ou plantes associées, habitat, niches écologiques), comportementaux (compétition inter/intra-spécifique, comportement d'accouplement), biologiques (traits d'histoire de vie), chimiques (phéromones sexuels, venins), ou géographiques (Padial *et al.*, 2010). Le terme de "taxonomie intégrative" a été récemment proposé comme une méthode taxonomique utile pour améliorer la délimitation des espèces et se réfère à la possibilité de combiner tous les types des informations pour examiner les limites des espèces (Dayrat, 2005; Will *et al.*, 2005; Schlick-Stieiner *et al.*, 2009; Padial *et al.*, 2010). D'après Dayrat (2005), l'intégration des multiples sources d'informations est nécessaire car la complexité de la biologie des espèces exige que les frontières des espèces doivent être définies à partir de preuves multiples et complémentaires. Trois constatations motivent le développement de la taxonomie intégrative. Premièrement, les caractères morphologiques échouent à délimiter les espèces dans certains cas, ce qui nécessite l'application d'autres sources d'informations. Deuxièmement, même si la morphologie réussit à délimiter les espèces, d'autres caractères peuvent aider de manière significative et accélérer le processus. Troisièmement, l'utilisation d'informations multiples aide la taxonomie à aller au-delà la seule dénomination des espèces

et permet la compréhension de leur origine évolutive (Schlick-Steiner *et al.*, 2010). D'une façon générale, la taxonomie intégrative a remarquablement amélioré le processus de la délimitation des espèces, en particulier pour des groupes ou complexes contenant des espèces étroitement liées et/ou cryptiques (Delvare *et al.*, 2014; Gebiola *et al.*, 2012; Lecocq *et al.*, 2015).

Padial *et al.* (2010) distingue deux manières de mettre en pratique la taxonomie intégrative dans la délimitation des espèces:

- **Intégration par concordance**: cette procédure basée sur l'idée que la concordance entre au moins deux types de caractères taxonomiques est nécessaire pour valider le statut taxonomique des espèces sous investigations. L'avantage majeur de cette approche est la stabilité des espèces définies, celles-ci étant acceptées par la plupart des taxonomistes. La limite principale de cette approche est le risque de sous-estimer le nombre d'espèces car le processus de spéciation n'est pas toujours accompagné par des changements pour les différents types de caractères. Une autre limite est le risque que cette approche ne soit surtout pertinente que pour la reconnaissance des espèces distantes ou ayant divergé depuis longtemps.

- **Intégration par cumulation** : le principe de cette approche est basé sur l'hypothèse que qu'au moins un caractère taxonomique "diagnostic" suffit à délimiter une espèce. Dans cette approche, la concordance est privilégiée mais n'est pas nécessaire. D'une façon générale, les preuves issues de chaque source d'information sont assemblées. Les éventuelles concordances et discordances sont ensuite expliquées dans une perspective évolutive. Finalement, les périmètres des espèces sont décidés. Le grand avantage de cette approche est que la délimitation des espèces n'est pas limitée a un caractère morphologique particulier; les taxonomistes peuvent donc sélectionner et se focaliser sur les caractères taxonomiques les plus informatifs et appropriés pour chaque groupe de taxa. Ainsi, la cumulation peut être considérée comme la procédure la plus adéquate pour découvrir les espèces inconnues ayant divergé récemment. Le défaut majeur de ce processus est que la délimitation des espèces peut être moins fiable, l'utilisation d'un seul caractère "discriminant" pouvant entrainer une sur-estimation du nombre d'espèces.

1.2.2. La phylogénie

1.2.2.1. Méthodes d'inférence en phylogénie

1.2.2.1.1. Généralités

La **phylogénie** se réfère à l'histoire évolutive d'un groupe d'organismes (taxa) (Harrison & Langdale, 2006). Le terme phylogénie est dérivé de deux mots grecs: "*phylon*" signifiant le tribu ou clan ou race et "*genesis*" signifiant l'origine ou la source (Patwardhan *et al.*, 2014). Les relations évolutives entre les taxa sont représentées par un diagramme de branchement ou un **arbre phylogénétique** qui est constitué des feuilles qui représentent les taxa descendants et des nœuds qui représentent les ancêtres communs hypothétiques de ces descendants. La phylogénie d'un groupe de taxa peut être reconstruite à partir des matrices des états des caractères morphologiques qui constituent une source importante d'informations pour une grande majorité des études actuelles et/ou à partir des alignements des caractères moléculaires (séquences nucléotidiques ou d'acides aminées) qui sont de plus en plus accessibles. La phylogénie combinée basée sur la concaténation des deux types de caractères dans une seule approche pourrait être plus robuste et résolutive que celle basée seulement sur la morphologie ou la moléculaire (Wahlberg *et al*. 2005; Wortly & Scotland, 2006).

Suivant la nature des informations (morphologiques et/ou moléculaires) et les méthodes utilisées, la longueur des branches peut représenter une distance évolutive, un nombre de mutations ou un nombre de changements de caractères et éventuellement, après calibration, des informations temporelles (date de divergence entre deux taxa par exemple). L'ordre relatif des branchements d'un arbre est appelé la topologie de l'arbre (Talavera, 2012).

Comme la Figure 1 présente, la reconstruction d'un arbre phylogénétique passe par plusieurs étapes (Talavera, 2012):

(i) l'identification, pour les approches basées sur la morphologie, des caractères homologues, c'est-à-dire des structures morphologiques comparables entre les taxa et, pour les caractères moléculaires, l'alignement des positions homologues;

(ii) dès que la matrice d'information ou l'alignement des séquences est disponible, la sélection d'un modèle d'évolution approprié;

(iii) ensuite, l'inférence des relations phylogénétiques au sein d'un groupe de taxa peut être réalisée via une diverse gamme d'algorithmes;

(iv) l'évaluation de la fiabilité de l'arbre.

En fait, chacune des étapes précédentes peut être accompagnée par des erreurs qui peuvent s'accumuler au cours du processus conduisant donc à une topologie erronée (Talavera, 2012). En ce qui concerne les données moléculaires par exemple, il ne faut utiliser que les séquences des gènes orthologues (gènes homologues ayant divergés par spéciation) et exclure toute autre sorte des gènes comme les paralogues (gènes liés par duplication) ou les Numts (copies mitochondriales dans le noyau) (Song *et al.*, 2008; Xiao *et al.*, 2010; Jordal & Kambestad, 2014). La sélection d'un modèle de substitution adéquat est également une procédure importante car l'utilisation d'un modèle d'évolution inadapté aux données peut changer les résultats de l'analyse phylogénétique (Bos & Possada, 2005).

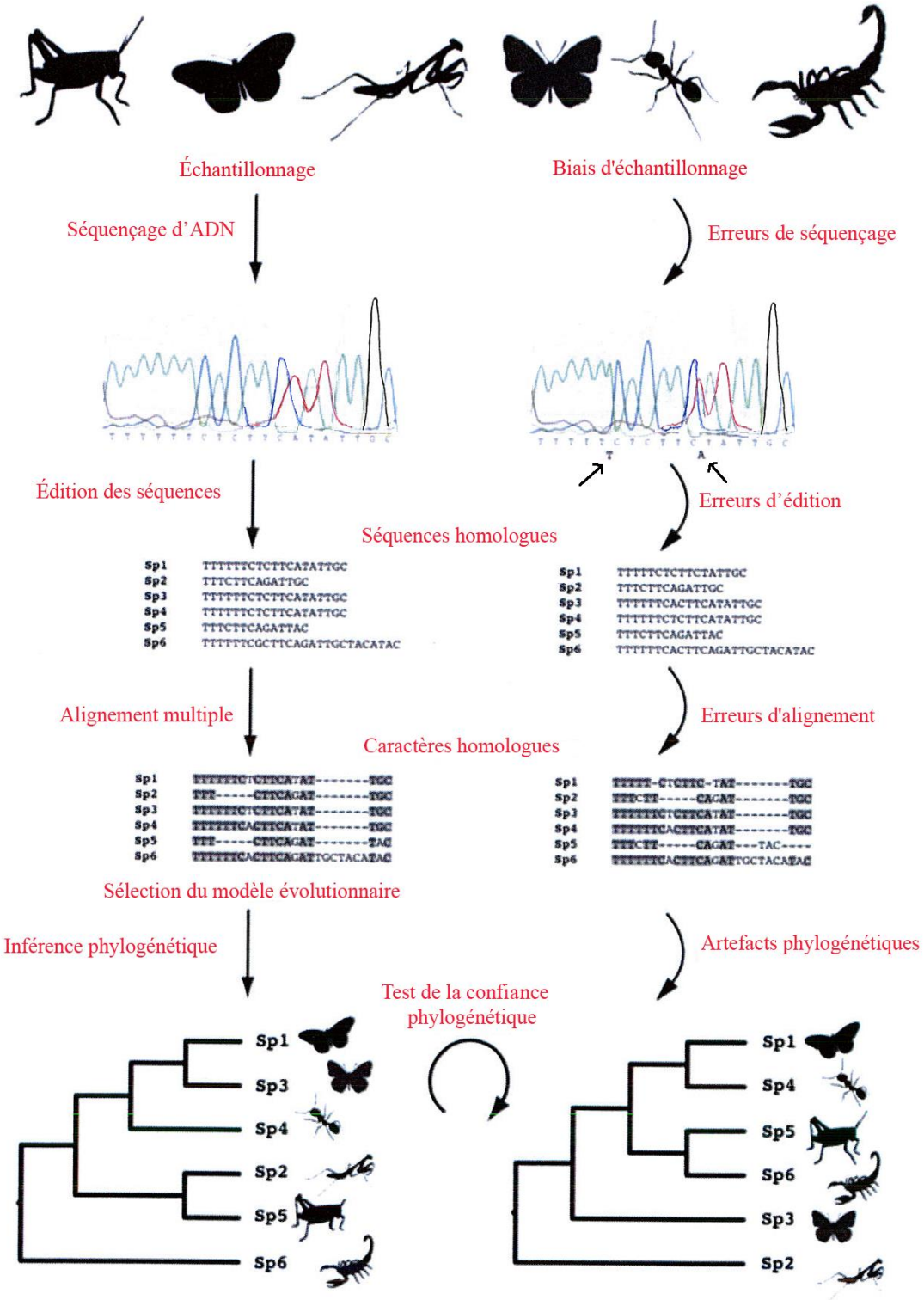

Figure 1: Diagramme résumant les différentes étapes nécessaires pour la reconstruction phylogénétique, les sources potentielles d'erreurs (Talavera, 2012).

Les méthodes de la reconstruction de l'arbre phylogénétique peuvent être classifiées en trois catégories décrites ci-dessous.

1.2.2.1.2. Méthodes basées sur les distances

Ces méthodes sont généralement appropriées pour la phylogénie moléculaire. Le principe de ces méthodes est basé sur l'idée de la transformation de la matrice de caractères en une matrice de distances qui représente la distance évolutionnaire entre chaque paire de séquences. Mais, les distances par paires (deux à deux ou *p*-distances) ne reflètent pas forcement les distances évolutionnaires réelles entre les séquences lointainement apparentées car multiples substitutions (multiples hits) peuvent se survenir dans le même site nucléotidique et donc une correction de ces distances observées deux à deux est nécessaire en utilisant un des modèles d'évolution disponibles comme JC69 (Jukes & Cantor, 1963), K2P (Kimura, 1980), TN93 (Tamura & Nei, 1993) etc. (Holder & Lewis, 2003). Sur la base de cette matrice de distance, un arbre phylogénétique peut être créé, en appliquant différentes méthodes: "unweighted pair-group method with arithmetic average" (UPGMA) (Sokalet & Michener, 1958); Neighbour-joining (NJ) (Saitu & Nei, 1987); Minimum d'évolution (ME) (Rzhetskyet & Nei, 1992) ou méthode des moindres carrés (Fitch & Margoliash, 1967). Un des avantages de ces méthodes est qu'elles sont rapides. Par contre, leur performance ou fiabilité est faible quant la diversité génétique des taxa analysés est grande car les grandes distances génétiques sont mal estimées (Yang, 2006).

1.2.2.1.3. Maximum de parcimonie

Cette méthode est basée directement sur la matrice des caractères (morphologiques et/ou moléculaires). Ces méthodes ont été initialement développées pour la phylogénie morphologique mais sont maintenant devenues populaires pour l'estimation de la phylogénie moléculaire (Futuyma, 2013). Ces méthodes sélectionnent, parmi tous les arbres phylogénétiques qui peuvent décrire les relations parmi un groupe de taxa, l'arbre qui implique le moins de changements évolutifs dans les caractères examinés. Autrement dit, les méthodes basées sur la parcimonie fonctionnent en choisissant l'arbre qui minimise la longueur totale des branches (c. à-d. le nombre de changements évolutifs nécessaires pour expliquer les données observées) (Xiong, 2006; Yang, 2006). La reconstruction des arbres par le maximum de parcimonie (MP) passe par trois étapes: (i) Calculer le nombre minimal de

substitutions à chaque site informatif, qui est un site ayant au moins de changements de caractère, pour une topologie donnée; (ii) Additionner le nombre total de changements à tous les sites informatifs pour chaque topologie possible; (iii) Choisir l'arbre ayant le nombre minimal de changements (Xiong, 2006). L'avantage du MP est que cette méthode est intuitive car son hypothèse est facile à comprendre. En plus, cette méthode peut fournir des informations sur les données observées comme l'intensité de l'homoplasie, qui se réfère à une similarité résultante soit d'une convergence évolutionnaire entre des taxa n'ayant pas un ancêtre commun ou soit d'une réversion entre des taxa ayant un ancêtre commun, et les états ancestraux des caractères (Xiong, 2006). Cependant, cette méthode ne considère que les sites informatifs et oublie les autres types de sites (variables, qui ont un changement, & constants, qui ne soumissent pas aux changements), et par conséquent certains signaux phylogénétiques peuvent être perdus (Xiong, 2006). Par ailleurs, cette méthode peut échouer à estimer correctement les relations phylogénétiques quand la quantité de la divergence génétique ou l'homoplasie est élevée car, dans ce cas-là, le principe de cette méthode, qui est basé sur l'hypothèse de rareté des changements, ne tient plus (Xiong, 2006; Hoy, 2013).

1.2.2.1.4. Méthodes probabiliste

Les méthodes probabilistes comme le **maximum de vraisemblance** (ML) et l'**inférence bayésienne** (BI) sont des méthodes puissantes, utilisées actuellement pour l'estimation des phylogénies à partir des séquences moléculaires (Futuyma, 2013).

Ces deux méthodes probabilistes sont fondées sur le concept de vraisemblance. La vraisemblance d'un arbre est la probabilité conditionnelle d'observer les données (la matrice de séquences, D) sous un ensemble d'hypothèses (la topologie de l'arbre T et le modèle d'évolution d'ADN) ce qui peut être résumé de la façon suivante (Delsuc & Douzery, 2004):

$$L\ (T) = Pr\ (D \mid T, Q)$$

La topologie, les longueurs des branches et les paramètres du modèle d'évolution qui maximisent la vraisemblance des données sont ensuite calculés (Talavera, 2012).

L'autre méthode adoptée récemment en phylogénie moléculaire est l'approche bayésienne (BI) (Delsuc & Douzery, 2004). Cette méthode utilise le théorème de Bayes qui combine la probabilité *a priori Pr (T)* d'un arbre *T* avec la vraisemblance *Pr (D | T, Q)* des données observées *D* sachant cet arbre *T* pour produire une distribution de probabilité postérieure *Pr (T | D)* sur les arbres.

$$Pr\ (T \mid D) = \frac{Pr\ (D \mid T, Q)\ Pr\ (T, Q)}{Pr\ (D)}$$

La probabilité postérieure d'un arbre pouvant être interprétée comme la probabilité que cet arbre soit vrai sachant les données, les inférences sur l'histoire du groupe des espèces sont ensuite basées sur la probabilité postérieure des arbres et l'arbre avec la plus haute probabilité postérieure peut être choisi comme la meilleure estimation de la phylogénie (Delsuc & Douzery, 2004; Bos & Possada, 2005). Puisque le calcul des probabilités postérieures des arbres phylogénétiques est analytiquement impossible, la technique de Markov Chaine Monte Carlo (MCMC) est utilisée.

D'un point de vue pratique, les méthodes de ML ne peuvent être utilisées qu'avec un jeu de données relativement petit. Par contre, l'analyse d'un large jeu de données est plus facile avec les méthodes BI (Hoy, 2013). En plus, alors que l'approche de ML génère un seul arbre qui représente la meilleure estimation des relations phylogénétiques et ignore l'incertitude qui pourrait être associée avec l'estimation finale, l'approche de BI produit une série des arbres dont un avec la plus haute probabilité postérieure sera accepté et préféré (Bos & Possada, 2005; Hoy, 2013).

Une fois que les arbres phylogénétiques ont été reconstruits, la robustesse de ces arbres ou l'adéquation entre les données et la topologie de l'arbre peut être mesurée. La confiance des arbres phylogénétiques, excepté ceux inférés via l'approche de BI dans laquelle la probabilité postérieure présente une évaluation directe de la robustesse phylogénétique, peut être évaluée en utilisant *a posteriori* des critères statistiques comme la procédure de bootstrapping (Felsenstein, 1985), le test du ratio de vraisemblance approximative (aLRT) (Anisimova & Gascuel, 2006) ou index de Bremer (BI) (Bremer, 1994).

1.3. Contexte méthodologique: marqueurs moléculaires chez les insectes

1.3.1. Généralités

Les approches moléculaires sont appliquées de manière efficace dans les études de la systématique des insectes depuis les années 1980 (Okiwelu & Noutcha, 2014). Ces techniques moléculaires ont inclus: l'électrophorèse des protéines; la cytologie moléculaire;

l'amplification aléatoire d'ADN polymorphe (RAPDs); l'analyse du polymorphisme de longueur des fragments amplifiés (AFLPs); l'analyse du polymorphisme de longueur des fragments de restriction (RFLPs); la technique du polymorphisme des nucléotides simples (SNPs); le séquençage d'ADN "classique"; techniques dites de "Nouvelles Générations de Séquençage". Parmi celle-ci, la technique du séquençage des gènes d'ADN voire de génome entier peut représenter l'approche la plus accessible et appropriée pour: (i) délimiter les groupes d'espèces distant ou cryptiques; (ii) étudier la variabilité intra-spécifique; (iii) étudier la variation géographique et écologique; et (iv) inférer l'histoire d'évolution des groupes d'espèces. Dans ce chapitre, nous présenterons les marqueurs classiquement utilisés pour la caractérisation moléculaire des insectes.

1.3.2. LôADN mitochondrial

Les mitochondries sont des organelles situées dans le cytoplasme des eucaryotes dont elles assurent la production d'énergie nécessaire. Chez les insectes, l'ADN mitochondrial (ADNmt) est une molécule circulaire compacte d'une taille de 15-18 kb (Cameron, 2014) composée de 37 gènes: 13 gènes codant pour des protéines (PCGs), 22 ARN de transfert (ARNt) impliqués dans la traduction des gènes (Crozier & Crozier, 1993) et 2 ARN ribosomiques (ARNr) (Figure 2). L'arrangement des gènes au sein du génome mitochondrial est hautement conservée (Avise *et al.*, 1987). En plus de ces gènes, l'ADN mitochondrial contient au moins une région non-codante (région riche en A-T) responsable du contrôle de la réplication et transcription. Malgré le fait que l'ADNmt ne représente qu'une petite fraction du génome d'un organisme, c'est le marqueur le plus populaire pour étudier la diversité moléculaire des animaux au cours de ces trois décennies (Cameron, 2014).

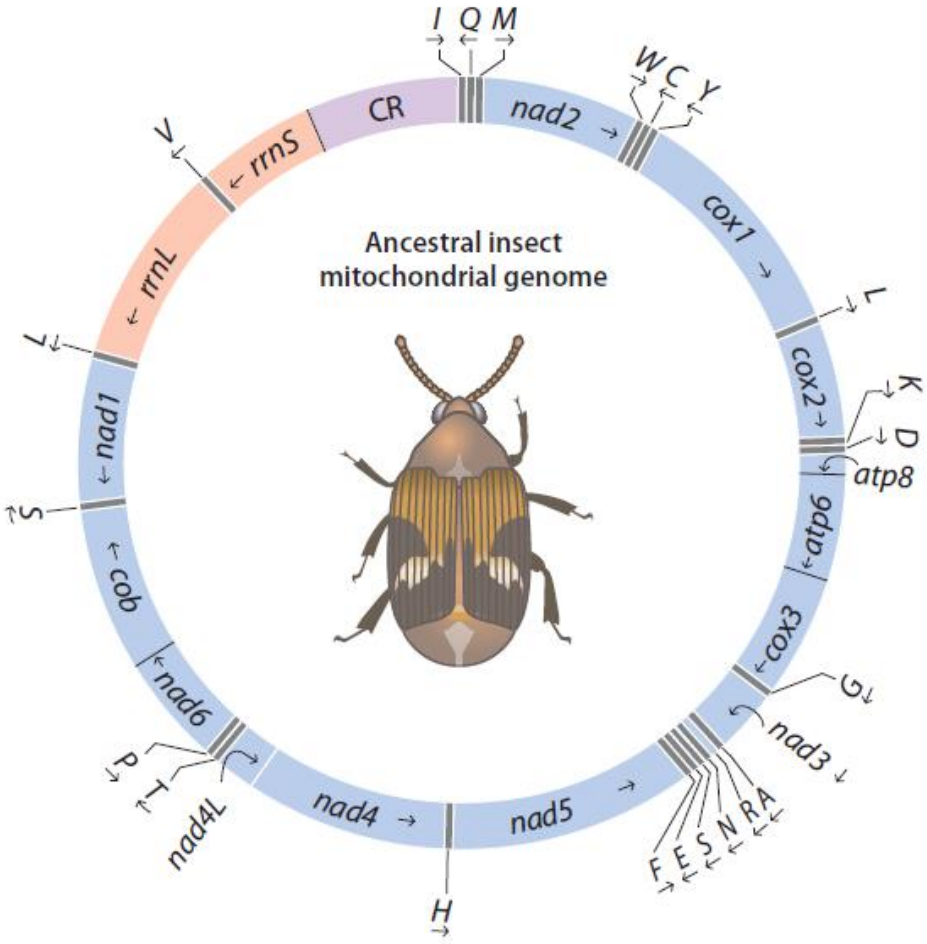

Figure 2: Diagramme illustrant le génome mitochondrial hypothétique de l'ancêtre des insectes (d'après Cameron, 2014).

Les gènes d'ARN transferts sont indiqués par les premières lettres des acides aminées correspondantes, la direction de la transcription des gènes est indiquée par une flèche.

Les gènes codant pour une protéine sont indiqués en bleu Les abréviations: *atp6*, *atp8*: les sous-unités 6 et 8 d'ATP-synthase; *cob*: le gène de cytochrome oxydase *b*; *cox1-cox3*: les sous-unités 1-3 de cytochrome oxydase *c*; *nad1-nad6*, *nad4L*: les sous-unités 1-6 et 4L de NADH-déshydrogénase.

Les deux sous-unités d'ARN ribosomiques (*rrnS*, *rrnL*) sont figurées en rouge.

La région non codante CR impliquée dans le contrôle de la transcription et de la réplication est présentée en violet.

Les avantages des séquences nucléotidiques de l'ADNmt pour les études de la systématique des insectes sont les suivants:

- Omniprésence de l'ADNmt chez tous les animaux (Avise *et al.*, 1987; Zhang & Hewitt, 1996).

- Comme les mitochondries existent en milliers dans chaque cellule, l'ADNmt est très abondant et donc le potentiel d'extraction d'ADNmt en bonne quantité et qualité même à partir des petits spécimens est élevé (Avise *et al.*, 1987; Harrison, 1989; Caterino *et al.*, 2000; Galtier *et al.*, 2009; Hoy, 2013).

- Absence des introns et faible nombre d'indels (d'un à quelques nucléotides) (Avise *et al.*, 1987), ce qui assure une conservation relative de la taille et de la structure des séquences générées et donc une facilité d'aligner et comparer les séquences homologues du même gène mitochondrial obtenues de différents taxa (Harrison, 1989).

- Facilité pour amplifier et séquencer des gènes mitochondriaux caractérisés par une forte variabilité (p.ex. région du contrôl*e, COI*, *Cytb*,…) grâce des amorces "universelles" définies dans des régions conservées flanquantes (Galtier *et al.*, 2009).

- Hérédité maternelle du génome mitochondrial. Il est mis en évidence que l'ADNmt est transmis de la mère aux descendants (Gyllensten *et al*. 1985). Par ailleurs, la transmission de l'ADNmt dans la lignée germinale des femelles est caractérisée par un fort goulot d'étranglement qui conduit souvent à réduire la diversité d'DNAmt intra-individuel *(*Shoubridge & Wai, 2007). Cette transmission maternelle et les goulots d'étranglement limitent ainsi les recombinaisons (Galtier *et al.*, 2009). En plus, l'absence de la recombinaison ou d'échange génétique a été considéré un trait utile car il implique que l'histoire évolutive d'ADN mitochondrial au sein des espèces pourra être présentée par un arbre unique qui retracera les origines et les mouvements géographiques des lignées (Galtier *et al.*, 2009).

- Fort taux de substitution qui conduit à une variabilité importante de l'ADNmt entre les populations naturelles ce qui peut générer des signaux sur l'histoire évolutive des populations des espèces proches sur de courtes périodes (Galtier *et al*., 2009).

- Taux d'évolution supposé constant dans le temps et l'espace ce qui permettrait d'estimer les temps de divergence entre différents taxas (Hoy, 2013).

Cependant, l'ADN mitochondrial a des défauts qui peuvent lui rendre un marqueur inapproprié pour les études de la systématique des insectes et ces limitations sont discutées dans le paragraphe qui traite "la démarche du barcoding".

Les gènes mitochondriaux les plus utilisés sont ceux codant pour des protéines (en particulier *COI*, *COII*, et *COIII* et *Cytb*) ainsi que les deux régions ribosomiques, *12S* et *16S*. *COI* et *COII* ont été séquencés dans une grande variété de taxa avec des séquences homologues disponibles pour a peu près tous les ordres d'insectes comme Coleoptera, Hemiptera, Hymenoptera, Lepidoptera, Neuroptera, Orthoptera et Siphanoptera (Caterino *et al.*, 2000) mais, dans le cas de *COI*, la région amplifiée de ce gène varie d'une étude à l'autre (Caterino *et al.*, 2000). Les séquences des gènes mitochondriaux peuvent être analysées individuellement pour étudier la diversité inter et/ou intra-spécifique (Hebert *et al*., 2004; Gebiola *et al.*, 2009; Xiao *et al.*, 2010; Delvare *et al.,* 2014; Jordal & Kambestad, 2014), ou en combinaison avec d'autres marqueurs moléculaires (mitochondriaux et/ou nucléaires) pour inférer l'histoire évolutive des espèces relativement proches, estimer le temps de divergence ou comparer les phylogénies basées sur l'ADN mitochondriaux et nucléaire pour détecter certains phénomènes tels que l'hybridation ou l'introgression (Deuve *et al*., 2012; Cruaud *et al*., 2013).

En plus des comparaisons des séquences nucléotidiques homologues, les réarrangements des gènes mitochondriaux peuvent également servir pour inférer les relations phylogénétiques chez les insectes (Cameron, 2014). La réorganisation du génome mitochondrial a reçu une attention considérable par les biologistes de l'évolution, d'une part, parce que ce phénomène pourrait être rare et, d'autre part, parce que la possibilité de convergence (même réarrangement dérivé dans des génomes mitochondriaux de deux taxa différents) semble faible à cause du nombre de gène (37) (Boore & Brown, 1998; Cameron, 2014). Les réarrangements des génomes mitochondriaux observés sont plus ou moins importants (nombre de gènes impliqués, implication ou non de gènes codants et/ou de gènes d'ADN ribosomaux) et, en général, les gènes codant pour des protéines et les ARN de transfert (ARNt) sont plus soumis aux changements (Cameron, 2014). La réorganisation des génomes mitochondriaux a ainsi été exploitée pour résoudre les relations phylogénétiques inférieures au niveau de l'ordre chez différents taxa d'insectes (Cameron, 2014). Les séquences du génome mitochondrial complet pour plus de 600 espèces d'arthropodes sont actuellement disponibles dans GenBank et d'autres bases de données (Cameron, 2014).

1.3.3. LôADN nucléaire:

Dans le cadre de ce paragraphe, nous distinguerons deux catégories de gènes nucléaires.

1.3.3.1. Gènes nucléaires ribosomiques

La popularité des gènes nucléaires ribosomiques (ADNr) vient de leur abondance dans les cellules et la facilité de leurs amplification et séquençage (Cameron *et al.*, 1992; Caterino *et al.*, 2000; Hoy, 2013). En plus, comme la plupart de ces gènes ont un taux d'évolution supérieur aux gènes nucléaires codant pour des protéines, ils sont considérés comme informatifs pour résoudre les relations phylogénétique au niveaux taxonomiques intermédiaires et inférieurs (Cameron *et al.*, 1992; Caterino *et al.*, 2000). Cependant, l'alignement des séquences de ces gènes peut être difficile voire impossible pour des espèces très distantes du fait de la présence des régions variables ayant des insertions et délitions (Cameron *et al.*, 1992; Caterino *et al.*, 2000; Hoy, 2013).

Les gènes nucléaires ribosomiques constituent des familles multi-géniques dans lesquelles tous les membres ont des séquences identiques ou proches qui rendent ces gènes faciles à être amplifiés et séquencés. Chez les eucaryotes, comme le montre la Figure 3, chaque cluster d'ADNr est constitué d'un gène codant (ARNr *18S*) pour la petite sous-unité d'ARN (SSU rRNA), un gène codant (ARNr *28S*) pour la grande sous-unité d'ARN (LSU rRNA), deux "espaceurs" transcrits mais non traduits internes (*ITS1* et *ITS2*) séparés par le gène d'ARNr *5.8S*,etet deux "espaceurs" transcrits externes (ETS) situés en amont de L'ADNr *18S* et en aval de l'ADNr *28S*. Les unités adjacentes des réplétions d'ADNr sont séparées par un espaceur non-transcrit (NTS) (Coleman, 2003; Dabert, 2006; Hoy, 2013). Les gènes nucléaires ribosomiques ont prouvé leur utilité dans la résolution des relations phylogénétiques à différents niveaux taxonomiques chez les insectes.

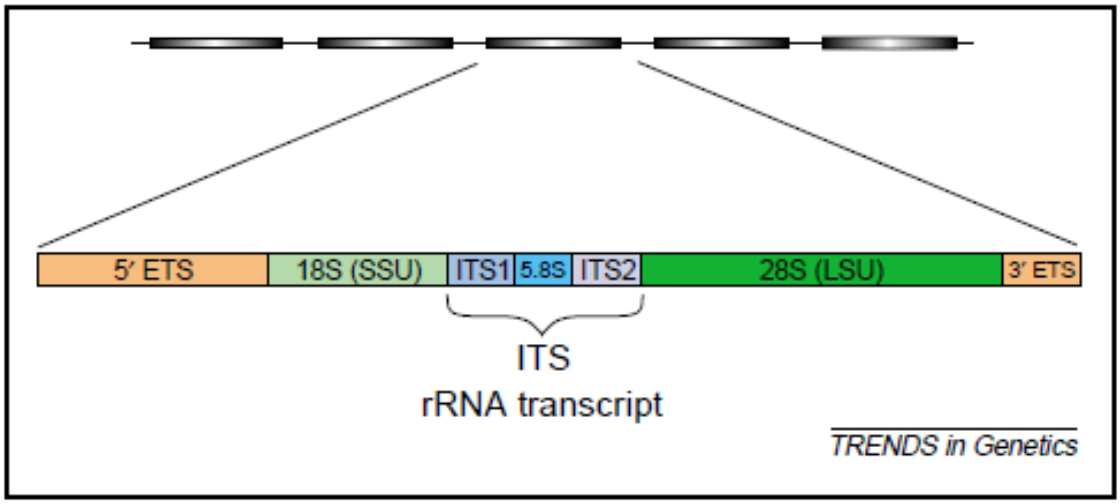

Figure 3: Diagramme illustrant l'organisation en clusters (boites grises) de l'ADN ribosomique d'un eucaryote (d'après Coleman, 2003).

Légende: ETS; espaceur non-transcrit externe; 18S: petite sous-unité d'ARN; ITS1 et ITS2 : "espaceurs" transcrits internes; 5.8S: sous-unité séparant ITS1 et ITS2; 28S: large sous-unité d'ARN.

Ainsi, les séquences nucléotidiques des espaceurs internes (*ITS1* & *ITS2*) sont très efficaces et utiles pour établir les relations phylogénétiques au niveau spécifique; inter-spécifique (incluant des cas d'espèces cryptiques ou d'hybridations) voire générique (Yara, 2006; Smith *et al.*, 2007; Gebiola *et al.*, 2009; Ercan *et al.*, 2011; Kol–Maimon *et al.*, 2014) car ces marqueurs évoluent plus rapidement que les autres marqueurs d'ADNr mais sont inadéquats pour étudier les relations phylogénétiques profondes (Coleman, 2003; Hillis & Dixon, 1991). En plus, ces marqueurs *ITS1* et *ITS2* ont été proposé comme des barcodes d'ADN au même titre que le gène mitochondrial, *COI*. Un des problèmes majeurs liés à ces marqueurs *ITS1* et *ITS2* est la difficulté d'aligner les séquences nucléotidiques de ces régions chez des espèces très divergentes (par exemple, des espèces appartenant à des familles différentes) (Caterino *et al.*, 2000; Rokas *et al.*, 2002; Coleman, 2003; Blaxter, 2004). Cette difficulté peut toutefois être surmontée pour le gène d'*ITS2* en alignant les séquences à partir de la structure secondaire de cette région (Coleman, 2003).

A cause de leur longueur, les séquences des gènes de *18S* et *28S* sont caractérisés par des régions très conservées et des régions plus variables (Hillis & Dixon, 1991; Cameron *et al.*, 1992; Caterino *et al.*, 2000). Le gène de la petite sous-unité d'ADNr *18S* est le gène nucléaire

ribosomique le plus séquencé et utilisé dans les études de systématique moléculaire chez les insectes (Caterino *et al.*, 2000). Le gène de *18S* est considéré comme un marqueur approprié pour les relations phylogénétiques au niveau taxonomique supérieur ou profond (inter-familles et inter-ordres) car les séquence de ce gène sont caractérisées par un faible taux de substitution (Hillis & Dixon, 1991; Rokas *et al.*, 2002). Un autre avantage encourageant l'utilisation du gène *18S* pour la phylogénie des taxons est la possibilité d'amplifier entièrement ce gène (≈ 1800 pb) via des amorces universelles (Hillis & Dixon, 1991; Dabert, 2006). Le gène de la large sous-unité d'ADNr *28S* est le gène nucléaire ribosomique le plus long (allant de 3000 à 5000 pb) (Dabert, 2006). Le gène de *28S* contient plusieurs domaines ou segments présentant des évolutions divergentes et il présente donc des tailles variables entre ou au sein des phylums (Hillis & Dixon, 1991). Le gène *28S* peut fournir un signal phylogénétique utile pour clarifier les relations phylogénétiques entre les espèces au niveau taxonomique supérieur (ordres et familles) ainsi qu'au niveau taxonomique inférieur (genres et espèces) (Hillis & Dixon, 1991; Hwang & Kim, 1999). Blaxter (2004) a proposé d'utiliser les séquences nucléotidiques des segments d'expansion hautement divergents des gènes de *18S* et *28S* comme des séquences du barcode d'ADN pour assurer un outil rapide d'identification des espèces. Le gène d'ADNr *5.8S* a les mêmes propriétés évolutives que *18S* et *28S* mais ce gène n'a pas été inclus dans les études de systématique moléculaire des insectes à cause de sa petite taille (≈ 150 pb) (Hillis & Dixon, 1991; Cameron *et al.*, 1992; Hwang & Kim, 1999; Rokas *et al.*, 2002). Pour exploiter de façon optimale le signal phylogénétique porté par les gènes nucléaires ribosomiques, les taxonomistes et phylogénéticiens combinent les séquences nucléotidiques des *18S* et *28S* avec les séquences nucléotidiques d'autres gènes ayant différentes vitesse d'évolution (Cruaud *et al.*, 2010; Deuve *et al.*, 2012; Heraty *et al.*, 2012; Cruaud *et al*., 2013; Farache *et al.*, 2013; Trizzino *et al*., 2013; Sriphirom *et al.*, 2014; Taekul *et al.*, 2014; Gebiola *et al.*, 2015).

1.3.3.2. Gènes nucléaires codant pour des protéines

Plusieurs gènes nucléaires codant pour des protéines ont été utilisés avec succès dans les études de systématique moléculaire des insectes (Friedlander *et al.*, 1991; Caterino *et al.*,2000; Rokas *et al.*, 2002; Danforth *et al.*, 2005). Comme ces gènes peuvent représenter une vaste source d'information complémentaire ou alternative aux autres marqueurs (gènes mitochondriaux et/ou des gènes nucléaires ribosomiques). Alors que certains gènes nucléaires codant pour des protéines (par exemple *EF-1Ŭ*, *RpS4*) ont prouvé leur utilité pour résoudre les

relations phylogénétiques anciennes (Cho *et al*., 1995; Belshaw and Quicke, 1997; Rokas *et al*., 2002; Mitchell *et al*., 1997; Mitchell *et al*., 2000; Lin & Danforth, 2004; Cruaud *et al*., 2013), d'autres peuvent représenter des marqueurs candidats porteurs du signal phylogénétique suffisant à détecter les événements récents de divergence (par exemple, *Wg*, *Rpl27a*) (Cruaud *et al*., 2013). Les séquences des gènes nucléaires sont ainsi fréquemment utilisées en combinaison avec des séquences des gènes mitochondriaux pour améliorer la résolution des arbres phylogénétiques ((Cruaud *et al*., 2010; Deuve *et al*., 2012; Cruaud *et al*., 2013; Farache *et al*., 2013; Taekul *et al*., 2014).

Cependant, l'utilisation des séquences des gènes nucléaires pose quelques problèmes potentiels incluant (i) l'hétérozygotie et le faible nombre de copies, qui peuvent empêcher leur amplification par PCR (Caterino *et al*., 2000; Hoy, 2013); (ii) l'absence de régions très conservées pour dessiner des amorces chez certains groupes de taxa (Danforth *et al*., 2005); (iii) la difficulté d'amplification de certains gènes par PCR à cause de la présence de larges introns; et (iv) la représentation de certains gènes nucléaires par plusieurs copies (paralogues) (Caterino *et al*., 2000; Hoy, 2013).

1.4. Cadre écologique et évolutionniste: Spéciation et spécialisation chez les insectes

1.4.1. Généralités sur les mécanismes de spéciation

Les espèces sont considérées des unités d'étude fondamentales pour aborder des enjeux tels que l'évaluation de la biodiversité, l'étude des communautés, la biologie de la conservation, etc. Cependant, la définition du concept de l'espèce reste toujours une question controversée, notamment à cause de la diversité des critères utilisables pour délimiter les espèces (Sites *et al*., 2004). Un de ces critères majeurs reste évidemment le critère "biologique" de Mayr (1963) qui définit l'espèce comme un ensemble d'individus/populations effectivement ou potentiellement interfécondes et isolés reproductivement d'autres groupes mais ce critère est souvent difficilement utilisable. A noter que la définition des espèces dans la plupart des études systématiques des insectes est basée sur la similarité morphologique et/ou sur la monophylie phylogénétique.

La diversité biologique observée chez les organismes vivants s'explique par le phénomène évolutif dit spéciation. **La spéciation** est le processus évolutif responsable de l'établissement des isolements reproductifs entre des individus conspécifiques et finalement de l'émergence

de nouvelles espèces (on les appellera “espèces-sœurs” dans la suite de ce paragraphe) à partir d’une espèce dite “ancestrale” (Ravigné, 2010). Classiquement, différents modes de spéciation sont identifiés selon le recouvrement géographique initial entre les deux espèces sœurs: (a) la spéciation allopatrique impliquant une séparation physique au sein de l’espèce ancestrale et l’apparition des “espèces-sœurs” dans des aires géographiques isolées; (b) la spéciation parapatrique impliquant une séparation géographique partielle au sein de l’espèce ancestrale et l’émergence des espèces-sœurs malgré du flux limité des gènes au travers d’une zone d’hybridation; (c) la spéciation sympatrique impliquant une formation des espèces-sœurs dans la même zone géographique sans isolation (Wiley & Lieberman, 2011). Des scénarios alternatifs et/ou complémentaires pouvant conduire à l’apparition de barrières reproductives peuvent être proposés (Schluter, 2001) comme la spéciation écologique qui était contreversé pendant longtemps. Ce mode de spéciation repose sur une **divergence écologique** initiale au sein de l’espèce ancestrale - c’est-à-dire une adaptation à des (micro/macro)environnements différents ou un changement dans l’utilisation des ressources ou des habitats - qui contribue à l’établissement des barrières aux flux des gènes entres les individus présentant des écologies contrastés et finalement à l’apparition des espèces sœurs distinctes (Rundel & Nosil, 2005). La spéciation écologique peut se produire dans n’importe quel arrangement géographique des populations (Matsubayashi *et al*., 2010). Le fonctionnement de la spéciation écologique nécessite trois principaux éléments: (i) une source de la sélection divergente incluant les habitats et les interactions entre espèces; (ii) une forme de la barrière reproductive qui peut être pré-zygotique ou post-zygotique; et (iii) un mécanisme génétique reliant la sélection divergente et l’isolement reproductif (Rundel & Nosil, 2005). A la lumière de la spéciation écologique, l’émergence des espèces spécialistes peut être déterminées par deux mécanismes (Hardy & Otto, 2014): (i) l’hypothèse d’oscillation, dans ce modèle, les espèces ancestrales généralistes sont la source de la génération des espèces spécialistes. En effet, l’apparition de ces espèces spécialistes est le résultat du changement de la largeur des niches (c. -à-d. spécialisation d’hôtes) chez certaines populations au sein de l’espèce ancestrale généraliste; (ii) l’hypothèse de chaises musicales (en anglais, “musical chairs”), dans ce modèle, les espèces ancestrales spécialistes constituent une source additionnelle pour l’apparition des espèces spécialistes. En effet, l’émergence des espèces spécialistes est le résultat du changement d’hôte “host switch” chez certaines populations au sein de l’espèce ancestrale spécialiste.

1.4.2. Spéciation et spécialisation chez les insectes herbivores

Les insectes phytophages sont considérés comme le groupe d'organismes le plus riche en espèces, le nombre total d'espèces étant estimé au moins à 500000 soit environ un quart des animaux multicellulaires décrits (Bernays, 2003). Les causes de cette diversité ont été intensivement étudiées et la spéciation écologique semble être une des principales causes de cette diversité (Abrahamson *et al.*, 2001; Schoonhoven *et al.*, 2005; Futuyma, 2008; Matsubayashi *et al.*, 2010). D'une façon générale, il est admis, d'une part, que la plupart des espèces d'insectes herbivores sont caractérisés par une spécificité d'hôte étroite, il est estimé que moins de 10% des insectes ravageurs se nourrissent sur des plantes appartenant aux plus de 3 différentes familles (Schoonhoven *et al.*, 2005), et, d'autre part, que les espèces généralistes peuvent être composées de populations spécialistes (Carletto *et al.*, 2009). Chez les espèces généralistes, il est évidemment tentant de voir dans les **ñraces hôtesò** une première étape vers la spéciation si la constitution des populations divergentes adaptés à une nouvelle plante-hôte crée également des accouplements d'homogamie (en anglais, "assortative mating") (Abrahamson *et al.*, 2001; Drès & Mallet, 2002). Un des meilleurs exemples qui illustre le rôle du changement d'hôtes dans l'apparition des nouvelles lignées est documenté chez la mouche téphritide *Rhagoletis pomonella* (Walsh, 1867) (Bush, 1969). Cette espèce se développe à l'origine sur les fruits d'aubépine *Crataegus spp*., (Rosaceae), mais quand la pomme *Malus pumila* (Rosaceae) a été domestiquée, cette mouche s'est développée sur les fruits des pommes. Donc, la spécialisation de certaines populations de cette mouche sur les pommiers a conduit à former des races d'hôtes et il est trouvé que les individus de chaque race s'accouplent et pondent sur leur hôte de préférence, fruits d'aubépine ou fruits de pomme. En conséquence, l'incorporation d'une nouvelle plante dans le régime alimentaire chez *R. pomonella* a favorisé la formation des races d'hôtes et donc la spéciation écologique à l'aide de spécificité d'hôtes. Une autre évidence sur la formation de races d'hôtes et donc des espèces sœurs distinctes a été documenté chez la téphritide *Eurosta solidaginis* (Fitch, 1855) qui induit des galles sur les tiges de *Solidago* (Asteraceae) (Craig *et al.,* 1993; Brown *et al.,* 1996; *Craig et al.,* 1997). Il est montré que *E. solidaginis* forment deux races d'hôtes sur deux espèces proches sympatriques de verge d'or, *S. altissima* et *S. gigantea* et ces deux races montrent des dates d'émergence différentes et s'exercent l'accouplement d'homogamie.

1.4.3. Spéciation et spécialisation chez les insectes parasitoïdes

Les insectes phytophages sont attaqués par un extraordinaire assemblage d'insectes parasitoïdes. Les **parasitoïdes** se définissent comme des insectes dont la phase adulte est libre et la phase pré-imaginale parasite. Suivant les espèces de parasitoïdes, les hôtes sont tués plutôt rapidement (parasitoïdes idiobiontes) ou après un délai relativement long durant lequel l'hôte continue à se développer (parasitoïdes koïnobiontes) (Godfray & Shimada, 1999). Les parasitoïdes sont mieux connus au sein des Hyménoptères mais peuvent se survenir dans d'autres ordres d'insectes comme les Diptères, Coléoptères, Lépidoptères, Neuroptères et Trichoptères (Quicke, 1997). Dans leur ensemble, leur diversité est estimé à 87,000 espèces, soit environ 10% de toute la diversité décrite d'insectes (Eggleton & Belshaw, 1992). Cependant, puisque la majorité des parasitoïdes sont des hyménoptères - un des groupes d'insectes les plus difficiles à identifier avec une haute fiabilité - cette estimation est probablement très incertaine. D'autres estimations avancent ainsi le chiffre de plus d'un million d'espèces (Godfray & Shimada, 1999).

Contrairement aux insectes phytophages, les mécanismes de spécialisation et de spéciation ont été encore relativement peu étudiés chez les insectes parasitoïdes chez qui, évidemment, les mécanismes généraux de spéciation évoqués précédemment s'appliquent. De façon originale, il est également proposé que la diversification chez les insectes parasitoïdes pourrait être la conséquence de celle de leurs hôtes (Stireman *et al.*, 2006). C'est ce qu'on appelle un effet de "cascade" (en anglais, "host-associated differentiation", HAD) qui peut aboutir à une "**spéciation sympatrique séquentielleò** ou une "**radiation séquentielleò** (Abrahamson *et al.*, 2003; Forbes *et al.*, 2009; Feder *et al.*, 2010). En effet, beaucoup de parasitoïdes localisent leurs insectes hôtes en utilisant des signaux chimiques émis par les plantes hôtes des insectes herbivores ou issus des interactions entre la plante et le phytophage (Vet & Dicke, 1992; Dicke, 2000; Dicke & van Loon, 2000). La spéciation sympatrique séquentielle a été documenté chez plusieurs hyménoptères parasitoïdes, comme chez *Diachasma alloeum* (Muesebeck, 1956) (Ichneumonoidea: Braconidae) qui a subi à une divergence écologique suite à la formation des races d'hôtes chez son insecte hôte *R. pomonella* (Feder *et al.*, 2010). Stiremann *et al.* (2006) ont aussi mis en évidence de l'importance du rôle de la cascade des différentiations d'hôtes associés (cascading HAD) observée chez l'insecte phytophage *Rhopalomyia solidaginis* (Loew, 1862) (Diptera: Cecidomyiidae) qui attaque des plantes hôtes proches de *Solidago altissima* dans la formation des races d'hôtes ou espèces naissantes correspondantes chez l'espèce parasitoïde *Platygaster variabilis* Fouts, 1924 (Platygastroidea:

Platygastridae). Cependant, l'absence de la radiation séquentielle a été documentée dans plusieurs études (p. ex. Cronin & Abrahamson, 2001).

1.5. L'étude de la systématique du genre *Eupelmus* comme un modèle biologique

1.5.1. Généralités

La superfamille des **Chalcidoidea** représente l'un des groupes, les plus abondants et riches en nombre d'espèces avec environs 23000 espèces décrites au niveau mondial, mais la diversité estimée de ce groupe peut atteindre plus de 500000 espèces, et les plus divers morphologiquement et biologiquement des insectes (Munro *et al.*, 2011; Heraty *et al.*, 2013; Noyes, 2013). Ce groupe d'hyménoptères contient actuellement 22 familles différentes (Heraty *et al.*, 2013) dont les membres varient en taille entre 0.11 mm et 45 mm ((Munro *et al.*, 2011). Alors que la phytophagie est connue chez six familles (Agaonidae, Eulophidae, Eurytomidae, Pteromalidae, Tanaostigmatidae et Torymidae), la plupart des Chalcidoidea sont des parasitoïdes attaquant des stades immatures ou adultes d'autres insectes-hôtes (Noyes & Valentine, 1989) et, à ce titre, peuvent donc constituer des agents de la lutte biologique contre différents insectes ravageurs (Heraty, 2009).

Les relations phylogénétiques au sein des Chalcidoidea ont été étudiées à plusieurs reprises à partir des caractères morphologiques ou moléculaires. L'étude la plus récente à ce sujet (Heraty *et al.*, 2013), basée sur l'analyse de la concaténation des caractères morphologiques et moléculaires, confirme la monophylie de la superfamille Chalcidoidea et supporte, avec certaines exclusions ou inclusions de certains taxa dans les analyses réalisées, la monophylie de la plupart des familles (à part pour les familles des Aphelinidae, Perilampidae, Pteromalidae et Tetracampidae). Cependant, la taxonomie de cette superfamille reste très difficile, entravée par la petite taille, l'extrême variabilité morphologique intra-spécifique et par la présences des espèces cryptiques (Gebiola *et al.*, 2012). En plus, les taxonomistes spécialistes en ce groupe sont peu nombreux et la description originale des espèces sont souvent basées sur des spécimens singletons, ignorant ainsi la variation intra-spécifique.

1.5.2. Biologie et statut systématique du genre *Eupelmus*

Au sein des Chalcidoidea, les membres de la famille des **Eupelmidae** partagent avec les Encyrtidae un certain nombre de caractères morphologiques dérivés, liés à l'adaptation au saut, notamment l'existence d'un éperon robuste sur le tibia médian. Mais ils s'en distinguent fortement par d'autres caractères, qui apparaissent comme dérivés chez les Encyrtidae: position avancé des cerques sur le métasoma, réduction du nombre de flagellomères, insertion avancée des coxae sur le deuxième segment thoracique, etc. Les Eupelmidae pourraient donc constituer un grade et non pas un groupe monophylétique du fait de l'absence de synapomorphies par rapport à l'ensemble Encyrtidae + Tanaostigmatidae Gibson (1989, 1995). Cette hypothèse a été confirmée par Munro *et al.* (2011) sur la base des séquences de deux gènes ribosomiques nucléaires *18S* et *28S* mais infirmée par Heraty *et al*. (2013) d'après une inférence basée sur une matrice combinée de 233 caractères morphologiques et des séquences nucléotidiques des deux gènes nucléaires précédents. Les Eupelmidae constituent une famille d'importance moyenne avec 45 genres et 907 espèces décrites (Noyes, 2015) et sont actuellement subdivisés en trois sous-familles, respectivement les **Calosotinae** Bouček, les **Neanastatinae** Kalina et les **Eupelminae** Walker (Gibson, 1990). Cette dernière sous-famille est la plus diversifiée avec 686 espèces décrites classifiées dans 33 genres (Noyes, 2015).

Les Eupelminae, à l'inverse des deux autres sous-familles présentent un fort dimorphisme sexuel. Comme chez les autres sous-familles d'Eupelmidae, les femelles d'Eupelminae présentent un mésosoma – le thorax apparent des Hyménoptères Apocrites – hautement modifié pour cette saltation: développement d'un système musculaire spécifique qui prend appui sur la paroi hypertrophiée de l'acropleuron, sclérite de taille réduite chez les autres hyménoptères. Le mésosoma des mâles d'Eupelmidae a retenu structure primitive, des mâles que l'on observe chez les autres chalcidiens (Gibson, 1995). Ils peuvent de ce fait être facilement confondus avec certains Pteromalidae.

Au sein des Eupelminae, les espèces du genre ***Eupelmus*** Dalman sont des ectoparasitoïdes primaires ou secondaires capables de parasiter une gamme variée d'insectes holométaboles (Coleoptera, Diptera, Hemiptera, Hymenoptera et Lepidoptera) et amétaboles comme Orthoptera. Les larves de ces parasitoïdes se développent comme des idiobiontes sur les stades immatures (souvent le dernier stade larvaire ou pupes) qui sont généralement cachés dans des habitats protégés comme les tiges, feuilles, fruits, semences et galles. Certaines espèces d'*Eupelmus* sont toutefois décrites comme des prédateurs ou parasitoïdes d'œufs de Cicadellidae, Mantidae, Curculionidae ou Saturnidae (Gibson, 1995). Le genre *Eupelmus* est

cosmopolite bien qu'il ne semble ni commun, ni diversifié dans la région Néotropicale (Gibson, 1995). Ce genre peut être considéré comme la lignée la plus riche en espèces au sein des Eupelmidae, avec environ 320 espèces décrites actuellement valides (Noyes, 2015).

Gibson (1995) a classifié les espèces d'*Eupelmus* en trois sous-genres: ***Episolindelia***, ***Eupelmus*** et ***Macroneura*** (Figure 4), ce dernier sous-genre ayant été classifié pendant longtemps comme un genre séparé: *Eupelmella*. En fait, la classification actuelle du genre *Eupelmus* est basée essentiellement sur la morphologie des femelles (Gibson, 1997). Cependant Gibson a lui-même exprimé des doutes sur sa pertinence: *Episolindelia* pourrait ne constituer qu'un grade à la base du genre et *Macroneura* un groupe spécialisé au sein du sous-genre nominal lui-même.

Gibson, dans une série de travaux novateurs, est de loin l'auteur qui a le mieux fait progressé nos connaissances sur les Eupelmidae et le genre *Eupelmus* en particulier: morphologie fonctionnelle des femelles d'Eupelminae (Gibson, 1986), phylogénie de la famille et révision générique des Calosotinae et Neastatinae (Gibson, 1989), phylogénie et revue des genres d'Eupelminae (Gibson, 1995 & 1997), la diversité des *Eupelmus* dans la région Néarctique (1990, 2011). D'autre recherches taxonomiques à mentionner sont: Ferrière (1954) qui a révisé les Eupelminae brachyptères d'Europe, Kalina (1981, 1988) qui a réalisé des clés de détermination des espèces Paléarctiques; Bouček (1988) qui a révisé les genres d'Eupelmidae de la région Australasienne et catalogué les espèces; Narendran & Anil (1995) qui ont révisé la faune d'Inde et Askew & Nieves-Aldrey (2000) qui se sont intéressés aux *Eupelmus* d'Espagne péninsulaire et des îles Canaries. Par ailleurs, des outils moléculaires et la cytogénétique ont déjà été utilisés en systématique des Eupelmides afin d'inférer une classification subgénérique du genre *Eupelmus* (Fusu, 2008) tandis que le même auteur a utilisé l'électrophorèse des protéines pour la différenciation des formes mélanisées et claires (espèces cryptiques) d'*E. vesicularis* (Retzius, 1783) (Fusu, 2009). Malgré ces apports, et d'une manière générale, la discrimination et l'identification des *Eupelmus* est restée délicate pour plusieurs raisons. Tout d'abord, les *Eupelmus*, comme les autres Eupelminae sont caractérisés par un fort dimorphisme sexuel. Comme on l'a vu ci-dessus, les mâles sont similaires morphologiquement aux mâles des Pteromalidae notamment des Cleonyminae. À cause de ce dimorphisme sexuel, l'association correcte des deux sexes de la même espèce est une tâche complexe qui nécessite en général de disposer de spécimens des deux sexes collectés au même endroit sur le même insecte hôte (Gibson, 2011). Enfin, le genre *Eupelmus* est susceptible de contenir des complexes d'espèces morphologiquement très proches.

Les *Eupelmus* n'ont pas seulement attiré l'attention des taxonomistes mais également celle des gents intéressés à la lutte biologique contre des insectes ravageurs des cultures. En effet, le genre *Eupelmus* renferme des espèces, notamment celles appartenant au groupe *urozonus*, pouvant contribuer à coté des autres parasitoïdes des autres familles à la limitation de la prolifération de certains insectes ravageurs présentant une certaine importance économique comme la mouche de l'olive *Bactrocera oleae* (Gmelin, 1790) (Tephritidae) (Neuenschwander *et al.*, 1983; Borowiec *et al.*, 2012) et le cynips du châtaigner *Dryocosmus kuriphilus* (Yasumatsu, 1951) (Cynipidae) (Aebi *et al.*, 2007; Quacchia *et al.*, 2013; Borowiec *et al.*, 2014). Par conséquent ces espèces d'*Eupelmus*, comme c'est expliqué dans la "Discussion et perspectives" de ma thèse, peuvent être exploitées comme des agents potentiels de lutte biologique dans des programmes de lutte par conservation.

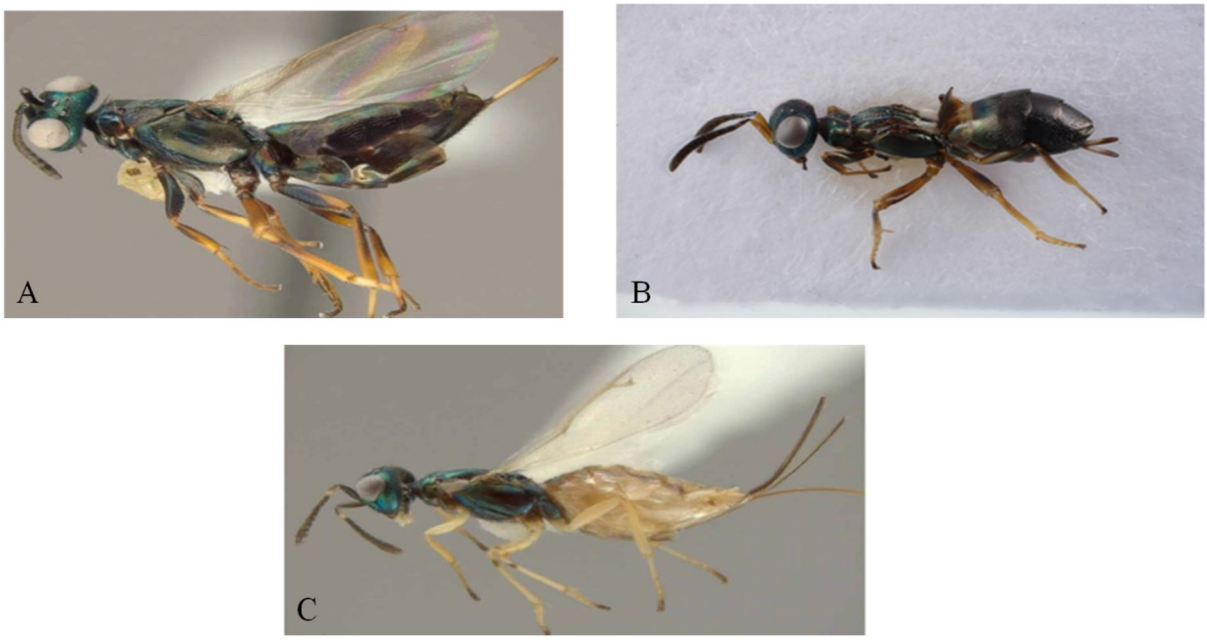

Figure 4: Femelles adultes des trois sous-genres d'*Eupelmus* (Gibson, 1995): (A) *Eupelmus* Dalman; (B) *Macroneura* Walker; (C) *Episolindelia* Girault.

2. OBJECTIFS DE LA THÈSE

L'objectif global de ma thèse était d'intégrer l'utilisation de marqueurs génétiques à des approches plus traditionnelles de façon à réviser les connaissances sur la systématique et l'écologie des espèces du genre *Eupelmus*.

La première partie de ma thèse a donc été centrée sur l'établissement des relations phylogénétiques au sein du genre *Eupelmus* avec pour objectif d'inférer la phylogénie au sein des membres du genre *Eupelmus* et, ainsi, confirmer ou infirmer la classification proposée par G. Gibson (1995). Dans ce but, nous avons cherché à intégrer par concordance des données moléculaires acquises essentiellement par moi-même et des données morphologiques acquises plus collectivement (G. Delvare, L. Fusu et moi-même). Ce travail a fait l'objet d'un article actuellement en préparation pour *Journal of Hymenoptera Research*.

La seconde partie de mon manuscrit s'est focalisée sur l'étude de l'histoire évolutive des espèces du groupe *urozonus* présentes dans la région Ouest-Paléarctique. La reconstruction des relations phylogénétiques a été réalisée sur la base d'une caractérisation multi-locus mise en place en étroite collaboration avec A. Cruaud, J-Y. Rasplus et N. Ris et d'analyses phylogénétiques actualisées grâce à A. Cruaud, J-Y. Rasplus et N. Ris. Sur cette phylogénie, nous avons cherché à reporter les informations concernant les spectres d'hôtes et la taille de l'ovipositeur (données principalement obtenues par G. Delvare, L. Fusu et moi) pour essayer de comprendre les processus de spécialisation à cette échelle et les éventuelles contraintes. Un article sur ce sujet est accepté dans *BMC Evolutionary Biology*.

La troisième partie de ma thèse synthétise le travail de taxonomie intégrative réalisée sur le groupe d'espèce *urozonus*, et le complexe d'espèces *vesicularis*. Ce travail a été réalisé sur un nombre limité de marqueurs moléculaires (données acquises principalement par moi-même en collaboration avec (A. Cruaud, J-Y. Rsplus et N. Ris) et l'étude de plusieurs caractères morphologiques (essentiellement, G. Delvare, L. Fusu et moi). Ce travail a fait l'objet de deux publications acceptées concernant le groupe *urozonus* (Al khatib *et al. Systematic Entomology* 2014 et Al khatib *et al. Zookeys* 2015) et d'une publication en préparation pour le complexe *vesicularis*.

Dans une dernière partie, nous concluons sur l'apport de notre étude et présentons ses conséquences concernant la compréhension du rôle potentiel des espèces d'*Eupelmus* contre deux ravageurs étudiés par l'Equipe "Recherche et Développement en Lutte Biologique"

(Institut Sophia-Agrobiotech), la mouche de l'olive *B. oleae* et le cynips du châtaignier *D. kuriphilus*.

3. Partie I: Inférence de la phylogénie du genre *Eupelmus* par lôintégration de caractères moléculaires et morphologiques.

Article 1: Combining the results of different data fields for phylogenetic reconstruction: an example with the genus *Eupelmus* (Hymenoptera: Eupelmidae). Soumission imminente.

Présentation de lôarticle

La classification du genre *Eupelmus* acceptée à ce jour est celle de Gibson (1995) qui a divisé ce genre en trois sous-genres: *Episolindelia*, *Eupelmus* et *Macroneura*. Cependant, cette classification infra-générique pose certaines questions. Par exemple, l'espèce *E. memnonius* Dalman, 1820 - l'espèce type du genre *Eupelmus* et du sous-genre *Eupelmus* - partage quelques états de caractères clés avec le sous-genre *Episolindelia*. De plus, alors que toutes les femelles des espèces assignées à *Macroneura* sont caractériséespar des ailles non développées, les mâles concernés sont difficilement différenciables de certaines espèces appartenant au sous-genre *Eupelmus*.

Dans ce contexte, cet article présente un premier essai pour la résolution phylogénétique du genre *Eupelmus* et la proposition d'une nouvelle classification infra-générique. Pour cela, deux approches complémentaires ont été utilisées: l'une est moléculaire basée sur l'analyse simultanée de plusieurs marqueurs, l'autre est morphologique basée sur une matrice des états de caractères morphologiques.

Plus précisément, nous avons tout d'abord établi un arbre phylogénétique moléculaire à partir de, au maximum, 7 marqueurs génétiques présentant des caractéristiques complémentaires (ADN nucléaire *versus* mitochondrial, ADN codant versus non-codant) et, au minimum, une trentaine d'espèces représentant les différents sous-genres (*Episolindelia*, *Eupelmus* et *Macroneura*) ou d'autres genres de la sous-famille des Eupelminae (*Anastatus* et *Reikosiella*). La topologie obtenue apparaît adéquate pour la phylogénie moléculaire du genre *Eupelmus* car tous les nœuds de cet arbre sont robustes.

Parallèlement, une phylogénie morphologique a été inférée avec la méthode du maximum de la parcimonie (PM) à partir d'une matrice de 57 caractères morphologiques retenus pour 55 espèces du genre *Eupelmus* et 4 espèces comme "out-groups" dont deux appartenant au genre *Anastatus* et deux assignées au genre *Reikosiella*.

Les résultats obtenus ont tout d'abord mis en évidence que la topologie moléculaire générée pour les 31 espèces est plus robuste et résolue que celle basée sur la morphologie de 59 espèces. De plus, une discordance entre les phylogénies moléculaire et morphologique est mise en évidence. Elle s'expliquerait par une homoplasie significative chez le genre *Eupelmus*. Ceci est en particulier visible lorsque l'on compare la longueur des branches de

l'arbre phylogénétique basé sur les données morphologiques seules et celui obtenu, toute chose étant égale, par ailleurs, sous la contrainte des données moléculaires.

De plus, quels que soient les caractères utilisés pour la phylogénie (moléculaires, morphologiques) et compte-tenu de notre échantillonnage, le genre *Eupelmus* apparaît comme une lignée monophylétique. Au niveau infra-genre, la phylogénie retenue rejette la monophylie des espèces classifiées dans le sous-genre *Episolindelia* qui, en fait, se structure en un ensemble de groupes d'espèces à la base de l'arbre retenu (Figs. 3, 4). La phylogénie obtenue rejette également la monophylie du sous-genre *Eupemus* dans lequel vient se nicher les espèces initialement identifiées comme appartenant au sous-genre *Macroneura*. Ce sous-genre représenterait donc plutôt un groupe d'espèce qu'un réel sous-genre.

Enfin, il apparaît que, le groupe *urozonus* est le groupe le plus riche en espèces et se structure en 3 clades (*urozonus*, *confusus* et *gemellus*) bien supportés, dans la topologie moléculaire. Par contre, une telle structuration n'a pas été retenue dans la topologie morphologique en raison d'absence des caractères dérivés pour chaque un de ces trois clades.

En conclusion, notre travail conduit à rejeter la classification actuelle du genre *Eupelmus* et proposer une nouvelle classification informelle basée sur le concept d'une mosaïque de groupes d'espèces (*antipoda*, *atropurpureus*, *hartigi, juniperinus*, *orientalis*, *peculiaris*, *pini*, *splendens, stramineipes*, *testaceiventris, urozonus*, *vesicularis*) et de quelques espèces, pour l'instant, isolées (*E. memnonius* et *E. microzonus*).

ARTICLE1: Combining the results of different data fields for phylogenetic reconstruction: an example with the genus Eupelmus (Hymenoptera: Eupelmidae)

Al khatib F.[1], Fusu L.[2], Ris N.[1] and Delvare G.[3]

(Imminent submission)

Affiliations:

1: INRA, Univ. Nice Sophia Antipolis, CNRS, UMR 1355-7254 Institut Sophia Agrobiotech, 06900 Sophia Antipolis, France

2: Faculty of Biology, Alexandru Ioan Cuza University, Bd. Carol I nr. 11, 700506, Iasi, Romania

3: CIRAD, UMR 55 CBGP, 755 avenue du Campus Agropolis, CS 30016 F-34988 Montferrier-sur-Lez Cedex, France

Corresponding author: fadel.alkhatib@sophia.inra.fr

Abstract

In order to infer the phylogeny of the genus *Eupelmus* Dalman (Hymenoptera: Eupelmidae), we used the procedure called "Taxonomic congruence" to compare and match the results of phylogenetic inferences using respectively (i) the concatenated nucleotide sequence alignment of seven genetic markers (4986 nucleotides) on 31 species and (ii) a morphological matrix including 57 characters coded to 59 species. Mapping the morphological characters on a well supported molecular phylogram revealed a large amount of homoplasy which prompted us to look for suboptimal instead of MP trees. Our results show that within a phylogenetic systematics framework, the present infra-generic classification into three subgenera cannot be retained. *Macroneura*, for a long time considered a valid genus and then a subgenus of *Eupelmus*, is treated as a species group as it renders *Eupelmus sensu stricto* paraphyletic. Furthermore, recognizing *Eupelmus sensu stricto* as a subgenus renders *Episolindelia* paraphyletic. We recognize a total of 14 species groups, the *urozonus* species group being by far the largest of them.

Keywords

Classification, derived morphological characters, integrative approach, molecular tree, morphological tree, phylogeny.

Introduction

Taxonomist and other biologists increasingly consider the need of an "Integrative Taxonomy" able to provide tools for accurate species discrimination and identification and ways to classify the taxa according to common descent, with the aim of providing a stable nomenclature (Dayrat 2005, Padial et al. 2010, Gebiola et al. 2012, Gómez-Zurita and Cardoso 2014). The approach used to infer phylogenies by considering several fields of data has been called "total evidence", an approach where the data – generally morphological and molecular – are concatenated into a 'supermatrix' to produce a 'supertree' (Jarvis et al. 2004, de Queiroz and Gatesy 2006, Sørensen and Giribet 2006, Fenwick et al. 2009, Winterton et al. 2010, Heraty et al. 2013, Wahlberg et al. 2015), after comparing the results achieved with all the data sets. Nevertheless, molecular data are used more and more, as their potential for providing characters (as nucleotide positions) are also increasing very quickly and this trend will be drastically accelerated when using the Next-Generation Sequencing (NGS) technology providing millions of data units (Misof et al. 2014). In fact when considering studies dealing with Hexapoda such a trend is not observed, or at least to a much lower rate (Bybee et al. 2010), the interest of still using morphology in the phylogenetic inference being reviewed by Wiens (2004). From the explanations suggested by Bybee et al. (2010), the main reasons that justify and promote the use of the morphology in phylogenetic inferences dealing with insects is their tremendous variation in the external morphological features and the preservation of most taxa in collections. Aside for the inclusion of fossils in the data matrices, which is still almost impossible or requiring extreme precautions, the analysis of extant species might also be quite problematic. This occurs when considering rare taxa, represented by a few old specimens in a single museum, which are therefore inadequate for DNA amplification. The problem is still bigger when the region of origin of the specimens is now inaccessible, the habitats destroyed, or collecting forbidden and organisms impossible to export because of state regulations. These situations are often encountered with insects and this is another reason why morphology is still broadly used in taxonomy and phylogeny in this group. When considering the number of specimens which can be examined by a traditional taxonomist, it is incommensurate in comparison with those included in molecular matrices. Also, molecular data are not exempt of artifacts and it is important to check the molecular results using another field of data (Lopardo et al. 2011, Beutel et al. 2010), for example by examining the morphology of the specimens grouped in a MOTU.

Because of the above mentioned disadvantage of incomplete sampling when using molecular data, it is often desirable to extend the sampling and then it is possible and useful to use morphology. Instead of inferring phylogeny with combined data we hence assumed the way described by Eernisse and Kluge (1993) as 'taxonomic congruence' which concentrates on deriving a consensus from the results obtained from different taxonomic characters. We applied such an approach to the genus *Eupelmus* Dalman because Al khatib et al (submitted) established a large molecular matrix for inferring the phylogeny and evolutionary history of the '*urozonus* group', the largest putative species group (SPG) of this genus. The existence of such a matrix and of the resulting tree, in which most of the nodes are well supported, appeared as an opportunity to extend the study to the whole genus by introducing additional data based on morphology.

The genus *Eupelmus* (Hymenoptera: Chalcidoidea: Eupelmidae) includes parasitoids of various holometabolous insects. The larvae develop as idiobionts, generally upon the last instar larvae or pupae of various organisms living in different parts of the plants (stems, twigs, fruits, flowers, seeds, and galls), in diverse habitats and all continents except Antarctica (for a review of their biology and economic importance, see Al khatib et al. 2014, 2015, Gibson and Fusu, submitted). The genus, which belongs to the subfamily Eupelminae, includes about 320 species worldwide representing alone nearly one third of the described Eupelmidae (Noyes 2015). Gibson published several revisional works on the family, especially on the phylogeny and reclassification of the Eupelminae (Gibson 1995), and revisions of the Nearctic species of *Eupelmus* (Gibson 1990, 2011), followed by a revision on Palaearctic Eupelmus (Gibson and Fusu 2015). Other noticeable works to be quoted are those of Kalina (1981, 1988) who keyed out the Palaearctic species, of Narendran and Anil (1995) who revised the Indian fauna and Bouček (1988) who keyed out the Australasian genera of Eupelmidae – together with most other families of Chalcidoidea – and catalogued the regional species.

Gibson (1995) classified *Eupelmus* in three subgenera respectively *Episolindelia* Girault, *Eupelmus* and *Macroneura* Walker. The last taxon has been incorrectly known for a long time as *Eupelmella* Masi (Bouček 1988, Gibson 1990) until it was downgraded to subgeneric level by Gibson (1995). *Episolindelia* was never used as a valid genus after the original description by Girault (1914), until used for a subgenus of *Eupelmus* by Gibson (1995). This classification is nevertheless far from being firmly established. For example *E. memnonius* Dalman, 1820, the type species of the genus and of the nominal subgenus, shares

some key character states with *Episolindelia* (Gibson 1995). Furthermore, while all females of the species classified in *Macroneura* are micropterous, and for this reason in combination with a characteristic structure of pronotum, metanotum and propodeum, easily separated from the rest of species, the relevant males are very difficult to distinguish from some *Eupelmus* males belonging to the nominal subgenus (Gibson 2011). Hence it is possible that the shift in the female morphology is secondarily derived and comes from micropterism, and the two subgenera represent a grade of structure and not monophyletic lineages (Gibson 2011). Most likely only *Macroneura* is monophyletic (nested within the nominal subgenus), and the three subgenera represent a nested paraphyletic series (Gibson 1995, 2011). Species of *Eupelmus*, as all Eupelminae in general, exhibit a striking sexual dimorphism. The sexes are so different that they would be classified in different families by non specialists. Therefore the morphological data includes actually two partitions figuring each the character states of the opposite sexes. Because the selection pressure is certainly different in males and females, it is expected that homoplasy would have a different pattern across the two sexes, and a classification based on females only might not accurately represent the phylogeny of the group.

The aims of this study are: 1) to infer the phylogeny of the genus *Eupelmus* using the tree established for the *urozonus* SPG and the out-group taxa by Al khatib et al. (submitted), which will form a frame and a starting point; 2) to propose an infra-generic structuring and classification for the genus; and 3) to evaluate the amount of homoplasy for some morphological characters.

Material and methods

Species sampling

Our knowledge of the genus *Eupelmus* includes over 150 species resulting from the molecular and/or morphological examination of specimens housed in various depositories:

- AICF: Al. I. Cuza University, Iasi, Romania, Lucian Fusu personal collection.
- CBGP: Center for Biology and Management of Populations, Montpellier, France.

- CNC: Canadian National Collection of Insects, Arachnids and Nematodes, Agriculture & Agri-food Canada, Ottawa, ON, Canada.
- CTPC Csaba Thuróczy Personal Collection, Koszeg, Hungary.
- FALPC Fadel Al khatib personal collection, Faculty of Agricultural Engineering, University of Aleppo, Syria.
- GDPC Gerard Delvare, personal collection, Montpellier, France.

Of the 150 species, 54 species (63 specimens) were used for the scoring of morphological characters (Table S1). When some specimens could not be identified at the species level, they were thus tentatively named according to the sampling location (country and, when necessary to avoid confusions, localities - i.e.: *Eupelmus* Yemen or *Eupelmus* Cameroon Mbe).

In addition to this set of species: Two species of *Anastatus* Motschulsky namely *A. sidereus* (Erdős, 1957) and *A. aff. temporalis* Askew, 2005 were also used as out-groups. Their molecular characterization was earlier obtained (Al khatib et al. submitted) and the morphological characterization was realized in this study.

Molecular study

In addition to the dataset (28 *Eupelmus*, one *Reikosiella* and two *Anastatus* species for a total of 91 individuals) obtained in Al khatib *et al.* (submitted), new sequences were taken into account including:

- 11 partial sequences of the mitochondrial gene *COI*, ten of them having been obtained by ourselves and the last one (*E. cushmani*) originating from Genbank;
- An extended characterization of one specimen of *E. muellneri* for another mitochondrial marker (*Cytb*) and three nuclear ones (*EF1-Ů*, *RpS4* and *Wg*) (see Al khatib et al. submitted for details about all these markers);
- One sequence of the *wingless* gene for *E. memnonius*.

The protocols for DNA extraction, PCR amplification, sequencing, sequences alignment and phylogenetic analysis (e.g. partitioning, evolutionary models used and phylogeny reconstruction) are fully explained in Al khatib et al. (submitted) and will not be detailed here. Accession numbers for all the sequences are given in Table S1.

The molecular concatenated matrix finally included 4986 bases pairs but, despite our efforts, this molecular dataset remained clearly unbalanced. Phylogenetic reconstructions

were consequently realized using two different sub-sets which leads to two complementary phylogenetic trees: (i) a first one called MOLTREE T31 (Table 2) which includes all the species for which we obtained a complete dataset for the 7 genes (Figure 1), (ii) a second one called MOLTREE T42 (Table 2) encompassing the dataset of the 31precedent species plus 11 ones for which the *COI* sequences were at least available (Figure 2).

Morphological investigation

Selection of specimens

A total of 59 species were introduced in the morphological matrix. Besides the 31 species (91 specimens) already studied in Al khatib *et al.* (submitted), other species were chosen according to the following criteria:

- The availability of morphological information for both sexes.
- The completion of the coverage of the *urozonus* SPG. *E. pervius* Gibson, 2011 was hence introduced to screen a possible relationship with *E. longicalvus*, Al khatib & Fusu, 2015 as the two species display long *linea calva* on the fore wing. We also wanted to check the placement of *E. afer* Silvestri, 1914, *E. cushmani* (Crawford, 1908), *E. elongatus* Risbec, 1951 and *E. stenozonus* Askew, 2000.
- The representativeness of other putative species groups: (i) *E. splendens* Giraud, 1872, supposedly the sister species of *E. matranus* Erdős, 1947; (ii) *E. stramineipes* Nikol'skaya, 1952 for screening a sister group relationship with *E. phragmitis* Erdős, 1955; (iii) *E. curvistylus* (Risbec, 1951) to check its relatedness to *E. testaceiventris*; (v) *E. vuilleti* (Crawford, 1913) and *E. orientalis* (Crawford, 1913), originally described in the genus *Bruchocida* Crawford, 1913.
- The presence of some particular morphological features, e.g. *E. peculiaris* Narendran, 2011 and the species called '*Eupelmus* Vietnam' which are both exhibiting some original combinations of character states.
- The exhibition of original ecological features: (i) representatives of the parasitoids of praying mantids: '*Eupelmus* Yemen', *Eupelmus orthopterae* (Risbec, 1951) and '*Eupelmus* PNG', this last species being possibly *E. antipoda* Ashmead, 1900; (ii) representatives of tropical or equatorial areas such as the specimens originating from Cameroon or French Guiana (Amazonian forest).

Specimen examination

Except for *E. pervius* which was coded from the original description (Gibson 2011), all specimens were examined by the authors. As DNA extraction was performed through lysis without crushing the individuals, it was possible to recover the sequenced specimens for morphological examination. Slide mountings were made for examining the detailed morphology of the male antenna (the number and distribution of the pores on the scape and the setation of the pedicel). In other cases SEM images were generated as quoted in Al khatib et al. (2014). The last abdominal segments of *E. linearis* Förster, 1860, *E. fuscipennis* Förster, 1860 and *E. cicadae* Giraud, 1872 were also examined through slide mounting to detect the possible presence of a median line on the penultimate tergite.

The morphological terminology is that used by Gibson (1995, 2011) and Al khatib et al. (2014). Because of the striking sexual dimorphism and possible contrasted morphological evolution between sexes (e.g. sex-specific homoplasy), the morphological data includes one partition for each sex. Most characters introduced in the morphological matrix were already quoted and discussed by these authors. As advocated by Scotland et al. (2003) and instead of building a large and exhaustive data matrix, we used only those characters that could be unambiguously scored and avoided those that form a continuum that cannot be clearly split into discrete states. We also did not introduce in the matrix obvious autapomorphies as they do not contribute to the resolution of the phylogenetic tree. The Table 1 contains the characters used and their states, and the Table S2 represents the morphology matrix.

Table 1. Morphological character states used to infer the phylogeny of the genus *Eupelmus*.

1 Female. Width of scrobal depression: Narrower than frons (0) (Al khatib et al. 2014: Fig. 17A); as broad as frons or nearly so (1) (Gibson, 1995: Fig. 87).
2 Female. Sculpture of scrobal depression: Entirely raised reticulate (0) (Al khatib et al. 2014: Fig. 19B); partly reticulate with bottom of antennal scrobes smooth (1) (Al khatib et al. 2014: Fig. 17C); mostly smooth, at most sides of depression narrowly reticulate (2) (Al khatib et al. 2014: Fig. 20D).
3 Female. Lateral margin of scrobal depression: Blunt without distinct margin (0) (Al khatib et al. 2014: Fig. 24A); sharp, forming evident ridge (1) (Gibson, 1995: Fig. 3).
4 Female. Sculpture of frontovertex: Frontovertex evidently reticulate, with a distinct raised network (0) (Gibson, 1995: Fig. 89; Gibson, 2011: Fig. 31); frontovertex very faintly reticulate, the walls of the cells hardly raised (1); frontovertex alutaceous to coriaceous, the network engraved or smooth (2) (Gibson, 2011: Fig. 27; Al khatib et al. 2014: Fig. 25A); frontovertex smooth (3) (Gibson, 1995: Fig. 76; Gibson, 2011: Fig. 26).
5 Female. Width of fronto-vertex: Vertex with usual width, 0.35-0.45X width of head (0) (Al khatib et al. 2014: Fig. 27A); vertex narrow, about 0.30-0.33× width of head (1) (Gibson, 1995: Fig. 69).
6 Female. Setae on lower face: Not especially enlarged (0); setae somewhat thickened, lanceolate (1); setae scale-like as on the rest of the body (2) (Gibson, 1995: Fig. 90).
7 Female. Palpi coloration: Palpi entirely pale (0); palpi entirely dark (1); palpi yellow but last segment of maxillary palpus dark (2) (Al khatib et al. 2014: Fig. 27A).
8 Female. Coloration of first flagellomere (=FL1): Flagellomere entirely dark, rarely orangey (0) (Al khatib et al. 2014: Fig. 27D); flagellomere light colored, contrasting with the rest of antenna (1).
9 Female. Mesosoma coloration: Mesosoma entirely dark with metallic reflections (0) (Al khatib et al. 2014: Fig. 27E); mesosoma with at least prepectus light colored (1) (Gibson, 2011: Fig. 1, 4).
10 Female. Pronotal collar anterior margin: Collar not delimited anteriorly (0) (Gibson, 1995: Fig. 180, 182); pronotal collar concave and delimited anteriorly by a faint ridge (1) (Gibson, 1995: Fig. 185, 186).
11 Female. Pronotal collar coloration: Collar without blue violet reflections (0) (Al khatib et al. 2014: Fig. 17D); collar with violet reflections (1) (Al khatib et al. 2014: Fig.

24E).
12 Female. Sculpture of median lobe of mesoscutum posteriorly: Sculptured, reticulate or coriaceous (0) (Al khatib et al. 2014: Fig. 17D); Smooth and shiny (1) (Gibson, 1995: Fig. 177).
13 Female. Metanotum: Transverse (0) (Gibson, 1995: Fig. 181); enlarged (1) (Gibson, 1995: Fig. 185).
14 Female. Sculpture of prepectus: Prepectus evidently reticulate (0) (Al khatib et al. 2014: Fig. 19F); prepectus smooth or coriaceous (1) (Gibson, 1995: Fig. 174).
15 Female. Setation of prepectus: Prepectus bare (0); prepectus with 1-5 setae on disc (1) (Al khatib et al. 2014: Fig. 21D); prepectus with 6-15 setae on disc (2); prepectus with 12-15 erect setae, some of them on edge (3) (Gibson, 2011: Fig. 43).
16 Female. Plical region of propodeum: Absent (0) (Gibson, 1995: Fig. 242); present and distinct, delimited laterally by curved carinae (1) (Gibson, 1995: Fig. 241).
17 Female. Wing development: At least some females macropterous (0); all females micropterous (1).
18 Female. Fore wing infuscation: Wing hyaline or uniformly and slightly infuscate (0) (Gibson, 2011: Fig. 48); wing strongly infuscate from parastigma, sometimes banded (1) (Gibson, 2011: Fig. 21-23; Al khatib et al. 2014: Fig. 6D).
19 Female. Relative length of costal cell: Costal cell elongate, 9-12× as long as broad and with mostly straight front margin (0) (Al khatib et al. 2014: Fig. 16F); costal cell relatively short, 6-8× as long as wide and with convex front margin (1).
20 Female. Setation of costal cell dorsally: Cell with 1 row of setae at apex (0) (Al khatib et al. 2014: Fig. 16F); cell with 1 row of setae and additional ones behind at mid length (1); cell with several rows of setae at apex (2) (Gibson, 2011: Fig. 47); cell without dorsal setae (3).
21 Female. Setation on apex of submarginal vein (=SMV), in front of parastigma: SMV with few setae (0-5) (0) (Al khatib et al. 2014: Fig. 16F); SMV moderately setose (6-10 setae) (1) (Al khatib et al. 2014: Fig. 17F); SMV somewhat inflated and bearing numerous setae (12-25) (2); SMV not inflated at apex but bearing numerous setae (3).
22 Female. Linea calva on fore wing: Absent (0); present, but quite short, at most as long as stigmal vein (=STV) (1); present and of usual length, distinctly longer than STV, not reaching posteriorly level of vanal lobe (2); present and long, reaching posteriorly level of vanal lobe (3) (Al khatib et al. 2014: Fig. 19G).

23 Female. Setation of basal cell, distribution: Setation similar to that of the disc of fore wing (0) (Al khatib et al. 2014: Fig. 17F); setation sparser (1); cell with a few setae or bare (2).
24 Female. Setation of basal cell, coloration: Similar to that on the disc of fore wing (0) (Al khatib et al. 2014: Fig. 17F); generally pale, contrasting to that on disc (1) (Al khatib et al. 2014: Fig. 16F).
25 Female. Stigmal vein (=STV) of fore wing: Straight (0) (Al khatib et al. 2014: Fig. 22G); at least slightly curved (1) (Al khatib et al. 2014: Fig. 17G).
26 Female. Relative length of postmarginal vein (=PMV) on fore wing: PMV not or hardly longer than STV (1.0-1.3X) (0) (Al khatib et al. 2014: Fig. 22G); PMV longer than STV (1.5-2.0X) (1); PMV intermediate in length between states 0 and 1 (1.3-1.5× as long as STV) (2).
27 Female. Mesotibia coloration: Mesotibia variously colored but different from alternate (0); mesotibia yellow with dark sub-basal ring (1).
28 Female. Mesotibia, apical groove: Present (0) (Gibson, 1995: Fig. 329); absent (1) (Gibson, 1995: Fig. 3).
29 Female. Mesotibia, apical pegs: Present (0) (Gibson, 1995: Fig. 336); absent (1) (Gibson, 1995: Fig. 332).
30 Female. Pegs of median basitarsus, coloration: Dark (0); light colored (1).
31 Female. Pegs of median basitarsus, distribution: Pegs on two parallel continuous rows (0) (Gibson, 1995: Fig. 333); pegs on two complete rows, and 1 or a few additional pegs between the rows such as sometimes to appear somewhat differentiated in two rows but never as symmetrical and densely packed as for state 3 (1) (Gibson, 2011: Fig. 18); pegs on unequal rows, sometimes quite distinctly so (2) (Gibson, 1995: Fig. 335; Gibson, 2011: Fig. 19); pegs on 2 partly overlapping rows on each side of the tarsus: 2 basal inner rows converging apically and 2 apical outer rows; (3) (Gibson, 1995: Fig. 334; Gibson, 2011: Fig. 32); pegs absent (4).
32 Female. Penultimate tergite (= GT6), median line: Absent (0) (Gibson, 1995: Fig. 311); present but incomplete (1); present and complete (2) (Gibson, 1995: Fig. 324).
33 Female. Penultimate tergite: Visible, not hidden by tergite 5 (0) (Gibson, 1995: Fig. 321, 322); mostly hidden below tergite 5 (1) (Gibson, 1995: Fig. 323); not hidden by tergite 5 and angulately protruding on posterior margin (2) (Gibson, 1995: Fig. 320).
34 Female. Syntergum: Flat or evenly convex and with convex or truncate apical margin

(0); strongly emarginate, with omega-like emargination (1) (Gibson, 1995: Fig. 322-324).
35 Female. Position of cerci: Cerci not advanced, located behind spiracle and on same level with it (0) (Gibson, 1995: Fig. 324); cerci advanced, located below spiracle (1) (Gibson, 1995: Fig. 310).
36 Female. Extension of valvifer 2: Valvifer not or slightly extended: exerted part shorter than apical width of metatibia (0) (Al khatib et al. 2014: Fig. 19I); valvifer evidently exerted: exerted part at least as long as apical width of metatibia (1) (Al khatib et al. 2014: Fig. 5E, H).
37 Female. Ovipositor sheaths coloration: Sheaths more or less uniformly colored, sometimes darkened progressively or toward basal or apical ends (0); sheaths with median to subapical light band between darker ends (1) (Al khatib et al. 2014: Fig. 20I); sheaths with narrow basal black band followed by long apical pale one (2).
38 Female. Relative length of exerted part of ovipositor (excluding valfifer 2 if projecting beyond gastral apex): Ovipositor evidently shorter than MV (0) (Al khatib et al. 2014: Fig. 5B); ovipositor from slightly shorter to longer than MV (1); ovipositor evidently longer than MV but shorter than metasoma (2) (Al khatib et al. 2014: Fig.5E); ovipositor at least as long as metasoma (3) (Gibson, 2011: Fig. 22, 24).
39 Male. Ridge behind vertex: No ridge or carina present, vertex roundedly merging to occiput (0); ridge or carina present, vertex angulate with occiput when examined laterally (1) (Al khatib et al. 2014: Fig. 12E, J).
40 Male. Setae on lower face above malar sulcus: Setation of lower face uniform and short (0) (Al khatib et al. 2014: Fig. 12C); a few longer setae present (1) (Al khatib et al. 2014: Fig. 13B); a tuft of setae with curved apex present (2) (Al khatib et al. 2014: Fig. 15A).
41 Male. Enlarged setae on gena: Absent (0) (Gibson, 1995: Fig. 377); only 1 long and curved seta present (1); gena with one conspicuously longer seta and with additional shorter but conspicuous setae (2) (Gibson, 1995: Fig. 403).
42 Male. Pit or shallow depression in scrobal depression at apex of the interantennal region: Absent (0) (Gibson, 1995: Fig. 403, 404); present (1) (Gibson, 1995: Fig. 407, 408).
43 Male. Palpi coloration: Maxillary palpi brown to black, at most last segment brownish (0) (Al khatib et al. 2014: Fig. 13C); maxillary palpi entirely yellow (1).
44 Male. Scape habitus: Scape not or slightly enlarged, more than 1.3× times as long as

broad (0) (Al khatib et al. 2014: Fig. 13I); scape enlarged, less than 1.3× as long as broad (1) (Al khatib et al. 2014: Fig. 13J, 14G).
45 Male. Scape ornamentation: Scape without pores (0); scape without or with few pores (less than 20) restricted to apico-ventral stripe along scapular scrobe (1) (Gibson, 2011: Fig. 79); scape with few pores (less than 20) distributed along scapular scrobe and on baso-ventral surface (2) (Al khatib et al. 2014: Fig. 13O); scape with numerous pores (over 20) distributed along scapular scrobe and baso-ventral surface (3) (Al khatib et al. 2014: Fig. 13E); scape with numerous pores (over 25) distributed on baso-ventral surface (4) (Al khatib et al. 2014: Fig. 14G); scape with a few pores (< 12) restricted to basal surface of scapular scrobe (5).
46 Male. Ventral setae on pedicel: Absent (0); 4-5 hook-like setae present (1) (Al khatib et al. 2014: Fig. 13I); at least 6 hook-like setae present (2) (Al khatib et al. 2014: Fig. 13F); a line of straight setae present, at most some of the basal setae slightly sinuate (3) (Gibson, 2011: Fig. 56).
47 Male. Flagellum habitus: Flagellum filiform (0) (Al khatib et al. 2014: Fig. 13H); flagellum long filiform, at least 1.5× as long as head width (1); flagellum subclavate, intermediate between state 1 and 3 (2); flagellum claviform with terminal flagellomeres much wider than basal ones (3) (Al khatib et al. 2014: Fig. 12D).
48 Male. First flagellomere (= FL1): Flagellomere short but not discoid (0) (Al khatib et al. 2014: Fig. 12D); flagellomere discoid (1) (Al khatib et al. 2014: Fig. 13D).
49 Male. Relative size of basal 2-4 flagellomeres: Flagellomere 2 (FL2) similar in length to FL3 and FL4 (0) (Al khatib et al. 2014: Fig. 13D); FL2 clearly shorter than FL4 (1) (Al khatib et al. 2014: Fig. 13A).
50 Male. Clava: Clava lanceolate with sharp apex (0) (Al khatib et al. 2014: Fig. 13H); clava truncate apically and more or less securiform (1) (Al khatib et al. 2014: Fig. 12D); clava ovoid (2).
51 Male. Tegula color: Tegula dark, sometimes with metallic reflections (0) (Al khatib et al. 2014: Fig. 14B); tegula yellowish to brown (1); tegula dark at base and then testaceous (2).
52 Male. Presence of differentiated dark setae on funicle: No differentiated setae present (0); in ventral view flagellomeres 2 to 3 or 2 to 4 each with region of short, appressed, lanceolate setae (1); stout and short dark setae visible in lateral view present ventrally on flagellomeres 2 to 3 or 2 to 4 (2); sparse stout dark setae interspersed

between the decumbent pale setae all over flagellomeres (3).
53 Male. Scape coloration: Scape uniformly dark (0) (Al khatib et al. 2014: Fig. 13J); scape yellow to brownish yellow basally and outer surface ventrally along longitudinal sensory region (1).
54 Male. Legs coloration: Mid and hind legs with at least tibiae yellowish to whitish, with variably extensively dark markings on femora and apices of tibiae (0); mid and hind legs darkened, sometimes tibiae lighter apically (1) (Al khatib et al. 2014: Fig. 14I); legs entirely pale, at most with reduced dark markings (2).
55 Male. Speculum on fore wing: Absent (0); present (1) (Al khatib et al. 2014: Fig. 14A).
56 Male. Basal cell setation on fore wing: Setose (0); bare or only with a few setae (1).
57 Male. Costal cell setation along leading margin: Setose for a length surpassing parastigma length (0) (Al khatib et al. 2014: Fig. 13K); setose only in front of parastigma (1).

Phylogenetic inferences

Analyses were run in PAUP* 4.0b10 (Swofford 2001), sometimes using the DOS version of this program with the graphical frontend by Calendini and Martin (2005), and by TNT (Goloboff et al. 2008). In a first step, all characters were treated as unordered and not weighted. Analyses with PAUP* were run using a heuristic search, with TBR (Tree Bisection and Reconnection) branch-swapping in conjunction with random addition of sequences, holding one tree at each step. Maxtrees was set to 1,000. Different algorithms were used in TNT such as 'Traditional search' and 'New Technology search' with the default settings. Nevertheless trees achieved with this program were curiously longer than those calculated by PAUP*; by a few steps when the characters were not weighted but clearly longer when an initial weighting was applied. This seems to be the result of the limitation of the tree-buffer in TNT when swapping on the trees during the calculation, which is limited to 100; PAUP* always stored more than 100 trees to swap. Hence, TNT was disused in the further analyses.

Phylogenetic trees were firstly reconstructed from the morphological matrix, either for the restricted dataset (31 species – see MP MORPHOTREE T31 in Table 2), or for the

largest one (42 species – see MP MORPHOTREE T42 in Table 2). Then, in order to quantify the morphological homoplasy, the morphological matrixes were scored on the correspondent molecular trees (MOLTREE T31 and MOLTREE T42 in Table 2) and for each type of generated trees, several parameters were estimated - number of steps (length=L), consistency (=CI), retention (=RI), rescaled retention (RS) and homoplasy indices (HI).

At last, we used the complete set of species (n=59) for the phylogenetic inference. As the molecular trees have shown not to be the most parsimonious according to our set of morphological data (Table 2), we looked for suboptimal trees proceeding to 100 successive runs beside the search for most parsimonious ones (MP). The 50% majority rule trees were calculated for each run and compared to the molecular tree MOLTREE T42. The morphological tree – called MORPHTREE T59 (Figure 3). – sharing the maximal common nodes with it was retained for further comparison and discussion.

Finally a manually edited tree (Figure 4) was built retaining the nodes supported in the different trees e.g. MOLTREE T31, MOLTREE T42 and MORPHTREE T59.

Results

Molecular-based phylogenetic reconstructions

The phylogenetic tree obtained from the restricted dataset (MOLTREE T31) (Figure 1) is well resolved with most of the nodes (83%) showing high bootstraps values. A few nodes only, within the *urozonus* SPG, are weakly supported, possibly as a result of the very quick radiations having occurred without leaving genetic marks. The tree provides thus a very strong frame for establishing an infrageneric structuring of the genus *Eupelmus*. In particular, the subgenus *Eupelmus* which includes in our sampling also *E. matranus*, and *E. pini* is found paraphyletic relative to the subgenus *Macroneura*. The subgenus *Episolindelia* – represented by *E. juniperinus* Bolivar y Pieltain, 1934, *E. testaceiventris* Motschulsky, 1863 and *E. linearis* – is retrieved monophyletic but few species are represented. This analysis especially supports the putative *urozonus* SPG which includes three clades respectively named here as *gemellus*, *confusus* and *urozonus* clades. Many species in this SPG were mixed together in the past (Kalina 1988, Askew and Nieves-Aldrey 2000) because of a high morphological similarity, so it is not surprising that these clades can hardly be recognized through the morphology. The tree also provides evidence for a sister group relationship between the

urozonus SPG and the clade formed by the species traditionally classified in the subgenus *Macroneura*, represented by the pair *E. falcatus* (Nikol'skaya, 1952) and *E. seculatus* (Ferrière, 1954), plus *E. microzonus* Förster, 1860 and *E. atropurpureus* Dalman, 1820.

The largest dataset only based on *COI* includes several new and relevant taxa, in particular: (i) *E. cicadae* Giraud, 1872 and *E. fuscipennis*, two other representatives of the subgenus *Episolindelia*; (ii) *E. memnonius*, type species of the genus and of the nominal subgenus; (iii) *E. muellneri,* an additional species in the subgenus *Macroneura*; (iv) representatives of equatorial or tropical areas that *a posteriori* group within the *urozonus* SPG. Although the support for the nodes is lower than with MOLTREE T31, MOLTREE T42 (Figure 2) mostly reinforces the paraphyly of the subgenus *Eupelmus* with regard to *Macroneura.* However, the monophyly of the subgenus *Episolindelia* was not observed insofar as, on one side, *E. cicadae* and *E. fuscipennis* cluster together at a basal position and with *Reikosiella aff. rostrata* Ruschka, 1921 (a possible artifact caused by long branch attraction) and, on the other hand, other representatives of this subgenus (*E. juniperinus*, *E.linearis* and *E. testaceiventris*) appears as a sister-group of the *Eupelmus-Macroneura* clades. Two putative relationships are also quite suspicious, the close relatedness between *Eupelmus* Cameroon Mbe, *E. urozonus* Dalman, 1820 and *E. minozonus* Delvare, 2015 and, to a lesser extent, the polytomy formed by *E. cushmani*, *E. annulatus* Nees, 1834 and *E. cerris* Förster, 1860.

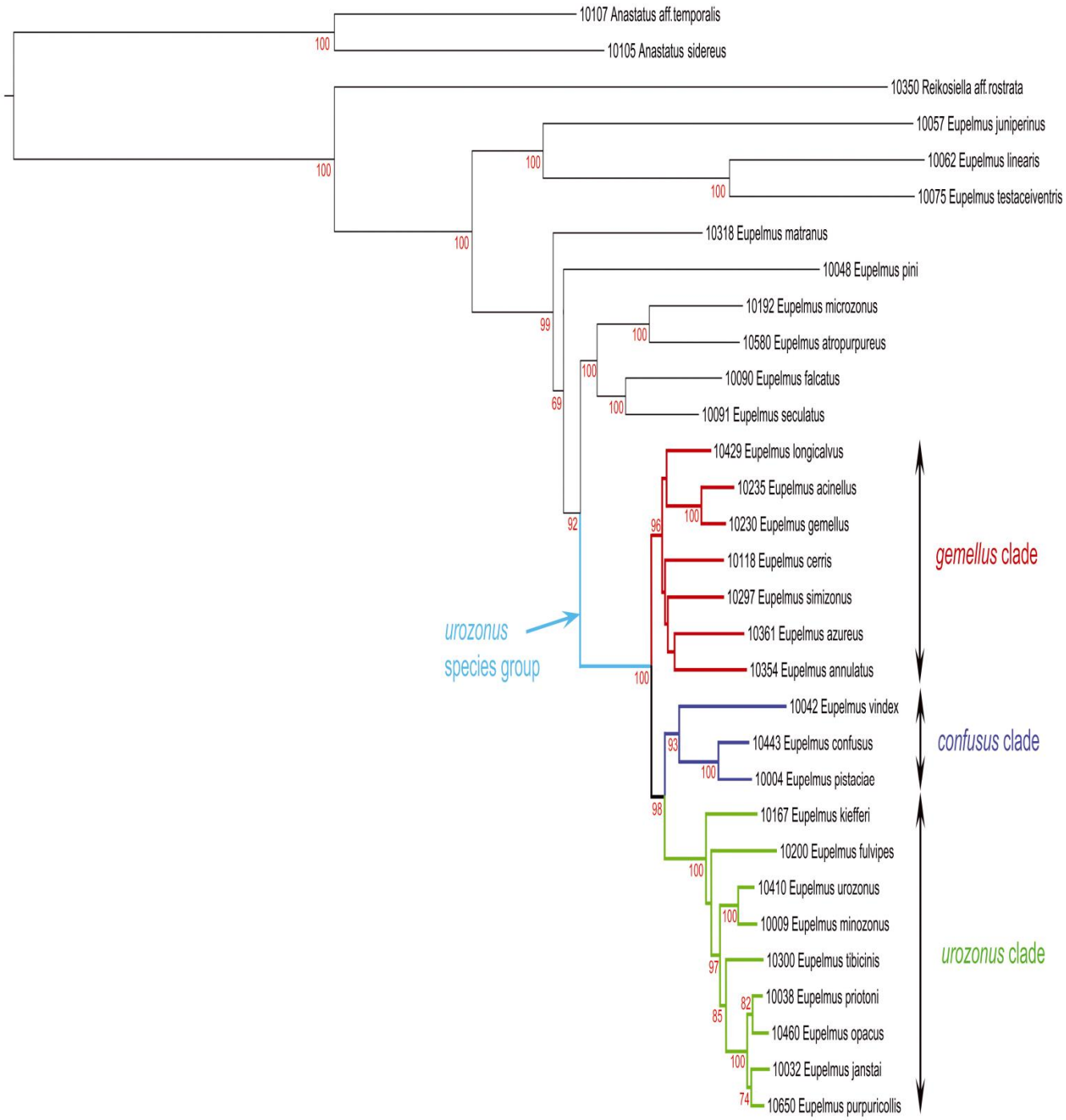

Figure 1. Phylogram of relationships among 31 species of the genus *Eupelmus* obtained from the concatenated dataset alignment (4986 bp) of 2 mitochondrial genes (*COI* and *Cytb*) and 5 nuclear genes (*Wg*, *EF-1Ŭ*, *Bub3*, *RpS4*, and *RpL27a*) using 9 partitions. Bootstrap values below the nodes.

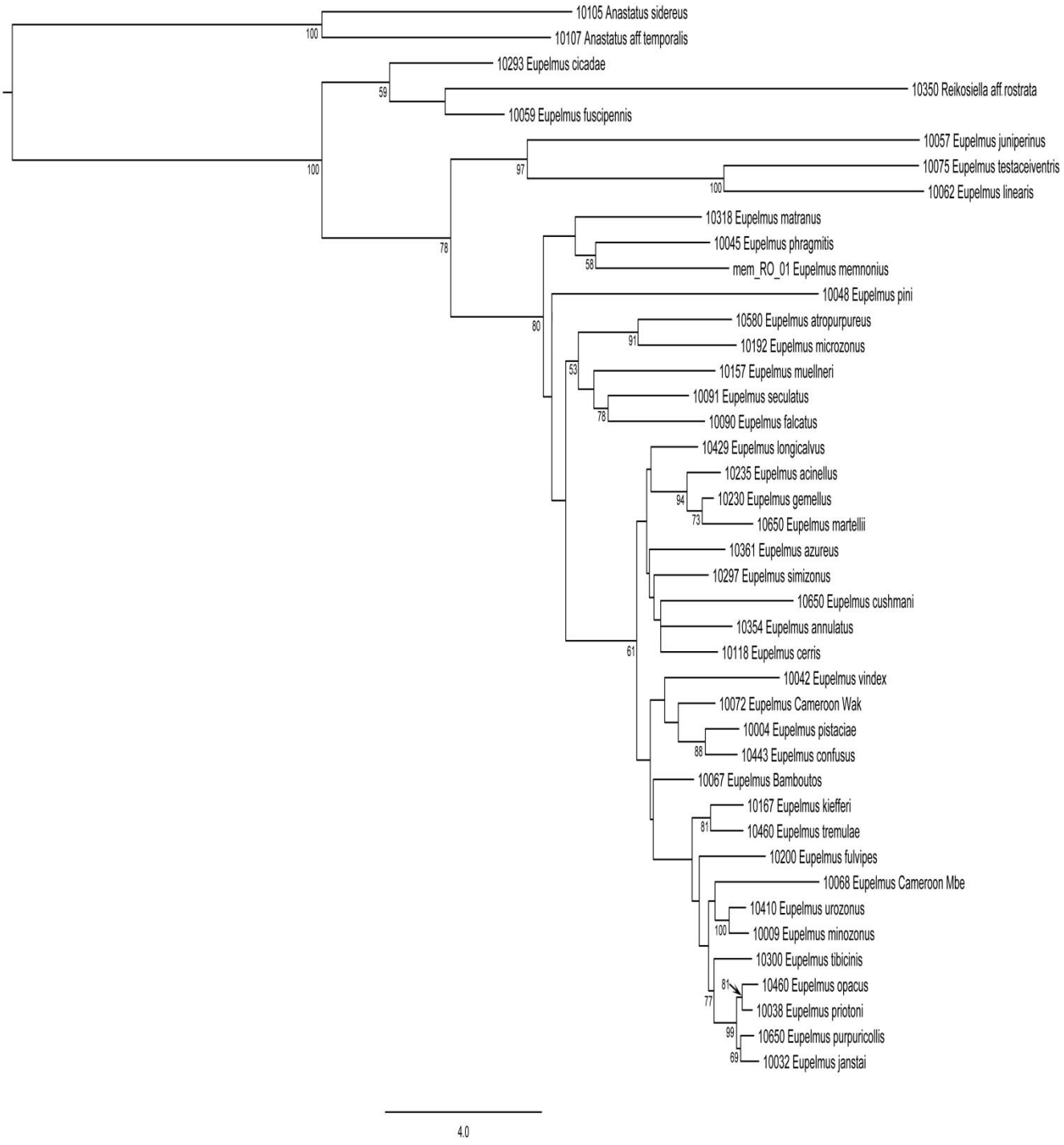

Figure 2. Phylogram of relationships among 42 species of the genus *Eupelmus*: 31 species from the previous phylogram using the complete molecular dataset and 9 species for which only the mitochondrial gene *COI* was sequenced, one species (*E. muellneri*) was sequenced for *COI*, *Cytb*, *Wg*, *EF-1Ŭ*& Rps4, and another one species (*E. memnonnius*) for which *COI* and *Wg* was sequenced.

Morphological-based phylogenetic reconstructions

The scores of the various trees are presented in Table 2, the molecular trees, on which morphological matrixes were mapped, (respectively MOLTREE T31 and MOLTREE T42) are much longer (206 steps versus 178 and 268 versus 228) than those obtained directly from the morphology (respectively MP MORPHOTREE T31 and MP MORPHOTREE T42) suggesting a significant homoplasy than expected. The MP trees resulting from the final analysis with the whole taxon sampling (59 species), respectively when using weighted and unweighted characters, were discarded and are not figured, as they strongly contradict the above molecular trees. They namely displayed two large clades and, in one of them, *Reikosiella* was the sister group of a series of *Eupelmus* forming a grade, which otherwise are retrieved on intermediate or terminal nodes in the molecular trees.

Table 2. scoring of the most parsimonious trees generated from morphological and molecular datasets.

	MP MORPHO TREE T31	MOLTREE T31	MP MORPHO TREE T42	MOLTREE T42	MP MORPHO TREE T59	Suboptimal MORPHO TREE T59	Edited TREE T59
Length = L	178	206	228	268	320	327	324
CI	0,470	0,403	0,386	0,328	0,294	0,287	0,290
RI	0,643	0,538	0,640	0,537	0,640	0,628	0,633
RC	0,300	0,217	0,247	0,176	0,188	0,181	0,184
HI	0,534	0,538	0,614	0,672	0,706	0,713	0,710

MP MORPHOTREE T31: Phylogenetic tree based on morphology of 31 species.

MP MORPHOTREE T42: Phylogenetic tree based on morphology of 42species.

MOLTREE T31: Phylogenetic tree based on molecular sequences of 31 species, and on which la morphology of these 31 species were mapped.

MOLTREE T42: Phylogenetic tree based on molecular sequences of 42 species, and on which la morphology of these 42 species were mapped.

Edited Tree T59: an integrative phylogenetic tree on retention of nodes supported in the different trees e.g. MOLTREE T31, MOLTREE T42 and MORPHTREE T59.

A suboptimal tree was thus preferred (Figure 3). This morphological tree firstly allows to confirm both the the paraphyly of the subgenus *Eupelmus* in which representatives of the subgenus *Macroneura* are nested as well as the paraphyly of the subgenus *Episolindellia* which splits into two clusters, the *hartigi* species group and the cluster formed by the *testaceiventris* and *juniperinus* species groups. Taken as a whole, the genus *Eupelmus* appears divided into numerous species groups (SPG), defined so as to merge preferably from well supported nodes. With our dataset, 12 SPGs can be identified together with two *species sola* (i.e. *E. memnonius* and *E. microzonus*). Each of these two species displays an original combination of character states that prevent them to be classified in the retrieved SPG.

This tree nevertheless contradicts the molecular ones especially in the absence of a sister group relationship between, on one side, the clade formed by the *atropurpureus* SPG, *E. microzonus* and the *vesicularis* SPG and, on the other side, the *urozonus* SPG. Looking in detail to the character changes allows establishing that the calculation privileges some series of reversals, for the characters structuring the pattern of the molecular trees: presence of apical pegs on the mesotibia, distribution and coloration of the pegs on the median basitarsus in the females (Gibson 1995); presence of enlarged genal setae, scape ornamentation and coloration, modified setae on the pedicel, habitus of the first flagellomere and of the clava in the males. Conversely, a series of characters which concern the setation of the fore wing were selected by the program to substantiate a node (node 14 in the Figure 3), which contradicts the topologies retrieved from the molecular datasets (Figures 1 and 2).

Instability in the morphological trees was also generated by missing data corresponding to unknown males. The lack of data sometimes occurs in combination with homoplasy, especially within the *urozonus* SPG. Hence, *E. simizonus* Al khatib, 2015 is always retrieved erroneously within the *urozonus* clade. *E. janstai* Delvare & Gibson, 2015 as sister species of *E. stenozonus* and *E. priotoni* Delvare, 2015 as sister species of *E. tremulae* Delvare, 2015 figure other cases of incorrect placements. An evident series of homoplastic characters is represented by the extension of the valvifer 2 in combination with long ovipositor sheaths; this led to the retrieval of the first of these wrong relationships and of some other ones.

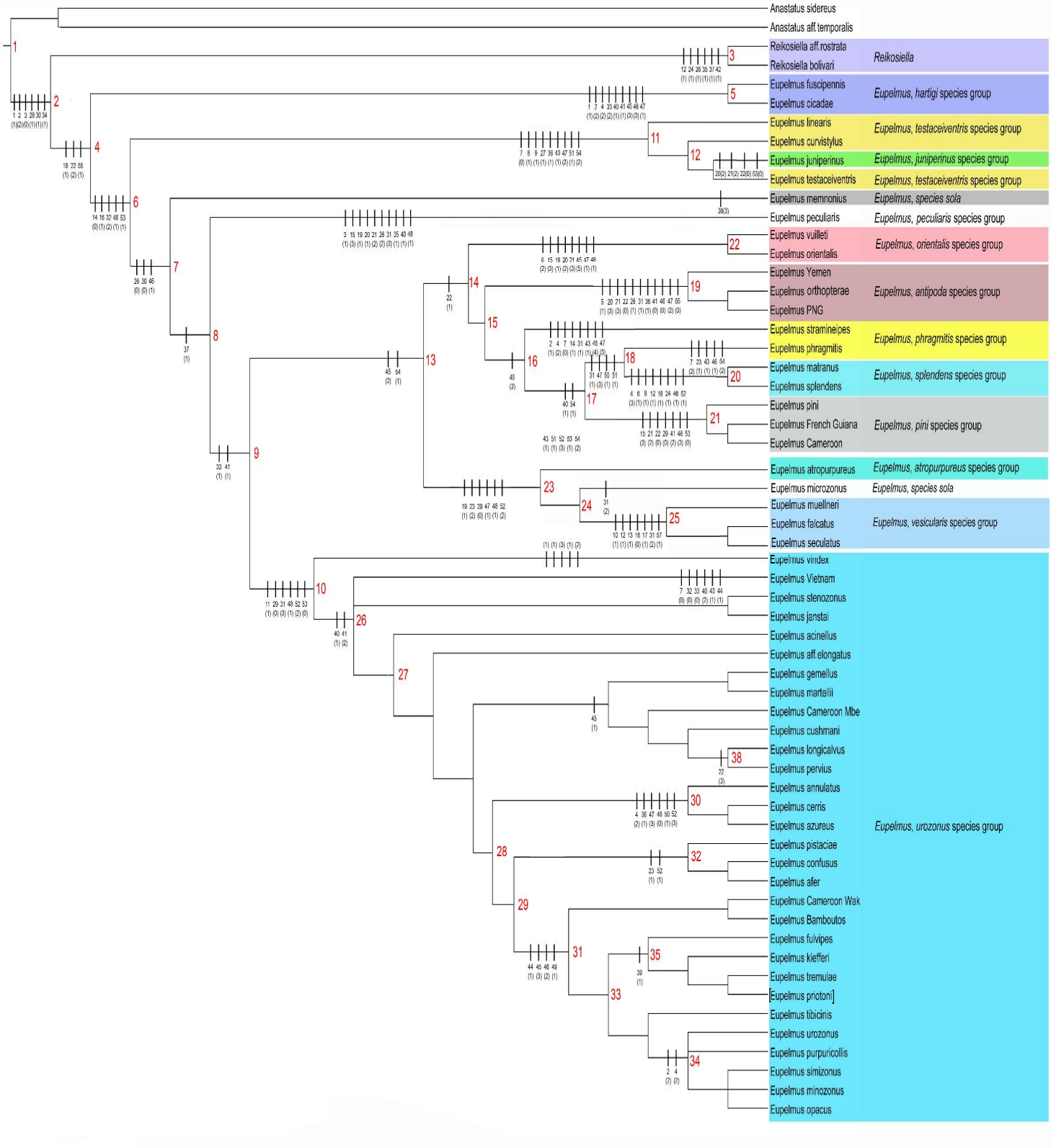

Figure 3. Suboptimal tree obtained from the morphological data for 59 species of *Eupelmus*, using 57 characters, which were weighted when assembling the molecular tree (31 species) with the morphology matrix. Bootstrap supports above 50 facing the nodes.

Towards an integrative tree

Taking into account the molecular trees obtained from restricted and largest datatsets respectively (MOLTREE T31 and MOLTREE T42) and complete morphological dataset (MP MORPHOTREE T59), an integrative tree (Edited TREE T59) was generated whose scores are detailed in Table 2. This tree (Figure 4), which maximizes the number of supported nodes, provides the support for a classification and evolutionary history of the genus *Eupelmus,* 36 nodes from 51 being well supported, at least from one of the data sources, sometimes by both of them. Taxonomic congruence lead hence to three main conclusions that are (i) the separation of the *Reikosiella* species from the genus *Eupelmus*; (ii) *Episolindelia* forms a grade with the *hartigi* SPG radiating from a basal node; (iii) the clustering of the subgenus *Macroneura* as a monophyletic and its emergence as a specialized species group within the subgenus *Eupelmus*.

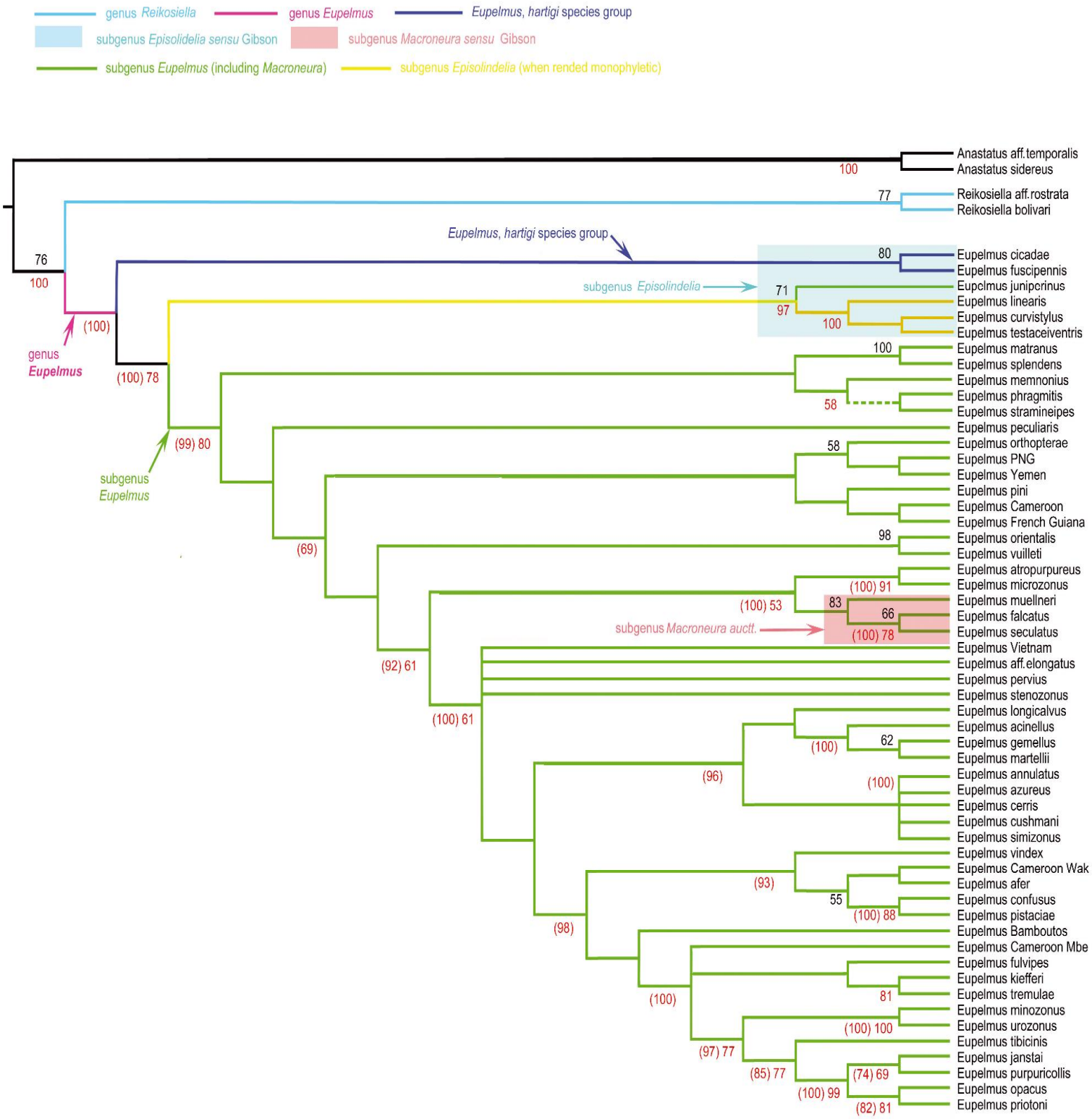

Figure 4. Integrative tree built from the suboptimal tree in Fig.3 when applying the results from the molecular data i.e. when reporting the nodes supported by high bootstraps and appearing in the Fig. 1 and 2. In black and above the nodes, bootstrap supports above 50 from the Fig. 3 (morphological data) in red and below the nodes from the Fig. 1 (in brackets) and Figure 2.

Discussion

Representativeness of the sampling

The revision of one diversified and globally-distributed taxa such as the *Eupelmus* genus is an actual challenge and the representativeness of our sampling is undoubtedly a possible issue. Of course, our dataset does not pretend to be exhaustive and is probably biased in favor of species from the West Palearctic or the Afrotropical ecozones but we nevertheless estimate that it can correctly cover the known and accessible global biodiversity.

In the Nearctic, eight of the fourteen species classified in the nominal subgenus belong to the *urozonus* SPG (Gibson 2011) and, hence, are not relevant for our analysis, this group being already well represented. From the remaining species of the nominal subgenus, three are shared with Europe and are present in our analysis. From the species classified in *Episolindelia* for all but *E. australiensis* (Girault) males are unknown or only tentatively associated (Gibson 2011) and hence unsuitable for our analysis. Though it seems that very few Neotropical species are included in our sampling, examination of samples trapped from French Guiana and thus well figuring the fauna of the Amazonian Basin, showed that *Eupelmus* is very rare there, being replaced by *Phlebopenes* Perty and *Brasema* Cameroon species. Although a number of *Eupelmus* were described from the Neotropical region, the descriptions were made a century ago and the relevant types never reexamined, or even if examined with a few exceptions formal taxonomic changes never published. It is hence possible that many of them will prove to actually belong to *Brasema* as is the case for a number of Nearctic species recently revised by Gibson (2011).

A clear limitation of our database is the bad coverage of the Oriental and Australasian realms. Hence, the present work should be seen as a first step only in the study of the genus. We deliberately avoided introducing in the data matrix species that can be coded only from females (and most species were described only from females), except in most situations if we had molecular data at least for *COI*. This was done because as outlined above the comparative analysis of trees based on comprehensive molecular data and those based on morphology showed a large amount of homoplastic characters that differentially affect the two sexes.

Evolutionary history of *Eupelmus*

The trees achieved from the two fields of data clearly show that within a phylogenetic systematics framework it is not possible to retain the subgeneric classification proposed by Gibson (1995). The author himself (Gibson 1995: 207-208) was doubtful about it, assuming that the subgenus *Eupelmus* might be paraphyletic relative to *Macroneura* and *Episolindelia* at its turn paraphyletic relative to *Eupelmus*. In order to avoid paraphyletic taxa and the presence of species that, by one character and/or sex, belong to one subgenus and, by other(s), to a different one, we thus propose to change the classification based on the three previous subgenera and propose a structuring according to informal species groups, the number of which being expected to increase with the inclusion of further investigations.

Our results, together with regional revisions or catalogues (Gibson 2011 for North America; Narendran and Anil 1995 for India; Bouček 1988 for Australasia) point out a strongly asymmetric patter in the partition of the species according to this grouping. The SPG merging on the basal and intermediate nodes – except for the *testaceiventris* SGP which is apparently relatively speciose – generally exhibit a low diversity both in term of species and hosts, each of the groups being specialist to a particular insect group. In contrast the clade *E. microzonus* + *atropurpureus* SPG + *vesicularis* SPG on one hand and *urozonus* SPG on the other hand, which branches on the terminal nodes, are quite diversified and include a number of generalists.

The features of the main species groups are reviewed in the following lines.

The *hartigi* species group

The group apparently only includes Palaearctic species, although undescribed species that likely belong here are known from the Afrotropical and Oriental regions. In addition to those appearing on Figure 3, *E. hartigi* Förster, 1841 itself, *E. pullus* Ruschka, 1921 and *E. cavifrons* Bouček, 1965 also belong here. The quoted hosts are Cecidomyiidae often living on conifers. Nevertheless *E. cicadae* is an oophagous parasitoid of *Cicada orni* Linnaeus, 1758 (Hemiptera, Cicadidae) according to Giraud (1872) and Silvestri (1921). Actually several specimens of *E. fuscipennis*, one female of *E. pullus* and another one, apparently belonging to an undescribed species, were sequenced for the *COI* gene. The relevant specimens are retrieved as monophyletic except *E. cicadae* which appears as the sister of *Reikosiella*. As discussed above this relationship is suspicious and even unrealistic

considering morphology; additionally *Reikosiella* appears on a long branch and the corresponding node is thus not supported. The females of *Reikosiella* and the *hartigi* SPG jointly share a broad and shallow scrobal depression and their penultimate tergite is exposed and does not show any median line, at most an impression being visible in some species of the *hartigi* SPG. In addition in some morphological trees the two taxa are retrieved as sister groups. Conversely the male characters strongly contradict for such a sister group relationship. In the absence of any other evidence we place the *hartigi* SPG on a basal node of *Eupelmus*. The females can well be separated from *Reikosiella* by the presence of a *linea calva*. In opposition to the other species classified in *Episolindelia* their body is entirely metallic.

The *testaceiventris* species group

The group forms the bulk of *Episolindelia*, *E. testaceiventris* being its type species. It is well supported both in the morphological and molecular trees. This group is cosmopolitan but some species were almost certainly introduced, like *E. australiensis* that is distributed from Australia to N. America. It is especially diverse in the Afrotropical Region and also presumably in the whole Old World tropics. It reaches the Mediterranean Basin at the North of its distribution range and one species (*E. linearis*) reaches as far north as Sweden (LF, unpublished data). Apart from the species included in our study, *E. australiensis* Girault, 1913, *E. australis* Girault, 1915, *E. greelyi* Girault, 1915, *E. moroderi* Bolivar y Pieltain, 1934, *E. mediterraneus*, Kalina 1988 come here. From the Nearctic fauna, besides the introduced species *E. australiensis, E. rubicola* (Ashmead, 1887) and *E. fuscipectus* Gibson, 2011 might also belong here. As far as it is known, they are almost all parasitoids of Cecidomyiidae developing on Poaceae. The development of savannahs and grasslands from 2.5 My before present in Africa might well explains their radiation here, since a number of species still await description. However, an undescribed species foraging on a dead trunk in a tropical forest of Cameroon was also collected. Hence, their habitat might be more diverse than previously expected. These *Eupelmus* are mostly small species with partially yellow body and long ovipositor sheaths in females, the mesotibia lacks apical pegs and the pegs on the basitarsus are pale and arranged in two regular rows; except for the Palaearctic *E. linearis* and the Nearctic *E. rubicola* and *E. fuscipectus* the apex of the pedicel and the first flagellomere are pale. The fore wing displays various patterns which are generally constant in other SPG: *linea calva* present or absent, stigmal vein straight or curved, postmarginal vein

not or evidently longer than stigmal vein. The scape of the male is linear and does not bear any pores, the pedicel lacks modified setae, and frequently the flagellum is somewhat clavate and formed of relatively short flagellomeres.

The *juniperinus* species group

This is a small Holarctic group including parasitoids of Cecidomyiidae within the seeds of *Juniperus* trees (Askew and Nieves-Aldrey 2000) or at least associated with *Juniperus* (Gibson 2011). Apart from the nominal species, *E. pallicornis* Gijswijt, 1993, *E. clavicornis* Askew, 2000 in Europe, *E. grisselli* Gibson, 2011 and *E. varicauda* Gibson, 2011 in North America come here. The females share most of the above quoted characters with the *testaceiventris* SPG but in the *juniperinus* SPG the body is squat, the flagellum short and evidently clavate and the ovipositor sheaths are not or only slightly exerted.

The *peculiaris* species group

The group was first mentioned and figured by Bouček (1988: 559 and figure 1007) and then characterized but not named by Gibson (1995: 204). Only *Eupelmus peculiaris* is described, but there is at least one other distinct undescribed species from Borneo (AICF). *E. peculiaris* is a geographically variable species, with specimens across Oriental and Palaearctic regions differing in minute details so this could be a group of cryptic species and rendering the group more speciose. Females of this SPG have a modified syntergum, conically protruding on either side of the anal plate and cercus advanced, located below spiracle; propodeum with long plical region and V-shaped plical depression; antenna has at least some white terminal or subterminal flagellomeres; face without lanceolate setae, all setae on head similar, hair-like, conspicuous and erect; fore wing densely setose with short *linea calva*; which is bordered anteriorly by several lines of setae differentiated in length and orientation; mesotibia without apical pegs, basitarsus with pegs somewhat to evidently differentiated on two overlapping rows on each side. Males are gracile, resembling those of *Reikosiella*; the antenna has the pedicel with a line of about 4 curved setae; basal funiculars with the articulation between them slightly offset so as to appear somewhat serrate basally; setation on head and wings similar to that of females, with speculum mesally along length filled with setae.

The *splendens* species group

Only the pair of closely related species *E. splendens* and *E. matranus* was introduced in the present sampling. They were even considered synonyms for some time. The group is apparently restricted to Europe and also includes *E. bulgaricus* Kalina, 1988. It is supported by a long series of derived states (see Figure 3).The females are easily recognized as their frontovertex, together with the concave posterior part of the mesoscutum, is smooth; the fore wing has a pattern of darkened areas. *E. splendens* is a parasitoid within galls of *Pediaspis aceris* (Gmelin, 1790) (Hymenoptera, Cynipidae) on *Acer* spp. (Askew and Nieves-Aldrey2000) while *E. matranus* is mentioned as a parasitoids of cynipids on oaks (Martelli and Arru 1958, Andriescu 1974).

***Eupelmus memnonius* Dalman, 1820 species sola**

This is the type species of the genus but its placement within the nominal subgenus is still problematic. Bouček (1988) considered it close to *Episolindelia*, our *testaceiventris* SPG. Gibson (1995) after discussing its placement finally included it in the subgenus *Eupelmus*. In the morphological trees we recovered both situations, while in the molecular tree MOLTREE T42 (Figure 2) it is the sister group of *E. phragmitis* thus definitely included in the nominal subgenus as hypothesized by Gibson (1995). The female of *E. memnonius* does not have any apical pegs on the mesotibia, furthermore the pegs on the basitarsus even if black are mostly arranged in two more or less regular rows, with a few additional pegs between the rows in large specimens such as they might appear inconspicuously differentiated into two rows. The dorsellum is partly protuberant over the propodeal plical depression. The penultimate tergite is fully exposed but shows a complete median line of flexion; the emargination of the syntergum does not reach its anterior margin; the exposed part of the second valvifer is long as well as the ovipositor sheaths. The females are collected on dead trunks hence *E. memnonius* certainly is a parasitoid of xylophagous insects but no precise host is known.

The *stramineipes* species group

E. phragmitis and *E. stramineipes* were not retrieved together in the suboptimal tree shown in Figure 3 but they appear as sister species in some other suboptimal trees. In the molecular tree MOLTREE T42 (Figure 2) – which does not include *E. stramineipes* – *E. phragmitis* surprisingly figures as the sister species of *E. memnonius* although they are quite different

morphologically. This relationship was hence never recovered when using morphological data. This putative group includes the two species quoted above and *E. levis* Nikol'skaya, 1952 described from Central Asia. All these species lack apical pegs on the mesotibia, the pegs on the basitarsus are distributed in two irregular rows, a few pegs being situated between these rows such as to appear sometimes inconspicuously differentiated into two rows; the prepectus is bare; the propodeal plical depression V-shaped, short, by far not reaching to the propodeal foramen; the maxillary palpi are at least partly pale, the legs excluding the coxae also tend to be pale in the females; the males exhibit a distinctly clavate flagellum and a long pedicel with about 6 long, straight or only slightly sinuate setae. The two European species are associated with *Phragmites australis*, *E. phragmitis* having been reared from *Tetramesa phragmitis* (Erdős, 1952).

The *antipoda* species group

The described species only include *E. antipoda* Ashmead from the Australasian Region and *E. orthopterae* from tropical Africa. As explained above *E. antipoda* might well figure among the species included in our sampling as *Eupelmus* PNG. *Eupelmus* rarely parasitize praying mantids according to the examination of extensive samples of parasitoids from these hosts examined by GD from all over the world. This group seemingly has a Palaeotropical distribution and appears relictual. The females have no apical pegs on the mesotibia, while the males have no enlarged genal setae, only a few pores on the scapular scrobe, no setae on the pedicel, first flagellomere being not discoid. The males also have no speculum on the fore wing, and because of this they are unique in the genus, no other described species with known males having this character. Because of this unusual combination of characters the males are similar to those of the genus *Brasema* Cameron (Gibson 1995: 207). Regarding the derived states of the females, the exerted part of the valvifer 2 and ovipositor sheaths are quite long; the fore wing is densely setose, the *linea calva* being very short or even absent, the apical section of the submarginal vein bears numerous setae; conversely the costal cell bears no dorsal setae. The males have a long pedicel and an ovoid clava.

The *orientalis* species group

The described species include only *E. orientalis* and *E. vuilleti*, both described by Crawford from India and Africa respectively. They are morphologically quite close and, except for a

few anomalous records from coccids, both are specialist parasitoids developing at the expense of bruchids infesting pods of Fabaceae. *E. orientalis* was intensively used as a model for studying various aspects of the biology and life traits of parasitic Hymenoptera (for a review of the relevant papers see Noyes 2015). The group is easy to recognize as the setae on the body are modified, scale-like. Hence these species were described in a separate genus, *Bruchocida* Crawford, now considered a synonym of *Eupelmus*. Otherwise the fore wing is densely setose, with a short *linea calva* and numerous setae on the inflated apical part of the submarginal vein. Conversely to the previous SPG the mesotibia bears apical pegs. The males have only one enlarged genal seta, few pores on the scape, the pores being restricted to the scapular scrobe, only 4 modified ventral setae on the pedicel, which is quite short in contrast with the very long and filiform flagellum.

The *pini* species group

Only the nominal species is described but the group is apparently cosmopolitan: we examined two other species, from French Guiana and Cameroon, collected in tropical forests and for the last one, on a dead tree. According to their morphology they were hypothesized to belong to the same SPG as *E. pini*. This species is recorded as a parasitoid of bark and wood-boring beetles (Gibson 2011). The male of *E. pini* is known but that quoted by Gibson (2011: 73) actually belongs to *E. vindex* according to the *COI* sequences (Table S1). The females may be recognized through the dense setation of the body, especially on the prepectus – linking the group with the *orientalis* SPG – and the fore wing which has no *linea calva*. Furthermore, in the two undescribed species examined here, the scrobal depression is margined laterally. The two known males of *E. pini* have a very unusual antenna, with a flagellum that combines a broad, not discoid, and setose anellus (characteristic of a clavate flagellum) with the flagellar structure of a typical filiform flagellum; the pedicel is long (more than two times as long as broad) and bears a line of 7–10 long white setae of which only the most basal are inconspicuously curved apically. The fore wing is conspicuously setose, with numerous setae on basal and costal cells and a speculum somewhat reduced in size.

The *atropurpureus* species group

Besides the nominal species, the group contains also an undescribed species from Korea (HNHM), of which only females are known. It is close to *E. atropurpureus* and differs in colour, sculptural characteristics and the setation pattern of the fore wing, so it definitely belongs to this SPG. Judging from the original description possibly also *E. rexonus* Narendran & Anil, 1998 described from a single specimen from India belongs here. The group is characterized by an ocello-ocular line more than 2 times the diameter of the small posterior ocellus, similar to species of the *vesicularis* SPG. In the Palaearctic, brachypterous females are known only in this group and in the *vesicularis* SPG. Though mostly brachypterous, females of *E. atropurpureus*, where long series were examined, may be conversely macropterous, in which case the fore wing has a broad costal cell (character 19, state 1) similar to that of *E. microzonus*, and a glabrous basal cell that has at most a few sparse setae. Probably because of the retention of rare winged females the brachypterism in this SPG is not associated with modifications in mesosomal structure as it is in the *vesicularis* SPG.

***Eupelmus microzonus* species sola**

E. microzonus is treated here as *species sola* as although the females of this species are superficially similar to females of the *urozonus* SPG, the males are extremely similar to those of the *vesicularis* SPG. Correlated with the strong support of a sister group relationship between the *urozonus* SPG and the clade formed by the *atropurpureus* SPG, *vesicularis* SPG and *E. microzonus*, this suggest that females of the common ancestor of this two large groups were similar to those of the *urozonus* SPG and all the characters of the *vesicularis* SPG could be secondarily derived following reduction of the wings.

In *E. microzonus* females the mesotarsal pegs are reduced in number and asymmetrically disposed, the anterior margin with at most 9 pegs and the posterior margin with about half the number of pegs on anterior margin; the pegs being shorter than usual, do not project beyond the surface of the ventral pads of setae that are well developed, forming cushion-like structure. This structure of the mesotarsus is almost identical to that found in many species of the *vesicularis* SPG, including *E. vesicularis* (Retzius, 1783). Otherwise the costal cell of the female is relatively short and broad while the basal one is sparsely setose.

Kalina (1988: 21), based on similarities in the mesotarsus structure, grouped *E. microzonus* in the same species group with three very close species he described in that paper

(*E. africanus*, *E. algiricus*, and *E. iranicus*). Unlike *E. microzonus* females of this 3 species have no mesotarsal pegs but the ventral pads of mesotarsal setae are cushion-like (similar to *E. microzonus* and many species in *vesicularis* SPG). Also, similarly to *E. microzonus*, they have a pale tegula. Males are unknown except for *E. algiricus*, and here again it is very similar to the males of the *vesicularis* SPG.

The three above species described by Kalina might indeed belong to the *E. microzonus* SPG. In this case *E. longicorpus*, described from Australia, is the fifth species to be included in the group as it is extremely close morphologically to the three Palaearctic species described by Kalina. Unlike *E. microzonus* these species have the ovipositor advanced, so that the gastral apex is conspicuously extending over the base of the third valvula.

The *vesicularis* species-group

This SPG contains all the species formerly included in the genus *Macroneura* (Bouček 1988) or the subgenus *Macroneura* of *Eupelmus* (Gibson 1995), the first described species being *E. vesicularis*. Females of all species are brachypterous and, correlated with brachypterism, conspicuous modifications of the pronotum, metanotum and propodeum occurred (Gibson 1995). The mesothorax of brachypterous or apterous Hymenoptera most often become dwarfed, following the reduction of the flight muscles, while the prothorax and the complex metathorax-propodeum are both enlarged, in correlation with the development of the groups of muscles used for walking. Since the mesothorax of Eupelminae is highly modified for jumping (Gibson 1986) and contains specialized and enlarged mesothoracic muscles, which are retained in *Macroneura*, this part of the thorax in not reduced comparative to the macropterous species. Yet the other mesosomal segments are here adjusted as for the other micropterous Hymenoptera, i.e. the pronotal collar and the metanotum are especially well expanded. The row of erect setae delimiting the pronotal collar, and characteristic for *Macroneura,* is most likely homologous with the admarginal setae (Al khatib et al. 2014) of the other *Eupelmus* species.

The males of this SPG have a gracile elongate body with the mesosoma at least 1.7 times longer than broad. Their flagellum is filiform, with stout and short dark setae visible in lateral view ventrally on flagellomeres 2-3 and frequently also on flagellomere 4.The scape is yellow on the outer side along the scapular scrobe and the baso-ventral surface conspicuously lighter than dorsally and on inner surface. The legs are extensively pale to brownish, but with

at least about basal half of meso- and metatibiae light-colored. The hind coxa is finely coriaceous, mostly smooth and shiny.

Macroneura was recovered as monophyletic in all our analyses, but although our data set included species from both subgenera of *Macroneura* proposed by Kalina (1981) it didn't include any Nearctic or Afrotropical species. Though *Macroneura* is monophyletic it renders the subgenus *Eupelmus sensu* Gibson (1995) paraphyletic as it is the sister group to (*atropurpureus* SPG + *E. microzonus*) and all the three form a monophyletic group strongly supported both in the molecular tree MOLTREE T31 and by a series of derived character states (Figure 3) such as brachypterism in most females, frequent reduction of the pegs on the mesobasitarsus, the cushion-like ventral pads of setae on mesotarsus, and the similarity in the morphology of the male antenna.

For historical and practical reasons we do not merge all these species in a single species group as suggested by the strong support for the monophyly of the clade and the male morphology, but rather propose a *vesicularis* SPG, an *atropurpureus* SPG and treat *E. microzonus* as *species sola*. These groups can be differentiated only based on females but not on males. If merged in a single SPG this would be diagnosable based on males but not on females.

The *urozonus* species group

This is by far the largest and most diversified SPG of the genus *Eupelmus*. It may include half of the described species. Al khatib et al. (2014) reviewed the Palaearctic species. In the Nearctic region *E. arizonensis* Gibson, 2011, *E. curticinctus* Gibson, 2011, *E. cushmani*, *E. cyaniceps* Ashmead, 1886, *E. pervius* and *E. utahensis* Girault, 1916 come here. Gibson (2011) also includes in the *urozonus* group the species *E. cynipidis* Ashmead, 1882 and *E. conigerae* Ashmead, 1885, that although have very atypical females for the group, the males are similar to those of other included species. The first six species can even be placed in the *gemellus* clade according to the morphology of the male antenna. The *confusus* clade is apparently quite diverse in tropical Africa and this might be true for the rest of the Old World tropics. The *gemellus* clade seems to be restricted to the Holarctic region, while we examined members of the *urozonus* clade only in the Palaearctic. The hosts basically exhibit the same habitats as for the *vesicularis* SPG but are still more diverse. The group was retrieved monophyletic in morphology only when weighting the characters, but it is well supported – at

least for the species included in the analysis – by molecular data. An apparently quick radiation, having left no or faint genetic trace, prevents a complete phylogenetic reconstruction within the clades. Females of this SPG can be identified by the presence of a double, partly overlapping, row of dense pegs on either side of the mid basitarsus, forming a symmetrical pattern (Gibson, 2011: Fig. 32). In females of other SPGs the mesotarsal peg pattern may sometimes approach the one characteristic for the *urozonus* SPG, but in the other groups the pegs are never so densely packed nor perfectly symmetrically arranged. Otherwise females of all species are winged, the fore wing always with a *linea calva*, the postmarginal vein is not or only slightly longer than the stigmal and the ovipositor sheaths have a median to subapical light band between darker ends. In addition, the pronotum has, not always but very often, violet reflections on the collar. Except for the species called '*Eupelmus* Vietnam' the last abdominal segments of the female are identical with those described for the bulk of *Eupelmus*: the penultimate tergite is hidden by the preceding one and shows a median line, and the syntergum is deeply emarginate, the emargination nearly reaching its anterior edge. It seems that reversals occurred in '*Eupelmus* Vietnam' and at least one another species from the Reunion Island. Nevertheless the male of the former species shows a number of states which are otherwise found in the *urozonus* clade, such as the presence of tufts of hook-like setae on the lower face, numerous pores on the enlarged scape, at least 6 ventral hook-like setae on the pedicel, etc. Hence the placement in this clade is mainly realized through the male morphology (head and antenna). Most members of the *confusus* clade are conversely recognized by examining the fore wing of the female, which has a bare stripe on the ventral side of the costal cell along the leading margin, a reduce number of setae (4-6) on the apical section of the submarginal vein, the basal cell more sparsely setose than in the rest of the wing and often bearing pale setae, in contrast with the dark ones observed elsewhere. Finally, unexpectedly, although *E. vindex* is relatively distant morphologically from other members of the group it merges on a basal node within the *confusus* clade in the molecular tree (Figure 1). However, the relative position of *E. vindex* within is not completely stable and depends on the concatenation of the molecular datasets (Al khatibe submitted). The *gemellus* clade is morphologically diversified and can hardly be recognized. In some species, such as *E. annulatus*, *E. azureus* Ratzeburg 1844 and *E. cerris*, the scape of the male is modified relatively to the usual case. In the pair *E. pervius* / *E. longicalvus* the *linea calva* is quite expanded. The other species cannot be readily placed according to their morphology, especially the females. The placement of the males may be deduced by elimination of the two other clades which exhibit more derived characters.

References

Al khatib F, Cruaud A, Fusu L, Rasplus J.-Y, Ris N, Delvare G (submitted) Ecological differentiation in the “Eupelmus urozonus species group” (Hymenoptera, Eupelmidae) occurring in the West-Palaearctic: first insights based on a multi-locus phylogeny and reliable host records. BMC Evolutionary Biology.

Al khatib F, Fusu L, Cruaud A, Gibson G, Borowiec N, Rasplus JY, Ris N, Delvare G (2015) Availability of eleven species names of Eupelmus (Hymenoptera, Eupelmidae) proposed in Al khatib et al. (2014). Zookeys 505: 137–145.

Al khatib F, Fusu L, Cruaud A, Gibson G, Borowiec N, Rasplus J-Y, Ris N, Delvare G (2014) An integrative approach to species discrimination in the *Eupelmus urozonus* complex (Hymenoptera, Eupelmidae), with the description of 11 new species from the Western Palaearctic. Systematic Entomology 39: 806–862.

Andriescu I (1974) Chalcidoidiens (Chalcidoidea, Hym., Insecta), d'importance economique de Roumanie (Catalogue hôte/parasite, parasite/hôte). Lucrarile Staţiunii 'Stejarul' (Ecologie Terestră şi Genetică) 1972–1973: 155–190.

Askew RR, Nieves-Aldrey JL (2000) The genus Eupelmus Dalman, 1820 (Hymenoptera, Chalcidoidea, Eupelmidae) in peninsular Spain and the Canary Islands, with taxonomic notes and descriptions of new species. Graellsia 56: 49–61.

Beutel RG, Friedrich F, Hörnschemeyer T, Pohl H, Hünefeld F, Beckmann F, Meier R, Misof B, Whiting MF, Vilhelmsen L (2010) Morphological and molecular evidence converge upon a robust phylogeny of the megadiverse Holometabola. Cladistics 26: 1–15.

Bouček Z (1988) Australasian Chalcidoidea (Hymenoptera). A Biosystematic Revision of Genera of Fourteen Families, with a Reclassification of Species. CAB International Institute of Entomology, The Cambrian News Ltd (Aberystwyth): 1-832.

Bybee EM, Zaspel JM, Beucke KA, Scott CH, Smith BW, Branham MA (2010) Are molecular data supplanting morphological data in modern phylogenetic studies. Systematic Entomology 35: 2–5.

Calendini F, Martin J-F (2005) PaupUP v1.0.2 Beta. A free graphical frontend for Paup* DOS Software. Montpellier, France. http://www.agro-montpellier.fr/sppe/Recherche/JFM/PaupUp/

Dayrat B (2005) Towards integrative taxonomy. Biological Journal of the Linnnean Society 85: 407–415.

de Queiroz A, Gatesy J (2006) The supermatrix approach to systematics. Trends in Ecology and Evolution 22: 34–39.

Eernisse DJ, Kluge AG (1993) Taxonomic congruence versus total evidence, and Amniote phylogeny inferred from fossils, molecules, and morphology. Molecular Biology and Evolution 10: 1170–1195.

Fenwick A, Gutberlet JR RL, Evans JA, Parkinson CL (2009) Morphological and molecular evidence for phylogeny and classification of South American pitvipers, genera Bothrops, Bothriopsis, and Bothrocophias (Serpentes: Viperidae). Zoological Journal of the Linnean Society 156: 617–640.

Gebiola M., Gómez-Zurita J., Monti M.M.P., Navone P. & Bernardo U. 2012. Integration of molecular, ecological, morphological and endosymbiont data for species delimitation within the Pnigalio soemius complex (Hymenoptera: Eulophidae). Molecular Ecology, 21: 1190–1208.

Gibson GAP (1986) Mesothoracic skeletomusculature and mechanics of flight and jumping in Eupelminae (Hymenoptera, Chalcidoidea: Eupelmidae). The Canadian Entomologist 118: 691–728.

Gibson GAP (1990) Revision of the genus Macroneura Walker in America North of Mexico (Hymenoptera: Eupelmidae). Canadian Entomologist 122: 837–873.

Gibson GAP (1995) Parasitic wasps of the subfamily Eupelminae: classification and revision of world genera (Hymenoptera: Chalcidoidea, Eupelmidae). Memoirs on Entomology, International, 5: i-v + 421 p.

Gibson GAP (2011) The species of Eupelmus (Eupelmus) Dalman and Eupelmus (Episolindelia) Girault (Hymenoptera: Eupelmidae) in North America north of Mexico. Zootaxa 2951: 1–97.

Gibson GAP, Fusu L (submitted) Revision of the Palaearctic species of Eupelmus (Eupelmus) Dalman (Hymenoptera: Chalcidoidea: Eupelmidae). Zootaxa.

Giraud J (1872) Miscellanées Hyménoptérologiques. III. Description d'Hyménoptères nouveaux avec l'indication des moeurs de la plupart d'entre eux et remarques sur quelques espèces déjà connues. Annales de la Société Entomologique de France 1: 389–419.

Girault AA (1914) Some new genera and species of chalcidoid Hymenoptera of the family Encyrtidae from Australia. Societas Entomologica 29: 22−24.

Goloboff PA, Farris JS, Nixon KC (2008) TNT, a free program for phylogenetic analysis. Cladistics 24: 774–786.

Gómez-Zurita J, Cardoso A (2014) Systematics of the New Caledonian endemic genus Taophila Heller (Coleoptera: Chrysomelidae, Eumolpinae) combining morphological, molecular and ecological data, with description of two new species. Systematic Entomology 39: 111–126.

Hebert PDN, Cywinska A, Ball SL, De Waard JR (2003) Biological identifications through DNA barcodes. Proceedings of the Royal Society Biological Sciences Series B 270: 313–321.

Heraty JM, Burks RA, Cruaud A, Gibson GAP, Liljeblad J, Munro J, Rasplus J.-Y, Delvare G, Jansta P, Gumovsky A, Huber J, Woolley JB, Krogmann L, Heydon S, Polaszek A, Schmidt S, Darling DC, Gates MW, Mottern J, Murray E, DalMolin A, Triapitsyn S, Baur H, Pinto JD, van Noort S, George J, Yoder M (2013) A phylogenetic analysis of the megadiverse Chalcidoidea (Hymenoptera). Cladistics 29: 1–77.

Jarvis KJ, Haas F, Whiting MF (2004) A phylogeny of earwigs (Insecta: Dermaptera) based on molecular and morphological evidence: reconsidering the classification of Dermaptera. Systematic Entomology 30: 1–12.

Kalina V (1981) The Palaearctic species of the genus Macroneura Walker, 1837 (Hymenoptera, Chalcidoidea, Eupelmidae), with descriptions of new species. Sbornik. Védeckého Lesnického Ustavu Vysoké Skoly Zemédélské v Praze 24: 83–111.

Kalina V (1988) Descriptions of new Palaearctic species of the genus Eupelmus Dalman with a key to species (Hymenoptera, Chalcidoidea, Eupelmidae). Silvaecultura Tropica et Subtropica 12: 3–33.

Lopardo L, Giribet G, Hormiga G (2011). Morphology to the rescue: Molecular data and the signal of morphological characters in combined phylogenetic analyses—A case study from mysmenid spiders (Araneae, Mysmenidae), with comments on the evolution of web architecture. Cladistics 27: 278–330.

Martelli M, Arru GM (1958) Ricerche premiminari sull'entomofauna della Quercia da sughero ("Quercus suber" L.) in Sardegna. Bollettino di Zoologia Agraria e Bachicoltura, Milano 1: 5–49.

Misof B, Liu S, Meusemann K, Peters RS, Donath A, Mayer C, Frandsen PB, Ware J, Flouri T, Beutel RG, Niehuis O, Petersen M, Izquierdo-Carrasco F, Wappler T, Rust J, Aberer AJ, Aspöck U, Aspöck H, Bartel D, Blanke A, Berger S, Böhm A, Buckley TR, Calcott B, Chen J, Friedrich F, Fukui M, Fujita M, Greve C, Grobe P, Gu S, Huang Y, Jermiin LS, Kawahara AY, Krogmann L, Kubiak M, Lanfear R, Letsch H, Li Y, Li Z, Li J, Lu H, Machida R, Mashimo Y, Kapli P, Duane D, McKenna DD, Meng G, Nakagaki Y, Navarrete-Heredia JS, Ott M, Ou Y, Pass G, Podsiadlowski L, Pohl H, von Reumont BM, Schütte K, Sekiya K, Shimizu S, Slipinski A, Stamatakis A, Song W, Su X, Szucsich NU, Tan M, Tan X, Tang M, Tang J, Timelthaler G, Tomizuka S, Trautwein M, Tong X, Uchifune U, Walzl MG, Wiegmann BM, Wilbrandt J, Wipfler B, Wong TKF, Wu Q, Wu G, Xie Y, Yang S, Yang Q, Yeates DK, Yoshizawa K, Zhang Q, Zhang R, Zhang W, Zhang Y, Zhao J, Zhou C, Zhou L, Ziesmann Z, Zou S, Li Y, Xu X, Zhang Y, Yang H, Wang J, Wang J, Kjer KM, Zhou X (2014) Phylogenomics resolves the timing and pattern of insect evolution. Science 346: 763–767.

Narendan TC, Anil K (1995) A key of Indian species of Eupelmus Dalman (Hymenoptera: Eupelmidae) with descriptions of eleven new species. Journal of the Zoological Society of Kerala 5: 1-15.

Noyes JS (2015) Universal Chalcidoidea database. Available from: http://www.nhm.ac.uk/research- curation/research/projects/chalcidoids/index.html.

Padial JM, Miralles A, De la Riva I, Vences M (2010) The integrative future of Taxonomy. Frontiers in Zoology 7: 2–14.

Scotland RW, Olmstead RG, Bennett JR (2003) Phylogeny Reconstruction: The Role of Morphology. Systematic Biology 52: 539–548.

Silvestri F (1921) Notizie sulla Cicada grigriastra (Tettigia orni L.) sulla Cicada maggiore (*Cicada plebeja* Scop.), sui loro parassiti e descrizione della loro larva neonata e della ninfa. Bollettino del Laboratorio di Zoologia Generale e Agraria della R. Scuola Superiore d'Agricoltura, Portici 15: 191–204.

Sørensen VM, Giribet G (2006) A modern approach to rotiferan phylogeny: Combining morphological and molecular data. Molecular phylogenetics and Evolution 40: 585–608.

Swofford DL. 2001. PAUP. Phylogenetic analysis using parsimony (*and other methods). Version 4.0 beta. Sinauer Associates, Sunderland, Massachusetts.

Wahlberg N, Braby MF, Brower AVZ, de Jong R, Lee M.-M, Nylin S, Pierce NE, Sperling FAH, Vila R, Warren AD, Zakharov E (2015) Proceeding of the Royal Entomological Society of London(B) 272: 1577–1586.

Wiens JJ (2004) The role of morphological data in phylogeny reconstruction. Systematic Biology 53: 653–661.

Winterton SL, Hardy NB, Wigmann BM (2010) On wings of lace: phylogeny and Bayesian divergence time estimates of Neuropterida (Insecta) base on morphological and molecular data. Systematic Entomology 35: 349–378.

Supporting Information

Table S1. Sample information for the specimens included in the study.

Table S2. Matrix of characters states for the genus *Eupelmus*. Outgroups are *Anastatus sidereus* and *A. aff. temporalis*. In-group includes 57 species.

Table S1. Sample information for the specimens included in the study.

Species	Collection code	Mol code and sex	ǁ sequenced	Sex morphology	Country	Province	Locality	Latitude	Longitude	Host
Anastatus aff. temporalis Askew, 2005	GDEL4100	10107 ♀	no	♀	France	Gard	Générac	43.71944°	4.35361°	unknown
Anastatus sidereus (Erdös, 1957)	GDEL4098	10105 ♀	no	♀	France	Alpes-Maritimes	Fontan	44.02639°	7.57778°	unknown
Eupelmus acinellus Askew, 2009	FAL1363	10235 ♀	yes	♀♂	France	Aude	Durban-Corbières	42.99825°	2.80690°	Mesophleps oxycedrella
Eupelmus afer Silvestri, 1914	-	-	no	♀♂	Namibia		Naukluft Mountains, Olive trail	-24.24327°	16.28350°	unknown
Eupelmus annulatus Nees, 1834	NB783	10354 ♀	yes	♀♂	France	Gard	Le Castanet	43.98925°	3.70094°	Dryocosmus kuriphilus
Eupelmus atropurpureus Dalman, 1820	PJ11159_23_1	10580 ♀	no	♀	Spain	Aragón	Huesca	-	-	unknown
Eupelmus atropurpureus Dalman, 1820	-	-	no	♂	Romania	Iași	Iași Botanical Garden	-	-	-
Eupelmus azureus Ratzeburg, 1844	NB773a	10361 ♀	yes	♀♂	France	Var	La Garde-Freinet	43.30487°	6.43701°	Dryocosmus kuriphilus
Eupelmus cerris Förster, 1860	GDEL4109	10118 ♀	no	♀♂	Hungary	Vezprém	Hegyesd	46.93333°	17.52278°	unknown
Eupelmus cicadae Giraud, 1872	GDEL4138	10293 ♀	no	♀	France	Ardèche	Les Vans	43.38722°	4.15444°	unknown
Eupelmus cicadae Giraud, 1872	-	-	no	♂	Romania	Galați	Gârboavele	-	-	unknown
Eupelmus confusus Al Khatib, 2015	FAL1278	10443 ♀	yes	♀♂	France	Ardèche	Saint-Georges-Montpellier	43.6104°	3.77227°	Bactrocera oleae
Eupelmus curvistylus (Risbec, 1951)	2880	-		♀♂	Burkina Faso		Banfora	-	-	Cecidomyiidae
Eupelmus cushmani (Crawford, 1908)	GBAH9086-14.COI-5P	-	yes, part	-	-	-	-	-	-	-
Eupelmus cushmani (Crawford, 1908)	2136	-	no	♀♂	Paraguay	-	Pirareta	-	-	Eutinobothrus brasiliensis
Eupelmus falcatus (Nikol'skaya, 1952)	GDEL4088	10090 ♀	no	♀♂	Hungary	Veszprém	Nagavászony	47.02167°	17.72417°	unknown
Eupelmus fulvipes Förster, 1860	FAL1221	10200 ♀	yes	♀♂	France	Alpes-Maritimes	Gréolières-les-Neiges	43.81584°	6.88711°	Diplolepis rosae
Eupelmus fuscipennis Förster, 1860	GDEL4066	10059 ♀	yes, part	♀	France	Hérault	Saint-Félix-de-l'Héras	43.82583°	3.32555°	unknown
Eupelmus gemellus Al khatib, 2015	FAL1359	10230 ♀	yes	♀♂	France	Alpes-Maritimes	Biot	43.63455°	7.08249°	Mesophleps oxycedrella
Eupelmus janstai Delvare & Gibson, 2015	GDEL4046	10032 ♀	no	♀	Czech Republic	Břeclav	Pavlov	48.86750°	16.65416°	unknown
Eupelmus juniperinus Bolivar y Pieltain, 1934	GDEL4064	10057 ♀	no	♀	France	Hautes-Alpes	Saint-Crépin	44.71056°	6.60639°	unknown
Eupelmus kiefferi De Stefani, 1898	FAL1109	10167 ♀	yes	♀♂	Spain	Logroño	La Rioja	-	-	Myopites stylata
Eupelmus linearis Förster, 1860	GDEL4069	10062 ♀	no	♀	France	Lozère	Cocurès	45.30555°	4.59194°	unknown
Eupelmus longicalvus Alkhatib & Fusus, 2015	LF.ma.SW 02	10429 ♀	no	♀	Sweden	Go	Gotlands	57.53908°	18.34092°	unknown
Eupelmus martellii Masi, 1940	LF.ma.LI.01	10659 ♀	yes, part	♀♂	Libya	-	Bukamash	-	-	unknown

Eupelmus matranus Erdös, 1947	FAL1491	10318 ♀	no	♀	France	Alpes-Maritimes	Sophia-Antipolis	43.61671°	7.07550°	unknown
Eupelmus memnonius Dalman, 1820	-	mem_RO_01 ♀	yes, part	♀	Romania	Olt	Piatra-Olt, Pădurea Sarului	44.378138°	24.19344°	unknown
Eupelmus memnonius Dalman, 1821	-		no	♀	Hungary	Veszprém	Devecseri Szeri Forest	-	-	-
Eupelmus microzonus (Förster, 1860)	GDEL4116	10192 ♀	no	♀ ♂	France	Haute-Corse	Aléria	42.12861°	9.46556°	Bruchophagus sp.
Eupelmus minozonus Delvare, 2015	GDEL4030	10009 ♀	no	♀	Hungary	Veszprém	Hegyesd	46.93333°	17.52278°	unknown
Eupelmus muellneri Ruschka, 1921	FAL1076	10157 ♀	no	♀ ♂	Italy	Liguria	Bussana-Vecchia	43.84026°	7.82905°	Myopites stylata
Eupelmus opacus Delvare, 2015	LF.ur.SW 02	10460 ♀	no	♀ ♂	Sweden	Og	Ödeshögs kommun	58.18452°	14.64053°	unknown
Eupelmus opacus Delvare, 2015	-	-	no	♂	Ukraine	Kiev	Kiev, Rybnoe lake	-	-	Rhabdophaga salicis
Eupelmus orientalis (Crawford, 1913)	17929	-	no	♀ ♂	Togo	-	Lomé	-	-	Callosobruchus maculatus
Eupelmus orthopterae (Risbec, 1951)	-	-	no	♀	Burkina Faso	-	Ouagadougou	-	-	Mantodea
Eupelmus orthopterae (Risbec, 1951)	-	-	no	♂	Cameroon	Adamaoua	Osséré Gadou	7.17306°	13.62306°	unknown
Eupelmus peculiaris Narendran, 2011	pe.KO 01	-	no	♀	S. Korea	Chungnam	Daejeon, Changdong-2-gu	-	-	unknown
Eupelmus peculiaris Narendran, 2011	pe.KO 02	-	no	♂	S. Korea	Chungnam	Daejeon, Wadong	-	-	unknown
Eupelmus pervius Gibson, 2011	-	-	no	♀ ♂	USA	-	-	-	-	-
Eupelmus phragmitis Erdös, 1955	GDEL4056	10045 ♀	yes, part	♀ ♂	Hungary	Veszprém	Várpalota	47.18361°	18.15555°	unknown
Eupelmus pini Taylor, 1927	GDEL4058	10048 ♀	yes	♀	France	Alpes Maritimes	Guillaumes	44.07083°	6.85306°	unknown
Eupelmus pini Taylor, 1928	ug.KO 47	ug.KO 47 ♂	yes, part	♂	S. Korea	Chungnam	Daejeon, Wadong	-	-	unknown
Eupelmus pistaciae Al khatib, 2015	GDEL4027	10004 ♀	yes	♀ ♂	France	Hérault	Cazevieille	43.75222°	3.77000°	Megastigmus pistaciae
Eupelmus priotoni Delvare, 2015	GDEL4051	10038 ♀	no	♀	France	Aveyron	Sauclières	43.96389°	3.35583°	unknown
Eupelmus purpuricollis Al khatib & Fusu, 2014	LF.ur.GR.02	10650 ♀	no	♀	Greece	Kerkini Lake N.P.	nr Neo Petritsi	41.31383°	23.27655°	unknown
Eupelmus seculatus (Ferrière, 1954)	GDEL4089	10091 ♀	no	♀ ♂	France	Gard	Beauvoisin	43.71250°	4.30722°	unknown
Eupelmus simizonus Al khatib, 2014	GDEL4142	10297 ♀	no	♀	France	Ardèche	Les Vans	44.38722°	4.15444°	unknown
Eupelmus splendens Giraud, 1872	-	-	no	♀	France	Hérault	Saint-Génies-de-Varensal, Albès	-	-	unknown
Eupelmus stenozonus Askew, 2000	-	-	no	♀ ♂	Canary Islands	-	-	-	-	unknown
Eupelmus stramineipes Nikol'skaya, 1952	-	-	no	♀	France	Hérault	Vias	-	-	unknown
Eupelmus testaceiventris (Motschulsky, 1863)	GDEL4078	10075 ♀	yes	♀	Cameroon	Adamaoua	Osséré Gadou	7.17305°	13.62305°	unknown
Eupelmus tibicinis Bouček, 1963	GDEL4149	10300 ♀	yes	♀ ♂	France	Ardèche	Berrias-et-Casteljau	44.39389°	4.19472°	unknown
Eupelmus tremulae Delvare, 2015	-	10569 ♀	yes	♀ ♂	Czech Republic	Jindóichùv Hradec	Veselí nad Lužnicí	49.15296°	14.70646°	Harmandia sp.
Eupelmus urozonus Dalman, 1820	FAL1518	10410 ♀	yes	♀ ♂	France	Haute-Corse	Lumio	42.55879°	8.81299°	Bactrocera oleae

Eupelmus vindex Erdös, 1955	GDEL4054	10042 ♀	yes	♀	Hungary	Veszprém	Hegyesd	-	-	unknown
Eupelmus vindex Erdös, 1955	LF.pi.RO 01	10543 ♂	yes	♂	Romania	Iaşi	Bârnova Forest	-	-	unknown
Eupelmus vuilleti (Crawford, 1913)	17928	-	no	♀♂	Togo	-	Lomé	-	-	Callosobruchus maculatus
Eupelmus aff. elongatus Risbec, 1951	4179	-	no	♀♂	Senegal	-	Ziguinchor, Djibelor	-	-	Bracon sp.
Eupelmus Bamboutos	GDEL4074	10067 ♀	yes, part	♀	Cameroon	Ouest	Bamboutos Mountains, Messang	5.65944°	10.09583°	unknown
Eupelmus Cameroon	-	-	no	♀	Cameroon	Centre	Nkolnguet, 5 km S Mbalmayo	-	-	unknown
Eupelmus Cameroon Mbe	GDEL4075	10068 ♀	yes, part	♀	Cameroon	Adamaoua	Mbé	7.68555°	13.58722°	unknown
Eupelmus Cameroon Wak	GDEL4077	10072 ♀	yes, part	♀♂	Cameroon	Adamaoua	Wak	7.68555°	13.58722°	unknown
Eupelmus French Guiana	-	-	no	♀	French Guiana	-	Roura, Montagne des Chevaux	-52.42033°	4.71191°	unknown
Eupelmus PNG	-	-	no	♀	PNG	Solomon	Guadalcanal Island, N Honiara	-9.43333°	159.95000°	Hierodula salomonis
Eupelmus Vietnam	17268	-	no	♀♂	Vietnam	-	Châu Thanh	-	-	Cecidomyiidae
Eupelmus Yemen	09445-09510	-	no	♀♂	Yemen	-	13 km Wadi Khamis Bani Sa'd	15.18333°	43.38333°	Sphodromantis viridis
Reikosiella aff. rostrata (Ruschka, 1921)	NB810	10350 ♀	yes	♀♂	France	Alpes Maritimes	Tende	44.05669°	7.57935°	Dryocosmus kuriphilus
Reikosiella bolivari (Kalina, 1988)	-	-	no	♀	France	Gard	Alès	-	-	Plagiotrochus australis

Table S1. Sample information for the specimens included in the study (continued).

Species	**Associate plant**	**Collection date**	**GenBank accessions *COI***	**GenBank accessions *Cytb***	**GenBank accessions *Wg***	**GenBank accessions *EF-1Ŭ***	**GenBank accessions *Bub3***	**GenBank accessions *Rps4***	**GenBank accessions *RpL27a***
Anastatus aff. temporalis Askew, 2005	unknown	August 2011	KR348752	KR348858	KR708338	KR708449	KR905352	KR905274	KR708469
Anastatus sidereus (Erdös, 1957)	unknown	July 2010	KR348751	KR348859	KR708337	KR708448	KR905351	KR905273	KR708468
Eupelmus acinellus Askew, 2009	Juniperius oxycedrus	March 2012	KJ018383	KR348783	KJ018562	KR708370	KR905287	KR905199	KR708481
Eupelmus afer Silvestri, 1914	Olaea africana	May 2005	-	-	-	-	-	-	-
Eupelmus annulatus Nees, 1834	Castanea sativa	February 2012	KJ018403	KR348773	KJ018579	KR708360	KR905278	KR905189	KR708496
Eupelmus atropurpureus Dalman, 1820	Poaceae	November 2011	KR348771	KR348850	KR708358	KR708438	KR905355	KR905267	KR708523
Eupelmus atropurpureus Dalman, 1820	-	September 2008	-	-	-	-	-	-	-

Eupelmus azureus Ratzeburg, 1844	Castanea sativa	February 2012	KJ018404	KR348777	KJ018580	KR708364	KR905281	KR905193	KR708497
Eupelmus cerris Förster, 1860	on Quercus cerris	June 2010	KJ018335	-	KJ018531	KR708372	KR905289	KR905201	KR708470
Eupelmus cicadae Giraud, 1872	on Quercus pubescens	July 2012	KT361610	-	-	-	-	-	-
Eupelmus cicadae Giraud, 1872	unknown	June 2005	-	-	-	-	-	-	-
Eupelmus confusus Al Khatib, 2015	Olea europaea	October 2011	KJ018424	KR348793	KJ018592	KR708381	KR905305	KR905213	KR708510
Eupelmus curvistylus (Risbec, 1951)	Sorghum vulgare	November 1982	-	-	-	-	-	-	-
Eupelmus cushmani (Crawford, 1908)	-	-	KF444812	-	-	-	-	-	-
Eupelmus cushmani (Crawford, 1908)	Gossypium hirsutum	February 1981	-	-	-	-	-	-	-
Eupelmus falcatus (Nikol'skaya, 1952)	unknown	June 2010	KR348749	KR348852	KR708335	KR708440	KR905357	KR905265	KR708466
Eupelmus fulvipes Förster, 1860	Rosa canina	March 2012	KJ018364	KR348845	KJ018548	KR708433	KR905346	KR905259	KR708478
Eupelmus fuscipennis Förster, 1860	-	June 2009	KT361611	-	-	-	-	-	-
Eupelmus gemellus Al khatib, 2015	Juniperus oxycedrus	March 2012	KJ018380	KR348789	KJ018503	KR708377	KR905294	KR905205	KR708480
Eupelmus janstai Delvare & Gibson, 2015	on T. platyphyllos	July 2010	KJ018330	KR348843	KJ018526	KR708431	KR905344	KR905257	KR708457
Eupelmus juniperinus Bolivar y Pieltain, 1934	on Juniperus thurifera	August 2008	KR348746	KR348857	KR708332	KR708445	KR905362	KR905275	KR708463
Eupelmus kiefferi De Stefani, 1898	Dittrichia viscosa	March 2012	KJ018354	KR348821	KJ018487	KR708409	KR905324	KR905236	KR708475
Eupelmus linearis Förster, 1860	unknown	July 2011	KJ018334	KR348854	KJ018530	KR708442	KR905359	KR905268	KR708464
Eupelmus longicalvus Alkhatib & Fusus, 2015	unknown	July 2004	KJ018418	KR348838	KJ018588	KR708426	KR905339	KR905251	KR708508
Eupelmus martellii Masi, 1940	unknown	February 2010	KJ018468	-	-	-	-	-	-
Eupelmus matranus Erdös, 1947	on Quercus ilex	October 2012	KR348759	KR348848	KR708345	KR708436	KR905354	KR905263	KR708490
Eupelmus memnonius Dalman, 1820	on dead standing Quercus	June 2014	KT352073	-	KT352069	-	-	-	-
Eupelmus memnonius Dalman, 1821	on dead trunk	May 2001	-	-	-	-	-	-	-
Eupelmus microzonus (Förster, 1860)	Asphodelus ramosus	September 2011	KR348754	KR348849	KR708340	KR708437	KR905353	KR905262	KR708476
Eupelmus minozonus Delvare, 2015	on Quercus cerris	June 2010	KJ018323	KR348815	KJ018521	KR708403	KR905318	KR905233	KR708452
Eupelmus muellneri Ruschka, 1921	Dittrichia viscosa	February 2012	KT361612	KT361618	KT361620	KT361619	-	KT361621	-
Eupelmus opacus Delvare, 2015	unknown	August 2005	KJ018435	KR348834	KJ018600	KR708422	KR905337	xxx	KR708512
Eupelmus opacus Delvare, 2015	Salix caprea	April-May 1973	-	-	-	-	-	-	-
Eupelmus orientalis (Crawford, 1913)	Vigna unguiculata	March 2002	-	-	-	-	-	-	-
Eupelmus orthopterae (Risbec, 1951)	-	November 1990	-	-	-	-	-	-	-
Eupelmus orthopterae (Risbec, 1951)	unknown	November 2008	-	-	-	-	-	-	-
Eupelmus peculiaris Narendran, 2011	unknown	May-June 2007	-	-	-	-	-	-	-
Eupelmus peculiaris Narendran, 2011	unknown	May-June 2008	-	-	-	-	-	-	-
Eupelmus pervius Gibson, 2011	-	-	-	-	-	-	-	-	-
Eupelmus phragmitis Erdös, 1955	-	June 2010	KT361614	-	-	-	-	-	-
Eupelmus pini Taylor, 1927	dead trunk of Pinus	August 2009	KR348745	KR348851	KR708331	KR708439	KR905356	KR905264	KR708462

	silvestris								
Eupelmus pini Taylor, 1928	unknown	April-May 2007	KT352074	-	-	-	-	-	-
Eupelmus pistaciae Al khatib, 2015	Pistacia terebinthus	October 2010	KJ018321	KR348785	KJ018519	KR708373	KR905290	KR905202	KR708450
Eupelmus priotoni Delvare, 2015	unknown	June 2011	KJ018332	KR348844	KJ018528	KR708432	KR905345	KR905258	KR708459
Eupelmus purpuricollis Al khatib & Fusu, 2014	unknown	July 2008	KJ018460	KR348835	KJ018616	KR708423	-	KR905249	KR708528
Eupelmus seculatus (Ferrière, 1954)	unknown	August 2011	KR348750	KR348853	KR708336	KR708441	KR905358	KR905266	KR708467
Eupelmus simizonus Al khatib, 2014	on Quercus pubescens	July 2012	KJ018388	KR348832	KJ018567	KR708420	KR905335	KR905247	KR708487
Eupelmus splendens Giraud, 1872	-	August 1999	-	-	-	-	-	-	-
Eupelmus stenozonus Askew, 2000	-	-	-	-	-	-	-	-	-
Eupelmus stramineipes Nikol'skaya, 1952	-	August 1999	-	-	-	-	-	-	-
Eupelmus testaceiventris (Motschulsky, 1863)	unknown	November 2008	KR348748	KR348856	KR708334	KR708444	KR905361	KR905270	-
Eupelmus tibicinis Bouček, 1963	unknown	July 2012	KJ018390	KR348842	KJ018569	KR708429	KR905342	KR905255	KR708489
Eupelmus tremulae Delvare, 2015	Populus tremula	June 2007	KJ018446	-	-	-	-	-	-
Eupelmus urozonus Dalman, 1820	Olea europaea	September 2012	KR348763	KR348806	KR708349	KR708394	KR905310	KR905221	KR708500
Eupelmus vindex Erdös, 1955	unknown	June 2010	KR348744	KR348802	KR708330	KR708390	KR905306	KR905218	KR708461
Eupelmus vindex Erdös, 1955	unknown	July 2006	KT361613	-	-	-	-	-	-
Eupelmus vuilleti (Crawford, 1913)	Vigna unguiculata	March 2002	-	-	-	-	-	-	-
Eupelmus aff. elongatus Risbec, 1951	Solanum aethiopicum	February 1984	-	-	-	-	-	-	-
Eupelmus Bamboutos	-	November 2008	KT361615	-	-	-	-	-	-
Eupelmus Cameroon	dead trunk	August 2012	-	-	-	-	-	-	-
Eupelmus Cameroon Mbe	Indigofera arrecta	November 2008	KT361616	-	-	-	-	-	-
Eupelmus Cameroon Wak	Indigofera arrecta	November 2008	KT361617	-	-	-	-	-	-
Eupelmus French Guiana	-	November 2009	-	-	-	-	-	-	-
Eupelmus PNG	-	-	-	-	-	-	-	-	-
Eupelmus Vietnam	Mangifera indica	June 2000	-	-	-	-	-	-	-
Eupelmus Yemen	-	-	-	-	-	-	-	-	-
Reikosiella aff. rostrata (Ruschka, 1921)	Castanea sativa	March 2012	KR348762	KR348861	KR708348	KR708447	KR905350	KR905272	KR708495
Reikosiella bolivari (Kalina, 1988)	Quercus ilex	February 1984	-	-	-	-	-	-	-

Table S2. Matrix of characters states for the genus *Eupelmus*. Outgroups are *Anastatus sidereus* and *A. aff. temporalis*. In-group includes 57 species.

	1 1111111112	2222222223	3333333334	4444444445	5555555
	1234567890	1234567890	1234567890	1234567890	1234567890	1234567
Anastatus sidereus	001000?010	00010011--	--00--0000	000000000?	??????????	????0??
Anastatus aff. temporalis	0010001000	0101000103	1021111000	000000000?	??????????	???????
Eupelmus acinellus	0100001000	1000210000	1200000100	3211011201	2000210100	0301100
Eupelmus afer	0100001000	1000210000	1211100100	3211001001	2000320110	0?01100
Eupelmus annulatus	0102001000	1000210000	1200100100	3211011202	2000313001	0101100
Eupelmus atropurpureus	0101001000	0000110013	1220100100	1211000000	1000211100	0200100
Eupelmus azureus	0202001000	1000210000	1200100100	3211011200	1000313001	0301100
Eupelmus cerris	0000001000	1000210100	1200100100	3211011201	1000313001	0301111
Eupelmus cicadae	1202001000	0001100000	1200010111	0021000201	1000331000	0001100
Eupelmus confusus	0101001000	1000210000	1211100100	3211001001	2000320110	0101100
Eupelmus curvistylus	0100000110	0000010000	0200010111	0201010300	0010002100	1010100
Eupelmus cushmani	0000002000	1000110000	1200100100	3211001101	2?00110100	0?01?00
Eupelmus falcatus	0000001001	01110011-3	0-2---0100	4211001000	1010211100	1210101
Eupelmus fulvipes	0100001000	1000210000	1200100100	3211001012	2001320110	0201100
Eupelmus fuscipennis	1202001000	0001000001	0201010111	00210002??	??????????	???????
Eupelmus gemellus	0100001000	0000210000	1200100100	3211001101	2000210110	0101100
Eupelmus janstai	0202001000	1000110000	1200000100	321101122?	??????????	???????
Eupelmus juniperinus	0100000110	0000010002	2000111111	0201000000	0??0?0????	??0?1??
Eupelmus kiefferi	0002001000	1000210000	1200100100	3211001012	2001320110	0201100
Eupelmus linearis	0100000010	0000010000	1200011111	0201010200	0010001100	1012100
Eupelmus longicalvus	0000001000	0000210000	1300100100	321100102?	??????????	???????
Eupelmus martellii	0100001000	0000210000	1200100100	3211001101	2000210110	0?01100
Eupelmus matranus	0003011010	0100010101	2101100110	1211001001	1000313001	1111100
Eupelmus memnonius	0001001000	0000010000	1200000110	020101032?	??????????	???????
Eupelmus microzonus	0101001000	0000210011	1201100100	2211001100	1010211100	1210100
Eupelmus minozonus	0202001000	0000110000	1200000100	321100102?	??????????	???????
Eupelmus muellneri	0000001001	11100010-3	--2---0100	2211001000	1000212002	1201111
Eupelmus opacus	0202001000	1000110000	1200000100	3211001002	2001?20110	0201100
Eupelmus orientalis	0000021000	0000310102	3101100100	1211001100	1000511100	0010100
Eupelmus orthopterae	1000101000	0000010103	3001010110	0211002100	0010502002	0010000

Table S2. Matrix of character states for the genus *Eupelmus* (continued)

	1 1111111112	2222222223	3333333334	4444444445	5555555
	1234567890	1234567890	1234567890	1234567890	1234567890	1234567
Eupelmus peculiarius	0110001000	0000310011	2200020110	3201101001	0000?11100	0011100
Eupelmus pervius	0001001000	?000210001	1310??0100	3211001101	2?00110100	0?01???
Eupelmus phragmitis	0000002000	0000010001	2110100110	1211000001	1010333001	1012100
Eupelmus pini	0202001000	0000310001	3000100100	0211001101	2000330002	0001100
Eupelmus pistaciae	0000001000	0000210000	1210100100	3211001001	2000320100	0101100
Eupelmus priotoni	0202001000	1000210000	1200000100	321100011?	??????????	???????
Eupelmus purpuricollis	0202001000	1000210000	1200100100	321100010?	??????????	???????
Eupelmus seculatus	0002001011	01110011-3	0-11--0100	2211000000	1010211110	1210100
Eupelmus simizonus	0202001000	1000110000	1200000100	321100010?	???????0??	???????
Eupelmus splendens	0003011010	0100010101	2101100110	121100010?	??????????	???????
Eupelmus stenozonus	0100001000	0000110000	1200100100	3211011200	1000110100	0?01100
Eupelmus stramineipes	0102000000	0001010001	2100100110	1211001000	1?10403002	???0???
Eupelmus testaceiventris	0101000110	0000010000	0200101111	0201011200	0010002100	1012100
Eupelmus tibicinis	0102001000	1000210000	1200100100	3211011202	2001320110	0?01100
Eupelmus tremulae	0102001000	1000210002	1200000100	3211001112	2001320110	2201100
Eupelmus urozonus	0202001000	0000210000	1200100100	3211001002	2001320110	0201100
Eupelmus vindex	0101001000	1000210000	1200100100	3211001000	1010211100	1312100
Eupelmus vuilleti	0000021000	0000310102	3100100100	1211?01200	1000511100	0010100
Eupelmus aff. elongatus	0000001000	1000210000	1211000100	3211001200	2000210100	0100110
Eupelmus Bamboutos	0100001000	1000210000	0200100100	321100010?	??????????	???????
Eupelmus Cameroon	0010002000	0000310001	1000000100	021100011?	??????????	???????
Eupelmus Cameroon Mbe	0100001000	1000210000	1200100100	321100011?	??????????	???????
Eupelmus Cameroon Wak	01010?1000	1000210000	0211100100	3211001001	2001320110	0?01111
Eupelmus French Guiana	0010101000	0000310001	1000110100	021100003?	??????????	???????
Eupelmus PNG	0010101000	0000010003	1100010110	121101122?	??????????	???????
Eupelmus Vietnam	0101000000	1000210000	1200000100	3001011102	1011210100	0201100
Eupelmus Yemen	0000101000	0000010003	3000010110	1211011300	0000502002	1010000
Reikosiella bolivari	1203000010	0101000101	0021000111	000110010?	??????????	???????
Reikosiella aff. rostrata	1200001000	0101000100	1001000101	0001101100	0100000000	0001000

4. Partie II: Apports de la phylogénie multi-locus du groupe urozonus à la compréhension des processus de spécialisation écologique.

Article 2: Multilocus phylogeny and ecological differentiation of the "*Eupelmus urozonus* species group" (Hymenoptera, Eupelmidae) in the West-Palaearctic. Accepté le 15 Decembre 2015 au journal « *BMC Evolutionary Biology* ».

Présentation de lôarticle

Les insectes, en particulier les phytophages et les parasitoïdes, présentent une diversité inter-spécifique très importante avec des gammes d'hôtes très contrastées incluant des espèces très généralistes et d'autres très spécialisées (Bernays, 2003; Schoonhoven *et al.*, 2005; Heraty, 2009). L'explication de cette biodiversité implique de mieux comprendre les processus de spéciation et de spécialisation écologique (échelle intra-spécifique et l'articulation entre les deux). En particulier, il s'agit de comprendre si les processus à l'échelle infra-spécifique peuvent favoriser la spéciation voire l'accompagner (cas de la spécialisation écologique) (Matsubayashi *et al.*, 2010; Hardy & Otto, 2014). Dans le cas d'insectes parasitoïdes (et d'autres organismes ayant d'autres modes de vie), la réussite du développement est également déterminée par des structures morphologiques qui, elles-mêmes, peuvent être contraintes par la phylogénie. C'est notamment le cas de l'ovipositeur, organe qui, d'une part, doit permettre le dépôt du descendant dans des conditions optimales pour son développement (Quicke *et al.,* 1995; Quicke, 1997; Sivinski & Aluja, 2003) et, d'autre part, constitue une structure relativement "accessible" pour des études quantitatives.

Dans ce cadre, nous avons exploré le lien entre phylogénie, spectre d'hôtes et taille de l'ovipositeur en nous focalisant sur le groupe d'espèce *urozonus*. Ce groupe nous a paru pertinent car: (i) nous avons mis en évidence une diversité étonnante dans ce groupe dans la région Paléarctique (cf. Parties I et III); (ii) nous disposions d'informations fiables sur le spectre d'hôtes de certaines espèces; et (iii) ce groupe contient des espèces citées comme des agents potentiels de lutte biologique contre des insectes ravageurs (cf. Partie "Discussion et Perspectives").

Sur la base d'un échantillon de 31 espèces dont 18 assignées au groupe *urozonus* (cf. Partie III), nous avons consacré la première partie de cette étude à l'obtention d'une phylogénie moléculaire du groupe *urozonus* en utilisant un alignement concaténé des séquences nucléotidiques issues de 7 marqueurs génétiques présentant des taux d'évolution *a priori* différents (mitochondriaux: *COI* & *Cytb*; nucléaires: *Wg*, *EF-1ŭ*, *Bub3*, *RpS4* & *RpL27a*). La reconstruction de l'arbre phylogénétique a été réalisée avec deux méthodes probabilistes (ML & BI), en testant partitions différentes et en testant l'impact de la conservation ou l'élimination des régions variables (introns des gènes *Bub3*, *RpS4* et *RpL27a*).

Dans une deuxième partie, nous avons reporté les informations concernant les spectres d'hôtes et les longueurs d'ovipositeurs (le ratio entre la longueur d'ovipositeur et celle de tibia postérieur) sur la phylogénie multi-locus. Pour étudier les relations entre phylogénie, écologie et morphologie, deux approches ont été utilisées: la première repose sur des tests de corrélations (test de Mantel) entre des matrices basées sur des distances moléculaires, des similitudes entre spectre d'hôte et des similitudes concernant la taille de l'ovipositeur; la seconde repose sur la détection d'un signal phylogénétique concernant (i) le statut des espèces (généralistes versus spécialistes), et (ii) la capacité des espèces d'*Eupelmus* à parasiter certains taxons hôtes.

D'un point de vue méthodologique, la procédure de comparaison des stratégies de partition (basée sur le facteur de Bayes) a favorisé le chemin le plus complexe (= 9 partitions), la topologie obtenue étant toutefois "robuste" vis-à-vis d'autres partitions. De plus, notre analyse montre une influence significative de la conservation (ou pas) des zones divergentes, puisque, d'une part, l'arbre phylogénétique obtenu sans élimination des zones divergentes (= 5000 pb) est plus résolu que celui obtenu après utilisation de Gblocks (= 3197 pb) et, d'autre part, il existe des conflits topologiques entre les deux arbres.

D'un point de vue évolutif, la phylogénie obtenue met tout d'abord en évidence une sous-structuration du groupe *urozonus* en trois clades bien supportés (***ñA** = gemellus**ò***; ***ñB** = confusus**ò***; ***ñC** = urozonus* – cf. Figure 1), la position relative pour la plupart des espèces au sein des clades "A et C" n'étant cependant pas résolue.

L'analyse croisée des données moléculaires, écologiques et morphologiques met en évidence des gammes d'hôtes très variées. Parmi les 11 espèces pour lesquelles nous avons des informations sur leurs gammes d'hôtes, nous avons en effet observé des espèces "spécialistes" telles que *E. pistaciae*, *E. acinellus* et *E. tibicinis* associées à un seul insecte hôte ou *E. azureus*, *E. cerris* et *E. fulvipes* spécialisées sur la famille de Cynipidae. Nous observons également en parallèle des espèces résolument généralistes, certaines (*E. confusus*, *E. gemellus*, *E. kiefferi* et *E. urozonus*) étant capables de parasiter plusieurs ordres d'insectes hôtes. De la même façon, les tailles relatives d'ovipositeurs sont très variables entre espèces (facteur de 1 à 3). Cependant, nous n'avons pas observé de corrélation significative entre les distances moléculaires, similarités entre spectres d'hôtes et/ou similarités entre longueurs d'ovipositeur. De même, les tests statistiques ne mettent pas en évidence l'existence d'un signal évolutif concernant la distribution des spectres d'hôtes, des capacités à parasiter des taxons particuliers ou des tailles d'ovipositeurs.

Al khatib et al. BMC Evolutionary Biology _####################_
DOI 10.1186/s12862-015-0571-2

BMC Evolutionary Biology

RESEARCH ARTICLE Open Access

Multilocus phylogeny and ecological differentiation of the "*Eupelmus urozonus* species group" (Hymenoptera, Eupelmidae) in the West-Palaearctic

F. Al khatib[1,3*], A. Cruaud[2], L. Fusu[4], G. Genson[2], J.-Y. Rasplus[2], N. Ris[1] and G. Delvare[3]

Abstract

Background: The ecological differentiation of insects with parasitic life-style is a complex process that may involve phylogenetic constraints as well as morphological and/or behavioural adaptations. In most cases, the relative importance of these driving forces remains unexplored. We investigate here this question for the "*Eupelmus urozonus* species group" which encompasses parasitoid wasps of potential interest in biological control. This was achieved using seven molecular markers, reliable records on 91 host species and a proxy of the ovipositor length.

Results: After using an adequate partitioning scheme, Maximum likelihood and Bayesian approaches provide a well-resolved phylogeny supporting the monophyly of this species group and highlighting its subdivision into three sub-groups. Great variations of both the ovipositor length and the host range (specialist versus generalist) were observed at this scale, with these two features being not significantly constrained by the phylogeny. Ovipositor length was not shown as a significant predictor of the parasitoid host range.

Conclusions: This study provides firstly the first evidence for the strong lability of both the ovipositor's length and the realised host range in a set of phylogenetically related and sympatric species. In both cases, strong contrasts were observed between sister species. Moreover, no significant correlation was found between these two features. Alternative drivers of the ecological differentiation such as interspecific interactions are proposed and the consequences on the recruitment of these parasitoids on native and exotic pests are discussed.

Keywords: Ecological specialization, Ectoparasitoid, Host range evolution, Molecular phylogeny, Morphological adaptation, Ovipositor, Phylogenetic constraint

Background

Ecological speciation is a process in which polymorphism within populations (e.g. in resource use or habitat preference) ultimately induces the appearance of two sister species, each adapted to a different niche [1–4]. According to Rundle and Nosil [2], three principal components must be involved: i) a source of divergent selection, ii) a form of reproductive isolation, and iii) a genetic mechanism linking divergent selection to reproductive isolation. Among plant-feeding insects, several empirical studies support this scenario [1, 5, 6], which can also occur for insects with a parasitic lifestyle, in particular within the upper trophic levels. For such organisms, ecological differentiation between sister species can also be driven by the ecological differentiation of their hosts *via* a process called sequential or cascading speciation [7–9]. If pervasive enough, such processes should lead to the clustering of phylogenetically related specialists.

Additionally, transitions between generalists to specialists (and vice-versa) are also occurring and, so far, empirical data provide a mixed picture about the

* Correspondence: fadel.alkhatib@sophia.inra.fr
[1]INRA, University Nice Sophia Antipolis, CNRS, UMR 1355-7254 Institut Sophia Agrobiotech, Sophia Antipolis 06900, France
[3]CIRAD, UMR 55 CBGP, 755 Avenue du Campus Agropolis, CS 30016 F-34988, Montferrier-sur-Lez Cedex, France
Full list of author information is available at the end of the article

relative frequencies of evolution toward specialisation and generalization [10–13]. However, transitions from generalist ancestors to specialized species are probably recurrent as (i) generalist species are unlikely to produce "jack-of-all trades-master of none" genotypes because of genetic or physiological trade-off [14–16]; (ii) the subsequent acquisition of specialized genotypes may be a primary step towards speciation [17–19]; and (iii) specialist species may be more prone to extinction [13, 20]. At a phylogenetic level, both kinds of transitions should lead to the mixing of both specialists and generalists within the same cluster.

Questions of (i) the host range (specialist versus generalist) of ancestral species of current specialists and (ii) the distribution of host ranges within a phylogeny were recently addressed by Hardy and Otto [21]. They illustrated them using two notions, respectively "the musical chairs hypothesis" (specialists originate from specialists through host switch) and the "oscillation hypothesis" (specialists originate from generalists, with some specialists widening their host range before the next speciation event). The extent to which one of these scenarios is more frequent has nevertheless still to be evaluated rigorously for the organisms with a parasitic lifestyle.

Parasitoids are organisms (mainly Hymenoptera and Diptera) whose pre-imaginal life depends on the successful exploitation of a single host [22, 23]. Behind this simple definition, a great diversity of life history strategies and physiological adaptations are observed. In particular, the ovipositor allows egg-laying by the female and is thus a key organ especially for species that are exploiting concealed or protected hosts [24, 25]. The features (in particular the length) of this organ and its ability to evolve could contribute to drive specialization and/or speciation. Focusing on the "*Eupelmus urozonus* species group" (Hymenoptera: Eupelmidae), we examine here whether the host range is subject to phylogenetic constraints and/or whether the ovipositor length is a significant driver of host use.

Within the subfamily Eupelminae (33 genera), the genus *Eupelmus* Dalman is the most diverse, with 91 available valid species names in the Palaearctic region [26]. Species of *Eupelmus* are primary or facultative secondary ectoparasitoids whose larvae develop as idiobionts on the immature stages (larvae, pupae and more rarely eggs) of many insects (beetles, flies, moths, wasps or cicadas) that are concealed or protected in plant tissues (stems, galls, fruits or seeds) [27]. Most *Eupelmus* are considered as generalist parasitoids [27, 28]. However, because of both the extreme sexual dimorphism characterizing the subfamily and the existence of species groups possibly hiding cryptic species, the systematics and the evolutionary ecology of these species remain poorly understood. This situation is well illustrated with the "*E. urozonus* species complex/group" which was repeatedly investigated [27, 29–31] until its recent revision within the Palaearctic region by Al khatib et al. [32, 33], which identified 11 new species in this region. Semantically, the term "complex" used in Al khatib et al. [32, 33] is substituted here by the term "species group" (Al khatib et al. in preparation). As a consequence of this unsuspected biodiversity, most of the published host records for these species are unreliable because all of the common species with a comparatively short ovipositor (*E. gemellus* Al khatib, 2015, *E. confusus* Al khatib, 2015, and especially *E. kiefferi* De Stefani, 1898) were misidentified as *E. urozonus* Dalman, 1820, while the two common species with a comparatively long ovipositor (*E. azureus* Ratzeburg, 1844 and *E. annulatus* Nees, 1834) were both frequently mistreated under *E. annulatus* [29, 34].

In the present study, we first provide a reliable molecular phylogeny of the "*E. urozonus* species group" using a multi-locus approach. Then, for most of the species, we compile host records and data on ovipositor length. We finally carry out a comparative analysis to evaluate the role of phylogenetic constraints in the evolution of ovipositor length and host range as well as the role of the ovipositor's length in determining the host range.

Methods

Sampling

A total of 31 species, with 91 individuals, sampled in the Palaearctic region were included in this study.

- Eighteen of the 21 species within the "*urozonus* group" that were recently revised using both morphological and molecular characters [32, 33]: *E. acinellus* Askew, 2009, *E. annulatus*, *E. azureus*, *E. cerris* Förster, 1860, *E. confusus*, *E. fulvipes* Förster, 1860, *E. gemellus*, *E. janstai* Delvare and Gibson, 2015, *E. kiefferi*, *E. longicalvus* Al khatib & Fusu, 2015, *E. minozonus* Delvare, 2015, *E. opacus* Delvare, 2015, *E. pistaciae* Al khatib, 2015, *E. priotoni* Delvare, 2015, *E. purpuricollis* Fusu & Al khatib, 2015, *E. simizonus* Al khatib, 2015, *E. tibicinis* Bouček, 1963 and *E. urozonus*.
- Thirteen species were used as outgroup including (i) species belonging to the three subgenera of *Eupelmus* sensu Gibson (1995): *Eupelmus* [*E. atropurpureus* Dalman, 1820, *E. matranus* Erdős, 1947, *E. microzonus* Förster, 1860, *E. pini* Taylor, 1927 and *E. vindex* Erdős, 1955]; *Macroneura* Walker [*E. falcatus* (Nikol'skaya, 1952) and *E. seculatus* Kalina, 1981], and *Episolindelia* Girault [*E. linearis* Förster, 1860, *E. testaceiventris* (Motschulsky, 1863) and *E. juniperinus thuriferae* Askew, 2000]; and (ii) species belonging to other

genera within Eupelminae, *Reikosiella* (*Hirticauda*) [*R. aff. rostrata* (Ruschka, 1921)] and *Anastatus* Motschulsky [*Anastatus sidereus* (Erdös, 1957) and *Anastatus aff. temporalis* Askew, 2005]. The species were identified by the authors using the available identification keys [29, 31, 35–37].

Specimens were killed with ethyl acetate and preserved in 95 % ethanol at −20 °C until DNA extraction. After the DNA extraction, the voucher specimens were prepared as explained in Al khatib et al. (2014) for the morphological examination. The vouchers are deposited in the following institutions and private collections: AICF, Lucian Fusu collection, Al. I. Cuza University, Iasi, Romania; BMNH, Natural History Museum, London, UK; CBGP, Centre for Biology and Management of Populations, Montpellier, France; CNC, Canadian National Collection of Insects, Arachnids and Nematodes, Agriculture & Agri-food Canada, Ottawa, ON, Canada; FALPC, Fadel Al khatib personal collection, Faculty of Agricultural Engineering, University of Aleppo, Syria; GDPC, Gérard Delvare personal collection, Montpellier, France; MNHG, Museum of Natural History of Geneva, Switzerland; MNHN, National Museum of Natural History, Paris, France; NHRS, Naturhistoriska riksmuseet, Stockholm, Sweden. The depository's acronyms of voucher specimens are included in (Additional file 1: Table S2; Additional file Dryad: doi:10.5061/dryad.115m1). Sampling information (host-plants, collection dates, and localities) is listed in Table 1.

Marker choice

Seven markers displaying various rates of molecular evolution were used: two coding portions of mitochondrial genes (Cytochrome oxidase I, *COI* and Cytochrome b, *Cytb*), two coding regions of nuclear genes (the F2 copy of elongation factor 1-alpha, *EF-1α* and *Wingless*, *Wg*) and three (at least partially) non-coding regions of other nuclear genes (the mitotic checkpoint control protein, *Bub3*; the ribosomal protein L27a, *RpL27a*, and the ribosomal protein S4, *RpS4*). All these markers were previously used for phylogenetic analyses in arthropods. *COI* and *Cytb* have been used to resolve insect molecular phylogenies at shallower taxonomic levels [38–41]. The *Wg* gene has provided a useful tool for the reconstruction of phylogenetic relationships at lower to intermediate taxonomic levels in different insect groups [32, 38, 41–45]. *EF-1α* has proven to evolve at slow rates and provide phylogenetic information at deeper levels (i.e. family relationships) [39, 46–51]. The *Bub3* gene is more rarely used [52, 53] for inferring phylogenetic relationships at a similar taxonomic level as *Wg*. Finally, ribosomal proteins *RpL27a* and *RpS4* have been used with success to infer the phylogeny of Hymenoptera associated with oak galls or figs [39, 54–56].

DNA extraction, PCR amplification and sequencing

Genomic DNA was extracted from a single individual using the Qiagen DNeasy kit (Hilden, Germany) with some minor modifications with regard to the manufacturer's protocol. Entire specimens were incubated at 56 °C for 15–17 h and DNA extraction was performed without destruction of the specimens, to allow subsequent examination of morphology (see § Sampling). Primer sequences are given in Additional file 1: Table S1.

For the two mitochondrial genes (*COI* and *Cytb*), the PCR mix was prepared in 20 μl as follows: 1 μl of DNA (1–55 ng/μl), 14.64 μl of Milli-Q water, 2 μl of 10x PCR buffer containing MgCl2 (1x), 1 μl of 10 μM primer cocktail (0.5 μM), 0.16 μl of dNTPs 25 mM each (0.2 mM) and 0.2 μl of 5 U/μl Taq DNA Polymerase (Qiagen, Hilden, Germany).

For the nuclear genes (*Bub3*, *EF1-α*, *RpL27a*, *RpS4* and *Wg*), the PCR mix was realised in 25 μl as follows: 2 μl of DNA (1–55 ng/μl), 19.825 μl of Milli-Q water, 2.5 μl of 10x PCR buffer containing MgCl2 (1x), 0.175 μl of 100 μM primer cocktail (0.7 μM), 0.2 μl of dNTPs 25 mM each (0.2 mM) and 0.125 μl of 5 U/μl Taq DNA Polymerase (Qiagen, Hilden, Germany).

PCR conditions for *Wg* and *COI* were as described in [32]. Those for other genes were as follows: *Cytb*: 94 °C for 5 min, followed by 40 cycles of (i) 94 °C for 1 min, (ii) 50 °C for 1 min, and (iii) 72 °C for 90 s with a final extension at 72 °C for 10 min; nuclear markers: 94 °C for 4 min, followed by 40 cycles of (i) 94 °C for 30 s, (ii) 58 °C for *EF-1α*, 48 °C for *Bub3*, 57 °C for *RpS4* and 55 °C for *RpL27a*, (iii) 72 °C for 5 min with final extension at 72 °C for 5 min.

In the absence of amplification or if the signal was too weak, we improved yields of PCRs by using 2x QIAGEN Multiplex PCR Master Mix (Qiagen, Hilden, Germany). In this case, PCRs were performed in a 25 μl reaction volume: 2 μl of DNA, 16.5 μl of Milli-Q water, 0.125 μl of 100 μM primer cocktail (0.5 μM) and 6.25 μl of 2x QIAGEN Multiplex PCR Master Mix (1x) and PCR conditions were as specified in the QIAGEN® Multiplex PCR kit: 95 °C for 15 min, followed by 40 cycles of (i) 95 °C for 30 s, (ii) 48 °C-58 °C for 90 s, (iii) 72 °C for 1 min, with final extension at 72 °C for 10 min.

All PCRs were performed on a GeneAmp 9700 thermocycler. PCR products were visualized using the QIAxcel Advanced System and QIAxcel DNA Fast Analysis Kit (Qiagen). PCR products were sent to GENOSCREEN (Lille, France) or to BECKMAN COULTER GENOMICS (Stansted, United Kingdom) for sequencing in both

Table 1 Sample information for the specimens included in the phylogenetic analysis

Species	Collection code	Molecular code	Country	Department	City	N°	E°	Host insect	Associated plant	Collection date
Eupelmus acinellus	FAL1363	10235	France	Aude	Durban-Corbières	42.99825°	2.80690°	*Mesophleps oxycedrella*	*Juniperus oxycedrus*	March 2012
Eupelmus acinellus	FAL1366	10237	France	Var	Fayence	43.65513°	6.68813°	*Mesophleps oxycedrella*	*Juniperus oxycedrus*	March 2012
Eupelmus annulatus	FAL1176	10198	France	Alpes-Maritimes	Gréolières-les-Neiges	43.81584°	6.88711°	*Diplolepis rosae*	*Rosa canina*	March 2012
Eupelmus annulatus	NB783	10354	France	Gard	Le Castanet	43.98925°	3.70094°	*Dryocosmus kuriphilus*	*Castanea sativa*	February 2012
Eupelmus annulatus	GDEL4053	10041	Hungary	Veszprém	Hegyesd	46.933333°	17.522778°	Unknown	On *Quercus cerris*	June 2010
Eupelmus annulatus	LF.an.SW 01	10471	Sweden	Öland	Mörbylånga	56.61670°	16.507617°	Unknown	Unknown	August 2006
Eupelmus azureus	FAL1323	10222	France	Ardèche	Saint-Georges-les-Bains	44.85028°	4.82433°	*Biorhiza pallida*	*Quercus pubescens*	June 2012
Eupelmus azureus	NB773a	10361	France	Var	La Garde-Freinet	43.30487°	6.43701°	*Dryocosmus kuriphilus*	*Castanea sativa*	February 2012
Eupelmus azureus	GDEL4048	10034	Italy	Piemonte/Cuneo	Palanfré	44.165833°	7.50361°1	Unknown	Unknown	August 2010
Eupelmus azureus	L.Loru713	10245	Italy	Sardinia	Aritzo	39.94743°	9.19968°	*Dryocosmus kuriphilus*	*Castanea sativa*	August 2011
Eupelmus azureus	PJ10077-21-4	10575	Hungary	Vezprém	Várpalota	47.19809°	18.21204°	*Andricus solitarius*	*Quercus pubescens*/ *Q. cerris*	June 2010
Eupelmus azureus	PJ11054-2-2	10578	Turkey	Bursa	Güneybudaklar	40.00560°	29.14982°	*Andricus fecundator*	*Quercus* sp.	-
Eupelmus azureus	MC-C4	10486	Switzerland	Stabio	Via Roccoletta	45.84722°	8.92638°	*Dryocosmus kuriphilus*	*Castanea sativa*	August 2012
Eupelmus cerris	GDEL4109	10118	Hungary	Vezprém	Hegyesd	46.93333°	17.52278°	Unknown	On *Quercus cerris*	June 2010
Eupelmus confusus	FAL1278	10443	France	Ardèche	Saint-Georges-Montpellier	43.6104°	3.77227°	*Bactrocera oleae*	*Olea europaea*	October 2011
Eupelmus confusus	FAL1519	10412	France	Haute-Corse	Lumio	42.55879°	8.81299°	*Bactrocera oleae*	*Olea europaea*	September 2012
Eupelmus confusus	FAL1051	10145	Italy	Liguria	Bussana-Vecchia	43.84026°	7.82905°	*Myopites stylata*	*Dittrichia viscosa*	January 2011
Eupelmus confusus	FAL1108	10250	Spain	Logroño	La Rioja	-	-	*Myopites stylata*	*Dittrichia viscosa*	March 2012
Eupelmus confusus	LF.ma.GR 01	10425	Greece	Seres	Kerkini Lake Nat.Park	41.27833°	23.21955°	Unknown	Unknown	June 2008
Eupelmus confusus	LF.ma.GR 02	10426	Greece	Seres	Kerkini lake	41.20180°	23.07747°	Unknown	Unknown	September 2007
Eupelmus confusus	GDEL4173	10596	France	Hérault	Laroque	45.91722°	3.74361°	Unknown	On *Quercus pubescens*	July 2013
Eupelmus confusus	LF.ma.IR 05	10424	Iran	Kerman	Bidkhan	29.59725°	56.48600°	Unknown	On *Salix alba*	May 2012

Table 1 Sample information for the specimens included in the phylogenetic analysis *(Continued)*

Eupelmus	*confusus*	LF.ma.CY 01	10427	Cyprus	Lemesos	Lemesos	34.73189°	33.05175°	*Apomyelois ceratoniae & Asphondylia gennadii*	*Ceratonia siliqua*	May 2009
Eupelmus	*fulvipes*	FAL1221	10200	France	Alpes-Maritimes	Gréolières-les-Neiges	43.81584°	6.88711°	*Diplolepis rosae*	*Rosa canina*	March 2012
Eupelmus	*fulvipes*	LF.ro.RO 02	10656	Romania	Constanţa	Hagieni & Negru Voda	-	-	*Diplolepis spinosissimae*	*Rosa* sp.	-
Eupelmus	*fulvipes*	LF.ro.GE 01	10657	Germany	Rottenburg-Wurmlingen		-	-	*Diplolepis rosae*	*Rosa* sp.	October 2011
Eupelmus	*gemellus*	FAL1260	10438	France	Var	Porquerolles	42.99534°	6.2044°	*Bactrocera oleae*	*Olea europaea*	-
Eupelmus	*gemellus*	FAL1359	10230	France	Alpes-Maritimes	Biot	43.63455°	7.082490°	*Mesophleps oxycedrella*	*Juniperus oxycedrus*	March 2012
Eupelmus	*gemellus*	NB441	10415	France	Haute-Corse	Bisinchi	42.48983°	9.32797°	*Dryocosmus kuriphilus*	*Castanea sativa*	June 2012
Eupelmus	*gemellus*	FAL1004	10130	Italy	Liguria	Bussana-Vecchia	43.84026°	7.82905°	*Myopites stylata*	*Dittrichia viscosa*	January 2011
Eupelmus	*gemellus*	FAL1508	10405	Italy	Sardinia	Province d'Oristano	39.70041°	8.739690°	Unknown	On *Pistacia lentiscus*	October 2012
Eupelmus	*janstai*	GDEL4046	10032	Czech Republic	Břeclav	Pavlov	48.867500°	16.654166°	Unknown	On *T. platyphyllos*	July 2010
Eupelmus	*kiefferi*	NB674b	10341	France	Alpes-Maritimes	Granile	44.03942°	7.57575°	*Dryocosmus kuriphilus*	*Castanea sativa*	March 2012
Eupelmus	*kiefferi*	NB666	10325	France	Haute-Corse	Muratu	42.55139°	9.30929°	*Dryocosmus kuriphilus*	*Castanea sativa*	December 2012
Eupelmus	*kiefferi*	FAL1070	10151	Italy	Liguria	Bussana-Vecchia	43.84026°	7.82905°	*Myopites stylata*	*Dittrichia viscosa*	January 2012
Eupelmus	*kiefferi*	FAL1109	10167	Spain	Logroño	La Rioja	-	-	*Myopites stylata*	*Dittrichia viscosa*	March 2012
Eupelmus	*kiefferi*	FAL1511	10406	Lebanon	Bakhoun	Fanar	-	-	*Myopites stylata*	*Dittrichia viscosa*	March 2012
Eupelmus	*kiefferi*	GDEL4045	10030	Hungary	Szombathely	Kőszeg	47.363888°	16.52500°	Unknown	On *Salix cinerea*	June 2010
Eupelmus	*kiefferi*	MC-C124	10492	Switzerland	Riviera	Monte Ceneri	46.136944°	08.902500°	*Dryocosmus kuriphilus*	*Castanea sativa*	July 2012
Eupelmus	*kiefferi*	LF.ma.RO 01	10423	Romania	Botoşani	Leorda	-	-	Unknown	Unknown	July 2007
Eupelmus	*kiefferi*	ZL.fu.RO 05	10585	Romania	Mures	Sovata	46.54482°	24.96769°	*Diplolepis mayri*	*Rosa canina*	March 2012
Eupelmus	*kiefferi*	LF.fu.GE 02	10658	Germany	Rottenburg-Wurmlingen		-	-	*Diplolepis rosae*	*Rosa* sp.	October 2013
Eupelmus	*kiefferi*	LF.fu.SL 01	10467	Slovakia	Muranska Planina	Predna Hora	-	-	Unknown	Unknown	July 2009
Eupelmus	*kiefferi*	GDEL4043	10028	Czech Republic	Trutnov	Vilantice	50.365833°	15.737222°	Unknown	Unknown	July 2010
Eupelmus	*kiefferi*	LF.fu.ES 01	10463	Estonia	Tartu	Rannu Parish	-	-	Unknown	Unknown	June 2010
Eupelmus	*kiefferi*	FAL1524	10593	Algeria	Tigzirt	Tigzirt	-	-	*Myopites stylata*	*Dittrichia viscosa*	Februry 2013
Eupelmus	*longicalvus*	GDEL4038	10019	Italy	Friuli Venezia Giulia	Chiusaforte	46.405277°	13.445000°	Unknown	Unknown	July 2008

Table 1 Sample information for the specimens included in the phylogenetic analysis *(Continued)*

Eupelmus	*longicalvus*	LF.ma.SW 02	10429	Sweden	Gotland	Gotlands commun	57°32.207′	18°20.273′	Unknown	Unknown	July 2004
Eupelmus	*longicalvus*	GDEL4191	10603	Italy	Friuli-Venezia Giulia	Chiusaforte	46.39944°	13.45944°	Unknown	Unknown	July 2008
Eupelmus	*minozonus*	GDEL4030	10009	Hungary	Veszprém	Hegyesd	46.93333°	17.52278°	Unknown	On *Quercus cerris*	June 2010
Eupelmus	*minozonus*	GDEL4030	10010	Hungary	Veszprém	Hegyesd	46.93333°	17.52278°	Unknown	On *Quercus cerris*	June 2010
Eupelmus	*minozonus*	GDEL4030	10011	Hungary	Veszprém	Hegyesd	46.93333°	17.52278°	Unknown	On *Quercus cerris*	June 2010
Eupelmus	*opacus*	LF.ur.GR 01	10459	Greece	Seres	Krousia Mts site	41°11′32,4″	23°03′59,5″	Unknown	Unknown	June 2007
Eupelmus	*opacus*	LF.ur.SW 02	10460	Sweden	Östergötland	Ödeshögs kommun	58°18.452′	14°37.859′	Unknown	Unknown	August 2005
Eupelmus	*pistaciae*	GDEL4027	10004	France	Hérault	Cazevieille	43.752222°	3.770000°	*Megastigmus pistaciae*	*Pistacia terebinthus*	October 2010
Eupelmus	*pistaciae*	GDEL4027	10005	France	Hérault	Cazevieille	43.752222°	3.770000°	*Megastigmus pistaciae*	*Pistacia terebinthus*	October 2010
Eupelmus	*pistaciae*	GDEL4027	10507	France	Hérault	Cazevieille	43.752222°	3.770000°	*Megastigmus pistaciae*	*Pistacia terebinthus*	October 2010
Eupelmus	*priotoni*	GDEL4051	10038	France	Aveyron	Sauclières	43.96389°	3.355833°	Unknown	Unknown	June 2011
Eupelmus	*purpuricollis*	LF.ur.GR 02	10650	Greece	Seres	nr Neo Petritsi	41°18′49,8″	23°16′35,6″	Unknown	Unknown	July 2008
Eupelmus	*purpuricollis*	LF.ur.GR 03	10651	Greece	Seres	Kerkini	41°11′32,4″	23°03′59,5″	Unknown	Unknown	July 2007
Eupelmus	*simizonus*	GDEL4142	10297	France	Ardèche	Les Vans	44.387222°	4.154444°	Unknown	On *Quercus pubescens*	July 2012
Eupelmus	*tibicinis*	GDEL4148	10299	France	Ardèche	Chassagnes	44.403888°	4.178333°	Unknown	On *Quercus pubescens*	July 2012
Eupelmus	*tibicinis*	GDEL4149	10300	France	Ardèche	Berrias-et-Casteljau	44.39389°	4.194722°	Unknown	Unknown	July 2012
Eupelmus	*tibicinis*	GDEL4175	10598	France	Hérault	Laroque	45.91722°	3.74361°	Unknown	On *Quercus pubescens*	July 2013
Eupelmus	*urozonus*	NB677	10333	France	Lot	Aynac	44.78155°	1.85896°	*Dryocosmus kuriphilus*	*Castanea sativa*	January 2012
Eupelmus	*urozonus*	FAL1518	10410	France	Haute-Corse	Lumio	42.55879°	8.81299°	*Bactrocera oleae*	*Olea europaea*	September 2012
Eupelmus	*urozonus*	FAL1060	10148	Italy	Liguria	Bussana-Vecchia	43.84026°	7.82905°	*Myopites stylata*	*Dittrichia viscosa*	January 2011
Eupelmus	*urozonus*	L.Loru235	10241	Italy	Sardinia	Desulo	39.99198°	9.23053°	*Dryocosmus kuriphilus*	*Castanea sativa*	July 2011
Eupelmus	*urozonus*	FAL1106	10165	Spain	Logroño	La Rioja	-	-	*Myopites stylata*	*Dittrichia viscosa*	March 2012
Eupelmus	*urozonus*	NB1117	10251	Greece	Crete	Gournes	35.32822°	25.28388°	*Myopites stylata*	*Dittrichia viscosa*	March 2012
Eupelmus	*urozonus*	MC-C100	10488	Switzerland	Riviera	Monte Ceneri	46.136944°	8.902500°	*Dryocosmus kuriphilus*	*Castanea sativa*	July 2012

Table 1 Sample information for the specimens included in the phylogenetic analysis *(Continued)*

Eupelmus urozonus	PJ10077-2-6	10573	Hungary	Vezprém	Várpalota	47.198091°	18.21204°	*Andricus lucidus*	*Quercus pubescens/ Q. cerris*	November 2010
Eupelmus urozonus	LF.fu.RO 01	10464	Romania	Neamț	Podoleni			Unknown	Unknown	September 2012
Eupelmus urozonus	LF.ur.IR 02	10457	Iran	Kerman	Bidkhan	-	-	Unknown	*Ephedra sp.*	March 2010
Eupelmus vindex	GDEL4054	10042	Hungary	Veszprém	Hegyesd	-	-	Unknown	Unknown	June 2010
Eupelmus vindex	LF.vi.RO 02	10468	Romania	Iaşi	Iaşi	-	-	Unknown	Unknown	June 2007
Eupelmus vindex	LF.vi.RO 01	10469	Romania	Tulcea	Letea	-	-	Unknown	Unknown	May 2007
Eupelmus microzonus	GDEL4116	10192	France	Haute-Corse	Aléria	42.128611°	9.465556°	*Bruchophagus* sp.	*Asphodelus ramosus*	September 2011
Eupelmus atropurpureus	PJ11159_23_1	10580	Spain	Aragón	Huesca			Unknown	Poaceae	November 2011
Eupelmus pini	GDEL4058	10048	France	Alpes-Maritimes	Guillaumes	44.070833°	6.853056°	Unknown	Dead trunk of *Pinus sylvestris*	August 2009
Eupelmus matranus	FAL1491	10318	France	Alpes-Maritimes	Sophia-Antipolis	43.61671°	7.07550°	Unknown	On *Quercus ilex*	October 2012
Eupelmus falcatus	GDEL4088	10090	Hungary	Veszprém	Nagavászony	47.021667°	17.724167°	Unknown	Unknown	June 2010
Eupelmus seculatus	GDEL4089	10091	France	Gard	Beauvoisin	43.712500°	4.307222°	Unknown	Unknown	August 2011
Eupelmus linearis	GDEL4069	10062	France	Lozère	Cocurès	45.30555°	4.59194°	Unknown	Unknown	July 2011
Eupelmus linearis	GDEL4073	10066	Hungary	Veszprém	Nagavászony	47.021667°	17.724167°	Unknown	Unknown	June 2010
Eupelmus testaceiventris	GDEL4078	10075	Cameroon	Adamaoua	Ossére Gadou	7.173056°	13.623056°	Unknown	Unknown	November 2008
Eupelmus juniperinus thuriferae	GDEL4064	10057	France	Hautes-Alpes	Saint-Crépin	44.710556°	6.606389°	Unknown	On *Juniperus thurifera*	August 2008
Reikosiella aff. rostrata.	NB670	10336	France	Drôme	Génissieux	45.09059°	5.07161°	*Dryocosmus kuriphilus*	*Castanea sativa*	February 2012
Reikosiella aff. rostrata.	NB810	10350	France	Alpes-Maritimes	Tende	44.056689°	7.579353°	*Dryocosmus kuriphilus*	*Castanea sativa*	March 2012
Anastatus sidereus	GDEL4098	10105	France	Alpes-Maritimes	Fontan	44.026389°	7.577778°	Unknown	Unknown	July 2010
Anastatus aff. temporalis	GDEL4100	10107	France	Gard	Générac	43.719444°	4.353611°	Unknown	Unknown	August 2011

directions. All sequences were deposited in GenBank (Additional file 1: Table S2).

Sequence alignment and phylogenetic analysis

Alignment

Sequences were aligned using Muscle [57] with the default settings as implemented in SeaView v4.4.1 [58] and subsequently visually checked. To assess the impact of indels on the phylogenetic resolution, highly divergent blocks present in *Bub3*, *RpS4* and *RpL27a* alignments were either included in or excluded from the analyses. These blocks were removed using Gblocks [59] with the default settings as implemented in SeaView. Alignments of *COI*, *Cytb*, *EF-1α* and *Wg* were translated to amino acids using Mega v5.1 [60] to detect potential frameshift mutations and premature stop codons, which may indicate the presence of pseudogenes.

Gene by gene analysis

To detect (i) possible inconsistencies linked to contamination during laboratory procedures, (ii) poor-quality sequences, (iii) possible pseudogenes or other artefacts, and (iv) to evaluate the impact of the Gblock procedure on the individual phylogenetic resolution, genes were first analysed separately using a maximum likelihood approach (ML).

Concatenated datasets analysis

Phylogenetic analyses were performed on concatenated nucleotide sequences using both ML and Bayesian methods. Four partitioning schemes were compared: (i) two partitions: one for the two mitochondrial genes (*COI* and *Cytb*) and another for all nuclear markers (*Wg*, *EF-1α*, *Bub3*, *RpS4 & RpL27a*); (ii) six partitions: one for the two mitochondrial markers (*COI* and *Cytb*) and one for each nuclear marker (*Wg*, *EF-1α*, *Bub3*, *RpS4* and *RpL27a*); (iii) seven partitions: one for the 1st and 2nd codon positions of the mtDNA, one for the 3rd codon positions of mtDNA, and one for each nuclear gene (*Wg*, *EF-1α*, *Bub*, *RpS4* and *RpL27a*); (iv) nine partitions: same as above with *Wg* and *EF-1α* further partitioned by codon position (1st and 2nd codon positions *versus* 3rd positions).

Bayes factors (BF) [61, 62] were used to compare the four partitioning schemes. Harmonic means of the likelihood scores were used as estimators of the marginal likelihoods. Following [61] and [63], Bayes factors were calculated using the following formula: $BF = 2 \times (\ln M1 - \ln M0) + (P1 - P0) \times \ln(0.01)$ where lnMi and Pi are the harmonic-mean of the ln likelihoods and the number of free parameters of the model i, respectively. BF values were interpreted following [61] and [62], with BF values between 2 and 6, between 6 and 10 and higher than 10 indicating positive evidence, strong evidence, and very strong evidence favouring one model over the others respectively.

Evolution models and phylogenetic reconstruction

For the separated and concatenated datasets, the best-fitting model was identified using the Akaike information criterion (AIC) as implemented in jModelTest v0.1.1 [64].

For both gene-by-gene and concatenated analyses, maximum likelihood analyses and associated bootstrapping were performed using RAxML v8.0.9 [65]. The GTRCAT approximation of models was used for ML bootstrapping (1000 replicates). Bootstrap percentages (BP) ≥85 % were considered as strong support and BP < 65 % as weak.

Bayesian analyses were performed only on the concatenated dataset using a parallel version of MrBayes v3.2.2 [66]. Model parameters for each data partition were independently estimated by unlinking parameters across partitions. Parameter values for the model were initiated with default uniform priors, and branch lengths were approximated using default exponential priors. Bayesian inferences were estimated using two simultaneous, independent runs of Markov Chain Monte Carlo (MCMC), including three heated and one cold chains. The Metropolis-coupled MCMC algorithm [67] was used to improve the mixing of Markov chains. Analyses were run for 20×10^6 generations with parameter values sampled every 2000 generations. To ensure convergence, 40×10^6 generations were used for the most complex partitioning scheme (9 partitions) with parameter values sampled every 4000 generations. To increase and improve the swap frequencies of states between cold and heated chains, the heating temperature (T) was set to 0.01 for the most complex partitioning scheme cleaned with Gblocks and to 0.02 for all other datasets. Convergence was assessed using the standard deviation of split frequencies given by MrBayes and the Effective Sample Size (ESS), as estimated using Tracer v1.6.0 [68]. The first 25 % of the tree samples from the cold chain were discarded and considered as *burn-in*. Posterior probabilities (PP) ≥ 0.95 were considered as strong support and PP < 0.90 as weak.

Analyses were conducted using the CIPRES Science Gateway (www.phylo.org) [69].

Evolutionary properties of marker sequences

For each partition of the concatenated datasets (without Gblocks cleaning), base composition, substitution rates, and among sites rate variation (α) were estimated and compared. We also compared rate variation among partitions, considering the parameter m (rate multiplier).

Comparative analysis

Evolution of ovipositor length

The ovipositor of Hymenoptera is a complex organ that exhibits great interspecific variation (see for instance

[23]). In species of *Eupelmus*, part of the ovipositor is easily visible at the extremity of the abdomen (the ovipositor sheaths), while the rest is concealed in the abdomen. The use of this visible part as a "proxy" of the total ovipositor length is *a priori* tempting in order to avoid damaging of specimens of newly described species known from very few individuals [32, 33]. In order to validate the use of this proxy, a total of 34 individuals of comparatively common species (e.g. *E. azureus*, *E. confusus*, *E. gemellus*, *E. kiefferi*, *E. pistaciae*, and *E. urozonus*) were dissected and, for each individual, we measured the length of the ovipositor stylet, the visible part of the ovipositor sheath and the metatibia (see dataset on Dryad: doi:10.5061/dryad.115m1). Measurements of the length of the ovipositor sheaths and hind tibia followed Al khatib et al. [32] (Additional file 2: Figure S18 A and C). The length of the ovipositor stylet (first and second valvulae) was measured from the articulation of the second valvula with the articulating bulb to the apex of the second valvula (Additional file 2: Figure S18 B). Using this dataset, we found evidence of linear relationships between the ovipositor sheath (response variable) and either the ovipositor stylet or the metatibia as predictors (data not shown). Moreover, no interaction was found between these two predictors and the host species (respectively $F_{5df,20df} = 1.23$ with $p = 0.34$ and $F_{5df,22df} = 1.20$ with $p = 0.34$). This suggests that the visible part of the ovipositor sheath can indeed be used as a reliable proxy of the entire ovipositor.

As a consequence, a first analysis was performed on the 19 species of the "*E. urozonus* species group" for which information about the ovipositor sheaths and the metatibia were available. This analysis includes a total of 121 individuals, with at least 2 individuals/species except for *E. priotoni* and *E. simizonus* (only one individual in each case). In most of the cases, we tried to select individuals from at least two geographical locations and/or, for generalist species, two host species (see dataset on Dryad: doi:10.5061/dryad.115m1). Both the absolute length of the ovipositor sheath ("AOS") and the ratio ("ROS") between the ovipositor sheaths and the metatibia were taken into account, the second one being potentially less sensitive to environmental-induced phenotypic plasticity (host and/or abiotic conditions). AOS/ROS medians were then calculated for each *Eupelmus* species and these medians were used for the subsequent analysis (see below).

Two tests were then performed: (i) a Mantel test of the correlation between pairwise genetic distances ("phylogenetic matrix") and pairwise differences in AOS/ROS ("morphological matrix"). (Dis) similarities were estimated as $|d_i\text{-}d_j|/[(d_i + d_j)/2]$ (d_i and d_j being the AOS/ROS medians obtained for species i and j respectively); (ii) the detection of a phylogenetic signal based on categories of AOS/ROS. For this purpose, "long ovipositors" (AOS/ROS exceeding the third quartile) were distinguished from "short ovipositors" (AOS/ROS below this threshold). Briefly, the sum of state changes was calculated, leading to a D statistic that could be tested against two theoretical distributions: a phylogenetic randomness and a Brownian distribution, this latter being underlain by a continuous trait evolving along the phylogeny at a constant rate [70].

Influence of phylogeny and ovipositor length on host range

A second analysis was restricted to a subset of 13 species for which host range was also available. Most of the information about host range was obtained from Al khatib et al. [32] and from Gibson and Fusu (in prep). Jean Lecomte (comm. pers.) communicated the rearing of *E. confusus* from curculionid larvae. Taken as a whole, our host survey is probably not exhaustive but nevertheless encompassed a total of several thousands of individuals of the "*E. urozonus* species group" and, with regard to the host's diversity, 95 insect species representing 22 families and 6 orders (see dataset on Dryad: doi:10.5061/dryad.115m1). Taken as a whole, these host insects were distributed on 18 plant families. Dissimilarities in host range were calculated—at three taxonomic levels (species, family and order) for the host insect and at one level (family) for the host plant—using the Bray-Curtis distance, each host taxon being treated qualitatively (at least one record *versus* none). This information was summarized and presented as "ecological matrices". Correlations between "phylogenetic", "morphological" and "ecological" matrices were tested using simple (2 matrices) or partial (3 matrices) Mantel tests, the relevance of these last tests having been repeatedly discussed (see for instance [71] and [72]).

Moreover, three kinds of traits were investigated using D-statistics (see previous paragraph):

(a) *Host specificity* ("specialists" which were reared from a single host species *versus* "generalists" that were reared from more than one host species). This specificity was evaluated at the order-family taxonomic level and at the species level. Because one may argue that our sampling underestimates specialists, we also performed this analysis under the assumption that all the rare species (*E. janstai*, *E. longicalvus*, *E. minozonus*, *E. priotoni*, *E. purpuricollis*, *E. vindex*) could be specialists.

(b) *Ability* ("Yes" or "No") to successfully parasitize some well-represented insect taxa at the ordinal level (Coleoptera, Diptera, Hymenoptera and Lepidoptera) or at the family level (Cynipidae within Hymenoptera and Cecidomyiidae within Diptera).

(c) *The ability* ("Yes" or "No") *to exploit some main host plants* (whatever the host insect), host plant being

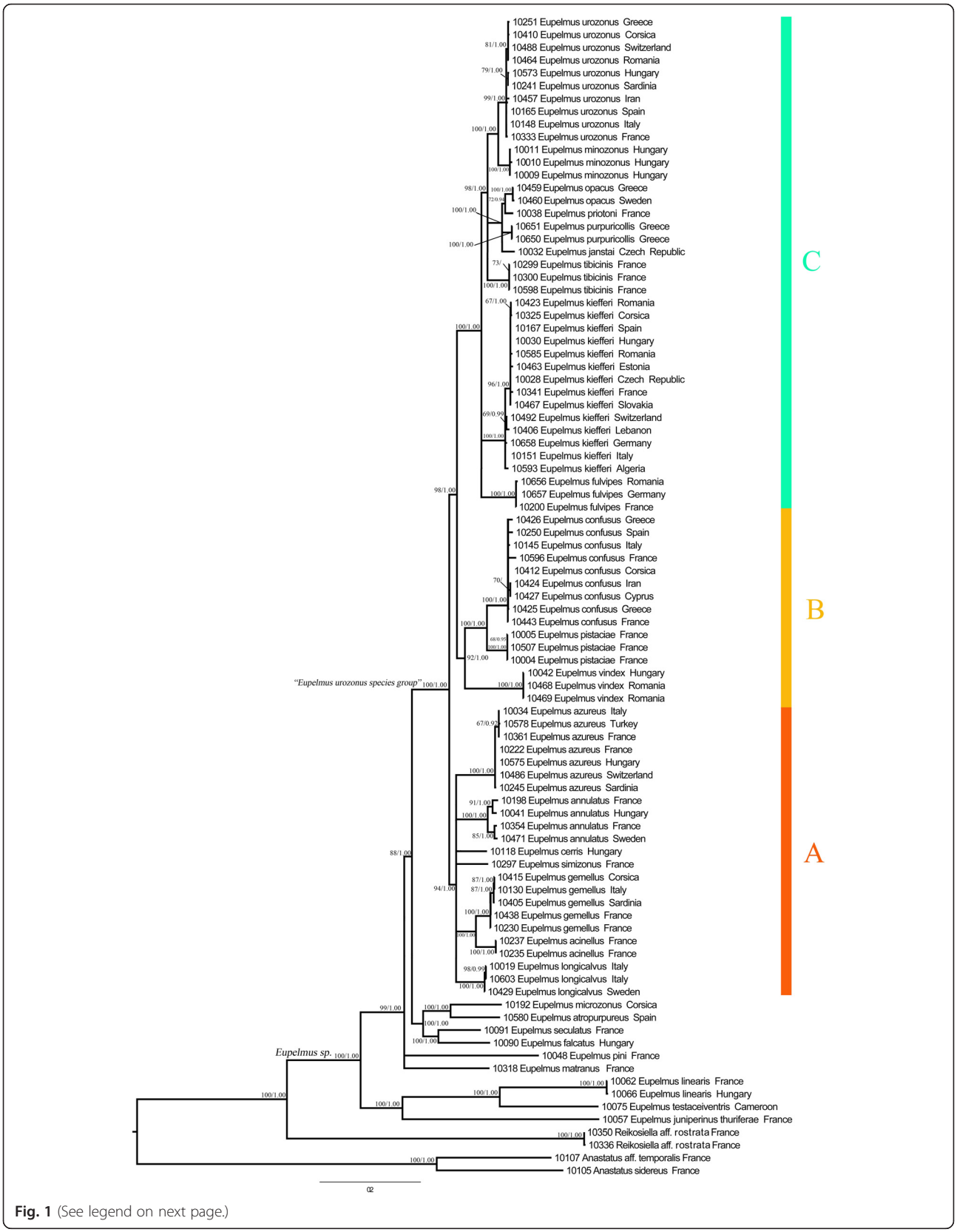

Fig. 1 (See legend on next page.)

(See figure on previous page.)
Fig. 1 Phylogram of relationships among species of the "*Eupelmus urozonus*-group" obtained from the concatenated dataset alignment (5000 bp and 9 partitions) without the Gblocks cleaning of divergent blocks. Uppercase letters refer to clades discussed in the text. Nodes with likelihood bootstrap (BP) values <65 have been collapsed. BP (≥65) and Bayesian posterior probabilities (≥0.90) are indicated at nodes. Each line represents a sequenced individual with information in the following order: molecular code, species and country

treated at the family level (Asteraceae, Fagaceae, Rosaceae, Salicaceae).

Software and packages

Manipulations of files and statistical tests were conducted using the software R (http://www.R-project.org - version 3.0.3 – 2014-03-06) with the following packages "ade4" (Euclidian transformation of matrices) [73], "ape" (phylogeny) [74], "caper" (comparative analysis), "ecodist" (Mantel tests) [75] and "vegan" (similarities between host ranges) [76].

Results

Alignments and single-marker analyses

Successful amplification and sequencing was completed for all gene regions used in this study. However, sequencing failures occurred for some markers for a few individuals. Genbank accessions of the sequences obtained for all analysed genes are given in Additional file 1: Table S2. The final matrix contained 91 specimens. No stop codons, frame shifts, insertions or deletions were observed in coding gene regions.

The numbers of aligned base pairs, variable sites and parsimony-informative sites for each gene are summarized in Table 2. As expected, mitochondrial genes showed more parsimony-informative sites compared to nuclear markers (472 out of 1085 bp). Among the nuclear markers, *EF-1α* exhibited the lowest number of variable and parsimony-informative sites (respectively 116 and 106 out of 517 bp). For *RpL27a*, removing the highly divergent alignment blocks significantly reduced the number of variable and parsimony-informative sites (from 54 to 38 % for variable sites and from 34 to 30 % for parsimony-informative sites). This loss consequently affected the resolution of the corresponding inferred topology (Additional file 2: Figure S16 and Figure S17). In contrast, the Gblocks procedure did not affect the number of variable and parsimony-informative sites for *Bub3* and *RpS4* and the resolution of the corresponding topologies (Additional file 2: Figures S12 – S15).

Evolution models and partitions in the concatenated dataset

Alignment lengths of the concatenated datasets with or without the exclusion of highly divergent blocks were 3197 bp and 5000 bp respectively. For all partitions, the best-fitting substitution model was the general time reversible model (GTR) with among-sites rate variation (ASRV) modelled by a discrete gamma distribution (Γ) [77] for which we used four categories. For all Bayesian analyses, after discarding 25 % of the samples as *burn-in*, the ESS value of each parameter largely exceeded 200, which indicated that convergence of runs was reached. Sixteen combined trees were obtained (Additional file 2: Figures S1 – S8). For all combined datasets, Bayes factors showed that the most complex partitioning scenario (9 partitions) was preferred over the three less complex ones (Table 3).

Evolutionary properties of the markers

Model parameter estimates for each partition of the Bayesian analysis of the "9 partitions without Gblocks cleaning dataset" are depicted in Table 4.

As expected, the mitochondrial partitions showed high base compositional bias (71.4 and 89.8 % of A/T for the first two positions and the third codon position respectively). Among the nuclear gene partitions, *RpL27a*, *Bub3* and *RpS4* were A/T-biased (77.9, 70 and 68.8 %) while

Table 2 Numbers and percentage of aligned base pairs, variable sites and parsimony-informative sites for the genes used in this study

Gene region	Total sites	Variable sites	Parsimony-informative sites
mtDNA	1085	530 (48.8 %)	472 (43.5 %)
Wg	433	157 (36.2 %)	147 (33.9 %)
EF-1a	517	116 (22.4 %)	106 (20.5 %)
Bub3 alignment without Gblocks	481	161 (33.4 %)	140 (29.1 %)
Bub3 alignment with Gblocks default	391	132 (33.7 %)	116 (29.7 %)
RpS4 alignment without Gblocks	1259	451 (35.8 %)	323 (25.6 %)
RpS4 alignment with Gblocks default	525	189 (36.0 %)	148 (28.1 %)
RpL27a alignment without Gblocks	1225	661 (53.9 %)	417 (34.0 %)
RpL27a alignment with Gblocks default	246	93 (37.8 %)	74 (30.0 %)

Table 3 Partitioning strategy selecting using Bayes factors (Harmonic-Mean) in Bayesian analyses

Dataset partitioning models	Harmonic-mean (LnL)	Bayes factor
Alignments without Gblocks		
M1: mtDNA, nucDNA (2 partitions, 19 free parameters)	−38664.20	*M2*, *M1* = 907.0
M2: mtDNA, *Wg*, *EF-1α*, *Bub3*, *RpS4*, *RpL27a* (6 partitions, 59 parameters)	−38118.57	*M3*, *M1* = 1909.5
M3: mtDNA 1&2, mtDNA 3, *Wg*, *EF-1α*, *Bub3*, *RpS4*, *RpL27a* (7 partitions, 69 parameters)	−37594.33	*M3*, *M2* = 1002.4
M4: mtDNA 1&2, mtDNA 3, *Wg* 1&2, *Wg* 3, *EF-1α* 1&2, *EF-1α 3*, *Bub3*, *RpS4*, *RpL27a* (9 partitions, 89 parameters)	−37261.28	*M4*, *M1* = 2483.5
		M4, *M2* = 1576.43
		M4, *M3* = 574
Alignments with Gblocks default	Harmonic Mean (LnL)	Bayes factor
M1: mtDNA, nucDNA (2 partitions, 19 free parameters)	−27676.75	*M2*, *M1* = 150.1
M2: mtDNA, *Wg*, *EF-1α*, *Bub3*, *RpS4*, *RpL27a* (6 partitions, 59 parameters)	−27509.59	*M3*, *M1* = 1210.5
M3: mtDNA 1&2, mtDNA 3, *Wg*, *EF-1α*, *Bub3*, *RpS4*, *RpL27a* (7 partitions, 69 parameters)	−26956.35	*M3*, *M2* = 1060.4
M4: mtDNA 1&2, mtDNA 3, *Wg* 1&2, *Wg* 3, *EF-1α* 1&2, *EF-1α* 3, *Bub3*, *RpS4*, *RpL27a* (9 partitions, 89 parameters)	−26691.65	*M4*, *M1* = 1647.8
		M4, *M2* = 1497.73
		M4, *M3* = 437.3

the A/T percentage in the 3rd codon positions in *Wg* and *EF-1α* was only 32 and 45 % respectively.

With the exception of *EF-1α* 1st and 2nd codon positions (18.9 %), there was an overall higher rate of A-G and C-T transitions (from 60.8 % for *RpL27a* up to 91.6 % for mtDNA 3rd codon positions). More precisely, mtDNA (all codon positions), *Bub3* and *Wg* 1st & 2nd codon positions were in excess of C-T transitions.

For protein-coding genes (mtDNA, *EF-1α* and *Wg*), the rate multiplier parameter (m) was higher for the 3rd

Table 4 Evolutionary properties of the partitions used in the study

Partitions	r (A↔C)	r (A↔G)	r (A↔T)	r (C↔G)	r (C↔T)	r (G↔T)
mtDNA 1&2	0.036 (0.015–0.059)	0.186 (0.134–0.241)	0.115 (0.089–0.141)	0.065 (0.034–0.099)	0.574 (0.503–0.642)	0.021 (0.010–0.034)
mtDNA 3	0.018 (0.006–0.029)	0.378 (0.310–0.445)	0.011 (0.00–0.014)	0.020 (0.00–0.048)	0.537 (0.464–0.608)	0.032 (0.021–0.046)
Wg 1&2	0.083 (0.021–0.149)	0.142 (0.057–0.240)	0.031 (0.000–0.079)	0.026 (0.000–0.064)	0.698 (0.565–0.827)	0.018 (0.000–0.056)
Wg 3	0.070 (0.042–0.100)	0.364 (0.274–0.459)	0.119 (0.072–0.171)	0.041 (0.024–0.058)	0.392 (0.300–0.484)	0.012 (0.000–0.029)
EF-1α 1&2	0.075 (0.–0.177)	0.070 (0.000–0.167)	0.040 (0–0.118)	0.182 (0.037–0.351)	0.197 (0.041–0.374)	0.432 (0.216–0.646)
EF-1α 3	0.052 (0.025–0.082)	0.481 (0.373–0.588)	0.072 (0.031–0.120)	0.018 (0.004–0.035)	0.342 (0.243–0.438)	0.031 (0.008–0.059)
Bub	0.084 (0.051–0.121)	0.289 (0.220–0.363)	0.069 (0.048–0.091)	0.036 (0.004–0.072)	0.456 (0.377–0.538)	0.062 (0.036–0.090)
RpS4	0.068 (0.047–0.090)	0.341 (0.296–0.388)	0.104 (0.085–0.123)	0.070 (0.042–0.099)	0.332 (0.288–0.378)	0.082 (0.062–0.104)
RpL27a	0.094 (0.070–0.119)	0.302 (0.257–0.348)	0.085 (0.070–0.101)	0.094 (0.054–0.138)	0.307 (0.260–0.353)	0.115 (0.089–0.141)
Partitions	pi A	pi C	pi G	pi T	α (Shape parameter)	m (Rtae multiplier)
mtDNA 1&2	0.271 (0.242–0.299)	0.137 (0.120–0.155)	0.147 (0.124–0.171)	0.443 (0.414–0.472)	0.133 (0.118–0.148)	0.580 (0.483–0.681)
mtDNA 3	0.418 (0.392–0.444)	0.049 (0.044–0.055)	0.051 (0.045–0.057)	0.480 (0.453–0.506)	0.635 (0.549–0.729)	8.929 (8.34–9.524)
Wg 1&2	0.284 (0.234–0.333)	0.215 (0.171–0.260)	0.288 (0.237–0.339)	0.211 (0.169–0.258)	0.076 (0–0.181)	0.034 (0.021–0.048)
Wg 3	0.151 (0.119–0.182)	0.402 (0.349–0.452)	0.278 (0.231–0.327)	0.168 (0.137–0.201)	1.086 (0.776–1.415)	1.254 (0.984–1.535)
EF-1α 1&2	0.307 (0.260–0.354)	0.212 (0.170–0.254)	0.258 (0.213–0.305)	0.222 (0.180–0.264)	0.093 (0–0.258)	0.029 (0.004–0.014)
EF-1α 3	0.178 (0.135–0.223)	0.373 (0.315–0.427)	0.176 (0.132–0.222)	0.270 (0.223–0.320)	0.769 (0.508–1.038)	0.336 (0.257–0.415)
Bub	0.351 (0.314–0.387)	0.129 (0.105–0.153)	0.169 (0.141–0.197)	0.349 (0.313–0.385)	0.222 (0.166–0.279)	0.190 (0.152–0.229)
RpS4	0.332 (0.308–0.354)	0.162 (0.146–0.180)	0.147 (0.131–0.163)	0.357 (0.334–0.380)	0.427 (0.364–0.496)	0.262 (0.224–0.303)
RpL27a	0.390 (0.367–0.412)	0.109 (0.096–0.123)	0.111 (0.097–0.124)	0.389 (0.366–0.410)	0.820 (0.693–0.946)	0.536 (0.455–0.619)

Mean and 95 % credibility intervals of the model parameters for each partition included in the Bayesian analyses of concatenated datasets without Gblocks cleaning (9 partitions) are reported

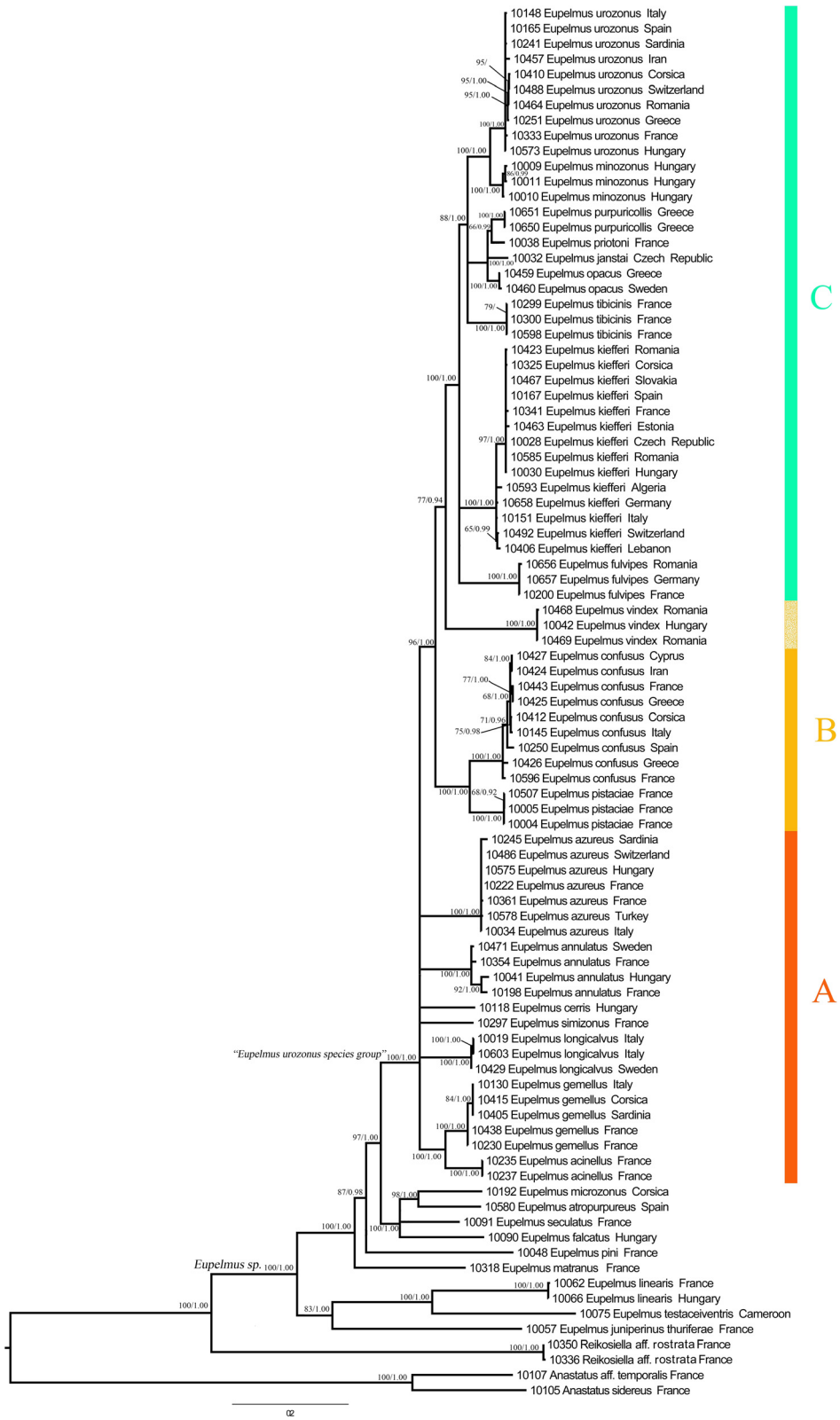

Fig. 2 (See legend on next page.)

(See figure on previous page.)
Fig. 2 Phylogram of relationships among species of the "*Eupelmus urozonus* group" obtained from the concatenated dataset alignment (3197 bp and 9 partitions) with Gblocks-default parameters. Uppercase letters refer to clades discussed in the text. Nodes with likelihood bootstrap (BP) values <65 have been collapsed. BP (≥65) and Bayesian posterior probabilities (≥0.90) are indicated at nodes. Each line represents a sequenced individual with information in the following order: molecular code, species, and country

codon positions. Thus, mtDNA 3rd codon positions evolved more than sixteen times faster than the fastest nuclear gene (*RpL27a*).

The shape parameter of the gamma distribution (α) was also higher for the 3rd codon position of the protein coding genes, indicating that these positions show lower rate heterogeneity among sites. Additionally, α was lower for *Bub3* than for *RpS4* and *RpL27a*, indicating that *Bub3* had a greater rate of heterogeneity among sites.

Phylogenetic trees inferred from concatenated datasets

Impacts of alignment strategy and reconstruction methods

ML and Bayesian topologies obtained from the concatenated alignments without Gblocks cleaning were more resolved than those obtained with removal of poorly aligned blocks. Whatever the partitioning scheme and regardless of whether or not divergent blocks were included in the analyses, most internal nodes were nevertheless statistically supported (BP value ≥ 65, PP value ≥ 90). Moreover, the 18 species recently defined by Al khatib et al. [32] and *E. vindex* were recovered as a monophyletic group.

Overall, topologies showed three major clades (A, B, C) that emerge on highly supported basal nodes (Figs. 1 and 2 and Additional file 2: Figures S1–S8). Three topological conflicts were observed depending on whether or not the Gblocks cleaning step was performed: (i) Clade A was not supported in topologies inferred from the datasets cleaned using Gblocks (Fig. 2 and Additional file 2: Figures S5–S8); (ii) *E. vindex* was sister to the rest of clade C in the topologies inferred from data sets cleaned using Gblocks (Fig. 2 and Additional file 2: Figures S5–S8), while it was sister to *E. confusus* and *E. pistaciae* (clade B) without Gblocks cleaning (Fig. 1 and Additional file 2: Figures S1–S4); (iii) the relationships of *E. matranus* and *E. pini* were resolved when Gblocks was used (PP = 1 and 0.98 respectively) (Fig. 2 and Additional file 2: Figures S5–S8), but not resolved without Gblocks cleaning of data sets (Fig. 1 and Additional file 2: Figures S1–S4). Taken as a whole, we decided to favour the alignment without the Gblocks procedure for the comparative analysis in order to favour the resolution for the terminal nodes.

Molecular relationships within the "Eupelmus urozonus species group"

ML and Bayesian analyses performed on the most complex partitioning scheme without Gblocks cleaning produced similar topologies with only a few differences for poorly supported nodes (Additional file 2: Figure S1). We therefore mapped all node support values (BP & PP) on the ML topology (Fig. 1).

In all analyses, the "*E. urozonus* species group" was recovered as monophyletic (Fig. 1) with a strong support. The group was subdivided into three clades, "clades" being defined here as a statistically-supported basal divergence including several species:

- Clade A included *E. acinellus*, *E. annulatus*, *E. azureus*, *E. cerris*, *E. gemellus*, *E. longicalvus* and *E. simizonus*, whose relative positions were not resolved to the exception of the sister species relationship between *E. acinellus* and *E. gemellus* (BP = 100, PP = 1).
- Clade B included three species with *E. vindex* being sister to *E. confusus* plus *E. pistaciae* with strong support (BP = 92, PP = 1).
- Clade C included the remaining species and namely *E. fulvipes*, *E. janstai*, *E. kiefferi*, *E. minozonus*, *E. opacus*, *E. priotoni*, *E. purpuricollis*, *E. tibicinis* and *E. urozonus*. Within clade C, two well-supported (in each case, BP = 100, PP = 1) subclades—"sub-clade" being defined as a more terminal divergence including at least 2 species—can be distinguished (i) *E. opacus*, *E. priotoni*, *E. purpuricollis* and *E. janstai*; (ii) *E. minozonus* and *E. urozonus*. These two subclades together with *E. tibicinis*, whose exact phylogenetic position remains unclear, form a well-supported monophyletic group (BP = 98, PP = 1).

Comparative analysis and host uses

There were significant interspecific differences for both the absolute (AOS—Kruskal-Wallis test: $\chi^2_{16df} = 93.7$; $p < 10^{-3}$; *E. priotoni* and *E. simizonus* discarded because of lack of replicates) and relative (ROS—Kruskal-Wallis test: $\chi^2_{16df} = 109.2$; $p < 10^{-3}$; *E. priotoni* and *E. simizonus* also discarded) ovipositor lengths (Fig. 3a). AOS ranged from 398 μm in *E. minozonus* to a maximum of 1179 μm in *E. cerris* while ROS ranged from a minimum of 0.58 in *E. fulvipes* to a maximum of 1.16 in *E. janstai*. Even if AOS and ROS medians were significantly correlated one with another (Kendall's rank correlation: $z = 2.73$; $p = 0.006$), some discrepancies were observed as for *E cerris* which exhibits the highest AOS but an intermediate ROS (Fig. 3a).

Within the "*Eupelmus urozonus*" species group, there was no significant correlation between similarity in ovipositor length and phylogenetic distance (Mantel test for

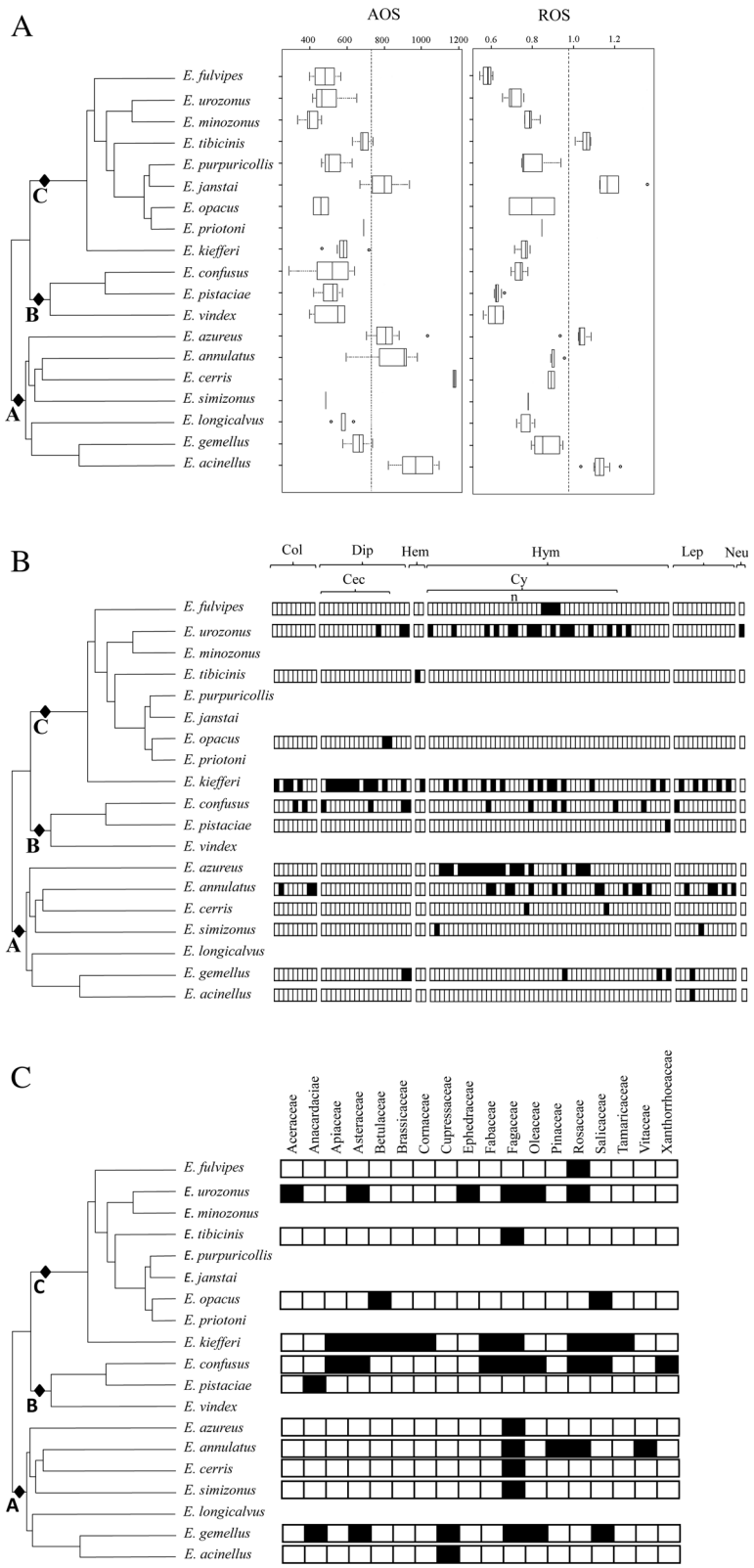

Fig. 3 (See legend on next page.)

(See figure on previous page.)
Fig. 3 Mapping of ovipositor size and host ranges (host insect and related plants) along the multi-locus phylogeny of the "*Eupelmus urozonus* group". The phylogenetic tree used is derived from the Fig. 1. For convenience, sizes of branches were modified but the topology remains unchanged. In Fig. 3a, boxplots are shown for the absolute (AOS in μm) and relative (ROS – no unit) lengths of the ovipositor for each Eupelmus species. In each case, the vertical dotted line separates "short" versus "long" ovipositors. In Fig. 3b, the host specificity is indicated at three levels (from up to down): order, family, and species. Each rectangle indicates a possible host and the black ones indicate that at least one *Eupelmus* specimen was obtained from this host. In Fig. 3c, the plant host is indicated at the family level

AOS: $r = 0.09$, $p = 0.39$ – Mantel test for ROS: $r = 0.08$, $p = 0.44$). When ovipositor length was treated as a binary variable with "long" ovipositors being those above the third quartile (4 or 5 cases among the 19 species), the observed D-statistics for AOS (0.13) and ROS (1.33) never departed from a random distribution (respectively p =0.13 and p =0.61) or a Brownian one (respectively p =0.48 and p =0.14). Consequently, it seems that no strong clustering existed on the length of the ovipositor sheaths. Remarkable differences in the length of the ovipositor sheaths were even observed between some sister species: *E. acinellus*—*E. gemellus* in clade A and *E. janstai*—*E. purpuricollis* in clade B (Fig. 3a).

Taken as a whole, our results indicated that both Cynipidae and Cecidomyiidae constitute the main host species for West Palearctic "*E. urozonus* species group" (Fig. 3b). Yet, contrasted feeding regimes (specialists versus generalists) were observed (Fig. 3b). Only three (*E. acinellus*, *E. pistaciae* and *E. tibicinis*) of the 13 species are strict specialists, with a distribution ($D = 2.38$) not significantly departing from both a random ($p = 0.79$) or a Brownian distribution (p =0.11). At the family and order level (same distributions), three other species were specialists of Cynipidae—*E. azureus* (reported on 21 host species), *E. cerris* (2 hosts) and *E. fulvipes* (4 hosts)—and one (*E. opacus*) on Cecidomyiidae. At these levels, the relative distribution of specialists and generalists ($D = 1.65$) does not differs from a random (p =0.72) or Brownian distribution (p =0.10) and, as shown in Fig. 33b, about 50–60 % of the described species in each of the three clades were specialists. The absence of a phylogenetic signal still holds under the assumption that all rare species (*E. janstai*, *E. longicalvus*, *E. minozonus*, *E. priotoni*, *E. purpuricollis*, *E. vindex*) are specialists. Departures from a random distribution is never significant (host species' level: D =1.04 with p =0.51 – host order's level: D =1.52 with p =0.76) while a significant departure is observed from a Brownian distribution at the host order's level (host species' level: p =0.12 – host order's level: p =0.031). Interestingly, contrasted host ranges were observed between sister species: *E. gemellus* (six host species distributed in 3 orders)—*E. acinellus* (one host species) within clade A and *E. confusus* (thirteen species distributed in four orders)—*E. pistaciae* (one host species) within clade B (Fig. 3b).

We investigated the ability of the "*E. urozonus* species group" to parasitize host species belonging to Coleoptera, Diptera, Hymenoptera and Lepidoptera (ordinal level) or Cecidomyiidae within Diptera and Cynipidae within Hymenoptera (familial level) (see Fig. 3b). However, in all these cases, we were not able to observe significant departures from a random or a Brownian distribution (See Additional file 3: Table S4).

Correlations between phylogenetic, morphometric (absolute or relative lengths of the ovipositor sheaths, AOS and ROS) and ecological (host ranges) matrices were also tested using simple or partial Mantel tests, at each of the three levels (species, family and order). Overall, the Mantel coefficients ranged between −0.07 and +0.14 and were never significantly different from zero (see Additional file 4: Table S3). At the host species level, such a result could be explained by the fact that only 24 % of the hosts (mostly Cynipidae) are shared by at least two species of the "*E. urozonus* species group". As a consequence, this level of investigation may be too precise to detect any signal. However, such a limit cannot be taken into account at the two other taxonomic levels since about half of the host families and all host orders except Neuroptera are shared by at least two species of *Eupelmus*. Taken as a whole, these results confirm those obtained using D-statistics about the absence of significant phylogenetic constraints on the host range evolution. The relative ovipositor length also does not appear to be a significant driver of the host use.

When host plants rather than host insects are taken into account, 18 plant families were identified (see Fig. 3c), eight of which being used by only one *Eupelmus* species. However, four main families were used by at least four *Eupelmus* species: Asteraceae (4 species), Fagaceae (9 species), Rosaceae (5 species) and Salicaceae (4 species). For each of these families, no phylogenetic signal was detected using the D-statistics (See Additional file 3: Table S4). Additionally, no correlation was found between the related ecological matrix and the phylogenetic, and/or morphometric (AOS/ROS) matrices (see Additional file 5: Table S5).

Discussion

Phylogenetic relationships within the "*E. urozonus* species group"

Phylogenetic inter-specific relationships within the "*E. urozonus* species group" occurring in the Palaearctic region were recently investigated by Al khatib et al. [32]

based on morphological characters and two genetic markers (mitochondrial *COI* and nuclear *Wg*). This study showed an unsuspected diversity but it (i) failed to resolve phylogenetic relationships at both deep and intermediate levels, (ii) highlighted some discrepancies among tree topologies at the shallowest nodes resulting from *COI* and *Wg* sequences, (iii) did not include morphologically divergent but potentially phylogenetically closely related species. By considering new species and adding more informative markers, the present study improved the knowledge on the evolutionary history of the "*E. urozonus* species group".

Although the phylogenetic resolution was proven to be sensitive to inclusion or exclusion of divergent blocks by using Gblocks procedure from the sequence alignments, we obtained a reliable phylogeny which strongly supported the monophyly of our focus group of *Eupelmus*, including the 18 species treated in Al khatib et al. [32] and *E. vindex*, which is morphologically distinct from other members of the group in the shape of the syntergum and the anterior displacement of the ovipositor sheaths (Gibson & Fusu, in prep). Additionally, the included species of the "*E. urozonus* group" were distributed in three strongly supported clades, referred here as A, B and C (Fig. 1).

The molecular monophyly of the Palaearctic "*E. urozonus* species group" reflected in our concatenated datasets can be also supported through morphology. Al khatib et al. (in prep.) recently compared and combined the results of phylogenetic inferences using the molecular data presented here with morphological data. The main conclusion of this complementary work seems to be the structuration of *Eupelmus* as a set of independent species groups (including our focus group). Their delineation and their morphological supports are therefore not detailed here.

Despite using several loci from both the nuclear and mitochondrial genomes, some of the focal taxa remain poorly resolved. We expect that newer methods that dramatically increase the number of loci will help to better resolve these relationships (see for instance [78]).

Ecological differentiation within the "*E. urozonus* species group"

The diversification of parasitic organisms has been explained by various processes linking ecological specialization and speciation. For parasitoids, phylogenetic information and reliable host ranges are necessary to describe the patterns (distribution of generalist and specialist species) and to understand the underlying processes (e.g. "musical chairs" *versus* "oscillation"). This motivated the present work. Although members of the genus *Eupelmus* are usually described as generalist ectoparasitoids [27, 28], our study nevertheless leads to a more complex pattern. Our results indeed showed the coexistence of "strict" specialists restricted to one specific host (i.e. *E acinellus*, *E. pistaciae*, *E. tibicinis*), intermediate specialists that can parasitize various species of Cynipidae (i.e. *E. azureus*, *E. cerris* and *E. fulvipes*) and generalists that are able to successfully develop on different insect orders (i.e. *E. annulatus*, *E. confusus*, *E. gemellus* and *E. kiefferi*).

This diversity in host use observed in the "*E. urozonus* species group" does not seem to be driven by phylogenetic history as generalists and specialists were recovered in each of the three clades. Moreover, some sister species exhibited fully contrasted ecologies (generalist species cited first): *E. confusus—E. pistaciae* and *E. gemellus—E. acinellus*. In this last case, because the facultative hyperparasitism lifestyle is recorded for some species of *Eupelmus*, we strongly suspect that *E. gemellus* develops as a hyperparasitoid of *E. acinellus* on *Mesophleps oxycedrella* (Lepidoptera). If this is true, it would mean that none of these generalists (*E. confusus* and *E. gemellus*) share any hosts with its sister species. Even if it is not the case, such contrasting patterns of host use remain, to our knowledge, rare in parasitoid species.

Quite similar conclusions arose when host plants instead hosts insects were taken into account. There was indeed no correlation between host plant ranges, phylogenetic and/or morphometric constraints. Moreover, the use of the four main plant families (Asteraceae, Fagaceae, Rosaceae and Salicaceae) did not seem to be constrained by the phylogenetic history. The underlying rationale of this complementary analysis was that host plants could at least partly determine ecological specialization of *Eupelmus* species insofar as the parasitoid species could use, innately or through learning, plant-linked cues in order to locate favourable environments, be the cues emitted passively (olfactory or visual information) or actively (synomones) (see for instance [79–81]). One criticism to this approach would, of course, be the level (plant family) at which our analysis was performed since it implies that only well-conserved cues could be detected.

A final facet of our investigation was the potential role of the ovipositor sheaths (as a proxy of the ovipositor length) as a driver of host use. The rationale was that (i) ovipositor structure could be constrained by the phylogenetic history of the species and, (ii) ovipositor length could determine accessibility to different hosts [82, 83]. None of these hypotheses was however verified, ovipositor length appearing to be a very labile trait within our focus group.

Another driver of host range evolution could be the complexity of gall communities exploited by the *Eupelmus* species. Indeed, in numerous cases, *Eupelmus* species are occurring with numerous parasitoid species belonging to different chalcid families (*e.g.* Torymidae, Eurytomidae or Pteromalidae) which seem to be more functionally

adapted to their hosts (see for instance [34, 84] and [85]). Such recurrent interspecific competitions may represent a potential limit for the abundance of *Eupelmus* but may also, ultimately, offer evolutionary opportunities. In particular, such an ecological intimacy could promote some switches towards unusual but ecologically related host insects and/or transitions towards other developmental modes (hyperparasitism or even predation). Such kind of adaptations may be illustrated by *E. tibicinis*, a specialist predator of the eggs of the red cicada, *Tibicina haematodes* (Scopoli, 1763) (Hemiptera: Tibicinidae).

Conclusions

This paper provides comprehensive information about the ecological differentiation within the Palaearctic species of the "*E. urozonus* group" and contributes to our understanding of ecological specialization in parasitoids. Although further investigations are required, the intimate mixing of generalist and specialist species along the phylogeny leans toward the "oscillation hypothesis" (*sensu* Hardy and Otto [21]). It also raises new questions at both the inter- and intra-specific levels. At the intra-specific level, more detailed population genetics studies would be useful to test the existence of "host races" within generalist species, which could be a way to, (i) explain the capacity of a single species to develop in different hosts and (ii) offer opportunities for the recurrent apparition of specialized lineages and ultimately species. At the interspecific level, the partitioning of the available resources within sympatric *Eupelmus* species and with other chalcid wasps remains unclear. This would probably require a better knowledge of potential and realised host ranges, interspecific interactions (e.g., competition and hyperparasitism) and investigations on the influence of host plants on the associated parasitoids (e.g., attraction/repellence; phenology and structure of galls). Finally, an agronomic output of such investigations would be a better knowledge of the actual potential of some *Eupelmus* species to regulate certain insect pests such as the olive fruit fly, *Bactrocera oleae* (Gmelin, 1790) [86–89] or the chestnut gall wasp *Dryocosmus kuriphilus* Yasumatsu, 1951 [90–92].

Availability of supporting data

The data sets supporting the results are available in Dryad (doi: 10.5061/dryad.115m1).

All sequences are available in Genbank (http://www.ncbi.nlm.nih.gov/genbank). Genbank accession numbers are given in Additional file 2: Table S2.

Additional files

Additional file 1: Table S1. Primer sequences used in the study and related references. **Table S2.** Information (including identification codes, taxonomic identity and Genbank accession numbers) related the specimens used in the phylogenetic analyses. (DOCX 50 kb)

Additional file 2: Figure S1. Trees from a) the ML and b) Bayesian analyses of the combined dataset (without Gblocks cleaning, 9 partitions). Likelihood bootstrap values and posterior probabilities are indicated at nodes. **Figure S2.** Trees from a) the ML and b) Bayesian analyses of the combined dataset (without Gblocks cleaning, 7 partitions). Likelihood bootstrap values and posterior probabilities are indicated at nodes. **Figure S3.** Trees from a) the ML and b) Bayesian analyses of the combined dataset (without Gblocks cleaning, 6 partitions). Likelihood bootstrap values and posterior probabilities are indicated at nodes. **Figure S4.** Trees from a) the ML and b) Bayesian analyses of the combined dataset (without Gblocks cleaning, 2 partitions). Likelihood bootstrap values and posterior probabilities are indicated at nodes. **Figure S5.** Trees from a) the ML and b) Bayesian analyses of the combined dataset (with Gblocks-default parameters, 9 partitions). Likelihood bootstrap values and posterior probabilities are indicated at nodes. **Figure S6.** Trees from a) the ML and b) Bayesian analyses of the combined dataset (with Gblocks-default parameters, 7 partitions). Likelihood bootstrap values and posterior probabilities are indicated at nodes. **Figure S7.** Trees from a) the ML and b) Bayesian analyses of the combined dataset (with Gblocks-default parameters, 6 partitions). Likelihood bootstrap values and posterior probabilities are indicated at nodes. **Figure S8.** Trees from a) the ML and b) Bayesian analyses of the combined dataset (with Gblocks-default parameters, 2 partitions). Likelihood bootstrap values and posterior probabilities are indicated at nodes. **Figure S9.** Tree from the ML analysis of the mitochondrial partition. Likelihood bootstrap values (1000 replicates) and posterior probabilities are indicated at nodes. **Figure S10.** Tree from the ML analysis of the *Wg* locus. Likelihood bootstrap values (1000 replicates) and posterior probabilities are indicated at nodes. **Figure S11.** Tree from the ML analysis of the *EF-1a* locus. Likelihood bootstrap values (1000 replicates) and posterior probabilities are indicated at nodes. **Figure S12.** Tree from the ML analysis of the *Bub3* locus (without Gblocks cleaning). Likelihood bootstrap values (1000 replicates) and posterior probabilities are indicated at nodes. **Figure S13.** Tree from the ML analysis of the *Bub3* locus (with Gblocks-default parameters). Likelihood bootstrap values (1000 replicates) and posterior probabilities are indicated at nodes. **Figure S14.** Tree from the ML analysis of the *RpS4* locus (without Gblocks cleaning). Likelihood bootstrap values (1000 replicates) and posterior probabilities are indicated at nodes. **Figure S15.** Tree from the ML analysis of the *RpS4* locus (with Gblocks-default parameters). Likelihood bootstrap values (1000 replicates) and posterior probabilities are indicated at nodes. **Figure S16.** Tree from the ML analysis of the *RpL27a* locus (without Gblocks cleaning). Likelihood bootstrap values (1000 replicates) and posterior probabilities are indicated at nodes. **Figure S17.** Tree from the ML analysis of the *RpL27a* locus (with Gblocks-default parameters). Likelihood bootstrap values (1000 replicates) and posterior probabilities are indicated at nodes. **Figure S18.** Illustrations of morphometric measurements on *Eupelmus* females. (A) ovipositor sheaths, (B) ovipositor stylet (second and third pairs of valvulae), and (C) hind tibia. (PDF 110496 kb)

Additional file 3: Table S4. Summary of information related to the detection of a phylogenetic signal (both host insects and plants). (DOCX 20 kb)

Additional file 4: Table S3. Summary of Mantel tests used for the comparative analysis dealing with host insects. (DOCX 21 kb)

Additional file 5: Table S5. Summary of Mantel tests used for the comparative analysis dealing with host plants. (DOCX 19 kb)

Competing interests

The authors declare that they have no competing interests.

Authors' contributions

AC, FAK, GD, LF, JYR and NR conceived the study. FAK, GD, LF and NR provided the biological material and related information. AC, FAK and GG performed the molecular characterization. FAK, GD and LF realised the morphological measurements. AC, FAK, GD and NR realised the analysis. FAK, GD and NR drafted the manuscript with input from the other authors. All authors read and approved the final manuscript.

Acknowledgements
This research was directly supported by the projects "EUPELMUS" (Scientific Department "Santé des Plantes et Environnement" of INRA—grant 2012-04-05-20), "INULA" (APR Pesticides 2011: "Changer les pratiques agricoles pour préserver les services écosystémiques") and 'BIOFIS' (number 1001-001) allocated by the French Agropolis Fondation (Montpellier). This project was supported by the network Bibliothèque du Vivant funded by the CNRS, the Muséum National d'Histoire Naturelle (MNHN) and the Institut National de la Recherche Agronomique (INRA), and technically supported by the Genoscope. This study also took benefits from field work conducted in the frame of the projects "BIOINV-4I" (ANR-06-BDIV-008 – Coordinator: Thomas Guillemaud), "Lutte biologique contre le Cynips du Châtaignier" (ONEMA 2011 – Coordinator: Nicolas Borowiec & Jean-Claude Malausa), and the Swedish Malaise Trap Project (SMTP).
The authors want to thank Sylvie Warot for her contribution to the molecular work as well as two anonymous reviewers who helped to improve the first draft.

Author details
[1]INRA, University Nice Sophia Antipolis, CNRS, UMR 1355-7254 Institut Sophia Agrobiotech, Sophia Antipolis 06900, France. [2]INRA, UMR 1062 CBGP, 755 avenue du Campus Agropolis, CS 30016 F-34988, Montferrier-sur-Lez Cedex, France. [3]CIRAD, UMR 55 CBGP, 755 Avenue du Campus Agropolis, CS 30016 F-34988, Montferrier-sur-Lez Cedex, France. [4]Faculty of Biology, Alexandru Ioan Cuza University, Bd. Carol I nr. 11, 700506 Iasi, Romania.

Received: 3 July 2015 Accepted: 15 December 2015

References

1. Matsubayashi KW, Ohshima I, Nosil P. Ecological speciation in phytophagous insects. Entomol Exp Appl. 2010;134:1–27.
2. Rundle HD, Nosil P. Ecological speciation. Ecol Lett. 2005;8:336–52.
3. Schluter D. Ecology and the origin of species. Trends Ecol Evol. 2001;16:372–80.
4. Schluter D. Evidence for ecological speciation and its alternative. Science. 2009;323:737–41.
5. Futuyma DJ. Sympatric speciation: norm or exception. In: Tilmon KJ editor. Specialization, speciation and radiation: the evolutionary biology of herbivorous insects. Berkeley: University of California Press; 2008. p. 136–48.
6. Nyman T, Vikberg V, Smith DR, Boeve JL. How common is ecological speciation in plant-feeding insects? A 'Higher' Nematinae perspective. BMC Evol Biol. 2010;10:266.
7. Feder JL, Forbes AA. Sequential speciation and the diversity of parasitic insects. Ecol Entomol. 2010;35:67–76.
8. Forbes AA, Powell THQ, Stelinski LL, Smith JJ, Feder JL. Sequential sympatric speciation across trophic levels. Science. 2009;323:776–9.
9. Stireman JO, Nason JD, Heard SB, Seehawer JM. Cascading host-associated genetic differentiation in parasitoids of phytophagous insects. Proc R Soc B-Biol Sci. 2006;273:523–30.
10. Armbruster WS, Baldwin BG. Switch from specialized to generalized pollination. Nature. 1998;394:632.
11. Moran NA. The evolution of host-plant alternation in aphids: evidence for specialization as a dead end. Am Nat. 1988;132:681–706.
12. Nosil P. Transition rates between specialization and generalization in phytophagous insects. Evolution. 2002;56:1701–6.
13. Vamosi JC, Armbruster WS, Renner SS. Evolutionary ecology of specialization: insights from phylogenetic analysis. Proc R Soc B-Biol Sci. 2014;281:20142004.
14. Futuyma DJ, Moreno G. The evolution of ecological specialization. Annu Rev Ecol Syst. 1988;19:207–33.
15. Jaenike J. Host specialization in phytophagous insects. Annu Rev Ecol Syst. 1990;21:243–73.
16. Via S. Ecological genetics and host adaptation in herbivorous insects: the experimental-study of evolution in natural and agricultural systems. Annu Rev Entomol. 1990;35:421–46.
17. Carletto J, Lombaert E, Chavigny P, Brevault T, Lapchin L, Vanlerberghe-Masutti F. Ecological specialization of the aphid *Aphis gossypii* Glover on cultivated host plants. Mol Ecol. 2009;18:2198–212.
18. De Barro PJ. Genetic structure of the whitefly *Bemisia tabaci* in the Asia-Pacific region revealed using microsatellite markers. Mol Ecol. 2005;14:3695–718.
19. Frantz A, Plantegenest M, Mieuzet L, Simon JC. Ecological specialization correlates with genotypic differentiation in sympatric host-populations of the pea aphid. J Evol Biol. 2006;19:392–401.
20. Colles A, Liow LH, Prinzing A. Are specialists at risk under environmental change? Neoecological, paleoecological and phylogenetic approaches. Ecol Lett. 2009;12:849–63.
21. Hardy NB, Otto SP. Specialization and generalization in the diversification of phytophagous insects: tests of the musical chairs and oscillation hypotheses. Proc R Soc B-Biol Sci. 2014;281:20132960.
22. Godfray HCJ. Parasitoids: Behavioral and Evolutionary Ecology. Princeton: Princeton University Press; 1994.
23. Quicke DLJ, Fitton MG, Tunstead JR, Ingram SN, Gaitens PV. Ovipositor structure and relationships within the Hymenoptera, with special reference to the Ichneumonoidea. J Nat Hist. 1994;28:635–82.
24. Sivinski J, Aluja M. The evolution of ovipositor length in the parasitic Hymenoptera and the search for predictability in biological control. Fla Entomol. 2003;86:143–50.
25. Vilhelmsen L, Turrisi GF. *Per arborem ad astra*: Morphological adaptations to exploiting the woody habitat in the early evolution of Hymenoptera. Arthropod Struct Dev. 2011;40:2–20.
26. Universal Chalcidoidea Database. http://www.nhm.ac.uk/research-curation/research/projects/chalcidoids/index.html.
27. Gibson GAP. Parasitic wasps of the subfamily Eupelminae: classification and revision of world genera (Hymenoptera: Chalcidoidea, Eupelmidae). Mem Entomol Intl. 1995;5:i-v + 421.
28. Gibson GAP. Revision of the genus *Macroneura* Walker in America north of Mexico (Hymenoptera: Eupelmidae). Can Entomol. 1990;122:837–73.
29. Askew RR, Nieves-Aldrey JL. The genus *Eupelmus* Dalman, 1820 (Hymenoptera, Chalcidoidea, Eupelmidae) in peninsular Spain and the Canary Islands, with taxonomic notes and descriptions of new species. Graellsia. 2000;56:58–60.
30. Bouček Z. Australasian Chalcidoidea (Hymenoptera). A Biosystematic revision of genera of fourteen families, with a reclassification of species. Aberystwyth: CAB International Institute of Entomology, the Cambrian News Ltd.; 1988.
31. Gibson GAP. The species of *Eupelmus* (*Eupelmus*) Dalman and *Eupelmus* (*Episolindelia*) Girault (Hymenoptera: Eupelmidae) in North America north of Mexico. Zootaxa. 2011;2951:1–97.
32. Al khatib F, Fusu L, Cruaud A, Gibson G, Borowiec N, Rasplus J-Y, et al. An integrative approach to species discrimination in the *Eupelmus urozonus* complex (Hymenoptera, Eupelmidae), with the description of 11 new species from the Western Palaearctic. Syst Entomol. 2014;39:806–62.
33. Al khatib F, Fusu L, Cruaud A, Gibson G, Borowiec N, Rasplus J-Y, et al. Availability of eleven species names of *Eupelmus* (Hymenoptera, Eupelmidae) proposed in Al khatib *et al.* (2014). Zookeys. 2015;505:137–45.
34. Kaartinen R, Stone GN, Hearn J, Lohse K, Roslin T. Revealing secret liaisons: DNA barcoding changes our understanding of food webs. Ecol Entomol. 2010;35:623–38.
35. Fusu L. A revision of the Palaearctic species of *Reikosiella* (*Hirticauda*) (Hymenoptera, Eupelmidae). Zootaxa. 2013;3636:01–34.
36. Kalina V. The Palearctic species of the genus *Macroneura* Walker, 1837 (Hymenoptera, Chalcidoidea, Eupelmidae), with descriptions of new species. Sbornik Vedeckeho Lesnickeho Ustavu Vysoke Skoly Zemedelske v Praze. 1981;24:83–111.
37. Kalina V. The Palearctic species of the genus *Anastatus* Motschulsky, 1860 (Hymenoptera, Chalcidoidea, Eupelmidae), with descriptions of new species. Silvaecultura Tropica et Subtropica. 1981;8:3–25.
38. Cruaud A, Jabbour-Zahab R, Genson G, Cruaud C, Couloux A, Kjellberg F, et al. Laying the foundations for a new classification of Agaonidae (Hymenoptera: Chalcidoidea), a multilocus phylogenetic approach. Cladistics. 2010;26:359–87.
39. Cruaud A, Underhill JG, Huguin M, Genson G, Jabbour-Zahab R, Tolley KA, Rasplus J-Y, van Noort S. A multilocus phylogeny of the world Sycoecinae fig wasps (Chalcidoidea: Pteromalidae). PLoS One. 2013. doi:10.1371/journal.pone.0079291.
40. Deuve T, Cruaud A, Genson G, Rasplus J-Y. Molecular systematics and evolutionary history of the genus *Carabus* (Col. Carabidae). Mol Phylogenet Evol. 2012;65:259–75.
41. Gomez-Zurita J, Cardoso A. Systematics of the New Caledonian endemic genus *Taophila* Heller (Coleoptera: Chrysomelidae, Eumolpinae) combining

morphological, molecular and ecological data, with description of two new species. Syst Entomol. 2014;39:111–26.
42. Brower AVZ, DeSalle R. Patterns of mitochondrial versus nuclear DNA sequence divergence among nymphalid butterflies: the utility of *wingless* as a source of characters for phylogenetic inference. Insect Mol Biol. 1998;7:73–82.
43. Campbell DL, Brower AVZ, Pierce NE. Molecular evolution of the *wingless* gene and its implications for the phylogenetic placement of the butterfly family Riodinidae (Lepidoptera : Papilionoidea). Mol Biol Evol. 2000;17:684–96.
44. Haine ER, Martin J, Cook JM. Deep mtDNA divergences indicate cryptic species in a fig-pollinating wasp. BMC Evol Biol. 2006;6:83.
45. Pilgrim EM, von Dohlen CD, Pitts JP. Molecular phylogenetics of Vespoidea indicate paraphyly of the superfamily and novel relationships of its component families and subfamilies. Zool Scr. 2008;37:539–60.
46. Rokas A, Nylander JAA, Ronquist F, Stone GN. A maximum-likelihood analysis of eight phylogenetic markers in gallwasps (Hymenoptera : Cynipidae): implications for insect phylogenetic studies. Mol Phylogenet Evol. 2002;22:206–19.
47. Belshaw R, Quicke DLJ. A molecular phylogeny of the Aphidiinae (Hymenoptera: Braconidae). Mol Phylogenet Evol. 1997;7:281–93.
48. Cho SW, Mitchell A, Regier JC, Mitter C, Poole RW, Friedlander TP, et al. A highly conserved nuclear gene for low-level phylogenetics - Elongation factor-1-alpha recovers morphology-based tree for heliothine moths. Mol Biol Evol. 1995;12:650–6.
49. Lin CP, Danforth BN. How do insect nuclear and mitochondrial gene substitution patterns differ? Insights from Bayesian analyses of combined datasets. Mol Phylogenet Evol. 2004;30:686–702.
50. Mitchell A, Cho S, Regier JC, Mitter C, Poole RW, Matthews M. Phylogenetic utility of elongation factor-1α in Noctuoidea (Insecta: Lepidoptera): the limits of synonymous substitution. Mol Biol Evol. 1997;14:381–90.
51. Mitchell A, Mitter C, Regier JC. More taxa or more characters revisited: combining data from nuclear protein-encoding genes for phylogenetic analyses of Noctuoidea (Insecta: Lepidoptera). Syst Biol. 2000;49:202–24.
52. Kawakita A, Ascher JS, Sota T, Kato M, Roubik DW. Phylogenetic analysis of the corbiculate bee tribes based on 12 nuclear protein-coding genes (Hymenoptera: Apoidea: Apidae). Apidologie. 2008;39:163–75.
53. Rasmussen C, Cameron SA. Global stingless bee phylogeny supports ancient divergence, vicariance, and long distance dispersal. Biol J Linn Soc. 2010;99:206–32.
54. Lohse K, Sharanowski B, Blaxter M, Nicholls JA, Stone GN. Developing EPIC markers for chalcidoid Hymenoptera from EST and genomic data. Mol Ecol Resour. 2011;11:521–9.
55. Lohse K, Sharanowski B, Stone GN. Quantifying the Pleistocene history of the oak gall parasitoid *Cecidostiba fungosa* using twenty intron loci. Evolution. 2010;64:2664–81.
56. Sharanowski BJ, Robbertse B, Walker J, Voss SR, Yoder R, Spatafora J, et al. Expressed sequence tags reveal Proctotrupomorpha (minus Chalcidoidea) as sister to Aculeata (Hymenoptera: Insecta). Mol Phylogenet Evol. 2010;57:101–12.
57. Edgar RC. MUSCLE: a multiple sequence alignment method with reduced time and space complexity. BMC Bioinformatics. 2004;5:1–19.
58. Gouy M, Guindon S, Gascuel O. SeaView version 4: a multiplatform graphical user interface for sequence alignment and phylogenetic tree building. Mol Biol Evol. 2010;27:221–4.
59. Castresana J. Selection of conserved blocks from multiple alignments for their use in phylogenetic analysis. Mol Biol Evol. 2000;17:540–52.
60. Tamura K, Peterson D, Peterson N, Stecher G, Nei M, Kumar S. MEGA5: molecular evolutionary genetics analysis using maximum likelihood, evolutionary distance, and maximum parsimony methods. Mol Biol Evol. 2011;28:2731–9.
61. Kass RE, Raftery AE. Bayes factors. J Am Stat Assoc. 1995;90(430):773–95.
62. Nylander JAA, Ronquist F, Huelsenbeck JP, Nieves-Aldrey JL. Bayesian phylogenetic analysis of combined data. Syst Biol. 2004;53:47–67.
63. Pagel M, Meade A. Mixture models in phylogenetic inferences. In: Gascuel O, editor. Mathematics of Evolution and Phylogeny. Oxford: Clarendon; 2005. p. 121–42.
64. Posada D. jModelTest: phylogenetic model averaging. Mol Biol Evol. 2008; 25:1253–6.
65. Stamatakis A. RAxML version 8: a tool for phylogenetic analysis and post-analysis of large phylogenies. Bioinformatics. 2014;30:1312–3.
66. Ronquist F, Teslenko M, van der Mark P, Ayres DL, Darling A, Hohna S, et al. MrBayes 3.2: efficient bayesian phylogenetic inference and model choice across a large model space. Syst Biol. 2012;61:539–42.
67. Geyer CJ. Markov chain Monte Carlo maximum likelihood. In Keramidas, E. M., Computing Science and Statistics. In: Proceedings of the 23rd Symposium on the Interface: 1991; Interface Foundation of North America, Fairfax. 156–163.
68. Tracer v1.6, [http://beast.bio.ed.ac.uk/Tracer].
69. Miller MA, Pfeiffer W, Schwartz T. Creating the CIPRES Science Gateway for inference of large phylogenetic trees. In: Gateway Computing Environments Workshop (GCE). New Orleans 2010; 1–8.
70. Fritz SA, Purvis A. Selectivity in mammalian extinction risk and threat types: a new measure of phylogenetic signal strength in binary traits. Conserv Biol. 2010;24:1042–51.
71. Legendre P, Fortin MJ. Comparison of the Mantel test and alternative approaches for detecting complex multivariate relationships in the spatial analysis of genetic data. Mol Ecol Resour. 2010;10:831–44.
72. Harmon LJ, Glor RE. Poor statistical performance of the Mantel test in phylogenetic comparative analyses. Evolution. 2010;64:2173–8.
73. Dray S, Dufour AB. The ade4 package: Implementing the duality diagram for ecologists. J Stat Softw. 2007;22:1–20.
74. Paradis E, Claude J, Strimmer K. APE: Analyses of Phylogenetics and Evolution in R language. Bioinformatics. 2004;20:289–90.
75. Goslee SC, Urban DL. The ecodist package for dissimilarity-based analysis of ecological data. J Stat Softw. 2007;22:1–19.
76. Oksanen JBF, Kindt R, Legendre P, Minchin PR, O'Hara RB, Simpson GL, Solymos P, Stevens MHH, Wagner H: "vegan" - Community ecology package. 2015. http://vegan.r-forge.r-project.org/FAQ-vegan.html#How-tocite-vegan_003f.
77. Yang ZH. Maximum-likelihood phylogenetic estimation from DNA-sequences with variable rates over sites: approximate methods. J Mol Evol. 1994;39:306–14.
78. Cruaud A, Gautier M, Galan M, Foucaud J, Saune L, Genson G, et al. Empirical assessment of RAD sequencing for interspecific phylogeny. Mol Biol Evol. 2014;31:1272–4.
79. Segura DF, Viscarret MM, Paladino LZC, Ovruski SM, Cladera JL. Role of visual information and learning in habitat selection by a generalist parasitoid foraging for concealed hosts. Anim Behav. 2007;74:131–42.
80. Turlings TCJ, Tumlinson JH, Eller FJ, Lewis WJ. Larval-damaged plants: source of volatile synomones that guide the parasitoid *Cotesia marginiventris* to the microhabitats of its hosts. Entomol Exp Appl. 1991;58:75–82.
81. Vinson SB. The general host selection behavior of parasitoid Hymenoptera and a comparison of initial strategies utilized by larvaphagous and oophagous species. Biol Control. 1998;11:79–96.
82. Austin AD, Field SA. The ovipositor system of scelionid and platygastrid wasps (Hymenoptera: Platygastroidea): comparative morphology and phylogenetic implications. Invertebr Taxon. 1997;11:1–87.
83. Ghara M, Kundanati L, Borges RM. Nature's swiss army knives: ovipositor structure mirrors ecology in a multitrophic fig wasp community. PLoS One. 2011. doi:10.1371/journal.pone.0023642.
84. László Z, Tóthmérész B. Parasitism, phenology and sex ratio in galls of *Diplolepis rosae* in the Eastern Carpathian Basin. Entomologia Romanica. 2011;16:33–8.
85. Delanoue P. The consequence of competition between indigenous chalcidoids and an introduced braconid (*Opius concolor*) in attempts to limit populations of *Dacus oleae* in the Alpes-Maritimes. Revue de Pathologie Végétale et d'Entomologie Agricole de France. 1964;43:145–51.
86. Boccaccio L, Petacchi R. Landscape effects on the complex of *Bactrocera oleae* parasitoids and implications for conservation biological control. Biocontrol. 2009;54:607–16.
87. Borowiec N, Groussier-Bout G, Vercken E, Thaon M, Auguste-Maros A, Warot-Fricaux S, et al. Diversity and geographic distribution of the indigenous and exotic parasitoids of the olive fruit fly, *Bactrocera oleae* (Diptera: Tephritidae), in Southern France. IOBC-WPRS Bull. 2012;79:71–8.
88. Neuenschwander P, Bigler F, Delucchi V, Michelakis S. Natural enemies of preimaginal stages of *Dacus oleae* Gmel. (Dipt., Tephritidae) in Western Crete. I. Bionomics and phenologies. Bollettino del Laboratorio di Entomologia Agraria 'Filippo Silvestri'. 1983;40:3–32.
89. Warlop F. Limitation of olive pest populations through the development of conservation biocontrol. Cah Agric. 2006;15:449–55.
90. Aebi A, Schonrogge K, Melika G, Quacchia A, Alma A, Stone GN. Native and introduced parasitoids attacking the invasive chestnut gall wasp *Dryocosmus kuriphilus*. Bull OEPP/EPPO Bull. 2007;37:166–71.

91. Borowiec N, Thaon M, Brancaccio L, Warot S, Vercken E, Fauvergue X, et al. Classical biological control against the chestnut gall wasp *Dryocosmus kuriphilus* (Hymenoptera, Cynipidae) in France. Plant Prot Q. 2014;29:7–10.
92. Quacchia A, Ferracini C, Nicholls JA, Piazza E, Saladini MA, Tota F, et al. Chalcid parasitoid community associated with the invading pest *Dryocosmus kuriphilus* in north-western Italy. Insect Conserv Divers. 2013;6:114–23.

Additional files

Additional file 1: Table S1. Primer sequences used in the study and related references. **Table S2.** Information (including identification codes, taxonomic identity and Genbank accession numbers) related the specimens used in the phylogenetic analyses.

Additional file 2: Figure S1 Trees from a) the ML and b) Bayesian analyses of the combined dataset (without Gblocks cleaning, 9 partitions). Likelihood bootstrap values and posterior probabilities are indicated at nodes. **Figure S2** Trees from a) the ML and b) Bayesian analyses of the combined dataset (without Gblocks cleaning, 7 partitions). Likelihood bootstrap values and posterior probabilities are indicated at nodes. **Figure S3** Trees from a) the ML and b) Bayesian analyses of the combined dataset (without Gblocks cleaning, 6 partitions). Likelihood bootstrap values and posterior probabilities are indicated at nodes. **Figure S4** Trees from a) the ML and b) Bayesian analyses of the combined dataset (without Gblocks cleaning, 2 partitions). Likelihood bootstrap values and posterior probabilities are indicated at nodes. **Figure S5** Trees from a) the ML and b) Bayesian analyses of the combined dataset (with Gblocks-default parameters, 9 partitions). Likelihood bootstrap values and posterior probabilities are indicated at nodes. **Figure S6** Trees from a) the ML and b) Bayesian analyses of the combined dataset (with Gblocks-default parameters, 7 partitions). Likelihood bootstrap values and posterior probabilities are indicated at nodes. **Figure S7** Trees from a) the ML and b) Bayesian analyses of the combined dataset (with Gblocks-default parameters, 6 partitions). Likelihood bootstrap values and posterior probabilities are indicated at nodes. **Figure S8** Trees from a) the ML and b) Bayesian analyses of the combined dataset (with Gblocks-default parameters, 2 partitions). Likelihood bootstrap values and posterior probabilities are indicated at nodes. **Figure S9** Tree from the ML analysis of the mitochondrial partition. Likelihood bootstrap values (1000 replicates) and posterior probabilities are indicated at nodes. **Figure S10** Tree from the ML analysis of the *Wg* locus. Likelihood bootstrap values (1000 replicates) and posterior probabilities are indicated at nodes. **Figure S11** Tree from the ML analysis of the *EF-1Ŭ* locus. Likelihood bootstrap values (1000 replicates) and posterior probabilities are indicated at nodes. **Figure S12** Tree from the ML analysis of the *Bub3* locus (without Gblocks cleaning). Likelihood bootstrap values (1000 replicates) and posterior probabilities are indicated at nodes. **Figure S13** Tree from the ML analysis of the *Bub3* locus (with Gblocks-default parameters). Likelihood bootstrap values (1000 replicates) and posterior probabilities are indicated at nodes. **Figure**

S14 Tree from the ML analysis of the *RpS4* locus (without Gblocks cleaning). Likelihood bootstrap values (1000 replicates) and posterior probabilities are indicated at nodes. **Figure S15** Tree from the ML analysis of the *RpS4* locus (with Gblocks-default parameters). Likelihood bootstrap values (1000 replicates) and posterior probabilities are indicated at nodes. **Figure S16** Tree from the ML analysis of the *RpL27a* locus (without Gblocks cleaning). Likelihood bootstrap values (1000 replicates) and posterior probabilities are indicated at nodes. **Figure S17** Tree from the ML analysis of the *RpL27a* locus (with Gblocks-default parameters). Likelihood bootstrap values (1000 replicates) and posterior probabilities are indicated at nodes. **Figure S18** Illustrations of morphometric measurements on *Eupelmus* females: (A) ovipositor sheaths, (B) ovipositor stylet (second and third pairs of valvulae), (C) hind tibia.

Additional file 3: Table S4 Summary of information related to the detection of a phylogenetic signal.

Additional file 4: Table S3 Summary of Mantel tests used for comparative analysisdealing with host insects.

Additional file 5: Table S5 Summary of Mantel tests used for comparative analysisdealing with host plants.

Additional file 1: Table S1 Primer sequences used in the study and related references.

Locus	Primer	F/R	Primer sequences	Primer sources
COI	LCO1490	F	GGTCAACAAATCATAAAGATATTGG	Folmer *et al.* (1994)
	HCO2198	R	TAAACTTCAGGGTGACCAAAAAATCA	
Cyt b	CB1	F	TATGTACTACCATGACGACAAATATC	Jermiin & Crozier (1994)
	CB2	R	ATTACACCTCCTAATTTATTAGGAAT	
Wg	wg1a	F	GARTGYAARTGYCAYGGYATGTCTGG	Brower & DeSalle (1998)
	LepWg2	R	ACTNCGCRCACCARTGGAATGTRCA	Danforth *et al.* (2004)
EF-1Ŭ	F2-557F	F	GAACGTGAACGTGGTTATYACSAT	Cruaud *et al.* (2011)
	F2-1118R	R	TTACCTGAAGGGGAAGACGRAG	
Bub3	Bub3F2	F	GATCCYAGAACACCYACYTGTGTWGG	Kawakita *et al*. (2008)
	Bub3Rev1	R	CGYTTYTTRTTRAARCCATCCC	
RpS4	11F	F	BAARGCATGGATGTTRGACA	Lohse *et al.* (2011)
	11R	R	GGTCWGGRTADCGRATRGT	
RpL27a	28Fb	F	CAAYTTYGACAARTACCATCCWG	Lohse *et al.* (2011)
	28R	R	CCYTTKCCYARRAGTTTGTA	

Additional file 1: Table S2 Information (including identification codes, taxonomic identity and Genbank accession numbers) related the specimens used in the phylogenetic analyses.

Collection code	**Molecular code**	**Species**	***COI***	***Cyt b***	***Wg***	***EF-1Ŭ***	***Bub3***	***RpS4***	***RpL27a***	**Voucher depository**
GDEL4100	10107	*Anastatus aff. temporalis*	KR348752	KR348858	KR708338	KR708449	KR905352	KR905274	KR708469	GDPC
GDEL4098	10105	*Anastatus sidereus*	KR348751	KR348859	KR708337	KR708448	KR905351	KR905273	KR708468	GDPC
GDEL4064	10057	*Eupelmus juniperinus thuriferae*	KR348746	KR348857	KR708332	KR708445	KR905362	KR905275	KR708463	GDPC
GDEL4069	10062	*Eupelmus linearis*	KJ018334	KR348854	KJ018530	KR708442	KR905359	KR905268	KR708464	GDPC
GDEL4073	10066	*Eupelmus linearis*	KR348747	KR348855	KR708333	KR708443	KR905360	KR905269	KR708465	GDPC
GDEL4078	10075	*Eupelmus testaceiventris*	KR348748	KR348856	KR708334	KR708444	KR905361	KR905270	_	GDPC
FAL1363	10235	*Eupelmus acinellus*	KJ018383	KR348783	KJ018562	KR708370	KR905287	KR905199	KR708481	FALPC
FAL1366	10237	*Eupelmus acinellus*	KJ018384	KR348784	KJ018563	KR708371	KR905288	KR905200	KR708482	FALPC
GDEL4053	10041	*Eupelmus annulatus*	KJ018333	KR348774	KJ018529	KR708361	KR905277	KR905190	KR708460	GDPC
FAL1176	10198	*Eupelmus annulatus*	KJ018363	KR348772	KJ018547	KR708359	KR905276	KR905188	KR708477	FALPC
NB783	10354	*Eupelmus annulatus*	KJ018403	KR348773	KJ018579	KR708360	KR905278	KR905189	KR708496	FALPC
LF.an.SW 01	10471	*Eupelmus annulatus*	KJ018439	KR348775	KJ018601	KR708362	KR905279	KR905191	KR708516	AICF
PJ11159_23_1	10580	*Eupelmus atropurpureus*	KR348771	KR348850	KR708358	KR708438	KR905355	KR905267	KR708523	FALPC
GDEL4048	10034	*Eupelmus azureus*	KJ018331	KR348778	KJ018527	KR708365	KR905282	KR905194	KR708458	GDPC
FAL1323	10222	*Eupelmus azureus*	KR348755	KR348776	KR708341	KR708363	KR905280	KR905192	KR708479	CBGP
L.Loru713	10245	*Eupelmus azureus*	KR348757	KR348779	KR708343	KR708366	KR905283	KR905195	KR708484	MNHN
NB773a	10361	*Eupelmus azureus*	KJ018404	KR348777	KJ018580	KR708364	KR905281	KR905193	KR708497	FALPC
MC-C4	10486	*Eupelmus azureus*	KR348769	KR348782	KR708356	KR708369	KR905286	KR905198	_	CBGP
PJ10077-21-4	10575	*Eupelmus azureus*	KJ018448	KR348780	KJ018606	KR708367	KR905284	KR905196	KR708521	MNHN
PJ11054-2-2	10578	*Eupelmus azureus*	KJ018449	KR348781	KJ018607	KR708368	KR905285	KR905197	KR708522	FALPC
GDEL4109	10118	*Eupelmus cerris*	KJ018335	_	KJ018531	KR708372	KR905289	KR905201	KR708470	GDPC
FAL1051	10145	*Eupelmus confusus*	KJ018345	KR348795	KJ018535	KR708383	KR905299	KR905214	KR708471	GDPC
FAL1108	10250	*Eupelmus confusus*	KR348758	KR348796	KR708344	KR708384	KR905304	KR905211	KR708485	GDPC
FAL1519	10412	*Eupelmus confusus*	KJ018409	KR348794	KJ018582	KR708382	KR905298	KR905210	KR708501	MNHN

LF.ma.IR 05	10424	*Eupelmus confusus*	KJ018474	KR348800	KJ018624	KR708388	_	KR905215	KR708504	AICF
LF.ma.GR 01	10425	*Eupelmus confusus*	KJ018416	KR348797	KJ018586	KR708385	KR905300	KR905216	KR708505	AICF
LF.ma.GR 02	10426	*Eupelmus confusus*	KJ018417	KR348798	KJ018587	KR708386	KR905301	KR905212	KR708506	AICF
LF.ma.CY 01	10427	*Eupelmus confusus*	KJ018473	KR348801	KJ018625	KR708389	KR905303	_	KR708507	AICF
FAL1278	10443	*Eupelmus confusus*	KJ018424	KR348793	KJ018592	KR708381	KR905305	KR905213	KR708510	MNHN
GDEL4173	10596	*Eupelmus confusus*	KJ018452	KR348799	KJ018608	KR708387	KR905302	KR905217	KR708525	GDPC
FAL1221	10200	*Eupelmus fulvipes*	KJ018364	KR348845	KJ018548	KR708433	KR905346	KR905259	KR708478	FALPC
LF.ro.RO.02	10656	*Eupelmus fulvipes*	KJ018465	KR348846	KJ018620	KR708434	KR905347	KR905260	KR708529	AICF
LF.ro.GE.01	10657	*Eupelmus fulvipes*	KJ018466	KR348847	KJ018621	KR708435	KR905348	KR905261	KR708530	AICF
FAL1004	10130	*Eupelmus gemellus*	KJ018338	KR348791	KJ018499	KR708379	KR905296	KR905208	_	MNHN
FAL1359	10230	*Eupelmus gemellus*	KJ018380	KR348789	KJ018503	KR708377	KR905294	KR905205	KR708480	MNHG
FAL1508	10405	*Eupelmus gemellus*	KJ018405	KR348792	KJ018506	KR708380	KR905297	KR905209	KR708498	CNC
NB441	10415	*Eupelmus gemellus*	KR348764	KR348790	KR708350	KR708378	KR905295	KR905206	KR708502	FALPC
FAL1260	10438	*Eupelmus gemellus*	KR348765	KR348788	KR708352	KR708376	KR905293	KR905207	KR708509	FALPC
GDEL4046	10032	*Eupelmus janstai*	KJ018330	KR348843	KJ018526	KR708431	KR905344	KR905257	KR708457	MNHG
GDEL4043	10028	*Eupelmus kiefferi*	KJ018328	KR348829	KJ018477	KR708417	KR905332	KR905244	_	GDPC
GDEL4045	10030	*Eupelmus kiefferi*	KJ018329	KR348823	KJ018478	KR708411	KR905326	KR905240	KR708456	GDPC
FAL1070	10151	*Eupelmus kiefferi*	KR348753	KR348820	KR708339	KR708408	KR905323	KR905235	KR708473	FALPC
FAL1109	10167	*Eupelmus kiefferi*	KJ018354	KR348821	KJ018487	KR708409	KR905324	KR905236	KR708475	FALPC
NB666	10325	*Eupelmus kiefferi*	KJ018393	KR348819	KJ018495	KR708407	KR905322	KR905234	KR708491	FALPC
NB674b	10341	*Eupelmus kiefferi*	KJ018397	KR348818	KJ018496	KR708406	KR905321	KR905239	KR708494	CNC
FAL1511	10406	*Eupelmus kiefferi*	KJ018406	KR348822	KJ018497	KR708410	KR905325	KR905237	KR708499	FALPC
LF.ma.RO 01	10423	*Eupelmus kiefferi*	_	KR348825	KR708351	KR708413	KR905328	KR905242	KR708503	AICF
LF.fu.ES 01	10463	*Eupelmus kiefferi*	KJ018436	KR348830	KJ018490	KR708418	KR905333	KR905245	_	AICF
LF.fu.SL 01	10467	*Eupelmus kiefferi*	KJ018437	KR348828	KJ018491	KR708416	KR905331	KR905243	KR708513	AICF
MC-C124	10492	*Eupelmus kiefferi*	KR348770	KR348824	KR708357	KR708412	KR905327	KR905241	KR708518	FALPC
ZL.fu.RO.05	10585	*Eupelmus kiefferi*	KJ018450	KR348826	KJ018492	KR708414	KR905329	KR905238	KR708524	GDPC

FAL1524	10593	*Eupelmus kiefferi*	KJ018451	KR348831	KJ018498	KR708419	KR905334	KR905246	_	FALPC
LF.fu.GE 02	10658	*Eupelmus kiefferi*	KJ018450	KR348827	KJ018492	KR708415	KR905330	_	KR708531	AICF
GDEL4038	10019	*Eupelmus longicalvus*	KJ018327	KR348837	KJ018525	KR708425	KR905338	KR905252	KR708455	GDPC
LF.ma.SW 02	10429	*Eupelmus longicalvus*	KJ018418	KR348838	KJ018588	KR708426	KR905339	KR905251	KR708508	NHRS
GDEL4191	10603	*Eupelmus longicalvus*	KJ018455	KR348839	KJ018611	KR708427	KR905340	KR905253	KR708527	FALPC
FAL1491	10318	*Eupelmus matranus*	KR348759	KR348848	KR708345	KR708436	KR905354	KR905263	KR708490	FALPC
GDEL4116	10192	*Eupelmus microzonus*	KR348754	KR348849	KR708340	KR708437	KR905353	KR905262	KR708476	GDPC
GDEL4030	10009	*Eupelmus minozonus*	KJ018323	KR348815	KJ018521	KR708403	KR905318	KR905233	KR708452	GDPC
GDEL4030	10010	*Eupelmus minozonus*	KJ018324	KR348817	KJ018522	KR708404	KR905319	KR905232	KR708453	MNHG
GDEL4030	10011	*Eupelmus minozonus*	KJ018325	KR348816	KJ018523	KR708405	KR905320	KR905231	KR708454	MNHN
LF.ur.GR 01	10459	*Eupelmus opacus*	KJ018434	KR348833	_	KR708421	KR905336	KR905248	_	AICF
LF.ur.SW 02	10460	*Eupelmus opacus*	KJ018435	KR348834	KJ018600	KR708422	KR905337	_	KR708512	NHRS
GDEL4058	10048	*Eupelmus pini*	KR348745	KR348851	KR708331	KR708439	KR905356	KR905264	KR708462	GDPC
GDEL4027	10004	*Eupelmus pistaciae*	KJ018321	KR348785	KJ018519	KR708373	KR905290	KR905202	KR708450	FALPC
GDEL4027	10005	*Eupelmus pistaciae*	KJ018322	KR348786	KJ018520	KR708374	KR905291	KR905203	KR708451	FALPC
GDEL4027	10507	*Eupelmus pistaciae*	KJ018444	KR348787	KJ018603	KR708375	KR905292	KR905204	KR708519	MNHG
GDEL4051	10038	*Eupelmus priotoni*	KJ018332	KR348844	KJ018528	KR708432	KR905345	KR905258	KR708459	MNHG
LF.ur.GR.02	10650	*Eupelmus purpuricollis*	KJ018460	KR348835	KJ018616	KR708423	_	KR905249	KR708528	AICF
LF.ur.GR.03	10651	*Eupelmus purpuricollis*	KJ018461	KR348836	KJ018617	KR708424	_	KR905250	_	GDPC
GDEL4142	10297	*Eupelmus simizonus*	KJ018388	KR348832	KJ018567	KR708420	KR905335	KR905247	KR708487	MNHG
GDEL4148	10299	*Eupelmus tibicinis*	KJ018389	KR348841	KJ018568	KR708428	KR905341	KR905254	KR708488	GDPC
GDEL4149	10300	*Eupelmus tibicinis*	KJ018390	KR348842	KJ018569	KR708429	KR905342	KR905255	KR708489	FALPC
GDEL4175	10598	*Eupelmus tibicinis*	KJ018454	KR348840	KJ018610	KR708430	KR905343	KR905256	KR708526	GDPC
FAL1060	10148	*Eupelmus urozonus*	KJ018346	KR348807	KJ018536	KR708395	KR905311	KR905225	KR708472	FALPC
FAL1106	10165	*Eupelmus urozonus*	KJ018353	KR348809	KJ018541	KR708397	KR905313	KR905227	KR708474	FALPC
L.Loru235	10241	*Eupelmus urozonus*	KR348756	KR348808	KR708342	KR708396	KR905312	KR905226	KR708483	CBGP
NB1117	10251	*Eupelmus urozonus*	KJ018387	KR348810	KJ018566	KR708398	KR905314	KR905228	KR708486	FALPC

NB677	10333	*Eupelmus urozonus*	KR348760	KR348805	KR708346	KR708393	KR905309	KR905224	KR708492	MNHN
FAL1518	10410	*Eupelmus urozonus*	KR348763	KR348806	KR708349	KR708394	KR905310	KR905221	KR708500	CNC
LF.ur.IR 02	10457	*Eupelmus urozonus*	KJ018433	KR348814	KJ018599	KR708402	_	KR905230	KR708511	AICF
LF.fu.RO 01	10464	*Eupelmus urozonus*	KR348766	KR348813	KR708353	KR708401	KR905317	KR905222	_	AICF
MC-C100	10488	*Eupelmus urozonus*	KJ018443	KR348811	KJ018602	KR708399	KR905315	KR905223	KR708517	FALPC
PJ10077-2-6	10573	*Eupelmus urozonus*	KJ018447	KR348812	KJ018605	KR708400	KR905316	KR905229	KR708520	FALPC
GDEL4054	10042	*Eupelmus vindex*	KR348744	KR348802	KR708330	KR708390	KR905306	KR905218	KR708461	FALPC
LF.vi.RO 02	10468	*Eupelmus vindex*	KR348767	KR348803	KR708354	KR708391	KR905307	KR905219	KR708514	FALPC
LF.vi.RO 01	10469	*Eupelmus vindex*	KR348768	KR348804	KR708355	KR708392	KR905308	KR905220	KR708515	AICF
GDEL4088	10090	*Eupelmus falcatus*	KR348749	KR348852	KR708335	KR708440	KR905357	KR905265	KR708466	GDPC
GDEL4089	10091	*Eupelmus seculatus*	KR348750	KR348853	KR708336	KR708441	KR905358	KR905266	KR708467	FALPC
NB670	10336	*Reikosiella aff. rostrata*	KR348761	KR348860	KR708347	KR708446	KR905349	KR905271	KR708493	FALPC
NB810	10350	*Reikosiella aff. rostrata*	KR348762	KR348861	KR708348	KR708447	KR905350	KR905272	KR708495	FALPC

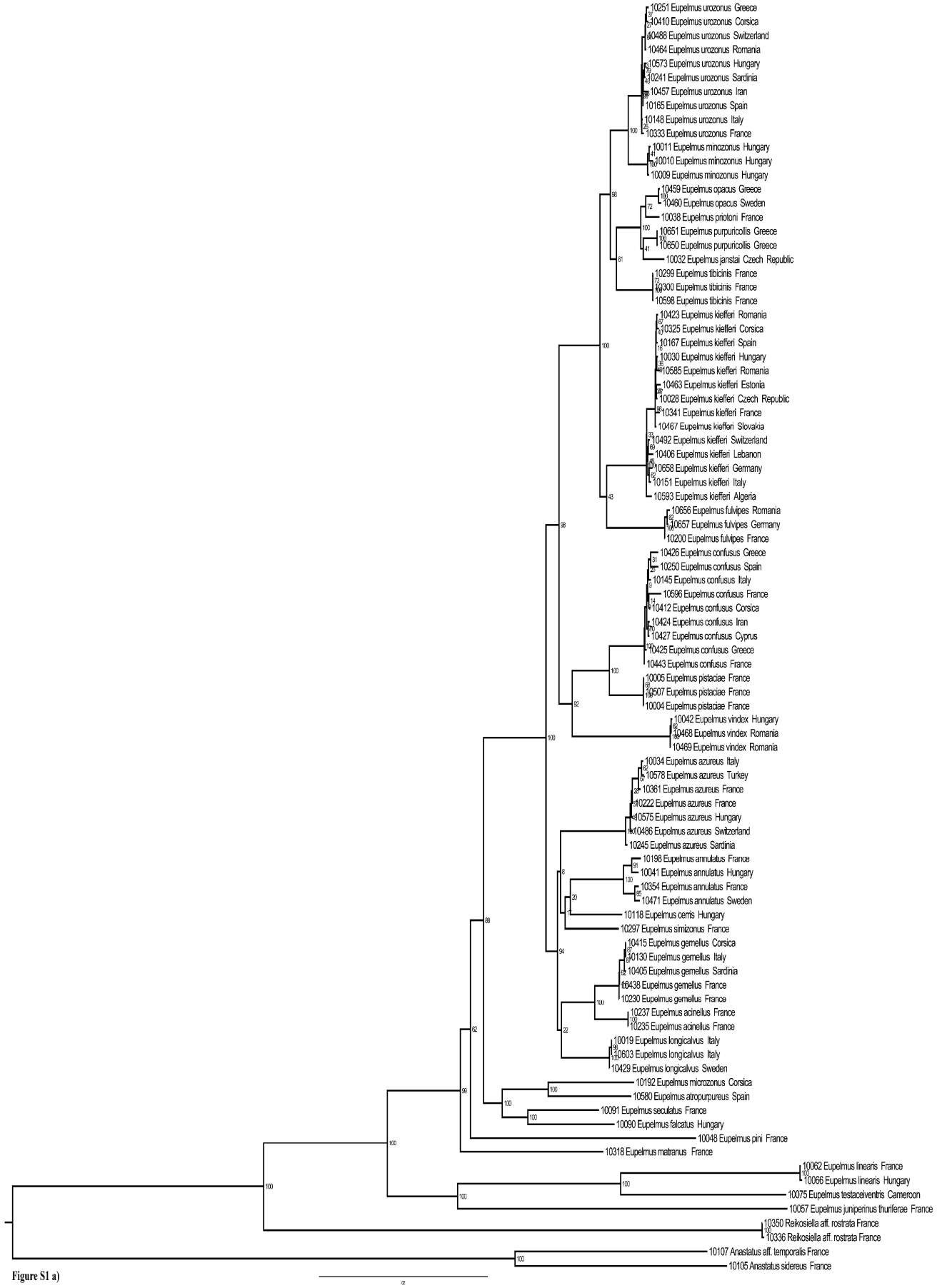

Additional file 2: Figure S1a Tree from the ml analysis of the combined dataset (without gblocks cleaning, 9 partitions). Likelihood bootstrap values are indicated at nodes.

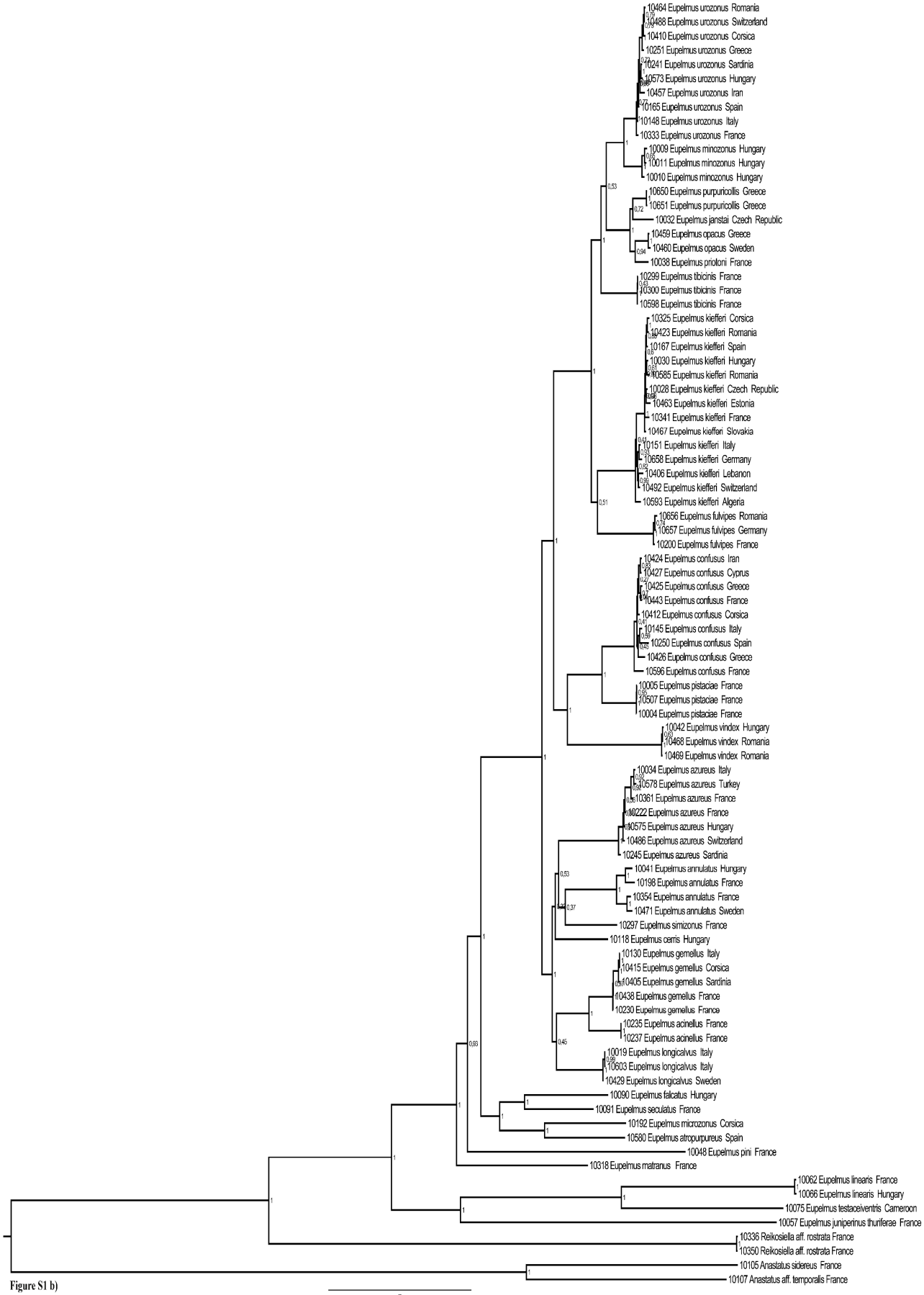

Additional file 2: Figure S1b tree from the bayesian analysis of the combined dataset (without gblocks cleaning, 9 partitions). Posterior probabilities are indicated at nodes.

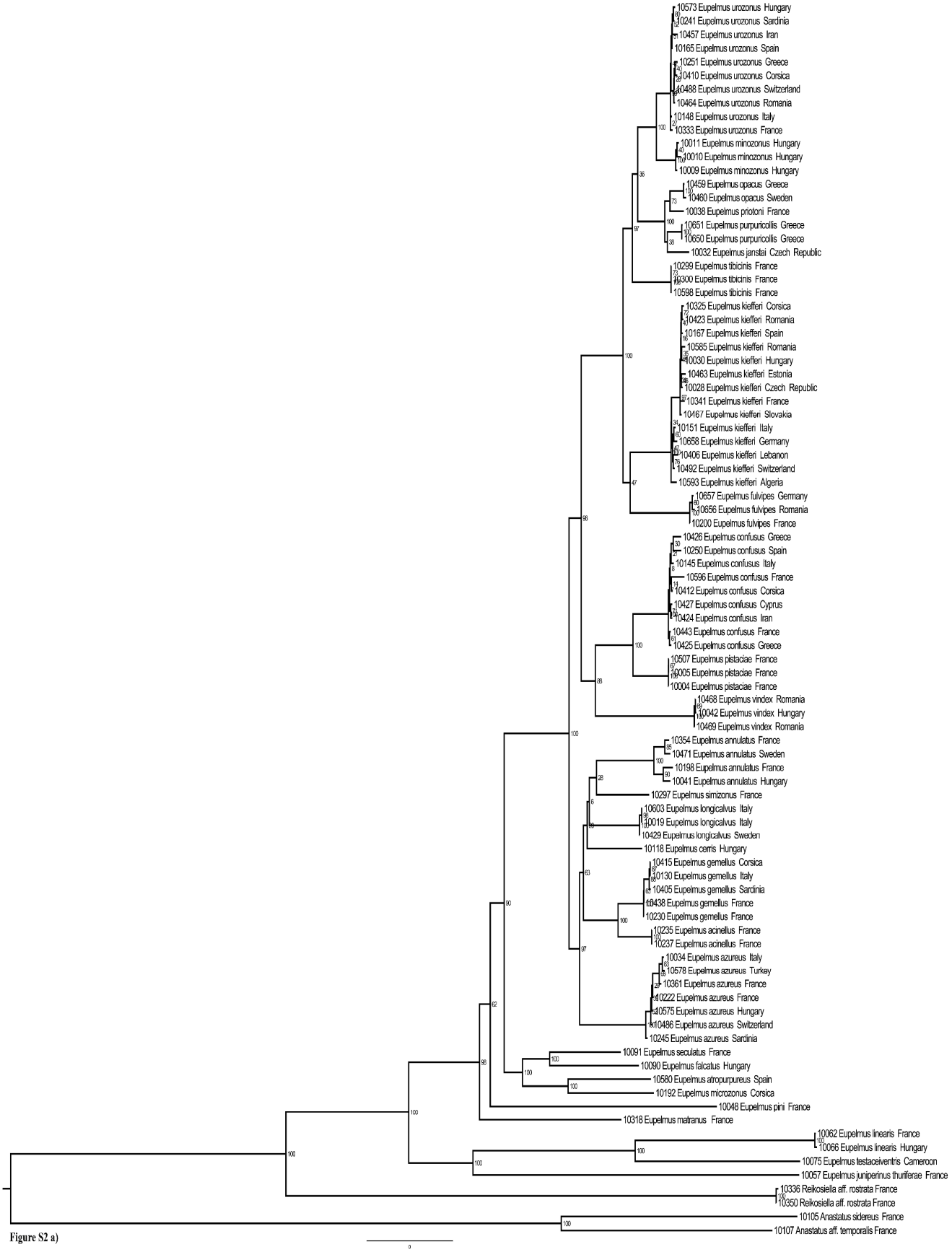

Additional file 2: Figure S2a Tree from the ML analysis of the combined dataset (without Gblocks cleaning, 7 partitions). Likelihood bootstrap values are indicated at nodes.

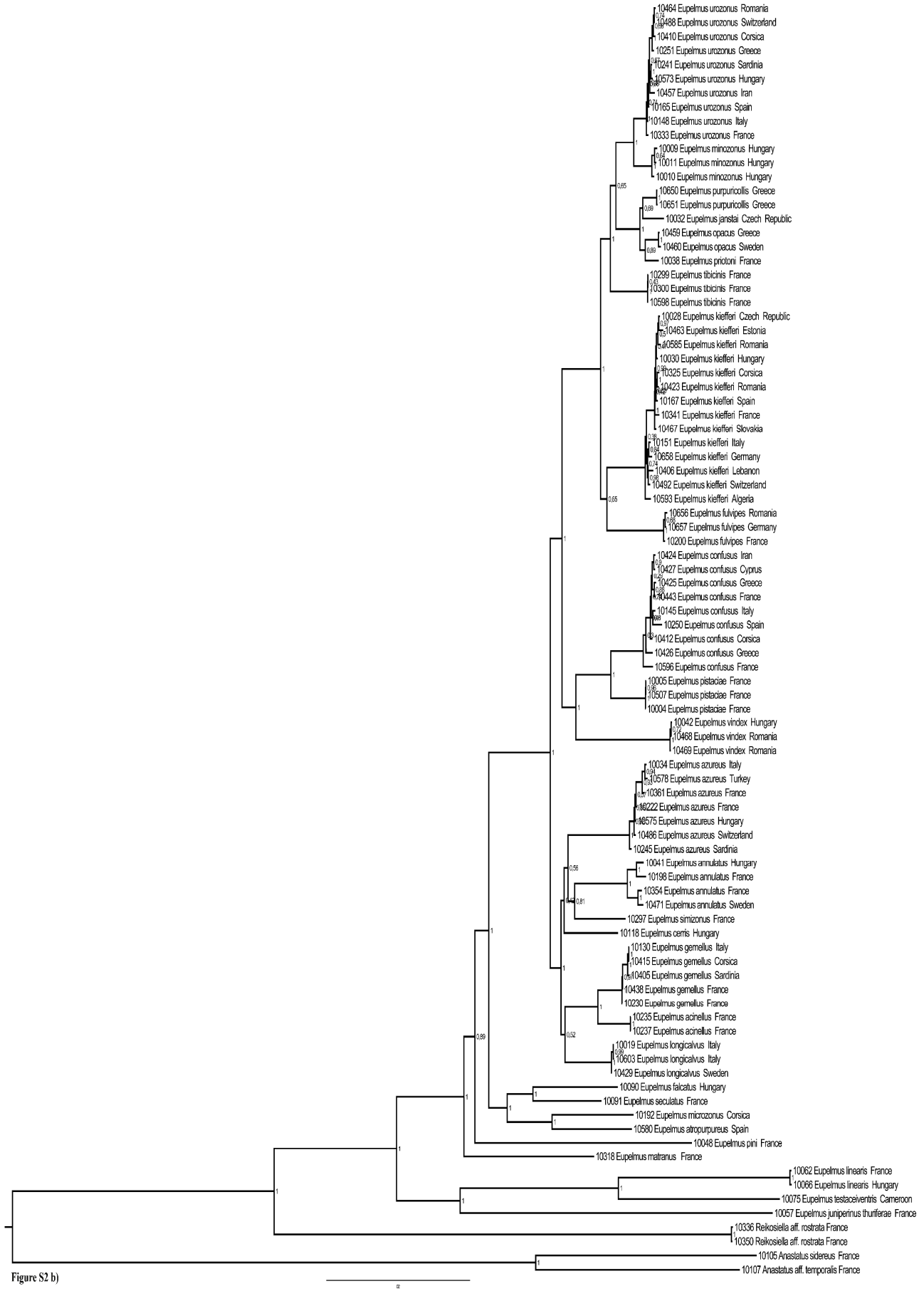

Additional file 2: Figure S2b Tree from the Bayesian analysis of the combined dataset (without Gblocks cleaning, 7 partitions). Posterior probabilities are indicated at nodes

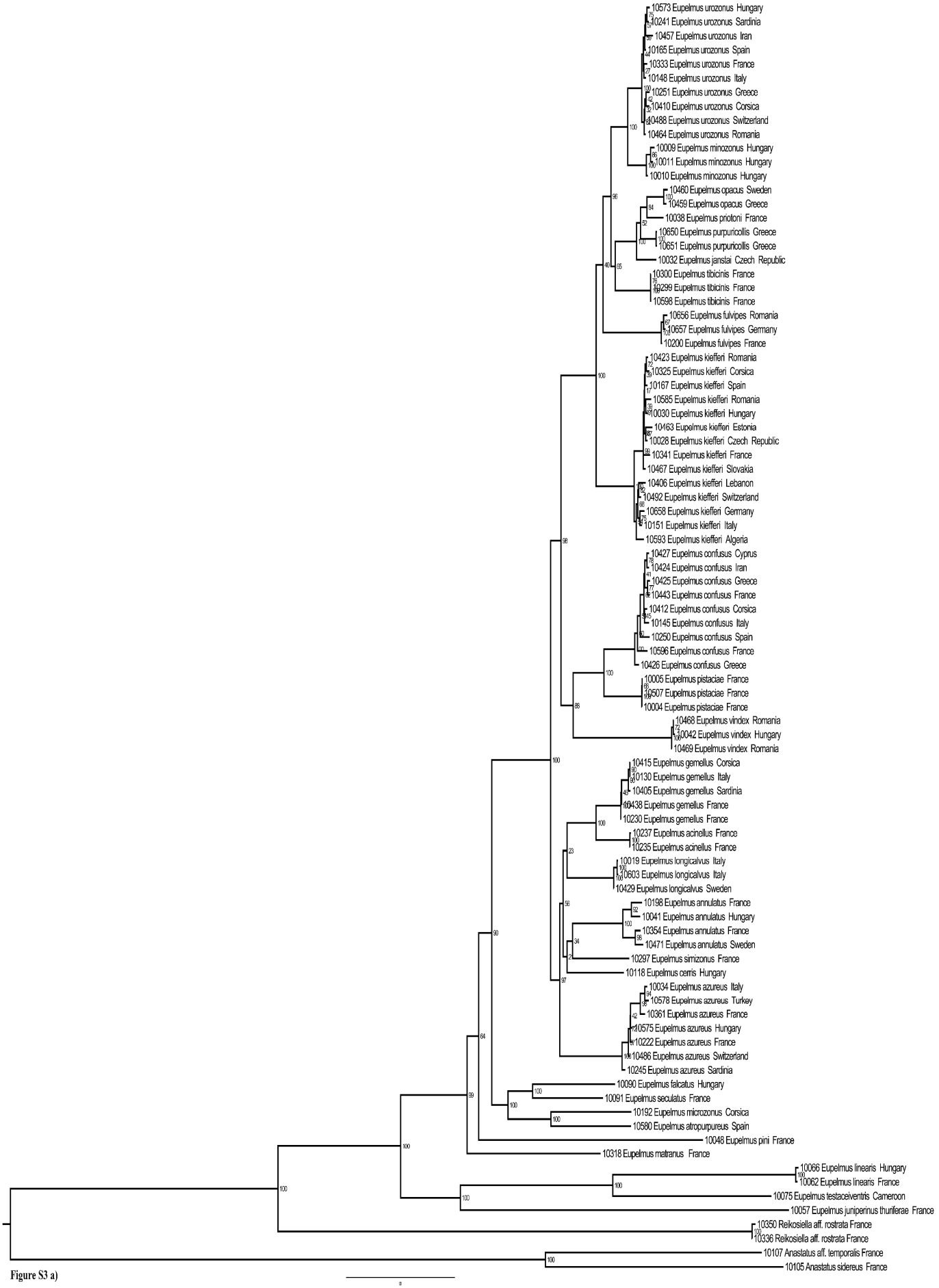

Figure S3 a)

Additional file 2: Figure S3a Tree from the ML analysis of the combined dataset (without Gblocks cleaning, 6 partitions). Likelihood bootstrap values are indicated at nodes.

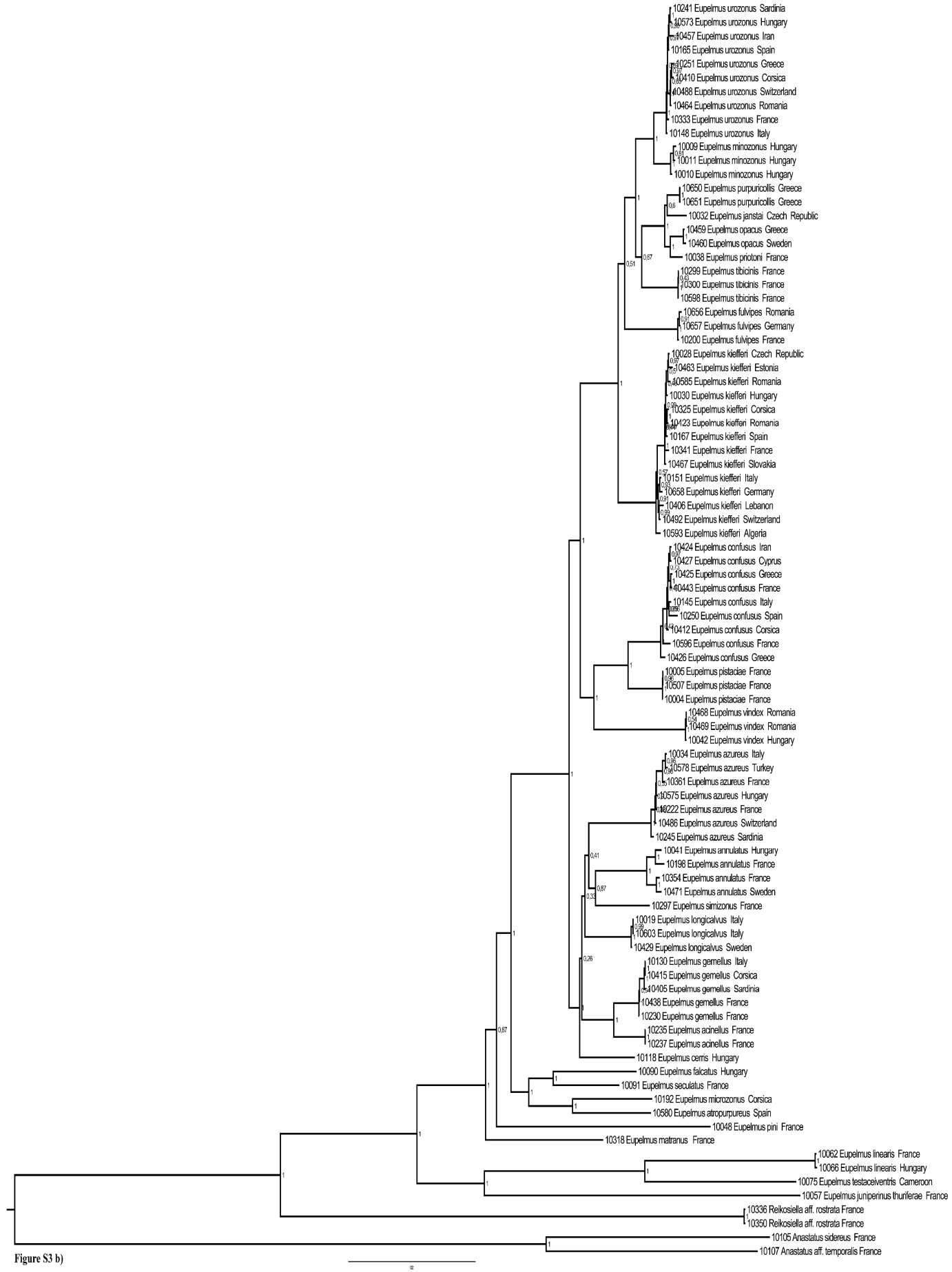

Additional file 2: Figure S3b Tree from the Bayesian analysis of the combined dataset (without Gblocks cleaning, 6 partitions) Posterior probabilities are indicated at nodes.

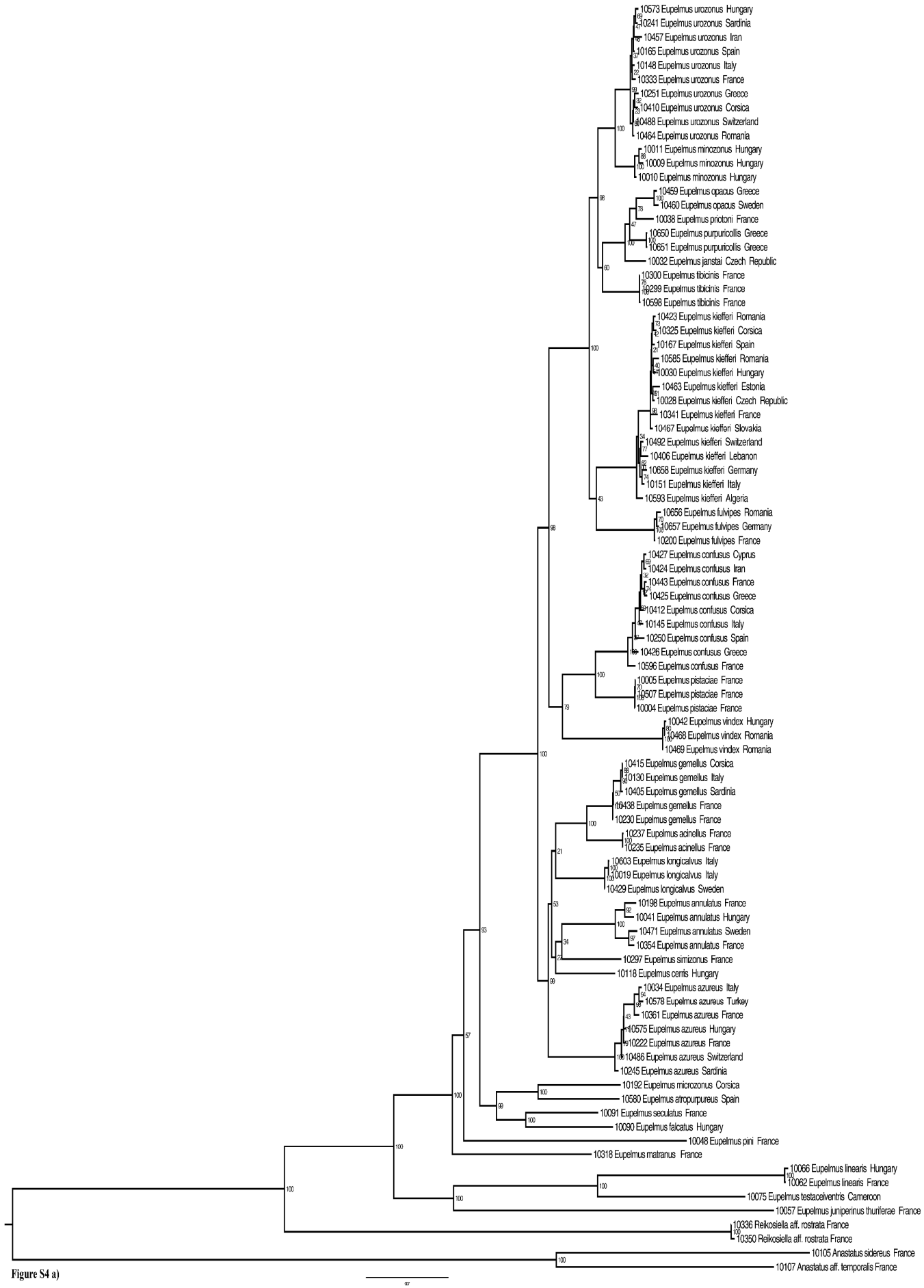

Additional file 2: Figure S4a Tree from the ML analysis of the combined dataset (without Gblocks cleaning, 2 partitions). Likelihood bootstrap values are indicated at nodes.

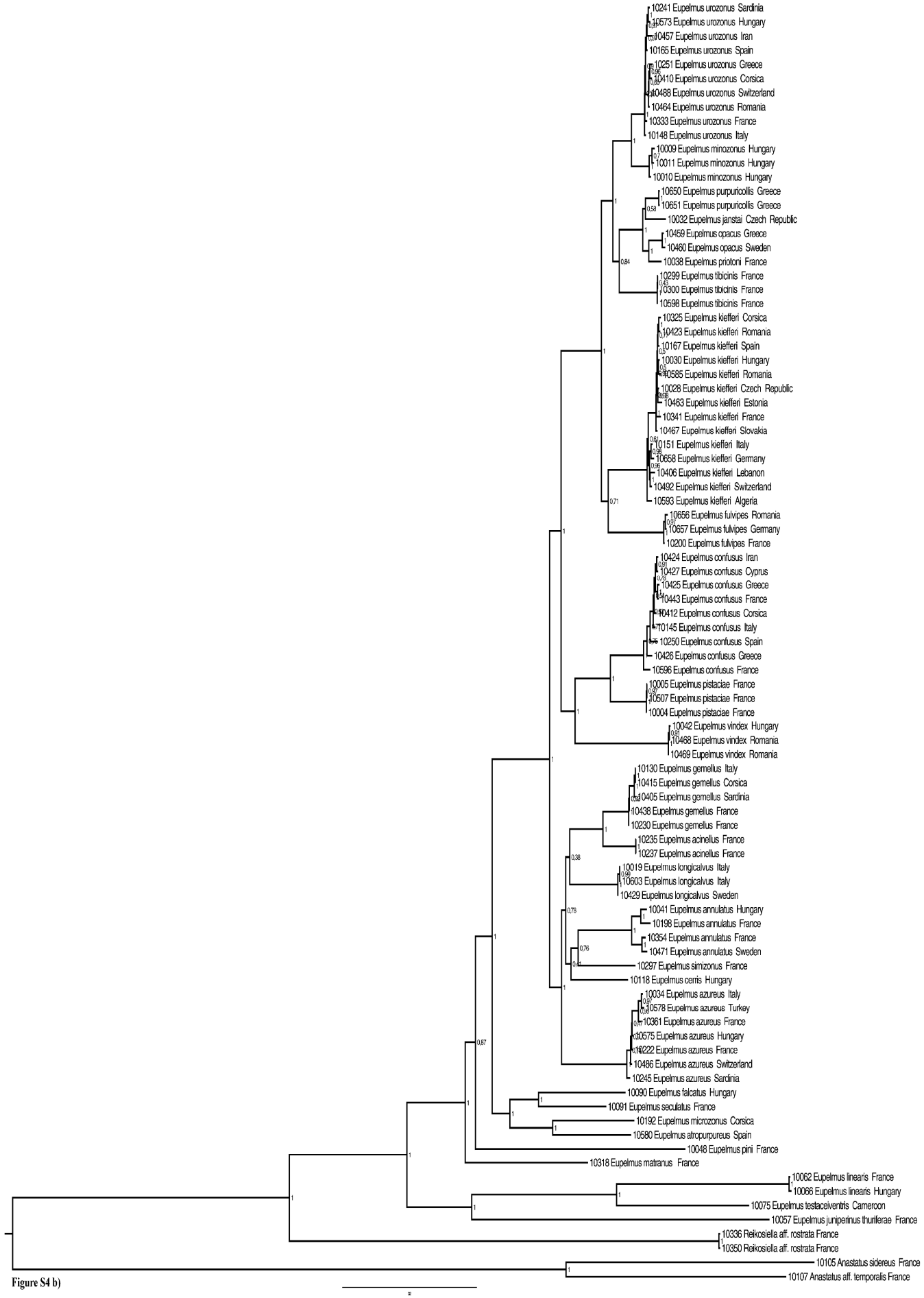

Additional file 2: Figure S4b tree from the Bayesian analysis of the combined dataset (without Gblocks cleaning, 2 partitions). Posterior probabilities are indicated at nodes.

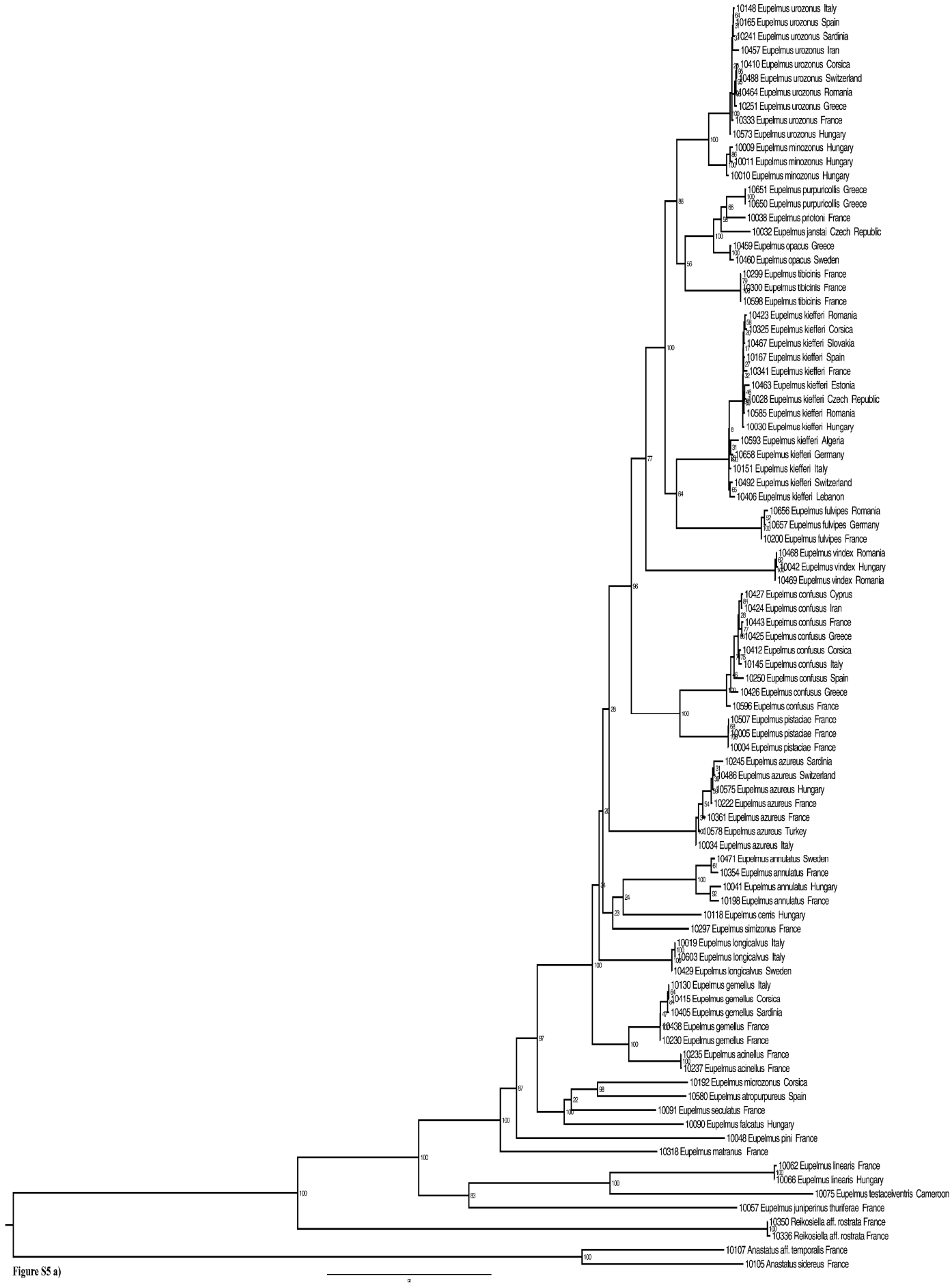

Additional file 2: Figure S5a Tree from the ML analysis of the combined dataset (with Gblocks-default parameters, 9 partitions). Likelihood bootstrap values are indicated at nodes.

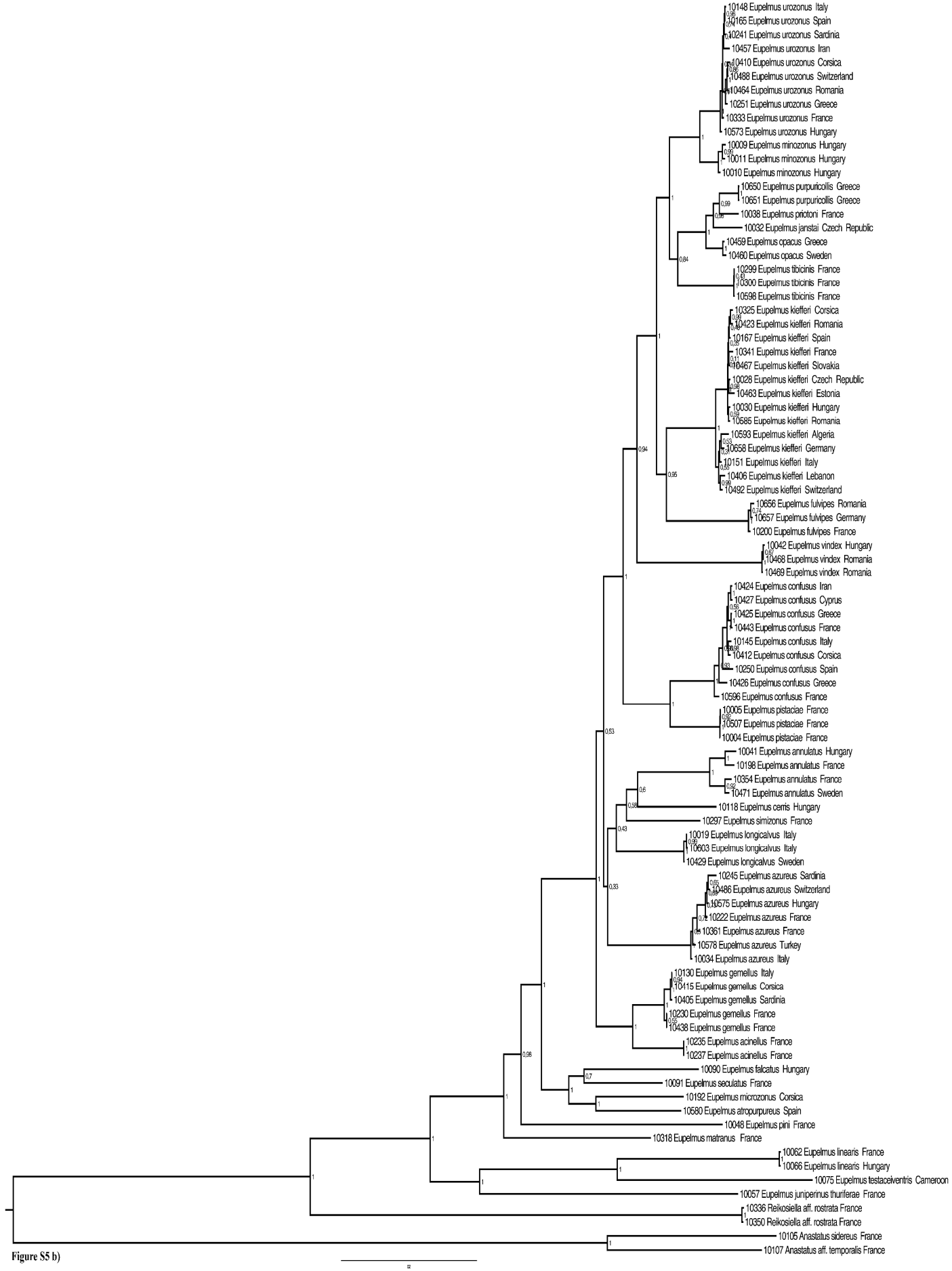

Additional file 2: Figure S5b Tree from the Bayesian analysis of the combined dataset (with Gblocks-default parameters, 9 partitions). Posterior probabilities are indicated at nodes.

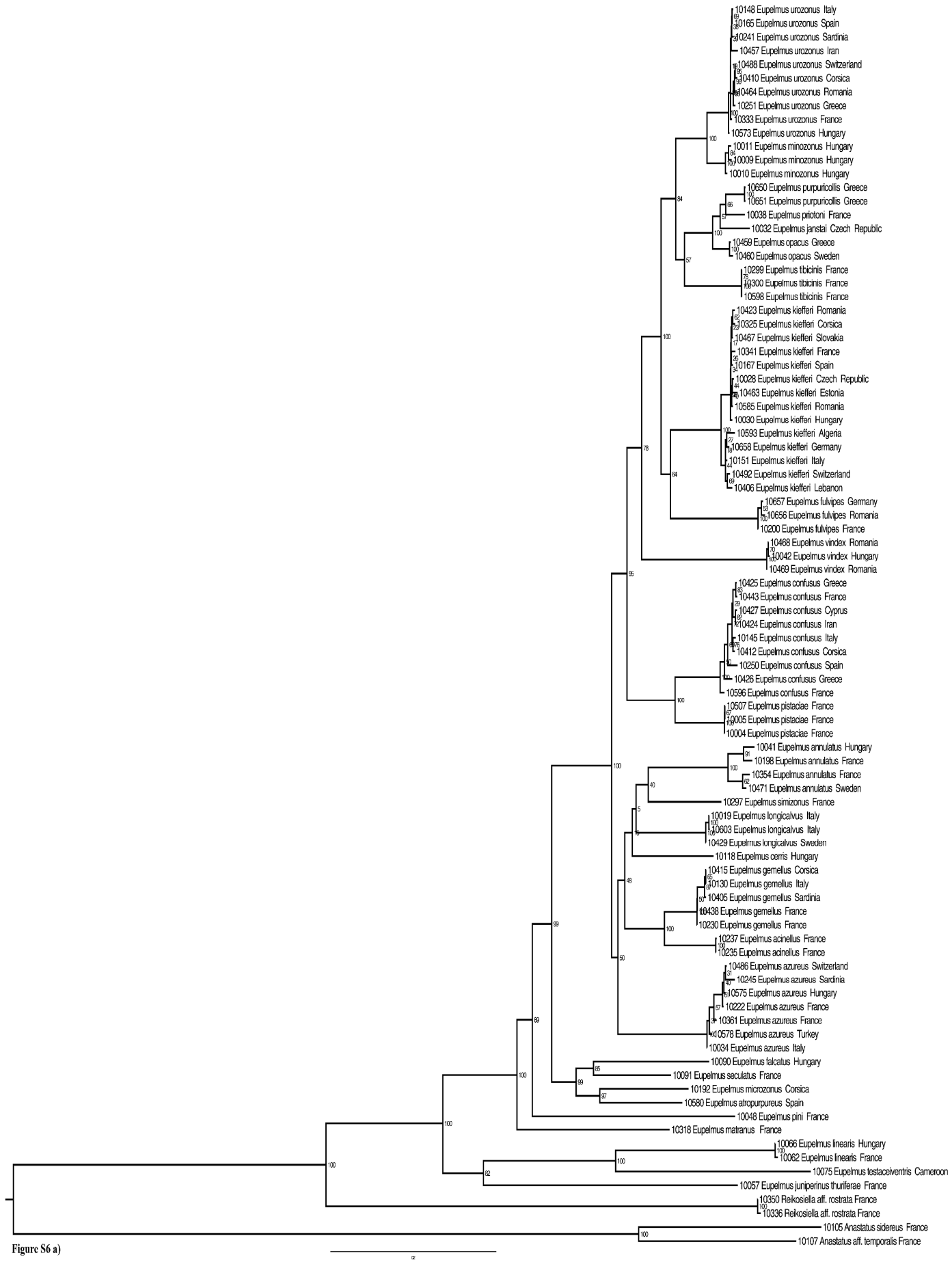

Additional file 2: Figure S6a Tree from the ML analysis of the combined dataset (with Gblocks-default parameters, 7 partitions). Likelihood bootstrap values are indicated at nodes.

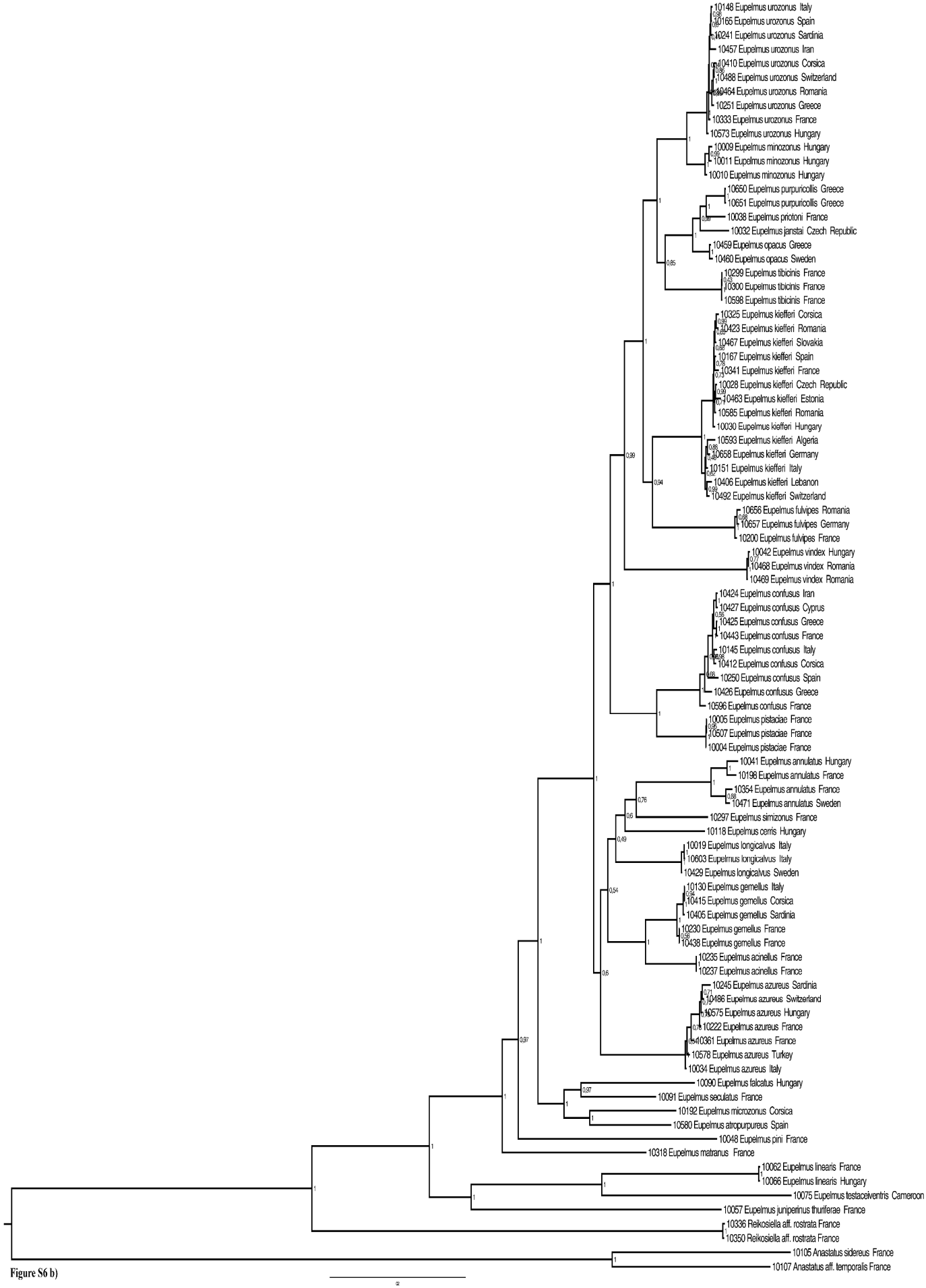

Additional file 2: Figure S6b Tree from the Bayesian analysis of the combined dataset (with Gblocks-default parameters, 7 partitions). Posterior probabilities are indicated at nodes.

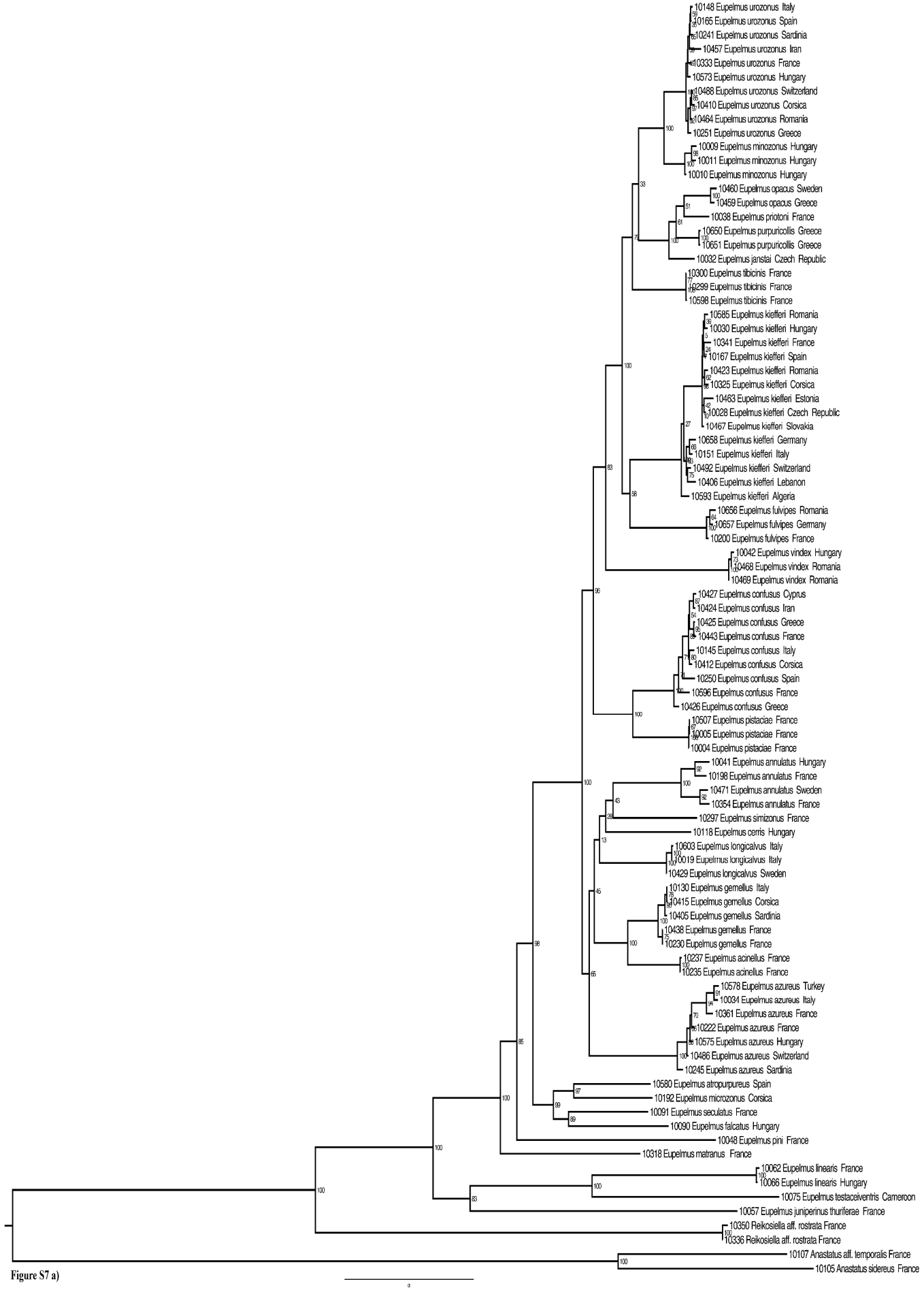

Additional file 2: Figure S7a Tree from the ML analysis of the combined dataset (with Gblocks-default parameters, 6 partitions). Likelihood bootstrap values are indicated at nodes.

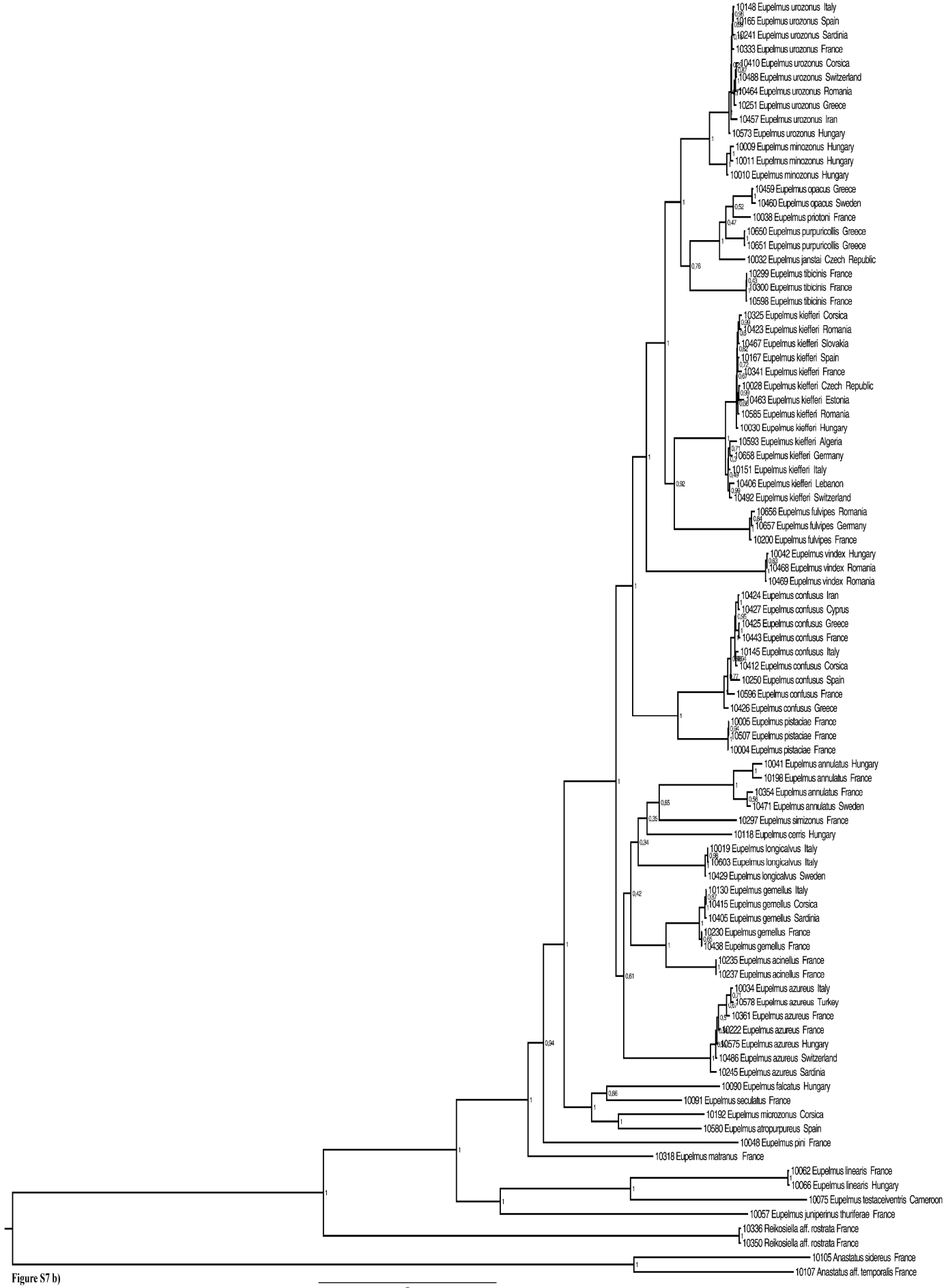

Figure S7 b)

Additional file 2: Figure S7b Tree from the Bayesian analysis of the combined dataset (with Gblocks-default parameters, 6 partitions). Posterior probabilities are indicated at nodes.

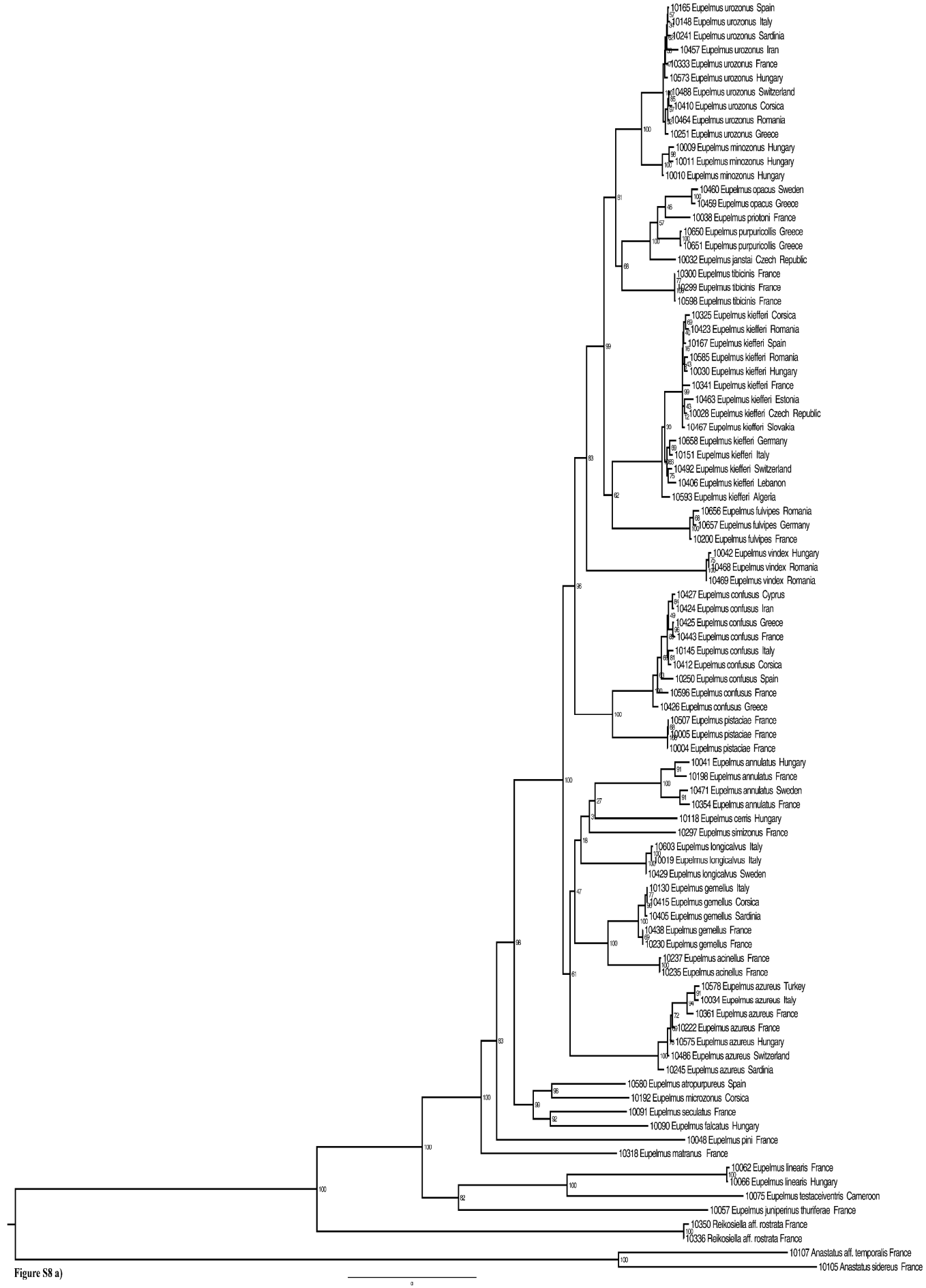

Figure S8 a)

Additional file 2: Figure S8a Tree from the ML analysis of the combined dataset (with Gblocks-default parameters, 2 partitions). Likelihood bootstrap values are indicated at nodes.

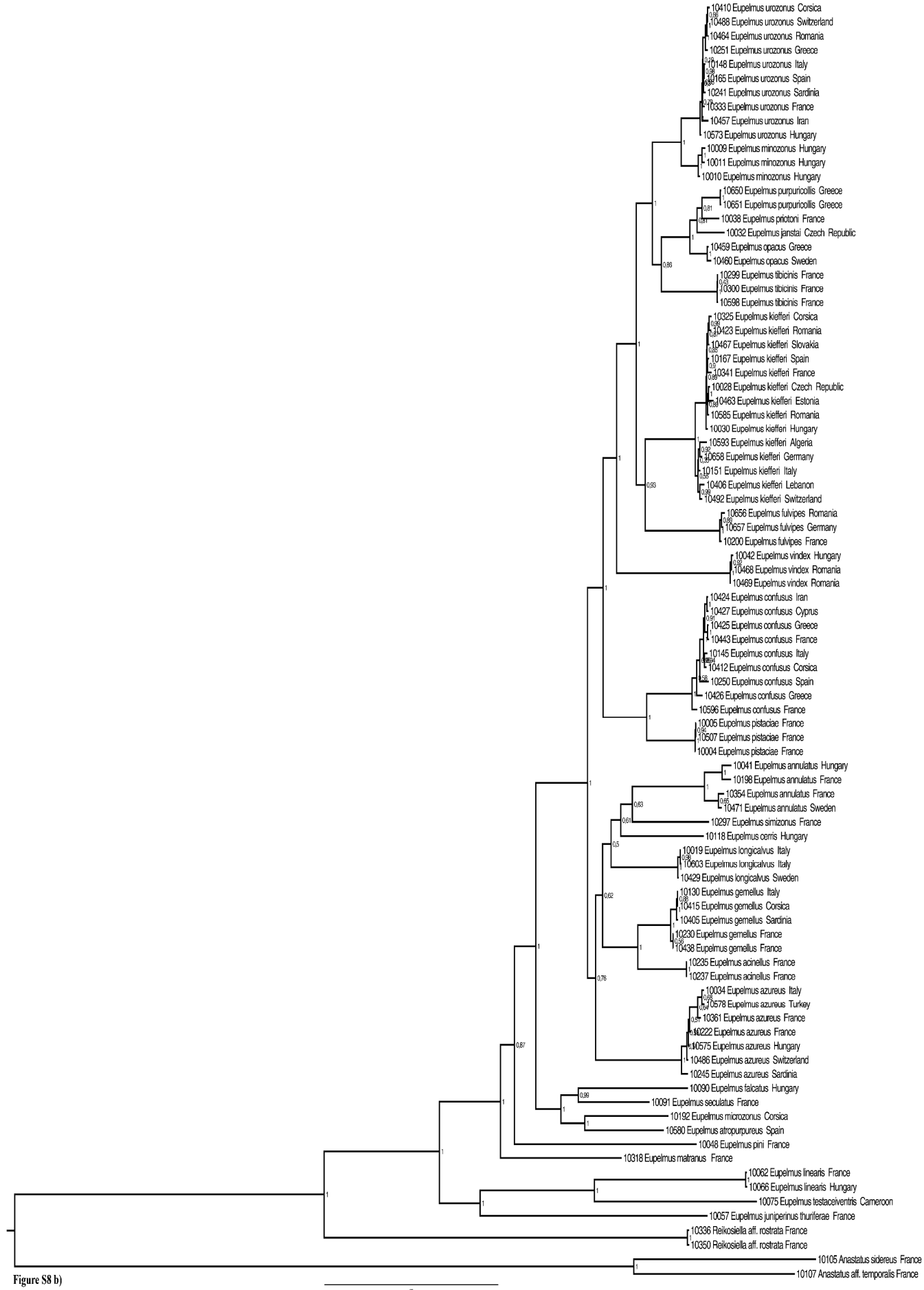

Additional file 2: Figure S8b Tree from the Bayesian analysis of the combined dataset (with Gblocks-default parameters, 2 partitions). Posterior probabilities are indicated at nodes.

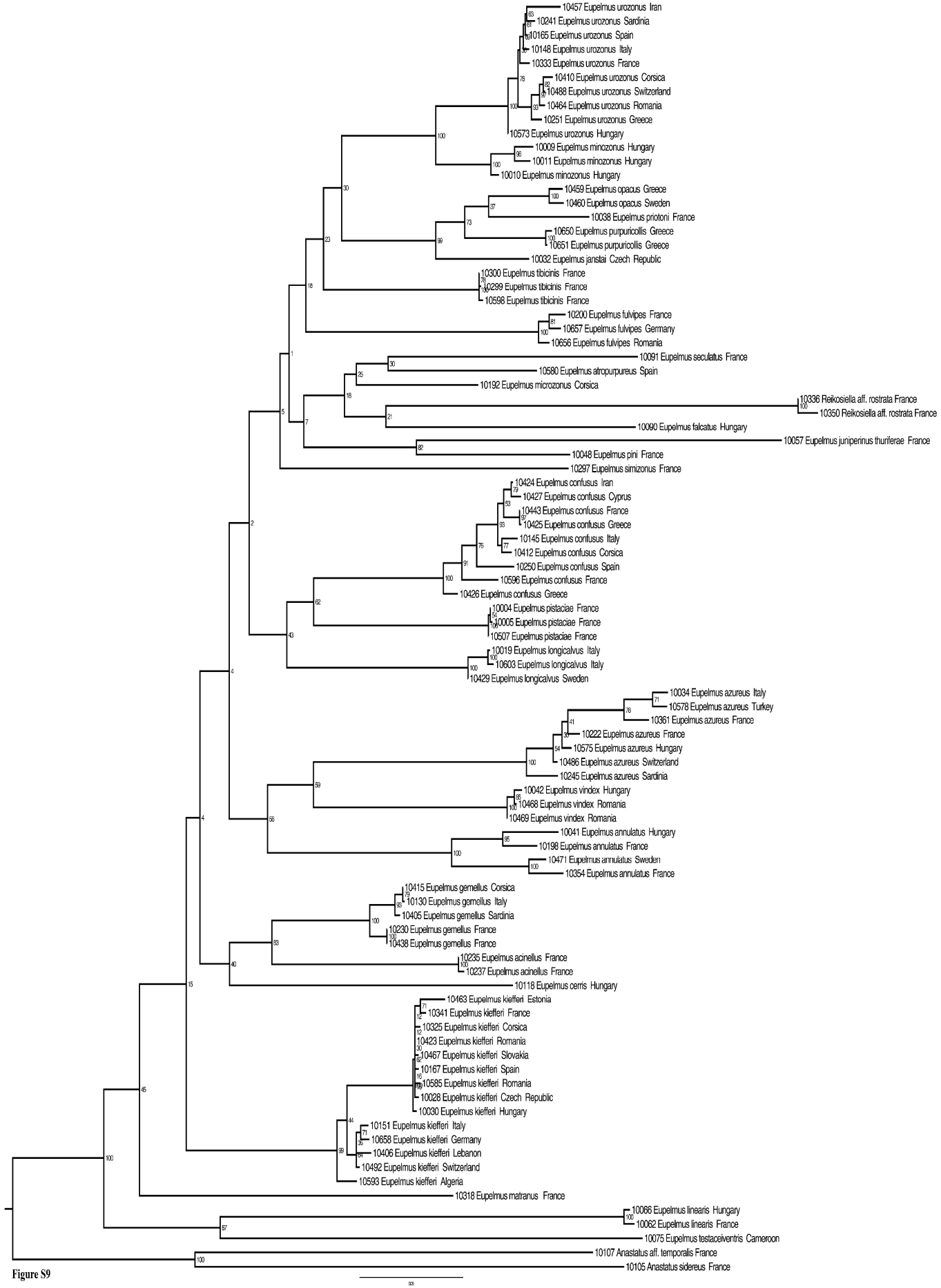

Figure S9

Additional file 2: Figure S9 Tree from the ML analysis of the mitochondrial partition. Likelihood bootstrap values (1000 replicates) and posterior probabilities are indicated at nodes.

Figure S10

Additional file 2: Figure S10 Tree from the ML analysis of the *Wg* locus. Likelihood bootstrap values (1000 replicates) and posterior probabilities are indicated at nodes.

Additional file 2: Figure S11 Tree from the ML analysis of the *EF-1Ū* locus. Likelihood bootstrap values (1000 replicates) and posterior probabilities are indicated at nodes.

Figure S12

Additional file 2: Figure S12 Tree from the ML analysis of the *Bub3* locus (without Gblocks cleaning). Likelihood bootstrap values (1000 replicates) and posterior probabilities are indicated at nodes.

Figure S13

Additional file 2: Figure S13 Tree from the ML analysis of the *Bub3* locus (with Gblocks-default parameters). Likelihood bootstrap values (1000 replicates) and posterior probabilities are indicated at nodes.

Additional file 2: Figure S14 Tree from the ML analysis of the *RpS4* locus (without Gblocks cleaning). Likelihood bootstrap values (1000 replicates) and posterior probabilities are indicated at nodes.

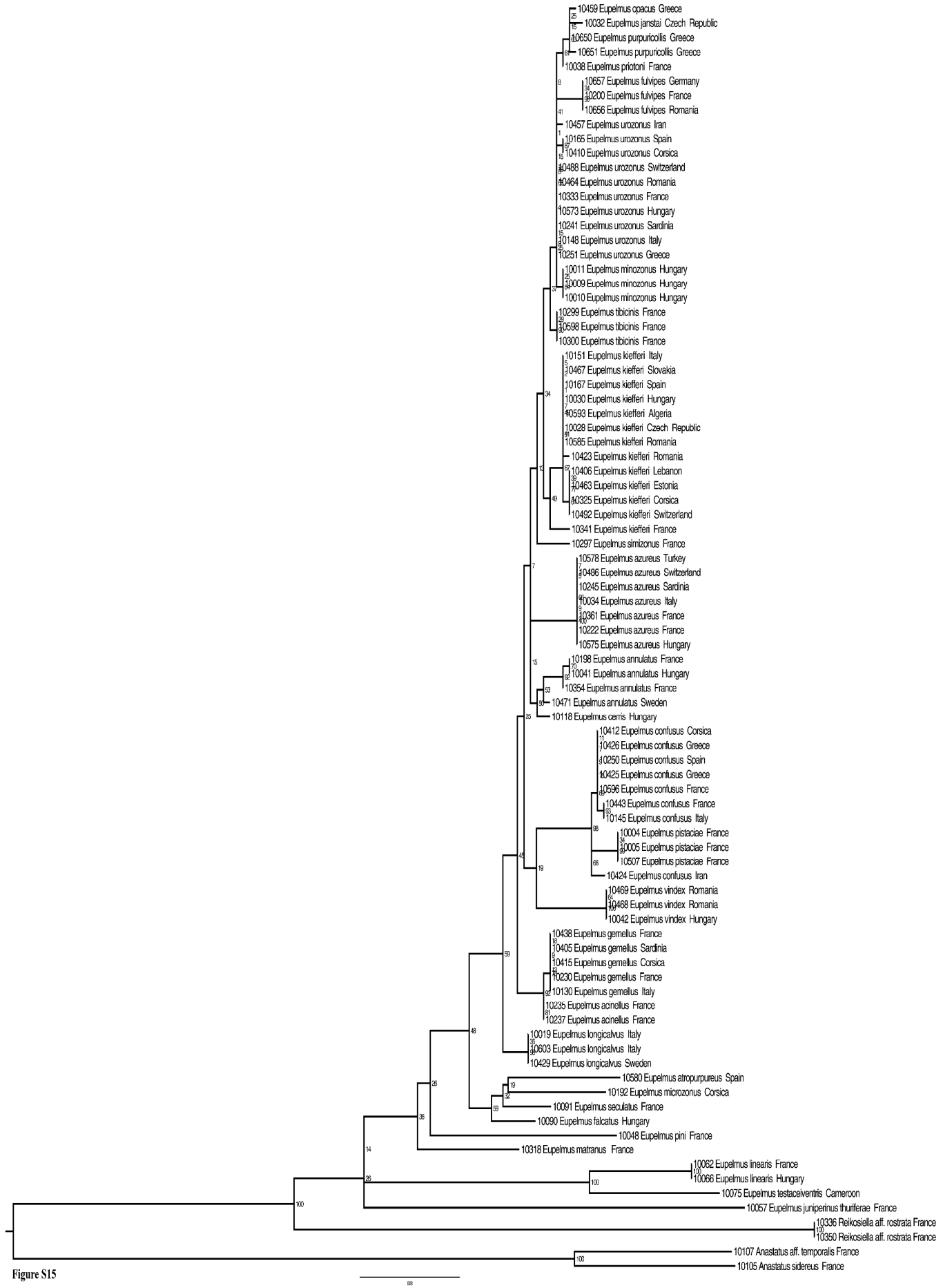

Additional file 2: Figure S15 Tree from the ML analysis of the *RpS4* locus (with Gblocks-default parameters). Likelihood bootstrap values (1000 replicates) and posterior probabilities are indicated at nodes.

Figure S16

Additional file 2: Figure S16 Tree from the ML analysis of the *RpL27a* locus (without Gblocks cleaning). Likelihood bootstrap values (1000 replicates) and posterior probabilities are indicated at nodes.

Additional file 2: Figure S17 Tree from the ML analysis of the *RpL27a* locus (with Gblocks-default parameters). Likelihood bootstrap values (1000 replicates) and posterior probabilities are indicated at nodes.

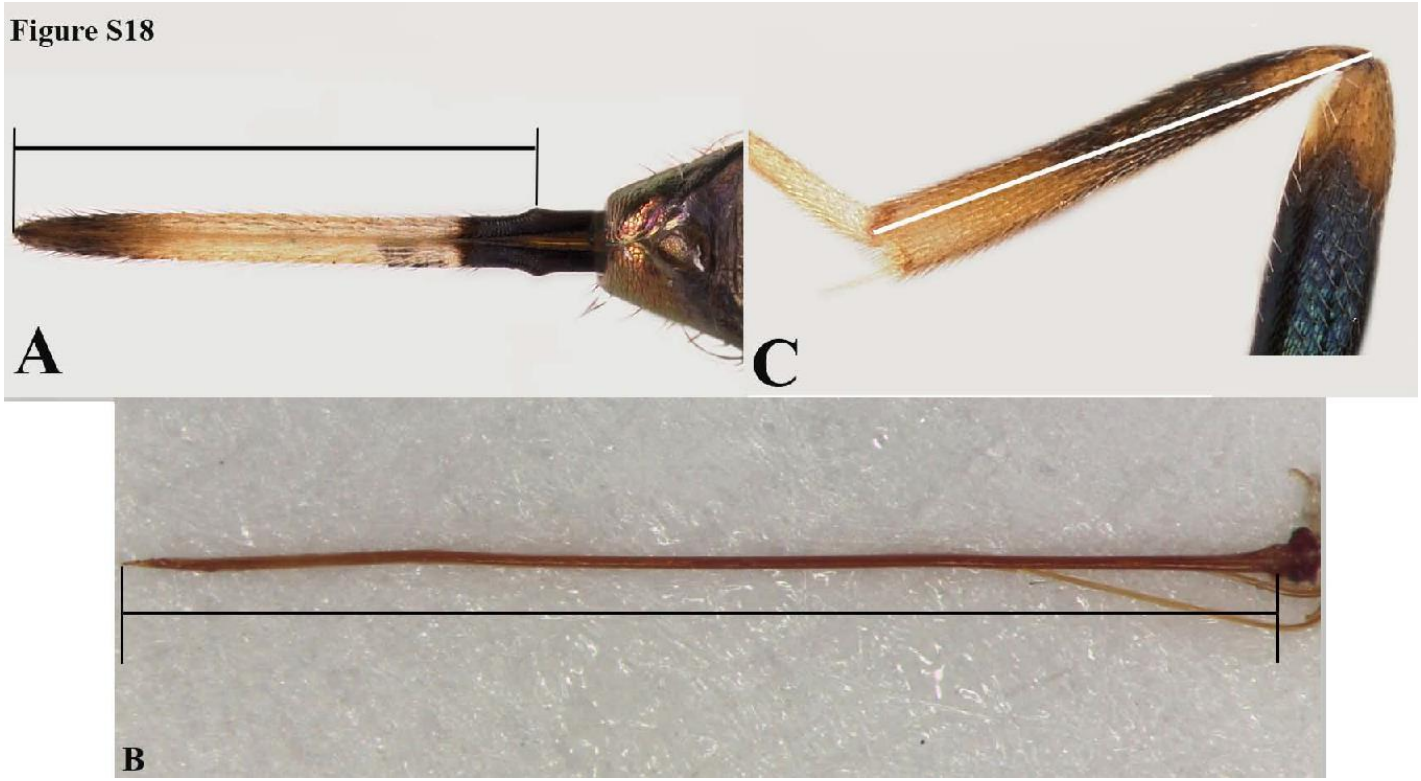

Additional file 2: Figure S18 Illustrations of morphometric measurements on Eupelmus females. (A) ovipositor sheaths, (B) ovipositor stylet (second and third pairs of valvulae), and (C) hind tibia

Additional file3: Table S4 Summary of information related to the detection of a phylogenetic signal (both host insects and plants).

Developmental ability	Distribution of states (no / yes)	D-statistics	p-value under a random distribution	p-value under a Brownian distribution
HOST INSECT				
Order's level				
Coleoptera	10 / 3	1.17	0.51	0.29
Diptera	8 / 5	1.26	0.55	0.17
Hymenoptera	3 / 10	-0.15	0.19	0.52
Lepidoptera	7 / 6	0.26	0.22	0.48
Family's level				
Cecidomyiidae (Dip.)	9 / 4	0.14	0.20	0.47
Cynipidae (Hym.)	4 / 9	0.66	0.33	0.42
HOST PLANT (Family's level)				
Asteraceae	9 / 4	0.91	0.42	0.32
Fagaceae	4 / 9	1.67	0.68	0.12
Rosaceae	8 / 5	1.06	0.48	0.23
Salicaceae	9 / 4	1.61	0.68	0.13

Additional file 4: Table S3 Summary of Mantel tests used for the comparative analysis dealing with host insects

Phylogeny	**Morphology**	**Ecology**			**Mantel r**	**p-value**
phylogenetic distances	AOS/ROS	Host species	Host family	Host order		
Simple Mantelós test						
Extended dataset (19 *Eupelmus* species)						
X	AOS				0.09	0.39
X	ROS				0.08	0.44
Restricted dataset (13 *Eupelmus* species)						
X		X			0.02	0.85
X			X		0.01	0.93
X				X	-0.01	0.91
	AOS	X			0.14	0.33
	AOS		X		-0.06	0.68
	AOS			X	-0.02	0.91
	ROS	X			0.14	0.34
	ROS		X		-0.06	0.68
	ROS			X	-0.02	0.92
Partial Mantelôs test (13 *Eupelmus* species)						
X	AOS	X			-0.02	0.89
X	AOS		X		0.03	0.81
X	AOS			X	-0.01	0.96
X	ROS	X			0.14	0.34
X	ROS		X		0.03	0.81
X	ROS			X	-0.01	0.96

Additional file 5: Table S5 Summary of Mantel tests used for the comparative analysis dealing with host plants**.**

	Phylogeny	**Morphology** AOS/ROS	**Ecology** (host plant at family's level)	**Mantel r**	**p-value**
Simple Mantelós test					
	X		X	0.08	0.45
		AOS	X	0.02	0.86
		ROS	X	0.02	0.88
Partial Mantelôs test					
	X	AOS	X	0.08	0.48
	X	ROS	X	0.08	0.51

5. Partie III: Caractérisation morphologique et moléculaire des espèces paléarctiques appartenant au groupe *ñE. urozonusò* et au complexe ñ*E. vesicularisò*

Article 3: An integrative approach to species discrimination in the *Eupelmus urozonus* complex (Hymenoptera, Eupelmidae), with the description of 11 new species from the Western Palaearctic. Systematic Entomology, **(2014), 39, 806ï 862.**

Article 4: Availability of eleven species names of *Eupelmus* (Hymenoptera, Eupelmidae) proposed in Al khatib *et al*. (2014). ZooKeys, **(2015), 505, 137ï 145.**

Article 5: An integrative approach to species differentiation in the "*vesicularis* complex" (Eupelmidae), with the description of two new species from Europe. **En préparation**.

Présentation des articles 3, 4 et 5

Dans cette partie, nous avons mis en évidence les apports de la combinaison de multiples caractères taxonomiques dans une seule approche dite de "taxonomie intégrative" afin de résoudre des relations phylogénétiques inférieures (= superficielles) et de clarifier les limites entre des taxons morphologiquement très semblables et/ou phylogénétiquement proches. La taxonomie intégrative a en effet été proposée comme une méthode ayant une grande fiabilité dans la différenciation des espèces très proches voire cryptiques (Schlick-Stieiner *et al.*, 2009; Padial *et al.*, 2010; Gebiola *et al.*, 2012; Delvare *et al.*, 2014; Lecocq *et al.*, 2015). Deux "complexes" ont retenu notre attention, le complexe "*urozonus*" (articles 3 & 4) et le complexe "*vesicularis*" (article 5).

Chronologiquement, il faut noter que ces travaux ont débuté avant la clarification de la structuration du genre *Eupelmus* présentée dans la Partie I et donc avant la mise en évidence des groupes d'espèces "*urozonus*" et "*vesicularis*" qui incluent respectivement les espèces de chacun des complexes initiaux. Pour chacun de ces deux complexes, deux types de marqueurs ont été combinés, des caractères morphologiques et des marqueurs moléculaires incluant au moins un gène nucléaire (*Wingless*) et au moins un gène mitochondrial (*COI*).

Concernant le complexe *urozonus*, plus de 300 spécimens (♀ & ♂) ont été échantillonnés en Europe et dans quelques pays méditerranéens sur divers insectes-hôtes et plante-hôtes. Une identification préliminaire a été réalisée en utilisant les clés disponibles d'identification des espèces du genre *Eupelmus* (Kalina, 1988; Askew & Nieves-Aldrey, 2000 ; Gibson, 2011 ; Gibson & Lucian, soumis) tandis que les individus ont été parallèlement séquencés sur deux gènes (*COI* & *Wg*), ces deux gènes étant analysés par la méthode des distances ou des approches probabilistes – Maximum de Vraisemblance et Inférence Bayésienne. Globalement, nous avons mis en évidence une bonne concordance concernant le nombre de clades détectés par *COI* et de *Wg*, à l'exception de 3 couples non différenciés sur *Wg* (*E. gemellus* ï *E. acinellus*; *E. kiefferi* ï *E. fulvipes*; *E. janstai* ï *E. priotoni* ï *E. purpuricollis*). Le nombre de clades observés du point de vue moléculaire étaient initialement supérieurs à ceux identifiés par les clés. Toutefois, après utilisations de caractères supplémentaires, une bonne concordance a été a posteriori observée entre les deux approches. Au final, nos résultats ont ainsi permis de : (i) confirmer la validité de 7 espèces déjà identifiés (*E. acinellus*, *E. annulatus*, *E. azueus*, *E. cerris*, *E. martellii*, *E. tibicinis*, *E. urozonus*); (ii) lever la synonymie entre deux taxons (*E. fulvipes* et *E. kiefferi*); (iii) décrire sur des bases morphologiques et

moléculaires, 11 nouvelles espèces (*E. confusus*, *E. gemellus*, *E. janstai*, *E. longicalvus*, *E. minozonus*, *E. opacus*, *E. pistaciae*, *E. priotoni*, *E. purpuricollis*, *E. simizonus* et *E. tremulae*). Ce travail permet donc de résoudre ce qui était perçu initialement comme un « complexe » et nous avons fourni une clé illustrée pour la reconnaissance morphologique des femelles et, parfois, des mâles pour 21 espèces ce qui permet de lever l'ambigüité et, éventuellement, mieux comprendre les confusions commises auparavant.

Concernant le complexe *vesicularis*, l'échantillonnage des spécimens a été effectué en Europe (France, Hongrie, Italie, Moldavie, Romanie, Slovaquie, Espagne et Suède) et au Canada, par fauchage et récolte de galles provoquées par des Cynips ou Téphritides. 84 individus ont été séquencés pour 2 gènes mitochondriaux (*COI & Cytb*) et 4 gènes nucléaires (*ITS2*, *EF-1a*, *RpL27a & Wg*) et environs 140 spécimens ont été examinés afin de relever leurs caractères morphologiques.-La discrimination des espèces a été réalisée en utilisant plusieurs approches: (i) l'approche phylogénétique en reconstruisant les arbres phylogénétiques individuels pour chacun des marqueurs utilisés et l'arbre combiné pour les 4 gènes nucléaires avec les méthodes de ML et BI; (ii) l'approche basée sur les distances génétiques calculées au niveau des séquences du gène *COI*, en utilisant deux modèles: SpeciesIdentifier of TAXONDNA et Automated Barcode Gap Discovery (ABDGD); (iii) l'approche basée sur l'hypothèse de la coalescence en utilisant la méthode de GMYC (Generalized Mixed Yule Coalescent) toujours au niveau du gène *COI*; (iv) l'approche basée sur la quantification de l'exclusivité généalogique sur l'ensemble des gènes nucléaires; et (iii) la caractérisation morphologique. D'un point de vue méthodologique, l'analyse du gène *ITS2* a été compliquée du fait de la présence de pseudogènes que nous avons tenté d'éliminer à partir d'une estimation de leur structure secondaire et de leur énergie libre en utilisant le serveur web "*mfold*" (Zuker, 2003). Au niveau phylogénétique, des discordances ont été observées entre les marqueurs mitochondriaux qui mettent tous deux en évidence 10 clades et les marqueurs nucléaires combinés, mettent seulement 5 clades en évidence. Les différentes topologies supportent la monophylie de 4 clades, représentant chacun une espèce, à savoir *E. vesicularis* lui-même, *E. albitarsis* Costa, *E. messene* et *E. vesimodicus* sp. n.) Au contraire, des divergences existent au niveau du clade appelé ***ñE. baraiò,*** non différenciés au niveau des marqueurs nucléaires (arbre combiné) mais structuré en six clades (*G1* à *G6*) sur les marqueurs mitochondriaux. Une deuxième source de discordances concerne les caractères moléculaires et les caractères morphologiques, ces derniers supportant plutôt la structuration observée sur marqueurs nucléaires. En effet, bien que le clade identifié comme *E. vesimodicus* soit supporté

moléculairement comme une lignée monophylétique avec les marqueurs utilisée, l'espèce est très difficile voire impossible à différencier de *E. vesicularis*. D'autre part, à l'exception des clades *G4* et *G5*, aucune différence morphologique n'a pu être trouvée entre les autres rameaux du "groupe *barai*" (groupes *G1-G6*). Par ailleurs, le nombre d'espèces putatives évalué via les distances génétiques ou la coalescence au niveau du gène *COI* a montré une grande variabilité suivant les paramètres choisis au départ, doublée d'une surestimation déraisonnable, d'une part par rapport aux gènes nucléaires, d'autre part en regard des données morphologiques. Ces approches se sont donc montrées inconciliables avec les autres champs de données et n'ont pas été retenues comme outils de délimitation des espèces. . Au niveau de la nomenclature, nos résultats amènent à revalider l'espèce *E. albitarsis* en la sortant de la synonymie avec *E. vesicularis*. Par ailleurs il est légitime de considérer les deux clades *G4* et *G5* comme deux espèces à part entière, décrites pour l'occasion sous les noms respectifs d'*Eupelmus maralpinus* et *Eupelmus myopitae*, tandis que nous sommes amenés à considérer et les autres clades *G1*, *G2* (d'Europe de l'Est) puis *G3* et *G6* (d'Europe Occidentale) comme appartenant à une seule et même espèce, décrite par ailleurs comme *Eupelmus barai* Fusu. Enfin, bien que morphologiquement similaires voire identiques *E. vesimodicus* et *E. vesicularis* sont génétiquement bien séparées et nous conduise à décrire la première.

En conclusion, l'ensemble de ces travaux met en évidence l'indéniable intérêt d'une démarche intégrative dans la caractérisation de la biodiversité. Dans les deux situations étudiées, elle a révélé une diversité insoupçonnée et procuré des outils pour la percevoir. Dans le cas particulièrement ardu du complexe *vesicularis*, où nous étions face à un ensemble de facteurs déroutants – dimorphisme sexuel peu banal, aptérisme des femelles, présence d'une espèce à parthénogénèse thélytoque, copies multiples d'un gène, spéciations récentes, etc. – cette approche intégrative, où d'autres types d'informations telles que écologie et distribution géographique sont aussi associées, fut la seule à pouvoir offrir une interprétation des faits et des résultats issus des modèles utilisés dans ce type de situation.

Systematic Entomology

Systematic Entomology (2014), **39**, 806–862

An integrative approach to species discrimination in the *Eupelmus urozonus* complex (Hymenoptera, Eupelmidae), with the description of 11 new species from the Western Palaearctic

FADEL AL KHATIB[1,2,3], LUCIAN FUSU[4], ASTRID CRUAUD[2], GARY GIBSON[5], NICOLAS BOROWIEC[1], JEAN-YVES RASPLUS[2], NICOLAS RIS[1] and GÉRARD DELVARE[3]

[1]INRA, UMR 1355 'Institut Sophia Agrobiotech', Sophia-Antipolis, France, [2]INRA, UMR 1062 CBGP, Campus International de Baillarguet, Montferrier-sur-Lez Cedex, France, [3]CIRAD, UMR 55 CBGP, Campus International de Baillarguet, Montferrier-sur-Lez Cedex, France, [4]Faculty of Biology, Alexandru Ioan Cuza University, Iasi, Romania and [5]Agriculture and Agri-Food Canada, Canadian National Collection of Insects, Arachnids and Nematodes, Ottawa, Canada

Abstract. The systematics of the European species of *Eupelmus* (*Eupelmus*) Dalman (Hymenoptera: Eupelmidae) belonging to the '*urozonus*-complex' is elucidated through combined molecular and morphological characterization. One mitochondrial gene fragment (*Cytochrome oxidase I*) and one nuclear protein-coding gene fragment (*Wingless*) were sequenced and the results compared with those of a detailed morphological study of the specimens from an extensive sampling. Knowledge of the biodiversity of *Eupelmus* in the Western Palearctic Region is significantly improved through the separation and description of 11 new species: *E.* (*Eupelmus*) *confusus* Al khatib **sp.n.**, *E. gemellus* Al khatib **sp.n.**, *E. janstai* Delvare & Gibson **sp.n.**, *E. longicalvus* Al khatib & Fusu **sp.n.**, *E. minozonus* Delvare **sp.n.**, *E. opacus* Delvare **sp.n.**, *E. pistaciae* Al khatib **sp.n.**, *E. priotoni* Delvare **sp.n.**, *E. purpuricollis* Fusu & Al khatib **sp.n.**, *E. simizonus* Al khatib **sp.n.** and *E. tremulae* Delvare **sp.n.** Illustrated keys to females and, when known, males of these new 11 species plus the other already described species considered to belong to the '*urozonus*-complex' (*E. acinellus* Askew, *E. annulatus* Nees, *E. azureus* Ratzeburg, *E. cerris* Förster, *E. fulvipes* Förster, *E. kiefferi* De Stefani, *E. martellii* Masi, *E. stenozonus* Askew, *E. tibicinis* Bouček and *E. urozonus* Dalman) are provided and all the species are described based on morphology. *Eupelmus kiefferi* is removed from synonymy under *E. urozonus* and *E. azureus* is recognized as the valid senior synonym of *Pteromalus cordairii* Ratzeburg, 1844 and *Eupelmus spongipartus* Förster, 1860 **syn.n.** The discrimination of the species included in this complex is particularly relevant because some are potential biological control agents and have been confused in the past.

This published work has been registered in ZooBank, http://zoobank.org/urn:lsid:zoobank.org:pub:F52CD199-C65F-43CC-B347-4E724096F2D5.

Correspondence: Fadel Al khatib, INRA, UMR 1355 'Institut Sophia Agrobiotech', 400 Route des Chappes, BP 167, 06903 Sophia-Antipolis, France. E-mail: fadel.alkhatib@sophia.inra.fr

Introduction

The superfamily Chalcidoidea (Hymenoptera) is a very large group with about 23 000 described species worldwide, although possibly more than 500 000 species exist (Munro *et al.*, 2011; Heraty *et al.*, 2013; Noyes, 2013). Currently, 22 families are recognized in the superfamily (Heraty *et al.*, 2013), whose members are generally very small insects that usually range from 1–4 mm, although some are up to 45 mm in length (Munro *et al.*, 2011). The combination of extreme taxonomic and morphological diversity, small size, presence of cryptic species and comparatively few taxonomists studying the group, make establishing systematics and the correct identification of species in the superfamily a real challenge.

Within the Chalcidoidea, Eupelmidae is a relatively small family with 45 extant genera and 907 described species (Noyes, 2013). The family is divided into three subfamilies: Eupelminae Walker, Calosotinae Bouček and Neanastatinae Kalina (Gibson, 1995). Within Eupelminae, Gibson (1995) divided the genus *Eupelmus* Dalman into three subgenera: *Eupelmus*, *Episolindelia* Girault and *Macroneura* Walker. Noyes (2013) listed 80 available valid names for *Eupelmus* in the Palaearctic region. Hosts of *Eupelmus* include various insect orders such as Coleoptera, Diptera, Hemiptera, Hymenoptera, Lepidoptera and Orthoptera. Species develop mostly as primary or secondary ectoparasitoids of larvae or pupae that are usually concealed within protected habitats such as cocoons, seeds, fruits or galls (Gibson, 1995; Gibson *et al.*, 1997). Egg parasitoids, such as *E. tibicinis* (Bouček, 1963), are less common.

As a consequence of their parasitic development, several *Eupelmus* species have been indicated as natural enemies of various pests worldwide. Thus, they are candidates as biocontrol agents of the emerald ash borer *Agrilus planipennis* (Fairmaire, 1888) (Duan *et al.*, 2009, 2012), bruchids such as *Callosobruchus maculatus* (Fabricius, 1775) and *Bruchidius atrolineatus* (Pic, 1921) (Gauthier *et al.*, 1999; Amevoin *et al.*, 2007), weevils such as *Cylindrocopturus adspersus* (LeConte, 1876) (Charlet *et al.*, 2002), the olive fruit fly *Bactrocera oleae* (Gmelin 1790) (Warlop, 2006; Boccaccio & Petacchi, 2009), the sorghum midge *Contarinia sorghicola* (Coquillet, 1899) (Gahukar, 1984), the chestnut gall wasp *Dryocosmus kuriphilus* (Yasumatsu, 1951) (Aebi *et al.*, 2007; Quacchia *et al.*, 2013), and the horse chestnut leafminer *Cameraria ohridella* (Deschka & Dimic, 1986) (Grabenweger & Lethmayer, 1999; Grabenweger, 2004).

Two practices can be considered in order to improve the regulation achieved by potential *Eupelmus* biocontrol agents. The first strategy (conservation biological control *sensu* Eilenberg *et al.*, 2001) is to identify and enhance environmental factors or practices promoting *Eupelmus* abundance (see for instance Boccaccio *et al.*, 2009). A second strategy is the release of mass-reared individuals (augmentation biological control *sensu* Eilenberg *et al.*, 2001) because some *Eupelmus* easily accept alternative hosts, which simplifies mass rearing (Arambourg, 1964; F. Al khatib, unpublished data). Whatever the underlying strategy for increasing biocontrol potential, the accurate identification of *Eupelmus* species and their host associations are necessary pre-requisites for improving pest regulation and to limit any unintended deleterious effects of the use or introduction of incorrect species.

The discrimination and identification of *Eupelmus* species is extremely difficult for several reasons, including: (i) as a genus of Eupelminae, the sexes are highly dimorphic, which might lead entomologists unfamiliar with them to classify males in a different family; (ii) because of sexual dimorphism, associating sexes of the same species correctly is difficult unless they are collected and reared from the same location and/or host species (Gibson, 1990, 1995, 2011); (iii) existing identification keys are almost entirely based only on the morphological characters of females; and (iv) the subgenus *Eupelmus* contains a complex of species, the '*urozonus*-complex', which are very close morphologically.

The '*urozonus*-complex' was first delimited by Bouček (1988) when he stated that *E. urozonus* Dalman, 1920 belongs to a very difficult species group and differentiated the complex based on a combination of morphological features of females. Askew & Nieves-Aldrey (2000) described the '*urozonus*-complex' species as an aggregate of morphologically poorly differentiated but biologically distinct forms. Gibson (2011) also defined the complex, but based on morphological features of males (see below in the results Circumscription of the *Eupelmus urozonus* complex). He discussed in detail the principal features that could be useful for the recognition of the *urozonus*-species group in North America, as well as in the Palaearctic region.

There is no recent and reliable taxonomic revision of the genus and the type material of the earliest species described in the 19th Century is only partly revised. There are very few recent treatments of regional faunas (Askew & Nieves-Aldrey, 2000; Ribes Escolà & Askew, 2009), and the only Palaearctic revision (Kalina, 1988) is outdated. Improved systematics of Palaearctic *Eupelmus* and of Eupelminae in general requires broad sampling, comprehensive morphological analyses such as the revision of the Nearctic fauna of *Eupelmus* by Gibson (2011), and molecular analyses to test morphological species concepts.

In morphologically cohesive groups such as the '*urozonus*-complex', DNA-based characterization can be a useful complementary approach (Blaxter, 2003; Tautz *et al.*, 2003) both to check the existence of cryptic species and to associate the highly dimorphic sexes. Many studies have indeed shown the efficiency of such methods (Hogg & Hebert, 2004; Pons, 2006; Smith *et al.*, 2006; Gariepy *et al.*, 2007; Gebiola *et al.*, 2009). In particular, DNA barcoding, based on the amplification of a short fragment of the mitochondrial cytochrome oxidase subunit I (*COI*) using a universal primer set (Folmer *et al.*, 1994; Blaxter, 2003; Hebert *et al.*, 2003a,b; Jinbo *et al.*, 2011) has proved its relevance to the discovery of new species, estimating biodiversity, disentangling species complexes, and the recognition of cryptic species (see for instance: Hebert *et al.*, 2004; Armstrong & Ball, 2005; Smith *et al.*, 2006; Fisher & Smith, 2008; Veijalainen *et al.*, 2011; Smith *et al.*, 2013).

In some cases, however, the routine use of *COI* can have drawbacks linked to introgression, heteroplasmy and integration of copies of mitochondrial DNA in the nucleus (referred to as 'numts') (e.g. Song *et al.*, 2008; Galtier *et al.*, 2009; Xiao

et al., 2010) and the infection by maternally inherited symbionts (Shoemaker *et al.*, 2004; Hurst & Jiggins, 2005; Yu *et al.*, 2011). It can be thus advantageous to add other sources of molecular information. Several nuclear coding genes have already been successfully tested for insect taxonomy (e.g. Caterino *et al.*, 2000; Rokas *et al.*, 2002; Danforth *et al.*, 2005). One of them is the *wingless* gene (*Wg*). This gene belongs to the *wnt* gene family and codes for a glycoprotein involved in the wing pattern formation of insects. Both the easy amplification and sequencing of *Wg* gene and its rate of evolution make it relevant for phylogenetic reconstructions at various taxonomic levels (Brower & DeSalle, 1998; Campbell *et al.*, 2000).

This study explores the inter- and intraspecific biodiversity of the Western Palearctic *Eupelmus* species included in the *Eupelmus urozonus* complex based on morphological characterization and molecular investigation using *COI* and *Wg* genes from an extensive sampling of reared specimens. We provide molecular information on the species treated herein and validate the morphological characters included by G. Gibson and L. Fusu in an ongoing revision of the Palaearctic species of *Eupelmus* (G. Gibson and L. Fusu, in preparation). Here, we describe 11 new species belonging to the '*urozonus*-complex' from the Western Palaearctic. We also briefly investigate the intraspecific variability of the most abundant species and the distribution of haplotypes according to their insect hosts.

Materials and methods

Sampling

More than 300 morphologically identified individuals of '*urozonus*-complex' were characterized for *COI* (see Appendix S1). Of these, 156 were selected for *COI* and *Wg* analysis in order to adequately cover geographic and biological ranges while limiting redundancy of 100% identical *COI* haplotypes sampled in the same locality or on the same host insect. Most of these individuals were sampled between 2007 and 2012 in Europe, North Africa and some Mediterranean countries (Algeria, Cyprus, Czech Republic, Estonia, France including Corsica, Germany, Greece, Hungary, Iran, Italy including Sardinia, Lebanon, Libya, Morocco, The Netherlands, Romania, Slovakia, Spain, Sweden, Switzerland and Turkey). Most of the *Eupelmus* used in this study were reared from naturally infested fruits/seeds or from galls. Consequently, in most cases, their hosts were identified. Some specimens were collected by sweeping, impeding the identification of the related hosts. Specimens were usually killed with ethyl acetate and stored in 95% ethanol within a freezer until DNA extraction. Host–plant systems, collection dates and localities with geographical coordinates are listed in Table S1.

DNA extraction, amplification and sequencing

Genomic DNA was isolated from single individuals using the DNeasy kit (Qiagen) following the manufacturer's protocol, with some modifications: Entire specimens were incubated at 56°C for 15–17 h and DNA extractions were performed without destruction of the specimens, to allow subsequent examination of morphology.

The *COI* barcoding fragment was amplified using the primers LCO1490 and HCO2198 (Folmer *et al.*, 1994). PCRs were performed on a GeneAmp 9700 thermocycler using the following reagents in a 20-μL reaction volume: 1 μL of DNA (1–55 ng/μL), 14.64 μL of Milli-Q water, 2 μL of 10× PCR buffer containing MgCl2 (1×), 1 μL of 10 μM primer cocktail (0.5 μM), 0.16 μL of dNTPs 25 mM each (0.2 mM), and 0.2 μL of 5 U/μL Taq DNA Polymerase (Qiagen) (1 U/reaction). *COI*-PCR conditions were as follows: 94°C for 5 min, followed by 35 cycles of (i) 94°C for 30 s, (ii) 45°C for 1 min, and 72°C for 1 min with a final extension at 72°C for 10 min.

Wingless (*Wg*) gene was amplified using the primers wg1a and lepwg2 (Brower & DeSalle, 1998). PCRs were performed on the same thermocycler with the following reagents in a 25-μL reaction volume: 2 μL of DNA (1–55 ng/μL), 19.825 μL of Milli-Q water, 2.5 μL of 10× PCR buffer containing MgCl2 (1×), 0.175 μL of 100 μM primer cocktail (0.7 μM), 0.2 μL of dNTPs 25 mM each (0.2 mM), and 0.125 μL of 5 U/μL Taq DNA Polymerase (Qiagen, Hilden, Germany) (0.625 U/reaction). *Wg*-PCR conditions were as follows: 94°C for 3 min, followed by 40 cycles of (i) 92°C for 45 s, (ii) 57°C for 1 min, and 72°C for 1 min with a final extension at 72°C for 10 min.

PCR products were visualized using the QIAxcel Advanced System and QIAxcel DNA Fast Analysis Kit (Qiagen). PCR products for *COI* and *Wg* genes were sent to GENOSCREEN (Lille, France) or to BECKMAN COULTER GENOMICS (Stansted, UK) for sequencing in both directions. Both strands for each fragment were assembled using Geneious v5.5 (Drummond *et al.*, 2010)

Sequence data analyses

The two gene regions were aligned using CLUSTALW (Thompson *et al.*, 1994). Alignments were translated to amino acids using Mega 5.0.5 (Tamura *et al.*, 2011) to detect frame-shift mutations and premature stop-codons, which may indicate the presence of pseudogenes. Although the monophyly of the three subgenera has yet to be documented, one species belonging to the subgenus *Episolindelia*, *E.* (*Episolindelia*) *linearis* (Förster, 1860), was used as the outgroup. Sequences of all individuals have been submitted to GenBank (see Table S1).

The most appropriate model of evolution for each gene region was identified using the Akaike information criterion implemented in MrAIC.pl 1.4.3 (Nylander, 2004). We performed both maximum likelihood (ML) and Bayesian analyses of the two gene regions. ML analyses were conducted using MPI-parallelized RAxML 7.2.8 (Stamatakis, 2006a). GTR-CAT approximation of models was used for ML bootstrapping (Stamatakis, 2006b) (1000 replicates). Bayesian analyses were performed using MrBayes v3.2.1 (Ronquist *et al.*, 2012). To improve mixing of the cold chain and avoid it converging on local optima, we used Metropolis-coupled Markov chain Monte Carlo (MCMC), with each run including a cold chain and three

incrementally heated chains. The heating parameter was set to 0.01 in order to allow swap frequencies from 20 to 70% (following recommendations in MrBayes manual). We ran two independent runs of 5 million generations. All values were sampled every 500 generations. For the initial determination of burn-in, we examined the plot of overall model likelihood against generation number to find the point where the likelihood started to fluctuate around a constant value. Convergence of all parameters was also evaluated using Tracer v1.5 (Rambaut & Drummond, 2007). The first 25% samples from the cold chains were discarded as burn-in. The results were based on the pooled samples from the stationary phases of the two independent runs. Analyses were conducted on a 150-core Linux Cluster at CBGP.

Intra- and interspecific sequence divergences on *COI* and *Wg* datasets were calculated in MEGA 5.0.5 (Tamura *et al.*, 2011), using a Kimura 2-parameter model (Kimura, 1980) which utilizes two different rates of substitution – one for transitions and another for transversions.

Morphological characterization

The bodies of female *Eupelmus* often distort into a U-shape when killed using ethyl acetate, the mesonotum becomes arched, and the head and metasoma reflex dorsally (Gibson, 1986). To avoid these artefacts, after the lysis of the specimen, we gently pressed the mesonotum dorso-ventrally using forceps in order to recover the natural habitus. After DNA extraction the specimens were dried using acetone vapour within an hermetic container for at least 12 h in order to avoid the drastic deformations due to air-drying of the now empty exoskeleton. Following desiccation, specimens were immediately prepared as recommended by Noyes (1982) for morphological examination. The morphological description of these species was guided using an unpublished key and descriptions of Gibson and Fusu's unpublished manuscript. The following abbreviations were used: F1–F7, first to seventh funicular segments; MPS, multiporous plate sensilla; OOL, minimal distance between a lateral ocellus and inner orbit; POL, minimal distance between the lateral ocelli (see also Table S4).

Terms for sculpture follow Gibson (2009, 2010, 2011). Here, we define some of the sculpture patterns on which the separating of most species of the '*urozonus*-complex' depends: **coriaceous** corresponds to a network of isodiametric cells defined by engraved edges; **alutaceous** is similar to coriaceous, but the engraved cells forming the network are more elongated; **reticulate** is a pattern of cells similar to coriaceous except that the cells forming the sculpture are defined by raised edges; **imbricate** or **imbricate-reticulate** is a reticulate pattern except that the cells composing the network appear slightly overlapping. Measurements of lengths of forewing veins, ovipositor sheaths, metatibia and other corporal structural terms (antenna, head and mesosoma) used in the morphological description of species are illustrated in Figs 3, 4. The measurement of the ovipositor sheaths excludes the exerted part of the second valvifer. The base of the sheaths is delimited by a constriction (Fig. 4G) that in dorsal view is indicated by a slight protrusion on either side (Fig. 4F). Length of metatibia is measured from the point of connection between femur and tibia to the metatibial spur excluding the apical setae (Fig. 4E). Length of marginal vein is considered between the base of marginal vein (the point of convergence of parastigma and marginal vein) and the point at which the postmarginal and stigmal veins diverge (Fig. 4B).

An accurate observation of the morphological characters described below, especially the sculpture of the frontovertex, requires caution in the choice of the light. The intense light necessary to examine small-bodied specimens generates strong reflections or glare on the body that inhibits the accurate observation of their real morphology. Avoiding this is possible in two ways: (i) using fluorescent light or (ii) intercepting the cold light of fibre optics or incandescent light through a filter such as a tracing paper that diffuses the light and prevents glare. Taping a piece of tracing paper to the objective lens (Gibson, 2011) or forming a miniature truncate 'umbrella' at the end of a handle are useful techniques, but placing it as close as possible to the specimen provides the best results.

The admarginal setae of the pronotum must be examined in full light; if they are in the shadow of the head, pale setae might be confused as dark setae.

Within size range of a particular species, smaller specimens can be very difficult, if not impossible, to identify correctly because the morphology of typical specimens is not expressed. The sculpture of smaller specimens becomes vestigial and hence difficult to appreciate. Also, the body tends to be uniformly dark, mostly dark bluish. Within a series of reared specimens, one should preferably use the largest ones to key.

Measurements were made using a Leica M205 C binocular stereomicroscope and the software Leica Application Suite v4 (LAS. v4). All measurements were taken at a high magnification, (125× or 160×). Most specimens were photographed with a JVC KY-75U 3CCD digital camera attached to an EntoVision binocular and the serial images obtained combined with Cartograph 5.6.0 (Microvision, Evry, France) software or with a Leica DFC 500 camera attached to a Leica M205 A stereomicroscope and Zerene Stacker 1.04 software. Observation and imaging of male antennae were made using the scanning electron microphotographs at the University Montpellier II, Montpellier, France, using FEI Quanta FEG 200 environmental-SEM. The photos were then digitally optimized (artefacts removal, background standardization) using Photoshop® V program. The measurements of some individuals of both sexes are given in Doc.S1.

The depository of voucher specimens is mentioned in the main text for the holotypes of the new species and in Appendix S1 for the nontype material and paratypes. Collection data for holotypes and paratypes are cited on the type labels, with a '/' distinguishing data on separate rows of the same label and a semicolon distinguishing data on separate labels. Unless noted otherwise, type material of all previously described species was examined by LF and/or GG in order to establish correct nomenclature. However, except for names for which we changed recent concepts, only abbreviated synonymy is provided; more comprehensive discussion of types and synonymy will be given in the Palaearctic revision of *Eupelmus* (G. Gibson and L. Fusu, in preparation).

Results

Molecular characterization

COI was successfully amplified for all 157 individuals (including the only outgroup), with most of the sequences ranging from 610 to 652 bp. A total of 150 sequences of 433 bp were successfully obtained for *Wg*. Missing sequences were for *E. opacus* **sp.n.** ♀10 459, *E. annulatus* (Nees, 1834) ♀10 470, *E. tremulae* **sp.n.** ♀10 569, *E. purpuricollis* **sp.n.** ♀10 653, *E. martellii* (Masi, 1941) ♀10 659, *E. confusus* **sp.n.** ♀10 660 and *E. urozonus* (Dalman, 1820) ♀10 458. Unfortunately, we could not get any DNA from *E. stenozonus* (Askew, 2000). Therefore, this species is represented only in the morphological analysis. No frame shifts, stop codons, insertions or deletions were detected in any of these sequences. As shown in Table S2, *COI* was more variable than *Wg* at both intra- and interspecific level.

Mean intraspecific pairwise distances ranged from 0.0 to 4.8% for *COI* and from 0.0 to 0.6% for *Wg* (Table S2). *COI* interspecific distances ranged from 6.7% (*E. opacus*/*E. priotoni* **sp.n**.) to 18.2% [*E. azureus* (Ratzeburg, 1844)/*E. simizonus* **sp.n.**]. With the exception of *E. acinellus* (Askew, 2009)/*E. gemellus* **sp.n.** (0.6%), *E. priotoni*/*E. purpuricollis* (0.2%) and *E. janstai* **sp.n.**/*E. purpuricollis* and *E. priotoni* (from 0.5 to 0.7%), *Wg* interspecific distances ranged between 1.5% (*E. confusus*/*E. pistaciae* **sp.n.**) and 8.6% [*E. annulatus*/*E. fulvipes* (Förster, 1860)].

Models chosen by MrAIC were as follows: GTR + I + Γ for *COI* and GTR + Γ for *Wg*. Given that α and the proportion of invariable sites cannot be optimized independently from each other (Gu *et al.*, 1995), we used a GTR + Γ model with four discrete rate categories for both *COI* and *Wg*. Shallow genetic clusters recovered by ML (Figs 1, 2) and Bayesian (Doc. S2, Figures 32, 33) analyses were identical. Topological conflicts occurred among deeper nodes, but all conflicting nodes had poor supports.

Phylogenetic analyses clearly indicated many more genetic clusters than expected based on the current taxonomy of this species complex. All *COI* sequences obtained from previously described species [*E. acinellus*, *E. annulatus*, *E. azureus*, *E. cerris* (Förster, 1860), *E. martellii*, *E tibicinis* and *E. urozonus*] clustered according to prior morphological concepts. However, the presence of additional clusters revealed the possible existence of previously unrecognized or confused species (Fig. 1). The discovery of differentiating morphological features (see Description of new species) supported 11 *COI* clusters as distinct species, which are described here as *E. confusus*, *E. gemellus*, *E. janstai*, *E. longicalvus*, *E. minozonus*, *E. opacus*, *E. pistaciae*, *E. priotoni*, *E. purpuricollis*, *E. simizonus* and *E. tremulae*. Moreover, *Eupelmus fulvipes* was recognized as a distinct species from *E. kiefferi* (De Stefani, 1898) primarily based on distinct *COI* sequences, both taxa being confused or misinterpreted by all previous authors. With only three exceptions (*E. gemellus*–*E. acinellus*; *E. kiefferi*–*E. fulvipes*; *E. janstai*–*E. priotoni*–*E. purpuricollis*), the same clustering of species was provided by the phylogenetic analysis of *Wg* (Fig. 2).

As presented in Table S3, the dataset exhibited a great diversity of nucleotidic haplotypes, in particular for *E. urozonus* and the newly described *E. confusus* and *E. gemellus* with about one haplotype per individual for each gene. The diversity in proteic haplotypes was expectedly reduced, yet polymorphism was observed in *COI* sequences, in particular in *E. annulatus*, *E. confusus*, *E. gemellus*, *E. longicalvus* and *E. urozonus.*

Our analyses revealed no mtDNA introgression between species. Moreover, *COI* minimum interspecific divergence exceeded the maximum intraspecific divergence for all species, showing that *COI* DNA barcodes should be valuable in routine identifications of *Eupelmus* species from the 'urozonus-complex' in the Western Palaearctic.

It is noteworthy that the topologies of *COI* and *Wg* genes trees diverged at several levels, likely because of different evolution rates. This clearly shows that inferring the phylogeny of the '*urozonus*-complex' requires more genes to mediate the discrepancies between the results achieved from both genes. This is one of the reasons why we do not infer here interspecific relationships.

Taxonomic results

Circumscription of the *Eupelmus urozonus* complex

For the purposes of this study the '*urozonus*-complex' is circumscribed by the following characters. **Female**. Macropterous; body with hair-like, not conspicuously lanceolate setae, except setae on face and parts of thorax slightly flattened; frons not angulate with vertex; postero-medial depression of mesoscutum sculptured; plical depression of propodeum reaching posterior margin; linea calva present on forewing; postmarginal vein not or only slightly longer than stigmal vein; mesotibia with black apical pegs; tarsomeres of mid leg with symmetrical paired rows of black pegs; ovipositor sheaths tricoloured, with basal and apical dark bands separated by median pale band. Syntergum and anal plate forming truncate or obliquely inclined surface, the syntergum not reflexed on either side of ovipositor sheaths. Ovipositor sheath 0.60–1.35× as long as metatibia and 0.70–1.50× as long as marginal vein. **Male**. Gena with 1–3 long, curved and somewhat thicker setae. Scape short and ovoid, bearing pores at least on outer band along scapular scrobe. Pedicel ventrally with a row of hook-like setae. First basal funicular segment often without MPS.

Most species included here also share a special pattern of colouration of the female mesosoma: lateral panels of pronotum and prepectus bluish, the latter often with bronze reflections on periphery, acropleuron bronze on either sides of the blue micro-sculptured surface (sometimes bluish anteriorly), mesepisternum bluish, metacoxa with bright coppery reflections dorsally, blue ventrally.

Key to European species of *Eupelmus* of the '*urozonus*-complex'

Females

1. Ovipositor sheaths (excluding exerted part of second valvifer) at least as long as marginal vein and slightly shorter to distinctly longer than metatibia (Fig. 5A) 2

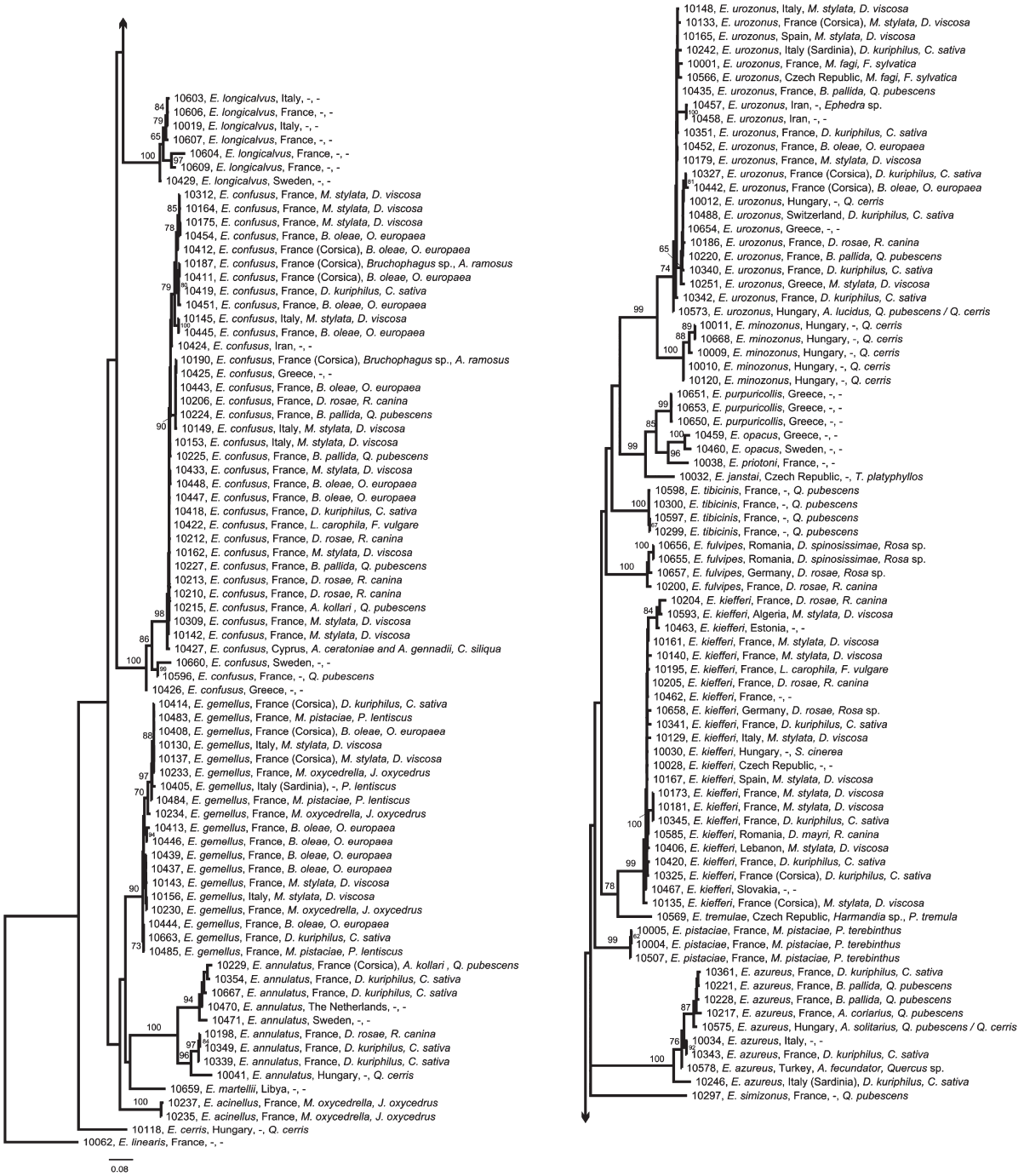

Fig. 1. ML tree figuring the relationships within the '*urozonus*-complex' of *Eupelmus* based on the barcoding fragment of the mitochondrial gene '*COI*'. *E. linearis* is used as outgroup. RAxML analysis with 1000 rbs bootstrap replicates (support >65% are indicated at nodes). Each line represents a sequenced individual with information in the following order: molecular code, species, country, insect host and associated plant.

1′. Ovipositor sheaths 0.65–0.95× as long as marginal vein and 0.60–0.90× as long as metatibia (Fig. 5B) 11

Note. Marginal cases will run both ways

2(1). Frontovertex reticulate, the sculpture delimiting meshes at least slightly raised (Fig. 5C, I) 3

2′. Frontovertex coriaceous, the sculpture delimiting meshes engraved, mostly superficial (Fig. 6G, J) 6

3(2). Ovipositor sheaths, excluding apex of second valvifer, much longer (1.35–1.70×) than marginal vein and at least slightly longer (1.05–1.20×) than metatibia (Fig. 5E). Head and

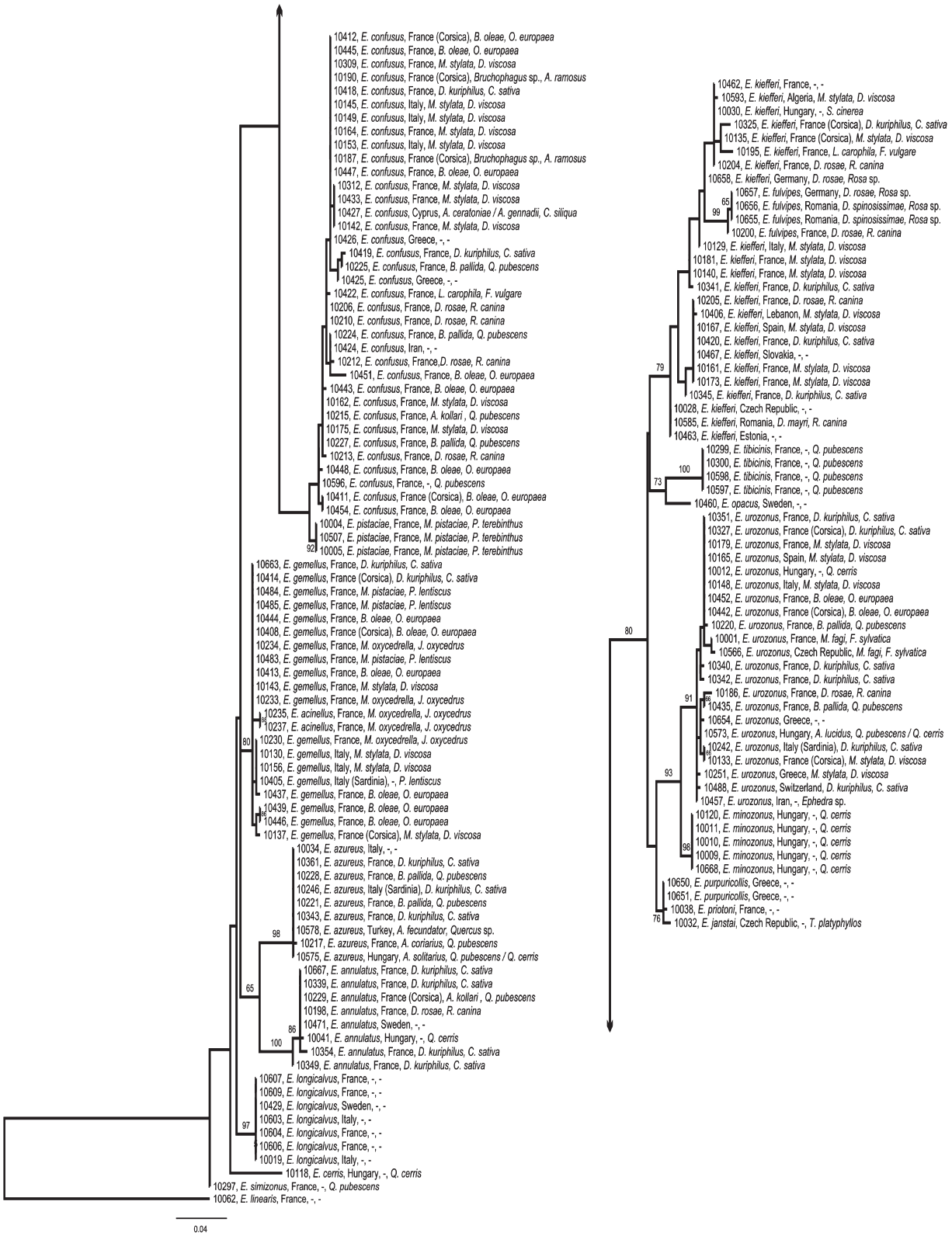

Fig. 2. ML tree figuring the relationships within the '*urozonus*-complex' of *Eupelmus* based on the nuclear gene '*Wingless*'. *E. linearis* is used as outgroup. RAxML analysis with 1000 rbs bootstrap replicates (support >65% are indicated at nodes). Each line represents a sequenced individual with information in the following order: molecular code, species, country, insect host and associated plant.

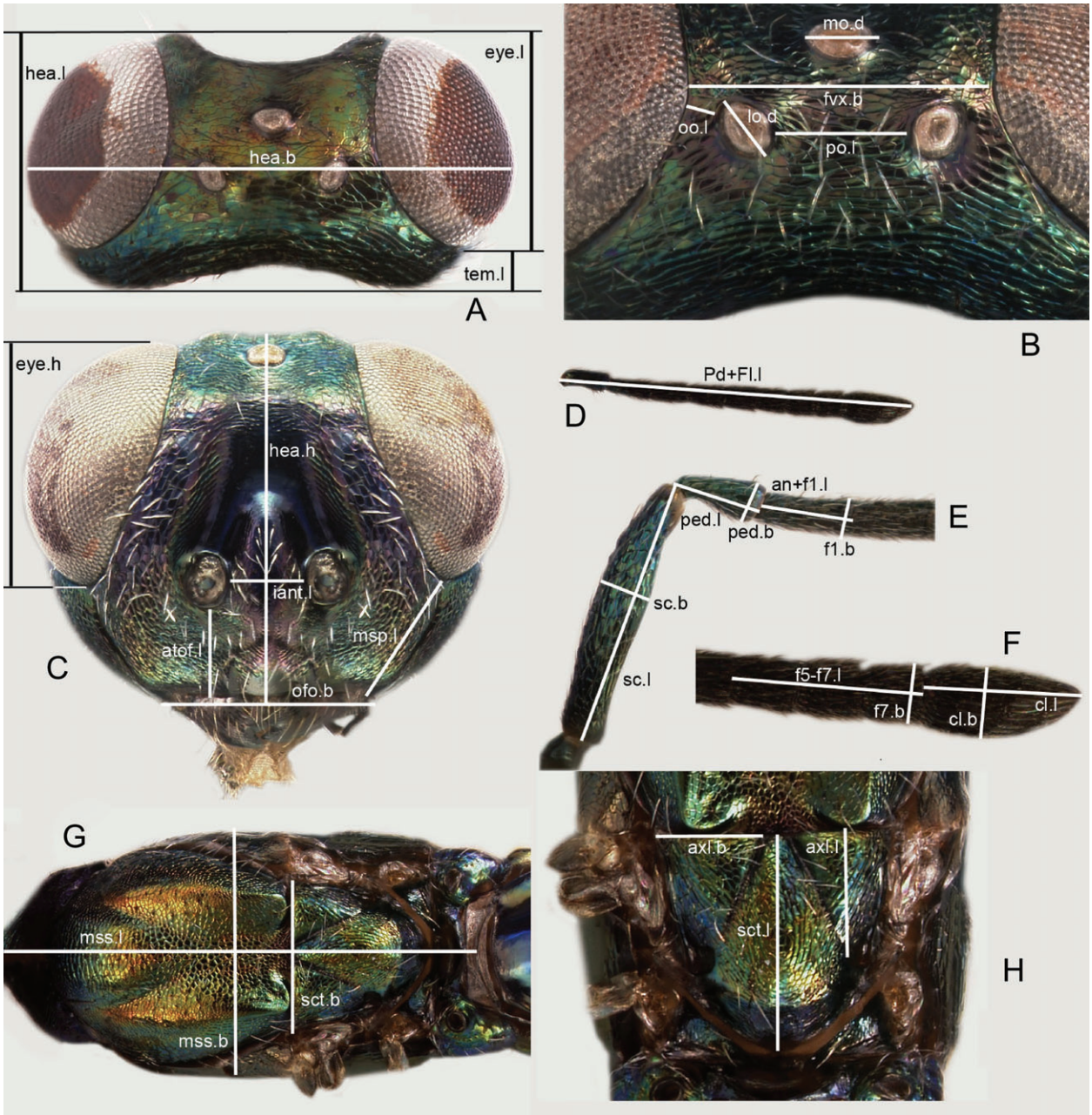

Fig. 3. Measurements of female *Eupelmus*. (A, G, H) *E. janstai*; (B, D, F) *E. gemellus*; (C, E) *E. confusus*. Head in dorsal view (A), vertex (B), head in frontal view (C), pedicel and flagellum (D); base of antenna (E); apex of flagellum (F); mesosoma in dorsal view (G); scutellar-axillar complex (H). Abbreviations in Table S4.

mesosoma entirely blue violet (Fig. 5C, D) . . . . . ***E. acinellus* Askew**

3′. Ovipositor sheaths shorter, 1.00–1.25× as long as marginal vein and 0.95–1.10× as long as metatibia (Fig. 5K). Head and mesosoma mostly bronze greenish (Fig. 5G, L), sometimes with bluish reflections (Fig. 5J) 4

4(3′). Scrobal depression mostly smooth, only a dorsal transverse strip and lateral margins imbricate-reticulate (Fig. 5F). Ovipositor sheaths with median pale band frequently shorter than or at most about as long as basal and apical dark bands (Fig. 5H). Head and mesosoma with dark bronze reflections (Fig. 5G) . . . . . ***E. stenozonus* Askew**

4′. Scrobal depression reticulate, only antennal scrobes (bottom of separate depressions above toruli) smooth (Fig. 5I). Ovipositor sheaths with median pale band always longer than basal and apical dark bands (Fig. 5K). Head and mesosoma mostly

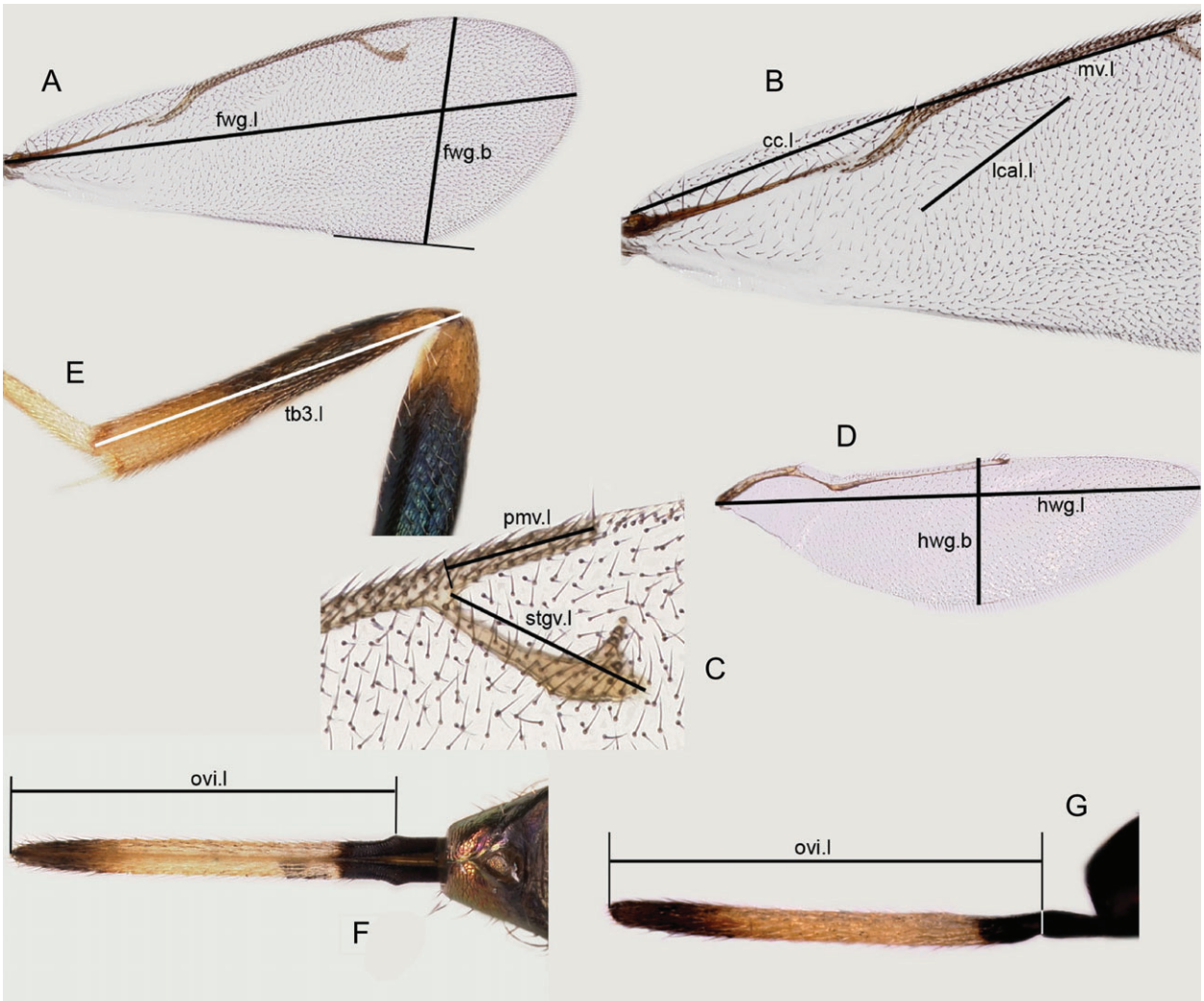

Fig. 4. Measurements of female *Eupelmus* (continued). (A–C) *E. gemellus*, (D) *E. urozonus*, (E) *E. priotoni*, (F, G) *E. janstai*. Forewing (A), base of forewing (B), stigmal and postmarginal veins (C), hindwing (D), metatibia (E), ovipositor sheaths in dorsal view (F), ovipositor sheaths in lateral view (G). Abbreviations in Table S4.

bronze greenish (Fig. 5L) to bluish green or sometimes with bluish reflections (Fig. 5J) 5

5(4′). Head and mesosoma metallic green to bluish green with slight coppery reflections (Fig. 5J) . . . . . ***E. gemellus* sp.n.** (part)

5′. Head and mesosoma greenish with distinct bronze reflections. Mesosoma entirely bronze greenish, without bluish reflections (Fig. 5L) . . . . . ***E. martellii* Masi** (part)

6(2′). Head and mesosoma predominantly blue (Fig. 6A, B), including mesosoma laterally (Doc. S3, Figure 40D, E). Body elongate, with gaster 1.15–1.25× as long as head + mesosoma (Fig. 6A). Forewing 2.50–2.70× as long as wide . . . . . ***E. tibicinis* Bouček**

6′. Head and mesosoma more extensively bronze to coppery, especially acropleuron (Doc. S3, Figures 36D, E, 37D). Body less elongate with gaster relatively shorter (Fig. 27G). Forewing 2.20–2.35× as long as wide 7

7(6′). Protibia dark except narrowly pale basally and apically. Axilla blue to violet blue, contrasting with green to bronze or bronze greenish scutellum (Fig. 6C). Ovipositor sheath with subapical dark region as longitudinal strip not extended to ventral and dorsal margins of valvula (Fig. 6E). Scape extensively to entirely orange . . . . . ***E. cerris* Förster**

7′. Protibia pale dorsolongitudinally along length and sometimes even more extensively pale. Axilla and scutellum similar in colour with a mixture of blue and bronze (Figs 6H, 18E; Doc. S3, Figure 35B). Ovipositor sheath colour different, sometimes hardly or progressively darker apically but if with distinct subapical dark region then as a band extending to dorsal and ventral margins of valvula (Figs 6I, 7B). Scape dark 8

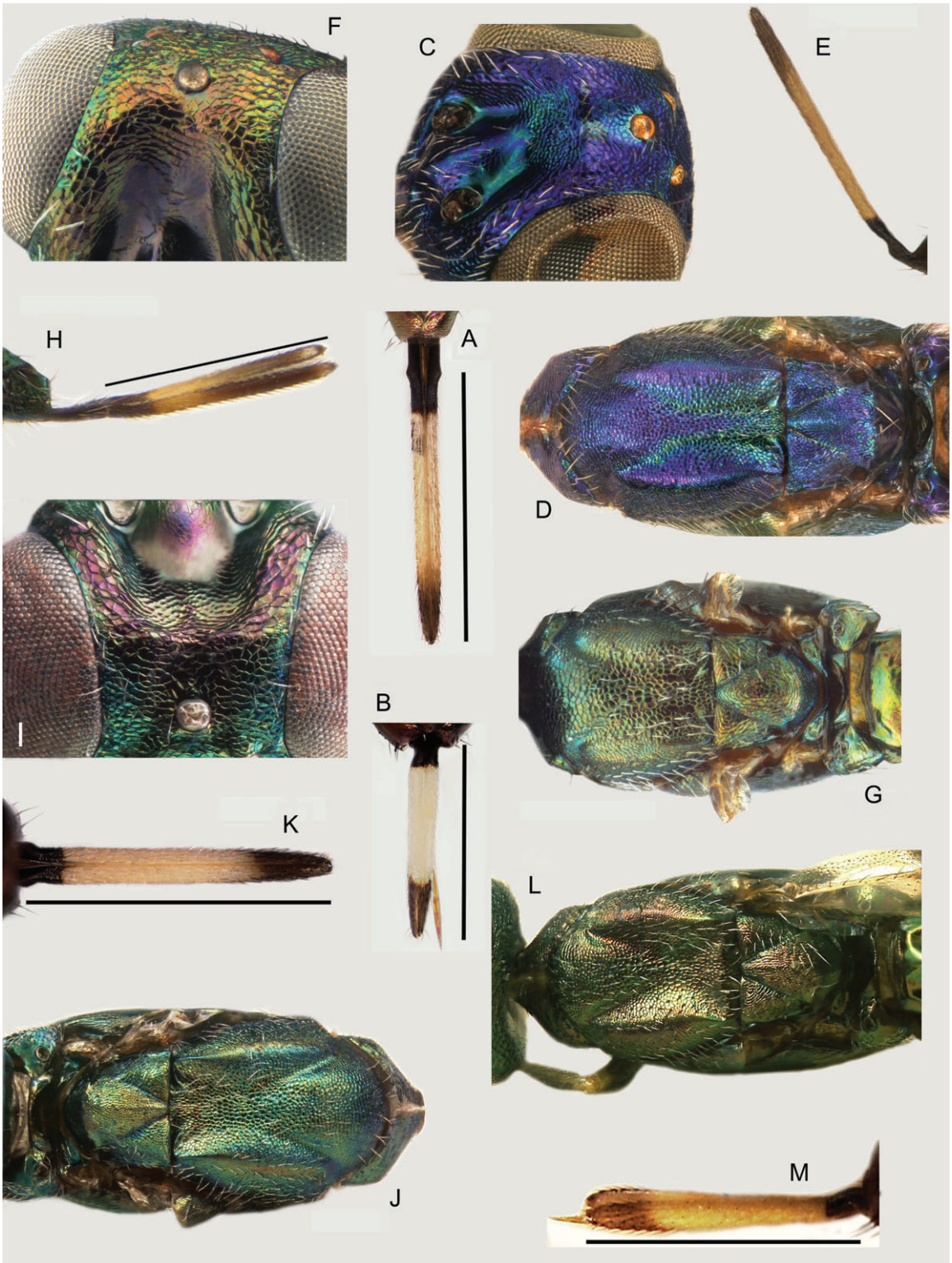

Fig. 5. Characters of female *Eupelmus* of the '*urozonus*-complex'. (A) *E. janstai*: ovipositor sheaths in dorsal view. (B) *E. confusus*: *ibidem*. (C–E) *E. acinellus*: head, in latero-dorsal view (C), mesosoma in dorsal view (D), ovipositor sheaths in lateral view (E). (F–H) *E. stenozonus*: frontovertex and scrobal depression in antero-dorsal view (F), mesosoma in dorsal view (G), ovipositor sheaths in lateral view (H). (I–K) *E. gemellus*: frontovertex and scrobal depression in antero-dorsal view (I), mesosoma in dorsal view (J), ovipositor sheaths in dorsal view (K). (L, M) *E. martellii*: mesosoma in dorsal view (L), ovipositor sheaths in lateral view (M).

8(7′). Scrobal depression mostly smooth, at most narrowly reticulate dorsally (Fig. 6G, K) 9

8′. Scrobal depression mostly to entirely reticulate (Fig. 7A, C) 10

9(8). Pro- and metafemora extensively dark with metallic reflections, and respective tibiae partly fuscous. Lateral ocellus large, separated from inner margin of eye by less than 0.50× its own diameter (Fig. 6F). Prepectus with 8–15 setae . . . . . ***E. azureus* Ratzeburg**

9′. Pro- and metafemora at most slightly fuscous, and respective tibiae pale. Lateral ocellus smaller, separated from inner margin of eye by about 0.80× its own diameter (Fig. 6J). Prepectus with 4–5 setae . . . . . ***E. janstai* sp.n.**

10(8′). Mid leg beyond coxa and metatibia entirely pale yellow (Fig. 7E, F). Flagellum somewhat clavate and relatively short, 1.20× as long as head width (Fig. 7D). Distance between lower edge of antennal torulus and margin of oral fossa 1.20–1.25× intertorular distance (Fig. 7C). Scrobal depression with sides bright blue. Ovipositor sheaths with apical darkened band distinctly delineated from whitish pale band (Fig. 7G) . . . . . ***E. tremulae* sp.n.**

10′. Mid and hind legs with tibiae and femora broadly fuscous. Flagellum hardly clavate, 1.35–1.45× as long as head width. Distance between lower edge of antennal torulus and margin of oral fossa at most as long as intertorular distance (Fig. 7A). Scrobal depression with sides dark bluish similar to most of frons. Ovipositor sheaths with pale band orange yellow and progressively darker apically, though sometimes hardly so (Fig. 7B) . . . . . ***E. annulatus* Nees**

11(1′). Scrobal depression mostly to entirely reticulate, at most with small part of each antennal scrobe just above torulus smooth (Figs 7H, 8A, D, I) 12

11′. Scrobal depression only partly reticulate, at least antennal scrobes (bottom of depressions above toruli) entirely smooth (Figs 5I, 9A) 15

12(11). Linea calva extended proximally to level equal with base of parastigma (Fig. 7J). Postmarginal vein 1.30–1.40× as long as stigmal vein (Fig. 7K). Mesosoma dark with faint bluish reflections (Fig. 7I). Scape entirely dark. Legs with femora and pro- and metatibiae mostly fuscous. Ovipositor sheaths 0.75–0.95× as long as marginal vein . . . . . ***E. longicalvus* sp.n.**

12′. Linea calva extended proximally to about level of apex of parastigma. Postmarginal vein not or slightly longer (1.00–1.20×) than stigmal vein. Mesosoma with mesonotum frequently greenish to bronze greenish with coppery reflections (Fig. 8K). Scape sometimes partly to completely reddish (Fig. 8F). Legs with mesofemur and meso- and metatibiae often reddish, not infuscate (Fig. 8H). Ovipositor sheaths 0.65–0.80× as long as marginal vein 13

13(12′). Head and mesosoma, including pronotal collar, extensively coppery bronze, rarely greenish bronze (Fig. 8A, C). Occiput without transverse ridge (Fig. 22D). Frontovertex distinctly reticulate (Fig. 8B). Scape partly and femora and tibiae extensively reddish testaceous (Fig. 8C) . . . . . ***E. pistaciae* sp.n.**

13′. Head with frons and lower face blackish, violet or dark blue (Fig. 8D, I; Doc. S3, Figures 38A, 39A), pronotal collar with blue violet reflections (Fig. 8K). Occiput sometimes with faint transverse ridge (Fig. 8E, J). Frontovertex often coriaceous. Scape orangey to dark and femora and tibiae variably extensively often dark (Fig. 8H) 14

14(13′). Frontovertex reticulate (Fig. 8D). Scape orange or nearly so (Fig. 8F). Ovipositor 0.65–0.75× as long as marginal vein. Legs beyond coxae almost completely reddish yellow except for variably developed dark spot on posterior surface of profemur (Fig. 8G, H) . . . . . ***E. fulvipes* Förster**

14′. Frontovertex coriaceous (Fig. 8I). Scape mostly dark. Ovipositor 0.75–0.80× as long as marginal vein. Legs sometimes with mesofemur infuscate and frequently with profemur extensively dark, protibia basally and metafemur at least basally, dark . . . . . ***E. kiefferi* De Stefani**

15(11′). Frontovertex and dorsal half and sides of scrobal depression reticulate (Figs 5I, 9A, B) 16

15′. Frontovertex coriaceous (Figs 9F, 10A, 11G) and scrobal depression mostly smooth (Figs 9G, 10B, G, 11A, F) 18

16(15). Ovipositor sheaths 0.73–0.90× as long as marginal vein (Fig. 5B). Pronotum with collar blue violet, contrasting with the mostly bronze, often dark bronze, mesonotum (Fig. 9C), and with, at least lateral, admarginal hairs dark, except frequently some of the lateral hairs light. Costal cell with broader bare strip along leading margin (Fig. 9D). Submarginal vein dorsally with apical, discoloured section along parastigma bearing 5–7 setae (exceptionally up to 8). Basal cell setation very often pale and less dense than on disc . . . . . ***E. confusus* sp.n.**

16′. Ovipositor sheaths almost as long as marginal vein (Fig. 5K). Pronotum with collar greenish, similarly coloured as mesonotum (Fig. 5J, L), and with light admarginal hairs. Costal cell with very narrow bare strip along leading margin (Fig. 9E). Submarginal vein dorsally with apical, discoloured section along the parastigma bearing 7–10 setae. Basal cell with setation dark and as dense as on disc 17

17(16′). Head and mesosoma greenish with bluish reflections especially laterally on frontovertex and convex parts of mesoscutum (Fig. 5J) . . . . . ***E. gemellus* sp.n.** (part)

17′. Head and mesosoma bronze greenish, without bluish reflections (Fig. 5L) . . . . . ***E. martellii* Masi** (part)

18(15′). Pronotal collar blue violet, contrasting with mostly greenish mesonotum, and lateral panel extensively blue (Figs 9I, 10C, E) 19

18′. Pronotal collar greenish, similarly coloured to mesonotum (Doc. S3, Figure 41E), and lateral panel at most with a small blue spot dorsally 22

19(18). Antennal toruli with ventral margins hardly below lower ocular line (Fig. 9G). Head in frontal view transverse, 1.35× as broad as high. Temples very short (Fig. 9F). Lateral ocellus

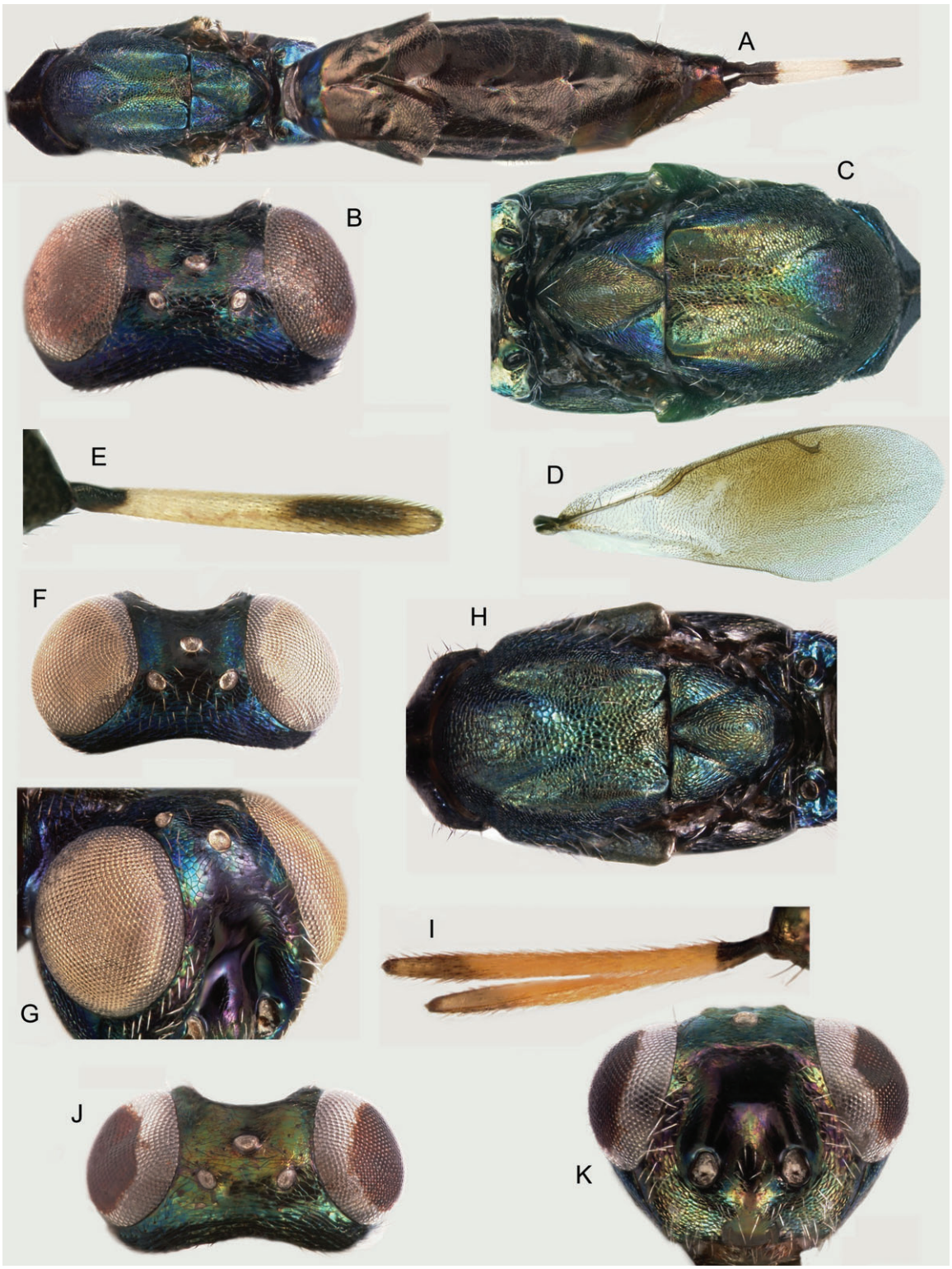

Fig. 6. Characters of female *Eupelmus* of the '*urozonus*-complex' (continued). (A, B) *E. tibicinis*: meso- and metasoma in dorsal view (A), head in dorsal view (B). (C–E) *E. cerris*: mesosoma in dorsal view (C), forewing (D), ovipositor sheaths in lateral view (E). (F–I) *E. azureus*: head in dorsal view (F), frontovertex and scrobal depression in latero-dorsal view (G), mesosoma in dorsal view (H), ovipositor sheaths in lateral view (I). (J, K) *E. janstai*: head in dorsal (J) and frontal view (K).

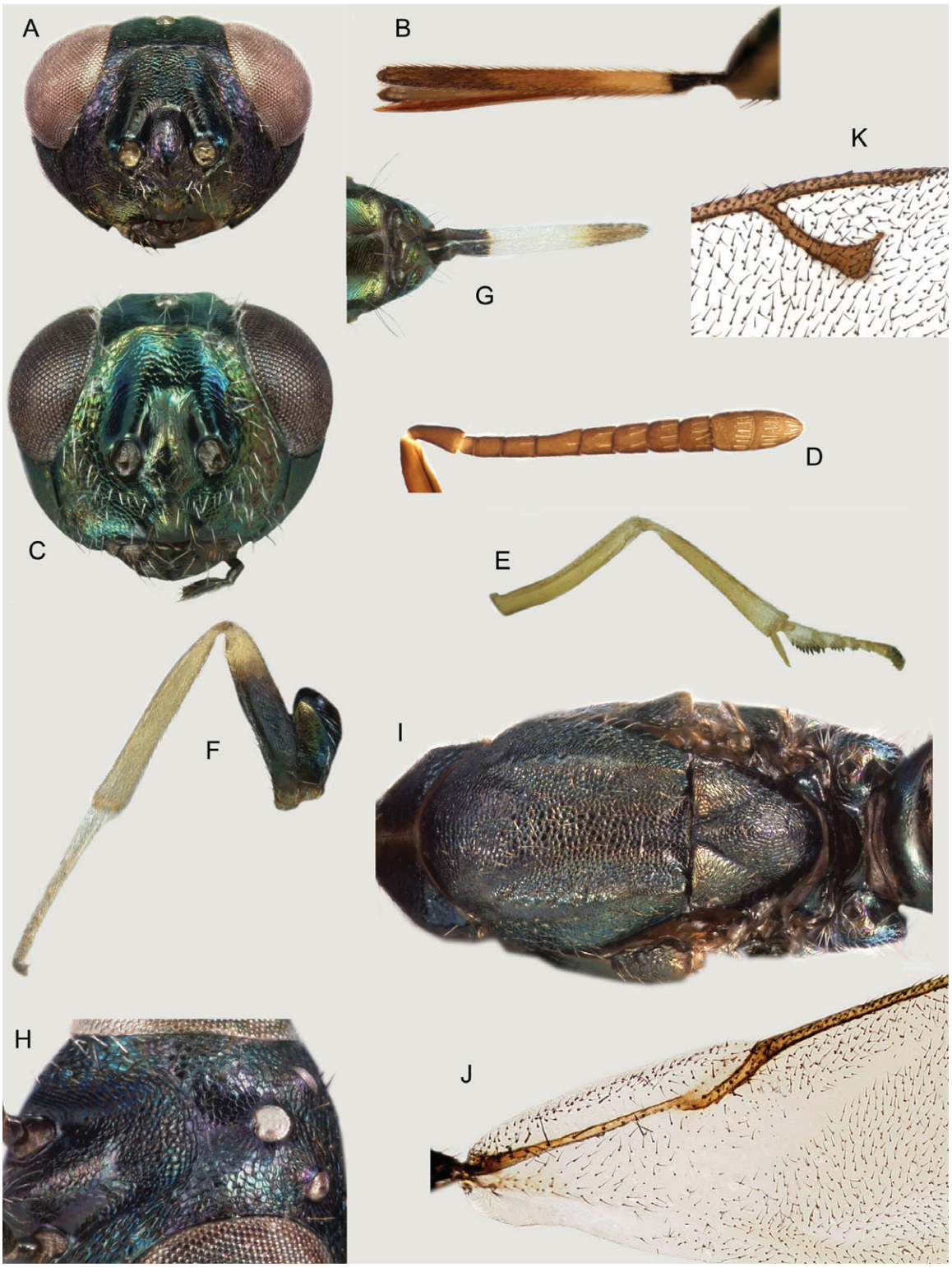

Fig. 7. Characters of female *Eupelmus* of the '*urozonus*-complex' (continued). (A, B) *E. annulatus*: head in frontal view (A), ovipositor sheaths in lateral view (B). (C–G) *E. tremulae*: head in frontal view (C), pedicel and flagellum (D), mid leg (E), hind leg (F), ovipositor sheaths in dorsal view (G). (H–K) *E. longicalvus*: frontovertex and scrobal depression in latero-dorsal view (H), mesosoma in dorsal view (I), base of forewing (J), stigmal and postmarginal veins (K).

separated from inner margin of eye by 0.50× own diameter. Prepectus with three or four setae . . . . . ***E. simizonus* sp.n.**

19′. Antennal toruli with ventral margins clearly below lower ocular line (Fig. 10B, D, G). Head in frontal view less transverse, about 1.25× as broad as high. Temples relatively longer (Fig. 10A). Lateral ocellus often separated from inner margin of eye by a longer distance. Prepectus often more densely setose 20

20(19′). Lateral ocellus small, distance to inner margin of eye 1.15–1.23× own diameter (Fig. 10A). Mesonotum predominantly bluish with greenish reflections on lateral bosses of mesoscutum (Fig. 10C). Frontovertex relatively large, 0.45× head width. Femora and tibiae extensively fuscous with metallic reflections . . . . . ***E. opacus* sp.n.**

20′. Lateral ocellus larger, distance to inner margin of eye 0.55–0.95× own diameter. Mesonotum predominantly greenish with anterior half of convex medial lobe of mesoscutum bluish (Fig. 10E). Frontovertex smaller than above, 0.37–0.40× head width. Femora and tibiae sometimes more extensively pale 21

21(20′). Ovipositor sheaths 0.93× as long as marginal vein (Fig. 10F). Lower ocular line in line with dorsal margins of toruli and distance between lower edge of torulus and margin of oral fossa only 0.85× intertorular distance (Fig. 10D) . . . . . ***E. priotoni* sp.n.**

21′. Ovipositor sheaths 0.73–0.78× as long as marginal vein. Lower ocular line intersecting toruli at about their mid height and distance between lower edge of torulus and margin of oral fossa 1.00–1.18× intertorular distance (Fig. 10G) . . . . . ***E. purpuricollis* sp.n.**

22(18′). Stigmal vein noticeably curved along posterior margin (Fig. 11I) . . . . . ***E. urozonus*** (part)

22′. Stigmal vein mostly to completely straight along posterior margin, only apex, at level of stigma, rounded (Fig. 11E) 23

23(22′). Eye small, height 1.45–1.50× length of malar space (Fig. 11A). Antennal toruli relatively high on head, distance between lower edge of torulus and margin of oral fossa 1.15–1.20× intertorular distance. Mesoscutum with cells on medial strip of posterior depression smaller than those on antero-medial lobe, and reticulation reaching top of sublateral bumps where as coarse as elsewhere (Fig. 11C). Legs with light parts extensive, all tibiae except for dorsobasal spot on protibia and mesofemur straw yellow . . . . . ***E. minozonus* sp.n.**

23′. Eye larger, height 1.60–1.95× length of malar space (Fig. 11F). Antennal toruli with distance between lower edge of torulus and margin of oral fossa at most as long as intertorular distance (0.65–1.00×). Mesoscutum with cells on medial strip of posterior depression larger than above, only slightly smaller than on slope of sublateral bumps, and reticulation not quite reaching top of bumps or there quite faint (Fig. 11H). Legs more extensively dark, pro- and metatibia plus mesofemur partly fuscous with metallic reflections, and light parts reddish-testaceous . . . . . ***E. urozonus*** (part)

Males (males of E. cerris, E. janstai, E. longicalvus, E. minozonus, E. opacus, E. priotoni, E. purpuricollis and E. simizonus are unknown)

1. Flagellum clavate and bearing relatively short and sparse setae (Figs 12D, 28I). Basal flagellomere (=anellus) usually only slightly broader than long, ring-like but not discoidal and with at least two rows of setae. Pedicel longer than in alternate, at least twice as long as broad 2

1′. Flagellum filiform and bearing long and most frequently dense setae (Figs 12H, 14D). Anellus discoidal, bare or at most with single row of setae (Figs 12O, 13F, N). Pedicel shorter, 1.20–1.65× as long as wide (Figs 12O, 13F, 14H) 3

2(1). Mesotibia largely pale on outer (anterior) surface (Fig. 12B). Lower face above malar sulcus with a patch of long, apically hooked setae (Fig. 12A). Mid leg with basitarsus whitish and following tarsomeres progressively darker or at least more yellowish than basal tarsomere . . . . . ***E. annulatus***

2′. Mesotibia infuscate except narrowly pale near apex. Lower face with shorter and sparse setae (Fig. 12C). Mid leg with basal three tarsomeres uniformly whitish . . . . . ***E. azureus***

3(1′). Head with transverse ridge or carina delimiting vertex from occiput (Fig. 12E, J, L) 4

3′. Head without such ridge, vertex progressively merging into occiput (Figs 28C, 29E; Doc. S3, Figure 42A) 6

4(3). Antenna and infuscate parts of legs dark brown, not metallic (Fig. 12H, I). Scape very broad, 1.50× as long as wide (Fig. 12F, G). Mesotibia with apical spur dark (Fig. 12I) . . . . . ***E. tremulae***

4′. Antenna and infuscate parts of legs with some metallic reflections. Scape more elongate, 1.80–1.90× as long as wide (Fig. 12K, M). Mesotibia with apical spur whitish 5

5(4′). Median carina of propodeum vestigial. Mid leg with only basitarsus whitish, the remaining tarsomeres fuscous . . . . . ***E. fulvipes***

5′. Median carina of propodeum percurrent (Fig. 29D). Mid leg with three basal tarsomeres whitish . . . . . ***E. kiefferi***

6(3′). Flagellum with F1 not much shorter than (0.75–1.00×) or as long as F3 and F4 (Figs 13A, D, H, 31D) 7

6′. Flagellum with at least F1 and sometimes F2 distinctly shorter (0.60–0.65×) than F3 and F4 (Figs 14F, 15B) 12

7(6). Maxillary palpi with last segment mostly yellowish to reddish (Fig. 13C). Lower face above malar sulcus with curved setae distinctly longer than others (Fig. 13C). Pedicel with first ventral, hook-like seta long, enlarged and forming a loop (Fig. 13F), and with a second row of straight setae. Scape with over 30 pores along scapular scrobe on outer band (Figs 13E, 31I) . . . . . ***E. pistaciae***

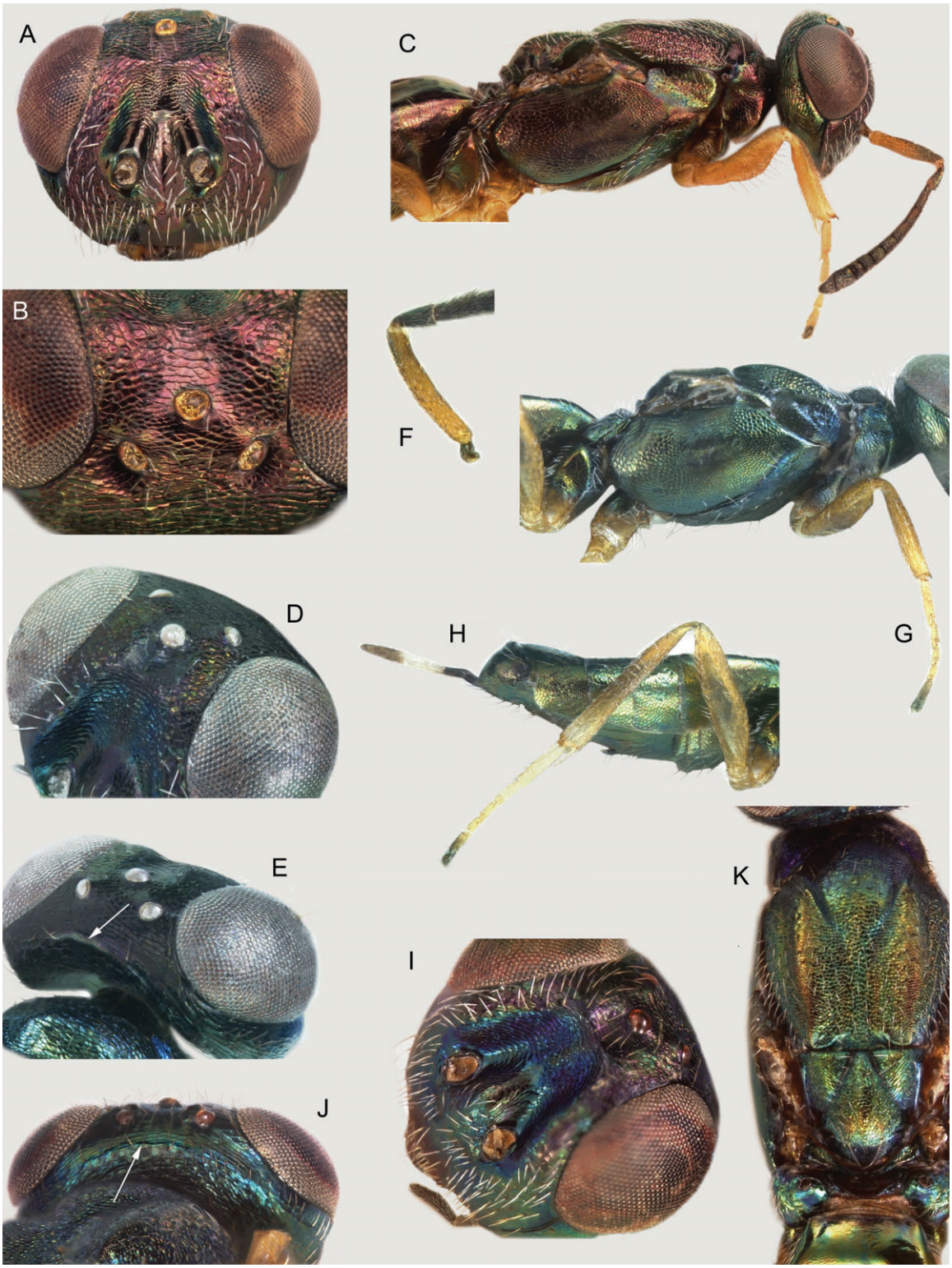

Fig. 8. Characters of female *Eupelmus* of the '*urozonus*-complex' (continued). (A–C) *E. pistaciae*: head in frontal view (A), frontovertex in antero-dorsal view (B), head and mesosoma in lateral view (C). (D–H): *E. fulvipes*: frontovertex and scrobal depression in latero-dorsal view (D), head in postero-dorsal view (E), base of antenna (F), mesosoma in lateral view (G), metasoma and hind leg in lateral view (H). (I–K) *E. kiefferi*: head respectively in latero-dorsal (I) and postero-dorsal view (J), mesosoma in dorsal view (K).

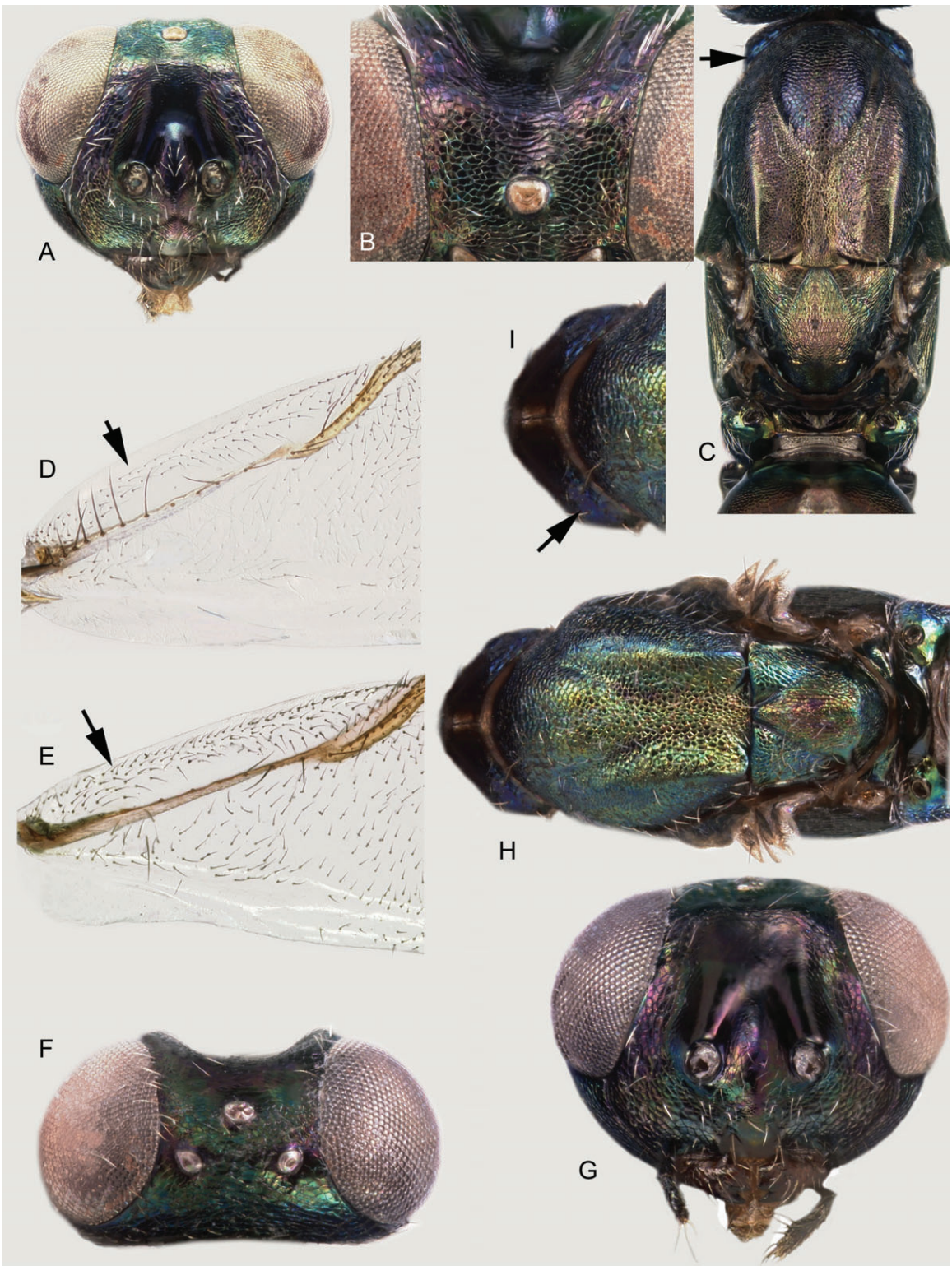

Fig. 9. Characters of female *Eupelmus* of the '*urozonus*-complex' (continued). (A–D) *E. confusus*: head in frontal view (A), frontovertex in antero-dorsal view (B), mesosoma in dorsal view (C), base of forewing (D). (E) *E. gemellus*: base of forewing. (F–I) *E. simizonus*: head in dorsal (F) and frontal view (G), mesosoma in dorsal view (H), pronotum (I).

7′. Maxillary palpi with last segment dark. Lower face above malar sulcus sometimes without curved setae (Figs 13L, 14C). Pedicel without second row of ventral setae, the first of the hook-like setae not so long and not forming a loop. Scape often with only 14–20 pores on outer side (Fig. 13O) 8

8(7′). Pronotum strongly sloping anteriorly, almost vertical (Fig. 12P). Pedicel with 5–7 ventral, hook-like setae (Fig. 12O). Scape with about 20 pores on outer band along scapular scrobe (Fig. 31A) . . . . . ***E. confusus***

8′. Pronotum sloping, but not vertical anteriorly (Fig. 14B). Pedicel with three or four ventral, hook-like setae plus sometimes a straight apical seta (Fig. 13N). Scape either with at most 14–16 (Figs 13O, 31F) or at least with 20 pores on outer band along scapular scrobe (Fig. 13J) 9

9(8′). Cubital fold bare behind speculum which is therefore completely open posteriorly (Fig. 13K). Costal cell ventrally with single complete row of setae (Fig. 13K). F1 about as long as F3 (Fig. 13H). Scape with at least 20 pores, arranged basally in 2–3 rows, on outer band along scapular scrobe (Fig. 13J) . . . . . ***E. acinellus***

9′. Cubital fold partly setose behind speculum (Fig. 14A). Costal cell ventrally often with two complete rows of setae (Fig. 14A). F1 somewhat shorter than F3 (Fig. 14D). Scape with at most 14–16 pores, arranged basally at most in two rows, on outer band along scapular scrobe (Figs 13O, 31F) 10

10(9′). Costal cell dorsally usually with less than 12 setae near leading margin apically over distance equal to or little more than length of parastigma, and ventrally usually with only a single row of setae basally or mesally (as in Fig. 13K), with ventral setae often paler and comparatively inconspicuous basally than apically. Middle leg usually and hind leg sometimes with three basal tarsomeres white . . . . . ***E. stenozonus***

10′. Costal cell dorsally with 12 or more dark setae near leading margin over at least apical half, and ventrally almost always with two distinct rows of uniformly dark and conspicuous setae along length (Fig. 14A). Middle and hind legs often with only one or two basal tarsomeres white (Fig. 29C) . . . . . ***E. gemellus*** **and** ***E. martellii***

12(6′). Mid and hind tarsi with the two basal tarsomeres whitish in contrast to the following, blackish tarsomeres (Fig. 14I). Scape with 30–35 pores on outer band along scapular scrobe (Fig. 14G). Pedicel with seven hook-like setae ventrally (Fig. 14H) . . . . . ***E. tibicinis***

12′. Mid and hind tarsi with basitarsus partly infuscate and followings tarsomeres progressively darker to black on telotarsus (Fig. 15D). Scape with 45–60 pores on outer band along scapular scrobe (Fig. 15C). Pedicel with six hook-like setae ventrally (Fig. 14K) . . . . . ***E. urozonus***

Description of new species

E. **(*Eupelmus*)** ***confusus*** **Al khatib sp.n.**

http://zoobank.org/urn:lsid:zoobank.org:act:E9A1F8A3-00D1-4DB6-9A04-5ACBEBDBFEA3

(Female: Figs 9A–D, 16A–H; male: Figs 12N–P, 13A, 28C–G, 31A–D)

Type material. **Holotype**. FRANCE: Var, Fayence, 43.61774°N, 06.69774°E, 17.iii.2012, emerged 25. iii.2012, ex *Diplolepis rosae* on *Rosa canina* (N. Ris) (1♀) [FAL1195/10206] (in MNHG). **Paratypes** are provided in Appendix S1.

Etymology. The name *confusus* refers to the possible confusion of this species with *E. martellii* because of extreme similarity.

Female. Length 2.00–4.60 mm (holotype 4 mm). Head dark with slight greenish to bluish lustre and bearing silvery slightly lanceolate setae. Antennal scrobes and interantennal boss dorsally with faint violet reflections, parascrobal area with violet to purple reflections. Scape and pedicel with greenish or bluish reflections. Flagellum and palpi blackish. Mesosoma dull dark but, when using intense artificial light, with dark bluish lustre on antero-median lobe of mesoscutum, bronze reflections on lateral lobes and postero-medial depression, and on scutellar-axillar complex. In contrast pronotum with bluish violet metallic reflections on collar and shoulders, even with slight light. Prepectus and mesepisternum black with slight bronze reflections when using intense artificial light. Acropleuron dark with very slight bluish to bronze reflections anterior to the dark bluish medial micro-sculptured region, bronze posteriorly. Forewing hyaline, venation yellowish-brown, setae generally dark, often whitish within basal cell. Procoxa black, femur dark brown to black at least dorsally, tibia testaceous except for dorsal and ventral brown strips, tarsus completely testaceous except for dark brown pulvillus and possibly telotarsus. Mesocoxa and femur brown at least ventro-laterally except for testaceous knee; tibia testaceous with a sub-basal brown ring or band and black apical pegs; apical spur and tarsus whitish except the brown telotarsus and the ventral black pegs on the four basal tarsomeres. Metacoxa and femur black with slight metallic tinge, tibia similar in colour except for the yellowish apical third, tarsus whitish but at least telotarsus brown. Gaster mostly dark with violet reflections when using intense artificial light, with distinct metallic green lustre anteriorly on basal tergum, and dark hair-like setae. Ovipositor sheaths tricoloured, with short black basal region abruptly delineate from whitish longer medial region, which is abruptly delineate from the short brownish apical region.

Frontovertex finely reticulate (raised network), imbricate-reticulate in front of median ocellus and on ocellar triangle. Vertex transversely reticulate behind ocellar triangle, roundly merging to occiput without transverse carina or ridge. Head with scrobes and scrobal depression above the interantennal boss smooth and shiny, but upper half and sloping edges of depression transverse reticulate to imbricate. Interantennal boss finely coriaceous. Lower face and parascrobal surfaces bearing slightly lanceolate setae. Antennal toruli with ventral margins below lower ocular line. Head 1.59–1.93× as broad as long, temples 0.10–0.25× length of eyes, POL 3.00–4.00× OOL, lateral ocelli separated from adjacent eye orbit by 0.46–0.94× their

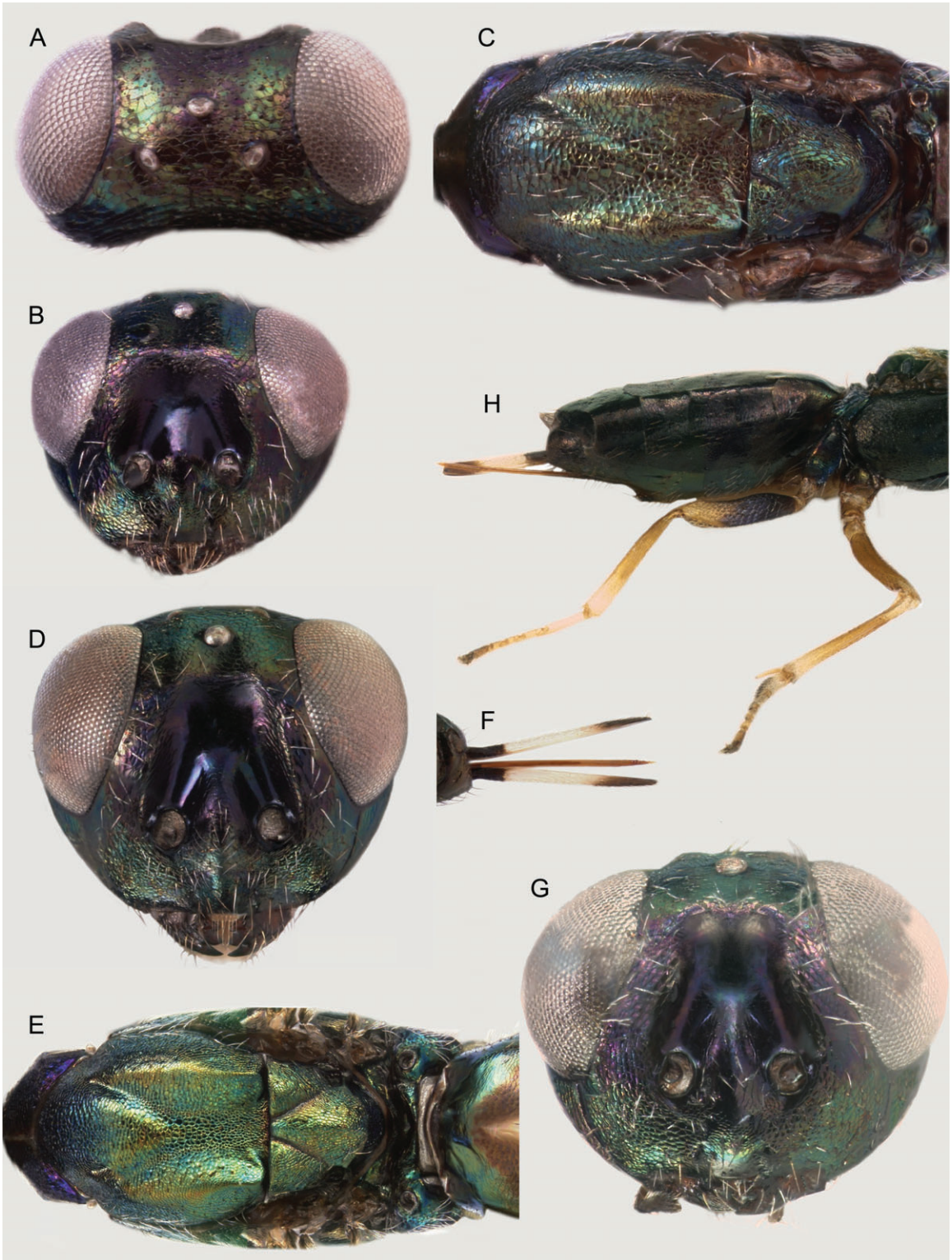

Fig. 10. Characters of female *Eupelmus* of the '*urozonus*-complex' (continued). (A–C) *E. opacus*: head in dorsal (A) and frontal view (B), mesosoma in dorsal view (C). (D–F) *E. priotoni*: head in frontal view (D), mesosoma in dorsal view (E), ovipositor sheaths in dorsal view (F). (G, H) *E. purpuricollis*: head in frontal view (G), apex of mesosoma and metasoma in lateral view (H).

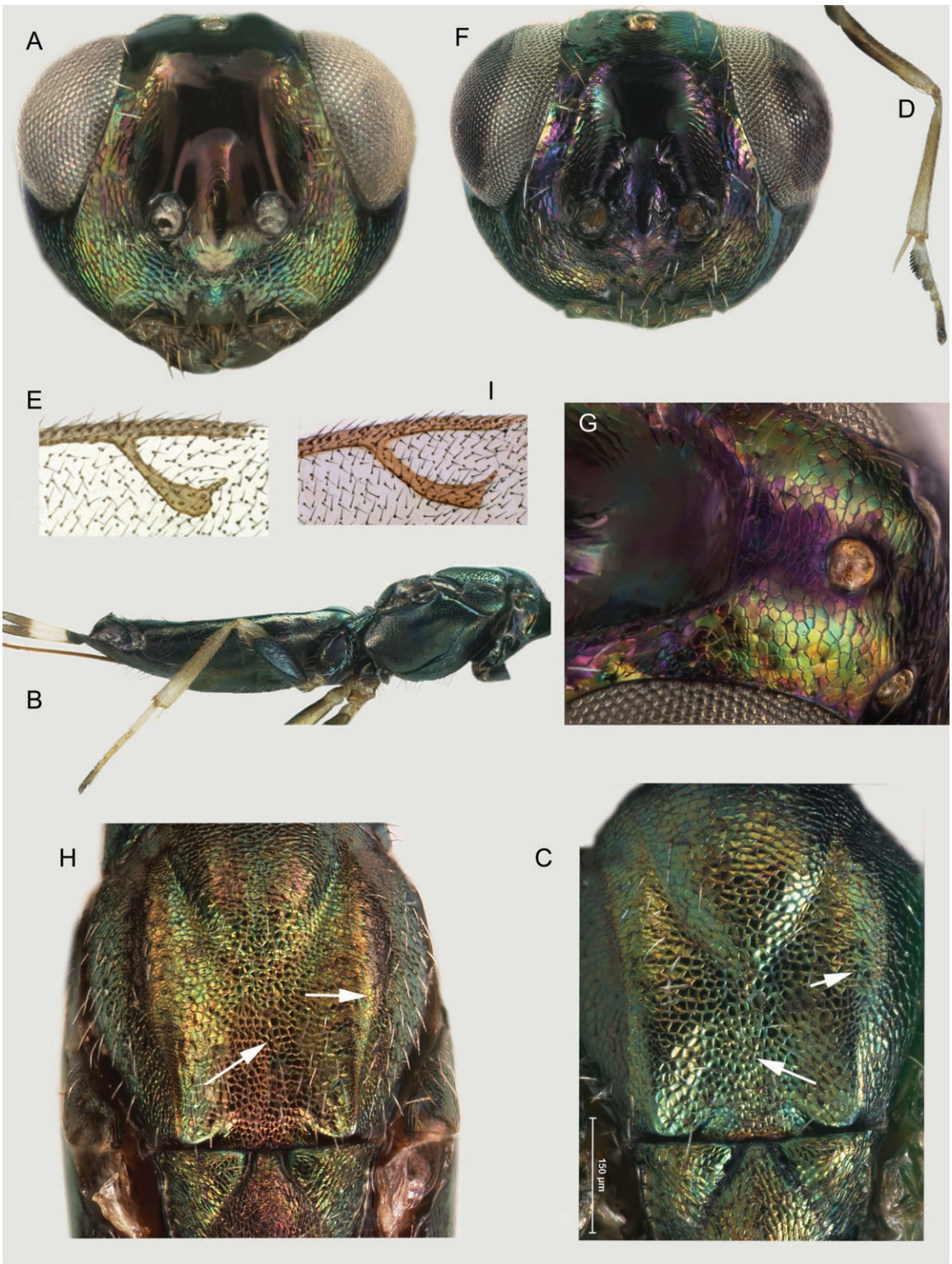

Fig. 11. Characters of female *Eupelmus* of the '*urozonus*- complex' (continued). (A–E) *E. minozonus*: head in frontal view (A), meso- and metasoma in lateral view (B), mesoscutum (C), mid leg (D), stigmal and postmarginal veins (E). (F–I) *E. urozonus*: head in frontal view (F), frontovertex and scrobal depression in antero-dorsal view (G), mesoscutum (H), stigmal and postmarginal veins (I).

own diameter which is 0.73–1.02× median ocellus diameter. Eyes separated by 0.36–0.50× head width, width of oral fossa 1.30–1.80× length of malar space. Antenna with combined length of pedicel and flagellum as 1.06–1.35× head width, scape 4.25–5.37(8.40)× as long as wide, pedicel 1.72–2.25× as long as wide and 0.91–1.44(1.76)× combined length of anellus and F1, the funicular segments shortening and widening distally, F7 1.40–1.90× as wide as F1, clava 1.98–2.70× as long as wide, 0.84–1.05× combined length of three apical funicular segments.

Mesosoma 1.60–1.90× as long as broad. Pronotum with dark admarginal hairs, but frequently some of the lateral hairs paler or white. Mesoscutum coarsely reticulate on convex antero-medial lobe, finely and densely so on postero-medial depression, lateral lobes finely reticulate to coriaceous. Scutellum 0.61–0.93× as long as wide. Scutellar-axillar complex densely reticulate-imbricate and with elongate cells, in contrast to the isodiametric reticulation of mesoscutum. Prepectus with variable number of white hair-like setae on centre of disc: 2–5 in small specimens, 7–15 in large ones, sometimes setal apices extending to dorsal margin. Acropleuron reticulate anterior and posterior of medial microsculptured region, the reticulation coarser posteriorly. Forewing moderately long, 2.42–2.51× as long as wide, with linea calva separated by several rows of setae from vanal area. Basal cell sometimes with setae irregularly and more sparsely setose than on disc (in that case they are white in contrast to the dark setae of the disc). Costal cell dorsally with line of setae over apical third and ventrally setose along whole length with two-three lines of setae medially, the first line of setae always somewhat distant from the front margin of the cell, the resulting bare strip evidently broader than the length of the adjacent setae. Discoloured apical section of the submarginal vein, along parastigma, generally bearing 5–7, exceptionally 7–8, dorsal setae. Marginal vein 0.84–0.99× length of costal cell, postmarginal 0.76–1.10× as long as stigmal. Stigmal vein curved apically on hind margin, stigma triangularly enlarged, basal sensillum distant from the other, adjacent to each other sensilla placodea. Mesotibia with apical row of 4–7 pegs. Mesotarsus ventrally with pegs on four basal tarsomeres, basitarsus with 17–29 pegs arranged distally in four rows , second tarsomere with 7–12 pegs in two rows, third with 4–6 pegs and fourth with 2–4 pegs. Propodeum with U-shaped plical depression extending to foramen, callus setose with white setae.

Gaster with apex of second valvifer not extending conspicuously beyond apex, ovipositor sheaths 0.70–0.78× length of metatibia and 0.77–0.89× length of marginal vein.

Male. Length 1.90–2.60 mm. Head blue with slight metallic greenish lustre, but lower face metallic green. Scape and pedicel often with greenish to bluish-green reflections. Flagellum and palpi dark brown. Mesosoma blue, mesoscutum dorsally with slight greenish lustre and scutellum sometimes with slight violet reflections under some angles of light. Tegula dark brown and often also variably metallic. Procoxa and femur dark blue except lighter knee, tibia dark blue with pale dorsal and ventral longitudinal strips, tarsus testaceous with dorsal infuscation but 1–2 apical tarsomeres brown. Mesofemur with blue reflections, mesotibia metallic greenish with incomplete pale dorsal and ventral longitudinal bands, tarsus white with 1–2 apical tarsomeres dark brown. Metafemur completely dark blue, tibia greenish with white apex, tarsus with the 2–3 basal tarsomeres white, the reminder progressively darkening. Forewing hyaline, venation testaceous, setae dark, setae on submarginal vein quite dark and conspicuous. Propodeum green to bluish-green. Gaster with basal tergum often metallic green to bluish-green basally, but remainder dark and with brown hair-like setae.

Frons reticulate, vertex clearly to transversely reticulate and roundly merging to occiput without transverse carina or ridge. Antennal scrobes and lower part of scrobal depression smooth, its upper part distinctly reticulate, interantennal region coriaceous. Head in dorsal view 1.86–2.02× as broad as long, temples 0.23–0.38× length of eye, POL 3.51–4.63× OOL, lateral ocelli separated from adjacent eye orbit by 0.61–0.89× their own diameter. Eyes separated by 0.49–0.52× head width, width of oral fossa 1.38–1.73× length of malar space. Lower face with sparse setae often white or sometimes brownish, the setae shortest mesally and variably longer laterally, but curved when long. Lower face above malar sulcus with apically curved setae. Gena with one seta brownish and much longer than the others. Antenna with combined length of pedicel and flagellum 1.40–1.47× head width. Scape ovoid, 1.94–2.38× as long as maximum width, the outer band along the scapular scrobe bearing about 20 pores arranged in several lines basally and in two lines apically; scapular scrobe also bearing 15–20 very small pores visible only with SEM photographs at high magnification (×7000). Pedicel compact, 1.10–1.42× as long as wide and ventrally with a line of 5–7 hook-like setae, frequently the apical one straight or nearly so. Flagellum densely setose and robust-filiform. Basal flagellomere (anellus) discoidal. F1 slightly shorter than F2, itself shorter than F3. Clava lanceolate with micropilose sensory region occupying apical two thirds of ventral surface, 1.91–2.38× as long as wide; combined length of apical three funicular segments 2.60–3.58× length of clava.

Pronotum strongly sloping anteriorly, nearly vertical. Mesoscutum and scutellar-axillar complex reticulate, but reticulation of posterior part of medial mesoscutal lobe usually much smaller and posterior part of scutellum coriaceous. Propodeum finely coriaceous and shiny; sublateral surface, between convex plical area and spiracle, evidently concave; groove in front of spiracle continuing along its outer rim, hence spiracle apparently raised relative to surrounding surface; callus similarly finely sculptured with setae originating from tiny bumps. Forewing with stigmal vein curved on hind margin, marginal vein 0.74–0.88× as long as costal cell and postmarginal 0.74–0.98× as long as stigmal. Costal cell dorsally with line of dark setae over apical third and ventrally with dark setae continuously along length, mesally on one line.

Variation. In the female coded [GDEL4173/10596] from Southern France the mesoscutum is bright bronze instead of dark; in the female coded [LF.u.SW.03/10660] from Sweden the lateral ocelli are smaller than in the rest of the sample, separated from the adjacent eye orbit by 1.1× their own diameter

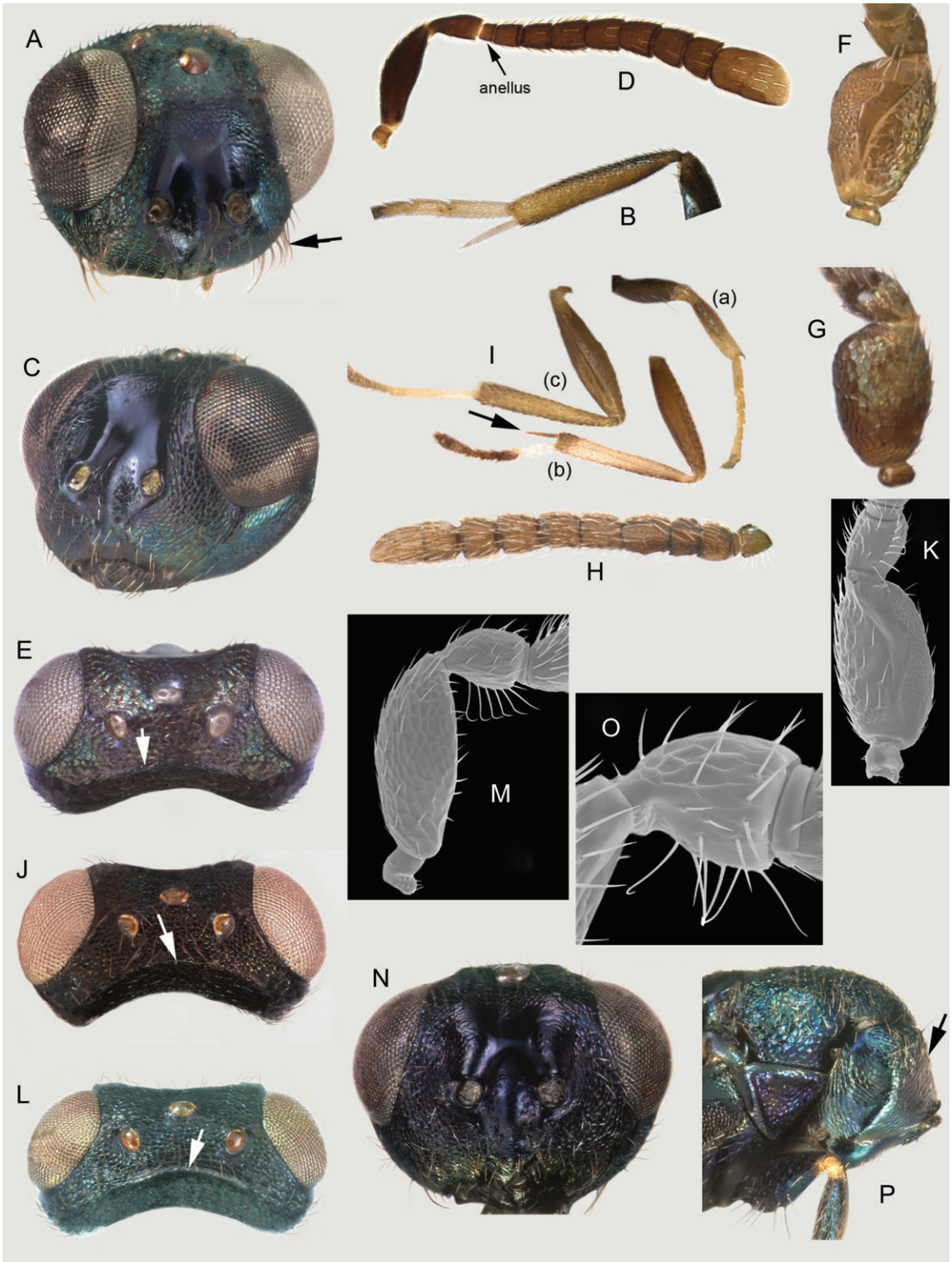

Fig. 12. Characters of male *Eupelmus* of the '*urozonus*-complex'. (A, B) *E. annulatus*: head in antero-lateral view (A), mesotibia (B). (C, D) *E. azureus*: head in antero-lateral view (C), antenna (D). (E–I) *E. tremulae*: head in dorsal view (E), scape respectively on outer (F) and inner side (G), pedicel and flagellum (H), (a) (b) (c) respectively fore, mid and hind legs (I). (J, K) *E. fulvipes*: head in dorsal view (J), scape and pedicel (K). (L, M) *E. kiefferi*: head in dorsal view (L), scape and pedicel (M). (N–P) *E. confusus*: head in frontal view (N), pedicel (O), pronotum in lateral view (P).

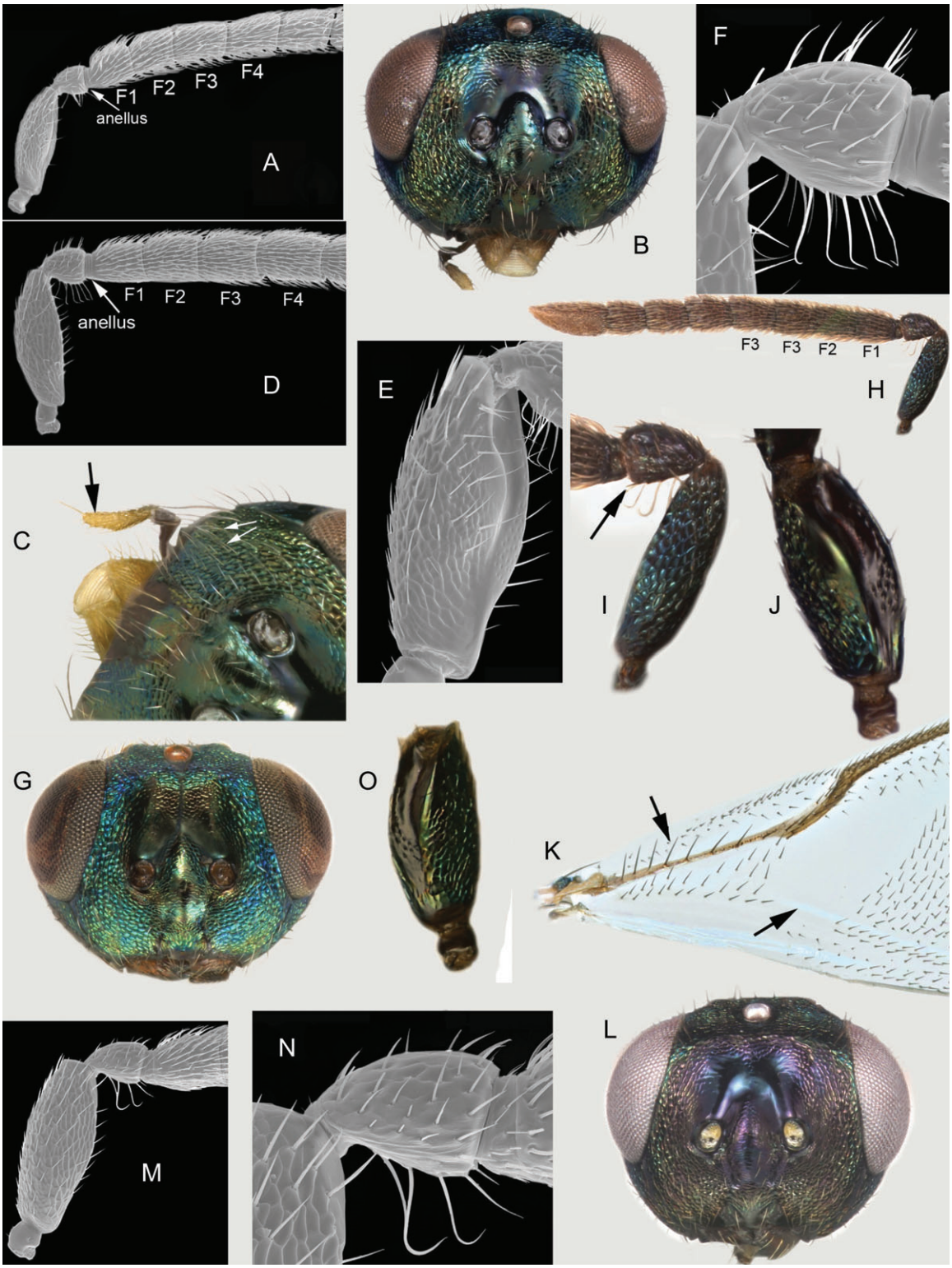

Fig. 13. Characters of male *Eupelmus* of the '*urozonus*-complex' (continued). (A) *E. confusus*: base of antenna. (B–F) *E. pistaciae*: head in frontal view (B), lower face and mouth parts (C), base of antenna (D), outer side of scape (E), pedicel (F). (G–K) *E. acinellus*: head in frontal view (G), antenna (H), scape and pedicel (I), outer side of scape (J), base of forewing (K). (L–N): *E. gemellus*: head in frontal view (L), base of antenna (M), pedicel (N). (O) *E. martellii* syntype: outer side of scape.

and the apical section of the submarginal vein bears 10 setae. These specimens are found at the base of the clade *E. confusus* in the *COI* tree and somewhat removed from it (see Fig. 1). Otherwise there is very little variation, except in the cases of very small specimens where the relative proportions of different parts of the body deviate from the means. Also the sculpture of the frontovertex and scrobal depression turns to vestigial; consequently it may be extremely difficult to identify them. An illustration is given in Doc.S1 with the female coded [FAL1088/10154].

Diagnosis. **Female.** Scrobal depression distinctly reticulate above interantennal boss and imbricate-reticulate laterally, but antennal scrobes smooth. Frontovertex superficially reticulate to level of lateral ocelli. Pronotal collar with violet reflections, in contrast to the rest of the dull dark mesosoma, which is at most dark bluish on antero-median lobe of mesoscutum, has bronze reflections on lateral lobes, postero-medial depression and scutellar-axillar complex, especially when using intense artificial light. Admarginal setae of pronotum black. Costal cell with a fairly wide bare strip along anterior margin, evidently broader than the length of the adjacent setae. Basal cell fairly sparsely setose, the setation often whitish. Discoloured section of submarginal vein generally bearing only a few setae (5–7). Stigmal vein at least slightly curved on hind margin. Postmarginal vein not longer than the stigmal vein. Ovipositor tricoloured, distinctly shorter than metatibia (0.70–0.78) and marginal vein (0.77–0.89); medial pale band whitish and longer than the apical dark band which is always very short. Apex of second valvifer not or hardly extending beyond apex of gaster. **Male**. Scrobal depression and frontovertex as for the female. Gena with one seta brownish and much longer than the others. Scape with outer band along the scapular scrobe bearing about 20 pores arranged into several lines basally and two lines apically; pedicel with a line of 5–7 hook-like setae. Pronotum strongly sloping anteriorly, almost vertical. Reticulation of posterior part of medial mesoscutal lobe with small and irregular meshes. Sublateral surface of propodeum, between convex plical area and spiracle, evidently concave; groove in front of spiracle continuing along its outer rim, hence spiracle apparently raised relative to surrounding surface. Mesotarsus white with 1–2 apical tarsomeres dark brown and metatarsus with the 2–3 basal tarsomeres white, the reminder progressively darkening.

Recognition. **Female.** The female of *E. confusus* is apparently similar to that of *E. martellii* and *E. gemellus* as those species have the same sculpture of frons (reticulate), scrobes (smooth and shiny) and scrobal depression (lower part smooth and shiny but upper part distinctly reticulate) and colouration of legs (femurs and tibias dark). In contrast, the females of *E. martellii* and *E. gemellus* have white admarginal hairs on pronotum, the pronotal collar is greenish, the costal cell has a very narrow anterior bare strip, the basal cell dense and dark setation, similar to that of the disc, apical section of the submarginal vein bears seven-nine setae, the ovipositor sheaths are longer. *E. confusus* is extremely close to the Afrotropical *E. afer* (Silvestri, 1914). The female syntypes of this species are badly crushed as they were initially slide-mounted; furthermore their colour was evidently modified by the medium used. Hence comparisons were made with a series of specimens reared from olives in Namibia which agree well with the original description and the characters visible on the syntypes. The body colour which is much brighter in *E. afer* in the two sexes; the smooth part of the scrobal depression in more reduced as the reticulation is better expanded on its lateral and dorsal surfaces; furthermore the sculpture on the interantennal boss is imbricate; the apical dark band of the ovipositor sheaths of *E. afer* is clearly longer than in *E. confusus* furthermore its medial pale band is lemon yellow. **Male**. The male of *E. confusus* can evidently be separated from that of *E. martellii* and *E. gemellus* by the strongly sloping, almost vertical, pronotum anteriorly. The characters of scape (number and distribution of pores) and pedicel (number of hook-like setae) and the colour of the tarsi of mid and hind legs is also useful. The male of *E. afer* also has a sloping pronotal collar; the meshes on the posterior part of mesoscutum are isodiametric and fairly large; the sublateral surface of the propodeum is here only slightly depressed and the rim of the spiracle is not elevated relative to the surrounding region.

Distribution. Mostly Mediterranean: Spain, Southern France, Corsica, Italy, Greece, Bulgaria, Cyprus and Iran, but one specimen collected in Sweden. Probably present in all countries bordering the Mediterranean Basin and also in the Near East.

Hosts. The following hosts have been definitively assessed: Diptera Cecidomyiidae: *Lasioptera carophila* (F. Low) on *Foeniculum vulgare* Miller (Apiaceae), *Asphondylia gennadii* (Marchal) on *Ceratonia siliqua* Linné (Fabaceae); Diptera Tephritidae: *Myopites stylata* (Fabricius) on *Dittrichia viscosa* (Linné) Greuter (Asteraceae), *B. oleae* on *Olea europaea* Linné (Oleaceae); Hymenoptera Cynipidae: *Andricus kollari* (Hartig), and *Biorhiza pallida* (Olivier) on *Quercus pubescens* Willdenow (Fagaceae), *Diplolepis rosae* (Linné) on *Rosa canina* Linné (Rosaceae), *D. kuriphilus* on *Castanea sativa* Miller (Fagaceae), *Timaspis phoenixopodos* (Mayr) on *Lactuca viminea* (Linné) J. Presl & C. Presl (Asteraceae); Hymenoptera Eurytomidae: *Bruchophagus* sp. (Eurytomidae) on *Asphodelus ramosus* Linné (Xanthorrhoeaceae); possibly Lepidoptera Pyralidae: *Apomyelois ceratoniae* (Zeller) on *Ceratonia siliqua*. It is quite possible, because of previous misidentifications under the name *E. urozonus*, that hosts recorded for this species actually concern *E. confusus*, especially cynipids galling Asteraceae.

***E.* (*Eupelmus*) *gemellus* Al khatib sp.n.**

http://zoobank.org/urn:lsid:zoobank.org:act:4BCB5C66-7AC7-431B-8F51-C76CF7D56AD4

(Female: Figs 9E, 17A–H; male: Figs 13L–N, 14A–B, 29A–C, 31E–G)

Type material. **Holotype**. FRANCE: Haute-Corse, Calenzana, 11.ix.2012, emerged 18.ix.2012, ex *Bactrocera oleae*

Fig. 14. Characters of male *Eupelmus* of the '*urozonus*-complex' (continued). (A, B) *E. gemellus*: base of forewing (A), mesosoma in dorsal view (B). (C–E) *E. martellii* syntype: head in frontal view (C), pedicel and flagellum (D), mesosoma in dorsal view (E). (F–I) *E. tibicinis*: base of antenna (F), outer side of scape (G), pedicel (H), hind leg (I). (J, K) *E. urozonus*: head in postero-lateral view (J), pedicel and base of flagellum (K).

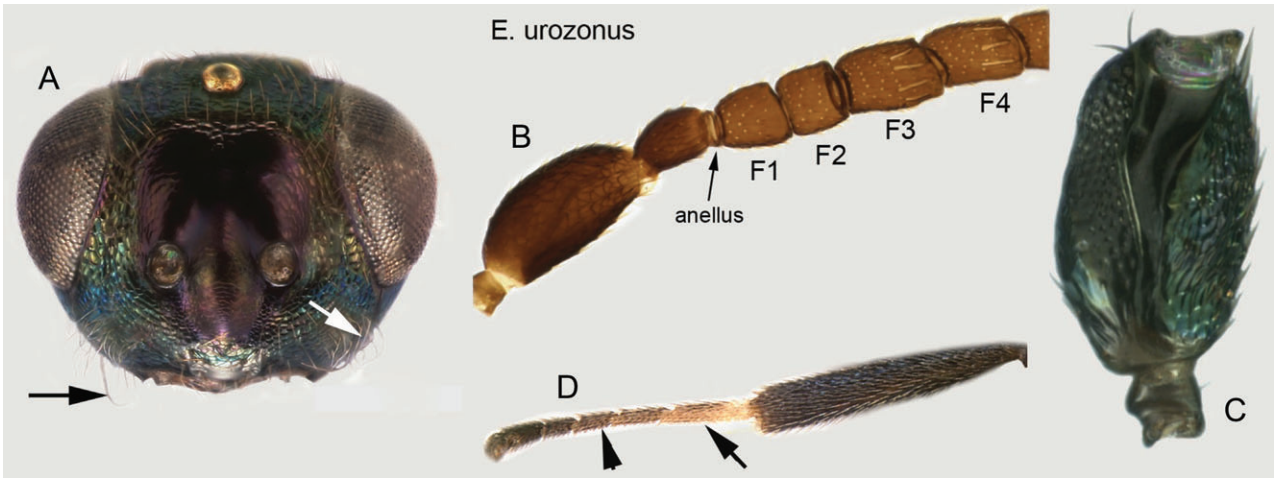

Fig. 15. Characters of male *Eupelmus* of the '*urozonus*-complex' (continued). (A–D) *E. urozonus*: head in frontal view (A), base of antenna (B), outer side of scape (C), metatibia and tarsus (D).

on *Olea europaea* (F. Ceccaldi) (1♀) [FAL1515/10408] (in MNHG). **Paratypes** are provided in Appendix S1.

Etymology. The name *gemellus* refers to the sister species for *E. martellii* because of their high degree of similarity.

Female. Length 3.46–4.10 mm. Head with greenish reflections, clearly green medially on frontovertex which shows distinct blue reflections laterally. Parascrobal area and scrobal depression often with distinct violet reflections. Setation silvery. Scape and pedicel with metallic greenish or bluish reflections. Flagellum and palpi blackish. Pronotum dark greenish on collar. All admarginal setae of pronotum pale. Mesonotum greenish with blue reflections variably distributed on mesoscutum, generally present on antero-medial lobe and sublateral bosses, occasionally on postero-medial depression; slight coppery reflections sometimes visible, especially on sublateral bumps. Tegula metallic greenish. Side of mesosoma mostly coppery bronze but lateral panel of pronotum with diffuse bluish spot ventrally and acropleuron with distinct blue spot on medial micro-sculptured region. Forewing hyaline, venation yellowish-brown, setae uniformly brown, but at least setae on submarginal vein quite dark and conspicuous. Procoxa and femur extensively dark with greenish tints except knee, yellowish to brownish, tibia yellowish-orange with dorsal and ventral band metallic greenish, tarsus completely orange-brownish except for pulvillus and sometimes with last apical tarsomere black. Mesocoxa dark with greenish lusters, femur brown at least ventro-laterally except for testaceous knee, tibia pale yellow to testaceous with a sub-basal brown to blackish ring and black apical pegs; apical spur and tarsus whitish to pale yellow at base and then gradually darkening except the brown telotarsus and the ventral black pegs on the four basal tarsomeres. Metacoxa with a large dorsal coppery spot, femur entirely, extensively dark with greenish reflections except knee lighter, brownish, tibia similar in colour to femur except for the last third apical part yellowish, basitarsus whitish, the followings segments progressively darkening with telotarsus blackish. Gaster mostly black, with distinct metallic green lustre anteriorly on basal tergum, and brown hair-like setae similar in colour to cuticle. Ovipositor sheaths with three distinct coloured regions, its basal and apical sections black and dark brown (respectively), the middle section pale yellow to whitish.

Frontovertex finely reticulate (raised network), imbricate-reticulate in front of median ocellus and on ocellar triangle. Vertex transversely reticulate behind ocellar triangle, merging into occiput without transverse carina or ridge. Head with scrobes and scrobal depression above the interantennal boss smooth and shiny, but upper half and sloping edges of depression transversely reticulate to imbricate. Interantennal boss finely coriaceous. Lower face and parascrobal surfaces with slightly lanceolate setae. Lower edge of antennal toruli somewhat below the lower ocular line. Head 1.57–1.84× as broad as long, temples 0.15–0.19× length of eyes, POL 2.67–3.33× OOL, lateral ocelli separated from adjacent eye orbit by 0.74–1.06× their own diameter which is 0.78–0.98× median ocellus diameter. Eyes separated by .0.38–0.43× head width, width of oral fossa 1.38–1.85× length of malar space. Antenna with combined length of pedicel and flagellum 1.21–1.33× head width, scape 5.22–5.90× as long as wide, pedicel 2.11–2.62× as long as wide and 0.83–1.25× combined length of anellus and F1, the funicular segments shortening and widening distally, F7 1.49–1.86× as wide as F1, clava 2.18–2.72× as long as wide, 0.82–0.93× combined length of three apical funicular segments.

Mesosoma 1.73–1.92× as long as broad. Pronotum with white admarginal hairs. Mesoscutum coarsely reticulate on convex antero-medial lobe, but finely reticulate on postero-medial depression, and lateral lobes finely reticulate to coriaceous mediolongitudinally. Scutellar-axillar complex 0.82–0.92× as long as wide, reticulate-imbricate and with elongate cells, in contrast to the isodiametric reticulation of mesoscutum. Prepectus with white hair-like setae (7–15 hairs) dorsolongitudinally,

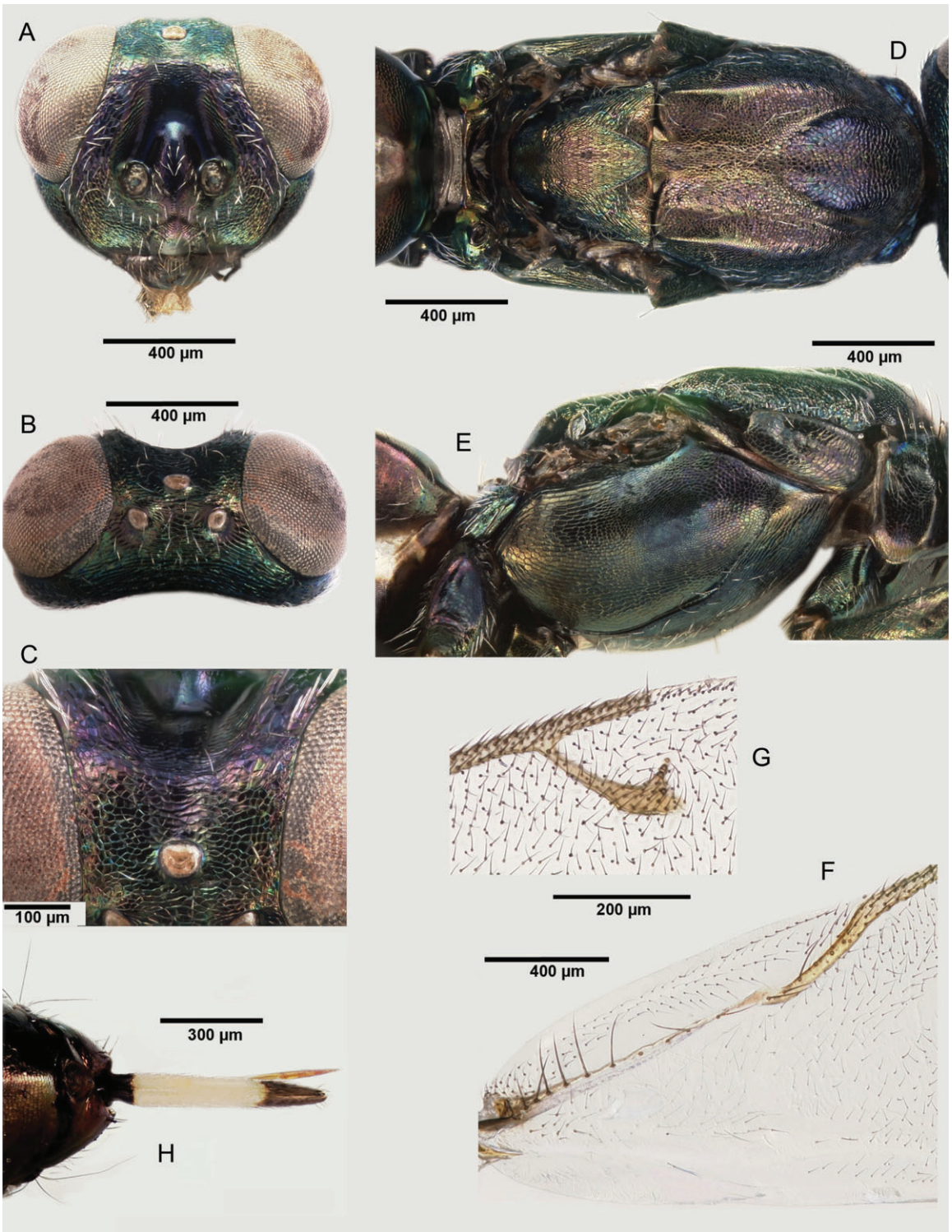

Fig. 16. Characters of female *Eupelmus confusus*. Head respectively in frontal (A) and dorsal view (B), frontovertex in antero-dorsal view (C), mesosoma respectively in dorsal (D) and lateral view (E), base of forewing (F), stigmal and postmarginal veins (G), ovipositor sheaths in dorsal view (H).

sometimes setal apices extending to dorsal margins. Acropleuron entirely, finely reticulate anterior and posterior of medial micro-sculptured region, the cells slightly larger posteriorly than anteriorly but with flat surfaces defined by slight raised ridges. Forewing with linea calva separated basally by several rows of setae from vanal area. Basal cell and disc uniformly setose, costal cell dorsally with line of setae over apical three quarters and ventrally setose along length with 2–3 lines of setae medially. Discoloured apical section of the submarginal vein, along parastigma, with 6–9 dorsal setae. Marginal vein 0.82–0.95× length of costal cell, postmarginal 1.00–1.15× as long as stigmal. Stigmal vein curved apically on hind margin. Mesotibia with apical row of 4–9 pegs. Mesotarsus ventrally with pegs on four basal tarsomeres, basitarsus with 30–34 pegs arranged distally in double row on either side, second tarsomere with 8–11 pegs in two rows, third with 4–5 pegs and apical tarsomere with one peg on one side. Propodeum with U-shaped plical depression extending to foramen, callus setose with white setae.

Gaster with apex of second valvifer not extending conspicuously beyond apex, ovipositor sheaths 0.80–0.96× length of metatibia and 0.97–1.24× length of marginal vein.

Male. Length 2.17–2.91 mm. Head dark greenish but frontovertex in front of median ocellus with faint violet spot and slight coppery lustres. Occiput bluish along edge of orbits. Scrobal depression and interantennal boss with distinct violet reflections. Scape and pedicel often with greenish to bluish-green reflections. Flagellum and palpi dark brown. Pronotum usually dark greenish on collar. Mesonotum commonly greenish with slight coppery reflections and sometimes with bluish reflections in particular on lateral mesoscutal lobes and axillae, notauli, transscutal line and scuto-scutellar sulcus occasionally brown to purplish. Tegula dark brown and often also variably metallic. Procoxa and femur dark green except lighter knee, tibia dark green with pale dorsal and ventral longitudinal strips, tarsus orange basally and brownish apically. Mesofemur dark green, mesotibia completely metallic greenish without pale dorsal or ventral longitudinal strips, tarsus whitish basally gradually darkening on the following segments. Metafemur and metatibia similar in colour to mesofemur and mesotibia, often dark with greenish reflections, tarsus with first basal tarsomere whitish, the reminder progressively darkening. Forewing hyaline. Propodeum metallic green to bluish-green. Gaster with basal tergum metallic green to bluish-green basally, but reminder black with slight violet lustres.

Frons reticulate, vertex clearly reticulate to transversely reticulate and merging into occiput without transverse carina or ridge. Antennal scrobes and lower part of scrobal depression smooth and shiny, but upper part and lateral edges distinctly reticulate, interantennal boss coriaceous to very slightly reticulate. Lower face with sparse setae often whitish to brownish, the setae shortest mesally and variably longer laterally, curved when long. Lower face without outstanding setae above malar sulcus. Gena with one seta brownish and much longer than the others. Head in dorsal view 1.71–1.96× as broad as long, temples 0.22–0.26× length of eye, POL 3.27–3.89× OOL, lateral ocelli separated from adjacent eye orbit by 0.75–0.98× their own diameter. Eyes separated by 0.46–0.50× head width, width of oral fossa 1.60–1.69× length of malar space. Antenna with combined length of pedicel and flagellum 1.32–1.39× head width. Scape ovoid, 2.67–3.03× as long as maximum width, the outer band along the scapular scrobe with 14–16 pores arranged in 2–3 lines basally and one line apically. Pedicel subglobular, 1.47–1.65× as long as wide and ventrally with a line of 3–4 hook-like setae and sometimes with one straight apical seta. Flagellum densely setose and robust-filiform. Basal flagellomere (anellus) discoidal. F1 sometimes with MPS, 0.85–1.06× as long as F3. Clava lanceolate with micropilose sensory region nearly along entire length on ventral surface, 2.08–2.40× as long as wide; combined length of apical three funicular segments 3.39–3.91× length of clava.

Mesoscutum and scutellar-axillar complex reticulate, but reticulation of posterior part of medial mesoscutal lobe usually much smaller and posterior part of scutellum coriaceous. Propodeum finely coriaceous and shiny with percurrent median carina; callus similarly finely sculptured with setae originating from tiny bumps. Forewing with stigmal vein curved on hind margin, marginal vein 0.70–0.75× as long as costal cell and postmarginal 0.90–0.99× as long as stigmal. Costal cell dorsally with line of dark setae extending at least to apical half and ventrally with dark setae continuously along length, mesally on two lines, so two complete rows of setae are present. Speculum closed posteriorly by 3–4 setae on cubital fold.

Variation. **Female**. Some specimens reared from certain hosts show morphological variability in comparison with most studied individuals. For example, some of the females reared from seeds of *Juniperus* barely have blue reflections on head and mesosoma and they are here mostly coppery bronze. Also, in most females reared from galls of *D. kuriphilus*, the parascrobal area and scrobal depression are metallic green without violet reflections or at most with very faint violet lustres. **Male**. Most males of *E. gemellus* reared from different insect hosts are metallic greenish with slight coppery reflections on the head and mesonotum. However, some males, such as the male [FAL1269/10439] which was reared from the olive fly, *B. oleae*, have a head metallic blue with slight coppery reflections on frontovertex, mesosoma metallic dark blue with slight greenish reflections on the antero-medial mesoscutal lobe and on the scutellum and femurs dark metallic blue.

Diagnosis. **Female**. Head with bluish reflections laterally on frontovertex and mesoscutum. Pronotum dark greenish on collar. Antennal scrobes smooth and shiny but upper part of scrobal depression distinctly reticulate to transversally reticulate. Frontovertex superficially reticulate to level of lateral ocelli. Vertex merging into occiput and without carina or ridge. Admarginal setae of pronotum white. Bare strip behind leading margin of costal cell very narrow. Basal cell setose and setae similar in colour to disc. Discoloured section of submarginal vein with 6–9 setae. Stigmal vein at least slightly curved on hind margin. Postmarginal vein as long as or barely longer than the stigmal vein. Ovipositor tricoloured, shorter than metatibia (0.80–0.96× length of metatibia) and of about same length as marginal vein

Fig. 17. Characters of female *Eupelmus gemellus*. Head in frontal view (A), frontovertex and scrobal depression in antero-dorsal view (B), head in dorsal view (C), mesosoma in dorsal (D) and lateral view (E), base of forewing (F), stigmal and postmarginal veins (G), ovipositor sheaths in dorsal view (H).

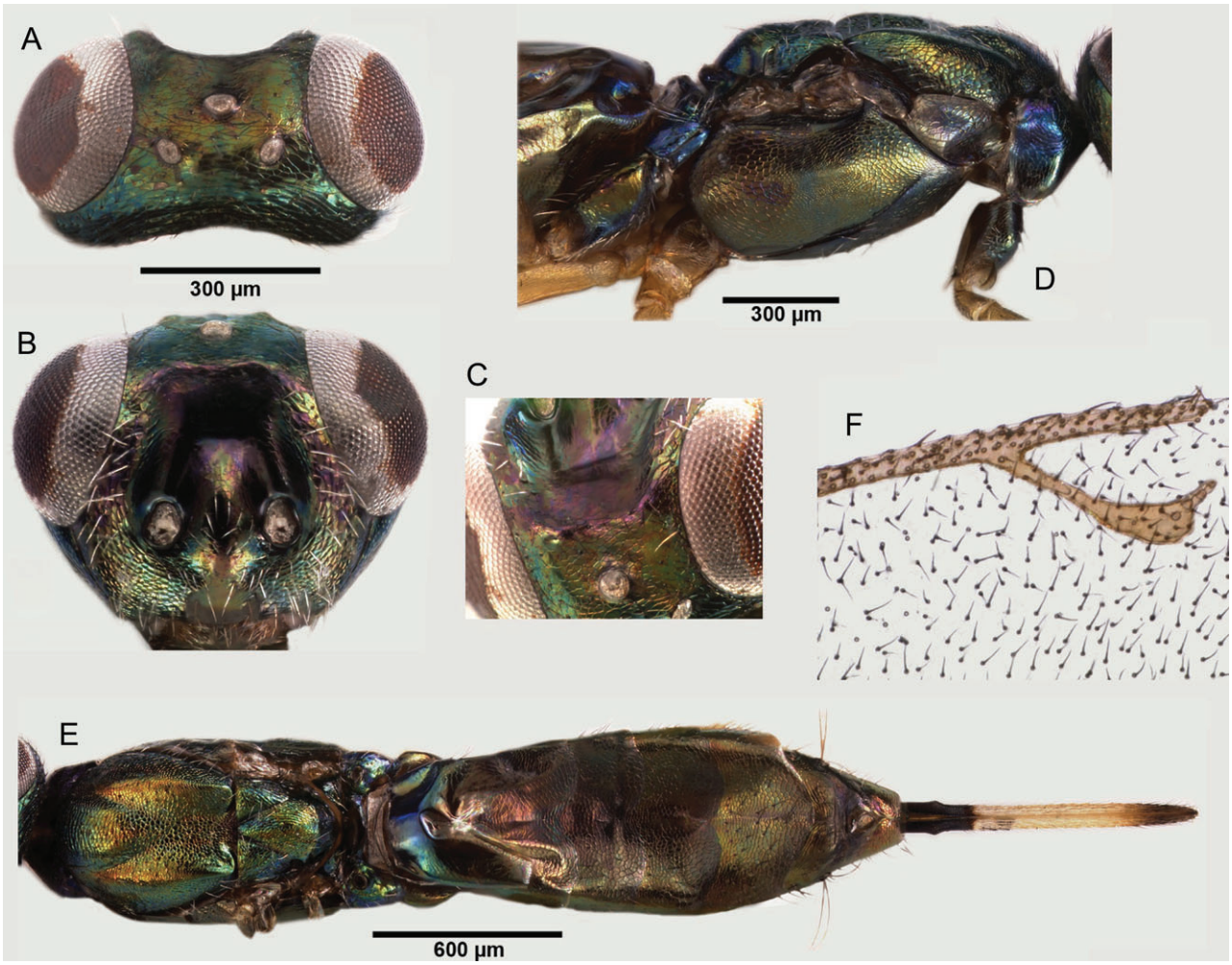

Fig. 18. Characters of female *Eupelmus janstai*. Head in dorsal (A) and frontal view (B), frontovertex and scrobal depression in antero-dorsal view (C), mesosoma in lateral view (D), meso- and metasoma in dorsal view (E), stigmal and postmarginal veins (F).

(0.97–1.24×). Medial pale band of ovipositor pale yellow to whitish. Apex of second valvifer not or hardly extending beyond apex of gaster. **Male**. Head and mesosoma mostly greenish with slight coppery lustres. Scrobes smooth and shiny but upper part of scrobal depression distinctly reticulate. Lower face without long and/or apically curved setae above malar sulcus. Gena with unique brown long and curved seta. Scape with few pores (14–15) on outer band along length of scapular scrobe region, distributed in one line apically. Pedicel ventrally with one line of 3–4 hook-like setae and sometimes with one straight apical seta. F1 occasionally with MPS. Costal cell dorsally with one line of dark setae over apical three-quarters and ventrally setose with at most three lines of dark setae mesally. Speculum closed posteriorly.

Recognition. **Female**. Very similar morphologically to *E. martellii* with which it is easily confused as the two species have the same structural characters. They are separated by the colour of the head and mesosoma. In *E. gemellus*, the head has blue reflections laterally on frontovertex, most often also on mesoscutum, whereas the head and mesosoma of *E. martellii* are entirely bronze greenish and without bluish reflections. **Male**. We are unable to find reliable morphological characters separating *E. gemellus* from *E. martellii*.

The distinctive characters between *E. gemellus* and *E. confusus* are reported above in the original description of that species.

Distribution. Widely distributed through Europe. Probably present in all countries bordering the Mediterranean basin.

Hosts. E. gemellus was reared from the following insect hosts : Diptera Tephritidae: *B. oleae* on *O. europaea* (Oleaceae), *M. stylata* on *D. viscosa* (Asteracae); Hymenoptera Cynipidae: *D. kuriphilus* on *C. sativa* (Fagaceae); Hymenoptera Tenthredinidae: *Pontania pedunculi* (Hartig) on *Salix elaeagnos* Scopoli (Salicaceae); Hymenoptera Torymidae: *Megastigmus pistaciae*

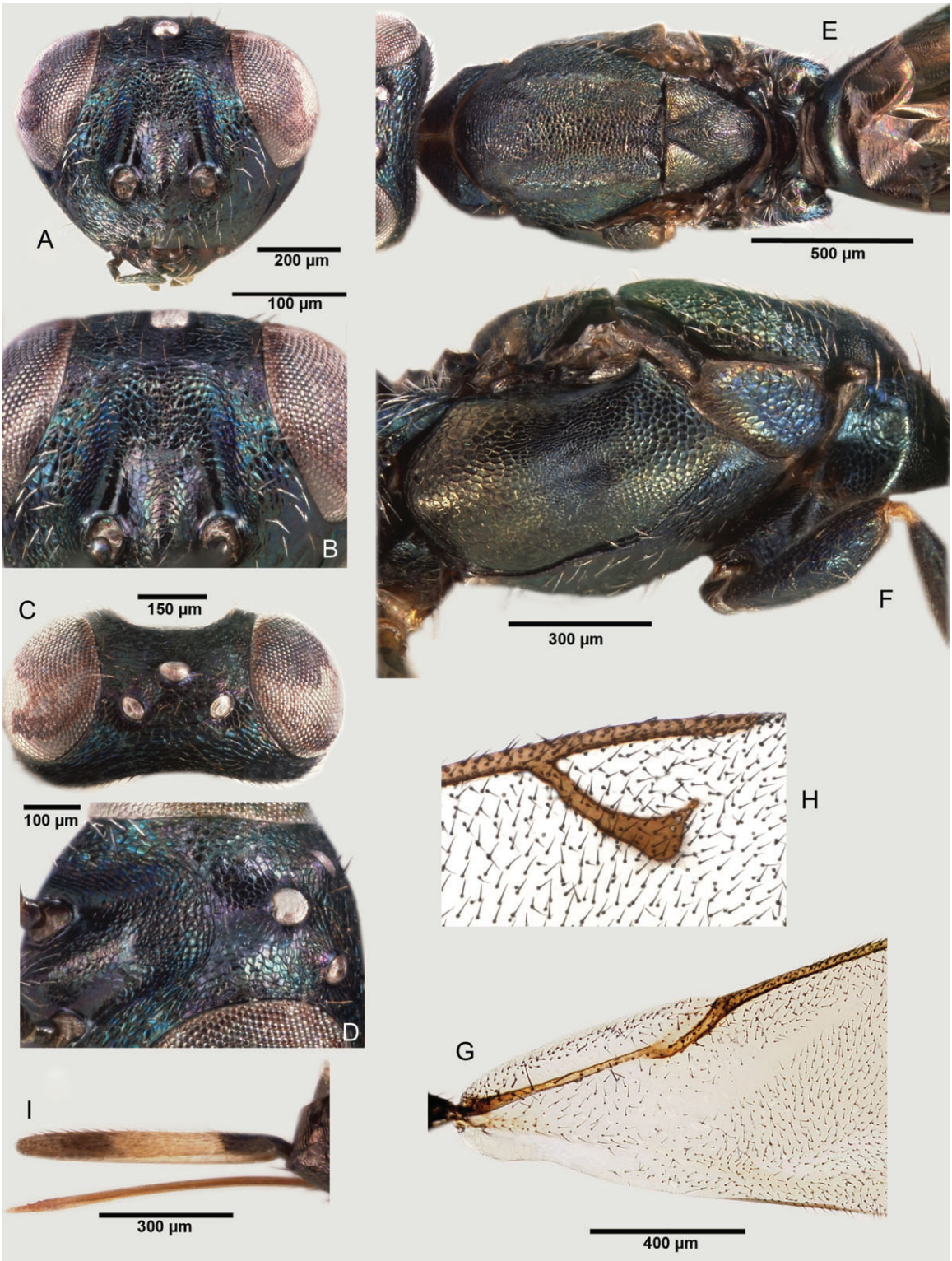

Fig. 19. Characters of female *Eupelmus longicalvus*. Head in frontal view (A), scrobal depression (B), head in dorsal view (C), frontovertex and scrobal depression in latero-dorsal view (D), mesosoma in dorsal (E) and lateral view (F), base of forewing (G), stigmal and postmarginal veins (H), ovipositor sheaths in lateral view (I).

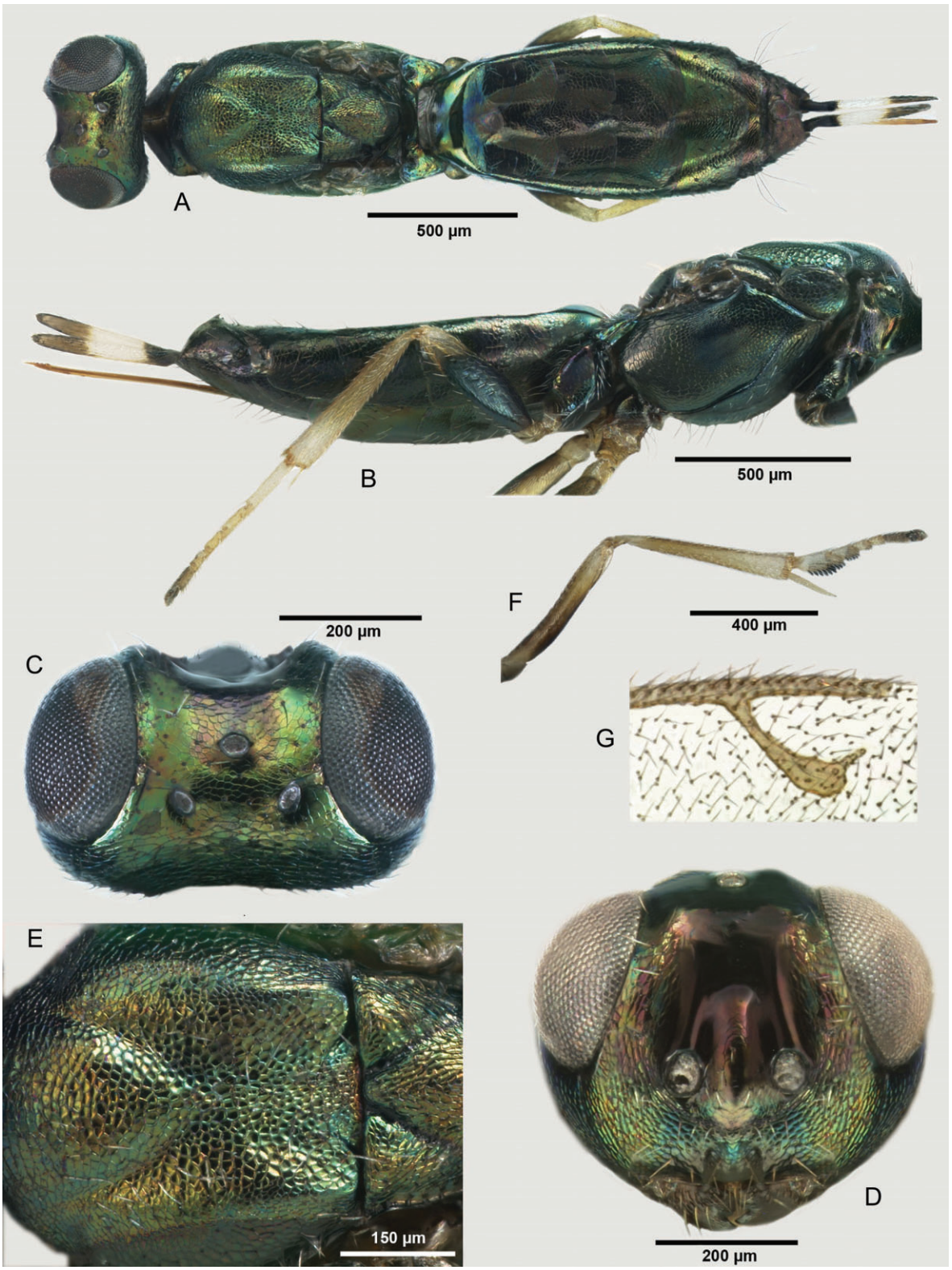

Fig. 20. Characters of female *Eupelmus minozonus*. Body in dorsal view (A), mesosoma, hind leg and metasoma in lateral view (B), head in dorsal (C) and frontal view (D), mesoscutum (E), mid leg (F), stigmal and postmarginal veins (G).

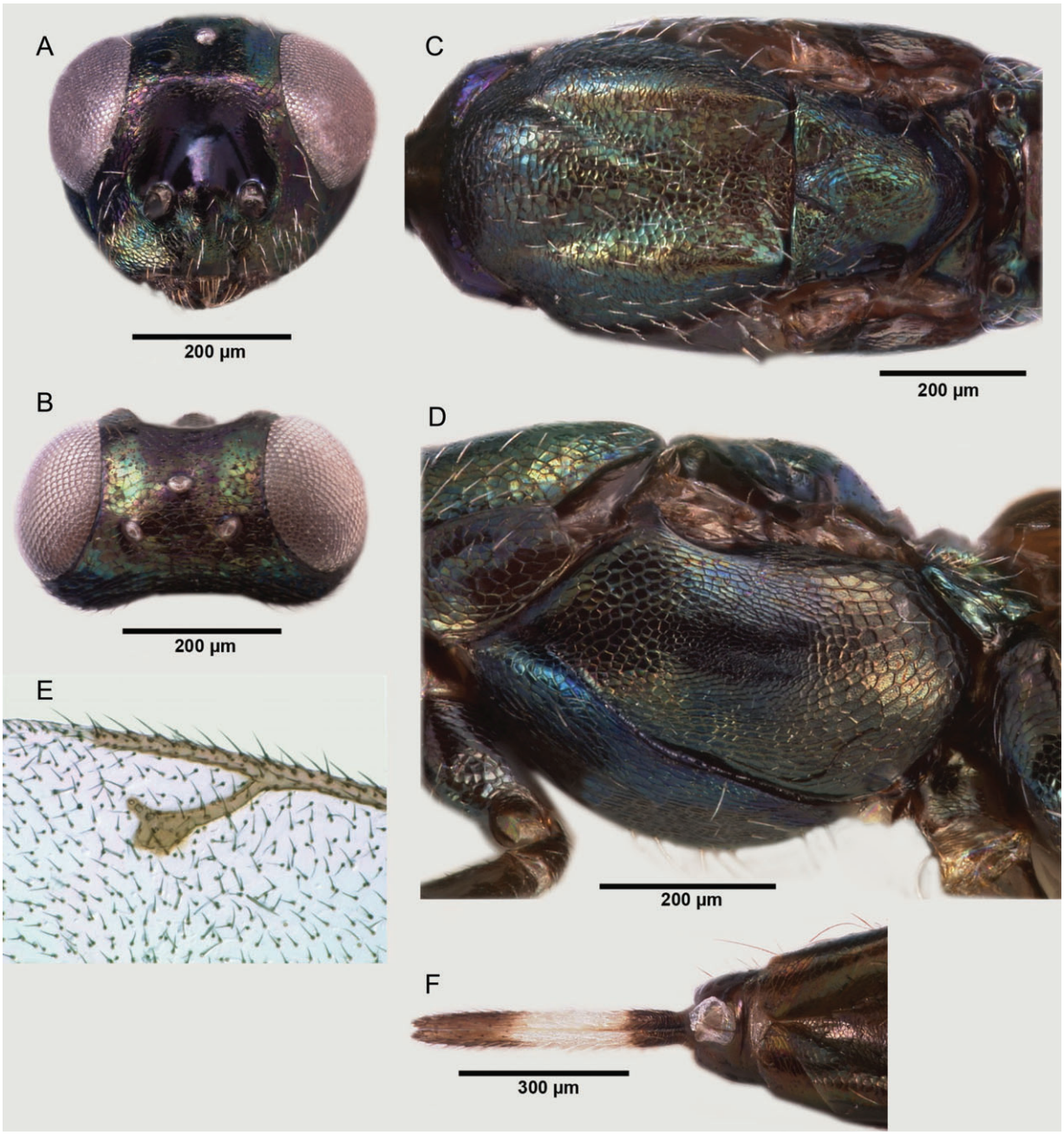

Fig. 21. Characters of female *Eupelmus opacus*. Head respectively in frontal (A) and dorsal view (B), mesosoma in dorsal (C) and lateral view (D), stigmal and postmarginal veins (E), ovipositor sheaths in dorsal view (F).

(Walker) on *Pistacia lentiscus* Linné (Anacardiaceae) and Lepidoptera Gelechiidae: *Mesophleps oxycedrella* (Millière) on *Juniperus oxycedrus* Linné (Cupressacae).

***E.* (*Eupelmus*) *janstai* Delvare and Gibson sp.n.**
http://zoobank.org/urn:lsid:zoobank.org:act:27BFFF36-E3EE-4B94-AC0B-D4AB07836E1B
(Female: Figs 6J, K, 18A–F)

Type material. **Holotype** ♀. CZECH REPUBLIC: Břeclav district, Pavlov, 48.86750°N, 16.65416°E, sweeping on *Tilia platyphyllos*, 03.vii.2010 (G. Delvare) [GDEL4046/10032] (in MNHG). **Paratypes**. Moravia, Vranov riv., Dyje, 48.89472°N, 15.81250°E, 13.viii.1991, riparian forest (L. Masner) (2♀ in CNC).

Etymology. Named in honour of our colleague Petr Jansta, in recognition of his kind welcome and his competence.

Female. Length of holotype 3.15 mm. Head metallic green, bearing whitish setae. Scrobal depression and upper half of interantennal boss violet, but boss greenish on lower half, occiput greenish-blue. Scape and pedicel very slightly bluish, flagellum and palpi dark brown. Pronotum bluish violet on collar and on lateral panels. Mesoscutum bronze with greenish reflections on periphery of antero-medial lobe and outer slopes of lateral bosses. Tegula dark brown with slight metallic reflections. Scutellar-axillar complex greenish with blue reflections on axillae and frenum. Metanotum and propodeum laterally bright blue, plical region black. Prepectus bluish with bronze reflections on margin. Acropleuron greenish bronze except the medial micro-sculptured region, blue. Mesepisternum bluish. Forewing hyaline, venation testaceous, setae brown, darker on submarginal vein. Procoxa with bluish metallic tints, trochanter blackish, femur except knee and baso-dorsal spot on tibia darkened with bluish reflections, the rest of the leg testaceous, except for the dark brown telotarsus and pulvillus. Mesocoxa dark brown, the rest of leg testaceous with tarsus turning to whitish, pegs on tibia and four basal tarsomeres black and pulvillus dark. Metacoxa with bright coppery-bronze reflections dorsally and bluish ventrally, trochanter brownish, femur with basal two thirds darkened, the rest of femur and tibia testaceous, tarsus yellowish-white except darkened telotarsus and pulvillus. Gaster dark brown (exhibiting faint coppery reflections when using intense artificial light) but first tergum with bright blue reflections anteriorly; setation dark everywhere. Ovipositor sheaths tricoloured, its basal and apical quarters respectively black and brown, the middle section testaceous.

Frontovertex finely and entirely coriaceous to lateral ocelli, distinctly reticulate to transversally reticulate-imbricate posteriorly and progressively merging into occiput without transverse ridge. Antennal scrobes and scrobal depression smooth and shiny with its periphery finely and superficially alutaceous, as well as interantennal boss. Lower margin of antennal toruli below lower ocular line. Head 1.88× as broad as long, 1.34× as broad as high, temples 0.18× length of eyes, POL 2.89× OOL, lateral ocelli separated from adjacent eye orbit by 0.80× their own diameter which is 0.85× median ocellus diameter. Eyes separated by 0.41× head width and 0.87× eye height, width of oral fossa 1.40× length of malar space. Antenna with combined length of pedicel and flagellum as 1.25× head width, scape 4.62× as long as wide, pedicel 2.18× as long as wide and 1.19× combined length of anellus and F1, the funicular segments shortening and widening distally, F7 1.74× as wide as F1, clava 2.45× as long as wide, 1.04× combined length of three apical funicular segments.

Mesosoma in dorsal view 1.86× as long as broad. Mesoscutum with fairly coarse reticulation on antero-medial lobe and postero-medial depression; lateral lobes with finer sculpture, coriaceous on top and reticulate on outer slopes. Scutellar-axillar complex 0.90× as long as broad, obliquely or longitudinally reticulate-imbricate in distinct contrast to isodiametric reticulation of mesoscutum. Prepectus with only a few (4–5) hair-like setae on centre of disc. Acropleuron finely reticulate anterior of medial micro-sculptured region, the reticulation coarser on posterior surface. Forewing 2.36× as long as broad, densely and uniformly setose except for linea calva; costal cell dorsally with one line of setae on apical two thirds, ventrally densely setose with three lines of setae close to anterior margin. Stigmal vein straight on hind margin, stigma hardly enlarged, sensilla placodea shortly distant from each other. Linea calva 0.45× length of marginal vein, marginal vein 0.96× as long as costal cell and postmarginal vein 1.05× as long as stigmal vein. Mesotibia with an apical row of four black pegs, ventral surfaces of mesotarsal segments 1–4 bearing black pegs, the basitarsus with 23 pegs arranged distally in double row on either side, second segment with nine in two rows, the third with five and fourth with two. Propodeum with U-shaped plical depression extending to foramen, callus setose with white setae.

Gaster with apex of second valvifer distinctly extending conspicuously beyond apex, ovipositor sheaths long, 1.52× length of marginal vein and 1.36× length of metatibia.

Male. Unknown.

Diagnosis. Body elongate; mesoscutum and acropleuron mostly bronze; legs, except coxae, extensively pale, including all tibiae and mesofemur, scrobal depression smooth, frontovertex coriaceous, lateral ocelli separated from adjacent eye orbit by 0.80× their own diameter, prepectus sparsely setose, stigmal vein straight on hind margin, ovipositor distinctly longer than metatibia and marginal vein and apex of second valvifer evidently exerted.

Recognition. The female of *E. janstai* is morphologically similar to that of *E. azureus* because of the identical sculpture on frontovertex and scrobal depression and relative length of ovipositor sheaths. Nevertheless in *E. azureus* the entire mesosoma is greenish to bluish, the diameter of the lateral ocelli is larger so that they are separated from the adjacent eye orbit by at most 0.50× their own major diameter, the prepectus is extensively setose and pro- and metafemora extensively dark with metallic reflections, and respective tibiae partly fuscous. *E. janstai* is otherwise similar to the *Eupelmus* species having a coriaceous frontovertex and a straight stigmal vein: *E. tibicinis*, *E. priotoni* **sp.n.** and *E. opacus* **sp.n.** *E. janstai* differs from the first species by the absence of sculpture on the scrobal depression and from the other species by its longer ovipositor, clearly longer than the metatibia and marginal vein.

Distribution. Czech Republic; the species is, for the time being, endemic to Southern Moravia. The holotype was collected in the Děvi-Kotel-Soutěska National Park, on the southern slope of a hill which harbours several representatives of the Mediterranean fauna, especially the famous *Saga pedo* (Pallas, 1771) (Tettigoniidae).

Host(s). Unknown.

***E.* (*Eupelmus*) *longicalvus* Al khatib & Fusu sp.n.**

http://zoobank.org/urn:lsid:zoobank.org:act:F83B5381-0448-4EE3-B42F-F9AD7749F964

(Female: Figs 7H–K, 19A–I)

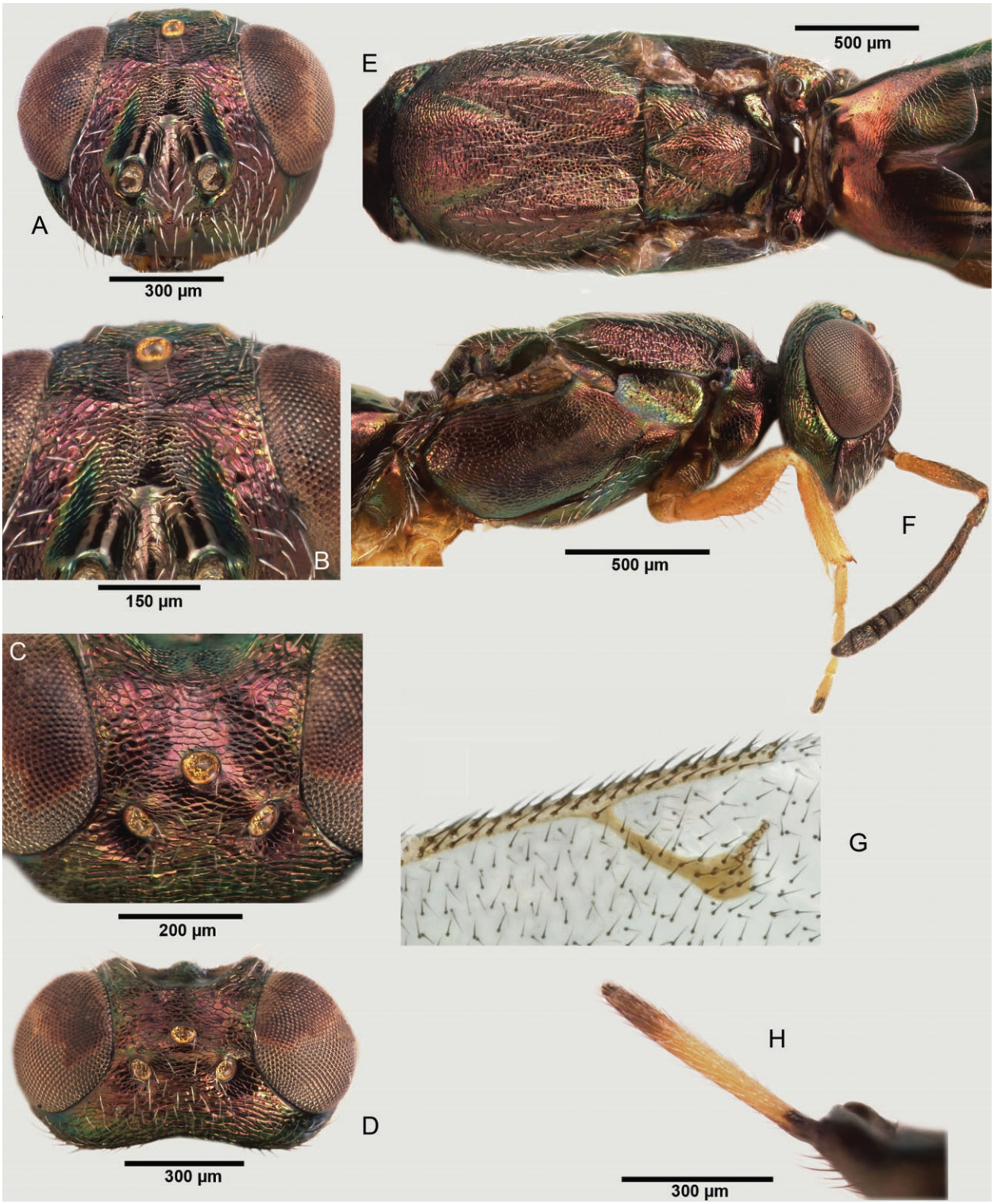

Fig. 22. Characters of female *Eupelmus pistaciae*. Head in frontal view (A), frons and scrobal depression in frontal view (B), frontovertex in antero-dorsal view (C), head in dorsal view (D), mesosoma in dorsal view (E), head, mesosoma and fore leg in lateral view (F), stigmal and postmarginal veins (G), ovipositor sheaths in lateral view (H).

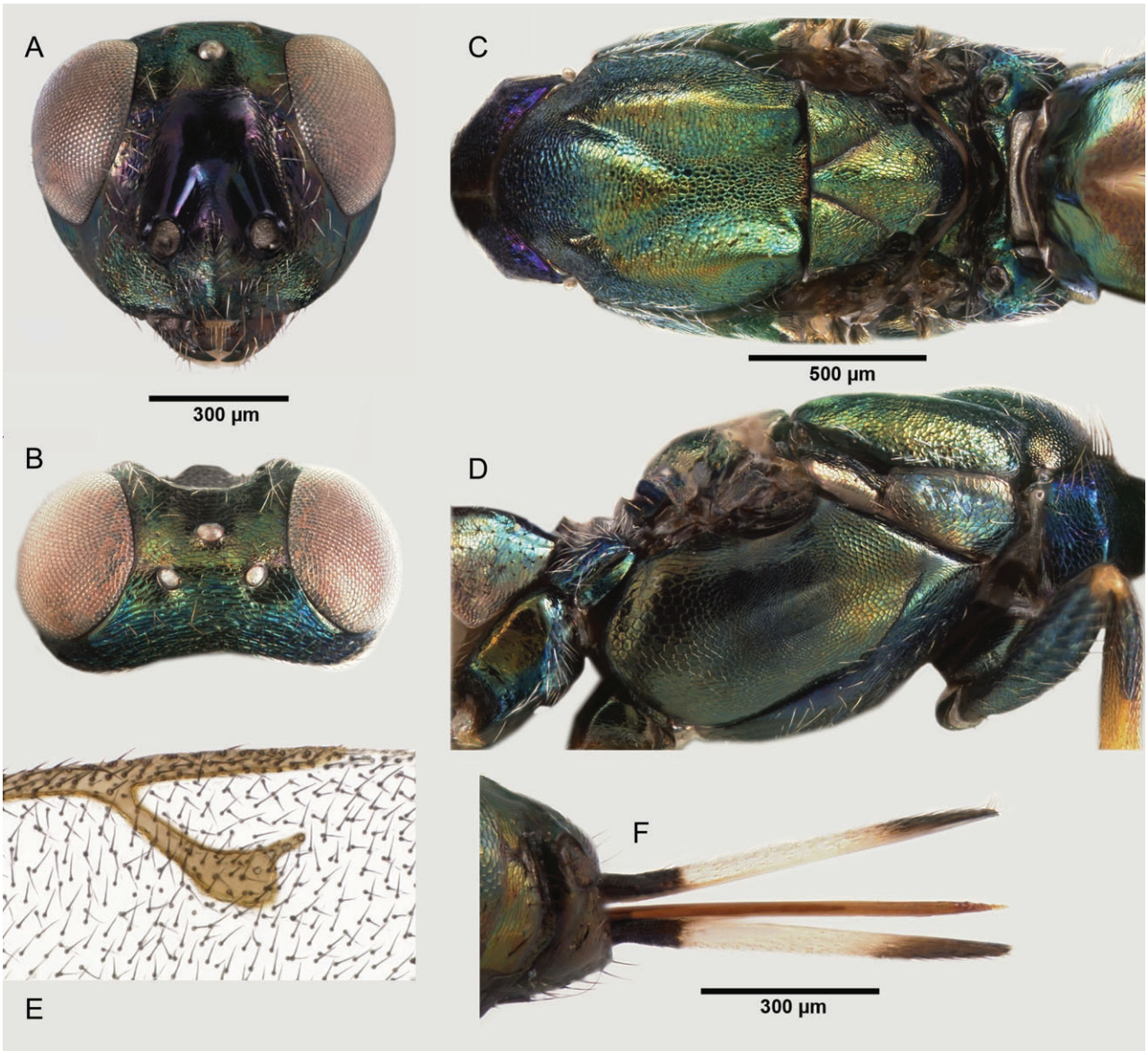

Fig. 23. Characters of female *Eupelmus priotoni*. Head in frontal (A) and dorsal view (B), mesosoma in dorsal (C) and lateral view (D), stigmal and postmarginal veins (E), ovipositor sheaths in dorsal view (F).

Type material. **Holotype.** ♀. SWEDEN: Gotlands, Go, Gotlands kommun, Roleks, grazed calcareous pine forest. 57°32.207′N, 18°20.273′E, 16.vii–02.viii.2004, Trap ID 28, Coll. event 1458 (SMTP) [LF.ma.SW 02/10429] (in NHRS). **Paratypes** are provided in Appendix S1.

Etymology. The name is a combination of the Latin words *longus* (long) and *calvus* (hairless) in reference to the linea calva of the females that is very long.

Female. Length 1.75–3.15 mm (holotype 3.15 mm). Head dark with slight bluish to dark-violet lustre, with parascrobal area and sometimes scrobal depression comparatively brighter bluish-green. Lower face and parascrobal area bearing white setae, frons with brown setae. Flagellum, palpi and mandibles dark, almost black. Scape and pedicel very slightly metallic bluish. Mesosoma dark and hardly metallic, bearing brown setae including the admarginal pronotal setae. Pronotum and mesoscutum with very slight bluish to bluish-green tinge and bronze reflections by places but pronotum with distinct metallic bluish violet tint on collar and on lateral panels. Scutellar-axillar complex dark-green with bronze reflections. Tegula dark brown with very faint metallic reflections. Propodeum slightly bluish but with coppery reflections around spiracles. Prepectus evidently bluish. Acropleuron dark with faint bronze lustre posteriorly and bluish-green anteriorly on either side of the dark-blue micro-sculptured region. Forewing with slight

brownish infumation (hyaline in small specimens), venation yellowish-brown, setae brown, those on submarginal vein quite dark. Procoxa black, femur extensively dark except brownish knee, tibia yellowish except dark brown dorsal and ventral strips, tarsus entirely brownish. Mesocoxa dark brown, femur dark except for brownish knee, tibia reddish with dark sub-basal longitudinal band and black apical pegs, tarsomeres testaceous with dorsal infumation which is progressively enlarged from base to apex, telotarsus dark and ventral pegs black. Metacoxa without coppery spot, dark with very slight metallic bluish lustre; femur mostly dark with brownish knee; tibia dark except for the orange apex, tarsus fuscous. Gaster dark brown with bluish metallic lustre, with very slight metallic green to blue lustre anteriorly on basal tergum and with brown hair-like setae. Ovipositor with three coloured regions, short black basal region delineated from much longer yellowish medial region, and variably conspicuously graduated brownish apical band.

Frontovertex distinctly superficially reticulate (network only slightly yet recognizably raised), transversely reticulate-imbricate posteriorly, merging to occiput without transverse carina. Scrobes and scrobal depression entirely reticulate. Interantennal boss imbricate-reticulate. Lower edge of antennal toruli evidently below lower ocular line. Lateral outline of gena slightly convex. Head 1.68–1.98× as broad as long and 1.28–1.32× as broad as high, temples 0.11–0.15× length of eyes, POL 2.48–3.33× OOL, lateral ocelli separated from adjacent eye orbit by 0.58–0.87× their own diameter which is 0.80–0.94× median ocellus diameter. Eyes separated by 0.42× head width, width of oral fossa 1.21–1.42× length of malar space. Distance between lower margins of antennal toruli from edge of oral fossa slightly larger than intertorular distance. Antenna with combined length of pedicel and flagellum as 1.37–1.49× head width, scape 3.95–5.45× as long as wide, pedicel 1.85–2.24× as long as wide and 0.69–0.86× combined length of anellus and F1. Funicular segments shortening and widening distally, F7 1.55–1.82× as wide as F1, clava 2.35–2.58× as long as wide, 0.77–0.81× the combined length of the three apical funicular segments.

Mesosoma 1.48–2.06× as long as broad. Mesoscutum transversely reticulate on convex antero-medial lobe, the reticulation progressively becoming coarser, with isodiametric cells, posteriorly on medial depression; lateral lobes minutely coriaceous on bosses. Scutellar-axillar complex 0.83–0.89× as long as wide, densely reticulate-imbricate, the small cells arranged in elliptic rows around the centre of scutellum. Prepectus with 3–8 setae. Acropleuron coarsely reticulate on each side of the medial micro-sculptured region. Forewing about 2.55× as long as wide, with a large bare to very sparsely setose area at the juncture of basal and cubital folds which continues with linea calva, making the linea calva appear much longer, 0.76–1.00× as long as marginal vein, reaching a level with base of parastigma and separated by only one to a few setae from the vanal area; basal cell and disc uniformly setose. Costal cell dorsally with line of setae near anterior margin on whole length and ventrally setose along length with at least three lines of setae. Marginal vein 0.96–1.15× as long as costal cell, postmarginal vein distinctly longer (1.33–1.42×) than the hardly curved on hind margin stigmal vein. Stigma hardly and triangularly enlarged. Sensilla placodea shortly distant from each other. Mesotibia with apical row of pegs, mesotarsus ventrally with pegs on basal four tarsomeres, basitarsus ventrally with pegs arranged distally in double row on either side, second and third segment with pegs arranged in one row on each side, and telotarsus with single or two pegs on either side. Propodeum with U-shaped plical depression extending to foramen, callus setose with curved setae.

Gaster reticulate with isodiametric cells, except most surface of first tergum basally smooth but merging to coriaceous. Apex of second valvifer extending slightly beyond apex of gaster, ovipositor sheaths 0.73–0.80× length of metatibia and 0.76–0.93× as long as marginal vein.

Variation. In small specimens the metallic lustre, as described for large specimens, is much reduced. Linea calva not quite reaching level with base of parastigma but nevertheless wing surface with sparse setae there. When the area between basal and cubital folds is sparsely setose instead of bare, linea calva appears shorter (0.76× as long as marginal vein), but its apparent proximal end is still defined and separated from vanal area by an area of sparse and irregularly distributed setae. Postmarginal vein occasionally fading with apex not easy to distinguish.

Male: unknown.

Diagnosis. Antennal scrobes and scrobal depression almost completely and distinctly reticulate. Frontovertex also reticulate. Linea calva extended proximally to level equal with base of parastigma. Postmarginal vein distinctly longer than stigmal vein. Ovipositor shorter than metatibia and slightly shorter than marginal vein. These characters allow to easily distinguish the species.

Recognition. Because of the comparatively long ovipositor sheaths with graduated yellowish-brown apex in combination with a reticulated scrobal depression, females of *E. longicalvus* are superficially similar to females of *E. annulatus* with shorter ovipositor sheaths. Besides the posteriorly expanded linea calva, they can be separated by the dark frons with some bluish and violet lustre and somewhat roughened, imbricate to imbricate-reticulate sculpture and bluish-green parascrobal area (in *E. annulatus* frons smooth and coriaceous and more or less distinctly tricoloured with green to bluish-green lustre along inner orbits and mesally dark violet below level of anterior ocellus and parascrobal area blue to purple).

Distribution. Sweden, French, Italian and Dinaric Alps. This disrupted distribution is typically a relict one, originating from a former larger one during the glaciations, as found in many plant species. The retreating of the glaciers fragmented the populations.

Host(s). Unknown.

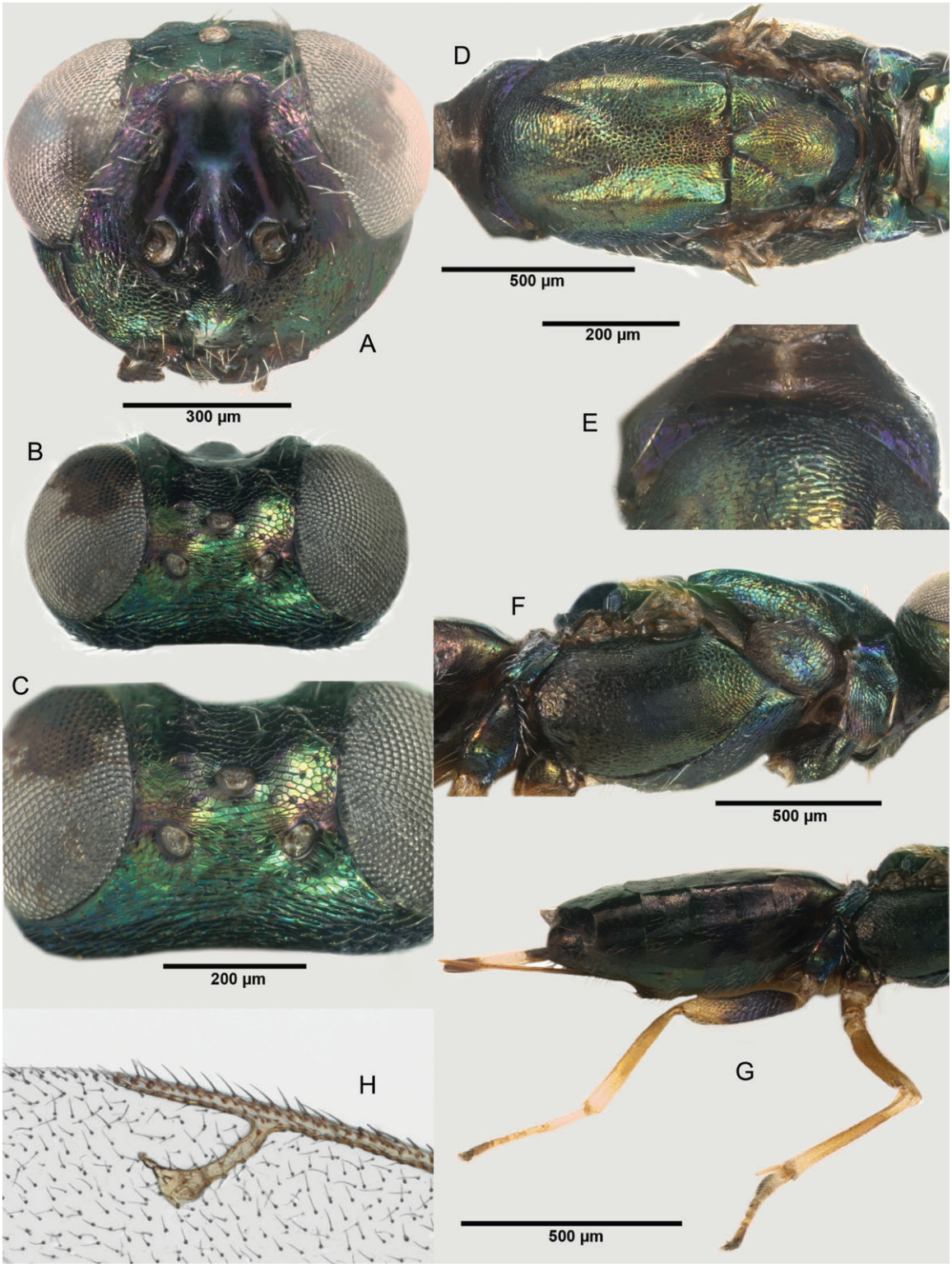

Fig. 24. Characters of female *Eupelmus purpuricollis*. Head respectively in frontal (A) and dorsal view (B), frontovertex (C), mesosoma in dorsal view (D), pronotum in dorsal view (E), mesosoma in lateral view (F), metasoma, mid and hind legs in lateral view (G), stigmal and postmarginal veins (H).

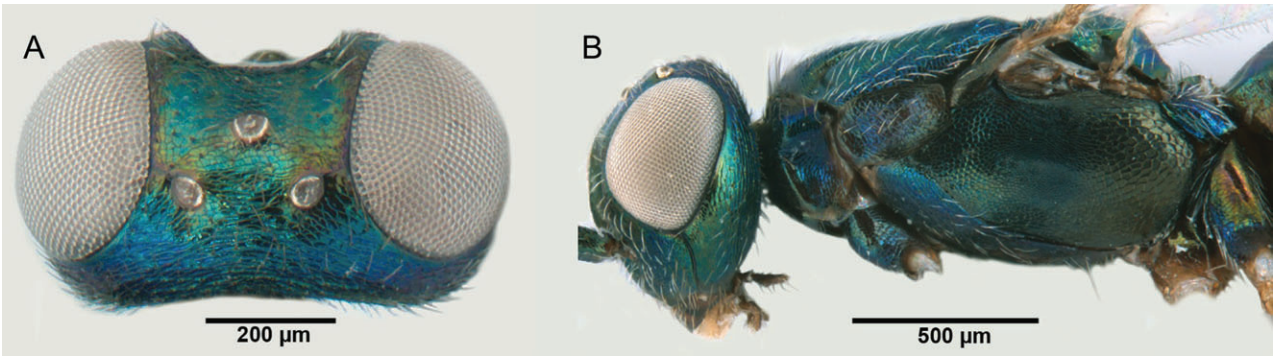

Fig. 25. Characters of female *Eupelmus purpuricollis* (alternate specimen). Head in dorsal view (A), mesosoma in lateral view (B).

***E.* (*Eupelmus*) *minozonus* Delvare sp.n.**
http://zoobank.org/urn:lsid:zoobank.org:act:B0EC22D2-129B-4A37-BF5C-FAE526CA3439
(Female: Figs 11A–E, 20A–G)

Type material. **Holotype** ♀. HUNGARY: Veszprém, Hegyesd, 175 m a.s.l., 46.93333°N, 17.52278°E, 27.vi.2010, sweeping *Quercus cerris* (G. Delvare) [GDEL4030/10010] (in MNHG). **Paratypes**. Same data as holotype (4♀) [GDEL4030/10009, GDEL4030/10120 & GDEL4031/1001 (in GDPC and MNHN), GDEL4030/10668 (in FALPC)]

Etymology. The name is a contraction of *minus* and *urozonus*, an allusion to the habitus of the new species, similar to a small specimen of *E. urozonus*.

Female. Length 2.35–2.70 mm (holotype 2.60 mm). Head greenish, bearing whitish setae; scrobal depression with faint coppery reflections. Antennae and palpi black. Pronotum weakly green, darker on collar, bearing black admarginal setae. Other setae of mesosoma white. Mesonotum bronze green with blue reflections anteriorly, on posterior margin of antero-medial convex lobes and on outer slopes of lateral bosses. Sloping parts of axillae and frenal area bluish. Tegula dark brown. Metanotum greenish. Propodeum blue on callus, black on plical area. Mesopleuron – including prepectus – dark and almost black, without metallic reflections, only acropleuron on either sides of micro-sculptured region with faint bronze lustre. Wings hyaline, venation testaceous and pilosity dark. Coxae blackish, the metacoxa with faint coppery lustre dorsally. Pro- and metafemur mostly dark, mesofemur straw yellow dorsally, slightly infuscate ventrally. Tibiae straw yellow but protibia with a dark baso-dorsal spot. Tarsi straw yellow except infuscate telotarsi. Gaster black with very slight bluish reflections on T1 and weak coppery lustre elsewhere. Ovipositor tricoloured, its basal and apical regions dark on either sides of the whitish median section.

Head long and moderately globose in dorsal view, 1.70–1.78× as broad as long, not especially transverse in frontal view, 1.25× as broad as high. Frontovertex finely and superficially coriaceous (engraved network), roundly merging to occiput without ridge, the sculpture turning to faintly imbricate-reticulate. Scrobal depression entirely smooth and shiny. Ventral margin of antennal toruli below the lower ocular line which crosses their centres. Lateral outline of genae distinctly convex. Temples relatively long, 0.28× length of eye, POL 3.08× OOL, lateral ocelli separated from adjacent eye orbit by about one time their own diameter. Eyes separated by 0.42× head width, width of oral fossa 1.48× length of malar space. Distance between lower margins of antennal toruli from edge of oral fossa 1.18× the intertorular distance. Antenna with combined length of pedicel and flagellum 1.32× head width, scape 4.20× as long as wide, pedicel 2.20× as long as wide, its length 1.20× combined length of anellus plus F1, the funicle segments clearly widening distally, F7 1.74× as wide as F1, clava 1.00× as long as combined length of three apical funicular segments.

Mesosoma short, only 1.70× as long as broad. Mesoscutum with finer reticulation on postero-medial depression than on antero-medial lobe and inner slopes of lateral bosses; outer slopes superficially reticulate. Scutellar-axillar complex 0.75× as long as wide, with imbricate sculpture, the meshes on scutellum arranged around its centre. Frenal area appearing very short in dorsal view. Prepectus sparsely setose with 2–5 white hair-like setae on disc. Acropleuron reticulate anterior and posterior of medial micro-sculptured region, the reticulation coarser posteriorly. Forewing with linea calva separated basally by several rows of setae from vanal area. Basal cell and disc uniformly and densely setose, costal cell ventrally densely setose with 3–4 lines of setae along margin, and dorsally with one line of setae along apical two thirds. Apical discoloured section of submarginal vein, along parastigma, bearing 7–8 setae. Linea calva 0.61× as long as marginal vein, marginal vein 0.87× as long as costal cell and postmarginal vein 1.12× as long as the hardly curved to straight stigmal vein on hind margin. Stigma a little enlarged. Sensilla placodea shortly distant from each other on the long uncus. Mesotibia with apical row of four pegs, mesotarsus ventrally with pegs on first four tarsomeres, basitarsus ventrally with pegs arranged in double row of 10–11 pegs on either side, second, third and fourth tarsomeres respectively with four, two and one peg arranged on each side; telotarsus without pegs. Propodeum with U-shaped plical depression extending to foramen, callus bearing a few setae.

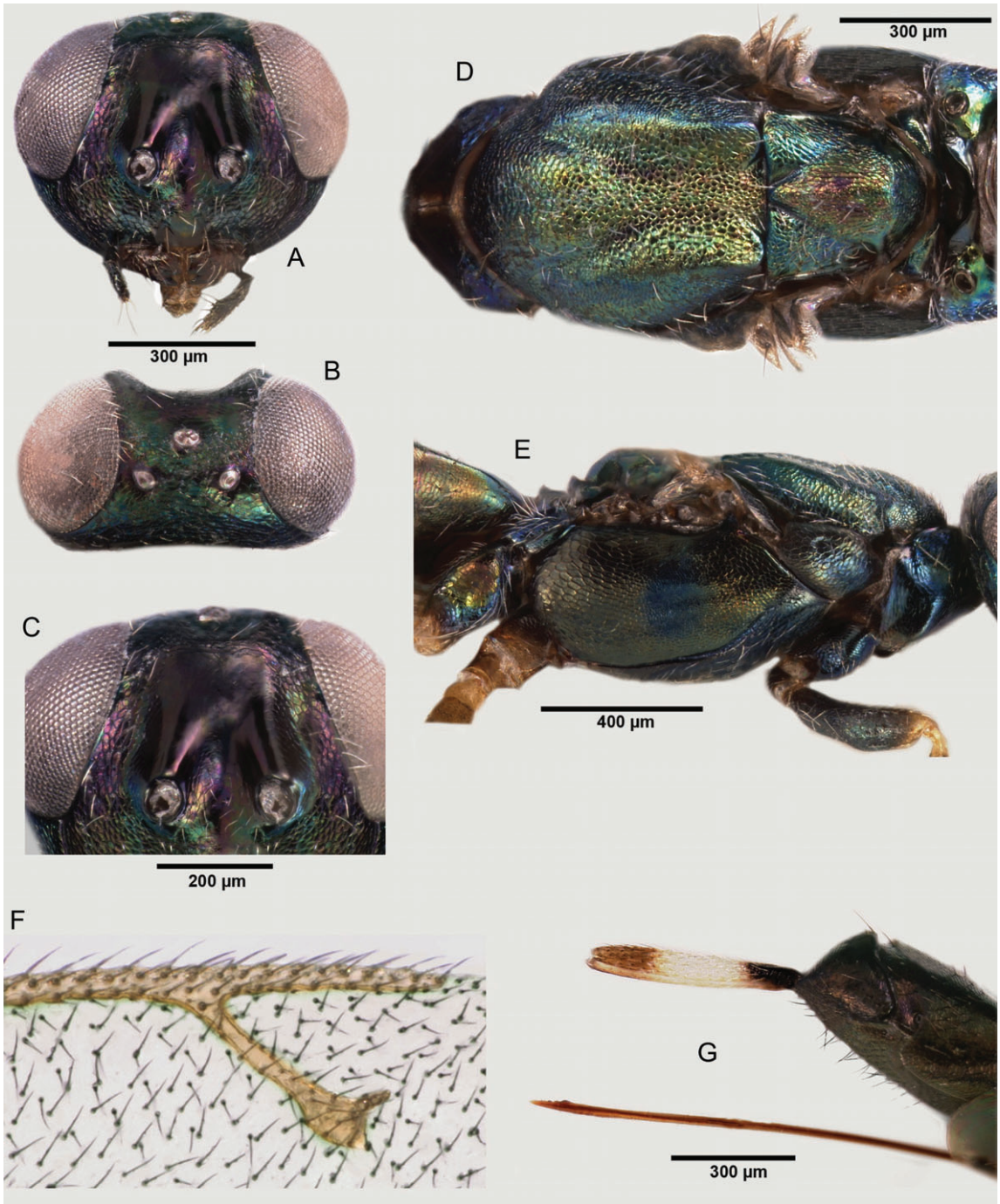

Fig. 26. Characters of female *Eupelmus simizonus*. Head in frontal (A) and dorsal view (B), frons (C), mesosoma in dorsal (D) and lateral view (E), stigmal and postmarginal veins (F), ovipositor sheaths in lateral view (G).

Gaster reticulate with isodiametric cells, except most surface of first tergum basally smooth but merging to coriaceous. Apex of second valvifer not extending beyond apex of gaster. Ovipositor sheaths 0.76× length of metatibia and 0.79× that of marginal vein.

Male. Unknown.

Diagnosis. Head and mesosoma for the most part green to bronze greenish. Head relatively long and with small ocelli, hence ocular-ocellar distance about as long as lateral ocelli diameter. Scrobal depression entirely smooth. Frontovertex delicately coriaceous. Lateral outline of genae distinctly convex. Mesosoma short and frenal area short in dorsal view. Prepectus

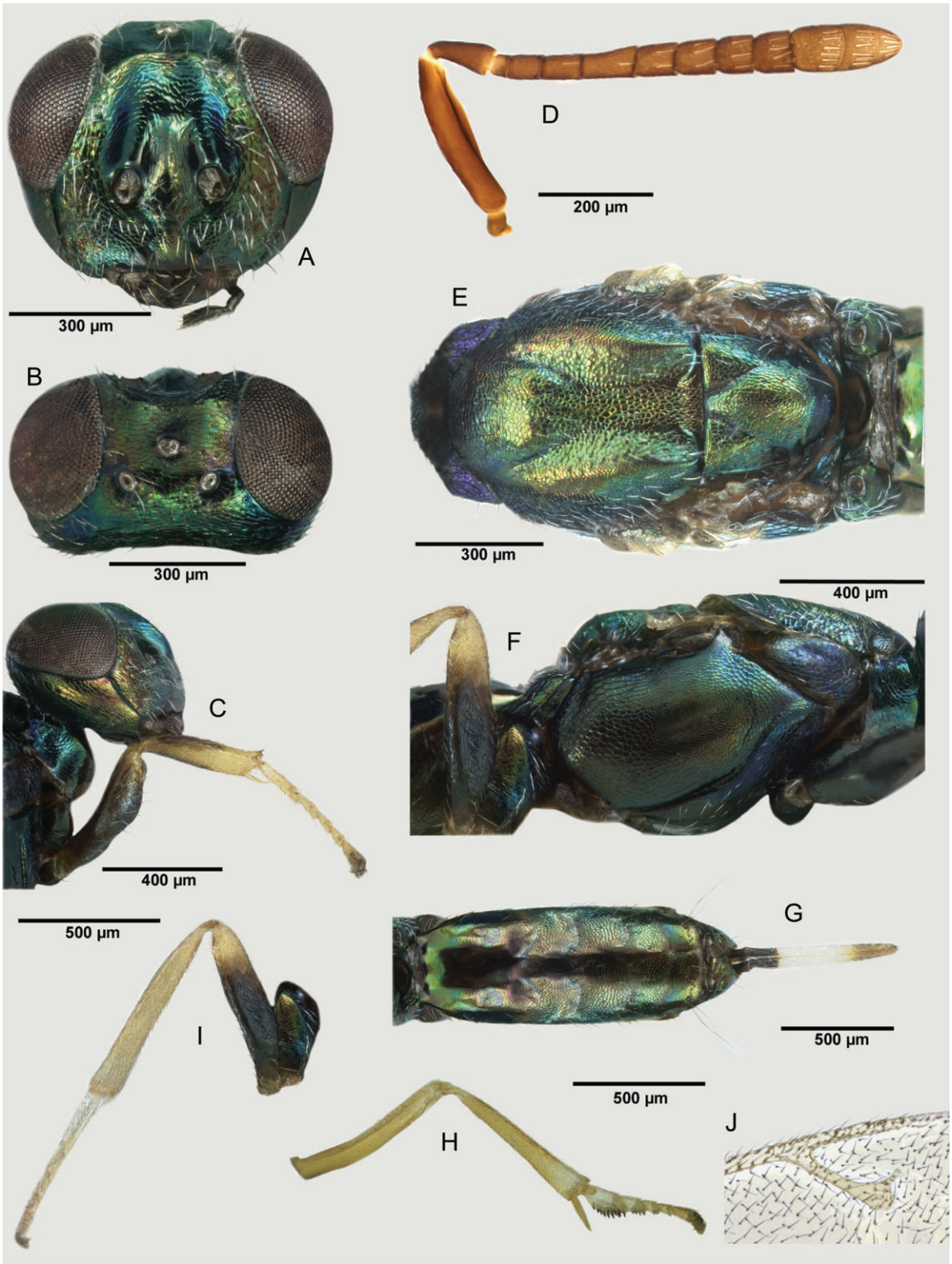

Fig. 27. Characters of female *Eupelmus tremulae*. Head in frontal (A) and dorsal view (B), head and fore leg in lateral view (C), antenna (D), mesosoma in dorsal (E) and lateral view (F), metasoma in dorsal view (G), mid leg (H), hind leg (I), stigmal and postmarginal veins (J).

black, without metallic reflections and sparsely setose (2–5 setae). Marginal vein virtually straight, with long uncus. Basitarsus of mid leg bearing 10–11 pegs on either side. Ovipositor sheaths shorter than metatibia and marginal vein. Apex of second valvifer not or hardly exerted.

Recognition. E. minozonus is quite similar and might easily be mixed with *E. urozonus*, especially with small specimens of that species. In *E. urozonus* the ocular-ocellar distance is often smaller relative to the lateral ocelli, eyes are larger (their height is 1.60–1.95× length of malar space compared to 1.45–1.50× in *E. minozonus*), the mesosoma and frenal area are longer (see Doc.S1). The prepectus is brownish or has coppery reflections and usually bears over seven setae. The anterior surface of acropleuron often has bluish lustre. The marginal vein in most cases is distinctly curved. The light parts of the legs are testaceous, the protibia always has a dark ventral streak in addition to the dorsal one and the metacoxa shows an evident metallic coppery spot dorsally.

Distribution. The species is known only from its type locality in Hungary.

Host(s). Unknown, but the type series was collected by sweeping on *Quercus cerris* Linné; it is therefore possible that *E. minozonus* is a parasitoid of oak cynipids and might have been previously mixed with the morphologically similar *E. urozonus*.

***E.* (*Eupelmus*) *opacus* Delvare sp.n.**
http://zoobank.org/urn:lsid:zoobank.org:act:23647401-C103-4AD7-ABA5-C41EC6126087
(Female: Figs 10A–C, 21A–F)

Type material. **Holotype** ♀. SWEDEN: Östergötland, Ög, Ödeshögs kommun, Omberg, Stocklycke äng, lime meadow, 58°18.452′N, 14°37.859′E, 23.viii/16.ix.2005, Trap ID 13, Coll. event 1648 (SMTP) [LF.ur.SW 02/10460] (in NHRS). **Paratype**. GREECE: Kerkini Lake N. Park, Kerkini, Krousia Mts site, Malaise tr., 06.vi–12.vii.2007, 41°11′32.4″N, 23°03′59.5″E, 190 m a.s.l., Leg. Gordon Ramel (1♀) [LF.ur.GR 01/10459] (in AICF).

Etymology. The name is derived from the Latin word *opacus* (dark) in reference to the darkened legs, a distinctive character from the morphologically similar *E. urozonus*.

Female. Length 2.3–2.7 mm (holotype 2.3 mm). Head bearing sparse setae, whitish on lower face and parascrobal areas, dark on frontovertex. Frontovertex, occiput and lower face greenish with violet reflections in some places; scrobal depression and parascrobal area violet. Scape and pedicel with slight metallic tints under some angles of light, flagellum and palpi dark brown. Mesosoma bearing whitish hair-like setae but admarginal pronotal setae dark. Pronotum distinctly metallic bluish violet on pronotal collar and most of lateral panels. Mesoscutum bluish on anterior half of convex medial lobe and outer slopes of lateral lobes, greenish elsewhere. Tegula dark brown with slight metallic reflections. Axillae bluish on inner angles and lateral slopes with small greenish spot on centre. Scutellum green but frenum bluish. Propodeum bluish to green laterally on callus, plical region black. Prepectus greenish. Acropleuron dark with metallic tints, greenish on reticulate surfaces on each side of the bluish micro-sculptured part. Mesepisternum distinctly blue. Forewing hyaline, venation yellowish-brown, setae uniformly brown, those on submarginal vein quite dark. Coxae metallic with greenish to bluish reflections, femora metallic bluish except narrowly at apices, as well as most part of tibiae which turn to reddish apically, but mesotibia more extensively reddish testaceous apically. Tarsi testaceous except darkened telotarsi and pulvilli. Gaster dark brown with distinct metallic green lustre anteriorly on basal tergum and bearing brown hair-like setae. Ovipositor tricoloured, its basal and apical region brown and its median section whitish.

Frontovertex finely and superficially coriaceous to lateral ocelli (engraved network), but ocellar triangle finely reticulate; roundly merging to occiput without ridge. Scrobes and scrobal depression mostly smooth and shiny; periphery of scrobal depression reticulate on narrow strip. Interantennal boss finely coriaceous. Lower margin of antennal toruli distinctly below lower ocular line. Head in dorsal view 1.74× as broad as long and 1.23× as broad as high, temples 0.16–0.19× length of eye, POL 2.17–2.31× OOL, lateral ocelli separated from adjacent eye orbit by 1.16–1.23× their own diameter which is 0.89–0.98× median ocellus diameter. Eyes separated by 0.46× head width, width of oral fossa 1.32–1.49× length of malar space. Distance between lower margins of antennal toruli from edge of oral fossa 0.89–0.97× the intertorular distance. Antenna with combined length of pedicel and flagellum 1.27× head width, scape 4.87× as long as wide, pedicel 2.08× as long as wide, its length 1.49× combined length of anellus plus F1, the funicle segments shortening and widening distally, F7 1.52× as wide as F1, clava 2.27× as long as wide and 1.17× as long as combined length of three apical funicular segments.

Mesosoma 1.85× as long as broad. Mesoscutum similarly reticulate on antero-medial lobe and postero-medial depression, lateral lobes minutely coriaceous. Scutellar-axillar complex 0.81–0.90× as long as wide, with imbricate sculpture, the meshes on scutellum arranged around its centre. Prepectus sparsely setose with 3–4 white hair-like setae on disc. Acropleuron reticulate anteriorly and posteriorly of medial micro-sculptured region, the reticulation coarser posteriorly. Forewing relatively short, 2.31–2.33× as long as wide, with linea calva separated basally by several rows of setae from vanal area. Basal cell and disc uniformly and densely setose, costal cell ventrally densely setose with 3–4 lines of setae along margin, and dorsally with one line of setae along apical two thirds. Discoloured section of submarginal vein, along parastigma, bearing 8–9 setae. Linea calva 0.55–0.70× as long as marginal vein, marginal vein 0.92–1.10× as long as costal cell and postmarginal vein 0.97–1.19× as long as the hardly curved stigmal vein on hind margin. Sensilla placodea adjacent to each other on short uncus. Mesotibia with apical row of four pegs, mesotarsus ventrally with pegs on basal four tarsomeres, basitarsus ventrally

with pegs arranged in double row on either side, second and third segment with pegs arranged in one line on each side, and apical tarsomere with single or two pegs on either side. Propodeum with U-shaped plical depression extending to foramen, callus bearing curved setae.

Gaster reticulate with isodiametric cells, except most surface of first tergum basally smooth but merging to coriaceous. Apex of second valvifer not extending conspicuously beyond apex of gaster. Ovipositor sheaths 0.69–0.91× length of metatibia and 0.73–0.92× that of marginal vein.

Male: unknown.

Variation. Very little except for the length of the ovipositor, much shorter in the Greek female.

Diagnosis. Head relatively long and globose in dorsal view, with small ocelli. Scrobal depression smooth, except narrowly at periphery. Frontovertex coriaceous. Pronotum distinctly metallic bluish violet on pronotal collar and most of lateral panels. Mesoscutum mostly greenish elsewhere but frenum bluish. Stigma enlarged. Femora metallic and most part of tibiae bluish. Ovipositor shorter than metatibia and marginal vein.

Recognition. The species would be easily mixed with other species close to *E. urozonus* as it exhibits a smooth scrobal depression and coriaceous frontovertex. Its short ovipositor separates it from *E. janstai* **sp.n.** and *E. tibicinis*. Its globose head and colour of pronotum distinguishes it from *E. urozonus* and *E. priotoni* **sp.n.** and the extensive darkened parts on the legs separates it from *E. minozonus* **sp.n.**

Distribution. Sweden and Greece.

Host(s). Unknown.

***E.* (*Eupelmus*) *pistaciae* Al khatib sp.n.**

http://zoobank.org/urn:lsid:zoobank.org:act:111A405E-470F-481A-A43D-663460CEC078

(Female: Figs 8A–C, 22A–H; male: Figs 13B–F, 29E–G, 30A, B, 31H–J)

Type material. **Holotype** ♀. FRANCE: Hérault, Cazevieille, 230 m a.s.l., 43.75222°N, 3.77000°E, 28.x.2011, emerged v.2012, ex *Megastigmus pistaciae* on *Pistacia terebinthus* (G. Delvare) [GDEL4027/10507] (in MNHG). **Paratypes** are provided in Appendix S1.

Etymology. Named after the primary plant associate *Pistacia terebinthus*.

Female. Length 3.30–4.50 mm (holotype 3.8 mm). Head generally coppery bronze with slight greenish tints, especially on fronto-vertex and parascrobal area. Gena, parascrobal area, scrobal depression and sometimes the area below antennal insertion, bronze with coppery reflections. Mandibles mostly reddish except on edges. Flagellum and palpi dark brown. Scape completely or at least dorso-basally light orange, apex of scape and pedicel brown with greenish reflections. Mesosoma bearing whitish setae. Pronotum coppery bronze with slight metallic greenish lustre. Mesoscutum and scutellum coppery bronze with slight greenish tints. Tegula coppery bronze. Propodeum entirely coppery. Prepectus greenish with coppery lustre medially. Lateral panel of pronotum and acropleuron coppery bronze with somewhat greenish lustre under some angles of light. Forewing hyaline, venation yellowish-brown, setae brown, but setae on submarginal vein dark. Coxae generally extensively green; pulvillus and claws brownish, the rest of legs yellowish-orange. Mesocoxa often yellow and sometimes front and middle legs with dark longitudinal marks or strips at femoral and tibial bases. Gaster coppery bronze with brown hair-like setae. Ovipositor sheaths with three distinct coloured sections, its basal and apical sections respectively black and brownish, and the middle section yellowish-white.

Lower face and parascrobal area bearing slightly lanceolate setae. Frontovertex distinctly reticulate laterally, imbricate-reticulate in front of median ocellus, reticulate-imbricate to transversely reticulate posterior to ocellar triangle and roundly merging to occiput without a transverse carina. Antennal scrobes narrowly smooth and shiny, the rest of scrobal depression broadly reticulate dorsally and scabrous reticulate laterally. Interantennal boss coriaceous. Lower margin of antennal toruli slightly below the lower eye margin. Head in dorsal view 1.68–1.85× as broad as long, temples 0.25–0.32× length of eyes, POL 2.85–3.91× OOL, lateral ocelli separated from adjacent eyes by 0.63–0.80× their diameter which is 0.86–1.12× median ocellus diameter. Eyes separated by 0.39–0.43× head width, width of oral fossa 1.43–1.58× length of malar space. Antenna with combined length of pedicel and flagellum 1.01–1.20× head width, scape 4.05–5.79× as long as wide, pedicel 1.95–2.45× as long as wide and 0.84–1.02× combined length of anellus plus F1. Funicular segments shortening and widening distally, F7 1.76–2.00× as wide as F1, clava 1.97–2.22(2.91×)× as long as wide, 0.87–1.02× combined length of the three apical funicular segments.

Mesosoma 1.59–1.90× as long as broad. Mesoscutum almost similarly reticulate on antero-medial lobe and postero-medial depression, lateral lobes on bosses and outer slopes minutely coriaceous to reticulate. Scutellar-axillar complex 0.83–0.96× as long as wide, longitudinally reticulate-imbricate in distinct contrast to sculpture of mesoscutum. Prepectus broadly setose on disc, bearing 12–15 setae, the apices of which nearly extend to dorsal margin. Acropleuron reticulate anterior of medial micro-sculptured region, more coarsely so on posterior surface. Forewing 2.34–2.48× as long as wide, with linea calva separated basally by several rows of setae from vanal area, basal cell with relatively sparse setae; costal cell dorsally with line of setae near anterior margin over apical third to half and ventrally setose along whole length with 2–3 lines of setae medially. Discoloured section of submarginal vein, along parastigma, bearing 7–8 hairs. Marginal vein 0.88–0.96× as long as costal cell, postmarginal vein 0.98–1.13× as long as stigmal vein. Stigmal vein straight on hind margin with uncus well expanded, first sensilla somewhat distant from the following, the others

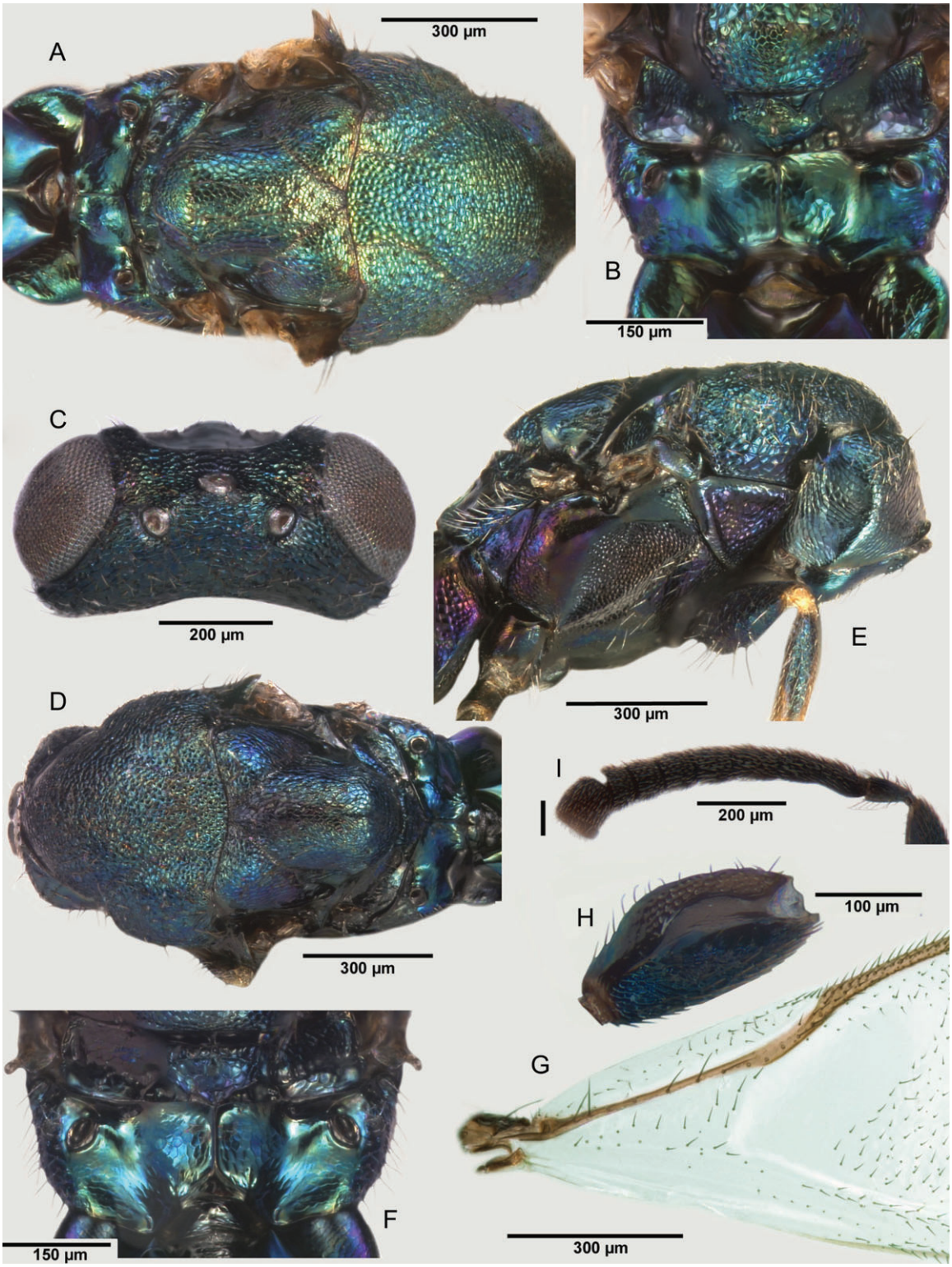

Fig. 28. Characters of male: *Eupelmus acinellus* (A, B), *E. confusus* (C, G) and *E. annulatus* (H, I). Mesosoma in dorsal view (A, D), propodeum (B, F), head in dorsal view (C), mesosoma in lateral view (E), base of forewing (G), scape (H), pedicel and flagellum (I).

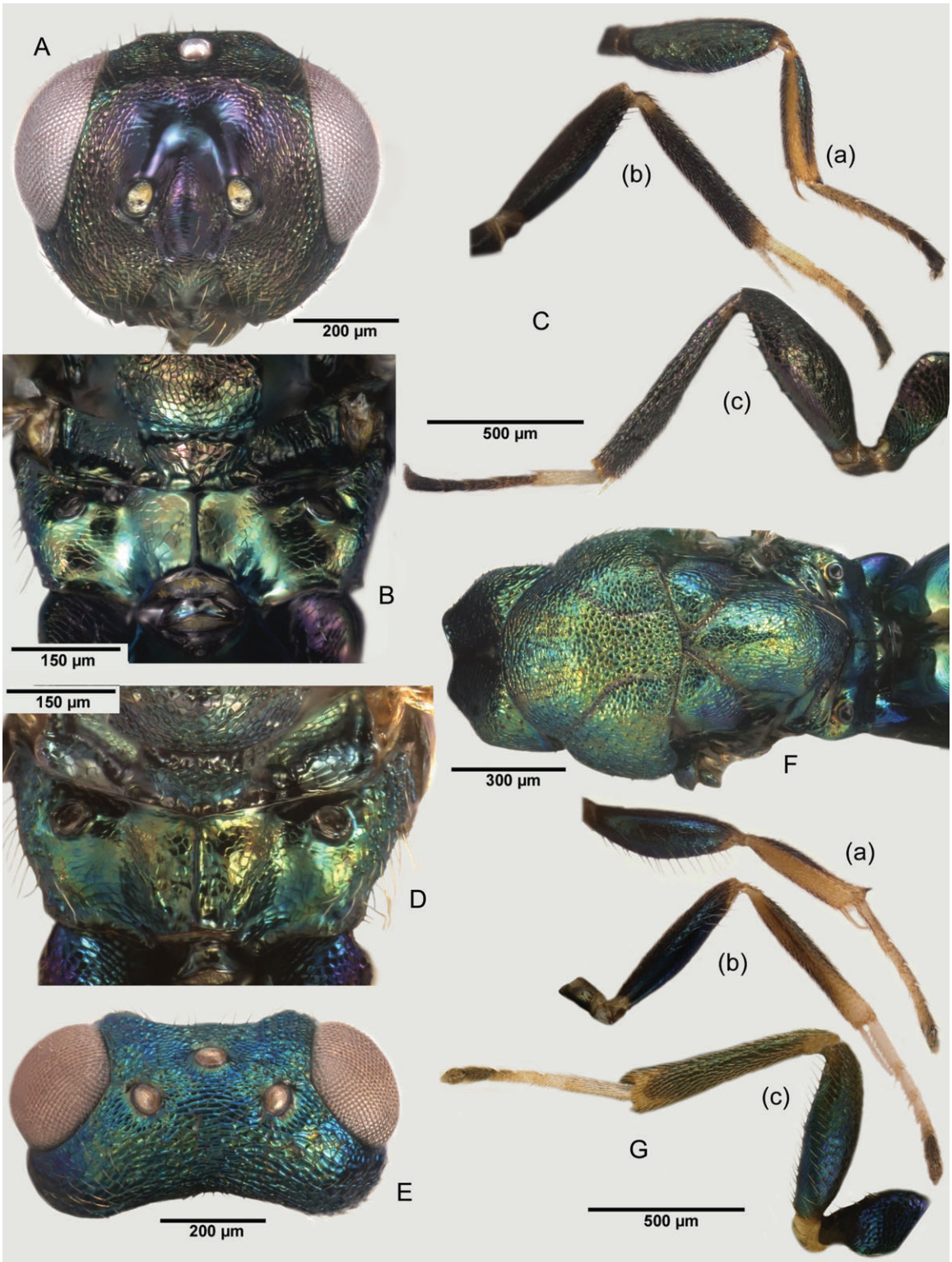

Fig. 29. Characters of male: *Eupelmus gemellus* (A–C), *E. kiefferi* (D) and *E. pistaciae* (E–G). Head in frontal view (A), propodeum (B, D), legs (C, G), head in dorsal view (E), mesosoma in dorsal view (F).

adjacent. Mesotibia with apical row of 6–7 pegs, mesotarsus ventrally with pegs on four basal tarsomeres, basitarsus ventrally with 13–16 pegs arranged distally in double row on either side, second tarsomere with 10–12 pegs, third tarsomere with 6–7 pegs, and telotarsus with single peg on either side. Propodeum with U-shaped plical depression extending to foramen, callus setose with curved setae.

Gaster reticulate with isodiametric cells, except basal half of first tergum initially smooth but merging to coriaceous. Apex of second valvifer not extending beyond apex of gaster, ovipositor sheaths 0.69–0.78× length of marginal vein and 0.60–0.67× length of metatibia.

Male. Length 2.70–3.00 mm. Head metallic green with slight coppery lustre especially on frons and parascrobal area along length of inner orbit, gena metallic green with slight coppery lustre. Flagellum brown with scape and pedicel metallic green. Maxillary palpi brown except the last segment yellowish to reddish. Mesosoma metallic green with bluish reflections, especially on mid lobe of mesoscutum. Propodeum green to bluish-green. Tegula dark brown and often also variably distinctly metallic. Procoxa and femur dark metallic green to bluish-green, tibia basally with longitudinal dorsal and ventral greenish strips, pulvillus dark brown; the reminder of leg yellowish-orange. Mesocoxa and femur blue except yellow knee, tibia yellow with metallic greenish surfaces especially basally, tarsus white except pulvillus and dark brown telotarsus. Hind leg similar in colour to middle leg, but tibia dark greenish except yellowish apex, tarsus white but at least telotarsus dark brown. Forewing hyaline, venation yellowish-brown, setae dark. Gaster with basal tergum often green to bluish-green basally, but remainder dark and with brown hair-like setae.

Lower face with sparse and often white setae, the shortest ones found mesally, the lateral setae conspicuously longer and curved. Gena with one curved, brownish and much longer seta. Frontovertex reticulate-imbricate, transversely reticulate-imbricate posteriorly and roundly merging to occiput. Antennal scrobes smooth and shiny, interantennal region finely coriaceous and shiny, scrobal depression reticulate to transversely reticulate. Head 1.86–1.92× as broad as long, temples 0.45–0.53× length of eyes, POL 4.04–4.20× OOL, lateral ocelli separated from adjacent eye orbit by 0.61–0.73× their own diameter. Eyes separated by 0.49–0.53× head width. Antenna with combined length of pedicel and flagellum 1.38–1.48× head width. Scape ovoid, 2.04–2.26× as long as maximum width, bearing ventrally over 30 pores on outer band along scapular scrobe, arranged in several rows basally and in single row apically. Scapular scrobe itself bearing numerous smaller pores visible only at high magnifications. Pedicel sub-globular, 1.25–1.50× as long as wide, and ventro-externally with a line of six or seven hook-like setae, the first basal seta quite long, enlarged and sometimes forming a loop, and another line of six straight or hardly curved setae on inner ventral surface. Flagellum conspicuously, densely setose and robust-filiform, with basal flagellomere (anellus) discoidal and funicular segments subequal, not much longer than wide. Clava lanceolate with micro-pilose sensory region occupying apical two-thirds of ventral surface, 2.16–2.61× as long as wide, 0.58–0.64× combined length of apical three funicular segments.

Mesoscutum and scutellar-axillar complex reticulate but reticulation of posterior part of medial mesoscutal lobe usually much finer and posterior part of scutellum coriaceous. Propodeum finely coriaceous and shiny, callus similarly finely sculptured with setae originating from tiny bumps. Forewing with marginal vein 0.78–0.84× as long as costal cell, postmarginal vein 0.95–1.07× as long as the curved stigmal vein on hind margin. Costal cell dorsally with line of dark setae extending over apical third and ventrally with dark setae continuous along whole length, mesally on two lines.

Diagnosis. **Female**. Body bronze with evident coppery reflections. Scape and legs extensively light, not or only slightly darkened. Scrobal depression entirely reticulate, frontovertex very distinctly – not superficially – reticulate. Ovipositor shorter than metatibia and marginal vein. **Male**. Head without ridge or carina delimiting the vertex posteriorly. Scape ovoid, 2.00–2.25× as long as broad, bearing ventrally over 30 pores on outer band along scapular scrobe, these pores arranged in several rows basally and in single row apically. Pedicel compact, with basal ventral seta loop-like, followed by five or six hook-like setae and also bearing another inner line of setae.

Recognition. **Female**. The species is easily distinguished with the characters provided above. It could be mixed with *E. confusus* and *E. martellii* but the body colour of the female together with the entirely reticulate scrobal depression clearly separated it from those species. **Male**. It can be distinguished by the number of pores on the scape, distributed on one row apically, the larger number of hook-like ventral setae and the loop-like basal seta. The scape and pedicel of *E. pistaciae* look somewhat similar to those of *E. kiefferi*, but in that species the vertex is distinctly delimited posteriorly by an evident ridge and angulate with occiput.

Distribution. Our molecular sampling was limited to France, but we have included additional museum specimens from Cyprus Greece, Iran, Tunisia and Turkey as part of the type series to better represent known distribution and host plant associations. The species is potentially present in all regions where pistachios are present, Mediterranean Basin and SW Asia.

Hosts. M. pistaciae (Torymidae) and possibly its eurytomid parasitoids, *Sycophila pistacina* (Rondani) and *Eurytoma pistaciae* (Rondani) on *Pistacia terebinthus* Linné (Anacardiaceae). Associated also with *P. lentiscus*, *Pistacia atlantica* Desfontaines (as *Pistacia mutica* Fischer & C.A. Meyer), and *Pistacia vera* Linné.

***E.* (*Eupelmus*) *priotoni* Delvare sp.n.**

http://zoobank.org/urn:lsid:zoobank.org:act:3565E30B-92D9-4DC4-BB94-7224D6BA3D22

(Female: Figs 10D–F, 23A–F)

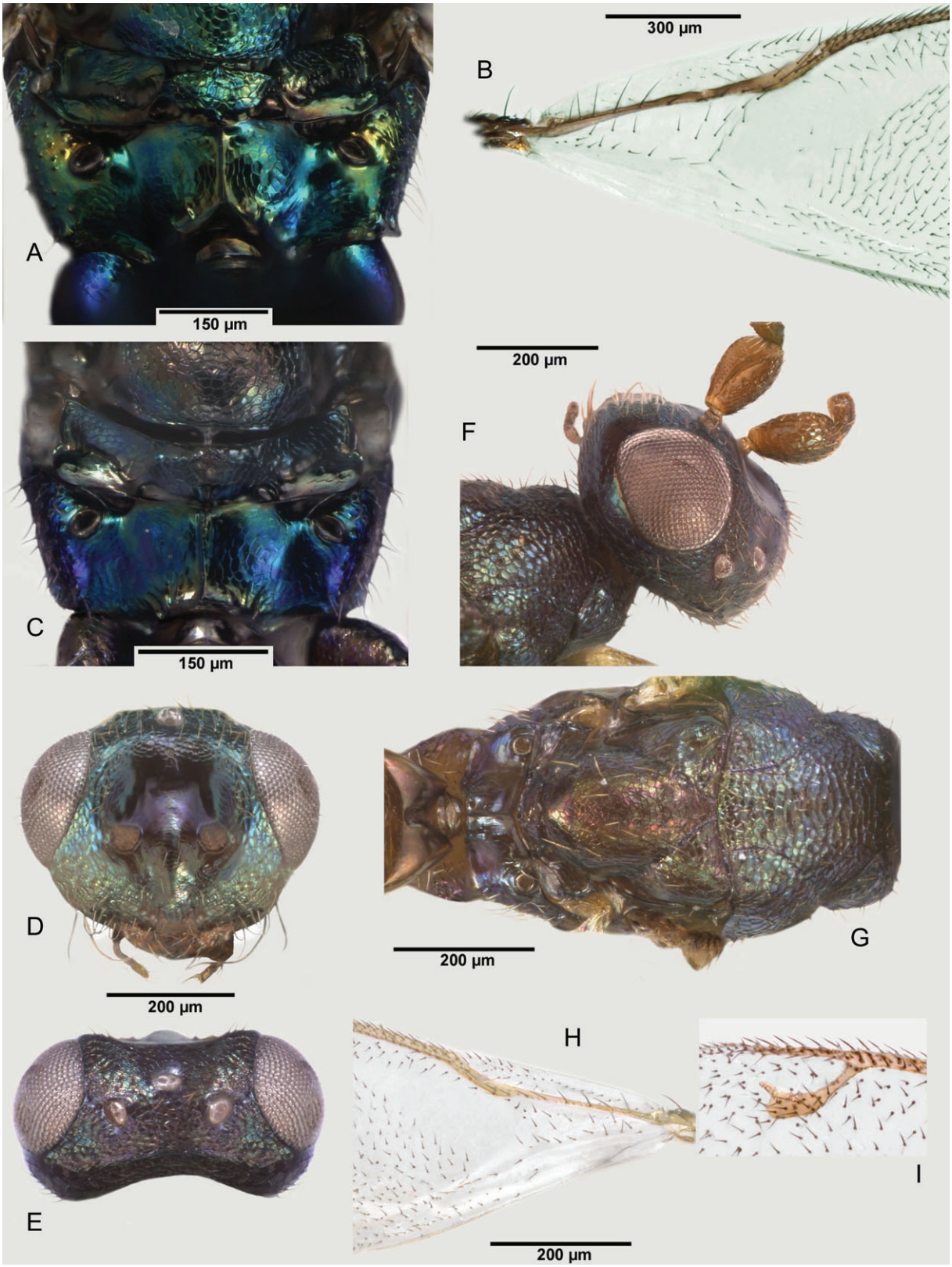

Fig. 30. Characters of male: *Eupelmus pistaciae* (A, B), *E. tibicinis* (C) and *E. tremulae* (D–I). Propodeum (A, C), base of forewing (B), head in frontal view (D), head in dorsal view (E), head in postero-dorsal view (F), mesosoma in dorsal view (G), base of forewing (H), stigmal and postmarginal veins (I).

Type material. **Holotype** ♀. FRANCE: Aveyron, Sauclières, 700 m a.s.l., Lit de la Virenque, 43.96389°N, 3.35583°E, 15.vi.2011 (G. Delvare) [GDEL4051/10038] (in MNHG).

Etymology. The species is dedicated to the late Jean Prioton who has been concerned with the vegetation of this region called 'Les Grands Causses' and especially revealed the floristic interest of the type locality.

Female. Length of holotype 3.7 mm. Head green with some small violet reflections by places. Lower face and parascrobal area bearing whitish setae, frontovertex with brownish setae. Scrobal depression, parascrobal area and upper half of interantennal boss violet, its lower half being greenish, occiput greenish-blue. Scape and pedicel very slightly bluish, flagellum and palpi dark brown, almost black. Mesosoma bearing whitish setae except admarginal setae of pronotum, dark. Pronotal collar and most of lateral panels with bright violet tinge, the rest of panels black. Mesoscutum dark bluish on anterior third, greenish posteriorly. Tegula with greenish reflections. Scutellar-axillar complex bright green. Propodeal callus with faint blue violet reflections and bearing white hair-like setae, plical region blackish. Prepectus greenish bronze on periphery and bluish on centre. Acropleuron with medial microsculptured region dark bluish, anterior and posterior regions greenish bronze, mesepisternum distinctly dark bluish. Forewing hyaline, venation yellowish-brown, setae dark brown. Procoxa and femur entirely dark with slight metallic lustre but knee orange, tibia orange with dark small baso-dorsal and ventral strips, tarsus brownish but pulvillus more darker. Mesocoxa greenish, trochanter brownish, femur and tibia brown except orange knee and apex of tibia, tarsus yellowish except dark telotarsus and pulvillus. Metacoxa broadly coppery dorsally and bluish ventrally, trochanter dark brown, femur dark with bluish reflections except for reddish knee, tibia reddish with broad sub-basal dark strip, basitarsus mostly whitish, the rest of tarsomeres slightly and progressively darkening to reddish, telotarsus blackish. Gaster entirely dark brown (exhibiting coppery to greenish reflections when using intense artificial light) but first basal tergum with metallic bluish-greenish lustre anteriorly, gaster dorsally bearing dark hair-like setae. Ovipositor tricoloured, with basal band short and black, median long and whitish, apical short and dark brownish.

Frontovertex coriaceous to lateral ocelli, distinctly reticulate to transversally reticulate-imbricate posteriorly and progressively merging into occiput without transverse ridge. Scrobes and lower scrobal depression smooth and shiny, interantennal boss, upper scrobal depression and its lateral edges finely and superficially coriaceous to reticulate-imbricate. Lower face and parascrobal area reticulate. Head 1.85× as broad as long, temples 0.18× length of eyes, POL 2.51× OOL, lateral ocelli separated from adjacent eye orbit by 0.83× their diameter which is 0.94× median ocellus diameter. Eyes separated by 0.40× head width, width of oral fossa 1.35× length of malar space. Antenna with combined length of pedicel and flagellum 1.25× head width, pedicel 2.42× as long as wide and 1.19× combined length of anellus and F1, the funicle segments shortening and widening distally, F7 1.82× as wide as F1, clava 2.18× as long as wide, 0.93× combined length of three apical funicular segments.

Mesosoma 1.83× as long as broad. Mesoscutum with fairly coarse reticulation on antero-medial lobe and postero-medial depression; lateral lobes entirely coriaceous and with finer sculpture. Scutellar-axillar complex 0.78× as long as broad, mostly coriaceous and with isodiametric cells, which are larger on centre of scutellum and inner angles of axillae, the cells finer and obliquely directed laterally where the sculpture progressively turns to imbrications. Prepectus with eight white hair-like setae on centre of disc. Acropleuron finely reticulate anterior of medial micro-sculptured region, the reticulation coarser on posterior surface. Forewing relatively elongate, 2.90× as long as wide, uniformly setose except for linea calva which is separated from vanal area by several rows of setae. Costal cell dorsally with 3–4 line of setae near anterior margin of cell on apical half, ventrally densely setose on several lines on apical half, leaving most of basal half bare. Discoloured section of submarginal vein, along parastigma, bearing 7–8 hairs. Linea calva 0.48× as long as marginal vein, marginal vein 0.96× as long as costal cell and postmarginal vein 1.04× length of stigmal vein. Stigmal vein straight on hind margin, stigma moderately enlarged. Sensilla placodea evidently distant from each other. Mesotibia with an apical row of pegs, ventral surfaces of tarsal segments 1–4 with pegs arranged into two rows distally on either side of basitarsus, and in one row on either side on followings segments. Propodeum with U-shaped plical depression extending to foramen, callus moderately setose with long and curved hair-like setae.

Gaster reticulate with isodiametric cells, except surface of first tergum basally smooth but merging to imbricate. Apex of second valvifer not distinctly extending beyond apex of gaster, ovipositor sheaths 0.85× length of metatibia and 0.93× length of marginal vein.

Diagnosis. Head and mesonotum for the most part greenish. Pronotum with bright bluish violet reflections on collar and lateral panels. Scrobal depression smooth, frontovertex superficially coriaceous. Lower ocular line in line with dorsal margins of toruli. Forewing relatively elongate. Stigmal vein straight on hind margin. Ovipositor sheaths shorter than metatibia and marginal vein.

Recognition. *E. priotoni* could be mixed with *E. urozonus* but its general colouration is more greenish and exhibits bright bluish-violet reflections on pronotal collar and lateral panels. Its ovipositor sheaths – although slightly shorter than the metatibia and marginal vein – are nevertheless longer than those of *E. urozonus* (see Doc. S1). The species is also close to *Eupelmus purpuricollis* (see Recognition under this species).

Male. Unknown.

Distribution. France, only known from the type locality.

Host(s). Unknown.

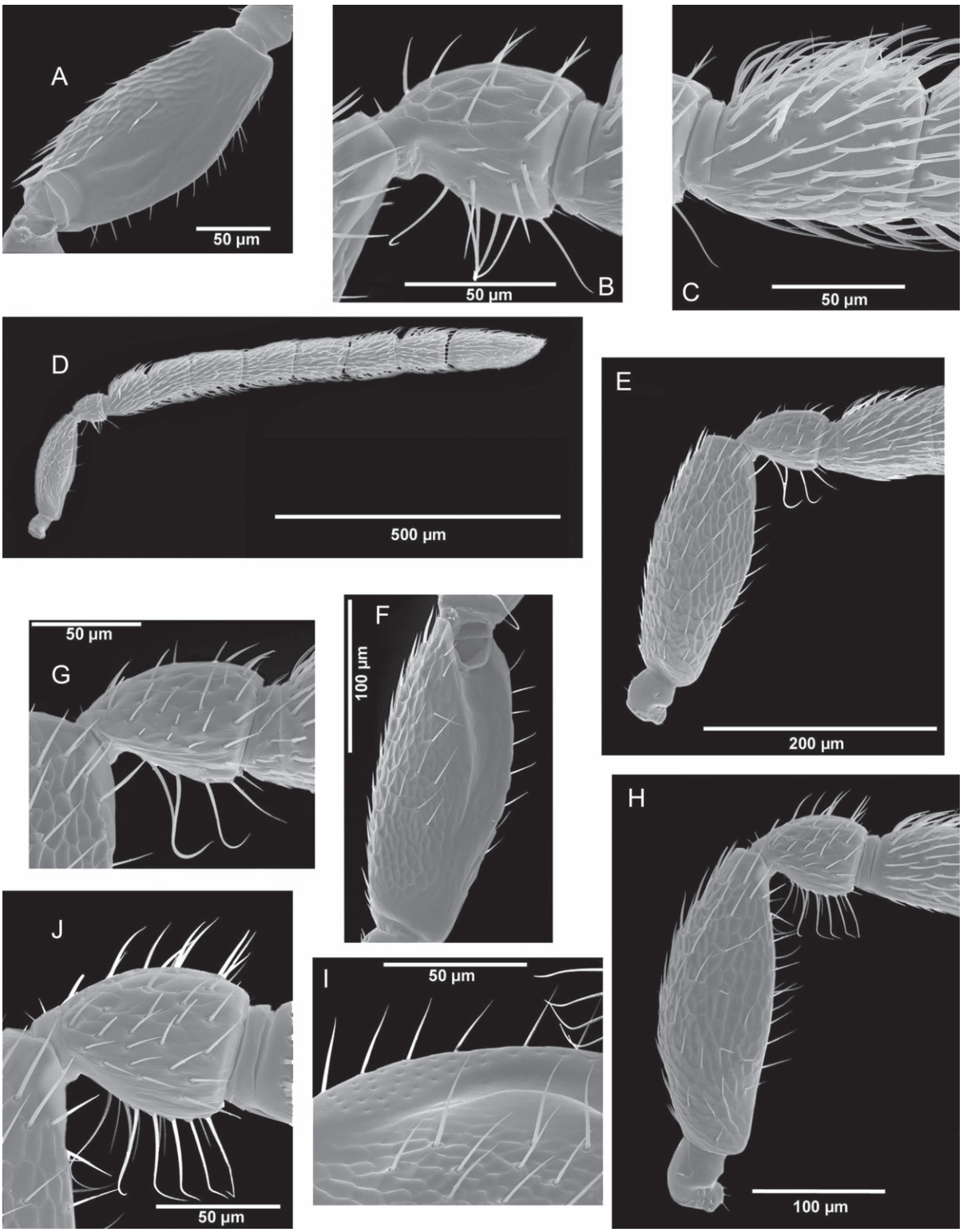

Fig. 31. SEM photographs of male antenna. *Eupelmus confusus* (A–D), *E. gemellus* (E–G) and *E. pistaciae* (H–J). Outer side of scape (A, F), pedicel (B, G, J), base of flagellum (C), antenna (D), base of antenna (E), ornamentation of scape enlarged (I).

***E.* (*Eupelmus*) *purpuricollis* Fusu & Al khatib sp.n.**
http://zoobank.org/urn:lsid:zoobank.org:act:1F354047-F041-4CD6-B1DA-1D53815B9B7C
(Female: Figs 10G, H, 24A–H, 25A, B)

Type material. **Holotype** ♀**.** GREECE: Kerkini lake nr Neo Petritsi; Malaise trap, Midway Site, 30.vii–06.vii.2008, 41° 18′49.8″N, 23°16′35.6″E, 750 m a.s..l, Leg. Gordon Ramel , [LF.ur.GR 02/10650] (in AICF). **Paratypes**: GREECE: same data as for holotype but 09–13.vii.2008 (1♀ not sequenced). Kerkini Lake N. Park, Kerkini, Krousia Mts site, Malaise tr., 11–17.vii.2007, 41°11′32.4″N, 23°03′59.5″E, 190 m a.s.l., Leg. Gordon Ramel, (1♀) [LF.ur.GR 05/10653] (in AICF); same data but 18–24.vii.2007 (1♀) [LF.ur.GR 03/10651] (in GDPC)

Etymology. From the Latin words *purpura*, purple, and *collis*, collar, in reference to the colour of the pronotal collar.

Female. Length 2.85–3.15 mm. Head mostly green to bluish-green with some bronze reflections and bright blue and violet lustre on vertex behind posterior ocelli and on occiput. In some specimens, frons inconspicuously tricoloured with bluish-green to golden-green lustre along inner orbits and mesally dark bronze-green below level of anterior ocellus. Lower face and parascrobal area bearing whitish setae, frontovertex with brownish setae. Scrobal depression, parascrobal area and interantennal boss violet to coppery-red, except sometimes lateral surface of scrobal depression and lower half of interantennal boss greenish. Scape and pedicel dark brown with some bluish to violet lustre, flagellum and palpi dark brown. Mesosoma bearing whitish setae except admarginal setae of pronotum dark. Pronotal collar and most of lateral panel with bright violet tinge, the rest of panel dark brown with reduced metallic shine. Mesoscutum bluish-green to bronze-green with outer surface of lateral lobe with strong violet and blue lustre along margin, similar to pronotal collar, and sometimes median lobe with coppery reflections anteriorly. Tegula with greenish reflections. Scutellar-axillar complex bright green with golden reflections mostly on scutellum and blue on axillae. Propodeal callus with blue and violet reflections and bearing white hair-like setae, plical region greenish. Prepectus greenish bronze on periphery and bluish to violet on centre. Acropleuron with medial microsculptured region dark violet, anterior and posterior surfaces bronze to bluish-green. Mesepisternum blue to dark bluish-green with small violet areas. Forewing hyaline, venation yellowish-brown, setae dark brown, whitish or at least somewhat paler within basal cell. Procoxa and femur entirely dark with slight metallic lustre but knee orange, tibia yellowish-orange with small to extensive dark baso-dorsal and ventral strips, tarsus brownish but pulvillus and last tarsomere darker. Mesocoxa yellowish-orange to dark brown, trochanter, femur and tibia yellowish-orange to light brown except whitish-yellow knee and apex of tibia, tarsus whitish-yellow except dark telotarsus and pulvillus. Metacoxa broadly coppery with green reflections dorsally and bluish ventrally, trochanter light-brown, femur dark with bluish reflections except for extreme base and apical third yellowish-orange to light-brown, tibia yellowish-orange to light-brown except barely darkened sub-basally, basitarsus mostly whitish-yellow, the rest of tarsomeres slightly and progressively darkening, telotarsus brown. Gaster entirely dark brown (exhibiting coppery to greenish reflections when using intense artificial light) but first basal tergum with metallic bluish-green lustre anteriorly, gaster dorsally bearing dark hair-like setae. Ovipositor tricoloured, with basal band short and black, median long and whitish, apical shorter than median and dark brownish.

Frontovertex coriaceous to lateral ocelli, distinctly reticulate to transversally reticulate-imbricate posteriorly and progressively merging into occiput without transverse ridge. Scrobes and lower scrobal depression smooth and shiny, interantennal boss, upper scrobal depression and its lateral surface finely and superficially coriaceous to reticulate-imbricate. Lower face and parascrobal area reticulate except coriaceous-imbricate along oral fossa margin. Head 1.72× as broad as long, temples 0.16–0.17× length of eyes, POL 3.05–3.73× OOL, lateral ocelli separated from adjacent eye orbit by 0.56–0.69× their diameter which is 0.92–1.07× median ocellus diameter. Eyes separated by 0.37–0.42× head width, width of oral fossa 1.47–1.61× length of malar space. Antenna with combined length of pedicel and flagellum 1.18–1.21× head width, scape 4.10–5.26× as long as wide, pedicel 2.17–2.52× as long as wide and 1.00–1.08× combined length of anellus and F1, the funicle segments shortening and widening distally, F7 1.79–1.84× as wide as F1, clava 2.19–2.56× as long as wide, 0.88–1.04× combined length of three apical funicular segments.

Mesosoma 1.60–1.76× as long as broad. Mesoscutum with fairly coarse reticulation on antero-medial lobe and postero-medial depression, lateral lobes entirely coriaceous and dorsally with finer sculpture with small mesh size. Mesh size medially along postero-medial depression similar to that of mesal surface of lateral lobes. Scutellar-axillar complex 0.77–0.79× as long as broad, mostly coriaceous and with isodiametric cells, which are larger on centre of scutellum and inner angles of axillae, the cells finer and obliquely directed laterally where the sculpture progressively turns to imbrications. Prepectus with 9–12 white hair-like setae on centre of disc. Acropleuron finely reticulate anterior of medial micro-sculptured region, the reticulation coarser on posterior surface. Forewing relatively elongate, 2.49–2.58× as long as wide, uniformly setose except for linea calva which is separated from vanal area by several rows of setae. Costal cell dorsally with one line of setae near anterior margin of cell on apical half, ventrally densely setose along length, on about 3–4 lines. Discoloured section of submarginal vein, along parastigma, bearing 4–6 setae. Linea calva 0.79–0.84× as long as marginal vein, marginal vein 0.86–0.96× as long as costal cell and postmarginal vein 1.18–1.29× length of stigmal vein. Hind margin of stigmal vein straight to slightly curved, stigma moderately enlarged. Sensilla placodea evidently distant from each other. Mesotibia with an apical row of 4–5 pegs, ventral surfaces of tarsal segments 1–4 with

pegs arranged into two rows distally on either side of basitarsus, and in one row on either side on followings segments. Propodeum with U-shaped plical depression extending to foramen, callus moderately setose with long and curved hair-like setae.

Gaster reticulate with isodiametric cells, except surface of first tergum basally smooth but merging to imbricate. Apex of second valvifer not extending beyond apex of gaster, ovipositor sheaths 0.75–0.94× length of metatibia and 0.78–1.09× length of marginal vein.

Diagnosis. Head and mesonotum for the most part greenish. Pronotum with bright bluish violet reflections on collar and lateral panels. Middle leg mostly pale. Lateral ocellus comparatively large. Scrobal depression smooth, frontovertex superficially coriaceous. Lower ocular line intersecting toruli at about their mid height. Sculpture of mesoscutum with mesh size medially along postero-medial depression similar to that of mesal surface of lateral lobes. Forewing relatively elongate. Hind margin of stigmal vein straight to slightly curved on hind margin. Ovipositor sheaths shorter than metatibia and marginal vein.

Male. Unknown.

Recognition. E. purpuricollis could be mixed with *E. urozonus* but it exhibits bright bluish-violet reflections on pronotal collar and lateral panels, prepectus, vertex behind posterior ocelli and along outer margin of mesoscutum. Frontovertex in *E. urozonus* is also generally distinctly tricoloured with mostly green lustre along inner orbits and mesally bronze or copper to dark-violet below level of anterior ocellus, while in *E. purpuricollis* this colour pattern is at most obscurely visible because area in front of median ocellus only slightly darker and less shiny than lateral areas along inner orbits. Because of this colour pattern combined with a smooth scrobal depression, the species is extremely close to *E. priotoni* and *E. opacus*. Ovipositor sheaths in *E. purpuricollis* are in the range of variation for *E. urozonus*, while in *E. priotoni*, although sheaths are slightly shorter than metatibia and marginal vein, they are nevertheless longer than those of *E. urozonus* and *E. purpuricollis*. In both *E. urozonus* and *E. purpuricollis*, sculpture of mesoscutum with mesh size medially along postero-medial depression similar to that of mesal surface of lateral lobes, while in *E. priotoni* this area has a band of small cells. Also in the former two species costal cell dorsally with a single line of setae near anterior margin on apical half, while in *E. priotoni* this area is much more setose, dorsally with 2–3 lines of setae on apical half. *Eupelmus purpuricollis* differs from *E. opacus* in having an extensively pale middle leg, a larger lateral ocellus and an extensively setose prepectus.

Distribution. Greece, only known from the Lake Kerkini area.

Host(s). Unknown.

***E.* (*Eupelmus*) *simizonus* Al khatib sp.n.**

http://zoobank.org/urn:lsid:zoobank.org:act:CCD5B87E-9C81-456A-9DD8-F737AE6AC2F3

(Female: Figs 9F–I, 26A–G)

Type material. **Holotype** ♀. FRANCE: Ardèche, Les Vans, 175 m a.s.l., Lit du Granzon, 44.38722°N, 4.15444°E, 15.vii.2012, sweeping on *Quercus pubescens*, (G. Delvare) [GDEL4142/10297] (in MNHG).

Etymology. Named for its high degree of apparent similarity with *E. urozonus*.

Female. Length of holotype 2.95 mm. Head metallic green with violet reflections and bearing white setae. Scrobal depression, parascrobal area and upper half of interantennal boss violet, its lower half being greenish. Scape and pedicel with slight metallic bluish tints, flagellum and palpi dark brown. Mesosoma bearing whitish hairs. Pronotum with white admarginal hairs. Pronotal collar and most of lateral panels evidently metallic blue violet, mesoscutum bluish anteriorly and on outer slopes of lateral lobes, greenish elsewhere. Scutellar-axillar complex blue on slopes of axillae and frenum, bronze greenish elsewhere. Propodeum blue to green on callus, black on plical region. Tegula dark brown with slight metallic reflections. Prepectus bluish on disc, with greenish reflections on margin. Acropleuron bronze greenish on each side of the bluish micro-sculptured part. Forewing hyaline, venation yellowish-brown, setae brown, those on submarginal vein quite dark. Procoxa and femur dark bluish, only narrowly at apex of latter testaceous, tibia reddish-testaceous with brown longitudinal dorsal and ventral strips, tarsus testaceous. Mesocoxa dark, trochanter brownish, femur and tibia reddish testaceous, the latter with lighter apex bearing black pegs, tarsus whitish except for testaceous telotarsus, brown pulvillus and black pegs on first four tarsomeres. Metacoxa and femur extensively dark metallic, trochanter and apex of femur reddish, tibia reddish but turning to whitish toward apex, tarsus yellowish-white except brownish telotarsus and brown pulvillus. Gaster dark brown with distinct metallic green to blue lustre anteriorly on basal tergum and with brown hair-like setae. Ovipositor sheaths distinctly banded, with medial whitish region delineated from black basal region and brown apical section.

Frontovertex finely and entirely coriaceous (engraved network) to lateral ocelli, reticulate to transversely reticulate posteriorly, roundly merging to occiput without transverse ridge. Scrobes and scrobal depression entirely smooth and shiny but the periphery of scrobal depression and interantennal area finely coriaceous. Ventral margin of antennal toruli hardly below lower eye margin. Head in dorsal view 1.81× as broad as long, temples 0.11× length of eye, POL 4.13× OOL, lateral ocelli separated from adjacent eye orbit by 0.49× their own diameter which is 1.00× median ocellus diameter. Eyes separated by 0.39× head width, width of oral fossa 1.45× length of malar space. Antenna with combined length of pedicel and flagellum as 1.25× head width, scape 5.40× as long as broad, pedicel 2.23× as long as wide and 0.89× combined length of anellus plus F1. Funicular segments shortening and widening distally, F7 1.78× as wide

as F1, clava 2.42× as long as wide, 0.86× as long as combined length of three apical funicular segments.

Mesosoma 1.86× as long as broad. Mesoscutum mostly uniformly reticulate except lateral lobes minutely coriaceous on bosses. Scutellar-axillar complex 0.85× as long as wide, densely reticulate-imbricate, the sculpture finer than on mesoscutum. Prepectus very sparsely setose, bearing four white setae. Acropleuron moderately reticulate anterior of medial micro-sculptured region, more coarsely reticulate on the broad posterior surface. Forewing moderately long, 2.40× as long as wide, uniformly setose except for linea calva. Costal cell ventrally setose with three lines of setae along length toward anterior margin and dorsally with line of setae on whole length. Discoloured section of submarginal vein, along parastigma, bearing eight hairs. Linea calva 0.80× as long as marginal vein, which itself is 0.97× as long as costal cell. Postmarginal vein 1.14× as long as the completely straight stigmal vein on hind margin which ends in subtriangular stigma. Sensilla placodea adjacent to each other on uncus. Mesotibia with apical row of 14 pegs, mesotarsus ventrally with pegs on four basal tarsomeres, pegs arranged distally in double row on either side of basitarsus, pegs arranged in one line on each side on second and third tarsomeres, fourth tarsomere with single or two pegs on either side. Propodeum with U-shaped plical depression extending to foramen, callus bearing straight setae.

Gaster reticulate with isodiametric cells, except most surface of first tergum basally smooth but merging to coriaceous. Apex of second valvifer not extending conspicuously beyond apex of gaster, ovipositor sheaths short, 0.78× length of metatibia and 0.81× length of marginal vein.

Diagnosis. Body on the whole with dimly metallic reflections. Head dark blue with greenish lustres, pronotum with collar and lateral panels violet bluish, mesonotum bronze with green. Scrobal depression smooth, frontovertex coriaceous. Head transverse in frontal view with ventral margins of antennal toruli at level with lower ocular line and lateral outline of genae evidently convex. Marginal vein straight. Ovipositor sheaths shorter than metatibia and marginal vein.

Recognition. The combination of smooth scrobal depression, transverse head, convex genae and antennal toruli situated high make this species similar to *E. tibicinis*. Nevertheless the ovipositor of that species is substantially longer, its body has brighter reflections and the scrobal depression is narrowly reticulate dorsally.

Male. Unknown.

Distribution. France, only known from the type locality.

Host(s). Unknown.

***E.* (*Eupelmus*) *tremulae* Delvare, sp.n.**

http://zoobank.org/urn:lsid:zoobank.org:act:3001FBF7-A5AF-4D65-A274-6673F34264F1

(Female: Figs 7C–G, 27A–J; male: Figs 12E–I, 30D–I)

Type material. **Holotype ♀.** CZECH REPUBLIC, Jindóichùv Hradec, Veselí nad Lužnicí, 1 km E of Charles University field station (Ruda), 422 m a.s.l., 49.15296°N, 14.70646°E, ex *Harmandia* sp. (Cecidomyiidae) on *Populus tremula*, 05.vi.2007, adult emergence 13.vi.2007 (P. Jansta) [PJ07003_1_1/10570] (in MNHG). Paratypes, same data (1♀) [PJ07003_1_1/10569] (in MNHN) (1♂) [PJ07003_1_1/10571] (in MNHN).

Etymology. The name derives from the associated plant on which the host develops.

Female. Length 2.65 mm. Head with lower face, parascrobal area and frontovertex bearing white setae. Frontovertex, parascrobal area, interantennal boss and lower face greenish with slight bluish reflections near oral fossa. Scrobal depression bright blue on sides, green above interantennal boss and dark bluish on antennal scrobes. Scape, pedicel, flagellum and palpi dark brown to black, without metallic reflections. Mesosoma bearing light setae including admarginal setae of pronotum. Pronotal collar and most of lateral panel with bluish violet tinge, the rest of panel greenish. Mesoscutum metallic green but outer surface of lateral lobe dark bluish. Tegula greenish anteriorly and on inner half, translucid yellow elsewhere. Scutellar-axillar complex metallic green dorsally, dark bluish on sloping surfaces. Propodeal callus bluish green. Prepectus bluish. Acropleuron with medial microsculptured region bronze green, anterior and posterior surfaces bluish. Mesepisternum distinctly bluish. Forewing hyaline, venation pale yellowish, all setae white. Procoxa and femur dark with slight bluish reflections except knee testaceous; tibia pale yellow with large antero-dorsal and ventral dark spots, tarsus pale yellow but telotarsus and pulvillus darkened. Mid leg pale yellow except coxa basally, apex of tibia and two basal tarsomeres, whitish, apical pegs of tibia and those of tarsus black. Metacoxa with a broad dorsal coppery spot, bluish ventrally, trochanter and most of femur except apical fifth, pale yellow as well as tibia, apical spur and basitarsus whitish, following tarsomeres yellowish. Gaster dark (but exhibiting green reflections mixed with small bluish spots when using intense artificial light), first basal tergum with evident metallic green lustre. Gaster dorsally bearing pale hair-like setae. Ovipositor tricoloured, with short basal band black, long and whitish median one, the apical brownish.

Frontovertex coriaceous to lateral ocelli, distinctly imbricate reticulate posteriorly and progressively merging into occiput but an almost imperceptible transverse ridge nevertheless present. Scrobal depression, except antennal scrobes ventrally, very distinctly reticulate. Interantennal boss and lower face finely and coriaceous to reticulate-imbricate, narrowly smooth along edge of oral fossa. Head 1.74–1.85× as broad as long, temples 0.20× length of eyes, POL 3.77–3.81× OOL, lateral ocelli separated from adjacent eye orbit by 0.56–0.63× their diameter which is of same size as median ocellus diameter. Eyes separated by 0.40× head width, width of oral fossa 1.47–1.56× length of malar space, distance from lower margin of antennal toruli to edge of oral fossa 1.19–1.26× the interantennal distance. Antenna with combined length of pedicel and flagellum 1.20×

head width, scape and pedicel respectively 4.52× and 2.15× as long as wide, pedicel 1.34× as long as combined length of anellus and F1, the funicle segments shortening and widening distally, F7 1.63× as wide as F1, clava 2.30× as long as wide and about as long as combined length of three apical funicular segments.

Mesosoma 1.60–1.76× as long as broad. Mesoscutum imbricate-reticulate anteriorly on convex median lobe and coarsely reticulate on postero-medial depression; top of sublateral bumps finely imbricate coriaceous with small mesh size. Mesh size medially along postero-medial depression similar to that of mesal surface of lateral lobes. Scutellar-axillar complex 1.17× as long as broad, mostly coriaceous and with isodiametric cells, which are larger on centre of scutellum and inner angles of axillae. Prepectus with 8–12 white hair-like setae on centre of disc. Acropleuron finely reticulate anterior of medial micro-sculptured region, the reticulation coarser on posterior surface. Forewing 2.31–2.55× as long as wide, uniformly setose except for linea calva which is separated from vanal area by a few rows of setae. Costal cell dorsally with 3–4 lines of setae near anterior margin of cell on apical half, ventrally densely setose along length, on 2–3 lines. Discoloured section of submarginal vein, along parastigma, bearing 5–7 setae. Linea calva 0.73–0.79× as long as marginal vein, marginal vein 0.81–0.86× as long as costal cell and postmarginal vein about as long as stigmal vein. Stigmal vein straight on his hind margin, stigma moderately enlarged. Mesotibia with an apical row of 5–6 pegs, ventral surfaces of tarsal segments with 12 pegs arranged into two rows distally on either side of basitarsus, and in one row on either side on following three segments. Propodeum with U-shaped plical depression extending to foramen, callus moderately setose with long and curved hair-like setae. Gaster reticulate with isodiametric cells, except surface of first tergum basally smooth but merging to imbricate. Tip of hypopygium at half length of gaster. Apex of second valvifer not distinctly extending beyond apex of gaster, ovipositor sheaths 0.94× length of metatibia and 1.09× length of marginal vein.

Male. Length 1.50 mm. Head bluish with faint irregular purple reflections on vertex, lower face greenish. Scrobal depression with violet reflections. Antenna and apical segment of palpi brown. Pro- and mesonotum bluish with coppery reflections medially on mesoscutum and dorsal surface of scutellum and axillae. Tegula dark basally, testaceous on rest of surface. Propodeum bluish with slight purple reflections on either side of plicae. Gaster dark brown. Venation testaceous. Procoxa and femur dark brown, tibia with antero-dorsal dark spot, the rest of tibia and tarsus testaceous. Mesocoxa, trochanter and femur entirely infuscate, tibia whitish, slightly fuscous on baso-dorsal half and at apex, apical spur dark and contrasting with the white basitarsus, the rest of tarsomeres blackish. Metacoxa black with slight bluish reflections, trochanter and femur dark brown, tibia moderately and uniformly infuscate, basitarsus white, second and third tarsomeres testaceous, and the last ones infuscate. Vertex with an evident transverse ridge delimiting it posteriorly. Vertex and edge of scrobal depression reticulate, antennal scrobes smooth. Parascrobal area reticulate, lower face imbricate to coriaceous. Lower face above malar sulcus with a few long and hook-like setae, not forming a patch. Gena bearing a long seta together with one or two shorter ones. Scape evidently enlarged, only 1.50× as long as broad, bearing numerous pores along scapular scrobe, distributed in several rows on whole length of scape. Pedicel 1.34× as long as broad, bearing seven hook-like setae ventrally. Flagellum filiform, bearing relatively sparse setae. F1 and F2 short and slightly transverse, the first one 0.82× as long as broad and 0.62× as long as F3. F1 without MPS, F2 bearing one MPS. Clava evidently two-segmented, 2.45× as long as wide and not broader than F1. Mesosoma 1.64× as long as broad. Mesoscutum entirely reticulate with isodiametric cells. Scutellum coriaceous on dorsum, with imbricate sculpture on sides. Propodeum entirely smooth with complete and percurrent median carina. Forewing 1.80× as long as broad, marginal vein 0.80× as long as costal cell. Postmarginal vein about as long as the stigmal vein which is curved on hind margin. Costal cell with one complete row of ventral setae. Cubital fold with three setae behind speculum.

Diagnosis. **Female**. Frontovertex coriaceous, scrobal depression, except lower half of antennal scrobes, reticulate. Combined length of pedicel and flagellum only 1.20× head width, pronotal collar with blue violet tinge contrasting with the green mesonotum. Legs with extensive pale yellow parts, especially whole tibiae and mesofemur. Hind margin of stigmal vein straight on hind margin. Ovipositor somewhat longer than marginal vein and hardly shorter than metatibia. **Male**. Vertex with evident ridge posteriorly separating it from occiput. Lower face above malar sulcus with some long hook-like setae not forming a patch. Gena bearing one long seta. Scape very short and broad bearing numerous pores arranged in several rows on outer band. Pedicel bearing seven hook-like setae. Flagellum filiform, basal flagellomere (anellus) discoidal, F1 and F2 very short, slightly transverse. Clava evidently two-segmented.

Recognition. **Female**. The species is easily recognized through the unique combination of characters quoted above, especially the coriaceous frontovertex, reticulate scrobal depression and yellow pale regions of legs. **Male**. It is easily recognized through the step-like ridge between vertex and occiput, the structure of scape and clava and the dark apical spur of mesotibia.

Distribution. Czech Republic, only known from the type locality.

Host (s). The two sexes have been reared from *Harmandia* sp. (Diptera: Cecidomyiidae) on *Populus tremula* Linné.

Discussion

Clarifying taxonomic concepts within *Eupelmus* is of utmost importance because this genus includes a large number of candidate biological control agents worldwide. Our results,

which focus on the *Eupelmus urozonus* complex, demonstrate the existence of previously unrecognized species with different host associations, contributing to a better understanding of the taxonomy of the genus. Within this framework, the combined use of morphological and molecular approaches was proven to be successful. Indeed, the morphological approach validated the systematic status of species already described, such as *E. acinellus*, *E. annulatus*, *E. azureus*, *E. cerris*, *E. fulvipes*, *E. kiefferi*, *E. martellii*, *E. tibicinis* and *E. urozonus*, and the morphological characters used for their discrimination. It also showed that – even for such a reduced taxonomic group occurring in a relatively well-studied region of the world that has been frequently sampled in biodiversity studies – the number of species still undiscovered and that were previously confused was very high.

In agreement with other recent studies such as Fisher & Smith (2008), Gebiola *et al.* (2009), Malausa *et al.* (2010), Veijalainen *et al.* (2011) and Gebiola *et al.* (2012), this paper advocates the necessity of combining morphological and molecular criteria in an integrative approach as an international standard for taxonomic studies.

Indeed, resolving species complexes gives a unique opportunity to more precisely define or even deeply revise ecological interactions (see, for instance, the following recent publications for case study involving arthropods: Chesters *et al.*, 2012; Knee *et al.*, 2012; Muirhead *et al.*, 2012; Miller *et al.*, 2013). In our study, almost all of the most common species (*E. confusus*, *E. kiefferi*, *E. gemellus* and *E. urozonus*) were confirmed to be generalist species with likely wide host ranges because they were recovered from at least two insect orders (Diptera and Hymenoptera) and in association with various plants (see Appendix S1 and Table S1).

Both the diversity of the '*urozonus*-complex' and the probable sympatry between some of the species brings into question their routine identification for taxonomic or applied purposes. Several new morphological characters are described in this study to characterize different species, in particular those that are morphologically very similar and that could be easily confused, such as *E. kiefferi* with *E. fulvipes* and *E. confusus* with *E. martellii* or *E. gemellus*. As a consequence, previous descriptions found in the literature have to be interpreted cautiously and it would be preferable that further morphological identifications are supervised by experts. For this purpose, two of the co-authors (GG & LF) studied the type material of Palearctic *Eupelmus* belonging to the nominal subgenus and are preparing a revision of all Palaearctic *E.* (*Eupelmus*) (G. Gibson and L. Fusu, in preparation), including other species not dealt with here. In addition, another paper treating the phylogeny of the *Eupelmus* of the '*urozonus*-complex' at the inter- and intraspecific levels is also in preparation by the same authors of this paper. Alternatively, development of molecular tools based on taxon-specific primers should be validated especially for the males, which show very small morphological differences (S. Warot, unpublished data). Consequently, specific primers combinations could be routinely used in laboratories with basic molecular biology equipment.

With regard to biological control applications, the discovery and description of *E. confusus* is of prime interest in France. This species appears, *a posteriori,* as the main *Eupelmus* species developing on the olive fruit fly *B. oleae* and probably has been repeatedly confused with other *Eupelmus* species. We ourselves erroneously identified it as *Eupelmus martellii* in a recent survey in French olive orchards (Borowiec *et al.*, 2012). Such confusion could negatively affect the efficiency of biological control programs, particularly those implying conservation methods that favour *Eupelmus* species by diversifying host plants and insects. In particular, the Asteraceae *D. viscosa* and the associated gall forming *M. stylata* are thought to be good candidates to locally support *Eupelmus* species in the absence of *B. oleae* (see for instance: Delucchi, 1957; Ferrière & Delucchi, 1957; Féron *et al.*, 1961; Neuenschwander *et al.*, 1983; Warlop, 2006; Boccaccio & Petacchi, 2009; Franco-Mican *et al.*, 2010; Gimilio, 2010). Such practices may only be effective if *Eupelmus* species do not have too marked host specificity/preferences.

Taken as a whole, our results clearly emphasize the need to study more precisely the systematics, phylogeny, population genetics and ecology of *Eupelmus* species, desirably through international initiatives with standardized and coordinated procedures.

Supporting Information

Additional Supporting Information may be found in the online version of this article under the DOI reference: 10.1111/syen.12089

Table S1. Collection information of specimens used in phylogenetic analysis and GenBank accessions.

Table S2. Kimura 2-parameter pairwise distances (indicated in %) for *COI* and *Wg* datasets.

Table S3. Haplotype diversity in the '*urozonus*-complex' species.

Table S4. Abbreviations of morphological structures used in the species description and measurements taken for adult *Eupelmus*.

Appendix S1. Review of previously described species and list of paratypes for some new species belonging to the '*urozonus*-complex' in the Western Palaearctic region.

Appendix S2. Information about collections, Museums and other institutions containing the observed specimens of *Eupelmus*.

Doc. S1. Raw measurements and selected ratios of some individuals of the '*urozonus*-complex' species.

Doc. S2. Trees from Bayesian analyses of *COI* and *Wg* datasets.

Doc. S3. Additional figures illustrating already described species of *Eupelmus*.

Acknowledgements

This research was directly supported by the projects 'EUPELMUS' (Scientific Department 'Santé des Plantes et Environnement' of INRA - grant 2012-04-05-20), 'INULA' (APR Pesticides 2011: 'Changer les pratiques agricoles pour préserver les services écosystémiques') and 'BIOFIS' (number 1001-001) allocated by the French Agropolis Fondation (Montpellier). This study also took benefits from field work realised in the frame of the projects 'BIOINV-4I' (ANR-06-BDIV-008 – Coordinator: Thomas Guillemaud), 'Lutte biologique contre le Cynips du Châtaignier' (ONEMA 2011 – Coordinator: Nicolas Borowiec & Jean-Claude Malausa), and the Swedish Malaise Trap Project (SMTP). The authors want to thank Sylvie Warot and Gwenaelle Genson for their contribution to the molecular work. We are grateful to Frédéric Fernandez for his technical assistance in using the SEM of the Sciences University at Montpellier. We thank the CBGP HPC computational platform on which phylogenetic analyses were performed. This work would have not been possible without the implication of colleagues from Museums for the loan of type material (see Appendix S2), several collaborators of the RDLB staff and the following distant persons: Richard Askew for the loan of the type of *E. stenozonus*, Maria Tavano and Roberto Poggi for their welcome during the visit of the Genova Museum, H.-P. Aberlenc (CIRAD), Martin Albers (Rottenburg), Julien Balajas (AREFLEC), Raquel Cantera-Rioja (Universidad de La Rioja), Frédérique Ceccaldi (Chambre d'Agriculture de Haute-Corse), Hélène Dumas (France), Jean Lecomte, Laura Loru (Istituto per lo Studio degli Ecosistemi), Seyed Massoud Madjdzadeh (University of Kerman), Pelle Magnusson (Station Linné, Sweden), J.-M. Maldès (CIRAD), Zinette Moussa (Lebanese Agriculture Research Institute), Ovidiu Popovici and Mircea Mitroiu (University of Iasi), Gordon Ramel, Ion Şchiopu (Constanta, Romania), Edy Spagnol (Conservatoire des Oliviers de Durban-Corbières), Anastasia Tsagkarakou (Plant Protection Institute of Heraklion), Giuseppe Fabrizio Turrisi (University of Catania), Villu Soon (University of Tartu) and Patrick Weill (Pau, France).

References

Aebi, A., Schönrogge, K., Melika, G., Quacchia, A., Alma, A. & Stone, G.N. (2007) Native and introduced parasitoids attacking the invasive chestnut gall wasp *Dryocosmus kuriphilus*. *Bulletin OEPP/EPPO Bulletin*, **37**, 166–171.

Amevoin, K., Sanon, A., Apossaba, M. & Glitho, I.A. (2007) Biological control of bruchids infesting cowpea by the introduction of *Dinarmus basalis* (Rondani) (Hymenoptera: Pteromalidae) adults into farmers' stores in West Africa. *Journal of Stored Products Research*, **43**, 240–247.

Arambourg, Y. (1964) Permanent rearing of *Eupelmus urozonus* Dalm. (Hym. Chalcididae), an ectophagous parasite of *Dacus oleae*, on a laboratory host. *Revue de Pathologie Végétale et d'Entomologie Agricole de France*, **43**, 183–190.

Armstrong, K.F. & Ball, S.L. (2005) DNA barcodes for biosecurity: invasive species identification. *Philosophical Transactions of the Royal Society B*, **360**, 1813–1823.

Askew, R.R. & Nieves-Aldrey, J.L. (2000) The genus *Eupelmus* Dalman, 1820 (Hymenoptera, Chalcidoidea, Eupelmidae) in peninsular Spain and the Canary Islands, with taxonomic notes and descriptions of new species. *Graellsia*, **56**, 49–61.

Blaxter, M. (2003) Counting angels with DNA. *Nature*, **421**, 122–124.

Boccaccio, L. & Petacchi, R. (2009) Landscape effects on the complex of *Bactrocera oleae* parasitoides and implications for conservation biological control. *Biological Control*, **54**, 607–616.

Borowiec, N., Groussier-Bout, G., Vercken, E. *et al.* (2012) Diversity and geographic distribution of the indigenous and exotic parasitoids of the olive fruit fly, *Bactrocera oleae* (Dipt., Tephritidae), in Southern France. *IOBC-WPRS Bulletin*, **79**, 71–78.

Bouček, Z. (1963) A new *Eupelmus* (Hymenoptera: Chalcidoidea), egg-parasite of the cicada *Tibicina haematodes*. *Acta Societatis Entomologicae Cechoslovenicae*, **60**, 277–279.

Bouček, Z. (1977) A faunistic review of the Yugoslavian Chalcidoidea (Parasitic Hymenoptera). *Acta Entomologica Jugoslavica*, **13** (Suppl.), 1–145.

Bouček, Z. (1988) *Australasian Chalcidoidea (Hymenoptera). A Biosystematic Revision of Genera of Fourteen Families, with a Reclassification of Species*. CAB International Institute of Entomology, The Cambrian News Ltd., Aberystwyth.

Brower, A.V.Z. & DeSalle, R. (1998) Patterns of mitochondrial versus nuclear DNA sequence divergence among nymphalid butterflies: the utility of *wingless* as a source of characters for phylogenetic inference. *Insect Molecular Biology*, **7**, 73–82.

Caleca, V. & Mineo, G. (1985) Profilo di un entomologo siciliano: Teodosio De Stefani-Perez (1853–1935). Atti XIV Congresso Nazionale Italiano di Entomologia, Palermo, Erice. Bagheria, pp. 17–29.

Campbell, D.L., Brower, A.V.Z. & Pierce, N.E. (2000) Molecular evolution of the *Wingless* gene and its implications for the phylogenetic placement of the butterfly family Riodinidae (Lepidoptera: Papilionoidea). *Molecular Biology and Evolution*, **17**, 684–696.

Caterino, M.S., Cho, S. & Sperling, F.A.H. (2000) The current state of insect molecular systematics: a thriving Tower of Babel. *Annual Review of Entomology*, **45**, 1–54.

Charlet, L.D., Armstrong, J.S. & Hein, G.L. (2002) Sunflower stem weevil and its larval parasitoids in the Central and Northern Plains of the USA. *Biological Control Journal*, **47**, 513–523.

Chesters, D., Wang, Y., Yu, F. *et al.* (2012) The integrative taxonomic approach reveals host specific species in an encyrtid parasitoid species complex. *PLoS One*, **7**, e37655.

Dalla Torre, K.W.V. (1898) *Catalogus Hymenopterorum hucusque descriptorum systematicus et synonymicus*, *Vol V: Chalcididae et Proctotrupidae*, Leipzig.

Dalman, J.W. (1820) Försök till uppställning af insect-familjen Pteromalini, i synnerhet med afseende på de i Sverige funne arter. *Kungliga Svenska Vetenskapsakademiens Handlingar*, **41**, 123–174, 177–182, 340–385.

Danforth, B.N., Linl, C. & Fang, J. (2005) How do insect nuclear ribosomal genes compare to protein-coding genes in phylogenetic utility and nucleotide substitution patterns? *Systematic Entomology*, **30**, 549–562.

Delucchi, V. (1957) Les parasites de la mouche des olives. *Entomophaga*, **2**, 107–118.

De Stefani, T. (1898) Note intorno ad alcuni zoocecidii del *Quercus robur* e del *Q. suber* raccolti nel territorio di Castelvetrano (Sicilia). *Naturalista Siciliano*, **2**, 156–174.

Drummond, A.J., Ashton, B., Buxton, S. *et al.* (2010) Geneious v5.5 [WWW document]. URL http://www.geneious.com [accessed on 21 June 2013].

Duan, J.J., Fuester, R.W., Wildonger, J., Taylor, P.B., Barth, S. & Spichiger, S.E. (2009) Parasitoids attacking the emerald ash borer

(Coleoptera: Buprestidae) in Western Pennsylvania. *Florida Entomologist*, **92**, 588–592.

Duan, J.J., Bauer, L.S., Abell, K.J. & van Driesche, R. (2012) Population responses of hymenopteran parasitoids to the emerald ash borer (Coleoptera: Buprestidae) in recently invaded areas in north central United States. *Biological Control*, **57**, 199–209.

Eilenberg, J., Hajek, A. & Lomer, C. (2001) Suggestions for unifyingthe terminology in biological control. *Biological Control*, **46**, 387–400.

Erdős, J. (1955) Megfigyelések a nád kártevőiről és azok parazitáiról. Observationes de insectis nocivis eorumque parasitis in *Phragmite vulgari* Lam. *Allattani Közlemények*, **45**, 33–48.

Féron, M., Bénard, R. & Poitout, S. (1961) La mouche de l'olive, *Dacus olea* Gmel. et ses parasites en Corse en 1959 et 1960. *Entomophaga*, **3**, 173–183.

Ferrière, C.H. & Delucchi, V. (1957) Les hymenoptères parasites de la mouche des olives. I. Les chalcidiens de la région méditerranéenne. *Entomophaga*, **2**, 119–124.

Fisher, B.L. & Smith, M.A. (2008) A revision of Malagasy species of *Anochetus* Mayr and *Odontomachus* Latreille (Hymenoptera: Formicidae). *PLoS One*, **3**, e1787.

Folmer, O., Black, M., Hoeh, W., Lutz, R. & Vrijenhoek, R. (1994) DNA primers for amplification of mitochondrial cytochrome c oxidase subunit I from diverse metazoan invertebrates. *Molecular Marine Biology and Biotechnology*, **3**, 294–299.

Förster, A. (1860) Eine Centurie neuer Hymenopteren. *Verhandlungen des Naturhistorischen Vereines der Preussischen Rheinlande und Westfalens*, **17**, 93–153.

Franco-Mican, S., Castro, J. & Campos, M. (2010) Preliminary study of the parasitic complex associated with *Dittrichia viscosa* in Andalusia. *IOBC/WPRS Bulletin*, **5**, 139–143.

Gahukar, R. (1984) Seasonal distribution of sorghum midge (*Contarinia sorghicola* Coq) and its hymenopterous parasites in Senegal. *Agronomie*, **4**, 393–397.

Galtier, N., Nabholz, B., Glémin, S. & Hurst, G.D.D. (2009) Mitochondrial DNA as marker of molecular diversity: a reappraisal. *Molecular Ecology*, **18**, 4541–4550.

Gariepy, T.D., Kuhlmann, U., Gillott, C. & Erlandson, M. (2007) Parasitoids, predators and PCR: the use of diagnostic molecular markers in biological control of Arthropods. *Journal of Applied Entomology*, **131**, 225–240.

Gauthier, N., Sanon, A., Monge, J.P. & Huignard, J. (1999) Interspecific relations between two sympatric species of hymenoptera, *Dinarmus basalis* (Rond) and *Eupelmus vuilleti* (Crw), ectoparasitoids of the bruchid *Callosobruchus maculatus* (F). *Journal of Insect Behavior*, **12**, 399–413.

Gebiola, M., Bernardo, U., Monti, M.M., Navone, P. & Viggiani, G. (2009) *Pnigalio agraules* (Walker) and *Pnigalio mediterraneus* Ferrière and Delucchi (Hymenoptera: Eulophidae): two closely related valid species. *Journal of Nature History*, **43**, 2065–2480.

Gebiola, M., Gómez-Zurita, J., Monti, M.M.,., Navone, P. & Bernardo, U. (2012) Integration of molecular, ecological, morphological and endosymbiont data for species delimitation within the *Pnigalio soemius* complex (Hymenoptera: Eulophidae). *Molecular Ecology*, **21**, 1190–1208.

Gibson, G.A.P. (1986) Mesothoracic skeletomusculature and mechanics of flight and jumping in Eupelminae (Hymenoptera, Chalcidoidea: Eupelmidae). *The Canadian Entomologist*, **118**, 691–728.

Gibson, G.A.P. (1990) Revision of the genus *Macroneura* Walker in America North of Mexico (Hymenoptera: Eupelmidae). *Canadian Entomologist*, **122**, 837–873.

Gibson, G.A.P. (1995) Parasitic wasps of the subfamily Eupelminae: classification and revision of world genera (Hymenoptera: Chalcidoidea, Eupelmidae). *Memoirs on Entomology, International*, **5**, i-v + 421 pp..

Gibson, G.A.P. (2009) Revision of New World Spalangiinae (Hymenoptera: Pteromalidae. *Zootaxa*, **2259**, 1–159.

Gibson, G.A.P. (2010) *Calosota* Curtis (Hymenoptera, Chalcidoidea, Eupelmidae) – review of the New World and European fauna including revision of species from the West Indies and Central and North America. *ZooKeys*, **55**, 1–75.

Gibson, G.A.P. (2011) The species of *Eupelmus* (*Eupelmus*) Dalman and *Eupelmus* (*Episolindelia*) Girault (Hymenoptera: Eupelmidae) in North America north of Mexico. *Zootaxa*, **2951**, 1–97.

Gibson, G.A.P., Huber, J.T. & Woolley, J.B. (1997) *Annotated Keys to the Genera of Nearctic Chalcidoidea (Hymenoptera)*. NRC Research Press, Ottawa.

Gimilio, R. (2010) L'inule visqueuse et la lutte biologique en oléiculture. *Annales de la Société d'Horticulture et d'Histoire Naturelle de l'Hérault*, **150**, 70–76.

Giraud, J. (1863) Mémoire sur les insectes qui vivent sur le roseau commun, *Phragmites communis* Trin. (*Arundo phragmites* L.) et plus spécialement sur ceux de l'ordre des Hymenoptères. *Verhandlungen der Zoologisch-Botanischen Gesellschaft in Wien*, **13**, 1251–1288.

Grabenweger, G. (2004) Poor control of the horse chestnut leafminer, *Cameraria ohridella* (Lepidoptera: Gracillariidae), by native European parasitoids: a synchronisation problem. *European Journal of Entomology*, **101**, 189–192.

Grabenweger, G. & Lethmayer, C. (1999) Occurrence and phenology of parasitic Chalcidoidea on the horse chestnut leafminer, *Cameraria ohridella* Deschka & Dimic (Lep.,Gracillariidae). *Journal of Applied Entomology*, **13**, 257–260.

Graham, M.W.R.d.V. (1969a) Some Eupelmidae (Hymenoptera: Chalcidoidea) new to Britain, with notes on new synonymy in this family. *Proceedings of the Royal Entomological Society of London B*, **38**, 89–94.

Graham, M.W.R.d.V. (1969b) The Pteromalidae of north-western Europe (Hymenoptera: Chalcidoidea). *Bulletin of the British Museum (Natural History) (Entomology), Supplement*, **16**, 1–908.

Gu, X., Fu, Y.-X. & Li, W.-H. (1995) Maximum likelihood estimation of the heterogeneity of substitution rate among nucleotide sites. *Molecular Biology and Evolution*, **12**, 546–557.

Hebert, P.D.N., Cywinska, A., Ball, S.L. & De Waard, J.R. (2003a) Biological identifications through DNA barcodes. *Proceedings of the Royal Society of London B*, **270**, 313–321.

Hebert, P.D.N., Ratnasingham, S. & deWaard, J.R. (2003b) Barcoding animal life: cytochrome oxidase subunit 1 divergences among closely related species. *Proceedings of the Royal Society of London B*, **270**, S96–S99.

Hebert, P.D.N., Penton, E.H., Burns, J.M., Janzen, D.H. & Hallwachs, W. (2004) Ten species in one: DNA barcoding reveals cryptic species in the neotropical skipper butterfly *Astraptes fulgerator*. *Proceedings of the National Academy of Sciences of the United States of America*, **101**, 14 812–14 817.

Heraty J. M., Burks, R. A., Cruaud A.*et al.* (2013) A phylogenetic analysis of the megadiverse Chalcidoidea (Hymenoptera). *Cladistics*, **29**, 1–77.

Hogg, I.D. & Hebert, P.D.N. (2004) Biological identification of springtails (Hexapoda: Collembola) from the Canadian Arctic, using mitochondrial DNA barcodes. *Canadian Journal of Zoology*, **82**, 749–754.

Hurst, G.D.D. & Jiggins, F.M. (2005) Problems with mitochondrial DNA as a marker in population, phylogeographic and phylogenetic studies: the effects of inherited symbionts. *Proceedings of the Royal Society B*, **272**, 1525–1534.

Jinbo, U., Kato, T. & Ito, M. (2011) Current progress in DNA barcoding and future implications for entomology. *Entomological Science*, **14**, 107–124.

Kalina, V. (1988) Descriptions of new Palearctic species of the genus *Eupelmus* Dalman with a key to species (Hymenoptera, Chalcidoidea, Eupelmidae). *Silvaecultura Tropica et Subtropica*, **12**, 3–33.

Kieffer, J.J. (1899) Description de quelques chalcidites nouveaux suivie d'une étude sur le genre *Euchalcis* Duf. (*Allocera* Sich.). *Annales de la Société Entomologique de France*, **68**, 368–378

Kimura, M. (1980) A simple method for estimating evolutionary rate of base substitutions through comparative studies of nucleotide sequences. *Journal of Molecular Evolution*, **16**, 111–120.

Knee, W., Beaulieu, F., Skevington, J.H., Kelso, S., Cognato, A.I. & Forbes, M.R. (2012) Species boundaries and host range of tortoise mites (Uropodoidea) phoretic on bark beetles (Scolytinae), using morphometric and molecular markers. *PLoS One*, **7**, e47243.

Lotfalizadeh, H., Rasplus, J.-Y. & Delvare, G. (2007) Rose gall wasps and their asssociated fauna (Hymenoptera) in Iran. *Redia*, **89**, 73–85.

Malausa, T., Fenis, A., Warot, S. *et al.* (2010) DNA markers to disentangle complexes of cryptic taxa in mealybugs (Hemiptera: Pseudococcidae). *Journal of Applied Entomology*, **135**, 142–155.

Masi, L. (1941) Un nuovo *Eupelmus* parassita del *Dacus oleae* nella cirenaica. (Hymen. Chacididae). *Bollettino della Società Entomologica Italiana*, **73**, 109–111.

Miller, A.D., Skoracka, A., Navia, D. *et al.* (2013) Phylogenetic analyses reveal extensive cryptic speciation and host specialization in an economically important mite taxon. *Molecular Phylogenetics and Evolution*, **66**, 928–940.

Muirhead, K.A., Murphy, N.P., Sallam, N., Stephen, C., Donnellan, S.T. & Austin, A.D. (2012) Phylogenetics and genetic diversity of the *Cotesia flavipes* complex of parasitoid wasps (Hymenoptera: Braconidae), biological control agents of lepidopteran stemborers. *Molecular Phylogenetics and Evolution*, **63**, 904–914.

Munro, J.M., Heraty, J.M., Burks, R.A. *et al.* (2011) Molecular phylogeny of the Chalcidoidea (Hymenoptera). *PLoS One*, **6**, e27023.

Nees ab Esenbeck, C.G. (1834) *Hymenopterorum ichneumonibus affinium monographiae, genera Europaea et species illustrantes*, 2, Stuttgart & Tubingen, 448 pp.

Neuenschwander, P., Bigler, F., Delucchi, V. & Michelakis, S. (1983) Natural enemies of preimaginal stages of *Dacus oleae* Gmel. (Dipt., Tephritidae) in Western Crete. I. Bionomics and phenologies. *Bollettino del Laboratorio di Entomologia Agraria Filippo Silvestri*, **40**, 3–32.

Noyes, J.S. (1982) Collecting and preserving chalcid wasps. *Journal of Natural History*, **16**, 315–334.

Noyes, J.S. (2013) Universal Chalcidoidea Database [WWW document]. URL http://www.nhm.ac.uk/research- curation/research/projects/chalcidoids/index.html [accessed on 15 July 2013].

Nylander, J.A.A. (2004) *MrAIC.pl*. Program Distributed by the Author, Evolutionary Biology Centre, Uppsala University, Uppsala.

Pons, J. (2006) DNA-based identification of preys from non-destructive, total DNA extractions of predators using arthropod universal primers. *Molecular Ecology Notes*, **6**, 623–626.

Puissant, S. & Sueur, R. (2011) *Dimissalna*, a cicada genus that remained unnoticed in France (Insecta: Hemiptera: Cicadidae). *Annales de la Société Entomologique de France (New Series)*, **47**, 519–523.

Quacchia, A., Ferracini, C., Nicholis, J.A. *et al.* (2013) Chalcid parasitoid community associated with the invading pest *Dryocosmus kuriphilus* in north-western Italy. *Insect Conservation and Diversity*, **6**, 114–123.

Rambaut, A. & Drummond, A.J. (2007) Tracer v1.5 [WWW document]. URL http://beast.bio.ed.ac.uk/Tracer [accessed on 30 November 2009].

Ratzeburg, J.T.C. (1844) *Die Ichneumonen der Forstinsekten in entomologischer und forstlicher Beziehung*, 1, 224 pp, 4 plates, Berlin.

Ratzeburg, J.T.C. (1852) Die Ichneumonen der Forstinsekten in entomologischer und forstlicher Beziehung, 3, v–xviii+272 pp, 3 tables, Berlin.

Ribes Escolà, A. & Askew, R.R. (2009) Chalcidoidea (Hymenoptera) reared from fruits of *Juniperus phoenicea*, with descriptions of three new species. *Boletín Sociedad Entomológica Aragonesa*, **45**, 109–121.

Rokas, A., Nylander, J.A.A., Ronquist, F. & Stone, G.N. (2002) A maximum-likelihood analysis of eight phylogenetic markers in gallwasps (Hymenoptera: Cynipidae): implications for insect phylogenetic studies. *Molecular Phylogenetics and Evolution*, **22**, 206–219.

Ronquist, F., Teslenko, M., van der Mark, P. *et al.* (2012) MrBayes 3.2: efficient Bayesian phylogenetic inference and model choice across a large model space. *Systematic Biology*, **61**, 539–542.

Ruschka, F. (1921) Chalcididenstudien I. *Verhandlungen der Zoologisch-Botanischen Gesellschaft in Wien*, **70**, 234–315.

Shoemaker, D.D., Dyer, K.A., Ahrens, M., McAbee, K. & Jaenike, J. (2004) Decreased diversity but increased substitution rate in host mtDNA as a consequence of a *Wolbachia* endosymbiont infection. *Genetics*, **168**, 2049–2058.

Smith, M.A., Woodley, N.E., Janzen, D.H., Hallwachs, W. & Hebert, P.D.N. (2006) DNA barcodes reveal cryptic host-specificity within the presumed polyphagous members of a genus of parasitoid flies (Diptera: Tachinidae). *Proceedings of the National Academy of Sciences of the United States of America*, **103**, 3657–3662.

Smith, M.A., Fernández-Triana, J.L., Eveleigh, E. *et al.* (2013) DNA barcoding and the taxonomy of Microgastrinae wasps (Hymenoptera, Braconidae): impacts after 8 years and nearly 20 000 sequences. *Molecular Ecology Resources*, **13**, 168–176.

Song, H., Buhay, J.E., Whiting, M.F., Keith, A. & Crandall, K.A. (2008) Many species in one: DNA barcoding overestimates the number of species when nuclear mitochondrial pseudogenes are coamplified. *Proceedings of the National Academy of Sciences of the United States of America*, **105**, 13486–13491.

Stamatakis, A. (2006a) RAxML-VI-HPC: maximum likelihoodbased phylogenetic analyses with thousands of taxa and mixed models. *Bioinformatics*, **22**, 2688–2690.

Stamatakis, A. (2006b) Phylogenetic models of rate heterogeneity: a high performance computing perspective. International Parallel and Distributed Processing Symposium (IPDPS 2006). Rhodes Island, p. 8.

Talitsky, V.I. (1966) The great singing cicadid (*Tibicina haematodes* Scop.) and its eupelmid egg predator (*Eupelmus tibicinis* Bck.). *Trudy Moldavskogo Nauchno-Issledovatel'skogo Instituta Sadovodstva, Vinogradarstva i Vinodeliya. Kishinev*, **13**, 223–230 (in Russian).

Tamura, K., Peterson, D., Peterson, N., Stecher, G., Nei, M. & Kumar, S. (2011) MEGA5: molecular evolutionary genetics analysis using maximum likelihood, evolutionary distance and maximum parsimony methods. *Molecular Biology and Evolution*, **28**, 2731–2739.

Tassi, F., Aberlenc, H.-P., Rasplus, J.-Y., Curletti, G., Dutto, M., Genson, G. & Lempérière, G. (2004) *Eupotosia mirifica*, la grande Cétoine bleue, joyau menacé du patrimoine naturel Européen. Propositions pour la protection de l'espèce et de ses biotopes (Coleoptera Cetoniidae Cetoniinae). *Lambillionea*, **104** (Suppl.), 1–32.

Tautz, D., Arctander, P., Minelli, A., Thomas, R.H. & Vogler, A.P. (2003) A plea for DNA taxonomy. *Trends in Ecology & Evolution*, **18**, 70–74.

Thompson, J.D., Higgins, D.G. & Gibson, T.J. (1994) CLUSTAL W: improving the sensitivity of progressive multiple sequence alignment

though sequence weighting, position-specific gap penalities and weight matrix choice. *Nucleic Acids Research*, **22**, 4673–4680.

Veijalainen, A., Broad, G.R., Wahlberg, N., Longino, J.T. & Sääksjärvi, I.E. (2011) DNA barcoding and morphology reveal two common species in one: *Pimpla molesta* stat. rev. separated from *P. croceipes* (Hymenoptera, Ichneumonidae). *ZooKeys*, **124**, 59–70.

Walker, F. (1839) *Monographia Chalciditum*, Vol. **1**, London.

Warlop, F. (2006) Limitation des populations de ravageurs de l'olivier par le recours à la lutte biologique par conservation. *Cahiers de l'Agriculture*, **15**, 1–7.

Xiao, J.-H., Wang, N.-X., Li, Y.-W. *et al.* (2010) Molecular approaches to identify cryptic species and polymorphic species within a complex community of fig wasps. *PLoS One*, **5**, e15067.

Yu, M.Z., Zhang, K.J., Xue, X.F. & Hong, X. (2011) Effects of *Wolbachia* on mtDNA variation and evolution in natural populations of *Tetranychus urticae* Koch. *Insect Molecular Biology*, **20**, 311–321.

Accepted 7 April 2014

ZooKeys 505: 137–145 (2015)
doi: 10.3897/zookeys.505.9021
http://zookeys.pensoft.net

RESEARCH ARTICLE

A peer-reviewed open-access journal
ZooKeys
Launched to accelerate biodiversity research

Availability of eleven species names of *Eupelmus* (Hymenoptera, Eupelmidae) proposed in Al khatib et al. (2014)

Fadel Al Khatib[1], Lucian Fusu[4], Astrid Cruaud[2], Gary Gibson[5], Nicolas Borowiec[1], Jean-Yves Rasplus[2], Nicolas Ris[1], Gérard Delvare[3]

1 *INRA, Univ. Nice Sophia Antipolis, CNRS, UMR 1355-7254 Institut Sophia Agrobiotech, 06900 Sophia Antipolis, France* **2** *INRA, UMR 1062 CBGP, 755 avenue du Campus Agropolis, Montferrier-sur-Lez Cedex, France* **3** *CIRAD, UMR 55 CBGP, 755 avenue du campus Agropolis, Montferrier-sur-Lez, Cedex, France* **4** *Faculty of Biology, Alexandru Ioan Cuza University, Iasi, Romania* **5** *Agriculture and Agri-Food Canada, Canadian National Collection of Insects, Arachnids and Nematodes, Ottawa, Canada*

Corresponding author: *Fadel Al Khatib* (fadel.alkhatib@sophia.inra.fr)

Academic editor: *M. Buffington* | Received 26 November 2014 | Accepted 20 May 2015 | Published 25 May 2015

http://zoobank.org/8292E6EE-70FF-42B6-B874-617B7DB0E2AD

Citation: Al khatib F, Fusu L, Cruaud A, Gibson G, Borowiec N, Rasplus J-Y, Ris N, Delvare G (2015) Availability of eleven species names of Eupelmus (Hymenoptera, Eupelmidae) proposed in Al khatib et al. (2014). ZooKeys 505: 137–145. doi: 10.3897/zookeys.505.9021

Abstract

This paper is an addendum for the availability of the names of 11 new species proposed in Al khatib et al. (2014).

Keywords

Eupelmus, ICZN, systematics, taxonomy

Introduction

Al khatib et al. (2014) described 11 new species of West Palaearctic *Eupelmus*, but only the acronyms of the depositories where the holotypes are deposited were given in the publication. The full names and location of the depositories were provided, but only in a Word document (Appendix S2) as part of the Supplementary Information

(SI) available on the website of *Systematic Entomology* (http://onlinelibrary.wiley.com/doi/10.1111/syen.12089/suppinfo). Article 16.4 of the International Code of Zoological Nomenclature states that "Every new specific and subspecific name published after 1999, ... must be accompanied in the original publication ... where the holotype or syntypes are extant specimens, by a statement of intent that they will be (or are) deposited in a collection and a statement indicating the name and location of that collection" (ICZN 2012). A museum acronym is not a statement of the location or even necessarily a clear indication of the name of a collection. Further, Appendix S2 cannot be considered as part of the publication or itself a publication because it is a Word document and thus contravenes ICZN Article 8.1.3, in addition to Articles 8.5.2 and 8.5.3. As a result, the new names published in Al khatib et al. (2014) are not available because the complete name and locality information of the holotype depositories are not provided in the publication, but only in a document that supplements the publication. For this reason, the authors provide in the present paper the new names published in Al khatib et al. (2014) with a precise statement (Table 1) as to the name and location of the collection in which the holotypes and other material listed in other supplementary files are deposited. Accordingly, the availability of the 11 names proposed in Al khatib et al. (2014) and given below takes the date of the present publication, as per ICZN Article 10.1. Al khatib et al. (2014) also did not include in the publication paratype information for new species with numerous paratypes, citing this information only in Appendix S1 on the *Systematic Entomology* website. We therefore also include here paratype designations to ensure this information is validly published.

Table 1. Collection acronyms, names and locations for specimen deposition cited in Al khatib et al. (2014).

AICF	Lucian Fusu collection, A1. I. Cuza University, Iasi, Romania.
BMNH	The Natural History Museum, London, United Kingdom.
CBGP	Center for Biology and Management of Populations, Montpellier, France.
CNC	Canadian National Collection of Insects, Arachnids and Nematodes, Agriculture & Agri-food Canada, Ottawa, ON, Canada.
FALPC	Fadel Al khatib personal collection, Faculty of Agricultural Engineering, University of Aleppo, Syria.
GDPC	Gérard Delvare personal collection, Montpellier, France.
MKUI	Plant Protection Department, Mustafa Kemal University, Antakya-Hatay, Turkey.
MNHG	Museum of Natural History of Geneva, Switzerland.
MNHN	National Museum of Natural History, Paris, France.
NHMW	Naturhistorisches Museum, Wien, Austria.
NHRS	Naturhistoriska riksmuseet, Stockholm, Sweden.
NMPC	Narodni Muzeum v Praze, Prague, Czech Republic.
RMNH	Rijksmuseum van Naturrlijke Historie collection, Naturalis Biodiversity Centre, Leiden, The Netherlands.

Results

***Eupelmus* (*Eupelmus*) *confusus* Al khatib**
http://zoobank.org/E9A1F8A3-00D1-4DB6-9A04-5ACBEBDBFEA3

Al khatib et al. (2014): 822–828.

Type material. Holotype ♀. **FRANCE**: Var, Fayence, 43.61774°N, 06.69774°E, 17.iii.2012, emerged 25.iii.2012, ex *Diplolepis rosae* on *Rosa canina* (N. Ris) (1 ♀) [FAL1195/10206] (in MNHG). **Paratypes**. **CYPRUS**: **Lemesos**, 6 km N of Lemesos, 24–25.V.2009, N34.73189°, E33.05175°, pods of carob tree with *Apomyelois ceratoniae* & *Asphondylia gennadii* (Fusu L. & Popovici O.) (5 ♀ 6 ♂ not sequenced) (in AICF) (1 ♀) [LF.ma.CY 01/10427] (in AICF); **6 km N of Lemesos**, 25. V. 2009, sweep net, N34.727028°, E33.052278° (Fusu L. & Popovici O.) (1 ♀ 10 ♂ not sequenced)(in AICF). **FRANCE**: **Alpes-Maritimes**, Biot, N43.63455°, E7.08249°, 11.iii.2012, emerged 27.iii.2012, ex *Andricus kollari* on *Quercus pubescens* (N. Ris) (2 ♀) [FAL1227/10215, FAL1227/10216] (in FALPC); **Alpes-Maritimes**, Opio, N43.64479°, E6.99957°, 04.x.2012, (F. Al khatib & P. Gory) (1 ♀) [FAL1485/10313] (in FALPC); **Alpes-Maritimes**, Pégomas, N43.58844°, E6.93612°, 08.vi.2012, emerged 11.vi.2012, ex *Myopites stylata* on *Dittrichia viscosa* (F. Al khatib & P. Gory) (1 ♀) [FAL1429/10433] (in GDPC); **Alpes-Maritimes**, Sophia--Antipolis, N43.62443°, E7.03667°, 21.ii.2012, emerged 27.ii.2012, ex *Myopites stylata* on *Dittrichia viscosa* (F. Al khatib) (1 ♀ 1 ♂) [FAL1029/10142, FAL1032/10432] (in MNHG); **Alpes-Maritimes**, Sophia-Antipolis, N43.61669°, E7.03722°, 07.vi.2012, emerged 16.vi.2012, ex *Biorhiza pallida* on *Quercus pubescens* (F. Al khatib & P. Gory) (1 ♀) [FAL1338/10227] (in MNHN); **Alpes-Maritimes**, Villars-sur-Var, N43.93730°, E7.08068°, 14.iii.2012, emerged 18.iii.2012, ex *Diplolepis rosae* on *Rosa canina* (F. Al khatib & N. Ris) (2 ♀) [FAL1198/10209 (in MNHG), FAL1198/10210 (in FALPC)]; **Ardèche**, Saint-Georges-les-Bains, N44.85028°, E4.82433°, 13.vi.2012, emerged 14.vi.2012, ex *Biorhiza pallida* on *Quercus pubescens* (F. Al khatib & M. Thaon) (2 ♀) [FAL1325/10224, FAL1325/10225] (in CBGP); **Ardèche**, Saint-Georges-les-Bains, N44.85028°, E4.82433°, 13.vi.2012, emerged 11.vii.2012, ex *Dryocosmus kuriphilus* on *Castanea sativa* (M. Thaon) (1 ♀ 1 ♂) [NB489/10418, NB489c/10419] (in GDPC); **Ardèche**, Saint-Georges-Montpellier, N43.6104°, E3.77227°, ix.2011, emerged ix.2011, ex *Bactrocera oleae* on *Olea europaea* (L. Brancaccio & M. Thaon) (1 ♀ 1 ♂) [FAL1278/10443, FAL1280/10445] (in MNHN); **Aude**, Durban-Corbières, N42.99825°, E2.80690°, 27.iii.2012, emerged 31.iii.2012, ex *Myopites stylata* on *Dittrichia viscosa* (F. Al khatib & N. Ris) (1 ♀) [FAL1122/10175] (GDPC); **Bouches-du-Rhône**, La Ciotat, garden, 09.I.2011 emerged 13-30.IV.2011, *Lasioptera carophila* on *Foeniculum vulgare* (H. Dumas) (5 ♀ 6 ♂ not sequenced, in AICF) (1♀) [LF.ma.FR 01/10422] (in AICF); **Gard**, Garons, N43.76371°, E4.42588°, 11.i.2012, emerged 27.ii.2012, ex *Myopites stylata* on *Dittrichia viscosa* (N. Ris) (1 ♀) [FAL1092/10162] (in MNHG); **Gard**, Roquemaure, N44.03148°, E4.72747°, x.2011, emerged x.2011, ex *Bactrocera oleae* on *Olea europaea* (N. Borowiec) (1 ♀) [FAL1274/10447] (in CBGP); **Haute-Corse**, Aléria, N42.12861°, E9.46555°,

22.ix.2011, ex seeds of *Asphodelus ramosus* infested by *Bruchophagus* sp. (J. Balajas) (2 ♀ 1 ♂) [GDEL4111/10187, GDEL4111/10188, GDEL4111/10189] (in MNHG); **Haute-Corse**, Lumio, N42.55879°, E8.81299°, 23.ix.2012, emerged 28.ix.2012, ex *Bactrocera oleae* on *Olea europaea* (F. Ceccaldi) (2 ♀) [FAL1519/10411, FAL1519/10412] (MNHN); **Haute-Corse**, Piedicorte di Gaggio, N42.22166°, E9.26527°, 22. ix.2011, ex seeds of *Asphodelus ramosus* infested by *Bruchophagus* sp. (J. Balajas) (2 ♀ 3 ♂) [GDEL4114/10190, GDEL4114/10191, GDEL4114a, GDEL4114b & GDEL4114c] (in MNHN); **Hérault**, Causses-et-Veyran, N43.47131°, E3.08508°, x.2011, emerged x.2011, ex *Bactrocera oleae* on *Olea europaea* (A. Auguste-Maros) (1 ♀) [FAL1254/10453] (in FALPC); **Hérault**, Frontignan, N43.43926°, E3.74145°, 17.vi.2012, emerged 19.vi.2012, ex *Myopites stylata* on *Dittrichia viscosa* (F. Al khatib & N. Ris) (1 ♀) [FAL1446/10309] (FALPC); **Hérault**, Laroque, 250-400 m, N45.91722°, E3.74361°, 05.vii.2013, sweeping on *Quercus pubescens* (G. Delvare), (1 ♀) [4173/10596] (in GDPC); **Hérault**, Mèze, N43.41670°, E3.6000°, x.2011, emerged x.2011, ex *Bactrocera oleae* on *Olea europaea* (N. Ris) (2 ♀) [FAL1257/10454 (in CNC), NB229/7052 (in FALPC)]; **Monaco**, Monaco, N43.73263°, E7.41369°, x.2010, ex *Bactrocera oleae* on *Olea europaea* (J.-C. Malausa & C. Roques) (1 ♀) [FAL1247/10436] (in CNC); **Pyrénées-Orientales**, Argelès-sur-Mer, N42.581000°, E3.010910°, x.2011, emerged x.2011, ex *Bactrocera oleae* on *Olea europaea* (N. Ris) (4 ♀ 1 ♂) [FAL1255/10449 & FAL1255/10450 (in GDPC), NB362v/7078, NB362w/7079, FAL1256/10451 (in FALPC)]; **Pyrénées-Orientales**, Banyuls-sur-Mer, 04.ii.2012, emerged 20.ii.2012, ex *Myopites stylata* on *Dittrichia viscosa* (J. Lecomte) (1 ♀) [FAL1100/10164] (in CBGP); **Pyrénées-Orientales**, Banyuls-sur-Mer, N42.47194°, E3.14333°, 250 m, 21.iii.2010 ex galls of *Timaspis phoenixopodos* on *Lactuca viminea* (G. Delvare & J. Lecomte) (2 ♀) [GDEL4001/3303, GDEL4002/3296] (in GDPC); **Pyrénées-Orientales**, Banyuls-sur-Mer, N42.46972°, E3.12388°, 10 m, 21.iii.2010 ex galls of *T. phoenixopodos* on *L. viminea* (G. Delvare & J. Lecomte) (1 ♀) [GDEL4003/3302] (in GDPC); **Pyrénées-Orientales**, Calce, N42.7348°, E2.75471°, x.2011, emerged x.2011, ex *Bactrocera oleae* on *Olea europaea* (N. Borowiec & L. Brancaccio) (2 ♂) [FAL1251/10448 (in GDPC), FAL1251/10283 (in FALPC)]; **Pyrénées-Orientales**, Perpignan, N42.67720°, E2.86912°, 18.vi.2012, emerged 19.vi.2012, ex *Myopites stylata* on *Dittrichia viscosa* (F. Al khatib & N. Ris) (1 ♀) [FAL1455/10312] (in FALPC); **Var**, Rians, N43.57352°, E5.77148°, 31.ii.2012, emerged 09.iii.2012, ex *Diplolepis rosae* on *Rosa canina*, (N. Ris) (2 ♀ 1 ♂) [FAL1204/10212 (in CNC), FAL1204/10213 & FAL1205/10280 (in MNHG)]; (1 ♀) [FAL1195/10207] (in MNHN), same data as holotype. **GREECE**: **Seres**, Kerkini Lake Nat.Park, Kerkini Mts near Vironeia, 300 m, N41.27833°, E23.21955°, sweep net 22.VI.2008 (Fusu, Popovici & Ramel) (1 ♀) (in AICF) (1 ♀) [LF.ma.GR 01/10425] (in AICF); **Seres**, Kerkini lake, Krousia Mts. Site, N41.20180°, E23.07747°, Malaise trap, 12-18.IX.2007 (G. Ramel) (1 ♀) [LF.ma.GR 02/10426] (in AICF); **Seres**, Kerkini Mts., Plateaux Beech, N41.28580°, E23.03368°, Malaise trap, 08.VIII to 13.VIII.2007, (G. Ramel) (1 ♀ not sequenced, in AICF); **Seres**, Kerkini Lake N. Park, nr Kerkini, Pumping St. Site, N41.19760°, E23.08883°, 13.VI to 19.VI.2007, Malaise trap (G. Ramel) (1♀ not sequenced, in AICF); **Seres**, Kerkini Lake N. Park, Kerkini, Krousia Mts site, 190 m, N41.20180°, E23.07747°, 06.VI-12. VI.2007, Malaise tr. (G. Ramel) (4 ♀ not sequenced, in AICF); same data but 13.VI-19.

VI.2007 (2 ♀ not sequenced, in AICF); same data but 20.VI-26.VI.2007 (4 ♀ not sequenced, in AICF). **IRAN**: **Kerman Prov.**, Bidkhan, 2897 m, N29°34.956' E 56°30.612', 11.v.2012, ex galls on *Salix alba* (M. Mahdavi) (1 ♀) [LF.ma.IR 05/10424] (in AICF). **ITALY**: **Liguria**, Bussana-Vecchia, N43.84026°, E7.82905°, 02.i.2012, emerged 20.ii.2012, ex *Myopites stylata* on *Dittrichia viscosa* (E. Spagnol) (4 ♀) [FAL1051/10145 (in GDPC), FAL1088/10154 & FAL1063/10149 (in CBGP), FAL1074/10153 (in MNHN)] and (3 ♂ not sequenced) [FAL1077a, FAL1077b, FAL1077c] (in MNHN); (3 ♀ not sequenced) [FAL1422d & FAL1422c, FAL1422b] (in FALPC) and (2 ♂ not sequenced) [FAL1418a, FAL1418b] (in CNC) same data but 06.vi.2012, emerged 07.vi.2012 (N. Ris). **SPAIN**: **Logroño**, La Rioja, 15.iii.2012, emerged 16.iii.2012, ex *Myopites stylata* on *Dittrichia viscosa* (R. Cantera Rioja) (2 ♀) [FAL1108/10250 (in GDPC), FAL1110/10168 (in FALPC)]. **SWEDEN**: **Skåne**, Sk, Höganäs kommun, Kullabergs naturreservat, between Hjortstugan and Ransvik, Oak forest in southern slope, N56.29421°, E12.48399°, 27.vi to 30.vii.2005, Trap ID 1004, Coll. event 1797 (SMTP) [LF.u.SW.03/10660] (in NHRS).

***E.* (*Eupelmus*) *gemellus* Al khatib**
http://zoobank.org/4BCB5C66-7AC7-431B-8F51-C76CF7D56AD4

Al khatib et al. (2014): 828–837.

Type material. Holotype ♀. **FRANCE**: Haute-Corse, Calenzana, 11.ix.2012, emerged 18.ix.2012, ex *Bactrocera oleae* on *Olea europaea* (F. Ceccaldi) (1 ♀) [FAL1515/10408] (in MNHG). **Paratypes**. **FRANCE**: **Alpes-Maritimes**, Biot, N43.63455°, E7.082490°, 29.x.2012, emerged 01.iii.2013, ex *Megastigmus pistaciae* on *Pistacia lentiscus* (F. Al khatib & N. Ris) (2 ♀ 1 ♂) [FAL1522/10483, FAL1522/10484, FAL1522/10485] (in MNHN); **Alpes-Maritimes**, Biot, N43.63455°, E7.082490°, 11.iii.2012, emerged 27.iii.2012, ex *Mesophleps oxycedrella* on *Juniperus oxycedrus* (N. Ris), (2 ♀) [FAL1359/10230 (in MNHG), FAL1359/10231 (in AICF)]; **Alpes-Maritimes**, Mont-Chauve, 476 m N 43.76578°, E7.27024°, 01.xi.2012, emerged 18.xii.2012, ex *Bactrocera oleae* on *Olea europaea* (M. Thaon) (1 ♀) [NB29/10413] (in FALPC); **Alpes-Maritimes**, Sophia-Antipolis, N43.624423°, E07.03667°, 21.ii.2012, emerged 27.ii.2012, ex *Myopites stylata* on *Dittrichia viscosa* (F. Al khatib) (1 ♀) [FAL1089/10143] (in FALPC); **Ardèche**, Saint-Georges-Montpellier, N43.6104°, E3.77227°, x.2011, ex *Bactrocera olea* on *Olea europaea* (L. Brancaccio & M. Thaon) (1 ♀) [FAL1279/10444] (in MNHG); **Aude**, Bize-Minervois, N43.32692°, E2.870750°, 27.iii.2012, emerged 11.iv.2012, ex *Mesophleps oxycedrella* on *Juniperus oxycedrus* (F. Al khatib & N. Ris), (1 ♀) [FAL1360/10233] (in MNHN); **Aude**, Durban-Corbières, N42.99825°, E2.80690°, 27.iii.2012, emerged 06.iv.2012, ex *Mesophleps oxycedrella* on *Juniperus oxycedrus* (F. Al khatib & N. Ris), (1 ♀) [FAL1362/10234] (in FALPC); **Aude**, Gruissan, N43.12105°, E3.09539°, x.2011, ex *Bactrocera oleae* on *Olea europaea* (N. Ris) (1 ♀) [FAL1266/10446] (in CBGP); **Bouches-du-Rhône**, Lançon-de-Provence, 33 m, N43.54818°, E5.16727°, x.2011, ex *Bactrocera oleae* on *Olea europaea*

(A. Auguste-Maros) (1 ♂) [FAL1269/10439] (in MNHN); **Bouches-du-Rhône**, La Ciotat, 53 m, N43.19011°, E5.65905°, x.2010, ex *Bactrocera oleae* on *Olea europaea* (A. Auguste-Maros) (1 ♂) [FAL1243/10437] (in MNHG); **Haute-Corse**, Bisinchi, 593 m, N42.48983°, E9.32797°, 18.vi.2012, emerged 03.vii.2012, ex *Dryocosmus kuriphilus* on *Castanea sativa* (N. Borowiec & M. Thaon) (4 ♀) [NB441/10414 (in MNHG), NB441/10415 & NB441/10416 (in FLAPC), NB441/10417 (in MNHN)]; **Haute-Corse**, Lumio, N42.55879°, E8.81299°, 13.i.2012, emerged 27.ii.2012, ex *Myopites stylata* on *Dittrichia viscosa* (F. Ceccaldi) (1 ♀) [FAL1013/10137] (in AICF); **Haute-Corse**, Muratu, 750 m, N42.5559°, E9.29929°, emerged 23.i.2013, ex *Dryocosmus kuriphilus* on *Castanea sativa* (N. Borowiec & M. Thaon) (1 ♀) [2013CYN355/10664] (in FALCP); **Var**, la Garde-Freinet, 366 m, N43.31597°, E6.47534°, emerged 28.ii.2013, ex *Dryocosmus kuriphilus* on *Castanea sativa* (N. Borowiec & M. Thaon) (1 ♂) [2013CYN448/10663] (in FALPC); **Var**, Porquerolles, 13 m, N42.99534°, E6.2044°, ex *Bactrocera oleae* on *Olea europaea* (J.-C. Malausa & M. Thaon) (2 ♀) [NB377c/7090 (in GDPC), FAL1260/10438 (in FALPC)]; **Var**, Puget-Ville, 143 m, N43.26728°, E6.10671°, ex *Bactrocera oleae* on *Olea europaea* (J.-C. Malausa & M. Thaon) (1 ♂) [FAL1273a, not sequenced] (in GDPC). **ITALY**: **Liguria**, Bussana-Vecchia, N43.84026°, E7.82905°, 02.i.2012, emerged 24.ii.2012, ex *Myopites stylata* on *Dittrichia viscosa* (E. Spagnol) (2 ♀) [FAL1004/10130, FAL1075/10156] (in MNHN); (1 ♀) [GDEL4122/10194] (in FALPC) same data except collected 25.i.2011 and emerged iv.2011; (1 ♀) [FAL1415/10481] (in CBGP) same data except collected 06.vi.2012 and emerged 07.vi.2012; **Sardinia**, Province Oristano, N39.70041°, E8.739690°, 20.x.2012, sweeping on *Pistacia lentiscus* (L. Brancaccio & M. Thaon) (1 ♀) [FAL1508/10405] (in CNC); **Sardinia,** Province Oristano, N39.70041°, E8.739690°, 20.x.2012, emerged 24.x.2012, ex *Megastigmus pistaciae* on *Pistacia lentiscus* (L. Brancaccio & M. Thaon) (1 ♀) [FAL1513/10407] (in CNC).

***E.* (*Eupelmus*) *janstai* Delvare & Gibson**
http://zoobank.org/27BFFF36-E3EE-4B94-AC0B-D4AB07836E1B

Al khatib et al. (2014): 837–838.

Type material. Holotype ♀. **CZECH REPUBLIC**: Břeclav district, Pavlov, 48.86750°N, 16.65416°E, sweeping on *Tilia platyphyllos*, 03.vii.2010 (G. Delvare) [GDEL4046/10032] (in MNHG). **Paratypes**. Moravia, Vranov riv., Dyje, 48.89472°N, 15.81250°E, 13.viii.1991, riparian forest (L. Masner) (2 ♀) (in CNC).

***E.* (*Eupelmus*) *longicalvus* Al khatib & Fusu**
http://zoobank.org/F83B5381-0448-4EE3-B42F-F9AD7749F964

Al khatib et al. (2014): 838–841.

Type material. Holotype ♀. **SWEDEN**: Gotlands, Go, Gotlands kommun, Roleks, grazed calcareous pine forest. 57°32.207'N, 18°20.273'E, 16.vii–02.viii.2004, Trap ID 28, Coll. event 1458 (SMTP) [LF.ma.SW 02/10429] (in NHRS). **Paratypes**. **FRANCE**: **Alpes-Maritimes**, La Bollène-Vésubie, 1700 m, N43.96778°, E7.38111°, 19.vii.2009 (G. Delvare) (2 ♀) [GDEL4196/10606, GDEL4197/10607] (in GDPC); **Aveyron**, Peyreleau, 850 m, N44.17528°, E3.23750°, 22.vi.2009 (G. Delvare) (1 ♀) [GDEL4194/10604] (in GDPC); **Hautes-Alpes**, Mont-Dauphin, 1869 m, N44.68972°, E6.6786°, 18.viii.2008 (G. Delvare) (1 ♀) [GDEL4199/10609] (in FALPC). **ITALY**: **Friuli Venezia Giulia**, Giulia, Chiusaforte, 1450 m, N46.40527°, E13.4450°, 12.vii.2008 (G. Delvare) (1 ♀) [GDEL4038/10019] (in GDPC); **Friuli Venezia Giulia**, Giulia, Chiusaforte, 1380 m, N46.39944°, E13.45944°, 12.vii.2008 (G. Delvare) (1 ♀) [GDEL4191/10603] (in FALPC). **SWEDEN**: **Södermanland**, **Sö**, Södertälje kommun, Tullgarns näs, Rävsalaviken, mixed forest next to pasture, N58.955217°, E17.607550°, 03.vii/19.viii.2004, Trap ID 30, Coll. event ID 1055 (SMTP) (4 ♀ not sequenced & 1 ♀ sequenced) [LF.ma.SW 01/10428]; same data but 16.vi/17.vii.2005 and coll. event ID 1717 (5 ♀); same data but 17.vii/08.ix.2005 and coll. event ID 1718 (4 ♀ not sequenced & 1 ♀ sequenced) [LF.ma.SW 03/10430] (in NHRS and AICF); **Södermanland, Sö**, Huddinge kommun, Pine forest with garbage, N59.1765333°, E17.9938500°, 13.vii/10 viii 2004, Trap ID 5, Coll. event ID 766 (SMTP) (1 ♀not sequenced) (AICF).

***E.* (*Eupelmus*) *minozonus* Delvare**
http://zoobank.org/B0EC22D2-129B-4A37-BF5C-FAE526CA3439

Al khatib et al. (2014): 843–846.

Type material. Holotype ♀. **HUNGARY**: Veszprém, Hegyesd, 175 m a.s.l, 46.93333°N, 17.52278°E, 27.vi.2010, sweeping *Quercus cerris* (G. Delvare) [GDEL4030/10010] (in MNHG). **Paratypes**. Same data as holotype (4 ♀) [GDEL4030/10009, GDEL4030/10120 & GDEL4031/1001 (in GDPC and MNHN), GDEL4030/10668 (in FALPC)].

***E.* (*Eupelmus*) *opacus* Delvare**
http://zoobank.org/23647401-C103-4AD7-ABA5-C41EC6126087

Al khatib et al. (2014): 846–847.

Type material. Holotype ♀. **SWEDEN**: Östergötland, Ög, Ödeshögs kommun, Omberg, Stocklycke äng, lime meadow, 58°18.452'N, 14°37.859'E, 23.viii/16.ix.2005, Trap ID 13, Coll. event 1648 (SMTP) [LF.ur.SW 02/10460] (in NHRS). **Paratype**. **GREECE**: Kerkini Lake N. Park, Kerkini, Krousia Mts site, Malaise tr., 06.vi–12.vii.2007, 41°11'32.4"N, 23°03'59.5"E, 190 m a.s.l., Leg. Gordon Ramel (1 ♀) [LF.ur.GR 01/10459] (in AICF).

***E.* (*Eupelmus*) *pistaciae* Al khatib**
http://zoobank.org/111A405E-470F-481A-A43D-663460CEC078

Al khatib et al. (2014): 847–850.

Type material. Holotype ♀. **FRANCE**: Hérault, Cazevieille, 230 m a.s.l, 43.75222°N, 3.77000°E, 28.x.2011, emerged v.2012, ex *Megastigmus pistaciae* on *Pistacia terebinthus* (G. Delvare) [GDEL4027/10507] (in MNHG). **Paratypes**. **FRANCE**: **Hérault**, same data as holotype (6 ♀) [GDEL4027/6390 (in GDPC), GDEL4027/6391 (in FALPC), GDEL4027/6392 (in AICF), GDEL4027/6393 (in MNHN), GDEL4027/10004 (in FALPC), GDEL4027/10506 (in BMNH)] (3 ♂) [GDEL4027/6394 & GDEL4027/6395 (in GDPC), GDEL4027/10005 (in FALPC)]; **Hérault**, Viols-le-Fort, 200 m, N43.74583°, E3.70389°, 28.x.2009, emerged v. 2010, ex *Megastigmus pistaciae* on *Pistacia terebinthus* (G. Delvare) (1 ♀) [GDEL4022/3704bis] (in GDPC).

***E.* (*Eupelmus*) *priotoni* Delvare**
http://zoobank.org/3565E30B-92D9-4DC4-BB94-7224D6BA3D22

Al khatib et al. (2014): 850–852.

Type material. Holotype ♀. **FRANCE**: Aveyron, Sauclières, 700 m a.s.l, Lit de la Virenque, 43.96389°N, 3.35583°E, 15.vi.2011 (G. Delvare) [GDEL4051/10038] (in MNHG).

Unfortunately, a mistake was included in the original description of *E. priotoni* in *Al khatib* et al. (2014). Like other *Eupelmus* species described in this paper, the upper surface of the costal cell on the fore wing has only one row of setae on the apical half and not 3-4 rows as previously written.

***E.* (*Eupelmus*) *purpuricollis* Fusu & Al khatib**
http://zoobank.org/1F354047-F041-4CD6-B1DA-1D53815B9B7C

Al khatib et al. (2014): 854–855.

Type material. Holotype ♀. **GREECE**: Kerkini lake nr Neo Petritsi; Malaise trap, Midway Site, 30.vi–06.vii.2008, 41°18'49.8"N, 23°16'35.6"E, 750 m a.s.l., Leg. Gordon Ramel, [LF.ur.GR 02/10650] (in AICF). **Paratypes**. **GREECE**: same data as for holotype but 09–13.vii.2008 (1 ♀ not sequenced). Kerkini Lake N. Park, Kerkini, Krousia Mts site, Malaise tr., 11–17.vii.2007, 41°11'32.4"N, 23°03'59.5"E, 190 m a.s.l., Leg. Gordon Ramel, (1♀) [LF.ur.GR 05/10653] (in AICF); same data but 18–24.vii.2007 (1♀) [LF.ur.GR 03/10651] (in GDPC).

***E.* (*Eupelmus*) *simizonus* Al khatib**
http://zoobank.org/CCD5B87E-9C81-456A-9DD8-F737AE6AC2F3

Al khatib et al. (2014): 855–856.

Type material. Holotype ♀. **FRANCE**: Ardèche, Les Vans, 175 m a.s.l., Lit du Granzon, 44.38722°N, 4.15444°E, 15.vii.2012, sweeping on *Quercus pubescens*, (G. Delvare) [GDEL4142/10297] (in MNHG).

***E.* (*Eupelmus*) *tremulae* Delvare**
http://zoobank.org/3001FBF7-A5AF-4D65-A274-6673F34264F1

Al khatib et al. (2014): 856–857.

Type material. Holotype ♀. **CZECH REPUBLIC**, Jindóichùv Hradec, Veselí nad Lužnicí, 1 km E of Charles University field station (Ruda), 422 m a.s.l, 49.15296°N, 14.70646°E, ex *Harmandia* sp. (Cecidomyiidae) on *Populus tremula*, 05.vi.2007, adult emergence 13.vi.2007 (P. Jansta) [PJ07003_1_1/10570] (in MNHG). **Paratypes**. Same data (1 ♀) [PJ07003_1_1/10569] (in MNHN) (1 ♂) [PJ07003_1_1/10571] (in MNHN).

Acknowledgements

The authors want to thank John Noyes (Natural History Museum, London, UK) and Svetlana Nikolaeva (Editor of the Bulletin of Zoological Nomenclature) for their useful comments and suggestions concerning the availability of the published new species names relative to ICZN rules concerning primary type depository statements.

References

Al khatib F, Fusu L, Cruaud A, Gibson G, Borowiec N, Rasplus J-Y, Ris N, Delvare G (2014) An integrative approach to species discrimination in the *Eupelmus urozonus* complex (Hymenoptera, Eupelmidae), with the description of 11 new species from the Western Palaearctic. Systematic Entomology 39: 806–862. doi: 10.1111/syen.12089

ICZN (2012) International Code of Zoological Nomenclature. Fourth Edition. http://www.iczn.org/iczn/index.jsp [accessed 19 October 2014]

ARTICLE 5: An integrative approach to species differentiation in the *Eupelmus vesicularis* species complex (Chalcidoidea: Eupelmidae), a group with extreme sexual dimorphism and flightless females: pitfalls in using single locus data

Al khatib F. et al.

(In preparation)

Abstract

Differentiation of closely related species is often hampered by the absence of discriminate morphological characters. Herein, we attempt to delimit the European species of *Eupelmus* (Hymenoptera: Eupelmidae) belonging to the *vesicularis* complex through multiple lines of evidence including molecular and morphological data. Two mitochondrial gene regions (*COI* and *Cytb*) and four nuclear gene regions (*ITS2*, *RpL27a*, *EF-1Ŭ* and *Wg*) were sequenced; phylogenetic trees were reconstructed and compared. The molecular results were then compared with those of a detailed morphological study of the examined specimens. We also tested the efficiency of several species delineation methods, including the generalized mixed Yule-coalescent (GMYC) method on the sequences of *COI* gene. The molecular results revealed an obvious bio-geographic discordance between the mtDNA and combined nucDNA trees concerning the number of genetic clades recovered in each dataset. However, the morphological differentiation opposes the mtDNA tree and supports generally those resulting from the combined nucDNA dataset. We show also the failure of GMYC approach and other methods in delimitation of species characterized by a high genetic divergence resulting from geographical isolation. An illustrated key is given to identify females of eight species. *Eupelmus albitarsis* Costa is removed from synonymy under *Eupelmus vesicularis* (Retzius) and considered as a valid distinct species. *Eupelmus maralpinus* sp. n., *Eupelmus myopitae* sp. n., and *Eupelmus vesimodicus* sp. n. are described as new species.

Keywords: *ITS2* paralogs, mito-nuclear discordance, *COI* tree, concatenated nucDNA tree, DNA barcoding, morphology, GMYC method

Introduction

In the groups or complexes comprising species whose morphological boundaries are not yet accurately resolved or established, DNA-based characterization can be a useful complementary approach (Blaxter, 2003; Tautz *et al*., 2003). It can be used to both ensure an accurate identification and check the existence of cryptic species which have no morphological differences, or where morphological differences are attributed to intraspecific variability. In this context, DNA-barcoding, typically based on the amplification and sequencing of the 5' fragment of the mitochondrial cytochrome oxidase subunit I (*COI*) using an universal primer set (Folmer *et al*., 1994; Blaxter, 2003; Hebert *et al*., 2003a, b; Jinbo *et al*., 2011), has proved to be a powerful tool to provide a precise allocation of unidentified specimens to previously described species, validate or revise the taxonomic status of the previously described species , facilitate the discovery of new species, assess the biodiversity and separate the species groups (Hebert *et al*., 2004; Armstrong & Ball, 2005; Smith *et al*., 2006; Fisher and Smith, 2008; Veijalainen *et al*., 2011; Smith *et al*., 2013; Al khatib *et al*., 2014; Delvare *et al.,* 2014).

The molecular information provided by *COI* sequences can be exploited in the species delimitation in two ways: i) assessment of the phylogenetic monophyly for all individuals of the same species by inferring a phylogenetic tree (Goldstein & DeSalle, 2010; Yassin *et al.,* 2010); ii) coalescent-based method, in particular adopting the generalized mixed Yule coalesent (GMYC) method which uses the distinct branching patterns between divergence (Yule model) and intraspecific diversification (coalescent model) to distinguish between species processes (speciation) and population processes (coalescent of alleles) (Fujita *et al*., 2012; Fujisawa & Barraclough, 2013). Despite the undoubted success for mtDNA-barcoding in taxonomy, it has shown that the mtDNA-barcoding can have technical and biological limitations including hybrid introgression (Rubinoff *et al*., 2006; Galtier *et al*., 2009), heteroplasmy (Magnacca and Brown, 2010; Berthier *et al*., 2011), integration of non-functional copies of *COI* in the nucleus (referred to as "numts") (Song *et al*., 2008; Xiao *et al*., 2010; Jordal and Kambestad, 2014), the infection with maternally inherited symbionts (Hurst & Jiggins, 2005; Yu *et al*., 2011; Shoemaker *et al*., 2004), species level paraphyly (Funk & Omland, 2003), and the extent of the geographic and taxon coverage (Bergsten *et al*., 2012; Meyer & Paulay, 2005). As a result, DNA barcoding is certainly not be prone to type II errors sensu Quicke (2003), i.e. failing to detect closely related species where they do exist (e.

g. Hickerson *et al.,* 2006). Likewise DNA barcoding is also affected by type I errors, i.e. oversplitting of one biological species into several molecular operational taxonomic units (MOTUs) (e. g. Hebert *et al.,* 2004 *versus* Brower, 2006; Dasmahapatra *et al.,* 2010).

Consequently, to overcome the problems associated with the *COI* gene and to ensure an accurate identification of species, many studies have advised to supplement the *COI* sequences with other resources of molecular information such as the sequences of certain nuclear genes which have proven to be valuable genetic markers in providing a sufficient resolution in species differentiation (Monaghan *et al*., 2005; Elias *et al*., 2007; Xiao *et al*., 2010; Gebiola *et al*., 2012; Al khatib *et al*., 2014). Several nuclear genes have already been successfully tested for insect taxonomy (e.g., Caterino *et al*., 2000; Rokas *et al*., 2002; Danforth *et al*., 2005). In this context, the most popular nuclear gene used for differentiating individuals of the same species or very closely related ones are the ribosomal internal transcribed spacers (*ITS1* and *ITS2*), which are characterized by a high rate of evolution (Smith *et al*., 2007; Yara, 2006; Gebiola *et al*., 2009; Ercan *et al*., 2011). Other nuclear genes such as the ribosomal protein *L27a* gene (*RpL27a*) and the *wingless* gene (*Wg*) have been proven to provide to some extent a useful genetic signal for the reconstruction of the phylogenetic relationships at lower to intermediate taxonomic levels in different insect groups (Campbell *et al*., 2000; Cruaud *et al*., 2010; Al khatib *et al*., 2014; .Al khatib *et al*., submitted).

Based on the morphological characters, Gibson (1995) classified the genus *Eupelmus* Dalman (Chalcidoidea: Eupelmidae) into three separate subgenera: *Eupelmus*, *Episolindelia* Girault and *Macroneura* Walker. However, Al khatib et al. (submitted) have proposed a new informal infrageneric classification for the genus *Eupelmus* based on the species group concepts and they have treated the members of *Macro*neura as a species group reffered to as *vesicularis* SPG. The genus *Eupelmus* may be considered the most speciose – with 103 recognised species in the Palearctic region (Gibson & Fusu, submitted) – compared to the other genera assigned to the subfamily Eupelminae. The members of *Eupelmus* are primary or secondary ectoparasitoids of a wide range of holometabolous insects concealed within the vegetal tissues such as galls, seeds, fruits and grass stems (Gibson, 1990 & 1995).

The members of *vesicularis* SPG (*Macroneura*) are cosmopolitan and mostly reared from galls on herbaceous plant species and grass stems (Fusu, submitted). The identification and discrimination of the species assigned to the ***ñ****vesicularis* SPG***ò***, as for other genera of Eupelminae, are extremely difficult. This is firstly because the females of *vesicularis* SPG are

brachypterous and could be easily confused by the non specialists with other genera of Eupelmidae with brachypterous females (Ferrière, 1954; Kalina, 1981; Gibson, 1990). The second difficulty is that, in many taxonomic revisions the species recognition is based largely on the female morphology (Ferrière, 1954; Kalina, 1981; Askew & Nieves-Aldrey, 2000). This may be explained by the following points: i) a high sexual dimorphism characterizing the Eupelminae; ii) a greater morphological similarity between the males compared to their females; iii) the difficulty of finding males in association with their females unless they are collected and reared from the same location or host species. The final difficulty is the presence of complexes of morphologically sibling species such as the *vesicularis* species complex or referred here after as *vesicularis* SC.

In this study, we are interested in studying the diversity of European species assigned to the *vesicularis* complex. We used the concept *vesicularis* SC to refer to the species which are close morphologically to *Eupelmus vesicularis* (Retzius, 1798). In other words, the *vesicularis* SC includes species either confused or synonymised with *E. vesicularis* such as *Eupelmus messene* Walker, 1839 and *Eupelmus albitarsis* Costa, 1883, and probably many other species due the extreme intraspecific morphological plasticity observed in *E. vesicularis sensu lato* and known for a long time (Giraud, 1863; Ruschka, 1921; Ferrière, 1954). Fusu (2010) showed that *Eupelmus vesicularis sensu lato* comprises two species but he did not solve the associated nomenclatural problems until Fusu (submitted) described two new species from the *vesicularis* SC and removed *E. messene* Walker, 1839 from synonymy under *E. vesicularis*. The latter study was based on an integrative approach that combined morphology, cytogenetics, host preferences, distribution data and DNA sequences from one mitochondrial and one nuclear locus. This study was possibly biased towards lineages that recolonized Central and Northern Europe at the end of the last glacial period because new sampling focused mainly on South France revealed even more cryptic diversity within this species complex.

In the present study, an integrative taxonomic approach including the morphological characterization and the molecular evidence from both mitochondrial and nuclear genomes was used to further discriminate the *Eupelmus* species from Europe included in the *vesicularis* SC. Here, we highlight some inconsistency between mitochondrial and nuclear phylogenies as well as some inconsistency between the molecular and morphological results concerning the number of putative species of the *vesicularis* SC. Furthermore, we resurrect one further

species which was previously synonymised with *E. vesicularis*. Finally we describe three new species belonging to the *vesicularis* SC from Europe.

Materials and Methods

Taxon sampling

This study comprised about 84 specimens, including 83 females and males identified by morphological criteria as belonging to the *vesicularis* SC used as in-groups and one female identified as *Eupelmus falcatus* (Nikol'skaya, 1952) used as an out-group, sampled between 2004 and 2013 in Europe (France, Hungary, Italy, Moldova, Romania, Slovakia, Spain and Sweden) and Canada (Fig. S7). Although most specimens were collected using a sweep net on herbaceous layer, a number of specimens were directly reared from an identified host (Table 1).

DNA extraction, PCR amplification and sequencing

Genomic DNA was isolated from single individuals using the Qiagen DNeasy kit (Hilden, Germany) as described in Al khatib *et al*. (2014). Our dataset included six gene regions consisting of two mitochondrial protein-coding genes: Cytochrome Oxidase Subunit I (*COI*) and Cytochrome b (*Cytb*) and four nuclear genes: Wingless (*Wg*), the F2 copy of elongation factor 1-alpha (*EF-1Ŭ*), the ribosomal protein L27a (*RpL27a*) and the internal transcribed spacer 2 (*ITS2*). All 84 specimens were amplified for *COI* and *Cytb*, 70 individuals were amplified for *EF-1Ŭ*, *RpL27a* and *ITS2*, and only 40 individuals were amplified for *Wg*. Primer sequences and PCR protocols followed Al khatib *et al*. (submited) for *COI*, *Cytb*, *Wg*, *EF-1a* and *RpL27a*. *ITS2* fragment was amplified using the primers ITS-F and ITS2-R2 (Yara *et al*., 2006). *ITS2*-PCRs were performed in a 24µl reaction volume: 1µl of DNA, 19,75µl of Milli-Q water, 2.5µl of 10x PCR buffer containing MgCl2 (1x), 1.75µl of 100µM primer cocktail (0.73µM), 0.2µl of dNTPs 25mM each (0.21mM), and 0.2µl of 5U/µl Taq DNA Polymerase (Qiagen, Hilden, Germany) (1U/reaction). *ITS2*-PCR conditions were as follows: 94°C for 5 min, followed by 40 cycles of (i) 94°C for 30 s, (ii) 45°C for 1 min, and 72°C for 1min with a final extension at 72°C for 10 min.

Except some *ITS2* sequences which have been successfully obtained with a direct sequencing method, the rest of the sequences presented multiple double peaks and were

unusable. Consequently, the *ITS2*-sequences for 1 to 3 individuals from each genetic clade obtained on mtDNA trees have been produced using a cloning approach. Cloning of the PCR products was performed using a pCR®2.1 Vector (Invitrogen) following the manufacturer's instructions. 1 to 3 transformed bacterial clones have been sequenced for each individual cloned. Surprisingly, intra-individual heterogeneity of *ITS2* gene has been detected in more than half of the cloned individuals (Fig. S2). For the multi-locus nuclear phylogenetic analysis, we selected a subset of these sequences such as every specimen cloned would be represented only once (Fig. S3). For this, the secondary structure and the free energy (dG [kcal/mol]) of each sequence have been estimated using the online version 3.5 of the *mfold* web server (Zuker, 2003). The idea of this method is based on that the putative pseudogene copies will have reduced secondary structure stability and a larger free energy (dG) (Kita and Ito, 2000). Consequently, for each specimen having intra-individual variability, the sequence with the smallest dG (highest secondary structure stability) was selected and the rest were discarded (Table S1). In three cases (differences in dG less than 0.1 kcal/mol) instead of the sequence with the smallest dG, we choose the less divergent sequence with a shorter branch length on the analysis containing all the obtained *ITS2* copies (Figs. S2).

PCR products were visualized using the QIAxcel Advanced System and QIAxcel DNA Fast Analysis Kit (Qiagen). PCR products were sent to BECKMAN COULTER GENOMICS (Stansted, United Kingdom) for sequencing in both directions. All the sequences were deposited in GenBank (Table S2).

Table 1. Sample information for the specimens included in the phylogenetic analyses.

Species/Clade	Collection code	Molecular code	Country	Departement	City	N	E	Host insect	Associated plante	Collection date
E. albitarsis	FAL1505	10324	Italie	Sardaigne	Province d'oristano	39.70041°	8.73969°	unknown	dried grass	October 2012
	FAL1504	10323	Italie	Sardaigne	Province d'oristano	39.70041°	8.73969°	unknown	dried grass	October 2012
	FAL1477	10311	France	Gard	Garons	43.76371°	4.42588°	Myopites stylata	galls on Dittrichia viscosa	June 2012
	FAL1398	10307	France	Aude	Sigean	43.06182°	2.92007°	unknown	dried grass	June 2012
	FAL1477	10310	France	Gard	Garons	43.76371°	4.42588°	Myopites stylata	galls on Dittrichia viscosa	June 2012
	FAL1486	10314	France	Alpes-Maritimes	Opio	43.64479°	6.99957°	unknown	dried grass	October 2012
	FAL1487	10315	France	Alpes-Maritimes	Opio	43.64479°	6.99957°	unknown	dried grass	October 2012
	FAL1398	10262	France	Aude	Sigean	43.06182°	2.92007°	unknown	dried grass	June 2012
	LF.B.FR 01	10528	France	Hérault	Saint-Guilhem-le-Désert	43.773051°	3.533166°	unknown	unknown	September 2012
	FAL1384	10257	France	Hérault	Vic-La-Cardiole	43.7331°	3.80687°	unknown	Papaver rhoeas	June 2012
	FAL1384	10305	France	Hérault	Vic-La-Cardiole	43.7331°	3.80687°	unknown	Papaver rhoeas	June 2012
	GDEL4183	10599	France	Hérault	Lespignan	43.254167°	3.163611°	unknown	salt meadows	July 2013
	FAL1398	10306	France	Aude	Sigean	43.06182°	2.92007°	unknown	dried grass	June 2012
	GDEL4184	10600	France	Hérault	Lespignan	43.254167°	3.163611°	unknown	salt meadows	July 2013
	GDEL4181	10626	France	Hérault	Lespignan	43.252778°	3.163611°	unknown	salt meadows	July 2013
E. messene	GDEL4255	10647	France	Aveyron	Saint-Privat	43.761944°	3.466667°	unknown	dried grass	July 2013
	GDEL4256	10648	France	Aveyron	Saint-Privat	43.761944°	3.466667°	unknown	dried grass	July 2013
	GDEL4254	10646	France	Aveyron	Saint-Privat	43.761944°	3.466667°	unknown	dried grass	July 2013
	LF.A.CA 05	10533	Canada	Ontario	5 km NW Almonte	-	-	unknown	unknown	May 2008
	LF.A.RO 05	10516	Romania	Iaşi	Iaşi	47.190944°	27.599261°	unknown	unknown	September 2012
	FAL1379	10256	France	Haut-Rhin	Colmar	48.0918°	7.3293°	Barbotinia oraniensis	galls on Papaver rhoeas	June 2012
	LF.A.RO 07	10514	Romania	Iaşi	Iaşi	47.187075°	27.549139°	unknown	unknown	July 2007
	GDEL4227	10621	France	Gard	Trèves	44.076111°	3.336667°	unknown	unknown	June 2011
	GDEL 4083	10084	France	Savoie	Lanslebourg	45.291389°	6.858056°	unknown	unknown	August 2007
	GDEL4216	10618	France	Aveyron	Nant	44.978611°	3.263056°	unknown	dried grass	June 2011
	GDEL4218	10635	France	Aveyron	Sauclières	43.963889°	3.355833°	unknown	unknown	June 2011
	GDEL4234	10639	France	Lozère	Saint-Pierre-des-Tripiers	44.215833°	3.259722°	unknown	dried grass	July 2011
	GDEL4195	10605	France	Aveyron	Peyreleau	44.175278°	3.237500°	unknown	unknown	June 2011
	LF.A.CA 07	10519	Canada	Nouveau-Brunswick	vic. Tracy	-	-	unknown	unknown	July 2008
	LF.A.CA 06	10534	Canada	Prince Eduard	Central Badeque	-	-	unknown	unknown	July 2008
	LF.A.CA 03	10531	Canada	Québec	Belle-Anse	-	-	unknown	unknown	July 2008
	LF.A.CA 04	10532	Canada	Terre-Neuve-Labrador	St-Andrew's	-	-	unknown	unknown	July 2008
E. vesicularis	LF.V.SL 02	10529	Slovakia	Muranska Planina	Predna Hora	48.765000°	20.103889°	unknown	unknown	August 2009
	LF.V.SW 03	10535	Sweden	Öl	Mörbylånga	56.616700°	16.507617°	unknown	unknown	August 2006

E. vesicularis	LF.V.SW 05m	10537	Sweden	Go	Gotlands	57.536783°	18.337883°	unknown	unknown	August 2004
E. vesimodicus	GDEL4236	10640	France	Lozère	Cocurès	44.349444°	3.611944°	unknown	unknown	July 2011
	GDEL4219	10636	France	Aveyron	Sauclières	43.946944°	3.355278°	unknown	unknown	June 2011
	GDEL4233	10624	France	Gard	Trèves	44.075278°	3.332778°	unknown	dried grass	June 2011
	GDEL4247	10643	France	Lozère	Belvezet	44.565845°	3.711934°	unknown	dried grass	July 2012
	GDEL4250	10645	France	Lozère	Altier	44.444722°	3.882778°	unknown	dried grass	July 2012
	GDEL42621	10561	France	Alpes Maritimes	Saint-Dalmas-le-Selvage	44.282559°	6.864681°	unknown	unknown	26.vi.2012
	GDEL4209	10629	France	Alpes Maritimes	Sospel	43.848056°	7.410278°	unknown	dried grass	August 2010
	GDEL4208	10616	France	Alpes Maritimes	Sospel	43.848056°	7.410278°	unknown	dried grass	August 2010
	GDEL4079	10123	France	Alpes-Maritimes	Lucéram	43.892778°	7.383611°	unknown	unknown	August 2011
	GDEL4198	10608	France	Alpes Maritimes	Belvédère	44.041389°	7.376111°	unknown	unknown	July 2009
	GDEL4207	10615	France	Alpes Maritimes	Moulinet	43.973611°	7.412778°	unknown	unknown	August 2010
	GDEL4204	10628	France	Alpes Maritimes	Lucéram	43.879444°	7.379167°	unknown	dried grass	August 2011
	GDEL4205	10613	France	Alpes Maritimes	Sospel	43.917778°	7.460833°	unknown	dried grass	August 2010
E. barai/G1	LF.A.RO 04	10512	Romania	Iași	Iași	47.190944°	27.599261°	unknown	unknown	September 2010
	LF.B.RM 01	10526	R. Moldova	Anenii-Noi	Chetrosu	46.889515°	29.044470°	unknown	unknown	August 2004
E. barai/G2	GDEL4085	10086	Hungary	Veszprém	Nagavászony	47.021667°	17.724167°	unknown	unknown	June 2010
	GDEL4087	10089	Hungary	Veszprém	Várpalota	47.183611°	18.155556°	unknown	unknown	June 2010
	GDEL4084	10085	Hungary	Kecskemét	Bócsa	46.696667°	19.530278°	unknown	unknown	June 2010
	GDEL4086	10088	Hungary	Veszprém	Nagavászony	47.021667°	17.724167°	unknown	unknown	June 2010
	PJ10077_31_3	10574	Hungary	Vezprém	Várpalota	47.198091°	18.21204°	Andricus quercustozae	Quercus pubescens/Q. cerris	November 2010
E. barai/G3	LF.B.SP 03	10523	Spain	Lleida	Omells na Gaia	-	-		galls on Lasioptera eringii	July 2007
E. maralpinus/G4	GDEL4206	10614	France	Alpes Maritimes	Sospel	43.892500°	7.449167°	unknown	dried grass	August 2010
	GDEL4212	10631	France	Alpes Maritimes	Sospel	43.856111°	7.408611°	unknown	dried grass	August 2010
	GDEL4210	10630	France	Alpes Maritimes	Sospel	43.854167°	7.408333°	unknown	dried grass	August 2010
	GDEL4203	10612	France	Alpes Maritimes	Lucéram	43.879444°	7.379167°	unknown	dried grass	August 2010
	GDEL4211	10617	France	Alpes Maritimes	Sospel	43.856111°	7.408611°	unknown	unknown	August 2010
	GDEL4240	10641	France	Alpes Maritimes	Breil-sur-Roya	43.925833°	7.485833°	unknown	unknown	June 2012
	GDEL4079	10077	France	Alpes-Maritimes	Lucéram	43.894444°	7.379167°	unknown	unknown	August 2010
	GDEL4202	10611	France	Alpes Maritimes	Lucéram	43.874722°	7.384444°	unknown	dried grass	August 2010
	GDEL4201	10627	France	Alpes Maritimes	Lucéram	43.892778°	7.383611°	unknown	dried grass d	August 2010
	GDEL4244	10642	France	Alpes Maritimes	Sospel	43.8860°	7.49558°	unknown	dried grass	June 2012
E. myopitae/G5	FAL1405	10303	France	Alpes-Maritimes	Gourdon	43.73168°	6.98859°	Myopites stylata	galls on Dittrichia viscosa	June 2012
	FAL1405	10304	France	Alpes-Maritimes	Gourdon	43.73168°	6.98859°	Myopites stylata	galls on Dittrichia viscosa	June 2012
	FAL1405	10264	France	Alpes-Maritimes	Gourdon	43.73168°	6.98859°	Myopites stylata	galls on Dittrichia viscosa	June 2012
	FAL1405	10265	France	Alpes-Maritimes	Gourdon	43.73168°	6.98859°	Myopites stylata	galls on Dittrichia viscosa	June 2012
E. barai/G6	GDEL4081	10081	France	Aveyron	Saint-Jean-du-Bruel	44.048056°	3.339444°	unknown	unknown	June 2011

	GDEL4228	10637	France	Gard	Trèves	44.076111°	3.336667°	unknown	unknown	June 2011
	GDEL4081	10080	France	Aveyron	Saint-Jean-du-Bruel	44.048056°	3.339444°	unknown	unknown	June 2011
	GDEL4080	10079	France	Aveyron	Saint-André-de-Vézines	44.137500°	3.228611°	unknown	unknown	June 2011
	GDEL4224	10620	France	Aveyron	Cornus	43.867222°	3.196111°	unknown	unknown	June 2011
	GDEL4082	10082	France	Lozère	Florac	45.305556°	4.591944°	unknown	unknown	July 2011
	GDEL4082	10083	France	Lozère	Florac	45.305556°	4.591944°	unknown	unknown	July 2011
E. barai/G6	GDEL4200	10610	France	Hautes-Alpes	Saint-Crépin	44.710556°	6.606389°	unknown	dried grass	August 2008
	DDEL4263	10562	France	Hérault	Riols	-	-	Diplolepis rosae	galls on Rosa canina	March 2013
	DDEL4263	10563	France	Hérault	Riols	-	-	Diplolepis rosae	galls on Rosa canina	March 2013
	GDEL4220	10619	France	Aveyron	Nant	44.040833°	3.283889°	unknown	dried grass	June 2011
	GDEL4229	10622	France	Gard	Trèves	44.075278°	3.332778°	unknown	dried grass	June 2011
	GDEL4080	10078	France	Aveyron	Saint-André-de-Vézines	44.137500°	3.228611°	unknown	unknown	June 2011
E. falcatus	GDEL4079	10076	France	Alpes-Maritimes	Lucéram	43.892778°	7.383611°	unknown	unknown	August 2010

Species boundaries delimitation

Phylogenetic species delimitation

All sequenced gene regions were aligned using Muscle algorithm (Edgar, 2004) with default settings as implemented in SeaView program v4.4.1 (Gouy *et al*., 2010) and then followed by manual adjustment. Alignments of protein-coding genes were translated to amino acids using Mega v5.1 (Tamura *et al*., 2011) to detect frame-shift mutations and premature stop codons, which may indicate the presence of pseudogenes.

The best-fitting evolution model for each gene region was selected using Akaike information criterion (AIC) as implemented in jModelTest v0.1.1 (Posada, 2008).

Phylogenetic trees were estimated individually for the two mitochondrial genes (*COI* and *Cytb*) using Maximum Likelihood (ML) and Bayesian Inferences (BI), then the nodes confidence (Bootstrap percentages; BP and Posterior probabilities; PP) values were mapped on the ML topology. Similarly, phylogenetic trees were firstly reconstructed individually for each sequenced nuclear gene regions (*EF-1Ŭ*, *ITS2*, *RpL27a* and *Wg*) using only the ML approach. Then the sequences of the four nuclear genes were concatenated together in one dataset (combined nucDNA dataset) in the following order (*Wg*, *EF-1Ŭ*, *Rpl27a* and *ITS2*). Only the specimens having at least 2 nuclear sequences were considered in combined nucDNA topologies. The Maximum Likelihood and Bayesian trees were estimated for the combined nucDNA dataset supposing one partition for each nuclear gene. All analyses were conducted on the CIPRES Science Gateway (www.phylo.org) (Miller *et al*., 2010).

Maximum likelihood analyses and associated bootstrapping were executed using RAxML v8.1.11. (Stamatakis, 2014). The parameters used were: GTRCAT approximation, rapid bootstrap with 1000 replicates, and search for the best scoring ML tree in one single program run. BP ≥85% were considered as strong support and BP <65% as weak.

Bayesian analyses were conducted using a parallel version of MrBayes v3.2.3. (Ronquist *et al*., 2012). For mitochondrial (*COI* and *Cytb*) and combined nucDNA datasets, parameter values for the model were initiated with default uniform priors and branch lengths were approximated using default exponential priors. For the combined nucDNA dataset, model parameters for each partition were independently estimated by unlinking parameters across partition. Bayesian trees were estimated using two simultaneous, independent runs of Markov Chain Monte Carlo (MCMC), including three heated chains and one cold chain. The

Metropolis-coupled MCMC algorithm (Geyer, 1991) was used to improve the mixing of Markov chains, moving chains from one peak to another and avoid the cold chain to be stuck on one local peak. The heating temperature (T) was set to 0.02 in order to increase and improve the swap frequencies of states between cold and heated chains. Each run contained 50 (*COI* and *Cytb*) or 60 (nucDNA) millions generations, and values for all parameters were sampled every 5000 or 6000 generations respectively. The first 25% tree samples from the cold chain were discarded and considered as *burn-in*, because the parameters values of this area are close to random values used to initialize the chain and the remaining trees of the two independent runs were included in calculating of posterior probability. Convergence of runs of MCMC was assessed based on the standard deviation of split frequencies given by MrBayes, Effective Sample Size (ESS), as estimated using Tracer v1.6.0 (Rambaut and Drummond, 2007), and generally by stabilization of tree likelihood after the *burn-in* phase. Posterior probabilities (PP) ≥ 0.95 were considered as strong support and PP < 0.90 as weak.

Distance-based species delimitation

We applied two different methods of distance based species delimitation. Since the topology of the *Cytb* tree (Fig. S1) is similar to that of the *COI* tree (Fig. 1) and the results obtained on this dataset are similar (data not presented), we discuss only the results for the *COI* dataset as these kinds of methods are traditionally used on the standard DNA barcoding region.

SpeciesIdentifier (SpeciesID) module of TAXONDNA v1.7.8 (Meier *et al.,* 2006) was used to identify the number of candidate species under an *a priori* assumed threshold value. We used the Cluster algorithm under a threshold value of 6.7%, which is the minimum interspecific difference between species of the *urozonus* SC (Al khatib *et al*., 2014) whose taxonomy is much better understood than that of *vesicularis* SC. The distance matrix was calculated using the Kimura 2-parameter (K2P) model (Kimura, 1980).

The Automated Barcode Gap Discovery (ABGD) (Puillandre *et al*., 2012) was used to automatically locate the genetic distance where the barcode gap is located. The method partitions the dataset into a number of clusters (candidate species) in such a way that the distance between two arbitrary sequences from different groups will always be larger than the distance within a group. To estimate the number of clusters under the barcoding gap hypothesis we used a distance matrix calculated with Mega v6.0.5 (Tamura *et al.,* 2011) using

the K2P model and the online version of ABGD available at www.abi.snv.jussieu.fr/public/abgd/abgdweb.html. We used both the default parameters (steps = 10 and relative gap width, X = 1.5) and also a larger number of steps (50) with X varying from 0.1 to 1 to avoid oversplitting.

Coalescent-based species delimitation

We tested the efficiency of the Generalized Mixed Yule Coalescent approach (GMYC) (Pons *et al*., 2006; Fujisawa & Barraclough, 2013) in the delineation of *vesicularis* SC using the standard DNA barcoding fragment (*COI*). The ultrametric tree based on *COI* sequences necessary to conduct the GMYC analysis was reconstructed using the Bayesian inference implemented in Beast v1.8.0 (Drummond & Rambaut, 2012) on the CIPRES Science Gateway (www.phylo.org) (Miller *et al*., 2010). The HKY + G was used as the best-fitting substitution model as identified by jModelTest v0.1.1 (see Results). We assumed a Yule speciation process as tree prior and uncorrelated lognormal relaxed clock and we used the default priors for all other parameters. The Bayesian tree was estimated using two separate runs of MCMC. Each run contained 150 million generations and values for all parameters were sampled every 15000 generations. The two separate runs were then combined using the LogCombiner v1.7.2. We checked for convergence using Tracer v1.6.0 (Rambaut & Drummond, 2007). Following the removal of 10% of trees as *burn-in*, the sampled posterior trees were summarized using TreeAnnotator v1.7.2 (Rambaut & Drummond, 2007) to generate a maximum clade credibility tree. Then, the ultrametric phylogeny recovered with Beast analysis was subjected to GMYC analysis implemented in the *splits* package (available from http://r-forge.r-project.org/projects/splits/) with the program R v3.1.2 (R Core Development Team, 2009). *Splits* is dependent on *ape* (Paradis *et al*., 2004), *MASS* (Venables & Ripley, 2002), and *paran* packages. A list of delimited ‘‘GMYC species’’ (described in the program’s output as ML entities) was compiled from the graphical output of the GMYC analysis in R.

Delimitations based on genealogical exclusivity

Biparentaly inherited nuclear loci coalesce four times more slowly than the maternally inherited mtDNA markers (Birky *et al.*, 1989; Palumbi *et al.*, 2001). If besides deep divergence in mtDNA sequences the nuclear markers exhibit patterns of exclusivity congruent

with those of the mitochondrial markers, the analyzed groups have a long history of restricted gene flow and can be considered distinct species (Avise & Ball, 1990; Handrixson *et al.,* 2013). The Genealogical Sorting Index (GSI) (Cummings *et al.,* 2008*),* that proved its efficiency in species delimitations attempts in other arthropod species with strong geographic structuring (Handrixson *et al.,* 2013; Parmakelis, 2013), is a statistic used to measure the exclusive ancestry of individuals from an *a priori* predefined group on a rooted tree. The statistical support for the index is obtained through a permutation test (Cummings *et al.,* 2008). We tested groups where those defined by Species ID except G5 was treated as a separate group from G6 because of its strong morphological distinctiveness. We also calculated the GSI for *E. vesimodicus* as a unitary group including the two groups differentiated by all the delimitation methods based on mtDNA (*E. vesimodicus* East and E. *vesimodicus* West). Prior to the analysis, trees were rooted using the *root* function and outgroup removed using the *drop.tip* function in R (v.3.2.2) using the *ape* package (Paradis *et al*., 2004). For single group analyses, we used the *gsi* and *permutationTest* functions in the g*enealogicalSorting* package (v0.92) written in the R language for statistical computing (Ihaka & Gentleman, 1996) that also requires the *ape* package. Larger analyses on all groups were performed using the GSI web service hosted at molecularevolution.org that uses GSI version 0.92 and grid computing through The Lattice Project (Bazinet & Cummings, 2008).

Because the different gene trees differ in the number and identity of included individuals, as all markers could not be sequenced for every specimen, instead of calculating the ensemble GSI that is a sum of the GSI values multiplied by the probability of each topology (Cummings *et al*., 2008), we computed a separate GSI for every group and every nuclear gene and looked for GSI values of 1 (indicating monophyly), or close to this value, for at least 2 independent loci. Computations were done only for the nuclear markers, as the groupings based on *COI* are evidently monophyletic (GSI = 1), this being the groups evaluated in the first place (see results for SpeciesID, ABGD and Fig. 1).

Morphological species characterization

After DNA extraction, specimens were dehydrated in acetone for 6 hours and then dried in an atmosphere saturated in acetone vapour within a hermetic container for at least 12 hours in order to avoid the radical deformations due to air-drying of the now empty

exoskeleton. Then, specimens were immediately mounted for morphological examination on rectangular cards, as recommended by Noyes (1982).

The number of the distinguished morphospecies was compared with the number of species recovered from phylogenetic and coalescence analyses (Fig. 1).

Detailed morphological descriptions were made for the different recovered putative specie not treated in Fusu (submitted). In the description of species, the following abbreviations were used: **F2-F8**, second to eighth funicular segments; **MPS**, multiporous plate sensilla; **MT2**, the second metasomal tergite situated immediately behind the membranous petiole; **MT3-MT6**, third to sixth metasomal tergites. Morphological terminology followed Gibson (1990, 1995 & 2011) and Al khatib *et al*. (2014). The measurements of ovipositor sheaths length and parts of the forewing followed Al khatib *et al*. (2014) and Fusu (2010) respectively. Accurate measurements of the fore wing rudiment are of utmost importance for the correct identification of the members of *vesicularis* SC. Since species identifications in Eupelmidae are usually done on card mounted specimens and not on slide mounted parts, the fore wing was measured in its normal bended position, using as landmarks the extreme proximal angle of the basal cell, the junction between the submarginal and marginal veins where the wing is folded and the wing apex. Because the apical part of the fore wing rudiment breaks easily, especially in specimens collected by sweeping, our first couplet in the key to females provides additional colour characters to help keying such specimens through the first couplet. For the analysis of the wing interference patterns (WIPs) (Shevtsova *et al*., 2011) on the male wing we used the method described in Shevtsova & Hansson (2011) as detailed in Fusu (submitted). Measurements were made using either a Leica M205 C binocular stereomicroscope using the software Leica Application Suite v4 (LAS. v4), at magnifications (×125 or ×160) (at INRA-PACA, Sophia-Antipolis, France), or an Olympus SZX9 stereomicroscope fitted with a 10 mm ocular grid having 100 divisions for measurements (at Al. I. Cuza University, Iasi, Romania). Specimens were photographed with a Leica DFC 500 camera attached to a Leica M205 A motorized stereomicroscope, illuminated with an Olympus KL1500 LCD light source and a Kruss 150-watt light source, and final images were produced by focus stacking using Zerene Stacker v1.04. All images were then edited using Adobe Photoshop to correct white balance and enhance clarity.

Vouchers specimens analysed in this study were deposited in the following institutions and private collections: **AICF**, Lucian Fusu collection, A1. I. Cuza University, Iasi, Romania; **BMNH**, The Natural History Museum, London, UK; **FALPC**, Fadel Al khatib

personal collection, Faculty of agricultural engineering, University of Aleppo, Syria; **GDPC**, Gérard Delvare personal collection, Montpellier, France; **MNHN**, National Museum of Natural History, Paris, France and **NHRS**, Naturhistoriska riksmuseet, Stockholm, Sweden.

Results

Molecular species discrimination

Completeness of the molecular dataset and model selection. Overall, successful amplification and sequencing were obtained for all genes used in this study. However, sequencing failure was observed in some individuals: 77 sequences from 84 individuals were obtained for *Cytb* (sequencing failure occurred in specimens 10640, 10636, 10643, 10645, 10526, 10081, and 10563); 38 sequences from 40 specimens were obtained for *Wg* (sequencing failure occurred in specimens 10535 and 10324); 62 sequences from 70 individuals were obtained for *RpL27a* (sequencing failure occurred in specimens 10537, 10561, 10624, 10089, 10562, 10082, 10622 and 10611); 64 sequences from 70 individuals were obtained for *EF-1Ŭ* (sequencing failure occurred in specimens 10533, 10618, 10636, 10624, 10622 and 10611) and finally only 15 sequences from 71 individuals were directly obtained for *ITS2* (Table S1) and this number of *ITS2* sequences was increased to 75 sequences by applying the cloning procedure in one to three individuals from each clade resulting from *COI* topology. No stop codons, frame shifts, insertions or deletions were observed in coding gene regions: *Wg*, *EF-1Ŭ*, *COI* and *Cytb*.

Evolution models selected by jModelTest were as follows: GTR+G+I for *COI*, HKY+G+I for *Cytb*, GTR+G for *Wg*, *EF-1Ŭ*, *RpL27a* and *ITS2*. Given that i) α and the proportion of invariable sites (I) cannot be optimized independently from each other (Gu *et al*., 1995) and ii) GTR is the sole available evolution model in RAxML program, for both *COI* and *Cytb* analyses, we used a GTR+G for ML topologies and a HKY+G which was the second evolution model proposed by jModelTest for Bayesian topologies.

Phylogenetic analysys of the mtDNA sequences. Overall, ML topologies obtained from both *COI* and *Cytb* sequences were largely similar to those produced from Bayesian analyses. However, certain topological conflicts could be detected in some nodes where bootstrap percentages (BP) ≥65 and posterior probabilities (PP) < 90 (Figs. 1, S1). Moreover, Phylogenetic tree resulting from *COI* dataset was exactly concordant concerning the number

of major clades with those resulting from *Cytb* sequences. The sole discordance is the major clade comprising two small clades *G5* and *G6*. In the *COI* tree, we found that these two small clades are monophyletic at least in the ML topology (BP≥65) (Fig. 1). In contrast for *Cyt b*, we observed that some individuals of *G6* nested with *G5* suggesting incomplete lineage sorting (Fig. S1).

Distance based methods. Using the algorithm implemented in the ABGD method (default settings) on the *COI* dataset resulted in finding 5 partitioning schemes. Of these the first two have 32 and 21 candidate species within *vesicularis* SC (prior maximal within-group distance P = 0.001 and 0.0017 respectively). The last three partitions have 16 potential species each (prior maximal distance P = 0.0027, 0.0046, and 0.0077 respectively), a value very close to that obtained by the GMYC single threshold method. By using a larger number of steps (50) and varying the relative gap width *X* from 0.1 to 1, the number of groups (candidate species) varies from 1 when all species are lumped together to 37 (for maximal distance P from 0.075 to 0.001), including the 16 groups obtained with the default parameters. However there were several values of P that consistently inferred 10 groups within *vesicularis* SC and for this value the number of groups in recursive partitions was frequently the same, i.e. no further splitting was possible (graph in Appendix S1). As primary partitions are closer to the number of taxa usually recognised by taxonomists and stable to variation of P (graph in Appendix S1) (Puillandre *et al*., 2012) we choose this number. The groups are the same as for SpeciesID approach (Fig. 1). For a value of P close to that found in other *Eupelmus* (*Eupelmus*) where maximal intraspecific distance is 4.8% (Al khatib *et al.,* 2014), there are 6 primary partitions (Appendix S1).

Based on prior knowledge of interspecific distances within another species complex in the genus *Eupelmus* (the *urozonus* SC) the algorithm implemented in the SpeciesIdentifier software (SpeciesID) identified 10 clusters. These clusters are the same as those identified by the most frequent grouping scheme by ABGD.

Coalescent based methods. When the multiple-threshold method of the general mixed Yule-coalescent (GMYC) model was applied on the *COI* dataset for delimitation of our *vesicularis* SC, it resulted in an unrealistically large number (twenty-six) of "GMYC species" (Fig. 1, graph in Appendix S2). The number of "GMYC species" recovered using the single-threshold approach, even if smaller than in the multiple-threshold method (Fig. 1, graph in Appendix S2) was still much larger than those recovered using the ABGD or SpeciesID methods. Indeed, this analysis recovered 15 "GMYC species" and this large number of

"GMYC species" was the result of splitting of certain clades exhibiting large variability into two or three "GMYC species". These clades were: *G4* divided into two "GMYC species", *G6* divided into two "GMYC species", *E. albitarsis* divided into two "GMYC species" and *E. vesimodicus* divided into three "GMYC species" (graph in Appendix S2). Overall, both the multiple- and single-threshold methods of GMYC had the tendency to identify as putative species groups of individuals that were the result of splitting the members of the same population (specimens with identical morphology and collected in the same locality).

In summary, as presented in the mitochondrial trees obtained from *COI* and *Cytb*, eleven non-overlapping clades (except for the major clade containing groups *G5* and *G6* which were not clearly resolved in the *Cytb* topology) were considered (Figs 1, S1). Among these eleven clades, three clades without geographical differentiation correspond perfectly to three previously confused and synonymised species on the morphological basis; these species are *E. albitarsis*, *E. messene* and *E. vesicularis*. The other remaining eight clades are *G1, G2, G3, G4, G5* and *G6*, (attributable by the combination of long forewing rudiment and a triangular spot on the mesoscutal plate to *E. barai*) and Eastern and Western clades of *E. vesimodicus* and they appear to correspond to a large extent to geographical isolates (Fig. S7). These clades correspond to the ten clades identified by the ABGD and SpeciesID methods, except group *G5* that is treated separately from *G6* because of its strong morphological differentiation.

Phylogenetic analysys of the nuclear markers. The individual topologies resulting from ML analysis of nuclear genes (*RpL27a*, *ITS2*, *EF-1Ŭ* and *Wg*) are given in supporting information (Figs. S2-S6). Overall, all the individual trees based on the nuclear datasets showed that the number of clades detected from the mitochondrial datasets (*COI* and *Cytb*) (Figs. 1, S1) is clearly an overestimation of the actual number of species. The individual trees resulting from the nuclear datasets were only somewhat similar and showed to some extent the same major clades exception for the *Wg* topology which was not well resolved (Fig. S6). However, certain discordances were identified, for example, clades of *E. messene* and *E. vesicularis* were resolved in *RpL27a* and *Wg* topologies (Figs. S4, S6), while these two clades nested together in one clade without any differences in *EF-1Ŭ* topology (Fig. S5) and many of *ITS* variants of *E. messene* were grouped within the *E. vesicularis* clade in the *ITS2* topology (Figs. S2, S3). Also in the *EF-1Ŭ* topology the eastern groups (*G1* and *G2*) and western groups (*G3* to *G6*), of what we provisionally identified as *E. barai* form two distinct clades, with no genetic differentiation within the clades (Fig. S5). In the *ITS2* topology *G1* and *G2*

are again nearly identical and rendered paraphyletic by a uniform group formed by *G4* and *G5*. The groups *G3* and *G6* form a distinct clade without substructuring (Figs. S2, S3).

The final matrix of concatenated nuclear genes (2389 bp: *Wg* = 433 bp, *EF-1Ŭ*= 517 bp, *Rpl27a* = 727 bp and *ITS2* = 712 bp) contained 69 specimens including one as out-group. The topology resulting from the ML and Bayesian analyses based on the concatenated nucDNA dataset is given in Figure 2. The six clades named as *G1* to *G6* and which were distinguished with *COI* sequences (Fig. 1), clustered together in one clade in the concatenated nucDNA topology (Fig. 2) and the assemblage of these six clades in one great clade on based on the concatenated nucDNA datasets could not be validated with the morphological characterization (see § Description of species). Moreover, the monophyly of the remaining clades discovered based on *COI* sequences and named as *E. albitarsis*, *E. vesimodicus*, *E. messene* and *E. vesicularis* were also supported in the concatenated nucDNA tree except for the *E. messene* clade which was with a low support value resulted from the nesting of part of *ITS2* clones of *E. messene* with *ITS2* variants of *E. vesicularis* (Figs S2, S3).

Genealogical exclusivity of the clades. The GSI values and corresponding P-value for the eleven mtDNA clades are presented in Table 2. Surprisingly, the clade supported by congruent patterns of monophyly for all four nuclear loci (GSI=1, P=0.0001) is the one that we describe as *E. vesimodicus* sp. n. It has the less support from the morphology being almost identical to *E. vesicularis* (Table 3, see also under Morphological species discrimination). The two clades composing the species and identified as putative species or even subdivided further by all mtDNA delimitation methods present complete lineage sorting only for *RpL27a* (Western clade) or *Wg* (Eastern clade; low support). The next well supported species is *E. albitarsis* that again is morphologically supported only by a combination of characters (Table 3). It presents congruent patterns of monophyly for three nuclear loci, though with low statistical support for *ITS2*, but this is because it is represented in this dataset by only two specimens due to sequencing failures. For the mitochondrial groups *G1* to *G6* there is support from the nuclear genes only for *G5* and *G6* that are monophyletic at the *RpL27a* locus while *G2* and *G4* have GSI values above 0.7 and with high support for the *ITS2* and *Wg* and *ITS2* and *RpL27a* respectively. The distinctivness of *E. messene* and *E. vesicularis* is highly supported as besides the mtDNA the species are also reciprocally monophyletic for *RpL27a* and *Wg*, with P-values slightly above 0.01 for *E. vesicularis* due to smaller sample size.

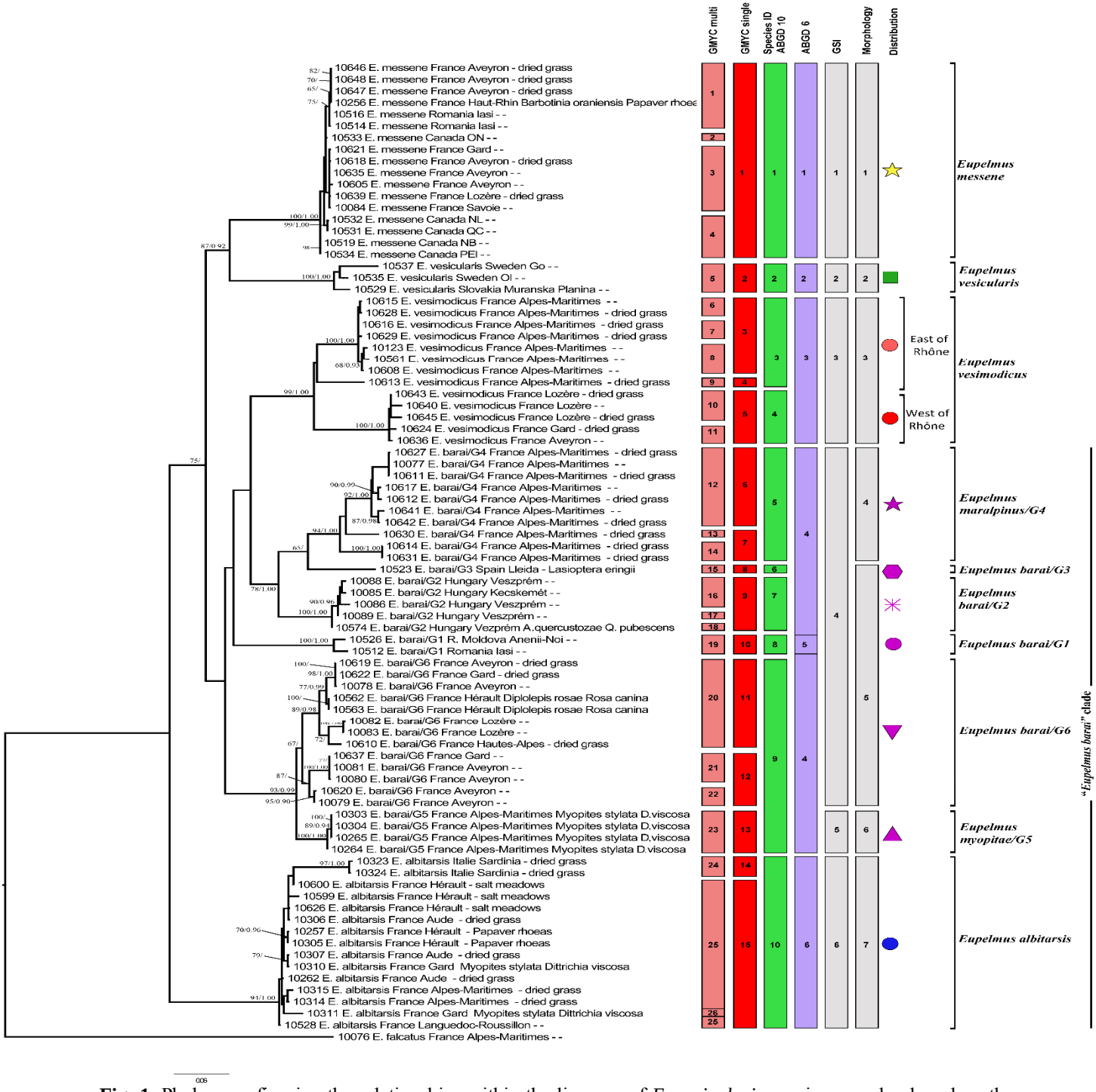

Fig. 1. Phylogram figuring the relationships within the lineages of *E. vesicularis* species complex based on the *COI* dataset alignment. Bootstrap Percentages (BP) ≥ 65 and Posterior Probabilities (PP) ≥ 0.90 are indicated at nodes. Each line represents a sequenced individual with information in the following order: molecular code, species/clade, country, insect host and associated plant. The vertical colored bars represent putative species suggested by different species boundaries delimitation methods: multiple-threshold method of GMYC (GMYC multi), single-threshold method of GMYC (GMYC single), SpeciesIdentifier (SpeciesID), ten and respectively six putative species identified by ABGD using different maximal P distances (ABDG 10 and ABDG 6), and genealogical exclusivity (GSI; lineages with complete lineage sorting for at least one mitochondrial and one nuclear locus). Distribution of different clades represented by same symbols as in the map in figure S7

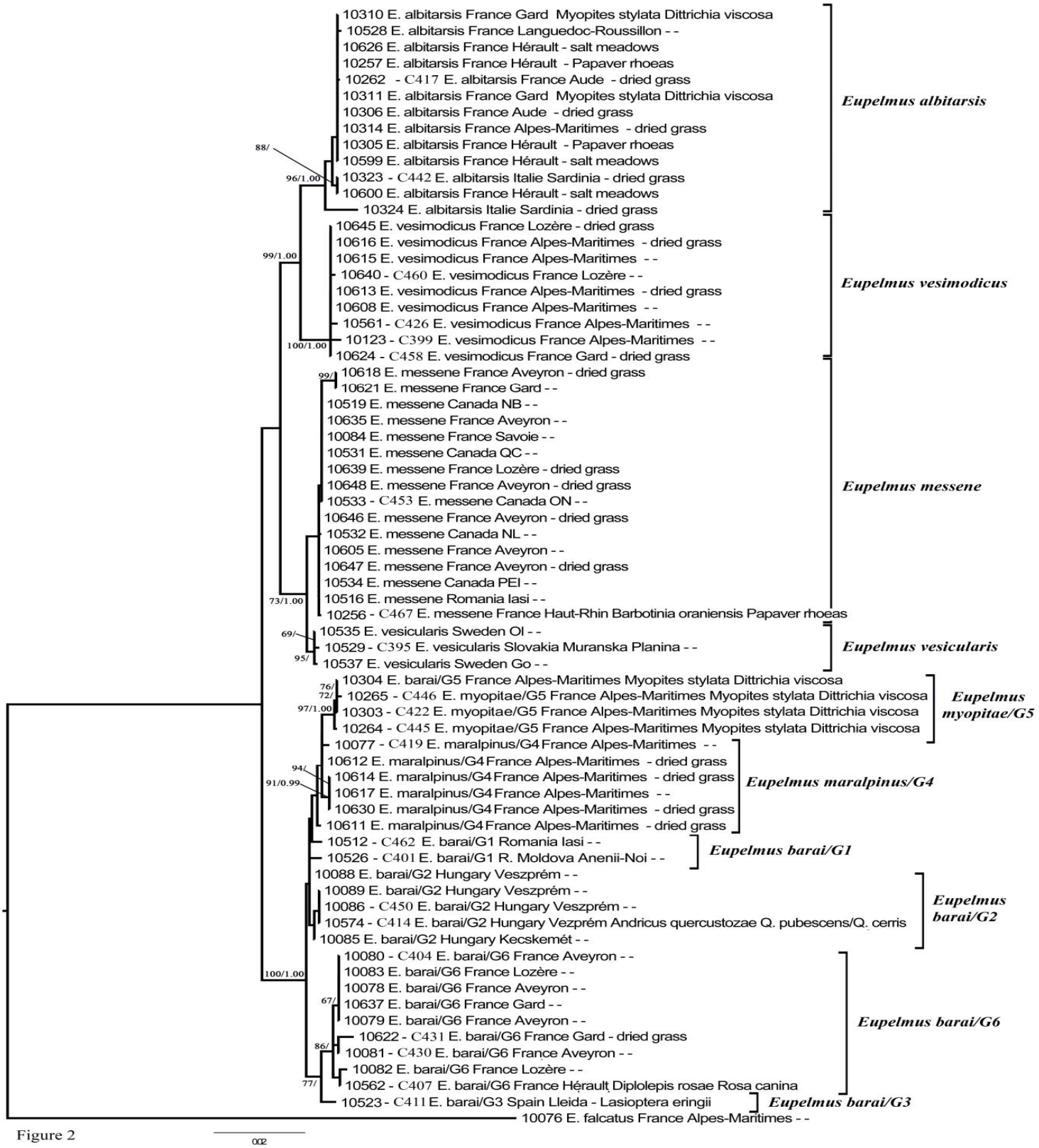

Fig. 2. Phylogram figuring the relationships within the *Eupelmus vesicularis* species complex based on the combined nucDNA dataset alignment (2389 bp and 4 partitions: *Wg*, *EF-1Ŭ*, *Rpl27a* and *ITS2*). Bootstrap Percentages (BP) ≥ 65 and Posterior Probabilities (PP) ≥ 0.90 are indicated at nodes. Each line represents an individual sequenced at least on two nuclear genes with information in the following order: molecular code, clone code for *ITS2* gene, species/clade, country, insect host and associated plant.

Morphological species discrimination

The number of clades belonging to *vesicularis* SC recovered through the different criteria used in this study is provided in Fig. 1. Based on the morphological differentiation using the characters from Fusu (2015), we found that the species delimitation of the *vesicularis* complex based on the concatenated nucDNA tree is more realistic than those obtained from both mitochondrial markers and GMYC or distance based methods. However, two discordances could be observed between these two approaches. The first one is that the clade *E. vesimodicus* is recovered as a distinct species in the concatenated nucDNA tree (Fig. 2), while this clade is hardly distinguished morphologically from the clade *E. vesicularis* (Table 3). The second discordance is that the clade *G5* could be considered as a distinct species based on the morphology alone if genetic data were unavailable. The strong support from the mtDNA and morphology for this clade is contradicted by the nuclear loci as this clade is grouped with clades *G1* to *G6* in the concatenated nucDNA tree (Fig. 2). *G5* is the most derived lineage of the *E. barai* clade, and its recognition as a species renders *E. barai* paraphyletic, except *G5* and *E. barai* are reciprocally monophyletic at the *RpL27a* locus. As a result, we revise the taxonomic status of *E. albitarsis* previously considered as synonyms of *E. vesicularis*, and consider it as a valid species. Moreover, although almost not morphologically differentiated from *E. vesicularis* we consider the clade *E. vesimodicus* as a new species. Finally, we describe the clades *G4* and *G5* as new species (*E. maralpinus* and *E. myopitae* respectively) based on morphological differences, support from the *COI* dataset correlated with congruent patterns of monophyly for one nuclear locus in *G5* and incomplete but significant lineage sorting for two loci in G4. In the following, we provide the diagnosis of *vesicularis* SC, a key to the validated species of *vesicularis* complex and a detailed morphological description for the new species and *E. albitarsis*.

Table 2. GSI values and P-value for *vesicularis* SC clades. The clades evaluated are those presented in Fig. 1 (for clade G3 represented by a single individual GSI values cannot be calculated). P-values indicate the probability of obtaining the corresponding GSI value or a larger one by chance alone.

Species or group	***EF-1ʊ***		***ITS2***		***RpL27a***		***Wg***	
	gsi	P-value	gsi	P-value	gsi	P-value	gsi	P-value
E. albitarsis	1	0.0001	1	0.0165	1	0.0001	0.775	0.0001
E. barai/G1	0.1868852	0.1026	0.483871	0.0506	0.2372881	0.0888	0.1771429	0.1925
E. barai/G2	0.6436782	0.0001	0.7241379	0.0007	0.5789474	0.0006	0.7272727	0.0003
E. maralpinus/G4	0.3586207	0.0013	0.7241379	0.0005	0.7857143	0.0001	0.5636364	0.0011
E. myopitae/G5	0.4745763	0.0004	0.4666667	0.0119	1	0.0001	0.7272727	0.0006
E. barai/G6	0.530303	0.0001	0.7241379	0.0005	1	0.0001	1	0.0001
E. messene	0.7627551	0.0001	0.5555556	0.0003	1	0.0001	1	0.0001
E. vesicularis	0.1545455	0.1404	0.4666667	0.012	1	0.0102	1	0.0143
E. vesimodicus	1	0.0001	1	0.0001	1	0.0001	1	0.0003
East	0.6892231	0.0001	0.311828	0.0982	0.7857143	0.0001	1	0.0153
West	0.4918033	0.0274	0.483871	0.0496	1	0.0001	0.4857143	0.0402

Table 3. Main morphological characters of the *vesicularis* SC clades identified using mtDNA.

Species or group	**Body colour pattern**	**Fore wing rudiment**	**Pilosity on gaster**	**Peg pattern on** anterior margin **of mesobasitarsus**	**Metallic spot on mesoscutal plate**	**Axillae and scutellum**
E. albitarsis	Uniform	Long	Dense	1 row	-	concolorous
E. barai/G1	Uniform	Long	Dense	2 rows	violet	contrasting
E. barai/G2	Uniform	Long	Dense	2 rows	violet	concolorous
E. barai/G3	Uniform	Long	Dense	2 rows	Blue to violet	contrasting
E. maralpinus/G4	Uniform	Long	Sparse	2 rows	violet	contrasting
E. myopitae/G5	Tricolored	Long	Moderate	2 rows	bronze	contrasting
E. barai/G6	Uniform	Long	Dense	2 rows	mainly blue	concolorous
E. messene	Tricolored	Short	Moderate	1-2 rows	-	contrasting
E. vesicularis	Uniform	Short	Dense	1-2 rows	-	contrasting
E. vesimodicus						
East	Uniform	Short	Dense	1-2 rows	-	concolorous
West	Uniform	Short	Dense	1-2 rows	-	concolorous

Diagnosis of vesicularis species complex

Diagnostic characters of *vesicularis* SC could be resumed as following. **Female**. brachypterous, apical part of forewing broad and not sharply pointed; mesotibia with one row of black begs apically; mesobasitarsus with asymmetrical peg pattern, with pegs along entire anterior margin but posterior margin with pegs only in about basal half or less and frequently with one peg apically.; scrobal depression distinctly reticulate and never smooth; antenna with scape contrasting with funicle, yellow to brownish; mesoscutal plate with flat, V-shaped anterior portion differentiated by minute reticulate mesh like sculpture and posteromedial portion coriaceous, shiny and shallowly concave mesally; mesoscutal plate entirely covered with white setae directed posteriorly, though setae denser anteriorly and progressively sparser posteriorly; ovipositor sheaths tricoloured, with small black basal and brown apical bands separated by an elongated median pale band or spot. **Male**. Males are known for some species and unlike females are macropterous and not distinguishable as a group from males of other species of *vesicularis* species group or even *atropurpureus* species group.

Key to European species of Eupelmus of the vesicularis complex

1. Fore wing rudiment short, with apical part less than 1.7× times longer than basal part and usually much shorter. Body tricoloured, with a metallic greenish head with bronze lusters, paler reddish brown to brownish yellow mesosoma and darker, brownish metasoma (Fig. 10) or dark brown with mostly dark green metallic luster (Figs. 11, 12) **and** postero-medial concave part of mesoscutum without a triangular violet to blue spot, at most narrowly violet near transscutal margin and bluish to violet on narrow longitudinal stripe mesally (Figs. 21, 23, 24)…….....2

- Fore wing rudiment long, with apical part at least 1.7× times longer than basal part and usually much longer. Body comparatively uniformly dark brown with green but also greenish-blue and violet lusters **or** mesoscutal plate with postero-medial concave part with a large, triangular violet to blue spot, under some angles of light sometimes overlaid by strong golden and bronze reflections……....…4

2(1). Body tricoloured, with a metallic green head with bronze lusters, paler reddish brown to brownish yellow mesosoma and darker, brownish metasoma (Fig. 10). Mesoscutal plate brownish along outer sides, without or with reduced metallic luster (Fig. 21). Metasoma with

short, sparse and comparatively inconspicuous hair-like setae. On median tergites distance between sockets of two adjacent setae usually about equal to setal length (Fig. 33)…….....……..……***E. messene*** **Walker**

- Body comparatively uniformly dark brown with dark, mainly green luster (Figs 11, 12). Mesoscutal plate with outer sides dark, with metallic luster (Figs 23, 24). Metasoma with dense, slightly lanceolate and conspicuous setae. On median tergites distance between sockets of two adjacent setae shorter than seta length (Fig. 36)…….....3

3(2). Axillae with a reddish-brown tint, at least slightly paler than the dark green scutellum; at least apical half of scutellum with whitish, reflective setae (Fig. 23)… ……..…….....***E. vesicularis*** **Retzius**

- Axillae and scutellum concolorous, dark brown to black with faint dark green luster; scutellum uniformly covered with dark setae (Fig. 24)……***E. vesimodicus*** **sp. n.**

4(1). Body tricoloured, with a metallic green head with bronze lusters, paler reddish brown to brownish yellow mesosoma and darker, brownish metasoma (Fig. 9). Mesoscutal plate with concave part having a large triangular bronze to golden spot, narrowly bordered on sides by violet (Fig. 22)…….....***E. myopitae*** **sp. n.**, **clade *G5***

- Body comparatively uniformly dark brown with green but also bluish-green and violet lusters (Figs. 3-8). Mesoscutal plate without such spot, only narrowly violet near transscutal margin and bluish to violet on narrow longitudinal stripe mesally (Figs. 14, 18), or with a largely violet spot (Fig. 20) or with more reduced golden reflections (Figs. 15, 16), or with a mostly blue spot, only narrowly violet posteriorly (Figs. 13, 17, 19)…….……5

5(4). Mesoscutal plate only narrowly violet along transscutal margin (Fig. 14) to having a variably developed blue triangular spot, with comparatively reduced violet colour posteriorly (Fig. 13) **and** basitarsus on anterior margin with pegs in single row and posterior margin with reduced peg count, with only 2 or sometimes 3 pegs basally and very rarely with 1 peg apically (Figs 37-39)…….....……...…….***E. albitarsis*** **Costa**

- Mesoscutal plate with concave part having a large triangular violet spot only narrowly bordered on outer sides by blue and bluish-green (Figs. 15, 16, 20) or rarely similar to above

(Figs 17, 18); basitarsus on anterior margin with pegs at least indistinctly differentiated into two medially overlapping rows and posterior margin usually with comparatively more numerous pegs, with 2 to 6 pegs basally and frequently with 1 or even 2 pegs apically (Figs. 40-44)…….……..…….…….....6

6(5). Metasoma sparsely setose, with short and very sparse hair-like setae, on median tergites distance between sockets of two adjacent setae greater than seta length (Fig. 32). Mesoscutal plate with concave part having a large triangular violet spot only narrowly bordered on outer sides by blue and bluish-green (Fig. 20) …….....…….7

- Metasoma densely setose, with lanceolate reflective setae, on median tergites distance between sockets of two adjacent setae much less than seta length (Figs. 27-31). Mesoscutal plate as described above (Figs 15, 16) or with a variably developed blue triangular spot, with comparatively reduced violet colour posteriorly (Figs 17-19).....……..8

7(6). Frontovertex with vertex and ocellar area coriaceous, appearing shiny under low magnification and frons mostly coriaceous-imbricate to slightly reticulate. Posterior margin of basitarsus with 2-4 (usually 3) pegs within basal half …….....***balcanicus* Fusu**

- Frontovertex coriaceous-imbricate to reticulate. Posterior margin of basitarsus with 3-5 (usually 4) pegs within basal half (Fig. 44)…….....…..***maralpinus* sp. n., clade *G4***

8(6). Mesoscutal plate with concave part having a large triangular violet spot, only narrowly bordered on outer sides by blue and bluish-green (Figs. 15, 16) ……..***E. barai* Fusu**, **clades *G1*** and ***G2***

Mesoscutal plate with concave part having a variably developed, mostly blue triangular spot, with comparatively reduced violet colour posteriorly (Figs. 17-19) ……..***E. barai* Fusu**, **clades *G3*** and ***G6***

<u>Species review</u>

***Eupelmus albitarsis*, Costa, 1883 revised status**

(Female: Figs. 3, 13-14, 25-26, 37-38)

Eupelmus albitarsis Costa, 1883: 101. Syntypes ♀, UDSN, examined. Type locality: Italy, Sardinia. Costa, 1884: 332 (subsequent description). Synonymy with *E. vesicularis* by Ruschka, 1921: 302.

Eupelmus vesicularis; Monaco, 1976: 135-142 (misidentification); Fusu, 2015 (synonym of *E. vesicularis*).

Material examined: **FRANCE**, **Alpes-Maritimes**, Masseboeuf, N 43.63339°, E 6.97492°, 26.ix.2014, ex sweeping on dry grass (F. Al khatib) (1 ♀) [not sequenced] (in FALPC); **Alpes-Maritimes**, Plascassier, N 43.64049°, E 6.97795°, 26.ix.2014, ex sweeping on dry grass (F. Al khatib) (1 ♀) [not sequenced] (in FALPC); **Alpes-Maritimes**, La Fontaine de l'Ormeau, N 43.651714°, E 6.976692°, 26.ix.2014, ex sweeping on dry grass (F. Al khatib) (2 ♀) [not sequenced] (in FALCP). **Aude**, Sigean, N 43.06182°, E 02.92007°, 19.vi.2012, (N.Ris & F. Al khatib) (1 + 2 ♀) [FAL1398/10306, FAL1398/10262, FAL1398/10307] (in FALPC, AICF); **Aude**, Peyriac-de-Mer, 28.vi.2004, (D. Gérard) (1 ♀) [not sequenced] (in MNHN); **Hérault**, Vic-la-Cardiole, N 43.7331°, E03.80687°, 17.vi.2012, (N.Ris & F. Al khatib) (1 ♀) [FAL1384/10305] (in MNHN); **Hérault**, Lespignan, le long canal, N 43.252778°, E 3.163611°, 2 m, 04.vii.2013, fauchage prés salés (G. Delvare) (1 ♀) [GDEL4181/10626] (in GDPC); **Hérault**, Lespignan near highway A9, N 43.254167°, E 3.163611°, 3 m, 04.vii.2013, fauchage prés salés, (G. Delvare) (2 ♀) [GDEL4183/10599, GDEL4184/10600] (in GDPC); **Hérault**, Vias, 07.viii.1999, (D. Gérard) (2 ♀) [not sequenced] (in GDPC); **Hérault**, Saint-Jean-Buèges, 29.vi.2000, (D. Gérard) (1 ♀) [not sequenced] (in GDPC); **Hérault**, Grabels, 03.viii.1999, (D. Gérard) (1 ♀) [not sequenced] (in FALPC); **Gard**, Garons, N 43.76371°, E 04.42588°, 17.ix.2012, ex *Myopites* stylata, on *Dittrichia viscosa*.(Ris & F. Al khatib) (2 ♀) [FAL1477/10310, FAL1477/10311] (in FALPC). **ITALY**, **Sardinia**, Oristano N 39.70041°, E 08.73969°, 20.x.2012, sweeping dried grass, (L. Brancaccio & M. Thon) (2 ♀) [FAL1505/10324, FAL1504/10323] (in MNHN, AICF); **Bari**, 20.x.73 (R. Monaco) (1♀, 1 ♂) (in BMNH).

Description. **Female**. Length 1.6–2.0 mm. Body dark brown to blackish, with slight metallic luster. Head dark brown to black, slightly metallic and bearing uniform white and brown setae on face and on frontovertex respectively; frontovertex black with dark violet metallic luster, especially below the level anterior ocellus and with very slight green reflections along the inner orbits; parascrobal area and interantennal area mostly with obviously violet metallic

luster; scrobal depression with greenish metallic luster and sometimes the luster is coppery; lower face below malar sulcus with coppery to violet metallic luster; gena dark green metallic. Antenna with scape yellow, pedicel and basal funiculars with greenish to bluish metallic luster, flagellum dark brown with faint violet metallic luster on apical funiculars.

Mesosoma brown to dark brown with greenish and violet metallic luster. Pronotum brown mostly with distinct violet metallic luster and sometimes with slight greenish metallic luster under some angles of light; pronotal collar with erect black setae; mesoscutal plate evenly dense setose except narrowly glabrous posteriorly, setae directed posteriorly, dark green metallic with slight bronze luster mesally and brownish to dark brown laterally, postero-medial part of mesoscutum with variably broad bluish to somewhat violet spot near or along transscutal line; axilla and scutellum uniformly dark brown with dark green luster, scutellar-axillar complex with brownish hair-like setae on axilla and base of scutellum and whitish slightly lanceolate setae on apical half of scutellum. Prepectus dark brown, setose, with violet metallic luster; tegula similar in colour to prepectus. Acropleuron dark brown, anteriorly with very slight green metallic reflections and the rest with bluish-violet metallic luster especially on the microsculptured region. Front leg with dark brown coxa with slight violet metallic luster; femur and tibia brown to dark brown except the paler knee and testaceous apical part of tibia and longitudinal ventral stripe on tibia; tarsus pale yellowish except brown telotarsus and pulvillus. Middle leg completely dark brown except paler knee, testaceous apical third of tibia and four basal tarsomeres of tarsus. Hind leg with dark brown coxa having violet metallic luster dorsally and with white dense setae dorsally and ventrally; femur dark brown with paler longitudinal band on dorsal margin; tibia dark brown except paler, testaceous apical third; tarsus completely pale, testaceous except brown telotarsus and pulvillus.

Metasoma dark brown to black with faint metallic luster and moderately to densely setose, setae long and lanceolate; Mt2 translucent, mostly yellowish apically and dark basally with green metallic luster, at most with two line of white setae subapically. Ovipositor sheaths banded dorsally, with short basal black section, long middle testaceous section and with short apical brownish section, but brown along ventral margin.

Frontovertex coriaceous-imbricate to reticulate. Scrobal depression reticulate and interantennal region finely coriaceous. Pronotal crest with erect setae shorter than pronotal collar.

Mesoscutal plate with flat, V-shaped anterior region differentiated by minute reticulate sculpture and posteromedial region evidently reticulate mesally and shallowly concave. Scutellum lowly convex, relatively broad, about anterior three-quarters elongate-reticulate to imbricate and posterior one-quarter coriaceous to smooth; axilla lowly convex, reticulate to imbricate. Forewing with apical part normally abruptly bent upward at level of petiole, comparatively long 1.90–2.00× as long as basal part; basal part hyaline with costal cell about 0.5× as wide as basal cell or slightly wider, basal cell densely setose dorsally; reflexed portion brown, setose, marginal and postmarginal veins extended along straight outer margin and without a trace of a stigmal vein and inner margin obliquely angled to obtuse point. Hind wing concealed beneath forewing and reflexed brownish apically. Middle leg with row of 4-7 mesotibial apical pegs; mesotarsus with asymmetrical peg pattern on basitarsus, anterior margin with 7-11 pegs in single row and basoposterior margin mostly with 2-3 pegs and very rarely with 1 peg apically, second tarsomere with 1-2 pegs on apicoanterior margin and 1 peg on apicoposterior margin, and third tarsomere with 1 apical peg on either side and fourth tarsomere without or with one single apical peg on either side.

Metasoma ovoid; Mt2 smooth to very finely coriaceous; Mt3-Mt5 coriaceous; Mt6 alutaceous-granular; Syntergum and anal plate forming truncate to somewhat obliquely inclined surface above ovipositor sheaths; Ovipositor sheaths 0.48–0.57× as long as metatibia and 0.25–0.30× as long as metasoma.

Male. Length = 2.15 mm. Body metallic dark-greenish. Head dark, frontovertex and scrobal depression dark-violet, with faint bronze and copper reflections under some angles of light and lower face, gena, and temples dark greenish with mostly bronze luster. Lower gena with one long seta. Maxillary palpus brown. Antenna with scape dark brown with faint dark green luster except yellow in basal one fifth and on outer surface ventrally along longitudinal sensory region, pedicel and flagellum brown; pedicel with line of 4 hooked setae ventrally; F2 to F8 with dense, strongly curved and more adpressed white setae such as the apical half of seta parallel with segment surface; F2–F4 with a group of 3–4 short, stout, black setae ventrally. Mesosoma with stronger metallic luster than head, mesoscutum dark green with some copper and bronze reflection; scutellar-axillar complex differently coloured than mesoscutum, dark with copper and bronze reflections, propodeum with comparatively strong green to copper luster. Tegula brown. Fore wing with a diffuse oval infuscate area behind marginal and stigmal veins. Setae of costal and basal cells, disc and venation all similarly brown to dark brown; costal cell dorsally with single line of 10–12 setae near leading margin

in distal third, and ventrally with 2 rows of setae along length except more setose distally in front of parastigma; basal cell similarly setose as disc, cubital fold setose along length. Front leg with coxa dark, femur dark except broadly yellow apically, tibia and tarsus yellow except last tarsomere brown. Middle leg with coxa and femur dark and tibia mostly yellow with about apical quarter comparatively abruptly dark brown, tarsus with basitarsus whitish, second and third frequently similarly only slightly darker than basitarsus and last two tarsomeres brown. Hind leg similar to middle leg except femur yellowish in about basal half, tibia dark on apical third and narrowly pale at extreme apex. Metasoma dark-brown with bluish-green luster basally on Mt2.

Antenna short, flagellum cylindrical, clava elongate with narrow ventral micropilose sensory region, pedicel plus flagellum 1.53× head width. Basal funiculars barrel-shaped, F2 1.76, F3 1.75, and F8 1.54× as long as wide. F2 to F8 with numeous MPS on 2–3 rows. Mesosoma 1.94× as long as broad. Fore wing 2.30× as long as broad. Propodeum superficially reticulated with percurent median carina.

Remarks. *E. albitarsis* was synonymised with *E. vesicularis* by Ruschka (1921, p. 302). The type was located in Costa's collection deposited in UDSN (Fusu, submitted). The unique female type is labelled "Tissi" (a commune in Sassari province, Sardinia) and has a handwritten label "*Eupelmus albitarsis*", but only one hind leg remains glued to the card rectangle (Fusu, submitted). According to the molecular phylogenetic analysis of specimens of the *vesicularis* SC from Sardinia, the type locality of *E. albitarsis* (Figs. 1, 2), and the morphological differences (see below), we remove the *E. albitarsis* from the synonymy under *E. vesicularis* and treat it as a valid species.

Recognition. Females of *E. albitarsis* could be readily confused with *E. vesicularis* and *E. vesimodicus* as these three species have the same comparatively uniformly dark body (dark brown to black) and the dark green metallic mesoscutal plate with an undifferentiated bluish to somewhat violet spot along transscutal margin of the mesoscutal plate. The main morphological differences between *E. albitarsis* and *E. vesicularis* or *E. vesimodicus* are i) the forewing comparatively longer with apical part more than1.8× as long as basal part in *E. albitarsis* whereas the forewing comparatively shorter with apical part 1.7× as long as basal part in *E. vesicularis* or *E. vesimodicus*; ii) frontovertex and pronotum in *E. albitarsis* largely with bronze to dark violet metallic luster whilst in *E. vesicularis* or *E. vesimodicus*, the

frontovertex and pronotum with reduced violet metallic tints. In addition, *E. albitarsis* is morphologically similar to *E. barai*. The females of two species are dark brown to black with violet luster and forewing relatively long (apical part more than 1.7× as long as basal part). However, females of *E. barai* can be discriminated by a large triangular violet metallic spot narrowly bordered by a blue and bluish-green metallic stripe (Eastern clades) or a similar blue spot with reduced violet lusters (Western clades) on the postero-medial concave portion of mesoscutum. In *E. albitarsis*, the postero-medial, concave portion of mesoscutal plate with a small bluish to violet metallic spot near or along transscutal line. Moreover, in *E. albitarsis* female's anterior margin of basitarsus with pegs in single row, while pegs are at least indistinctly differentiated into two medialy overlapping rows in *E. barai* females.

Our concept of the males of *E. albitarsis* is based on a single specimen and characters that we currently use to differentiate it from the males of *E. vesicularis* and *E. vesimodicus* could prove unreliable when more specimens will become available. Similar to the males of *E. vesicularis* and *E. vesimodicus* the male of *E. albitarsis* has comparatively short antennae (pedicel plus flagellum 1.53× head width), with barrel-shaped basal funiculars with adpressed setae and numerous MPS on multiple rows, but foretibia and tarsus in *E. albitarsis* are yellow except last tarsomere brown, the fore wing has a conspicuous diffuse oval infuscate area behind marginal and stigmal veins, and fore wing interference pattern with a apical magenta spot. In both *E. vesicularis* and *E. vesimodicus* males the fore tibia is dark ventrally and sometimes also subbasally and fore wing variably conspicuously infuscate beyond parastigma, with a diffuse oval infuscate area behind marginal and stigmal veins only in large specimens; additionally in *E. vesicularis* fore wing interference pattern with a yellow to orange and reddish band in apical third. As both the infuscation and the wing interference pattern are influenced by specimen size, it is possible that these characters are not reliable.

Distribution. Sequenced specimens originate in South France and Sardinia. One unsequenced specimens that we attribute to this species based on morphology is from Italy.

Hosts. Although most specimens were collected by sweeping on the herbaceous layer, some females were reared from the galls of *Myopites stylata* (Fabricius, 1794) on *Dittrichia viscosa* (L.) Greuter (Asteraceae).

***Eupelmus barai* Fusu (submitted)**

(Female: Figs. 4-7, 15-19, 27-31, 40-43)

Material examined:

"***E. barai/G1***": **R. MOLDOVA**, **Anenii-Noi**, Chetrosu, N 46.889515°, E 29.044470°, viii.2004 (1 ♀) [LF.B.RM 01/10526] (in AICF). **ROMANIA**, **Iaşi**, Bârnova forest, 01.vii.2010 (Leg. Popovici O.) (1 ♂) [not sequenced] (in FALPC); **Iaşi**, Breazu village, Mîrzești, steppic vegetation, N 47.244278°, E 27.482806° to N 47.233228°, E 27.473389°, 07.viii.2010 (Leg. Fusu L. & Popovici O) (1 ♀) [not sequenced] (in FALPC); **Iaşi**, giade on the border of Ciric lake, N 47.187561°, E 27.601708°, 30.vii.2010 (Leg. Popovici O) (1 + 2 ♀) [not sequenced] (in FALPC & GDPC); **Iaşi**, Iași, Botanical Garden, 19.ix.2012 (Fusu L. & Popovici O) **(**1 ♀) [LF.B.RO 04m/10522] (in FALPC); **Iasi [county]**, Iasi, Ciric, N 47.190944°, E 27.599261°, 19.ix.2010 (**Fusu L. & Popovici O.**) (1 ♀) [LF.A.RO 04/10512] (in AICF); **Mehedinit**, Iron Gates, Dubova vill., Ciucaru Mare, N 44.600500°, E 22.259667°, 300 m, 14-16.vii.2009, sweep net (Leg. Fusu & Popovici) (1 ♂) [not sequenced] (in GDPC);

"***E. barai/G2***": **HUNGARY**, **Kecskemét**, Bócsa, 10 km NNE village, N 46.69669°, E 19.53034°, 100m, 29.vi.2010 (G. Delvare) (1 ♀) [GDEL4084/10085] (in GDPC); **Veszprém**, Várpalota, 2km SSE village, N 47.18453°, E 18.15362, 116 m, 28.vi.2010 (G. Delvare) (1 ♀) [GDEL4087/10089] (in MNHN); **Veszprém**, Nagavászony, 4.5 km NNE village, N 47.01925°, E 17.71442°, 300m, 27.vi.2010 (G. Delvare) (1 + 1 ♀) [GDEL4086/10088, GDEL4085/10086] (in FALPC, AICF); **Veszprém**, Várpalota, 5.5 km E of Varpalota, N 47.198091°, E 18.21204°, 138m, 17.xi.2010, em. 03.iv.2011, ex *Andricus quercustozae* on *Quercus pubescens/cerris* (P. Jansta) (1 ♀) [PJ10077_31_3/10574] (in AICF).

"***E. barai/*G3**": **SPAIN**, **Lleida**, Omells na Gaia, 06.vii.2007, ex. *Lasioptera eringii* galls (1 ♀) [LF.B.SP 03/10523] (in AICF).

"***E. barai/*G6**": **FRANCE**, **Aveyron**, Saint-André-de-Vézines, Roquesaltes 825 m, N 44.137500°, E 3.228611°, 20.vi.2011 (G. Delvare) (1 ♀) [GDEL4080/10079] (in FALPC); **Aveyron**, Cornus 750 m, GR71 Mas Raynal-, Roc Blanc, N 43.867222°, E 3.196111°, 21.vi.2011, herbaceous layer (G. Delvare) (1 ♀) [GDEL4224/10620] (in MNHN); **Aveyron**, Nant, Maison Forestière, des Canalettes, N 44.978611°, E 3.263056°, 680 m, 12.vi.2011, strate herbacée (G. Delvare) (1 + 1 ♀) [GDEL4215/10633, GDEL4217/10634] (in GDPC, AICF); **Aveyron**, Saint-Jean-du-Bruel, Œil de Bœuf, N 44.048056°, E 3.339444°, 800m,

14.vi.2011 (G. Delvare) (2 ♀) [GDEL4081/10080, GDEL4081/10081] (in AICF); **Aveyron**, Nant, Le Causse des Cuns, N 44.040833°, E 3.283889°, 800m, 19.vi.2011 (G. Delvare) (1 ♀) [GDEL4220/10619] (in FALPC); **Aveyron**, Saint-André-de-Vézines, Roquesaltes, N 44.137500°, E 3.228611°, 825m, 20.vi.2011 (G. Delvare) (1 ♀) [GDEL4080/10078] (in GDPC); **Gard**, Trèves, Gorges du Trévezel à Saint-Sulpice, N 44.075278°, E 3.332778°, 510m, 22.vi.2011 (G. Delvare) (1 ♀) [GDEL4229/10622] (in AICF); **Gard**, Trèves, Gorges du Trévezel NE, Saint-Sulpice, N 44.076111°, E 3.336667°, 530 m, 22.vi.2011, herbaceous layer (G. Delvare) (1 ♀) [GDEL4228/10637 (in GDPC); (1 ♀) [GDEL4231/10638] (in GDPC) the same data as the precedent except the altitude is 510 m; **Hautes-Alpes**, Saint-Crépin, Malpasset, N 44.710556°, E 6.606389°, 950 m, 22.viii.2008, sweeping on herbaceous layer (G. Delvare) (1 ♀) [GDEL4200/10610] (in GDPC); **Hérault**, Riols, N-D de Trédos, 580 m, 03.iii.2013,ex gall *Diplolepis rosae* on *Rosa canina* (P. Jansta & G. Delvare) (2 ♀) [GDEL4263/10562, GDEL4263/10563] (in MNHN); **Lozère**, Florac, S Viala de Grimoald, 680 m, 07.vii.2011 (G. Delvare) (2 ♀) [GDEL4082/10082, GDEL4082/10083] (in FALPC).

Eupelmus maralpinus Delvare, Fusu & Al khatib sp. n.

(Female: Figs. 8, 20, 32, 44)

Type material. Holotype: **FRANCE**, **Alpes-Maritimes**, Lucéram, , N 43.874722°, E 7.384444°, trail between points 177 and 178, 1100 m, 01.viii.2010 (1 ♀) (G. Delvare) [GDEL4202/10611] (in MNHN). Paratypes: **Alpes-Maritimes**, Ablé Mount, N 43.894444°, E 7.379167°, Lucéram 1230-1260 m, 01.viii.2010 (G. Delvare) (1 ♀) [GDEL4079/10077] (in FALPC); **Alpes-Maritimes**, Lucéram, trail Col de l'Ablé- Caire de Braus (point 179), N 43.879444°, E 7.379167°, 1150 m, 01.viii.2010 (G. Delvare) (1 ♀) [GDEL4203/10612] (in FALPC); **Alpes-Maritimes**, Lucéram, environs Col de l'Ablé, N 43.892778°, E 7.383611°, 01.viii.2010 (G. Delvare) (1 ♀) [GDEL4201/10627] (in AICF); **Alpes-Maritimes**, Breil-sur-Roya, GD128 = Versant N Cime du Bosc, N 43.925833°, E 7.485833°, 1000m, 17.vi.2012 (G. Delvare) (1 ♀) [GDEL4240/ 10641] (in AICF); **Alpes-Maritimes**, Sospel, near Mont Scardélans, N 43.856111°, E 7.408611°, 1025 m, 06.viii.2010, herbaceous layer (G. Delvare) (1 + 1 ♀) [GDEL4211/10617, GDEL4212/10631] (in GDPC, AICF); **Alpes-Maritimes**, Sospel, N 43.892500°, E 7.449167°, 700 m between, points 75 et 84, 03.viii.2010, herbaceous layer (G. Delvare) (1 ♀) [GDEL4206/10614] (in MNHN); **Alpes-Maritimes**, Sospel, Baisse

du Pape, N 43.854167°, E 7.408333°, 1025m, 06.viii.2010, herbaceous layer (G. Delvare) (1 ♀) [GDEL4210/10630] (in FALPC); **Alpes-Maritimes**, Sospel, sentier botanique vers, Olivetta 280 m, N 43.8860°, E 07.49558°, old olive orchard, 17.vi.2012 (5G. Delvare) (1 ♀) (GDEL4244/10642] (in GDPC).

Description. **Female**. Body mostly brown, with some metallic luster. Head dark violet to bronze, with dark green to bluish-green luster mostly on occiput, vertex behind posterior ocelli, scrobal depression, lower face and temples; frons only indistinctly tricoloured with dark green luster along inner orbits except immediately near them where narrowly dark violet and mesally copper to dark violet below level of anterior ocellus. Antenna with scape yellow, pedicel and flagellum dark brown with green luster on pedicel and variably distinct bronze to violet lusters on basal funiculars. Mesosoma similar in colour to head, mostly dark brown with slight dark greenish, bronze and violet luster under some angles of light; mesoscutal plate moderately densely setose with setation progressively sparser posteriorly and broadly glabrous in front of scutellum, dark bronze-green to coppery and concave part with a large triangular violet spot narrowly bordered on sides by blue and bluish green; the spot reaches with its pointed apex the anterior V-shaped sculptured region; axillae dark brown with faint green luster anteriorly and only slightly contrasting with the dark brown to greenish-black scutellum or axillae and scutellum anteriorly reddish-brown, conspicuously contrasting with the rest of scutellum that is dark brown with dull green luster; scutellar-axillar complex uniformly covered with brownish hair-like setae except setae lighter and slightly lanceolate toward frenal line. Front leg mostly dark brown, except coxa with violet and copper to green metallic luster and knee, apex and dorsal edge of tibia, and basal tarsomeres pale. Middle leg similar in colour to front leg except coxa less metallic, apex of tibia more broadly pale with distal third to distal half whitish-yellow and anterodorsal angle of femur with a whitish spot or femur more extensively pale along anterior edge of dorsal and ventral surfaces; mesotarsal pegs dark. Hind leg with similar colour pattern as front leg except knee at most obscurely lighter in colour and tibia paler along ventral surface. Metasoma with short and sparse hair-like setae, on median tergites distance between sockets of two adjacent setae larger to slightly shorter than seta length; dark brown except Mt2 translucent in distal half with the underlying yellowish-white internal structures visible in variable extent and dark basally with strong greenish-blue with violet to golden-green metallic luster or at least with a pair of dark, metallic subbasal spots; Mt3 sometimes also extensively metallic dorsally. Ovipositor sheaths

dark brown in about apical third, along ventral margin and at extreme base, with a yellowish elongate spot in basal half.

Head with frontovertex coriaceous-imbricate to reticulate. Pronotal crest with erect setae shorter than pronotal collar. Mesoscutal plate with flat, V-shaped anterior region differentiated by minute reticulate sculpture and posteromedial region mostly smooth and shiny or with almost effaced sculpture and shallowly concave. Scutellum and axillae lowly convex. Forewing base extended to near petiole, with costal cell about 0.5× as wide as basal cell or slightly wider; basal cell densely setose dorsally; apical part normally abruptly bent upward, comparatively long, more than 1.7× an usually up to 2× as long as basal part with marginal and postmarginal veins extended along straight leading margin and without a trace of the stigmal vein, posterior and leading margins obliquely angled to rounded point. Hind wing concealed beneath forewing and apically reflexed. Middle leg with row of 5-8 mesotibial apical pegs; mesotarsus with asymmetrical peg pattern on basitarsus, anterior margin with 8-12 pegs differentiated into two medially overlapping rows and posterior margin with 3-5 pegs (usually 4) within basal half and with 1 peg apically, second tarsomere with 2-3 pegs on anterior margin and one peg on posterior margin, and third and fourth tarsomeres with 1 apical peg on either side. Metasoma ovoidal and comparatively narrow, Mt6 alutaceous-granular. Syntergum and anal plate forming truncate to somewhat obliquely inclined surface above ovipositor sheaths and gastral apex extending to about apex of second valivfer. Ovipositor sheaths about 0.5-0.6× as long as metatibia and 0.3-0.4× as long as metasoma.

Male. Unknown.

Recognition: Because of the long fore wing rudiment and the colour of the mesoscutal plate females of *E. maralpinus* are most similar to those of *Eupelmus barai* and *E. balcanicus*. Both *E. maralpinus* and *E. balcanicus* have very sparse setae on gaster which helps easily differentiate them from *E. barai*. *E. maralpinus* can further be separated from *E. balcanicus* by its coriaceous imbricate to reticulate frontovertex and a slightly more pubescent gaster, on median tergites distance between sockets of two adjacent setae being mostly slightly shorter than seta length (in *E. balcanicus* vertex finely coriaceous, appearing shiny under low magnification and frons mostly coriaceous-imbricate to slightly reticulate; setae on gaster very short, on median tergites distance between sockets of two adjacent setae mostly larger than seta length). Although variable, the number of pegs on basitarsus can also be used to

discriminate the two species. In *E. maralpinus* posterior margin of basitarsus with 3-5 pegs (usually 4) within basal half while in *E. balcanicus* with 2-4 (usually 3).

Etymology. From the type locality situated in the Maritime Alps. Noun in apposition.

Hosts. Unknown.

Distribution. SE France, Maritime Alps.

Eupelmus messene Walker, 1839

(Female: Figs. 10, 21, 33, 45)

Material examined: **CANADA: Nouveau-Brunswick**, vic. Tracy, 24.vii.2008 (**Goulet, Boudreault & Badiss**) (1 ♀) [LF.A.CA 07/10519] (in AICF); **Prince Eduard**, Central Badeque, 20.vii.2008 (Goulet, Boudreault & Badiss) (1 ♀) [LF.A.CA 06/ 10534] (in AICF); **Québec**, Belle-Anse, 26.vii.2008 (Goulet, Boudreault & Badiss) (1 ♀) [LF.A.CA 03/10531] (in AICF); **Terre-Neuve-Labrador**, St-Andrew's,18. vii.2008 (Goulet, Boudreault & Badiss) (1 ♀) [LF.A.CA 04/10532] (in AICF); **Ontario**, 5 km NW Almonte, 29.v.2008 (Goulet & Fernandez) (1 ♀) [LF.A.CA 05/10533] (in AICF). **FRANCE**, **Alpes-Maritimes**, La Fontaine de l'Ormeau, N 43.651714°, E 6.976692°, 26.ix.2014, sweeping on dry grass (F. Al khatib) (1 ♀) [not squenced] (in FALPC); **Aveyron**, Peyreleau, Forêt Domaniale Causse Noir, piste du champignon, préhistorique, N 44.175278°, E 3.237500°, 850 m, 22.vi.2009 (G. Delvare) (1 ♀) [GDEL4195/10605] (in MNHN); **Aveyron**, Nant, Maison Forestière des Canalettes, N 44.978611°, E 3.263056°, 680 m, 12.vi.2011, herbaceous layer (G. Delvare) (1 ♀) [GDEL4216/10618] (in FALPC); **Gard**, Trèves, Gorges du Trévezel NE, Saint-Sulpice, N 44.076111°, E 3.336667°, 530 m, 22.vi.2011, herbaceous layer (G. Delvare) (1 ♀) [GDEL4227/10621] (in MNHN); **Haut-Rhin**, Colmar, 08.vi.2012, émergence 28.vi.2012, ex capsule, Papaver rhoeas (A. Fleisch) (1 ♀) [FAL1379/10256] (in FALPC); **Hérault**, Saint-Privat, Causse du Larzac, N 43.761944°, E 3.466667°, 26.vii.2013, 700 m, herbaceous layer (G. Delvare) (3 ♀) [GDEL4254/10646, GDEL4255/10647 & GDEL4256/10648] (in GDPC); **Lozère**, Saint-Pierre-Tripiers, sentier Arcs de Pierre, N 44.215833°, E 3.259722°, 920 m, 09.vii.2011, forest Pinus sylvestris (G. Delvare) (1 ♀) [GDEL4234/10639] (in FALPC); **Savoie**, Lanslebourg, Chemin du Pré Vaillant, 1900 m, 21.viii.2007 (G. Delvare) (1 ♀) [GDEL4083/10084] (in GDPC). **ROMANIA**, **Iasi [county]**, Iasi, Ciric, N 47.190944°, E

27.599261°, 19.ix.2012 (Fusu L. & Popovici O.) (1 ♀) [LF.A.RO 05/10516] (in AICF); **Iasi [county]**, Iasi, Botanical Garden, N 47.187075°, E 27.549139°, 20.vi.2007 (Popovici O.) (1 ♀) [LF.A.RO 07/10514] (in AICF).

Eupelmus myopitae Al khatib, Delvare & Fusu sp. n.

(Female: Figs. 9, 22, 34, 46)

Type material. **Holotype**: **FRANCE**, **Alpes-Maritimes**, Gourdon, N 43.73168°, E 06.98859, 08.vi.2012, emergence 11.vi.2012, ex *Myopites stylata*, on *Dittrichia viscosa* (F. Al khatib & P. Gory) (1 ♀) [FAL1405/10304] (in MNHN). **Paratypes**: Same data as holotype except different codes: (3 ♀) [FAL1405/10264, FAL1405/10264 (in FALPC); FAL1405/10265 (AICF)]; (1 ♀) [FAL1405 (not sequenced) (in GDPC) same data as the precedent].

Description. **Female**. Body tricoloured, with a metallic greenish head, largely reddish-brown or brownish-yellow mesosoma and brown metasoma. Head dark violet to bronze, with dark green to bluish-green lusters mostly on occiput, vertex behind posterior ocelli, scrobal depression, lower face and temples; frons only indistinctly tricoloured with dark green luster along inner orbits except immediately near them where narrowly dark violet and mesally copper to dark violet below level of anterior ocellus. Antenna with scape yellow, pedicel pale brownish to dark brown and flagellum dark brown, with green luster on pedicel and variably distinct bronze to violet lusters on basal funiculars. Mesosoma lighter than head; dorsal surface of pronotum, prepectus, acropleuron and mesopectus brownish yellow to reddish brown with at most a very faint metallic luster; lateral panel of pronotum, prosternum and metapleuron brown with green to copper metallic luster; mesoscutal plate moderately uniformly setose except narrowly glabrous posteriorly, brownish laterally with reduced metallic luster, bronze-green to coppery in rest and concave part with a large triangular bronze to golden spot, narrowly bordered on sides by violet and then blue and bluish green; the spot reaches with its pointed apex the anterior V-shaped sculptured region; axillae and scutellum anteriorly yellow to reddish-brown, conspicuously contrasting with the rest of scutellum that dorsally is dark brown with dull green luster; scutellar-axillar complex with brownish hair-like setae except setae lighter and slightly lanceolate toward frenal line. Front leg mostly pale reddish-brown, except coxa with slight green metallic luster and knee, apex and dorsal edge

of tibia, and basal tarsomeres pale-yellow. Middle leg almost uniformly pale reddish-brown, except coxa brownish and about apical third of tibia and 4 basal tarsomeres lighter, yellowish-white; mesotarsal pegs dark. Hind leg with similar colour pattern as front leg except knee at most obscurely lighter in colour and tibia paler along ventral surface to almost uniformly pale, only slightly darkened mesally on anterior surface. Metasoma with short and sparse hair-like setae, on median tergites distance between sockets of two adjacent setae equal to slightly shorter than seta length; brown to dark brown and darker than mesosoma except Mt2 almost completely translucent, appearing uniformly brownish-yellow, at most with a pair of darker subbasal spots with indiscernible metallic hue. Ovipositor sheaths dark brown in about apical third, along ventral margin and at extreme base, with a yellowish elongate spot in basal half.

Frontovertex coriaceous-imbricate to reticulate. Pronotal crest with erect setae shorter than pronotal collar. Mesoscutal plate with flat, V-shaped anterior region differentiated by minute reticulate sculpture and posteriorly finely coriaceous and shallowly concave. Scutellum and axillae lowly convex. Forewing base extended to near petiole, with costal cell about 0.5× as wide as basal cell or slightly wider; basal cell densely setose dorsally; apical part normally abruptly bent upward, comparatively long, more than more than 1.7× an usually up to 2× as long as basal part, with marginal and postmarginal veins extended along straight leadin margin and without a trace of a stigmal vein; leading and posterior margins obliquely angled to rounded point. Hind wing concealed beneath forewing and apically reflexed. Middle leg with row of 5-8 mesotibial apical pegs; mesotarsus with asymmetrical peg pattern on basitarsus, anterior margin with 10-14 pegs differentiated into two medially overlapping rows and posterior margin with 4-6 pegs within basal half and with 1-2 pegs apically, second tarsomere with 2 pegs on anterior margin and 1 peg on posterior margin, and third and fourth tarsomeres with 1 apical peg on either side. Metasoma ovoid and comparatively narrow, Mt6 alutaceous-granular. Syntergum and anal plate forming truncate to somewhat obliquely inclined surface above ovipositor sheaths and gastral apex extending to about apex of second valvifer. Ovipositor sheaths about 0.5-0.6× as long as metatibia and 0.3-0.4× as long as metasoma.

Male. Unknown.

Recognition. Because of the tricoloured body, with a darker greenish head, reddish brown or brownish yellow mesosoma and darker brown metasoma females of *E. myopitae* are similar to *E. messene*, but can be recognized because of the long fore wing rudiment and the presence on the concave part of mesoscutum of a large, triangular, bronze to golden spot, narrowly

bordered on sides by violet. Also, the apical part of fore wing more than 1.7× as long as basal part in *E. myopitae* and less than 1.7× in *E. messene*. From all the species with a long fore wing rudiment *E. myopitae* can be separated by the tricoloured body and by the colour of the spot on the mesoscutal plate. In *E. maralpinus*, *E. balcanicus* and *E. barai* the spot is violet or blue, with at most some bronze shine under some angles of light, while in *E. albitarsis* the spot is undifferentiated: concave part of mesoscutum bluish-green medially, conspicuously violet only along transscutal margin.

Etymology. Named for the host of the type series, *Myopites stylata*. Noun in apposition.

Hosts. Reared from galls of *M. stylata* on *Dittrichia viscosa*.

Distribution. SE France, Maritime Alps.

Eupelmus vesicularis (Retzius, 1798)

(Female: Figs. 11, 23, 35, 47)

Ichneumon vesicularis Retzius, 1783: p 70 [type material not found in DeGerr collection in Stockholm]

Eupelmus degeeri Dalman, 1820: p. 379; synonymy by Ruschka (1921: 301)

Eupelmus maculipes Walker, 1837; ♂ designated as lectotype by Graham (1969: 93)

Material examined: **SLOVAKIA**, **Muranska Planina**, Preda Hora, 24.vii/01.viii.2009 (M. Mitroiu) (1 ♀) [LF.V.SL 02/10529] (in FALPC); **Muránska Planina Nat. Park**, Predná Hora, N 48°45′54″, E 20°06′14″, 865m, 25.vii-31.vii.2009, Malaise trap meadow, Leg. M. Mitoiu (1 ♂) [not sequenced] (in FALPC). **SWEDEN**, **Öland**, Mörbylånga kommun, Gamla, Skogsby (Kalkstad), meadow with bushes, 26-29.V.2011, Leg. Fusu L (1 ♀) [not sequenced] (in FALPC); **Öl**, Mörbylånga, N 56.616700°, E 16.507617°, 20.viii.2006/15.viii.2006 (SMTP project 1731) (1 ♀) [LF.V.SW 03/10535] (in AICF); **Go**, Gotlands, N 57.536783°, E 18.337883°, 16.vii/02.viii.2004 (SMTP project 1458) (1 ♂) [LF.V.SW 05m/10537] (in AICF).

Eupelmus vesimodicus Al khatib, Delvare & Fusu sp. n.

(Female: Figs. 12, 24, 36, 48)

Type material: **Holotype**: **FRANCE**, **Alpes-Maritimes**, Sospel, trail Baisse du Pape - Col du Farguet, N 43.848056°, E 7.410278°, 1025 m, 06.viii.20110, herbaceous layer (G. Delvare) (1 ♀) [GDEL4208/10616] (in MNHN). **Paratypes**: **FRANCE**, **Alpes-Maritimes**, Sospel, trail Baisse du Pape - Col du Farguet, N 43.848056°, E 7.410278°, 1025 m, 06.viii.20110, herbaceous layer (G. Delvare) (1 ♀) [GDEL4209/10629] (in FALPC); **Alpes-Maritimes**, Sospel, Baisse de Levens, N 43.917778°, E 7.460833°, 1090 m, 03.viii.2010, herbaceous layer, (G. Delvare) (1 ♀) [GDEL4205/10613] (in FALPC); **Alpes-Maritimes**, Moulinet, trail RG Bévéra S point 28, N 43.973611°, E 7.412778°, 1100 m, 04.viii.2010, herbaceous layer, (G. Delvare) (1 ♀)[GDEL4207/10615] (in MNHN); **Alpes-Maritimes**, Lucéram, trail Col de l'Ablé- Caire de Braus (point 179), N 43.879444°, E 7.379167°, 1150 m, 01.viii.2010 (G. Delvare) (1 ♀) [GDEL4204/10628] (in GDPC); **Alpes-Maritimes**, Belvédère, Vallon de la Gordolasque point 271, N 44.041389°, E 7.376111°, 1370 m, 22.vii.2009, (G. Delvare) (1 ♀) [GDEL4198/10608] (in GDPC); **Aveyron**, Sauclières Virenque, Pont de Grailhes,N 43.946944°, E 3.355278°, 700 m, 15.vi.2011, (G. Delvare) (1 ♀) [GDEL4219/10636] (in GDPC); **Alpes-Maritimes**, Lucéram, Mont l'Ablé, N 43.892778°, E 7.383611°, 1230-1260, 01.viii.2010, (1 ♀) [GDEL4079/10123] (in AICF); **Alpes Maritimes**, Saint-Dalmas-Selvage, Bois de Sestrière, 1850 m, 26.vi.2012, sur éboulis grossiers (G. Delvare) (1♀) [GDEL4262/10561] (in GDPC); **Gard**, Trèves, Gorges du Trévezel à Saint-Sulpice, N 44.075278°, E 3.332778°, 510m, 22.vi.2011 (G. Delvare) (1 ♀) [GDEL4233/10624] (in AICF); **Gironde**, Badet, Salles, 10-25.v.2005, Malaise trap (M. van Helden) (1♀) (V.FR.02) (in AICF); **Lozère**, Altier, GR68, 500 m E Habitarelle, N 44.444722°, E 3.882778°, 850 m, 20.vii.2012, herbaceous layer (G. Delvare) (1 ♀) [GDEL4250/10645] (in MNHN); **Lozère**, Cocurès Ravin de l'Agude, N 44.349444°, E 3.611944°, 600 m, 14.vii.2011, herbaceous leyer (G. Delvare) (1 ♀) [GDEL4236/10640] (in FALPC); **Lozère**, Belvezet, N Gouffre des Crozes, N 44.565845°, E 3.711934°, 1210m, 20.vii.2012, herbaceous leyer (G. Delvare) (1 ♀) [GDEL4247/10643] (in AICF). **BELGIUM**: **Tervuren**, Museum park, 16-18.v.2010, grass near shrubs, YPT (M. Mitroiu) (1 ♀) (V.BE.01) (in AICF).

Non type material. FRANCE: **Allier**, Broût-Vernet, H. du Buysson (1 ♀); **Côte-d'Or**, Esbarres: 14.ix.1952 (1 ♀), 10.viii.1954 (1 ♀), 23.viii.1955 (1 ♀), 11.vii.1956 (1 ♀), 11.viii.1956 (3 ♀, 2 ♂), 6.vii.1958 (1 ♀), 12.vii.1958 (1 ♀), 14.vii.1958 (3 ♀), 31.vii.1958 (1 ♀), 31.viii.60 (1 ♂), 9.ix.1961 (1 ♀), 16.vii.1962 (1 ♀), 19.vii.1962 (1 ♀), 13.vii.1963 (1

♀), 22.vii.1964 (1 ♀) (J. Barbier); **Côte-d'Or**, Gevrolles: 4.ix.1951 (1 ♀), 9.ix.1955 (1 ♀), 27.viii.1957 (1 ♀), 28.viii.1957 (1 ♀), 31.viii.1957 (1 ♀, 1 ♂); 29.vii.1964 (1 ♀) (J. Barbier); **Côte-d'Or**, Messigny-et-Vantoux, 7.ix.1968 (1 ♀) (J. Barbier); **Côte-d'Or**, La Maison-Dieu, 9.vi.1969 (1 ♀) (J. Barbier); **Côte-d'Or**, Saint-Usage, 9.viii.1954 (1 ♀) (J. Barbier); **Côte-d'Or**, Corcelotte, 13.vi.1969 (1 ♀) (J. Barbier); **Finistère**, Blancs Sablons, 17.vi.1962 (1 ♀) (J. Barbier) (in MNHN). **ITALY**: Genova, Righi, 12.vii.1927 (1 ♀) (in NHMV). **SPAIN**: Santander, Castro Urdinales, 02.VII.1973 (1 ♀) (Z. Bouček) (in BMNH). **SWITZERLAND**: WA, Gampel, Jeizinen-Matte, Wagrander 1520-1400 m, 13.vii.2005 (1 ♀) (H. Baur & P. Jansta) (in CNC) (improperly mounted/preserved or contorted specimens excluded from the type series).

Description. Female. Identical in all respects to females of *E. vesicularis* except axillae and scutellum concolorous, dark brown to black with faint dark green luster and setae on scutellum dark; mesoscutal plate and gaster evenly and densely setose.

Male. Males of *E. vesimodicus* are indistinguishable from those of *E. vesicularis* except perhaps the fore wing interference pattern with a magenta to blue band in apical third, but in smaller specimens with more golden and yellowish and then more similar to that of *E. vesicularis*.

Recognition. Females of *E. vesimodicus* are very similar to those of *E. vesicularis*. Besides the characters provided in the key, *E. vesimodicus* is also more densely pubescence on gaster and mesoscutal plate.

Etymology. A combination of ***ñvesiò*** (from *E. vesicularis*) and the Latin word "*modicus**ò*** (indistinguishable), in reference to the close morphological resemblance of this species to *E. vesicularis*. Noun in apposition.

Distribution. The sequenced specimens were collected in South of France. Judging from unsequenced specimens that we attribute to this species it has a Western European distribution: Spain, France, Switserland, and Belgium.

Hosts. The host insect associations for this species are unknown. All specimens included in this study were collected by sweeping on herbaceous layer.

Figs. 3-10. Habitus of females in the *Eupelmus vesicularis* species complex: *E. albitarsis* 10314 from France (**3**); *E. barai/G2* 10574 from Hungary (**4**); *E. barai/G3* 10523 from Spain (**5**); *E. barai/G6* 10080 from France (**6**); *E. barai/*G6 10634 from France (**7**); *E. maralpinus/G4* 10641 from France (**8**); *E. myopitae/G5* 10265 from France (**9**); *E. messene* 10514 from Romania (**10**).

Figs. 11-12. Habitus of females in the *Eupelmus vesicularis* species complex (continued): *E. vesicularis* 10535 from Sweden (**11**); *E. vesimodicus* 10643 from France (**12**). Scale bar 1 mm.

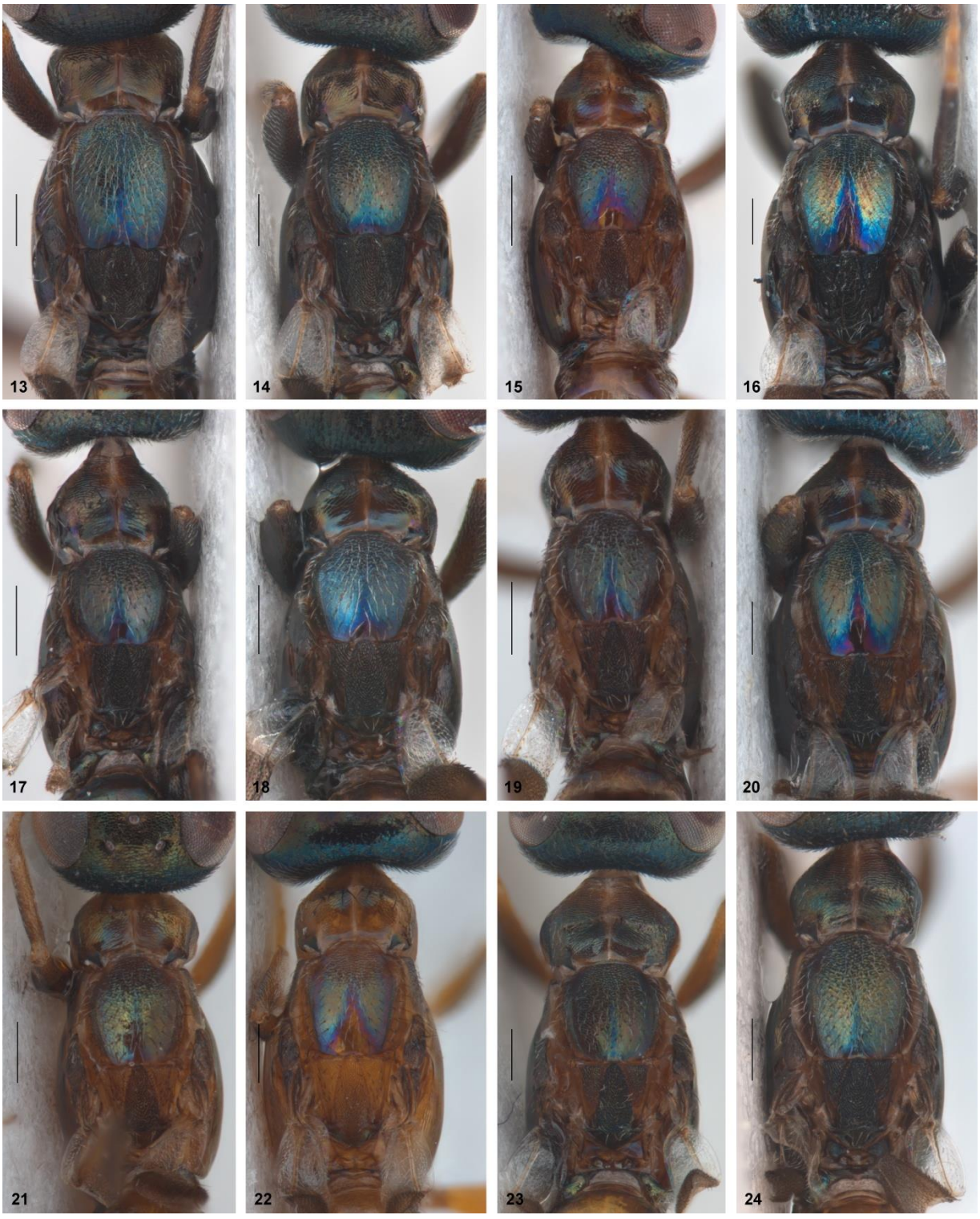

Figs. 13-24. Mesosoma in females of the *Eupelmus vesicularis* species complex: *E. albitarsis* 10262 from France (**13**); *E. albitarsis* 10307 from France (**14**); *E. barai/G1* 10525 from Moldova (**15**); *E. barai/G2* 10574 from Hungary (**16**); *E. barai*/G6 10080 from France (**17**); *E. barai*/G6 10634 from France (**18**); *E. barai/G3* 10523 from Spain (**19**); *E. maralpinus/G4* 10641 from France (**20**); *E. messene* 10514 from Romania (**21**); *E. myopitae/G5* 10265 from France (**22**); *E. vesicularis* 10535 from Sweden (**23**); *E. vesimodicus* 10643 from France (**24**). Scale bar 0.2 mm.

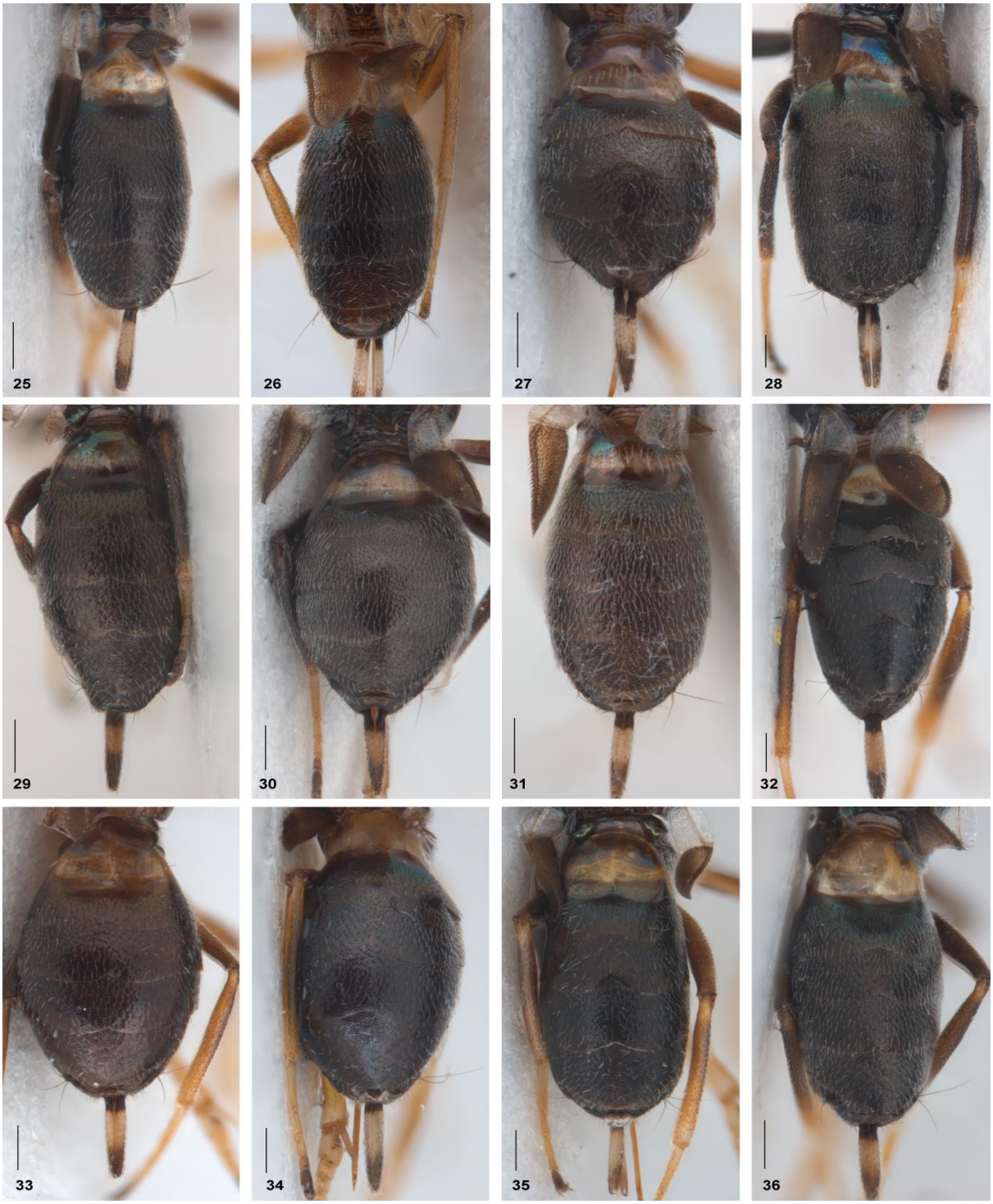

Figs. 25-36. Metasoma in females of the *Eupelmus vesicularis* species complex: *E. albitarsis* 10314 from Ftance (**25**); *E. albitarsis* from Italy (**26**); *E. barai/G1* 10525 from Moldova (**27**); *E. barai/G2* 10574 from Hungary (**28**); *E. barai/G6* 10080 from France (**29**); *E. barai/G6* 10634 from France (**30**); *E. barai/G3* 10523 from Spain (**31**); *E. maralpinus/G4* 10641 from France (**32**); *E. messene* 10514 from Romania (**33**); *E. myopitae/G5* 10303 from France (**34**); *E. vesicularis* 10535 from Sweden (**35**); *E. vesimodicus* 10643 from France (**36**). Scale bar 0.2 mm.

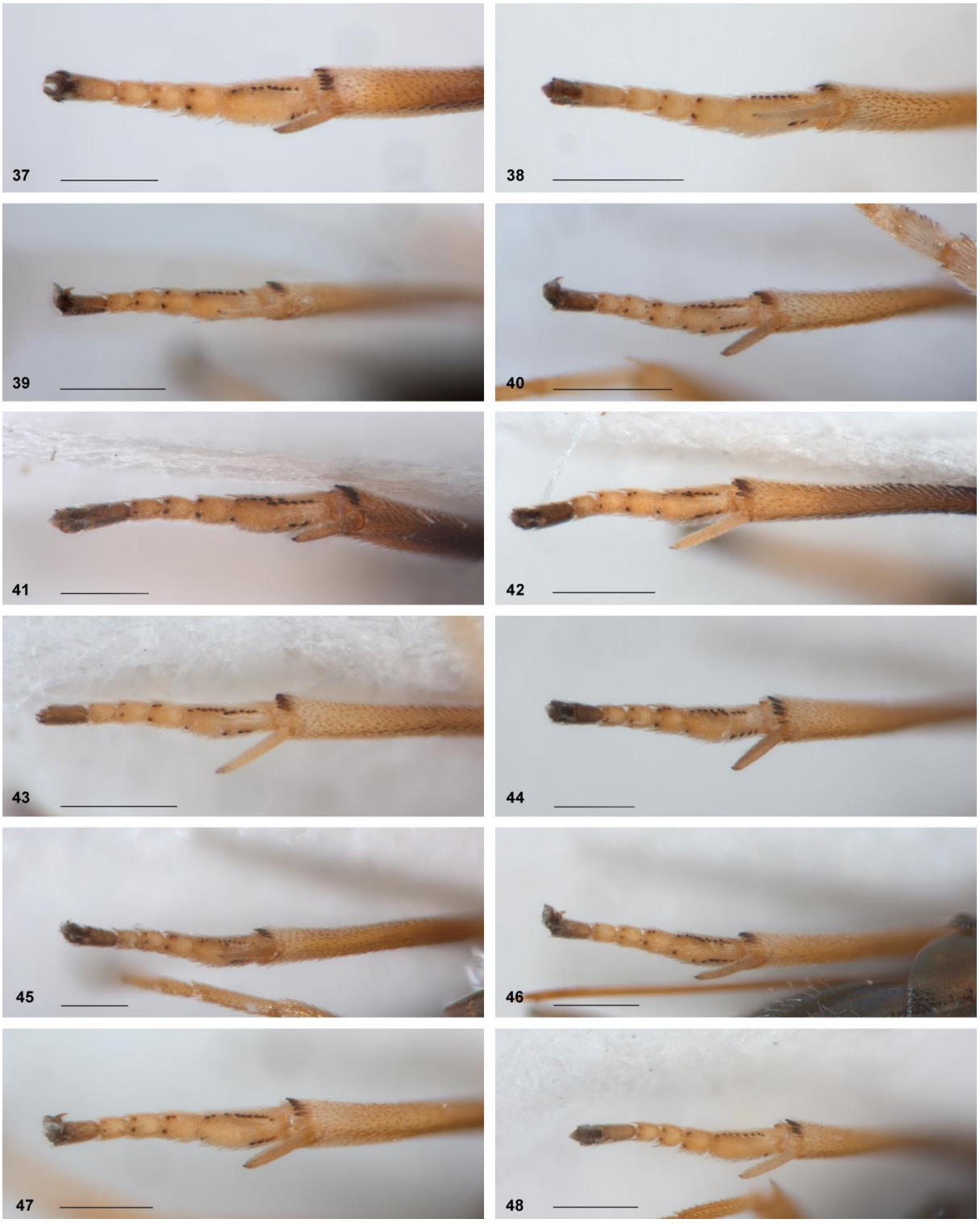

Figs. 37-48. Mesotarsus in females of the *Eupelmus vesicularis* species complex: *E. albitarsis* 10262 from Ftance (**37**); *E. albitarsis* from Italy (**38**); *E. albitarsis* 10528 from Ftance (**39**); *E. barai/G1* 10525 from Moldova (**40**); *E. barai/G2* 10086 from Hungary (**41**); *E. barai/G6* 10634 from France (**42**); *E. barai/G3* 10523 from Spain (**43**); *E. maralpinus/G4* 10641 from France (**44**); *E. messene* 10514 from Romania (**45**); *E. myopitae/G5* 10265 from France (**46**); *E. vesicularis* 10535 from Sweden (**47**); *E. vesimodicus* 10643 from France (**48**). Scale bar 0.2 mm.

Discussion

Face to the drawbacks emerged from using the mitochondrial DNA markers alone − especially the *COI* gene sequences − as an ideal genetic markers for species identification and investigation of biodiversity (Mortiz & Cicero, 2004; Rubinoff *et al*., 2006; Galtier *et al*., 2009), many studies have shown the great necessity to combine different types of data in one approach known as integrative taxonomy to improve the species delimitation (Dayrat, 2005; Will *et al.*, 2005, Padial *et al.,* 2010). In fact, the integrative taxonomy has proven to be an efficient approach in the disentangling of species groups/complexes containing closely related species (Al khatib *et al.*, 2014; Delvare *et al.*, 2014; Lecocq *et al.*, 2015; Gebiola *et al*., 2015a), cryptic species which are indistinguishable morphologically (Gebiola *et al.*, 2012 & 2015b) or in revealing the discordance between the different types of data such as the mito-nuclear discordance (Dasmahapatra *et al.*, 2010; Wiens *et al.*, 2010; Deuve *et al.*, 2012; Toews and Brelsford, 2012).

In the present study, we have compared the performance of several information sources including mtDNA markers (*COI* and *Cytb*), nucDNA markers (*ITS2*, *RpL27a*, *EF-1Ŭ* and *Wg*) and morphological diagnosis in disentangling of the *vesicularis* SC. Our results from the *vesicularis* SC show a general concordance and three cases of inconsistencies between the different types of data used in this study as will be discussed below.

Both the phylogenetic trees produced from the mitochondrial genes *COI* and *Cyt*b and the concatenated nuclear genes revealed congruent genetic divisions between three clades (Figs. 1, 2, S1). These clades represent species – namely *E. albitarsis*, *E. messene* and *E. vesicularis* – the first two being confused with *E. vesicularis* and considered its synonyms (e.g., Ruschka, 1921; Gibson, 1990). Also morphological evidence re-enforced the molecular discrimination. While the specific status of *E. messene* was recently re-established (Fusu, submitted) we here removed *E. albitarsis* from synonymy with *E. vesicularis* and consider it a valid species.

- Discripancies between mitochondrial markers and nuclear markers in the "*E. barai*" clade

The clade named "*E. barai*" was found to be monophyletic in the mtDNA trees but with deep divisions between the 6 clades and coded *G1* to *G6*, suggesting that each clade could be a putative species (Figs. 1, S1). This impression is re-enforced by the use of the Generalized

Mixed Yule Coalescent approach (GMYC) which leads to even a larger number of putative species. However, the monophyly for most of these clades was not supported neither with the combined nucDNA markers nor with morphology. In addition, unlike mtDNA markers, neither individual nuclear markers nor combined nucDNA dataset did not support the monophyly of all of the clades referred as "*E. barai*" (Figs. 2, S2-S6), although clade *G5* is supported by a congruent pattern of monophyly for the *RpL27a* and *COI*. Conversely, all these six clades nested together in a single large cluster in the combined nucDNA tree (Fig. 2). Clades *G3* and *G6* are part of a single monophyletic lineage. Contrary to the expectations, clades *G4* and *G5* instead of being close to clades *G3* and *G6* as it would be expected giving the close geographic proximity (Fig. S7) are nested within the Eastern clades *G1* and G2 (Fig. 2). This suggests a long separation history and migration of clades *G4* and G5 from distinct glacial refuges, perhaps along Southern Alps from the Balkan Peninsula and not local differentiation.

How to explain the discordance between mtDNA and combined nucDNA datasets concerning the number of clades here included in the "*E. barai*" clade? It might be hypothesized that the nuclear DNA genes used may not be variable enough to detect small differences between such closely related species detected by more rapidly evolving mtDNA markers. However several nuclear genes used in this study and especially *ITS2* and *RpL27a* are known to have an elevated rate of substitution allowing them to be appropriate nuclear markers to detect interspecific divergences among closely related species (Campbell *et al.*, 1993; Wilkerson *et al*., 2004; Yara, 2006; Ercan *et al*., 2011; Cruaud *et al.*, 2013; Kol-Maimon *et al.*, 2014). Nevertheless there is some evidence indicating that the information from the mitochondrial genes might be erroneous. The six clusters included within the "*E. barai* clade" correspond to populations sampled in different geographic areas (Table 1; Figs 1, S7). The brachypterous females of the *vesicularis* SPG exhibit limited capacities of dispersion. Consequently restricted gene flows of mitochondrial genes should occur between these isolated populations. As the mitochondrial genome is maternally transmitted, it might be assumed that the relevant populations accumulate mutations in their mitochondrial genome over the time, which increased to high frequency via genetic drift. As a result these genetically divergent populations could end up with a large genetic distance in their mtDNA (Toews & Brelsford, 2012). Conversely to the females, males of the "*E. barai* clade" are winged and are known for clades *G1*, *G2* and *G3* (Fusu, submitted). Winged insects exhibit powerful dispersal capacities, allowing a regular gene flow of the nuclear genome of different

gene pools, leading to homogenization of the nuclear genes among these populations, and the pattern observed on the combined nucDNA dataset could be a result of historical introgression between the six groups. This mito-nuclear genomic dissociation in species of male-biased dispersal is expected and not surprising, given that it was detected even in such large species as elephants (Roca *et al.*, 2005). In addition, the morphological data mostly support the molecular clustering based on the combined nucDNA dataset except for clades G4 and G5. As a result, we conclude that the mtDNA genes used in this study fail in providing a correct picture of species diversity and molecular discrimination of the populations in such a group of taxa as the "*E. barai* clade" could be misleading.

Though introgression between species of *vesicularis* SG cannot be completely excluded, we think that it is not the most likely explanation of the observed high level of paraphyly at the nuclear loci for many of the mtDNA clades of the "*E. barai* clade". The species pair *E. vesicularis* and *E. messene* is retrieved as sister species in our analyses of both mtDNA markers (Figs. 1, S1) and of two nuclear loci (*RpL27a* and *Wg*; Figs. S4, S6). Otherwise the two species are identical for *EF-1Ŭ*(Fig. S5) and *28S-D2* (Fusu, submitted) loci and there is a pattern of polyphyly for the *ITS2* locus (Figs. S2, S3). We attribute this pattern to incomplete lineage sorting following a comparatively recent speciation event rather than to recent introgression, as hybridisation between this two species is highly improbable. Though this is unknown for *E. messene*, in other species that reproduce by thelytokous parthenogenesis for long enough this can become irreversible, as for the well documented case of *Muscidifurax uniraptor* Kogan & Legner (Gottlieb & Zchori-Fein, 2001). The explanation is that if purifying selection on characters involved in mating ceases, this leads after some time to loss of function and to irreversible thelytoky. Though we did not use a molecular clock in our phylogenetic analyses due to the lack of an adequate calibration point, if we apply a molecular clock of 3.5% per myr (Papadopoulou *et al.,* 2010), this would translate into 2.9 myr divergence time, given the 10% mean uncorrected pairwise distance between the *COI* sequences of *E. vesicularis* and *E. messene*.

A pattern of paraphyly is a normal step during the incipient stages of speciation due to incomplete lineage sorting (Avise & Ball, 1990; Cummings *et al.,* 2008) and it is frequent between closely related species (Funk & Omland, 2003). In correlation with other sources of data, a distinct monophyletic lineage that renders its parental species paraphyletic should not be declined species status for this reason alone (Bond & Stockman, 2008) and on this ground we recognise lineages G4 and G5 as species (*E. maralpinus* and *E. myopitae*).

As suggested by Petit & Excoffier (2009) the accuracy in species delimitation is higher when based on genetic markers that exhibit stronger intraspecific gene flow. Though their finding is explained by the assumption that higher gene flow will minimise the effect of introgression from closely related species, this is true also in our case but for different reasons. As females of our model group are flightless and with the exception of *E. messene* that was transported due to human activities (Fusu, submitted) have reduced mobility, the genetic drift in small isolated populations can relatively rapidly generate a pattern of reciprocal monophyly for the mtDNA marker and produce an inflation of putative species. For this reason we give more weight to the nuclear markers. Hence we do not interpret mtDNA lineages as distinct species, but distinctiveness for nucDNA in parapatry, even if paraphyletic, correlated with morphological differentiation are considered sufficient to recognise a lineage as a species.

- Discrepancies between nuclear genes exhibiting different rates of evolution

The individual topologies resulting from the nuclear markers used in this study (*Wg*, *EF-1Ŭ*, *RpL7a* and *ITS2*) revealed some discordance suggesting a diverse rate of evolution among the different nuclear loci (Figs. S2-S6) and thereby these inconsistencies could be as a result of incomplete lineage sorting. Unlike *EF-1Ŭ* and *Wg* gene sequences which showed a weak power in differentiating the species of the *vesicularis* SC (Figs. S5, S6) and which could be consistent to some extent with previous findings especially for to *EF-1Ŭ* (Cho *et al.*, 1995; Rokas *et al.*, 2002; Cruaud *et al.*, 2013), *RpL27a* and *ITS2* gene sequences revealed a good resolution of the species (Figs. S3, S4) and these results might be concordant with those found in previous studies (references indicated above). However, problems of amplification and intra-individual sequence heterogeneity reflecting *ITS2* paralogs or pseudogenes were detected in the *ITS2* gene and it was documented that this phenomenon could be common in both nuclear as and mitochondrial genomes (Tang *et al.*, 1996; Sword *et al.*, 2007; Magnacca & Brown, 2010; Berthier *et al.*, 2011). The gene topology resulting from the reduced set of *ITS2* sequences (Fig. S3) selected for the combined nucDNA dataset using the estimation of both secondary structure and the free energy (dG) for each *ITS2* variant (Kita & Ito, 2000) was quite similar to those based empirically on the eliminating the clones placed on a long branch or grouped with the wrong clade (tree not published). Moreover, this reduced topology was essentially the same with that based on the complete *ITS2* sequences (Fig. S3; Table S1). As a result, we consider that our approach of selecting between the multiple variants of *ITS2* could be applicable to other taxa with intra-individual sequence heterogeneity in *ITS*.

- Discripancies between molecular results and morphological characters

The clade *E. vesimodicus* was monophyletic in both mitochondrial and combined nuclear trees and is not the sister species of *E. vesicularis* (Figs. 1, 2), showing that *E. vesimodicus* diverged as a distinct species since the process of lineage sorting is complete for all investigated mtDNA and nucDNA loci. Nevertheless the females of the two species, *E. vesimodicus* and *E. vesicularis*, are hardly morphologically differentiable.

On the other hand, four of the six clusters included in "*E. barai*" are to a large extent morphologically identical but especially the specimens reared from *M. stylata* (lineage G5) differ in the colouration of their mesoscutum, a tricoloured body pattern, and sparser setation on metasoma. The influence of the host on the imaginal morphology of the parasitoids – especially on their colouration – has already been documented in other families (Delvare, 2005; Delvare *et al.*, 2014). In this case we tend to exclude this explanation as we also obtained a specimen of *E. albitarsis* from *M. stylata* and it is morphologically similar to other members of its species. Also lineage G5, similar to lineage *G4*, is closer phylogenetically to the Eastern lineages *G1* and *G2* (Fig. 2), thus indicating that the presence of this morphologically differentiated lineages in South France could be also explained by recent colonisation from a different glacial refugium. This hypothesis is also sustained by the complete lineage sorting for *RpL27a* between *G5* and G6 that is hard to explain for parapatric populations of the same species when it is absent for example within lineages *G1*, *G2* and *G3* separated by much larger distances (Fig. S4).

- Evaluation of the generalized mixed Yule-coalescent (GMYC), ABGD and SpeciesID methods

Beside the phylogenetic reconstructions based on the mtDNA and nucDNA datasets and morphological differentiation used in delimitation of the *vesicularis* SC, we tested the performance of the generalized mixed Yule-coalescent (GMYC) method and two distance based methods (ABGD and SpeciesID) using the *COI* dataset in the disentangling the species of this complex. Because GMYC method has been particularly developed for single-locus sequences and does not require any previous information about the species under investigation, it became one of the most popular approaches for species delimitation and biodiversity assessments (Pons *et al.*, 2006; Ceccarelli *et al.*, 2012; Fujita *et al.*, 2012; Fujisawa & Barraclough, 2013; Talavera *et al.*, 2013). In the present study, the total number of species/entities estimated by GMYC method was higher than the number of putative

species recognised based on both genetic (mtDNA and nucDNA genes) and morphological differentiations. This is especially true for the multiple-threshold version of the method, and we can confirm the demonstration on simulated data that the single-threshold method outperforms the multiple-threshold method of GMYC (Fujisawa and Barraclough, 2013). Indeed, it has been claimed that GMYC method is sensitive to detect potential cryptic species when morphospecies are divided into two or more GMYC entities (Ceccarelli *et al.*, 2012). However, as discussed above that the clades or the species recovered in mtDNA phylogeny (Fig. 1) are characterized by a great genetic diversity due the limited flow of mtDNA between the different geographically isolated populations, we think that GMYC method similar to distance based algorithms fail in species delimitation in groups characterized by male-biased dispersal as in *vesicularis* SC whose females brachypterous and have a low dispersal ability. The ABGD and SpeciesID performed relatively better but this is due, at least for SpeciesID, to a previous knowledge of inter- and intraspecific differences within a species complex of the same genus.

As a final remark we emphasise that in cases of recent or on-going speciation events where there is incomplete lineage sorting, as seemingly is the case of *vesicularis* SC, genetic data alone are not sufficient for sound species delimitations. In such cases additional, non-genetic data such as geographical, morphological or ecological data can be used (Bond & Stockman, 2008; Padial *et al.*, 2010, Puillandre *et al*., 2012, Hendrixson *et al.,* 2013). The present study evidenced the relevance of including multiple information sources in the segregation of closely related species suffering from a lake of discriminatory morphological characters and displaying particular biological features such as the low mobility in females and male-biased dispersal, as in our case of *vesicularis* SC which otherwise could result in inconsistencies between the different adopted approaches of species delimitation.

Acknowledgements:

This research was directly supported by the projects “EUPELMUS” (Scientific Department “Santé des Plantes et Environnement” of INRA - grant 2012-04-05-20), “INULA” (APR Pesticides 2011: “Changer les pratiques agricoles pour préserver les services écosystémiques”) and ‘BIOFIS’ (number 1001-001) allocated by the French Agropolis Fondation (Montpellier). This study also took benefits from field work realised in the frame

of the projects “BIOINV-4I” (ANR-06-BDIV-008 – Coordinator: Thomas Guillemaud), “Lutte biologique contre le Cynips du Châtaignier” (ONEMA 2011 – Coordinator: Nicolas Borowiec and Jean-Claude Malausa), and the Swedish Malaise Trap Project (SMTP). Part of the collectings in the Alps were supported by the European Network "EDIT" Work package 7 (European Distributed Institute of Taxonomy) during the ATBI+M (All Taxa Biodiversity Inventory + Monitoring) activities in National Park of Mercantour and Alpi Marittime. We are especially relevant to Marie-France Leccia, head of this ATBI, for facilities given during the different trips and kind assistance. The authors want to thank Sylvie Warot and Gwenaelle Genson for their contribution to the molecular work.

References

Al khatib, F., Fusu, L., Cruaud, A., Gibson, G., Borowiec, N., Rasplus, J-Y., Ris, N., Delvare, G. (2014) An integrative approach to species discrimination in the *Eupelmus urozonus* complex (Hymenoptera, Eupelmidae), with the description of 11 new species from the Western Palaearctic. *Systematic Entomology*, 39, 806–862.

Al khatib, F., Cruaud, A., Fusu, L., Rasplus, J.-Y., Ris, N. & Delvare, G. (submitted) Ecological differentiation in the “*Eupelmus urozonus* species group” (Hymenoptera, Eupelmidae) occurring in the West-Palaearctic: first insights based on a multi-locus phylogeny and reliable host records. *BMC Evolutionary Biology*.

Armstrong, K.F. & Ball, S.L. (2005) DNA barcodes for biosecurity: invasive species identification. *The Philosophical Transactions of the Royal Society*, 360, 1813–1823.

Askew, R.R. & Nieves-Aldrey, J.L. (2000) The genus *Eupelmus* Dalman, 1820 (Hymenoptera, Chalcidoidea, Eupelmidae) in peninsular Spain and the Canary Islands, with taxonomic notes and descriptions of new species. *Graellsia*, 56, 49–61.

Avise, J.C. & Ball Jr., R.M. (1990) Principles of genealogical concordance in species concepts and biological taxonomy. *Oxford Surveys in Evolutionary Biology* 7, 45–67.

Bazinet, A.L. & Cummings, M.P. (2008) The Lattice Project: a grid research and production environment combining multiple grid computing models. Pages 2-13. In Weber, M. H. W. (Ed.) Distributed & Grid Computing - Science Made Transparent for Everyone. Principles, Applications and Supporting Communities. Rechenkraft.net, Marburg.

Bergsten, J., Bilton, D.T., Fujisawa T *et al*. (2012) The effect of geographical scale of sampling on DNA barcoding. *Systematic Biology*, 61, 851–869.

Berthier, K., Chapuis, M.-P., Moosavi, S.M., Tohidi-Esfahani, D. & Sword, G.A. (2011) Nuclear insertions and heteroplasmy of mitochondrial DNA as two sources of intra-individual genomic variation in grasshoppers. *Systematic Entomology*, 36, 285–299.

Birky, C.W., Fuerst, P. & Maruyama, T. (1989) Organelle gene diversity under migration, mutation and drift: equilibrium ex-pectations, approach to equilibrium, effects of heteroplasmic cells, and comparison to nuclear genes. *Genetics*, 121, 613–627.

Blaxter, M. (2003) Counting angels with DNA. *Nature*, 421, 122–124.

Bond, J. E., Stockman, A. K. (2008) An integrative method for delimiting cohesion species: finding the population-species interface in a group of Californian trapdoor spiders with extreme genetic divergence and geographic structuring. Systematic Biology, 57, 628–646.

Bouček, Z. (1988) Australasian Chalcidoidea (Hymenoptera). A Biosystematic Revision of Genera of Fourteen Families, with a Reclassification of Species. CAB International Institute of Entomology, The Cambrian News Ltd., Aberystwyth.

Brower, A. V. Z. (2006) Problems with DNA barcodes for species delimitation: 'ten species' of *Astraptes fulgerator* reassessed (Lepidoptera: Hesperiidae). Syst Biodivers 4 (2), 127–32.

Campbell, B.C., Steffen-Campbell, J.D. & Werren, J.H. (1993) Phylogeny of the *Nasonia* species complex (Hymenoptera: Pteromalidae) inferred from an internal transcribed spacer (*ITS2*) and *28s* rDNA sequences. *Insect Molecular Biology*, 2, 225–237.

Campbell, D.L., Brower, A.V.Z. & Pierce, N.E. (2000) Molecular evolution of the Wingless gene and its implications for the phylogenetic placement of the butterfly family Riodinidae (Lepidoptera: Papilionoidea). *Molecular Biology and Evolution*, 17, 684–696.

Caterino, M.S., Cho, S. & Sperling, F.A.H. (2000) The current state of insect molecular systematics: a thriving Tower of Babel. *Annual Review of Entomology*, 45: 1–54.

Ceccarelli, F.S., Sharkey, M.J. & Zaldívar-Riverón, A. (2012) Species identification in the taxonomically neglected, highly diverse, neotropical parasitoid wasp genus *Notiospathius* (Braconidae: Doryctinae) based on an integrative molecular and morphological approach. *Molecular Phylogenetics and Evolution*, 62, 485–495.

Cho, S., Mitchell, A., Regier, J.C., Mitter, C., Poole, R.W. *et al*. (1995) A highly conserved nuclear gene for low-level phylogenetics: Elongation Factor-1α recovers morphology-based tree for heliothine moths. *Molecular, Biology and Evolution,* 12, 650–656.

Cruaud, A., Jabbour-Zahab, R., Genson, G., Cruaud, C., Couloux, A. *et al*. (2010) Laying the foundations for a new classification of Agaonidae (Hymenoptera: Chalcidoidea), a multilocus phylogenetic approach. Cladistics, 26, 359–387.

Cruaud, A., Underhill, J.-G., Huguin, M., Genson, G., Jabbour-Zahab, R., Tolley, K.A., Rasplus, J.-Y. & Noort, S.V. (2013) Multilocus Phylogeny of the World Sycoecinae Fig Wasps (Chalcidoidea: Pteromalidae). PLoS ONE. 8, e79291. doi:10.1371/journal.pone.0079291.

Cummings, M.P., Neel, M.C. & Shaw, K.L. (2008) A genealogical approach to quantifying lineage divergence. *Evolution*, 1–12. doi:10.1111/j.1558-5646.2008.00442.x.

Danforth, B.N., Linl, C. & Fang, J. (2005) How do insect nuclear ribosomal genes compare to protein-coding genes in phylogenetic utility and nucleotide substitution patterns? *Systematic Entomology*, 30, 549–562.

Dasmahapatra, K.K., Elias, M., Hill, R.I., Hoffman, J.I. & Mallet, J. (2010) Mitochondrial DNA barcoding detects some species that are real, and some that are not. *Molecular Ecology Resources*, 10, 264–273.

Dayrat, B. (2005) Towards integrative taxonomy. *Biological Journal of the Linnean Society*, 85, 407–415.

Delvare, G. (2005) A revision of the West-Palearctic *Podagrion* (Hymenoptera: Torymidae), with the description of *Podagrion bouceki* sp. nov. *Acta Societatis Zoologicae Bohemoslovenicae*, 69, 65–88.

Delvare, G., Gebiola, M., Zeiri, A. & Garonna, A.P. (2014) Revision and phylogeny of the European species of the *Eurytoma morio* species group (Hymenoptera: Eurytomidae), parasitoids of bark and wood boring beetles. *Zoological Journal of the Linnean Society*, 171, 370–421.

Deuve, T., Cruaud, A., Genson, G., Rasplus, J.-R. (2012) Molecular systematics and evolutionary history of the genus *Carabus* (Col. Carabidae*). Molecular Phylogenetics and Evolution*, 65, 259–275.

Drummond, A.J. & Rambaut, A. (2007) "BEAST: Bayesian evolutionary analysis by sampling trees." *BMC Evolutionary Biology*, 7:214.

Edgar, R.C. (2004) MUSCLE: Multiple sequence alignment with high accuracy and high throughput. *Nucleic Acids Research*, 32, 1792–1797.

Elias, M., Hill, R.I., Willmott, K.R., Dasmahapatra, K.K., Brower, A.V.Z., Mallet, J. & Jiggin, C.D. (2007) Limited performance of DNA barcoding in a diverse community of tropical butterflies. *Proceedings of the Royal Society B*, 274, 2881–2889.

Ercan, F.S., Oztemiz, S., Tuncbilek, A.S. & Stouthamer, R. (2011) Sequence analysis of the ribosomal and *ITS2* region in two *Trichogramma* species (Hymenoptera: Trichogrammatidae). *Archives of Biological Science*, 63, 949–954.

Ferrière, Ch. (1954) Eupelmides brachyptères (Hym. Chalcidoidea). *Mitteilungen der Schweizerischen Entomologischen Gesellschaft*, 27, 1−21.

Fisher, B.L. & Smith, M.A. (2008) A revision of Malagasy species of *Anochetus* Mayr and *Odontomachus* Latreille (Hymenoptera: Formicidae). *PLoS ONE*, 3, e1787.

Folmer, O., Black, M., Hoeh, W., Lutz, R. & Vrijenhoek, R. (1994) DNA primers for amplification of mitochondrial cytochrome c oxidase subunit I from diverse metazoan invertebrates. *Molecular Marine Biology and Biotechnology*, 3, 294–299.

Fujisawa, T. & Barraclough, T.G. (2013) Delimiting species using single-locus data and the generalized mixed Yule coalescent approach: A revised method and evaluation on simulated data sets. *Systematic Biology*, 62, 707–724.

Fujita, M.K, Leaché, A.D., Burbrink, F.T., McGuire, J.A. & Moritz, C. (2012) Coalescent-based species delimitation in an integrative taxonomy. *Trends in Ecology and Evolution*, 27, 480–488.

Funk, D.J. & Omland, K.E. (2003) Species-level paraphyly and polyphyly: frequency, causes, and consequences, with insights from animal mitochondrial DNA. *Annual Review of Ecology, Evolution and Systematics*, 34, 397–423.

Fusu, L. (2010) Species status of two color morphs of *Eupelmus vesicularis* (Hymenoptera: Eupelmidae) as revealed by allozyme electrophoresis, morphometric and host preference data. *Journal of Natural History*, 44, 1113–1129.

Fusu, L. (Submitted) A revision of European *Eupelmus* (*Macroneura*) (Hymenoptera, Chalcidoidea, Eupelmidae), with a molecular and cytogenetic analysis of *Eupelmus* (*Macroneura*) *vesicularis*: several species hiding under one name for 240 years.

Galtier, N., Nabholz, B. Glémin, S. & Hurst, G.D.D. (2009) Mitochondrial DNA as marker of molecular diversity: a reappraisal. *Molecular Ecology*, 18, 4541–4550.

Gebiola, M., Bernardo, U., Monti, M.M., Navone, P. & Viggiani, G. (2009) *Pnigalio agraules* (Walker) and *Pnigalio mediterraneus* Ferriere and Delucchi (Hymenoptera: Eulophidae): two closely related valid species. *Journal of Nature History*, 43, 2065–2480.

Gebiola, M., Gomez-Zurita, J., Monti, M.M., Navone, P. & Bernardo, U. (2012) Integration of molecular, ecological, morphological and endosymbiont data for species delimitation within the *Pnigalio soemius* complex (Hymenoptera: Eulophidae). *Molecular Ecology*, 21, 1190–1208.

Gebiola, M., Bernardo. U., Ribes, A., Gibson, G.A.P. (2015a) An integrative study of *Necremnus* Thomson (Hymenoptera: Eulophidae) associated with invasive pests in Europe and North America: taxonomic and ecological implications. *Zoological Journal of the Linnean Society*, 173, 352–423.

Gebiola, M., White, J.A., Cass, B.N., Kozuch, A., Harris, L.R., Kelly, S.E., Karimi, J., Giorgini, M., Perlman., S.J. & Hunter, M.S. (2015b) Cryptic diversity, reproductive isolation and cytoplasmic incompatibility in a classic biological control success story. *Biological Journal of the Linnean Society* (in press).

Geyer, C.J. (1991) Markov chain Monte Carlo maximum likelihood. In Keramidas, E. M., Computing Science and Statistics: Proceedings of the 23rd Symposium on the Interface. Interface Foundation, Fairfax Station, pp. 156–163.

Gibson, G.A.P. (1990) Revision of the genus *Macroneura* Walker in America North of Mexico (Hymenoptera: Eupelmidae). *Canadian Entomologist*, 122, 837–873.

Gibson, G.A.P. (1995) Parasitic wasps of the subfamily Eupelminae: classification and revision of world genera (Hymenoptera: Chalcidoidea, Eupelmidae). *Memoirs on Entomology, International*, 5, i-v + 421 pp.

Gibson, G.A.P. (2011) The species of *Eupelmus (Eupelmus*) Dalman and *Eupelmus* (*Episolindelia*) Girault (Hymenoptera: Eupelmidae) in North America north of Mexico. *Zootaxa*, 2951, 1–97.

Gibson, G.A.P. & Fusu, L. (submitted) Revision of the Palaearctic species of *Eupelmus* (*Eupelmus*) Dalman (Hymenoptera: Chalcidoidea: Eupelmidae). *Zootaxa*.

Gibson, G.A.P., Huber, J.T. & Woolley, J.B. (1997) Annotated Keys to the Genera of Nearctic Chalcidoidea (Hymenoptera). NRC Research Press, Ottawa.

Giraud J. (1863) Mémoire sur les insectes qui vivent sur le roseau commun, *Phragmites communis* Trin. (*Arundo phragmites* L.) et plus spécialement sur ceux de l'ordre des Hyménoptères. *Verhandlungen der Zoologisch-Botanischen Gesellschaft in Wien*, 13, 1251–1288.

Goldstein, P.Z. & DeSalle, R. (2011) Integrating DNA barcode data and taxonomic practice: Determination, discovery, and description. *Bioessays*, 33, 135–147.

Gottlieb, Y. & Zchori-Fein, E. (2001) Irreversible thelytokous reproduction in *Muscidifurax uniraptor*. *Entomologia Experimentalis et Applicata*, 100, 271–278.

Gouy, M., Guindon, S. & Gascuel, O. (2010) SeaView version 4: A multiplatform graphical user interface for sequence alignment and phylogenetic tree building. *Molecular Biology and Evolution*, 27, 221–224.

Gu, X., Fu, Y.-X. & Li, W.-H. (1995) Maximum likelihood estimation of the heterogeneity of substitution rate among nucleotide sites. *Molecular Biology and Evolution*, 12, 546–557.

Hebert, P.D.N., Cywinska, A., Ball, S.L. & De Waard, J.R. (2003a) Biological identifications through DNA barcodes. *Proceedings of the Royal Society Biological Sciences Series B*, 270, 313–321.

Hebert, P.D.N., Penton, E.H., Burns, J.M., Janzen, D.H. & Hallwachs, W. (2004) Ten species in one: DNA barcoding reveals cryptic species in the neotropical skipper butterfly *Astraptes fulgerator*. *Proceedings of the National Academy of Sciences of the United States of America*, 101, 14812–14817.

Hebert, P.D.N., Ratnasingham, S. & deWaard, J.R. (2003b) Barcoding animal life: cytochrome oxidase subunit 1 divergences among closely related species. *Proceedings of the Royal Society Series B*, 270, S96–S99.

Hendrixson, B.E., DeRussy, B.M., Hamilton, C.A., Bond, J.E. (2013) An exploration of species boundaries in turret-building tarantulas of the Mojave Desert (Araneae, Mygalomorphae, Theraphosidae, Aphonopelma). *Molecular Phylogenetics and Evolution*, 66, 327-340.

Hickerson, M.J., Meyer C.P. & Moritz C. (2006) DNA barcoding will often fail to discover new animal species over broad parameter space. *Systematic Biology*, 55, 729–739.

Hurst, G.D.D. & Jiggins, F.M. (2005) Problems with mitochondrial DNA as a marker in population, phylogeographic and phylogenetic studies: the effects of inherited symbionts. *Proceedings of the Royal Society B*, 272, 1525–1534.

Ihaka, R. & Gentleman, R. (1996) R: a language for data analysis and graphics. *Comput Graph Stat*, 5, 299–314.

Jinbo, U., Kato, T. & Ito, M. (2011) Current progress in DNA barcoding and future implications for entomology. *Entomological Science*, 14, 107–124.

Jordal, B. & Kambestad, M. (2014) DNA barcoding of bark and ambrosia beetles reveals excessive NUMTs and consistent east-west divergence across Palearctic forests. *Molecular Ecology Resources*, 14, 7–17.

Kalina, V. (1981) The Palearctic species of the genus *Macroneura* Walker, 1837 (Hymenoptera, Chalcidoidea, Eupelmidae), with descriptions of new species. Sbornik Vedeckeho Lesnickeho Ustavu Vysoke Skoly Zemedelske v Praze, 24, 83–111.

Kimura, M. (1980) A simple method for estimating evolutionary rates of base substitutions through comparative studies of nucleotide sequences. *Journal of Molecular Evolution*, 16, 111–120.

Kita, Y. & Ito, M. (2000) Nuclear ribosomal *ITS* sequences and phylogeny in East Asian *Aconitum* subgenus Aconitum (Ranunculaceae), with special reference to extensive polymorphism in individual plants. *Plant Systematics and Evolution*, 225, 1–13.

Lecocq, T., Dellicour, S., Michez, D., Dehon, M., Dewulf, A., De Meulemeester, T., Brasero, N., Valterová, I., Rasplus, J.-Y. & Rasmont, P. (2014) Methods for species delimitation in bumblebees (Hymenoptera, Apidae, *Bombus*): towards an integrative Approach. *Zoologica Scripta*, doi:10.1111/zsc.12107.

Magnacca, K. & Brown, M.J.F. (2010) Mitochondrial heteroplasmy and DNA barcoding in Hawaiian *Hylaeus* (*Nesoprosopis*) bees (Hymenoptera: Colletidae). *BMC Evolutionary Biology*, 10:174.

Meier, R., Kwong, S., Vaidya, G. & Ng, P.K.L. (2006) DNA Barcoding and taxonomy in Diptera: a tale of high intraspecific variability and low identification success. *Systematic Biology*, 55, 715–728.

Meyer, C.P. & Paulay, G. (2005) DNA barcoding: error rates based on comprehensive sampling. *PLOS Biology*, 3, 1–10.

Miller, M.A., Pfeiffer, W. & Schwartz, T. (2010) Creating the CIPRES Science Gateway for inference of large phylogenetic trees. New Orleans, 1–8.

Monaghan, M.T., Balke, M., Pons, J. & Vogler, A.P. (2006) Beyond barcodes: complex DNA taxonomy of a South Pacific Island radiation. *Proceedings of the Royal Society B*, 273, 887–893.

Mortiz, C. & Cicero, C. (2004) DNA Barcoding: Promise and Pitfalls. *PLoS Biology*, 2: e354.

Noyes, J.S. (1982) Collecting and preserving chalcid wasps. *Journal of Natural History*, 16, 315–334.

Padial, J.M., Miralles, A., De la Riva, I., Vences, M. (2010) The integrative future of taxonomy. *Frontiers in Zoology*, 7, 16.

Papadopoulou, A., Anastasiou, I. & Vogler, A. P. (2010) Revisiting the insect mitochondrial molecular clock: The Mid-Aegean Trench calibration. *Molecular Biology and Evolution*, 27, 1659–1672.

Paradis, E., Claude, J. & Strimmer, K. (2004) APE: Analyses of Phylogenetics and Evolution in R language. *Bioinformatics*, 20, 289–90.

Parmakelis, A., Kotsakiozi, P., Stathi, I., Poulikarakou, S. & Fet, V. (2013) Hidden diversity of *Euscorpius* (Scorpiones: Euscorpiidae) in Greece revealed by multilocus species-delimitation approaches. *Biological Journal of the Linnean Society*, 110, 728–748.

Petit, R. J. & Excoffier L. (2009). Gene flow and species delimitation. *Trends in Ecology and Evolution*, 24, 386–393.

Palumbi, S.R., Cipriano, F. & Hare, M.P. (2001) Predicting nuclear gene coalescence from mitochondrial data: the three-times rule. *Evolution*, 55, 859–868.

Pons, J., Barraclough, T., Gomez-Zurita, J., Cardoso, A., Duran, D., Hazell, S., Kamoun, S., Sumlin, W. & Vogler, A. (2006) Sequence-based species delimitation for the DNA taxonomy of undescribed insects. *Systematic Biology*, 55, 595–610.

Posada, D. (2008) jModelTest: phylogenetic model averaging. *Molecular Biology and Evolution*, 25; 1253–1256.

Puillandre, N., Lambert, A., Brouillet S. & Achaz, G. (2012) ABGD, Automatic Barcode Gap Discovery for primary species delimitation. *Molecular Ecology*, 21, 1864–1877

Quicke, D. (2003) The world of DNA barcoding and morphology -collision or synergism and what of the future? *The Systematist*, 23, 8–16.

R Core Development Team, (2009) R: A language and environment for statistical computing. R Foundation for Statistical Computing, Vienna, Austria.

Rambaut, A., Suchard, M.A., Xie, D. & Drummond, A.J. (2014) Tracer v1.6, Available from [http://beast.bio.ed.ac.uk/Tracer].

Roca, A.L., Georgiadis, N. & O'Brien, S.J. (2005) Cytonuclear genomic dissociation in African elephant species. *Nature Genetics,* 37, 96–100.

Rokas, A., Nylander, J.A.A., Ronquist, F. & Stone, G.N. (2002) A Maximum-Likelihood analysis of eight phylogenetic markers in gallwasps (Hymenoptera: Cynipidae): Implications for insect phylogenetic studies. *Molecular Phylogenetics and Evolution*, 22, 206–219.

Ronquist, F., Teslenko, M., van der Mark, P., Ayres, D.L., Darling, A. *et al*. (2012) MrBayes 3.2: efficient Bayesian phylogenetic inference and model choice across a large model space. *Systematic Biology*, 61, 539–542.

Rubinoff, D., Cameron, S. & Will, K. (2006) A Genomic perspective on the shortcomings of mitochondrial DNA for ''barcoding'' identification. *Journal of Heredity*, 97, 581–594.

Ruschka, F. (1921) Chalcididenstudien I. *Verhandlungen der Zoologisch-Botanischen Gesellschaft in Wien,* 70, 234−315.

Shevtsova, E. & Hansson, C. (2011) Species recognition through wing interference patterns (WIPs) in *Achrysocharoides* Girault (Hymenoptera, Eulophidae) including two new species. *ZooKeys*, 154, 9-30.

Shevtsova, E., Hansson, C., Janzen, D.H. & Kjærandsen, J. (2011) Stable structural color patterns displayed on transparent insect wings. *Proceedings of the National Academy of Sciences of the United States of America*, 108, 668-673.

Shoemaker, D.D., Dyer, K.A., Ahrens, M., McAbee, K. & Jaenike, J. (2004) Decreased diversity but increased substitution rate in host mtDNA as a consequence of a *Wolbachia* endosymbiont infection. *Genetics*, 168, 2049–2058.

Smith, M.A., Fernández-Triana, J.L., Eveleigh, E., Gómez, J., Guclu, C., Hallwachs, W., Hebert, P.D.N., Harcek, J., Huber, J.J., Janzen, D., Mason, P.G., Miller, S., Quicke, D.L.J., Rodriguez, J.J., Rougerie, R., Shaw, M.R., Várkonyi, G., Ward, D.F., Whitfield, J.B. & Zaldívar-Riverón, A. (2013) DNA barcoding and the taxonomy of Microgastrinae wasps (Hymenoptera, Braconidae): impacts after 8 years and nearly 20 000 sequences. *Molecular Ecology Resources*, 13, 168−176.

Smith, M.A., Wood, D.M., Janzen, D.H., Hallwachs, W. & Hebert, P.D.N. (2007) DNA barcodes affirm that 16 species of apparently generalist tropical parasitoid flies (Diptera, Tachinidae) are not all generalists. *Proceedings of the Royal Society USA*, 104, 4967–4972.

Smith, M.A., Woodley, N.E., Janzen, D.H., Hallwachs, W. & Hebert, P.D.N. (2006) DNA barcodes reveal cryptic host-specificity within the presumed polyphagous members of a genus of parasitoid flies (Diptera: Tachinidae). *Proceedings of the National Academy of Sciences of the United States of America*, 103, 3657−3662.

Song, H., Buhay, J.E., Whiting, M.F., Keith A. & Crandall, K.A. (2008) Many species in one: DNA barcoding overestimates the number of species when nuclear mitochondrial pseudogenes are coamplified. *Proceedings of the National Academy of Sciences of the United States of America*, 105, 13486−13491.

Stamatakis, A. (2014) RAxML Version 8: A tool for Phylogenetic Analysis and Post-Analysis of Large Phylogenies. *Bioinformatics*, doi: 10.1093/bioinformatics/btu033.

Sword, G.A., Senior, L.B., Gaskin, J.F. & Joern, A. (2007) Double trouble for grasshopper molecular systematics: intra-individual heterogeneity of both mitochondrial 12S-valine-

16S and nuclear internal transcribed spacer ribosomal DNA sequences in *Hesperotettix viridis* (Orthoptera: Acrididae). *Systematic Entomology*, 32, 420–428.

Talavera, G., Dincă, V. & Vila, R. (2013) Factors affecting species delimitations with the GMYC model: insights from a butterfly survey. *Methods in Ecology and Evolution*, 4, 1101–1110.

Tamura, K., Peterson, D., Peterson, N., Stecher, G., Nei, M., Kumar, S. (2011) MEGA5: Molecular evolutionary genetics analysis using maximum likelihood, evolutionary distance, and maximum parsimony method. *Molecular Biology and Evolution*, 28, 2731–2739.

Tamura, K, Stecher, G, Peterson, D, Filipski, A, Kumar, S. (2013) MEGA6: Molecular Evolutionary Genetics Analysis Version 6.0. *Molecular Biology and Evolution*, 30, 2725-2729.

Tang, J., Toè, L., Back, C. & Unnasch, T.R. (1996) Intra-specific Heterogeneity of the rDNA Internal Transcribed Spacer in the *Simulium damnosum* (Diptera: Simuliidae) Complex. *Molecular, Biology and Evolution*, 13, 244–252.

Tautz, D., Arctander, P., Minelli, A., Thomas, R.H. & Vogler, A.P. (2003) A plea for DNA taxonomy. *Trends in Ecology and Evolution*, 18, 70−74.

Toews, D.P.L. & Brelsford, A. (2012) The biogeography of mitochondrial and nuclear discordance in animals. *Molecular Ecology*, doi: 10.1111/j.1365-294X.2012.05664.x.

Veijalainen, A., Broad, G.R., Wahlberg, N., Longino, J.T. & Sääksjärvi, I.E. (2011) DNA barcoding and morphology reveal two common species in one: *Pimpla molesta* stat. rev. separated from *P. croceipes* (Hymenoptera, Ichneumonidae). *ZooKeys*, 124, 59−70.

Venables, W.N. & Ripley, B.D. (2002) Modern applied statistics with S. Fourth Edition. Springer, New York.

Wiens, J., Kuczynski, C.A. & Stephens, P.R. (2010) Discordant mitochondrial and nuclear gene phylogenies in emydid turtles: implications for speciation and conservation. *Biological Journal of the Linnean Society*, 99, 445–461.

Wilkerson, R.C., Reinert, J.F. & Li, C. (2004) Ribosomal DNA *ITS2* Sequences Differentiate Six Species in the *Anopheles crucians* Complex (Diptera: Culicidae). *Molecular Biology/Genomics*, 41, 392–401.

Will, K.W., Mishler, B.D. & Wheeler, Q.D. (2005) The perils of dna barcoding and the need for integrative taxonomy. *Systematic Biology*, 54, 844–851.

Xiao, J-H., Wang, N-X., Li, Y-W., Murphy, R.W, Wan, D-G., Niu1, L-M., Hu, H-Y., Fu, Y-G. & Huang, D-W. (2010) Molecular approaches to identify cryptic species and polymorphic species within a complex community of fig wasps. *PLoS ONE*, 5: e15067.

Yara, K. (2006) Identification of *Torymus sinensis* and *T. beneficus* (Hymenoptera: Torymidae), introduced and indigenous parasitoids of the chestnut gall wasp *Dryocosmus kuriphilus* (Hymenoptera: Cynipidae), using the ribosomal *ITS2* region. *Biological Control*, 36, 15–21.

Yassin, A., Markow, T.A., Narechania, A., O'Grady, P.M. & DeSalle, R. (2010) The genus *Drosophila* as a model for testing tree- and character-based methods of species identification using DNA barcoding. *Molecular Phylogenetics and Evolution*, 57, 509–517.

Yu, M.Z., Zhang, K.J., Xue, X.F. & Hong, X. (2011) Effects of *Wolbachia* on mtDNA variation and evolution in natural populations of Tetranychus urticae Koch. *Insect Molecular Biology*, 20, 311–321.

Zuker, M. (2003) Mfold web server for nucleic acid folding and hybridization prediction. *Nucleic Acids Research*, 31, 3406–3415.

Supporting Information

Table S1. Selection of *ITS2* sequences used in combined nucDNA analysis based on stability of their secondary structure and their free energy.

Table S2. Genbank accession numbers for the specimens used in the phylogenetic analyses. The submission of sequences will be achieved as soon as possible.

Fig. S1. Phylogram figuring the relationships within the*vesicularis* complex based on the *Cytb* dataset alignment. Bootstrap Percentages (BP) ≥ 65 and Posterior Probabilities (PP) ≥ 0.90 are indicated at nodes. Each line represents a sequenced individual with information in the following order: molecular code, species/clade, country, insect host and associated plant.

Fig. S2. Topology obtained from ML analysis of the complete *ITS2* dataset. Bootstrap Percentages (BP) ≥65 are indicated at nodes. Each line represents a sequenced individual with information in the following order: molecular code, clone code, species/clade, country, insect host and associated plant.

Fig. S3. Topology obtained from ML analysis of the reduced *ITS2* dataset. Bootstrap Percentages (BP) ≥65 are indicated at nodes. Each line represents a sequenced individual with information in the following order: molecular code, clone code, species/clade, country, insect host and associated plant.

Fig. S4. Topology obtained from ML analysis of the *RpL27a* dataset. Bootstrap Percentages (BP) ≥65 are indicated at nodes. Each line represents a sequenced individual with information in the following order: molecular code, species/clade, country, insect host and associated plant.

Fig. S5. Topology obtained from ML analysis of the *EF-1Ŭ* dataset. Bootstrap Percentages (BP) ≥65 are indicated at nodes. Each line represents a sequenced individual with information in the following order: molecular code, species/clade, country, insect host and associated plant.

Fig. S6. Topology obtained from ML analysis of the *Wg* dataset. Bootstrap Percentages (BP) ≥65 are indicated at nodes. Each line represents a sequenced individual with information in the following order: molecular code, species/clade, country, insect host and associated plant.

Fig. S7. Geographical distribution of different mitochondrial clades of *vesicularis* SC.

Appendix S1. Recursive and primary partitions resulted from ABGD (Automated Barcode Gap Discovery) method based on *COI* dataset and with number of steps = 50 and X = 0.1

Appendix S2. Putative species within *vesicularis* SC detected using the GMYC (Generalized Mixed Yule Coalescent) method.

Table S1. Selection of *ITS2* sequences used in combined nucDNA analysis based on stability of their secondary structure and their free energy.

Molecular code-clone code	**mtDNA clade**	Molecular code-clone code mtDNA clade	dG (kcal/mol). Recalculated value	Structure nr according to initial dG	Absolute difference between the sequences with the smallest and largest free energy of the same specimen.
10516	E. messene	10516 E. messene	-214,15	3	
10621	E. messene	10621 E. messene	-210,25	4	
10618	E. messene	10618 E. messene	-210,25	4	
10532	E. messene	10532 E. messene	-214,95	4	
~~10533-C452~~	~~E. messene~~	~~10533-C452 E. messene~~	~~-213,45~~	3	0,4
10533-C453	E. messene	10533-C453 E. messene	-213,85	3	
10256-C467	E. messene	10256-C467 E. messene	-211,65	5	
10537	E. vesicularis	10537 E. vesicularis	-217,37	2	
10535	E. vesicularis	10535 E. vesicularis	-215,75	3	
~~10529~~	~~E. vesicularis~~	~~10529 E. vesicularis~~	~~-216,1~~	3	14,54
10529-C395	E. vesicularis	10529-C395 E. vesicularis	-218,59	2	
~~10529-C396~~	~~E. vesicularis~~	~~10529-C396 E. vesicularis~~	~~-204,05~~	4	
~~10529-C397~~	~~E. vesicularis~~	~~10529-C397 E. vesicularis~~	~~-214,15~~	4	
10624-C458	E. vesimodicus	10624-C458 E. vesimodicus	-214,19	2	5,68
~~10624-C465~~	~~E. vesimodicus~~	~~10624-C465 E. vesimodicus~~	~~-208,51~~	2	
~~10624-C466~~	~~E. vesimodicus~~	~~10624-C466 E. vesimodicus~~	~~-211,43~~	1	
~~10640-C459~~	~~E. vesimodicus~~	~~10640-C459 E. vesimodicus~~	~~-211,28~~	2	3,07
10640-C460	E. vesimodicus	10640-C460 E. vesimodicus	-211,28	2	
~~10640-C461~~	~~E. vesimodicus~~	~~10640-C461 E. vesimodicus~~	~~-208,21~~	2	
10561-C426	E. vesimodicus	10561-C426 E. vesimodicus	-213,91	2	1,12
~~10561-C427~~	~~E. vesimodicus~~	~~10561-C427 E. vesimodicus~~	~~-212,79~~	2	
~~10123-C398~~	~~E. vesimodicus~~	~~10123-C398 E. vesimodicus~~	~~-209,84~~	2	1,59
10123-C399	E. vesimodicus	10123-C399 E. vesimodicus	-211,43	1	
~~10123-C400~~	~~E. vesimodicus~~	~~10123-C400 E. vesimodicus~~	~~-209,84~~	2	
10526-C401	E. barai/G1	10526-C401 E. barai/G1	-220,69	1	8
~~10526-C402~~	~~E. barai/G1~~	~~10526-C402 E. barai/G1~~	~~-212,69~~	1	
10512-C462	E. barai/G1	10512-C462 E. barai/G1	-216,4	4	0,37

~~10512-C463~~	~~E. barai/G1~~	~~10512-C463 E. barai/G1~~	~~-216,03~~	2	
~~10080~~	~~E. barai/G6~~	~~10080 E. barai/G6~~	~~-207,21~~	1	0,78
10080-C404	E. barai/G6	10080-C404 E. barai/G6	-207,83	1	
~~10080-C405~~	~~E. barai/G6~~	~~10080-C405 E. barai/G6~~	~~-207,13~~	1	
~~10080-C406~~	~~E. barai/G6~~	~~10080-C406 E. barai/G6~~	~~-207,91~~	1	
~~10081-C428~~	~~E. barai/G6~~	~~10081-C428 E. barai/G6~~	~~-203,91~~	3	4,1
~~10081-C429~~	~~E. barai/G6~~	~~10081-C429 E. barai/G6~~	~~-208,01~~	1	
10081-C430	E. barai/G6	10081-C430 E. barai/G6	-208	1	
10562-C407	E. barai/G6	10562-C407 E. barai/G6	-202,7	1	1,04
~~10562-C408~~	~~E. barai/G6~~	~~10562-C408 E. barai/G6~~	~~-202,56~~	2	
~~10562-C409~~	~~E. barai/G6~~	~~10562-C409 E. barai/G6~~	~~-201,66~~	2	
10622-C431	E. barai/G6	10622-C431 E. barai/G6	-206,53	1	4,85
~~10622-C432~~	~~E. barai/G6~~	~~10622-C432 E. barai/G6~~	~~-204,11~~	2	
~~10622-C433~~	~~E. barai/G6~~	~~10622-C433 E. barai/G6~~	~~-201,68~~	2	
~~10523-C410~~	~~E. barai/G3~~	~~10523-C410 E. barai/G3~~	~~-211,46~~	3	3,85
10523-C411	E. barai/G3	10523-C411 E. barai/G3	-215,31	1	
~~10523-C412~~	~~E. barai/G3~~	~~10523-C412 E. barai/G3~~	~~-215,31~~	1	
~~10574~~	~~E. barai/G2~~	~~10574 E. barai/G2~~	~~-220,69~~	1	N/A
~~10574-C413~~	~~E. barai/G2~~	~~10574-C413 E. barai/G2~~	~~-220,69~~	1	
10574-C414	E. barai/G2	10574-C414 E. barai/G2	-220,69	1	
~~10574-C415~~	~~E. barai/G2~~	~~10574-C415 E. barai/G2~~	~~-220,69~~	1	
10085	E. barai/G2	10085 E. barai/G2	-218,96	2	
10089	E. barai/G2	10089 E. barai/G2	-222,06	2	
~~10086-C449~~	~~E. barai/G2~~	~~10086-C449 E. barai/G2~~	~~-215,76~~	3	N/A
10086-C450	E. barai/G2	10086-C450 E. barai/G2	-215,76	3	
~~10086-C451~~	~~E. barai/G2~~	~~10086-C451 E. barai/G2~~	~~-215,76~~	3	
~~10262-C416~~	~~E. albitarsis~~	~~10262-C416 E. albitarsis~~	~~-212,01~~	2	1,4
10262-C417	E. albitarsis	10262-C417 E. albitarsis	-213,41	2	
~~10262-C418~~	~~E. albitarsis~~	~~10262-C418 E. albitarsis~~	~~-213,41~~	2	
~~10323-C440~~	~~E. albitarsis~~	~~10323-C440 E. albitarsis~~	~~-211,35~~	5	0,99
~~10323-C441~~	~~E. albitarsis~~	~~10323-C441 E. albitarsis~~	~~-211,8~~	3	
10323-C442	E. albitarsis	10323-C442 E. albitarsis	-212,34	2	
10617	E. maralpinus/G4	10617 E. maralpinus/G4	-220,14	1	
10611	E. maralpinus/G4	10611 E. maralpinus/G4	-217,43	2	

10614	E. maralpinus/G4	10614 E. maralpinus/G4	-218,24	2	
10077-C419	E. maralpinus/G4	10077-C419 E. maralpinus/G4	-218,44	1	5,46
~~10077-C420~~	~~E. maralpinus/G4~~	~~10077-C420 E. maralpinus/G4~~	~~-212,98~~	1	
~~10077-C421~~	~~E. maralpinus/G4~~	~~10077-C421 E. maralpinus/G4~~	~~-213,74~~	2	
~~10264-C443~~	~~E. myopitae/G5~~	~~10264-C443 E. myopitae/G5~~	~~-217,07~~	1	5,75
~~10264-C444~~	~~E. myopitae/G5~~	~~10264-C444 E. myopitae/G5~~	~~-219,24~~	1	
10264-C445	E. barai/G5	10264-C445 E. barai/G5	-222,82	1	
10265-C446	E. barai/G5	10265-C446 E. barai/G5	-218,5	2	1,03
~~10265-C447~~	~~E. myopitae/G5~~	~~10265-C447 E. myopitae/G5~~	~~-217,47~~	2	
~~10265-C448~~	~~E. myopitae/G5~~	~~10265-C448 E. myopitae/G5~~	~~-218,5~~	2	
10303-C422	E. myopitae/G5	10303-C422 E. myopitae/G5	-220,64	1	0,13
~~10303-C423~~	~~E. myopitae/G5~~	~~10303-C423 E. myopitae/G5~~	~~-220,64~~	1	
~~10303-C424~~	~~E. myopitae/G5~~	~~10303-C424 E. myopitae/G5~~	~~-220,77~~	2	
10076	E. falcatus	10076 E. falcatus			

- Sequences derived from the same individual are shaded in the same tone of grey.
- Strikethrough text indicate sequences eliminated from the final analysis (larger dG).
- Values highlighted in red indicate the three instances where the selected sequence was not the one with the smallest dG value, but the sequence on a shorter branch (see main text).
- **Minimum and maximum absolute difference in dG between the ITS sequences of the same individual**:

Minimum difference	**0,13**	(E. myopitae (G5) 10303)
Maximum difference	**14,54**	(E. vesicularis 10529)
Mean	**3,376315789**	
stdev	**3,561558976**	

Table S2. Genbank accession numbers for the specimens used in the phylogenetic analyses.

The submission of sequences will be achieved as soon as possible.

Collection code	**Molecular code-Clone code for *ITS2***	**Clades/Species**	***COI***	***Cyt b***	***Wg***	***EF-1Ŭ***	***RpL27a***	***ITS2***
FAL1505	10324	E. albitarsis			xxx			xxx
FAL1504	10323-C442	E. albitarsis						
FAL1504	10323-C440	E. albitarsis						
FAL1504	10323-C441	E. albitarsis						
FAL1477	10311	E. albitarsis						xxx
FAL1398	10307	E. albitarsis						xxx
FAL1477	10310	E. albitarsis						xxx
FAL1486	10314	E. albitarsis						xxx
FAL1487	10315	E. albitarsis						xxx
FAL1398	10262-C417	E. albitarsis						
FAL1398	10262-C416	E. albitarsis						
FAL1398	10262-C418	E. albitarsis						
LF.B.FR 01	10528	E. albitarsis						xxx
FAL1384	10257	E. albitarsis						xxx
FAL1384	10305	E. albitarsis						xxx
GDEL4183	10599	E. albitarsis						xxx
FAL1398	10306	E. albitarsis						xxx
GDEL4184	10600	E. albitarsis						xxx
GDEL4181	10626	E. albitarsis						xxx
GDEL4255	10647	E. messene						xxx
GDEL4256	10648	E. messene						xxx
GDEL4254	10646	E. messene						xxx
LF.A.CA 05	10533-C452	E. messene						
LF.A.CA 05	10533-C453	E. messene				xxx		
LF.A.RO 05	10516	E. messene						
FAL1379	10256-C467	E. messene						
LF.A.RO 07	10514	E. messene						xxx
GDEL4227	10621	E. messene						
GDEL 4083	10084	E. messene						xxx

GDEL4216	10618	E. messene				xxx		
GDEL4218	10635	E. messene						xxx
GDEL4234	10639	E. messene						xxx
GDEL4195	10605	E. messene						xxx
LF.A.CA 07	10519	E. messene						xxx
LF.A.CA 06	10534	E. messene						xxx
LF.A.CA 03	10531	E. messene						xxx
LF.A.CA 04	10532	E. messene						
LF.V.SL 02	10529-C395	E. vesicularis						
LF.V.SL 02	10529-C396	E. vesicularis						
LF.V.SL 02	10529-C397	E. vesicularis						
LF.V.SW 03	10535	E. vesicularis			xxx			
LF.V.SW 05m	10537	E. vesicularis					xxx	
GDEL4236	10640-C460	E. vesimodicus		xxx				
GDEL4236	10640-C459	E. vesimodicus						
GDEL4236	10640-C461	E. vesimodicus						
GDEL4219	10636	E. vesimodicus		xxx		xxx		xxx
GDEL4233	10624-C458	E. vesimodicus				xxx	xxx	
GDEL4233	10624-C465	E. vesimodicus						
GDEL4233	10624-C466	E. vesimodicus						
GDEL4247	10643	E. vesimodicus		xxx				xxx
GDEL4250	10645	E. vesimodicus		xxx				xxx
DDEL-… 1 (FAL)	10561-C426	E. vesimodicus					xxx	
DDEL-… 1 (FAL)	10561-C427	E. vesimodicus						
GDEL4209	10629	E. vesimodicus						xxx
GDEL4208	10616	E. vesimodicus						xxx
GDEL4079	10123-C399	E. vesimodicus						
GDEL4079	10123--C398	E. vesimodicus						
GDEL4079	10123-C400	E. vesimodicus						
GDEL4198	10608	E. vesimodicus						xxx
GDEL4207	10615	E. vesimodicus						xxx
GDEL4204	10628	E. vesimodicus						xxx
GDEL4205	10613	E. vesimodicus						xxx

LF.A.RO 04	10512-C462	E. barai/G1						
LF.A.RO 04	10512-C463	E. barai/G1						
LF.B.RM 01	10526-C401	E. barai/G1		xxx				
LF.B.RM 01	10526-C402	E. barai/G1						
GDEL4085	10086-C450	E. barai/G2						
GDEL4085	10086-C449	E. barai/G2						
GDEL4085	10086-C451	E. barai/G2						
GDEL4087	10089	E. barai/G2					xxx	
GDEL4084	10085	E. barai/G2						
GDEL4086	10088	E. barai/G2						xxx
PJ10077_31_3	10574-C414	E. barai/G2						
PJ10077_31_3	10574	E. barai/G2						
PJ10077_31_3	10574-C413	E. barai/G2						
PJ10077_31_3	10574-C415	E. barai/G2						
LF.B.SP 03	10523-C411	E. barai/G3						
LF.B.SP 03	10523-C410	E. barai/G3						
LF.B.SP 03	10523-C412	E. barai/G3						
GDEL4206	10614	E. maralpinus/G4						
GDEL4212	10631	E. maralpinus/G4						xxx
GDEL4210	10630	E. maralpinus/G4						xxx
GDEL4203	10612	E. maralpinus/G4						xxx
GDEL4211	10617	E. maralpinus/G4						
GDEL4240	10641	E. maralpinus/G4						xxx
GDEL4079	10077-C419	E. maralpinus/G4						
GDEL4079	10077-C420	E. maralpinus/G4						
GDEL4079	10077-C421	E. maralpinus/G4						
GDEL4202	10611	E. maralpinus/G4				xxx	xxx	
GDEL4201	10627	E. maralpinus/G4						xxx
GDEL4244	10642	E. maralpinus/G4						xxx
FAL1405	10303-C422	E. myopitae/G5						
FAL1405	10303-C423	E. myopitae/G5						
FAL1405	10303-C424	E. myopitae/G5						
FAL1405	10304	E. myopitae/G5						xxx
FAL1405	10264-C445	E. myopitae/G5						

FAL1405	10264-C443	E. myopitae/G5						
FAL1405	10264-C444	E. myopitae/G5						
FAL1405	10265-C446	E. myopitae/G5						
FAL1405	10265-C448	E. myopitae/G5						
FAL1405	10265-C447	E. myopitae/G5						
GDEL4081	10081-C430	E. barai/G6		xxx				
GDEL4081	10081-C428	E. barai/G6						
GDEL4081	10081-C429	E. barai/G6						
GDEL4228	10637	E. barai/G6						xxx
GDEL4081	10080-C404	E. barai/G6						
GDEL4081	10080	E. barai/G6						
GDEL4081	10080-C405	E. barai/G6						
GDEL4081	10080-C406	E. barai/G6						
GDEL4080	10079	E. barai/G6						xxx
GDEL4224	10620	E. barai/G6						xxx
GDEL4082	10082	E. barai/G6					xxx	xxx
GDEL4082	10083	E. barai/G6						xxx
GDEL4200	10610	E. barai/G6						xxx
DDEL4263	10562-C407	E. barai/G6					xxx	
DDEL4263	10562-C408	E. barai/G6						
DDEL4263	10562-C409	E. barai/G6						
DDEL4263	10563	E. barai/G6		xxx				xxx
GDEL4220	10619	E. barai/G6						xxx
GDEL4229	10622-C431	E. barai/G6				xxx	xxx	
GDEL4229	10622-C432	E. barai/G6						
GDEL4229	10622-C433	E. barai/G6						
GDEL4080	10078	E. barai/G6						xxx
GDEL4079	10076	E. falcatus						

- xxx: Sequencing failure
- Cases shaded indicate specimens non sequenced on certain genes

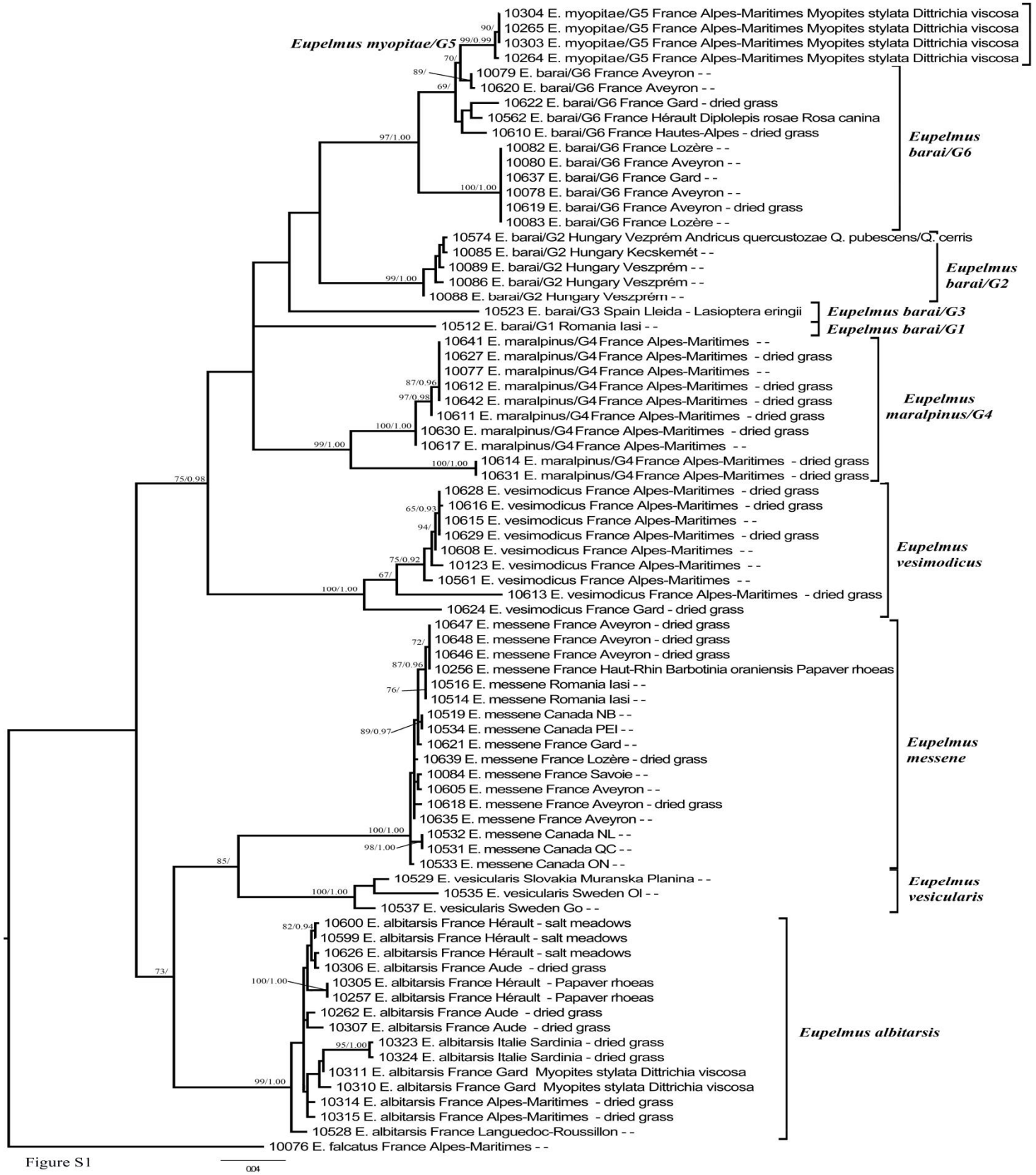

Fig. S1. Phylogram figuring the relationships within the *vesicularis* complex based on the *Cytb* dataset alignment. Bootstrap Percentages (BP) ≥ 65 and Posterior Probabilities (PP) ≥ 0.90 are indicated at nodes. Each line represents a sequenced individual with information in the following order: molecular code, species/clade, country, insect host and associated plant.

Fig. S2. Topology obtained from ML analysis of the complete *ITS2* dataset. Bootstrap Percentages (BP) ≥65 are indicated at nodes. Each line represents a sequenced individual with information in the following order: molecular code, clone code, species/clade, country, insect host and associated plant.

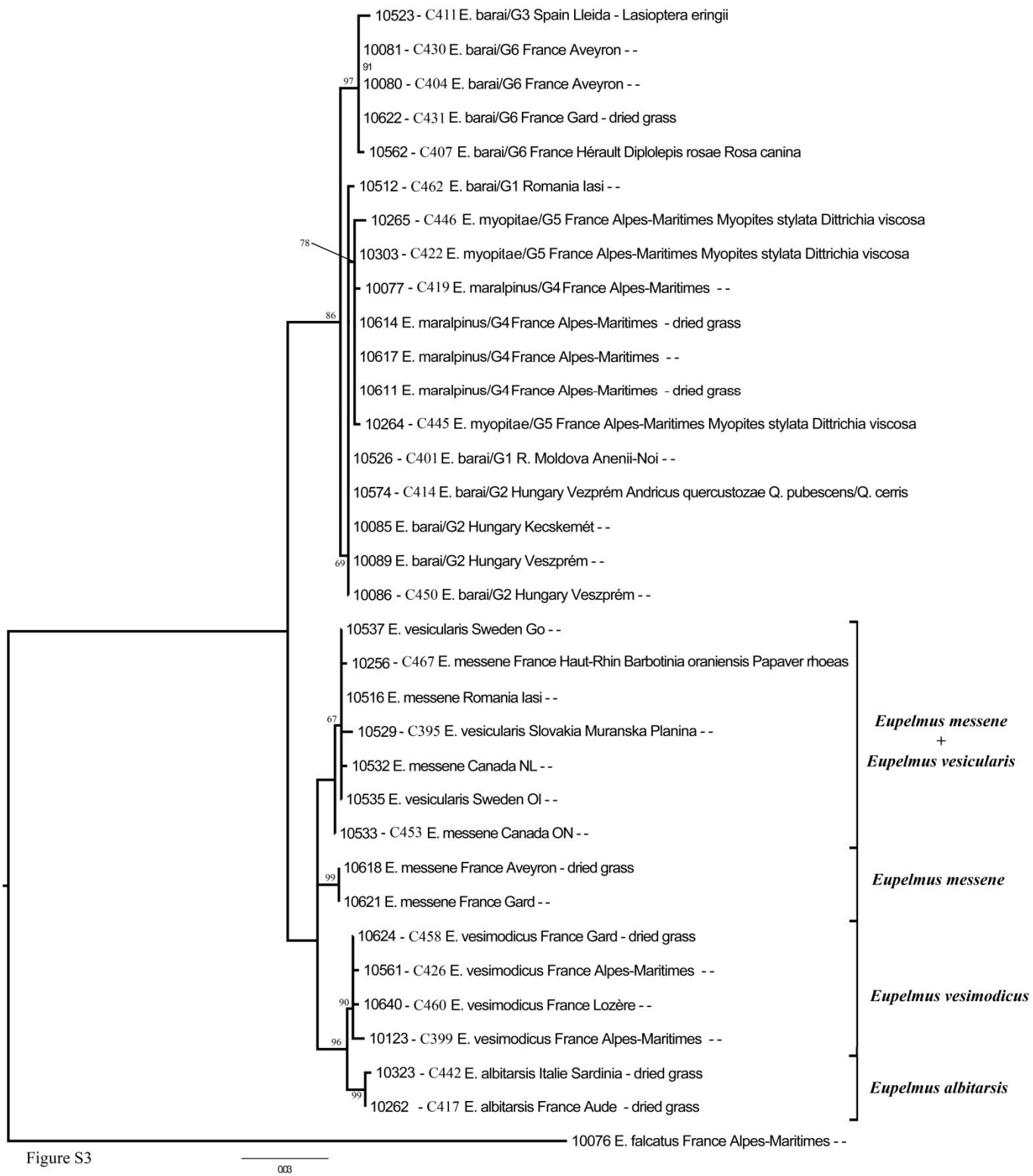

Fig. S3. Topology obtained from ML analysis of the reduced *ITS2* dataset. Bootstrap Percentages (BP) ≥65 are indicated at nodes. Each line represents a sequenced individual with information in the following order: molecular code, clone code, species/clade, country, insect host and associated plant.

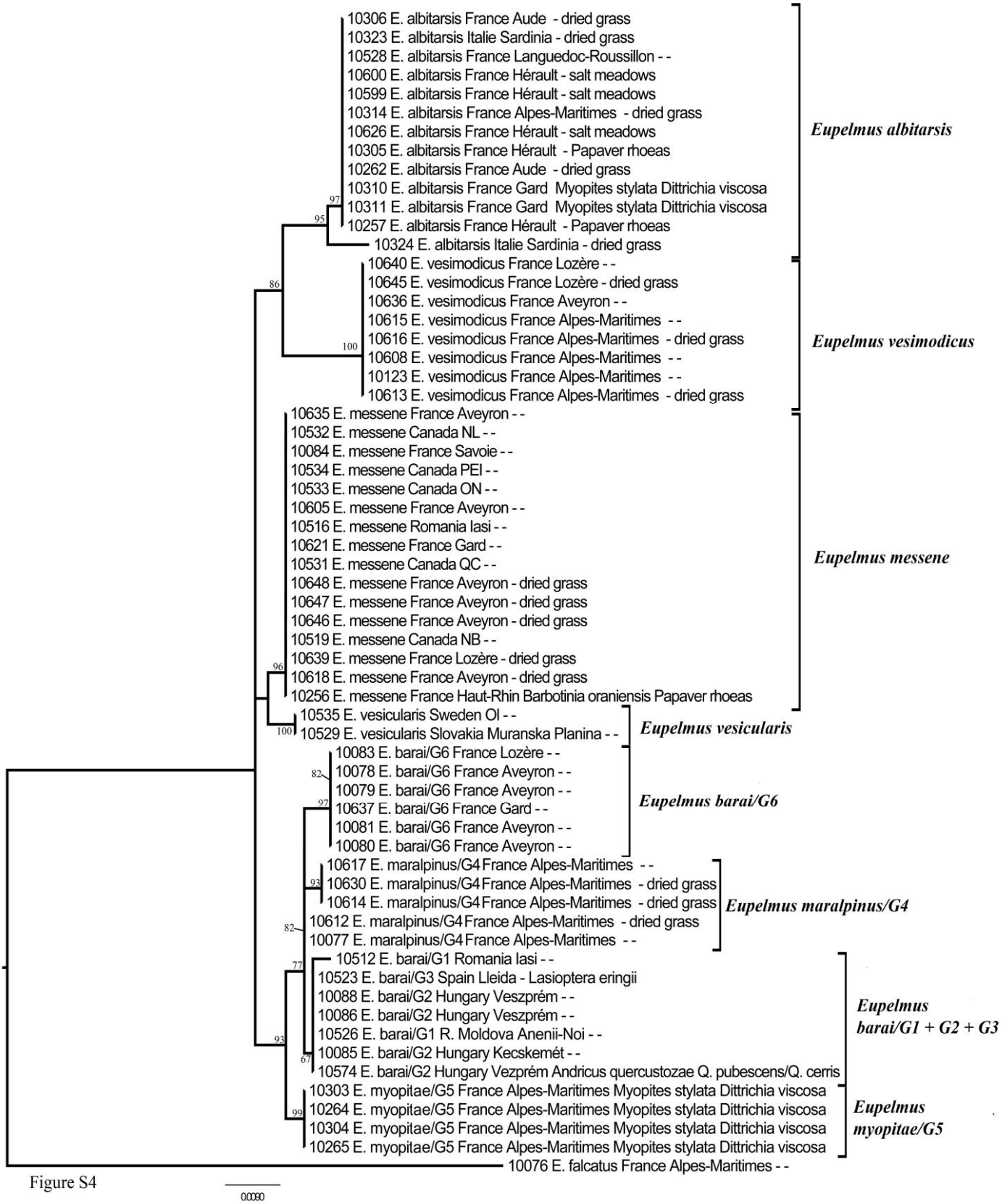

Figure S4

Fig. S4. Topology obtained from ML analysis of the *RpL27a* dataset. Bootstrap Percentages (BP) ≥65 are indicated at nodes. Each line represents a sequenced individual with information in the following order: molecular code, species/clade, country, insect host and associated plant.

Fig. S5. Topology obtained from ML analysis of the *EF-1Ŭ* dataset. Bootstrap Percentages (BP) ≥65 are indicated at nodes. Each line represents a sequenced individual with information in the following order: molecular code, species/clade, country, insect host and associated plant.

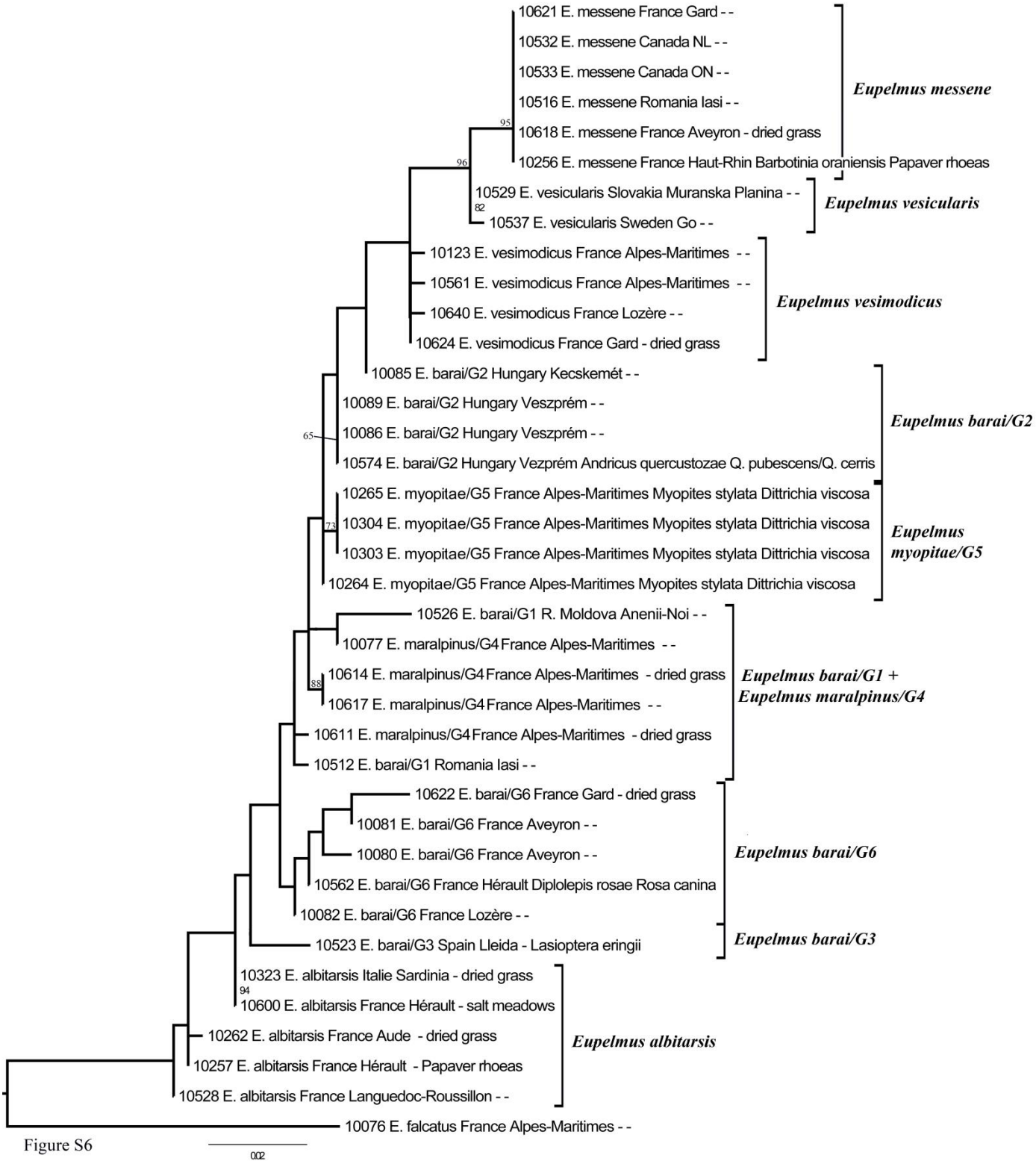

Fig. S6. Topology obtained from ML analysis of the *Wg* dataset. Bootstrap Percentages (BP) ≥65 are indicated at nodes. Each line represents a sequenced individual with information in the following order: molecular code, species/clade, country, insect host and associated plant.

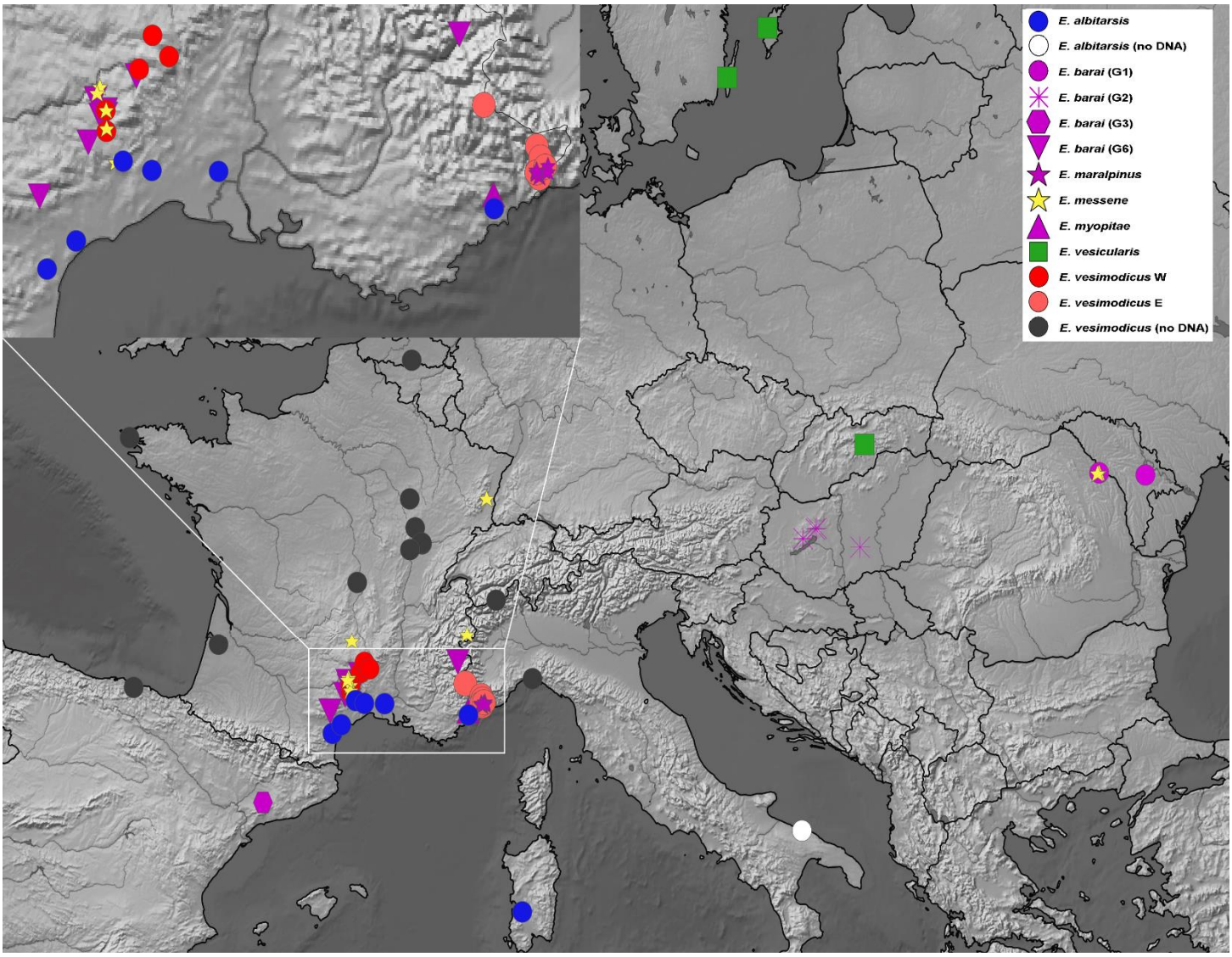

Fig. S7. Geographical distribution of different mitochondrial clades of *vesicularis* SC. Included in the distribution are also not sequenced (no DNA) specimen from BMNH and MNHN collections identified as *E. albitarsis* and *E. vesimodicus*.

Appendix S1. Recursive and primary partitions resulted from ABGD (Automated Barcode Gap Discovery) method based on *COI* dataset and with number of steps = 50 and X = 0.1

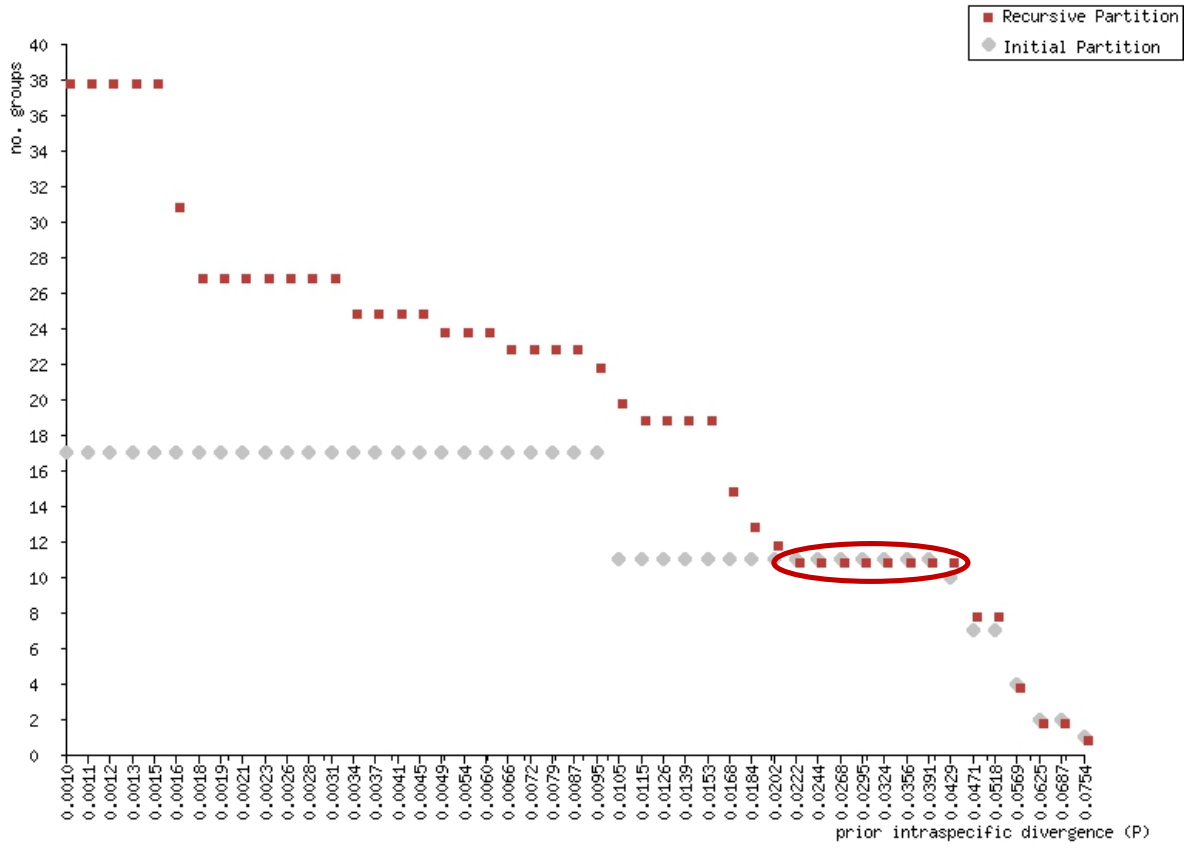

Recursive partitions and number of groups

Partition 1 : found 38 groups (prior maximal distance P= 0.001000)

Partition 2 : found 38 groups (prior maximal distance P= 0.001099)

Partition 3 : found 38 groups (prior maximal distance P= 0.001207)

Partition 4 : found 38 groups (prior maximal distance P= 0.001326)

Partition 5 : found 38 groups (prior maximal distance P= 0.001456)

Partition 6 : found 31 groups (prior maximal distance P= 0.001600)

Partition 7 : found 27 groups (prior maximal distance P= 0.001758)

Partition 8 : found 27 groups (prior maximal distance P= 0.001931)

Partition 9 : found 27 groups (prior maximal distance P= 0.002121)

Partition 10 : found 27 groups (prior maximal distance P= 0.002330)

Partition 11 : found 27 groups (prior maximal distance P= 0.002560)

Partition 12 : found 27 groups (prior maximal distance P= 0.002812)
Partition 13 : found 27 groups (prior maximal distance P= 0.003089)
Partition 14 : found 25 groups (prior maximal distance P= 0.003393)
Partition 15 : found 25 groups (prior maximal distance P= 0.003728)
Partition 16 : found 25 groups (prior maximal distance P= 0.004095)
Partition 17 : found 25 groups (prior maximal distance P= 0.004498)
Partition 18 : found 24 groups (prior maximal distance P= 0.004942)
Partition 19 : found 24 groups (prior maximal distance P= 0.005429)
Partition 20 : found 24 groups (prior maximal distance P= 0.005964)
Partition 21 : found 23 groups (prior maximal distance P= 0.006551)
Partition 22 : found 23 groups (prior maximal distance P= 0.007197)
Partition 23 : found 23 groups (prior maximal distance P= 0.007906)
Partition 24 : found 23 groups (prior maximal distance P= 0.008685)
Partition 25 : found 22 groups (prior maximal distance P= 0.009541)
Partition 26 : found 20 groups (prior maximal distance P= 0.010481)
Partition 27 : found 19 groups (prior maximal distance P= 0.011514)
Partition 28 : found 19 groups (prior maximal distance P= 0.012649)
Partition 29 : found 19 groups (prior maximal distance P= 0.013895)
Partition 30 : found 19 groups (prior maximal distance P= 0.015264)
Partition 31 : found 15 groups (prior maximal distance P= 0.016768)
Partition 32 : found 13 groups (prior maximal distance P= 0.018421)
Partition 33 : found 12 groups (prior maximal distance P= 0.020236)
Partition 34 : found 11 groups (prior maximal distance P= 0.022230)
Partition 35 : found 11 groups (prior maximal distance P= 0.024421)
Partition 36 : found 11 groups (prior maximal distance P= 0.026827)
Partition 37 : found 11 groups (prior maximal distance P= 0.029471)
Partition 38 : found 11 groups (prior maximal distance P= 0.032375)
Partition 39 : found 11 groups (prior maximal distance P= 0.035565)
Partition 40 : found 11 groups (prior maximal distance P= 0.039069)
Partition 41 : found 11 groups (prior maximal distance P= 0.042919)
Partition 42 : found 8 groups (prior maximal distance P= 0.047149)
Partition 43 : found 8 groups (prior maximal distance P= 0.051795)
Partition 44 : found 4 groups (prior maximal distance P= 0.056899)
Partition 45 : found 2 groups (prior maximal distance P= 0.062506)

Partition 46 : found 2 groups (prior maximal distance P= 0.068665)

Partition 47 : found 1 groups (prior maximal distance P= 0.075431)

Groups and their membership for partitions 34 to 41

Group[1] n: 17; id: 10647 10648 10646 10533 10516 10256 10514 10621 10084 10618 10635 10639 10605 10519 10534 10531 10532

Group[2] n: 3; id: 10537 10529 10535

Group[3] n: 8; id: 10561 10616 10123 10608 10613 10615 10628 10629

Group[4] n: 5; id: 10640 10636 10624 10643 10645

Group[5] n: 2; id: 10512 10526

Group[6] n: 1; id: 10523

Group[7] n: 5; id: 10086 10089 10085 10088 10574

Group[8] n: 17; id: 10081 10637 10080 10079 10620 10082 10083 10610 10562 10563 10619 10078 10622 10264 10265 10303 10304

Group[9] n: 15; id: 10324 10323 10311 10307 10310 10314 10315 10262 10528 10257 10305 10599 10306 10600 10626

Group[10] n: 1; id: 10614 10631 10612 10617 10641 10077 10611 10627 10630 10642

Group[11] n: 1; id: 10076 (outgroup)

Groups and their membership for partitions 42 and 43 (initial partitions)

Group[1] n: 17; id: 10647 10648 10646 10533 10516 10256 10514 10621 10084 10618 10635 10639 10605 10519 10534 10531 10532

Group[2] n: 3; id: 10537 10529 10535

Group[3] n: 13; id: 10561 10616 10123 10608 10640 10636 10624 10643 10645 10613 10615 10628 10629

Group[4] n: 2; id: 10512 10526

Group[5] n: 33; id: 10523 10086 10089 10085 10088 10574 10081 10637 10080 10079 10620 10082 10083 10610 10562 10563 10619 10078 10622 10264 10265 10303 10304 10614 10631 10612 10617 10641 10077 10611 10627 10630 10642

Group[6] n: 15; id: 10324 10323 10311 10307 10310 10314 10315 10262 10528 10257 10305 10599 10306 10600 10626

Group[7] n: 1; id: 10076 (outgroup)

Appendix S2. Putative species within *vesicularis* SC detected using the GMYC (Generalized Mixed Yule Coalescent) method.

Single-Threshold Method

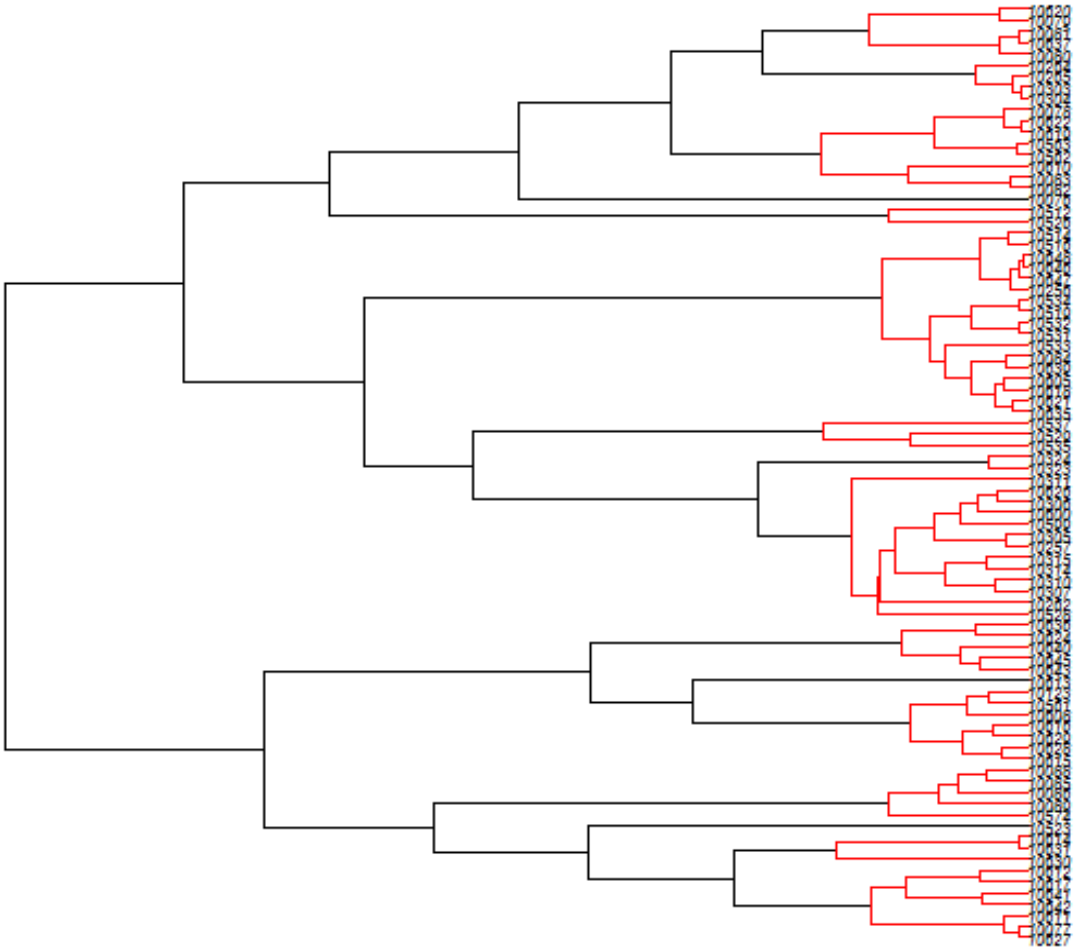

COI_GMYC Species List

1	1	10627
2	1	10077
3	1	10611
4	1	10642

5	1	10641
6	1	10617
7	1	10612
8	2	10630
9	2	10631
10	2	10614
11	3	10574
12	3	10089
13	3	10086
14	3	10085
15	3	10088
16	4	10615
17	4	10628
18	4	10629
19	4	10616
20	4	10608
21	4	10561
22	4	10123
23	5	10643
24	5	10645
25	5	10640
26	5	10624
27	5	10636
28	6	10528
29	6	10262
30	6	10307
31	6	10310
32	6	10314
33	6	10315
34	6	10257
35	6	10305
36	6	10599
37	6	10600
38	6	10306
39	6	10626

40	6	10311
41	7	10323
42	7	10324
43	8	10535
44	8	10529
45	8	10537
46	9	10635
47	9	10621
48	9	10618
49	9	10605
50	9	10639
51	9	10084
52	9	10533
53	9	10531
54	9	10532
55	9	10519
56	9	10534
57	9	10256
58	9	10647
59	9	10646
60	9	10648
61	9	10516
62	9	10514
63	10	10526
64	10	10512
65	11	10082
66	11	10083
67	11	10610
68	11	10562
69	11	10563
70	11	10619
71	11	10622
72	11	10078
73	12	10304
74	12	10303

75	12	10265
76	12	10264
77	13	10080
78	13	10637
79	13	10081
80	13	10079
81	13	10620
82	14	10076
83	15	10523
84	16	10613

Multiple-Threshold Method

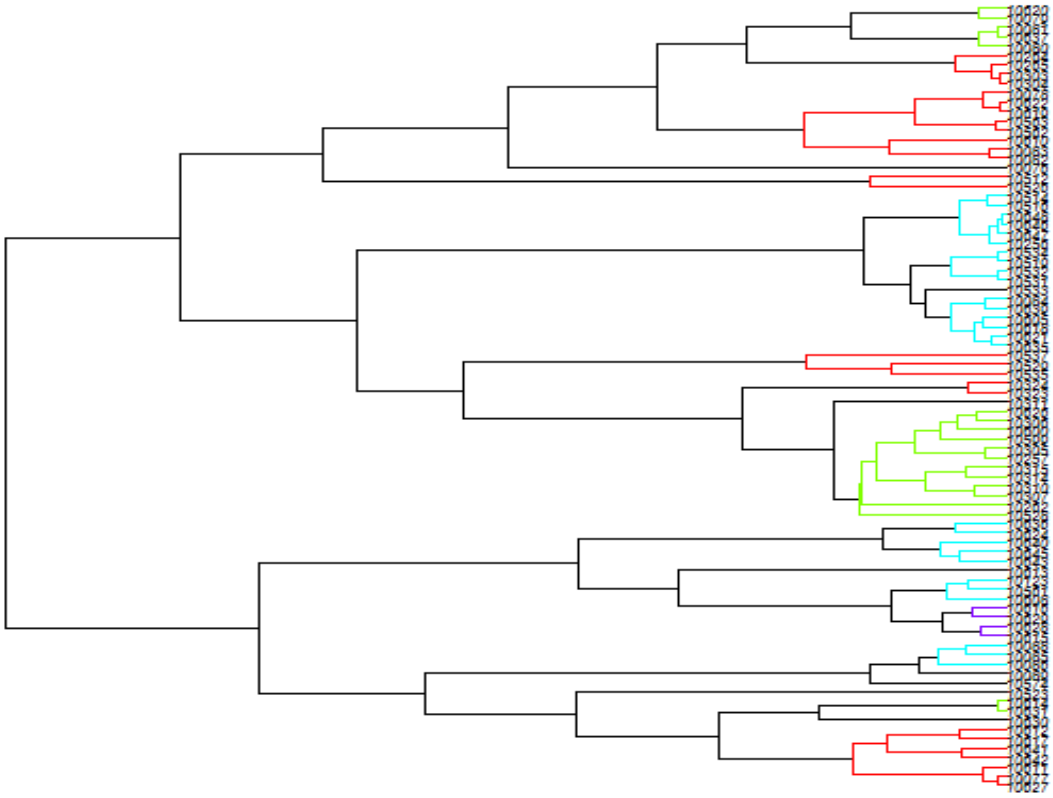

GMYC Species List

1	1	10535
2	1	10529
3	1	10537
4	2	10526
5	2	10512
6	3	10608
7	3	10561
8	3	10123
9	4	10627
10	4	10077
11	4	10611
12	4	10642
13	4	10641
14	4	10617
15	4	10612
16	5	10323
17	5	10324
18	6	10643
19	6	10645
20	6	10640
21	7	10624
22	7	10636
23	8	10256
24	8	10647
25	8	10646
26	8	10648
27	8	10516
28	8	10514
29	9	10086
30	9	10085
31	9	10088
32	10	10082
33	10	10083
34	10	10610

35	10	10562
36	10	10563
37	10	10619
38	10	10622
39	10	10078
40	11	10304
41	11	10303
42	11	10265
43	11	10264
44	12	10631
45	12	10614
46	13	10531
47	13	10532
48	13	10519
49	13	10534
50	14	10635
51	14	10621
52	14	10618
53	14	10605
54	14	10639
55	14	10084
56	15	10528
57	15	10262
58	15	10307
59	15	10310
60	15	10314
61	15	10315
62	15	10257
63	15	10305
64	15	10599
65	15	10600
66	15	10306
67	15	10626
68	16	10080
69	16	10637

70	16	10081
71	17	10079
72	17	10620
73	18	10615
74	18	10628
75	19	10629
76	19	10616
77	20	10076
78	21	10089
79	22	10311
80	23	10523
81	24	10533
82	25	10574
83	26	10613
84	27	10630

6. DISCUSSION ET PERSPECTIVES

6.1 Synthèse des résultats et perspectives

6.1.1. Intérêt du barcoding moléculaire pour la taxonomie

Le barcoding moléculaire a été proposé comme un outil idéal et prometteur pour assigner les spécimens étudiés à des espèces déjà décrites, découvrir et décrire des nouvelles espèces et plus faciliter et accélérer la découverte de la biodiversité (Hebert *et al.*, 2003; Hajibabaei *et al.*, 2007; Frézal & Leblois, 2008; Goldstein & DeSalle, 2010). Malgré des succès évidents (Hebert *et al.* 2004; Janzen *et al.*, 2005; Smith *et al.*, 2006; Veijalainen *et al.*, 2011), cette approche a subi des critiques en raison des inconvénients biologiques et techniques qui peuvent fausser les résultats taxonomiques obtenus de ce marqueur (Meyer & Paulay, 2005; Rubinoff *et al.*, 2006; Galtier *et al.*, 2009). En conséquence, il est nécessaire de compléter le barcoding en utilisant d'autres données (ex: ADN nucléaire, morphologie, etc.) dans une approche taxonomique intégrative (Mortiz & Cicero, 2004; Dayrat, 2005; Will *et al.*, 2005). Dans le cadre de mon travail, cette approche a été utilisée pour étudier deux complexes/groupes d'espèces particuliers, l'un incluant les espèces morphologiquement ou (supposées) phylogénétiquement associées à l'espèce *E. urozonus* et l'autres incluant les espèces confondues ou synonymies avec l'espèce *E. vesicularis* (cf. Partie III). Si, dans les deux cas, notre étude montre une diversité insoupçonnée dans chaque groupe/complexe, des résultats différents ont été obtenus quant à la concordance entre gènes mitochondriaux, gènes nucléaires et caractères morphologiques.

Concernant le groupe *urozonus*, les arbres basés sur les séquences de *COI* et *Wg* et la structuration basée sur les caractères morphologiques s'avèrent globalement concordants. En fait, 3 cas de contradiction, entre le gène de *COI* et celui de *Wg*, ont été mis en évidence concernant la monophylie des espèces suivantes: *E. gemellus*/*E. acinellus*; *E. kiefferi*/*E. fulvipes*; et *E. priotoni*/*E. jansati*/*E. purpuricollis*. En effet, alors que chaque une des espèces composant les couples précédents a été avérée d'être un clade distinct et monophylétique dans l'arbre de *COI*, la variation des séquences de *Wg* n'était pas suffisante pour différencier les espèces de ces couples. Mais, la validation de la nomenclature de ces espèces a été supportée avec la caractérisation morphologique.

Concernant le complexe *vesicularis*, la situation est finalement plus complexe, d'une part, on observe une discordance entre la caractérisation basée sur les séquences des gènes mitochondriaux *COI* ou *Cytb* et celle basée sur soit les séquences individuelles de quatre gènes nucléaires (*EF-1Ŭ*, *Wg*, *ITS2* et *RpL27a*) ou sur la concaténation des leurs séquences. D'autre part, la discrimination basée sur les marqueurs mitochondriaux s'oppose aussi à la délimitation effectuée sur des critères morphologiques. Ce comportement particulier des marqueurs mitochondriaux pourrait être, ici, le résultat d'un isolement géographique important entre des populations de femelles appartenant à une même espèce et à une divergence génétique de l'ADN mitochondrial amplifiée par la faible dispersion résultant du brachyptérisme de ces femelles. Un tel exemple souligne la limite à n'utiliser que ce type d'information pour des approches de taxonomie.

Au final, notre travail a significativement contribué à une meilleure connaissance de la diversité du genre *Eupelmus* au niveau de la Région Paléarctique avec notamment (i) une délimitation des espèces cryptiques morphologiquement ou sœurs phylogénétiquement sur une base morphologique et génétique (*E. minozonus*/*E. urozonus*, etc.); (ii) la découverte des nouvelles espèces qui auraient été confondues avec d'autres espèces déjà décrites (ex: *E. martelli*/*E. gemellus*/*E. confusus*, *E. longicalvus*/*E. annulatus*); (iii) la validation du statut taxonomique de certaines espèces qui étaient mises en synonymies auparavant (ex: *E. kiefferi*/*E. fulvipes* et *E. albitarsis*/*E. vesicularis*); (iv) quand c'est possible, une sélection des caractères morphologiques discriminant pour l'ensemble des espèces analysées; (v) une association hautement fiable entre les femelles et les males dimorphiques des espèces pour lesquelles les deux sexes étaient disponibles; et/ou (vi) une précision sur les spectres d'hôtes et la répartition géographique pour les espèces d'*Eupelmus* étudiées.

Suite à ce travail, il serait utile d'utiliser les techniques de séquençage de nouvelles générations afin de résoudre précisément l'histoire évolutive des espèces du complexe v*esicularis* et apporter donc plus d'informations sur l'identité taxonomique des clades observés au sein de ce complexe. En plus, il serait également intéressant d'étendre l'échantillonnage, notamment en région méditerranéenne et en zones de montagne, susceptibles d'héberger des lignées isolées géographiquement et génétiquement. Par conséquent, ce complexe d'espèces serait un très bon modèle pour une étude bio- et phylogéographique du "modelage" des populations à travers les épisodes de glaciation.

6.1.2. Intégration de caractères morphologiques et moléculaires en phylogénie

Comme mentionné dans le paragraphe précédent, l'intégration des caractères provenant de différents champs de données (ici morphologiques et moléculaires) est souvent nécessaire, aussi bien quant à la délimitation des espèces que pour l'inférence phylogénétique. Ils peuvent amener des informations complémentaires et évoluer à des vitesses différentes. Elle permet aussi d'exploiter des jeux de données plus importants pouvant inclure des individus documentés seulement sur un type de caractères (des fossiles par exemple).

Dans le cadre de mon travail, l'intégration de caractères morphologiques et moléculaires dans une perspective de phylogénie a été appliquée pour ré-évaluer la classification infra-générique du genre *Eupelmus* proposée par Gibson (1995) sur la base de caractères morphologiques (cf. Partie I). L'étude est fondée sur: (i) d'un échantillonnage aussi représentatif que possible considérant les moyens et temps disponibles et incluant notamment des représentants des 3 sous-genres retenus par Gibson dans sa classification infra-générique; (ii) d'une matrice des états de caractères morphologiques basée sur les deux sexes, sachant qu'ils sont fortement dimorphiques et qui a concerné 57 caractères; (iii) d'une matrice concaténée des séquences nucléotidiques (avec un nombre variable de marqueurs suivant les individus). La comparaison des arbres moléculaires et morphologiques montrent que les deux champs de données apportent des informations soit complémentaires soit convergentes. La topologie profonde est essentiellement soutenue via les données moléculaires, qui structurent également le groupe *urozonus*, de loin le plus diversifié, en trois clades. Les données morphologiques viennent en complément et soutiennent certains groupes d'espèces pour lesquels les données moléculaires faisaient défaut. Finalement le genre *Eupelmus* peut être structuré en une douzaine de groupes d'espèces, respectivement les groupes (*hartigi*, *testaceiventris*, *juniperinus*, *peculiaris*, *splendens*, *stramineipes*, *antipoda*, *orientalis*, *pini*, *atropurpureus*, *vesicularis* et *urozonus*) plus quelques espèces isolées telle que *E. memnonius* – l'espèce type du genre – et *E. microzonus*). Enfin, la classification infra-générique de Gibson (1995) ne peut plus être retenue, puisque le sous-genre *Episolindelia* apparaît comme paraphylétique et que le sous-genre *Macroneura* apparaît comme un groupe d'espèces niché à l'intérieur du sous-genre *Eupelmus*.

En conclusion, cette étude démontre une fois de plus l'intérêt d'intégrer des données morphologiques et moléculaires ici dans une approche de "congruence taxonomique" en maximisant ici la concordance des résultats issus des deux champs de données. Toutefois, notre étude reste limitée en termes d'espèces analysées et de couverture géographique, en

particulier pour ce qui concerne l'approche moléculaire. L'ajout d'individus provenant notamment des Régions Est-Paléarctique et Pacifique serait donc particulièrement utile. Plus généralement, il conviendrait également d'étudier les relations phylogénétiques entre le genre *Eupelmus* et des taxons proches, en particulier avec le genre *Ecnomocephala* Gibson, 1995 qui semble le genre le plus apparenté au niveau évolutif en raison du partage d'un même caractère morphologique clé, la division du 7ème tergite du metasoma (Mt7) par une ligne et le recouvrement partiel ou total de cette tergite par le tergite précédente (MT6).

6.1.3 Apports de la phylogénie multi-locus à la systématique

L'utilisation de plusieurs marqueurs moléculaires pour la reconstruction des relations phylogénétiques répond à plusieurs nécessités. Tout d'abord, l'augmentation du nombre de sites améliore, toute chose étant égale par ailleurs, d'être plus résolu et robuste. Deuxièmement, le choix de marqueurs présentant des taux d'évolution contrastés permet de documenter à la fois des divergences récentes et plus anciennes (Rokas *et al.,* 2002; Lin & Danforth, 2004; Cruaud *et al.,* 2013). Enfin, la multiplication des marqueurs permet également de détecter des événements évolutifs particuliers tel que le phénomène de "incomplete lineage sorting" (le maintien d'un polymorphisme ancestral au travers des événements de spéciation) ou les phénomènes d'hybridation/'introgression qui peuvent survenir entre des espèces proches (Degnan & Rosenberg, 2009; Knowles & Kubatko, 2010; Deuve *et al.,* 2012).

La reconstruction des arbres phylogénétiques basés sur de multiples gènes peut être réalisée de deux façons (Gadackar *et al.,* 2005): (i) l'approche par consensus qui est basée sur l'inférence des arbres individuels pour tous les gènes, suivie d'un arbre de consensus résumant les arbres individuels; (ii) l'approche par concaténation qui est basée sur la combinaison des séquences des gènes analysés dans un seul alignement dit "super-gène", cet alignement étant ensuite analysé pour l'estimation d'un arbre combiné. C'est cette deuxième approche que nous avons utilisée ici pour étudier les relations phylogénétiques au sein du groupe. *urozonus* (cf. Partie II).

Du point de vue méthodologique, ce travail m'a permis d'étudier la sensibilité des reconstructions phylogénétiques à l'inclusion ou l'exclusion des régions divergentes des gènes combinés et les modèles de partitionnement des séquences analysées. Mon étude a montré que l'inclusion dans l'alignement des séquences des régions les plus divergentes

aboutissait à une résolution meilleure et davantage robuste que celle les excluant (par utilisation du programme Gblocks). Ainsi, l'exploitation (ou non) de régions divergentes et l'utilisation de logiciels de traitement appropriés doivent être prudentes, en particulier lorsque les relations phylogénétiques aux niveaux taxonomiques intermédiaires et inférieurs sont envisagées. Un deuxième point méthodologique important pour l'analyse de ce type de données concerne la stratégie de partitionnement via la comparaison de modèles de complexité croissante, incluant de plus en plus de réalisme par rapport à l'évolution des marqueurs voire des sites. Dans notre cas, bien que le chemin de partitionnement le plus complexe (composé de 9 partitions) a été préféré au niveau des "facteurs de Bayes" pour l'inférence finale des relations phylogénétiques au sein du groupe étudié, les arbres phylogénétiques inférés à partir des différents modèles de partitionnements (4 modèles testés) étaient identiques mais avec quelques discordances mineures concernant les nœuds ou les branches non ou faiblement supportés. Des résultats similaires à les nôtres ont été obtenus dans des précédentes études phylogénétiques (ex. Cruaud *et al.,* 2013).

Au niveau biologique, l'arbre phylogénétique obtenu a prouvé la monophylie du groupe *urozonus* et sa sous-structuration en trois clades principaux ("A = *gemellus*", "B = *confusus*" et "C = *urozonus*"). Comme discuté dans la partie II et dans le paragraphe suivant, cette information nous a permis de mieux comprendre les processus de spécialisation écologique chez ce groupe diversifié des parasitoïdes. Cependant, les positions relatives de quelques espèces analysées restent encore non résolues, en particulier pour les espèces assignées phylogénétiquement aux clades "A = *gemellus*" et "C = *urozonus*". Pour aborder de telles divergences récentes, d'autres approches comme la technique du séquençage de RAD (restriction-site-associated DNA sequencing) (Cruaud *et al.,* 2014) seraient nécessaires. De telles approches pourraient également permettre d'aborder des questions de structuration à l'échelle des populations.

6.1.4. Utilisation de la phylogénie pour la compréhension des processus de spécialisation

La prise en compte des relations phylogénétiques sont des éléments indispensables pour comprendre des processus évolutifs tels que la spécialisation écologique (Nyman *et al.,* 2010; Jousselin *et al.,* 2013; Hardy & Otto, 2014; Vamosi *et al.,* 2014). Ainsi que mentionné en "Introduction", l'étude des phénomènes de spécialisation écologique se sont principalement

portés sur l'étude des insectes phytophages et, à ce jour, peu de données sont disponibles pour les parasitoïdes. L'obtention d'une phylogénie multi-locus bien résolue pour le groupe *urozonus* (cf. Partie II et § précédent) et la compilation de nombreuses informations concernant le spectre d'hôtes, ont permis de documenter cette question à une échelle évolutive pertinente. Nos résultats indiquent tout d'abord une très forte disparité au niveau des spectres d'hôtes incluant quelques rares espèces strictement spécialistes (*E. acinellus*, *E. pistaciae* et *E. tibicinis*) et de nombreux généralistes. Parmi ces derniers, 4 espèces au moins (c.-à-d. *E. annulatus*, *E. confusus*, *E. kiefferi* et *E. urozonus*) apparaissent capables de parasiter des espèces de différents ordres. A cette échelle, des variations significatives de la taille relative d'ovipositeur (le ratio entre la longueur d'ovipositeur et celle de tibia postérieur) ont été mises en évidence (de 0.58% chez *E. fulvipes* à 1.36% chez *E. janstai*).

L'analyse comparative réalisée n'a toutefois pas pu mettre en évidence de corrélation significative entre la divergence moléculaire et la similarité entre spectres d'hôtes. Cette même analyse n'a également pas pu mettre en évidence de corrélation entre la largeur du spectre d'hôtes et la longueur l'ovipositeur, contrairement à ce qui a pu être observé dans d'autres communautés telle que celle associée aux pollinisateurs de figuiers (Ghara *et al.*, 2011). Au final, nous n'avons donc pas pu mettre en évidence de contraintes particulières liées à l'évolution des spectres d'hôtes, qui présentent une "labilité" plutôt étonnante. De plus, la proche proximité phylogénétique entre des espèces spécialistes et généralistes pose la question de l'origine évolutive des espèces spécialistes. Même si ce résultat doit être confirmé, cette observation penche plutôt en faveur du scenario de "l'oscillation" proposé par Hardy & Otto (2014). A ce titre, il serait particulièrement intéressant de poursuivre cette analyse en complétant l'étude des spectres d'hôtes de certaines espèces décrites récemment dans le groupe *urozonus* telles que *E. janstai*, *E. longicalvus*, *E. minozonus*, *E. opacus*, *E. priotoni*, *E. purpuricollis*, *E. simizonus*, et *E. vindex*) voire dans d'autres groupes ou à l'échelle plus globale du genre.

6.2. Implications en lutte biologique

6.2.1. Généralités

La lutte biologique vise à réduire la densité des populations des ravageurs et/ou leurs dommages à un niveau acceptable *via* l'utilisation d'organismes vivants (parasitoïdes,

prédateurs et pathogènes) appelés auxiliaires. Quatre stratégies principales de lutte biologique peuvent être distinguées (Eilenberg *et al.*, 2001): (i) la lutte biologique par introduction qui vise à introduire intentionnellement un auxiliaire exotique en vue de son établissement permanent et d'un contrôle durable du ravageur; (ii) la lutte biologique par inoculation basée sur des lâchers intentionnels d'auxiliaires en vue de leur multiplication et d'un contrôle transitoire du ravageur ciblé; (iii) la lutte biologique par inondation qui consiste à produire et relâcher massivement des auxiliaires en vue d'un impact rapide et significatif des populations de ravageurs; (iv) la lutte biologique par conservation qui vise à aménager l'environnement ou modifier les pratiques culturales afin de protéger et favoriser la présence d'ennemis naturels locaux.

Quelle que soit la stratégie visée, l'identification correcte et précise des espèces nuisibles et des auxiliaires est déterminante pour l'échec ou le succès des programmes de lutte biologique (Narendran, 2008; Rosen, 1973 & 1986). Plus généralement, la compréhension des interactions précises entre les auxiliaires potentiels, les ravageurs ciblés, les éventuels hôtes-relais ainsi que d'autres espèces non-cibles sont importants pour garantir l'efficacité et l'innocuité des auxiliaires potentiels. Par conséquent, sans l'aide de taxonomistes spécialistes, les chercheurs intéressés par la lutte biologique contre des ravageurs des cultures risquent de commettre des erreurs dans l'identification des insectes impliqués et donc de compromettre la réussite de la stratégie de lutte biologique.

Grâce à leur mode de la vie "parasitoïde", plusieurs espèces d'*Eupelmus* ont été présentées comme des ennemis naturels des divers insectes ravageurs présentant une certaine importance économique. Dans ce contexte et à ce titre, mes travaux ont permis d'apporter un éclairage nouveau sur deux programmes de lutte biologique en cours, à savoir la limitation des populations de la mouche de l'olive *B. oleae* et celles du cynips du châtaigner *D. kuriphilus*. Dans chacun des cas, mes résultats ont contribué à (i) apporter des éléments de reconnaissance (morphologiques et/ou moléculaires) pour une identification précise des *Eupelmus* impliqués; (ii) expliquer voire anticiper le rôle des *Eupelmus* dans la régulation du ravageur-cible; et (iii) éventuellement, fournir des recommandations pour améliorer le contrôle du ravageur.

6.2.2 Lutte biologique contre la mouche de l'olive, *Bactrocera oleae*

La mouche de l'olive est actuellement le ravageur principal sur olivier dans le monde et ses dégâts peuvent être estimés à 5% de la production totale des olives (Nardi *et al*., 2005). Plusieurs méthodes de lutte ont été déployées ou envisagées incluant l'utilisation d'insecticides, le piégeage massif, différentes stratégies en lutte biologique voire, plus récemment, des méthodes analogues aux lâchers de mâles stériles. Concernant la lutte biologique, deux stratégies de lutte biologique méritent d'être mentionnées. La première concerne la lutte biologique par augmentation à l'aide du parasitoïde *Psyttalia concolor* (Szepligeti, 1910). Dans cette stratégie, ce parasitoïde apparaît comme un auxiliaire efficace dans la limitation des populations de *B. oleae* (Monastero & Delanoue, 1966; Kapatos *et al.,* 1977; Danne & Johnson, 2010) mais l'augmentation du coût d'élevage de ce parasitoïde sur *Ceratitis capitata* (Wiedemann, 1824) et la nécessité de lâchers saisonniers limitent l'application de cette approche de manière durable. L'autre stratégie repose sur la tentative d'acclimatation d'autres espèces du genre *Psyttalia*, en particulier *P. lounsburyi*, originaire d'Afrique tropicale. Le taux de la réussite avec cet auxiliaire varie suivant la région géographique. Appliquée avec succès en Californie grâce au bon établissement du parasitoïde *P. lounsburyi* dans cette région (Danne & Johnson, 2010), l'acclimatation de ce parasitoïde en France a échoué en raison d'absence d'une capacité d'adaptation de *P. lounsburyi* au nouvel environnement (Sud de France) (Borowiec *et al.*, 2012).

Une troisième stratégie en lutte biologique est basée sur l'utilisation d'une plante-relais, l'astéracée *Dittrichia viscosa* (Linné) appelée communément "inule visqueuse" (Delucchi, 1957; Ferriere & Delucchi, 1957; Neuenschwander *et al.*, 1983; Warlop, 2006; Franco-Mican *et al.*, 2010). En effet, cette plante est naturellement infestée par un diptère galligène, *Myopites stylata*, lui-même parasité par *Eupelmus urozonus*. *E. urozonus* étant également capable de parasiter la mouche de l'olive, la plantation d'inule visqueuse à proximité des oliviers est censée renforcer la présence d'*E. urozonus* dans les oliveraies, augmenter le taux de parasitisme sur la mouche de l'olive et, donc, réduire les dégâts occasionnés par ce ravageur (Figure 5).

A l'occasion de l'introduction de *P. lounsburyi* dans le Sud de la France et en Corse, l'étude des parasitoïdes indigènes avait montré l'abondance relative du genre *Eupelmus* sur *B. oleae* (2ème genre fréquent après *Pnigalio* Schrank, 1802) mais également la présence de deux "taxons", identifiés à l'époque comme *E. urozonus* et *E. martellii* (Borowiec *et al.,* 2012). L'étude des communautés d'*Eupelmus* associées à *B. oleae* et à *M. stylata* a donc fait l'objet d'étude dans le cadre de ma thèse et du programme INULA (https://www6.paca.inra.fr/inula).

En l'état, l'examen de plusieurs centaines d'individus met en évidence une grande diversité interspécifique des *Eupelmus* sur *M. stylata* et *B. oleae* avec 6 espèces recensées: *E. kiefferi*, *E. confusus*, *E. urozonus*, *E. gemellus*, *E. microzonus* et *E. muellneri*. De plus, les espèces majoritaires d'*Eupelmus* sur chacun des hôtes diffèrent. Tandis que *E. kiefferi* est prédominant sur *M. stylata* (sauf apparemment en Corse), *E. urozonus* et *E. confusus* semblent majoritaires sur *B. oleae* ce qui tend à invalider la complémentarité entre l'inule et l'olivier.

A posteriori, il apparaît également que les espèces principales sur *B. oleae* et *M. stylata* (*E. kiefferi*, *E. confusus*, *E. urozonus* et *E. gemellus*) sont toutes des "super-généralistes" (cf. Partie II) et qu'aucune ne semble spécialisée sur Tephritidae voire sur Diptera. A partir des spectres d'hôtes connus de ces espèces et d'observations réalisées par G. Delvare en Sicile, une piste pour l'augmentation des *Eupelmus* en oliveraie pourrait être le l'implantation de l'asphodèle *Asphodelus ramosus* (Linné). Cette plante est en effet est infestée par un eurytomide du genre *Bruchophagus*, lui-même parasité à des taux importants par *E. confusus*.

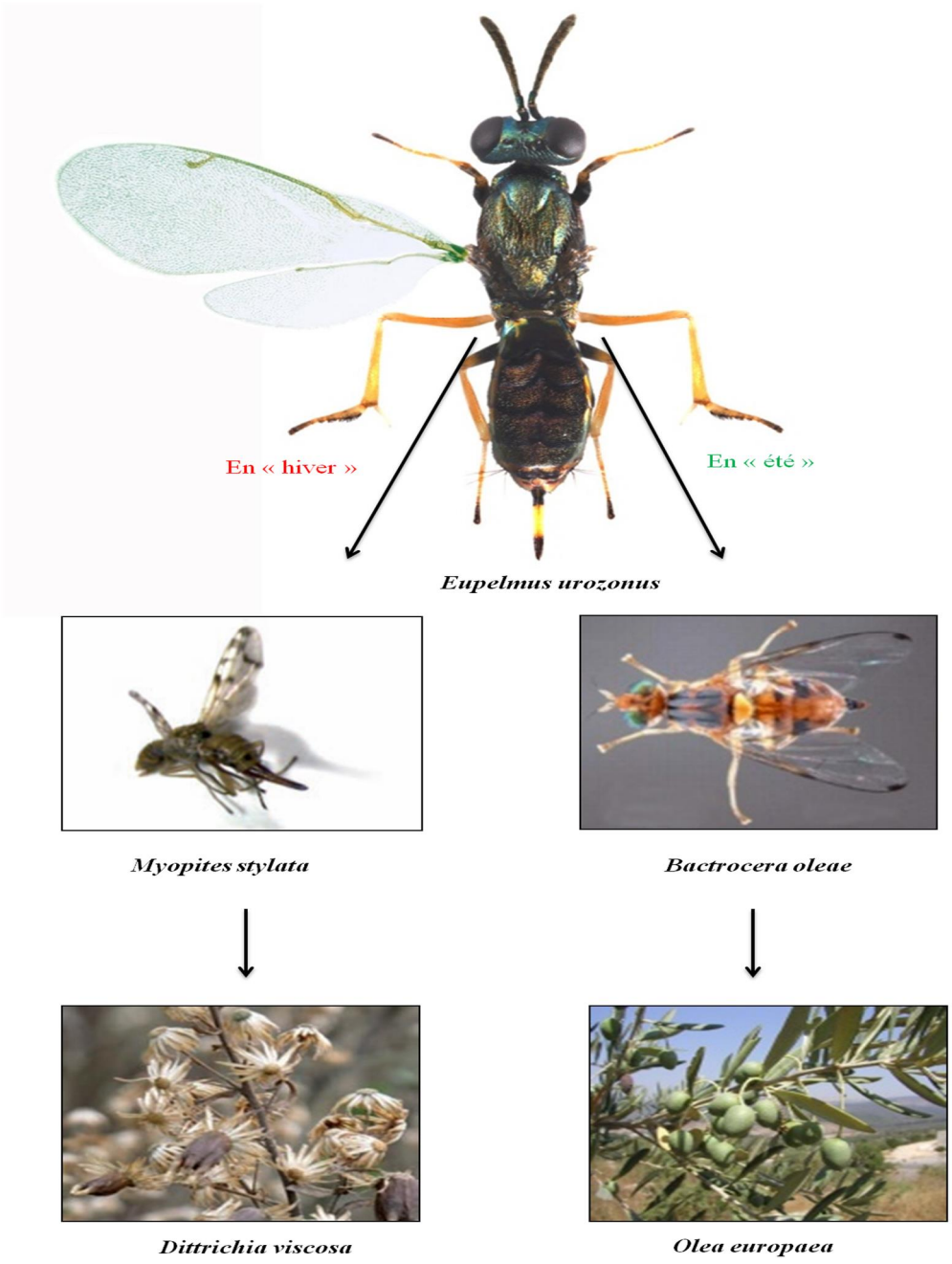

Figure 5: l'hypothèse de la favorisation de la présence d'*E. urozonus* dans les oliveraies grâce à la plante de *D. viscosa*.

6.2.3. Lutte biologique contre le cynips du châtaignier, *Dryocosmus kuriphilus*

Le cynips du châtaignier *D. kuriphilus* est un ravageur de réelle importance économique (Moriya *et al.,* 1989; Murakami *et al.,* 1995) puisqu'il peut occasionner une baisse de production estimée à 60%-80% (EFSA, 2010). Cette guêpe galligène est un membre de la tribu des Cynipini dont la plupart des membres induisent des galles sur les chênes (*Quercus* sp.) et elle est le seul membre de cette tribu qui est spécifique aux châtaigniers (Stone *et al.,* 2002). Ce cynips originaire de la Chine a pu s'installer avec une rapidité impressionnante dans plusieurs aires géographiques (Japon en 1941, Corée en 1958, Sud-est des Etats-Unis en 1974, Europe à partir de 2002) (Aebi *et al.,* 2007). En France, ce cynips invasif a colonisé toutes les régions françaises où la châtaigne est présente (vergers cultivés ou massifs forestiers) (Borowiec *et al.,* 2013).

D'après les expériences antérieures, un moyen efficace du contrôle des populations de *D. kuriphilus* peut être assuré par la lutte biologique par acclimatation du parasitoïde *Torymus sinensis* (Kamijo, 1982) (Matošević *et al.,* 2014). L'introduction de cette espèce a cependant été faite en Europe dans un contexte relativement polémique compte-tenu de risques éventuels d'hybridation entre espèces de *Torymus* et d'impacts non intentionnels sur les communautés associées à d'autres galligènes. Dans le cadre du projet de la "Lutte biologique contre le cynips du châtaigner à l'aide de *T. sinensis* en France" (financements ECOPHYTO, 2011-2014), ces craintes ont justifié la mise en place, au niveau français, d'un suivi sur le terrain pour documenter la dynamique de *T. sinensis* et celles d'espèces indigènes.

En fait, malgré le taux faible du parasitisme naturel exercé par les cortèges de parasitoïdes indigènes – < 2 % – il a été mis en évidence que le cynips du châtaigner peut recruter une grande variété des parasitoïdes chalcidiens qui attaquent initialement d'autres cynipides galligènes, notamment des chênes (Aebi *et al.,* 2007; Quacchia *et al.,* 2013). Quacchia *et al.* (2013) ont pu précisément identifier en Italie, sur une base morphologique et moléculaire, une trentaine d'espèces appartenant à six familles: Eurytomidae, Pteromalidae, Torymidae, Eupelmidae, Ormyridae et Eulophidae. Parmi les Eupelmidae et selon ces auteurs, *E. urozonus* et *E. annulatus* semblent être les espèces les plus abondantes sur le cynips du châtaigner. Les résultats encore préliminaires obtenus en France semblent confirmer ces conclusions. Nous avons ainsi observé que le recrutement de chalcidiens augmente au cours du temps en termes de diversité (18 chalcidiens obtenus en 2014 contre 6 en 2011) et de quantité. Parmi ceux-ci, les *Eupelmus* représentent la moitié des parasitoïdes indigènes émergés des galles de *D. kuriphilus* récoltés en hiver. Il apparaît de plus que toutes les espèces

d'*Eupelmus* élevées de *D. kuriphilus* (*E. urozonus*, *E. azureus*, *E. kiefferi*, *E. confusus* et *E. gemellus*) font en fait partie du groupe *urozonus* et que *E. urozonus* et *E. azureus* sont les deux espèces prédominantes, avec plus de 80% des *Eupelmus* émergés des galles sèches récoltées en hiver, sur les quatre années de suivi (2011-2014). Contrairement aux résultats de Quacchia *et al.* (2013), *E. annulatus* est une espèce très marginale sur *D. kuriphilus* dans nos relevés et, en raison du grand niveau de similarité morphologique entre *E. azureus* et *E. annulatus*, nous supposons que ces deux espèces ont été confondues par Quacchia *et al.* (2013) sur la base de précédentes études (Kaartinen *et al.*, 2010; Askew *et al.*, 2013). Les spectres d'hôtes établis durant mon travail de thèse pour ces *Eupelmus* (cf. Partie II) montrent que deux types d'espèces ont donc été recrutées par le cynips de châtaigner: les "super-généralistes" connues pour parasiter différents ordres d'insectes hôtes (c'est-à-dire, *E. urozonus*, *E. kiefferi*, *E. confusus* et *E. gemellus*) et une espèce spécialisée sur les cynipides du chêne (*E. azureus*). Si le recrutement de ces différentes espèces apparaît donc logique, ces observations démontrent l'opportunisme de ces espèces et suggèrent également des dynamiques locales différentes pour *a minima* les deux types de parasitoïdes. Les suivis actuellement en cours devraient permettre de tester cette hypothèse. D'une façon plus générale, le genre *Eupelmus* s'avère donc être également un bon modèle pour étudier la réponse d'une communauté indigène à une espèce invasive.

7. BIBLIOGRAPHIE GÉNÉRALE

Abrahamson, W.G., Eubanks, M.D., Blair, C.P., Whipple, A.V., 2001. Gall flies, inquilines, and goldenrods: a model for host-race formation and sympatric speciation. *Americain Zoologist*, 41, 928–938.

Abrahamson, W.G., Blair, C.P., Eubanks, M.D., Morehead, S.A., 2003. Sequential radiation of unrelated organisms: the gall fly *Eurosta solidaginis* and the tumbling flower beetle *Mordellistena convicta*. *Journal of Evolutionary Biology*, 16, 781–789.

Aebi, A., Schonrogge, K., Melika, G., Quacchia, A., Alma, A., Stone, G.N., 2007. Native and introduced parasitoids attacking the invasive chestnut gall wasp *Dryocosmus kuriphilus*. *Bulletin OEPP/EPPO Bulletin*, 37, 166–171.

Ahrens, D., Monaghan, M.T., Vogler, A.P., 2007. DNA-based taxonomy for associating adults and larvae in multi-species assemblages of chafers (Coleoptera: Scarabaeidae. *Molecular Phylogenetics and Evolution*, 44, 436–449.

Anisimova, M., Gascuel, O., 2006. Approximate Likelihood-Ratio Test for Branches: A Fast, Accurate, and Powerful Alternative. *Systematic Biology*, 55, 539–552.

Askew, R.R., Melika, G., Pujade-Villar, J., Schönrogge, K., Stone, G.N., Nieves-Aldrey, J.L., 2013. Catalogue of parastoids and inquilines in cynipid oak galls in the West Palaearctic. *Zootaxa*, 3643, 1–133.

Askew, R.R., Nieves-Aldrey, J.L., 2000. The genus *Eupelmus* Dalman, 1820 (Hymenoptera, Chalcidoidea, Eupelmidae) in peninsular Spain and the Canary Islands, with taxonomic notes and descriptions of new species. *Graellsia*, 56, 49–61.

Avise, J.C., Arnold, J., Ball, R.M., Bermingham, E., Lambt, T., Neigel, J.E., Reeb, C.A., Saunders, N.C., 1987. Intraspecific phylogeography: the mitochondrial DNA bridge between population genetics and systematics. *Annual Review of Ecology, Evolution and Systematics*, 18, 489–522.

Bashasab, F., Vijaykumar, Kambalpally, K.B., Patil, B.V., Kuruvinashetti, M.S., 2006. DNA-based marker systems and their utility in entomology. *Entomologica Fennica*, 17, 21–33.

Belshaw, R., Quicke, D.L.J., 1997. A molecular phylogeny of the aphidiinae (Hymenoptera: Braconidae). *Molecular Phylogenetics and Evolution*, 7, 281–293.

Bergsten, J., Bilton, D.T., Fujisawa, T., Elliot, M., Monaghan, M.T., Balke, M., Hendrich, L., Geijer, J., Herrmann, J., Foster, G.N., *et al.*, 2012. The effect of geographical scale of sampling on DNA barcoding. *Systematic Biology*, 61, 851–869.

Bernays, E.A., 2003. Phytophagous Insects. In: Resh, V.H., Cardé, R.T. Encyclopedia of insects. Academic Press, Elsevier Science, pp. 902-905.

Berthier, K., Chapuis, M-P., Moosavi, S.M., Tohidi-Esfahani, D., Sword, G.A., 2011. Nuclear insertions and heteroplasmy of mitochondrial DNA as two sources of intra-individual genomic variation in grasshoppers. *Systematic Entomology*, 36, 285–299.

Blaxter, M.L., 2004. The promise of a DNA taxonomy. *Philosophical Transactions of the Royal Society of London B*, 359, 669–679.

Boore, J.L., Brown,W.M., 1998. Big trees from little genomes: mitochondrial gene order as a phylogenetic tool. Current Opinion in Genetics and Development, 8, 668–674.

Borowiec, N., Groussier-Bout, G., Vercken, E. *et al.*, 2012. Diversity and geographic distribution of the indigenous and exotic parasitoids of the olive fruit fly, *Bactrocera oleae* (Dipt., Tephritidae), in Southern France. *IOBC-WPRS Bulletin*, 79, 71–78.

Borowiec, N., Groussier-Bout, G., Vercken, E. *et al.*, 2012. Diversity and geographic distribution of the indigenous and exotic parasitoids of the olive fruit fly, *Bactrocera oleae* (Dipt., Tephritidae), in Southern France. *IOBC-WPRS Bulletin*, 79, 71–78.

Borowiec, N., Thaon, M., Brancaccio, L., Warot, S., Risso, S., Bertoncello, E., Quacchia, A., Ris, N., Malausa, J.-C., 2013. Lutte biologique contre le cynips du châtaignier: Objectifs et enjeux de cette lutte biologique dite « classique ». *Phytoma*, 662, 32–35.

Borowiec, N., Thaon, M., Brancaccio, L., Warot, S., Vercken, E., Fauvergue, X., Ris, N., Malausa, J.-C., 2014. Classical biological control against the chestnut gall wasp *Dryocosmus kuriphilus* (Hymenoptera, Cynipidae) in France. *Plant Protection Quarterly*, 29, 7–10.

Bosa, D.H., Posadab, D., 2005. Using models of nucleotide evolution to build phylogenetic trees. *Developmental and Comparative Immunology*, 29, 211–227.

Bouček, Z., 1988. Australasian Chalcidoidea (Hymenoptera). A Biosystematic Revision of Genera of Fourteen Families, with a Reclassification of Species. CAB International Institute of Entomology, the Cambrian News Ltd., Aberystwyth, pp. 832.

Bremer, K., 1994. Branch support and tree stability. *Cladistics*, 10, 295–304.

Brown, J.M., Abrahamson, W.G., Way, P.A., 1996. Mitochondrial DNA phylogeography of host races of the goldenrod ball gallmaker, *Eurosta solidaginis* (Diptera: Tephritidae). *Evolution*, 50, 777–786.

Bush, G.L., 1969. Sympatric host race formation and speciation in frugivorous flies of the genus *Rhagoletis* (Diptera, Tephritidae). *Evolution*, 23, 237–251.

Cameron, S.A., Austin, A.D., Derr, J.N., Wharton, R.A., 1992. The application of nucleotide sequence data to phylogeny of the Hymenoptera: a review. *Journal of Hymenoptera Research*, 1, 63–79.

Cameron, S.L., 2014. Insect Mitochondrial Genomics: Implications for Evolution and Phylogeny. *Annual Review of Entomology*, 59, 95–117.

Carletto, J., Lombaert, E., Chavigny, P., Brévault, T., Lapchin, L., Vanlerberghe-Masutti, F., 2009. Ecological specialization of the aphid *Aphis gossypii* Glover on cultivated host plants. *Molecular Ecology*, 18, 2198–2212.

Caterino, M.S., Cho, S., Sperling, F.A.H., 2000. The current state of insect molecular systematics: a thriving Tower of Babel. *Annual Review of Entomology*, 45, 1–54.

Cho, S.W., Mitchell, A., Regier, J.C., Mitter, C., Poole, R.W., Friedlander, T.P. *et al.,* 1995. A highly conserved nuclear gene for low-level phylogenetics - Elongation factor-1-alpha recovers morphology-based tree for heliothine moths. *Molecular Biology and Evolution*, 12, 650–656.

Craig, T.P., Horner, J.D., Itami, J.K., 1997. Hybridization studies on the host races of Eurosta solidaginis: implications for sympatric speciation. *Evolution*, 51, 1552–1560.

Craig, T.P., Itami, J.K., Abrahamson, W.G., Horner, J.D., 1993. Behavioral evidence for host race formation in *Eurosta solidaginis*. *Evolution*, 47, 1696–1710.

Cronin, J.T., Abrahamson, W.G., 2001. Do parasitoids diversify in response to host-plant shifts by herbivorous insects? *Ecological Entomology*, 26, 347–355.

Crozier, R.H., Crozier, Y.C., 1993. The mitochondrial genome of the honeybee *Apis mellifera*: complete sequence and genome organization. *Genetics*, 133, 97–117.

Cruaud, A., Gautier, M., Galan, M., Foucaud, J., Saune, L., Genson, G. *et al.,* 2014. Empirical assessment of RAD sequencing for interspecific phylogeny. *Molecular Biology and Evolution*, 31, 1272–1274.

Cruaud, A., Jabbour-Zaha,b.R., Genson, G., Cruaud, C., Couloux, A., Kjellberg, F. *et al.,* 2010. Laying the foundations for a new classification of Agaonidae (Hymenoptera: Chalcidoidea), a multilocus phylogenetic approach. *Cladistics*, 26, 359–387.

Cruaud, A., Underhill, J.-G., Huguin, M., Genson, G., Jabbour-Zahab, R., Tolley, K.A., Rasplus, J.-Y., Noort, S. V., 2013. Multilocus Phylogeny of the World Sycoecinae Fig Wasps (Chalcidoidea: Pteromalidae). *PLoS ONE*. 8, e79291.

Daane, K.M., Johnson, M.W., 2010. Olive Fruit Fly: Managing an Ancient Pest in Modern Times. *Annual Review of Entomology*, 55, 151–69.

Dabert, M., 2006. DNA markers in the phylogenetics of the Acari. *Biological Letters*, 43, 97–107.

Danforth, B.N., Linl, C., Fang, J., 2005. How do insect nuclear ribosomal genes compare to protein-coding genes in phylogenetic utility and nucleotide substitution patterns? *Systematic Entomology*, 30, 549–562.

Dasmahapatra, K.K., Elias, M., Hill, R.I., Hoffman, J.I., Mallet, J., 2010. Mitochondrial DNA barcoding detects some species that are real, and some that are not. *Molecular Ecology Resources*, 10, 264–273.

Dasmahapatra, K.K., Mallet, J., 2006. DNA barcodes: recent successes and future prospects. *Heredity*, 97, 254–255.

Dayrat, B., 2005. Towards integrative taxonomy. *Biological Journal of the Linnean Society*, 85, 407–415.

Degnan, J.H., Rosenber, N.A., 2009. Gene tree discordance, phylogenetic inference and the multispecies coalescent. *Trends in Ecology and Evolution*, 24, 332–340.

Delsuc, F., Douzerye, J.P., 2004. Les méthodes probabilistes en phylogénie moléculaire. (1) Les modèles d'évolution des séquences et le maximum de vraisemblance. *Biosystema*, 22, 59–74.

Delucchi, V., 1957. Les parasites de la mouche des olives. *Entomophaga*, 2, 107–118.

Delvare, G., 2005. A revision of the West-Palearctic *Podagrion* (Hymenoptera: Torymidae), with the description of *Podagrion bouceki* sp. nov. *Acta Societatis Zoologicae Bohemoslovenicae*, 69, 65–88.

Delvare, G., Gebiola, M., Zeiri, A., Garonna, A.P., 2014. Revision and phylogeny of the European species of the *Eurytoma morio* species group (Hymenoptera: Eurytomidae), parasitoids of bark and wood boring beetles. *Zoological Journal of the Linnean Society*, 171, 370–421.

Deuve, T., Cruaud, A., Genson, G., Rasplus, J.-R., 2012. Molecular systematics and evolutionary history of the genus *Carabus* (Col. Carabidae*). Molecular Phylogenetics and Evolution*, 65, 259–275.

Dicke, M., 2000. Chemical ecology of host-plant selection by herbivorous arthropods: A multitrophic perspective. *Biochemical Systematics and Ecology*, 28, 601–61.

Dicke, M., van Loon, J.J.A., 2000. Multitrophic effects of herbivore-induced plant volatiles in an evolutionary context. *Entomologia Experimentalis et Applicata*, 97, 237–249.

Drès, M., Mallet, J., 2002. Host races in plant-feeding insects and their importance in sympatric speciation. *Philosophical Transactions of the Royal Society of London B*, 357, 471–492.

EFSA, 2010. Risk assessment of the oriental chestnut gall wasp, *Dryocosmus kuriphilus* for the EU territory and identification and evaluation of risk management options. *European Food Safety Authority Journal*, 8, 1–114.

Eggleton, P., Belshaw, R., 1992. Insect parasitoids: an evolutionary overview. *Philosophical Transactions of the Royal Society of London B*, 337, 1–20.

Eilenberg, J., Hajek, A., Lomer, C., 2001. Suggestions for unifyingthe terminology in biological control. *Biological Control*, 46, 387–400.

Enghoff, H., 2009. What is taxonomy? An overview with myriapodological examples. *Soil Organisms*, 81, 441–451.

Ercan, F.S., Oztemiz, S., Tuncbilek, A.S., Stouthamer, R., 2011. Sequence analysis of the ribosomal and *ITS2* region in two *Trichogramma* species (Hymenoptera: Trichogrammatidae). *Archives of Biological Science*, 63, 949–954.

Farache, F.H.A., Cruaud, A., Genson, G., Pereira, R.A.S., Rasplus, J.-R., 2013.Taxonomic revision and molecular phylogeny of the fig wasp genus *Anidarnes* Bouček, 1993 (Hymenoptera: Sycophaginae). *Systematic Entomology*, 38, 14–34.

Feder, J.L., Forbes, A.A., 2010. Sequential speciation and the diversity of parasitic insects. *Ecological Entomology*, 35, 67–76.

Felsenstein, J., 1985. Confidence limits on phylogenies: an approach using the bootstrap. *Evolution*, 39, 783–791.

Ferrière, C.H., 1954. Eupelmides brachyptères (Hym. Chalcidoidea). *Mitteilungen der Schweizerischen Entomologischen Gesellschaft*, 27, 1−21.

Ferriere, C.H., Delucchi, V., 1957. Les hymenopteres parasites de la mouche des olives. I. Les chalcidiens de la région méditerranéenne. *Entomophaga*, 2, 119–124.

Fitch, W.M., Margoliash, E., 1967. Construction of phylogenetic trees. *Science*, 155, 279–284.

Forbes, A.A., Powell, T.H.Q., Stelinski, L.L., Smith, J.J., Feder, J.L., 2009. Sequential sympatric speciation across trophic levels. *Science*, 323, 776–779.

Franco-Mican, S., Castro, J., Campos, M., 2010. Preliminary study of the parasitic complex associated with *Dittrichia viscosa* in Andalusia. *IOBC/WPRS Bulletin*, 5, 139–143.

Frézal, L., Leblois, R., 2008. Four years of DNA barcoding: Current advances and prospects. *Infection, Genetics and Evolution*, 8, 727–736.

Friedlander, T.P., Regier, J.C., Mitter, C., 1992. Nuclear Gene Sequences for Higher Level Phylogenetic Analysis: 14 Promising Candidates. *Systematic Biology*, 41, 483–490.

Fusu, L., 2008. The usefulness of chromosomes of parasitic wasps of the subfamily Eupelminae (Hymenoptera: Chalcidoidea: Eupelmidae) for subfamily systematics. *European Journal of Entomology*, 105, 823–828.

Fusu, L., 2009. Romanian Eupelmidae (Hymenoptera, Chalcidoidea): new cytogenetic, faunistic and host records. *North-Western Journal of Zoology*, 5, 307−320.

Futuyma, D.J., 2008. Sympatric speciation: norm or exception. In: Tilmon, K. Specialization, speciation and radiation: the evolutionary biology of herbivorous insects. Berkeley, University of California Press, pp. 136–148.

Futuyma, D.J., 2013. Evolution. 3rd ed., Sunderland, Massachusetts, Sinauer Associates.

Gadagkar, S.R., Rosenberg, M.S., Kumar, S., 2005. Inferring species phylogenies from multiple genes: concatenated sequence tree versus consensus gene tree. *Journal of Experimental Zoology*, 304B, 64–74.

Galtier, N., Nabholz, B., Glemin, S., Hurst, G.D.D., 2009. Mitochondrial DNA as marker of molecular diversity: a reappraisal. *Molecular Ecology*, 18, 4541–4550.

Gebiola, M., Bernardo, U., Monti, M.M., Navone, P., Viggiani, G., 2009. *Pnigalio agraules* (Walker) and *Pnigalio mediterraneus* Ferriere and Delucchi (Hymenoptera: Eulophidae): two closely related valid species. *Journal of Nature History*, 43, 2065–2480.

Gebiola, M., Bernardo, U., Ribes, A., Gibson, G.A.P., 2015. An integrative study of *Necremnus* Thomson (Hymenoptera: Eulophidae) associated with invasive pests in Europe and North America: taxonomic and ecological implications. *Zoological Journal of the Linnean Society*, 173, 352–423.

Gebiola, M., Gomez-Zurita, J., Monti, M.M., Navone, P., Bernardo, U., 2012. Integration of molecular, ecological, morphological and endosymbiont data for species delimitation within the *Pnigalio soemius* complex (Hymenoptera: Eulophidae). *Molecular Ecology*, 21, 1190–1208.

Gebiola, M., Gomez-Zurita, J., Monti, M.M., Navone, P., Bernardo, U., 2012. Integration of molecular, ecological, morphological and endosymbiont data for species delimitation within the *Pnigalio soemius* complex (Hymenoptera: Eulophidae). *Molecular Ecology*, 21, 1190–1208.

Ghara, M., Kundanati, L., Borges, R.M., 2011. Nature's Swiss army knives: Ovipositor structure mirrors ecology in a multitrophic fig wasp community. *PLoS ONE*, 6: e23642.

Gibson, G.A.P., 1986. Mesothoracic skeletomusculature and mechanics of flight and jumping in Eupelminae (Hymenoptera, Chalcidoidea: Eupelmidae). *The Canadian Entomologist*, 118, 691–728.

Gibson, G.A.P., 1989. Phylogeny and classification of Eupelmidae, with revision of the world genera of Calosotinae and Metapelmatinae (Hymenoptera: Chalcidoidea). *Memoirs of the Entomological Society of Canada*, 149, pp. 121.

Gibson, G.A.P., 1990. Revision of the genus *Macroneura* Walker in America North of Mexico (Hymenoptera: Eupelmidae). *Canadian Entomologist*, 122, 837–873.

Gibson, G.A.P., 1995. Parasitic wasps of the subfamily Eupelminae: classification and revision of world genera (Hymenoptera: Chalcidoidea, Eupelmidae). *Memoirs on Entomology, International*, 5, pp. i-v + 421.

Gibson, G.A.P., 2011. The species of *Eupelmus* (*Eupelmus*) Dalman and *Eupelmus* (*Episolindelia*) Girault (Hymenoptera: Eupelmidae) in North America north of Mexico. *Zootaxa*, 2951, 1–97.

Gibson, G.A.P., Heraty, J.M., Woolley, J.B., 1999. Phylogenetics and classification of Chalcidoidea and Mymarommatoidea – a review of current concepts (Hymenoptera: Apocrita). *Zoologica Scripta*, 28, 87–124.

Gibson, G.A.P., Huber, J.T., Woolley, J.B., 1997. Annotated keys to the genera of nearctic Chalcidoidea (Hymenoptera). Ottawa, NRC Research Press.

Godfray, H.C.J., Shimada, M., 1999. Parasitoids: a model system to answer questions in behavioral, evolutionary and population ecology. *Researches on Population Ecology*, 41, 3–10.

Goldstein, P.Z., DeSalle, R., 2010. Integrating DNA barcode data and taxonomic practice: Determination, discovery, and description. *Bioessays*, 33, 135–147.

Guerra-García, J.M., Espinosa, F., García-Gómez J.C., 2008. Trends in taxonomy today: an overview about the main topics in taxonomy. *Zoologica baetica*, 19, 15–49.

Gyllensten, U., Wharton, D., Wilson, A.C., 1985. Maternal inheritance of mitochondrial DNA during backcrossing of two species of mice. *The Journal of Heredity*, 76, 321–324.

Hajibabaei, M., Singer, G.A.C., Paul, D.N., Hebert, P.D.N., Donal, A., Hickey, D.A., 2007. DNA barcoding: how it complements taxonomy, molecular phylogenetics and population genetics. *Trends in Genetics*, 23, 167–172.

Hardy, N.B., Otto, S.P., 2014. Specialization and generalization in the diversification of phytophagous insects: tests of the musical chairs and oscillation hypotheses. Proceedings of the Royal Society B, 281: 20132960.

Harrison, C.J., Langdale, J.A., 2006. A step by step guide to phylogeny reconstruction. *The Plant Journal*, 45, 561–572.

Harrison, R., 1989. Animal mitochondrial DNA as a genetic marker in population and evolutionary biology. *Tree*, 4, 6–11.

Hebert, P.D.N., Cywinska, A., Ball, S.L., DeWaard, J.R., 2003. Biological identifications through DNA barcodes. *Proceedings of the Royal Society of London B*, 270, 313–321.

Hebert, P.D.N., Penton, E.H., Burns, J., Janzen, D.H., Hallwachs, W., 2004. Ten species in one: DNA barcoding reveals cryptic species in the neotropical skipper butterfl y, *Astraptes fulgerator*. *Proceedings of the National Academy of Sciences of the United States of America*, 101, 14812–14817.

Heraty J.M., Burks, R.A., Cruaud A. *et al.,* 2013. A phylogenetic analysis of the megadiverse Chalcidoidea (Hymenoptera). *Cladistics*, 29, 1–77.

Heraty, J., 2009. Parasitoid biodiversity and insect pest management. In: Foottil, R.G., Adler, P.H. Insect biodiversity: science and society. UK, Wiley- Blackwell, pp. 445–462.

Heraty, J.M., Burks,R. A., Cruaud A. *et al.,* 2012. A phylogenetic analysis of the megadiverse Chalcidoidea (Hymenoptera). *Cladistics*, 29, 1–77.

Hillis, D.M., 1987. Molecular versus morphological approaches to systematics. *Annual Review of Ecology and Systematics*, 18, 23–42.

Hillis, D.M., Dixon, M.T., 1991. Ribosomal DNA: molecular evolution and phylogenetic inference. *The Quarterly Review of Biology*, 66, 411–453.

Holder, M., Lewis, P.O., 2003. Phylogeny estimation: traditional and Bayesian approaches. *Nature*, 4, 275–284.

Hoy, M.A., 2013. Insect molecular genetics: an introduction to principles and applications. 3rd ed., Academic Press, Elsevier Science.

Hwang, U.-W., KIM, W., 1999. General properties and phylogenetic utilities of nuclear ribosomal DNA and mitochondrial DNA commonly used in molecular systematics. *The Korean Journal of Parasitology*, 37, 215–228.

Janzen1, D.H., Hajibabaei, M., Burns, J.M., Hallwachs, W., Remigio, E., Hebert, P.D.N., 2005. Wedding biodiversity inventory of a large and complex Lepidoptera fauna with DNA barcoding. *Philosophical Transactions of the Royal Society B*, 360, 1835–1845.

Jordal, B.H., Kambestad, M., 2014. DNA barcoding of bark and ambrosia beetles reveals excessive NUMTs and consistent east-west divergence across Palearctic forests. *Molecular Ecology Resources*, 14, 7–17.

Jousselin, E., Cruaud, A., Genson, G., Chevenet, F., Foottit, R.G., 2013. Is ecological speciation a major trend in aphids? Insights from a molecular phylogeny of the conifer-feeding genus *Cinara*. *Frontiers in Zoology*, 10:56.

Kaartinen, R., Stone, G.N., Hearn, J., Lohse, K., Roslin, T., 2010. Revealing secret liaisons: DNA barcoding changes our understanding of food webs. *Ecological Entomology*, 35, 623–638.

Kalina, V., 1981. The Palearctic species of the genus *Macroneura* Walker, 1837 (Hymenoptera, Chalcidoidea, Eupelmidae), with descriptions of new species. *Sbornik Vedeckeho Lesnickeho Ustavu Vysoke Skoly Zemedelske v Praze*, 24, 83–111.

Kalina, V., 1988. Descriptions of new Palearctic species of the genus *Eupelmus* Dalman with a key to species (Hymenoptera, Chalcidoidea, Eupelmidae). *Silvaecultura Tropica et Subtropica*, 12, 3–33.

Kapatos, E., Fletcher, B.S., Pappas, S., Laudeho, Y., 1997. The release of *Opius concolor* and *O. concolor var. siculus [Hym.*: Braconidae] against spring generation of *Dacus ole*ae [Dipt.: Trypetidae] on Corfu. *Entomophaga*, 22, 265–270.

Knowles, L.L., Kubatko, L.S., 2010. Estimating species trees: an introduction to concepts and models. In: Knowles, L.L., Kubatko, L.S. Estimating species trees: practical and theoretical aspects. Wiley-Blackwell, pp. 163-172.

Kol-Maimon, H., Ghanim, M., Franco, J.C., Mendel, Z., 2014. Evidence for Gene Flow between Two Sympatric Mealybug Species (Insecta; Coccoidea; Pseudococcida. *PLoS One*, 9, 88433.

Lecocq, T., Dellicour, S., Michez, D., Dehon, M., Dewulf, A., De Meulemeester, T., Brasero, N., Valterová, I., Rasplus, J.- Y., Rasmont, P., 2014. Methods for species delimitation in bumblebees (Hymenoptera, Apidae, *Bombus*): towards an integrative Approach. *Zoologica Scripta*, doi:10.1111/zsc.12107.

Lin, C.P., Danforth, B.N., 2004. How do insect nuclear and mitochondrial gene substitution 683 patterns differ? Insights from Bayesian analyses of combined datasets. *Molecular Phylogenetics and Evolution*, 30, 686–702.

Magnacca, K.N., Brown, M.J.F., 2010. Mitochondrial heteroplasmy and DNA barcoding in Hawaiian *Hylaeus* (*Nesoprosopis*) bees (Hymenoptera: Colletidae). *BMC Evolutionary Biology*, 10:174.

Matošević, D., Quacchia, A., Kriston, É., Melika, G., 2014. Biological control of the invasive *Dryocosmus kuriphilus* (Hymenoptera: Cynipidae) - an overview and the first trials in Croatia. *South-east European forestry*, 5, 3–12.

Matsubayashi, K.W., Ohshima, I., Nosil, P., 2010. Ecological speciation in phytophagous insects. *Entomologia Experimentalis et Applicata*, 134, 1–27.

Mayr, E., 1963. Animal species and evolution. Belknap Press of Harvard University Press, Cambridge, Massachusetts.

Meyer, C.P., Paulay, G., 2005. DNA barcoding: error rates based on comprehensive sampling. *PLOS Biology*, 3, 1–10.

Mitchell, A., Cho, S., Regier, J.C., Mitter, C., Poole, R.W., Matthews, M., 1997. Phylogenetic utility of elongation factor-1 alpha in Noctuoidea (Insecta: Lepidoptera): the limits of synonymous substitution. *Molecular Phylogenetics and Evolution*, 14, 381–390.

Mitchell, A., Mitter, C., Regier, J.C., 2000. More taxa or more characters revisited: Combining data from nuclear protein-encoding genes for phylogenetic analyses of Noctuoidea (Insecta: Lepidoptera). *Systematic Biology*, 49, 202–224.

Monastero, S., Delanoue, P., 1966. Lutte biologique expérimentale contre la mouche de l'olive (*Dacus oleae* Gmel.) au moyen d'*Opius concolor* Szepl. *Siculus* Mon. dans les iles éolinnes (Sicile) en 1965. *Entomophaga*, 11, 411–432.

Moriya, S., Inoue, K., Mabuchi, M., 1989. The use of *Torymus sinensis* to control chestnut gall wasp, *Dryocosmus kuriphilus*. *Food Fertil Technol Cent FFTC Tech Bull*, 118, 1–12.

Mortiz, C., Cicero, C., 2004. DNA barcoding: promise and pitfalls. *PLoS Biology*, 2: e354.

Munro, J.M., Heraty, J.M., Burks, R.A. *et al.*, 2011. Molecular phylogeny of the Chalcidoidea (Hymenoptera). *PLoS One*, 6, e27023.

Murakami, Y., Ohkubo, N., Moriya, S., Gyoutoku, Y., Kim, C.H., Kim, J.K., 1995. Parasitoids of *Dryocosmus kuriphilus* (Hymenoptera, Cynipidae) in South Korea with particular reference to ecologically different types of *Torymus* (*Syntomaspis*) *sinensis* (Hymenoptera, Torymidae). *Applied Entomology and Zoology*, 30, 277–284.

Nardi, F., Carapelli, A., Dallai, R., Roderick, G.K., Frati, F., 2005. Population structure and colonization history of the olive fly, *Bactrocera oleae* (Diptera, Tephritidae). *Molecular Ecology*, 14, 2729–2738.

Narendan, T.C., Anil, K., 1995. A key of Indian species of *Eupelmus* Dalman (Hymenoptera: Eupelmidae) with descriptions of eleven new species. *Journal of the Zoological Society of Kerala*, 5, 1–15.

Narendran, T.C., 2008. Taxonomy and its relevance. *Government Arts & Science College Researche Journal*, 9–14.

Neuenschwander, P., Bigler, F., Delucchi, V., Michelakis, S., 1983. Natural enemies of preimaginal stages of *Dacus oleae* Gmel. (Dipt., Tephritidae) in Western Crete. I. Bionomics and phenologies. *Bollettino del Laboratorio di Entomologia Agraria Filippo Silvestri*, 40, 3–32.

Noyes, J.S., 2013. Universal Chalcidoidea database. Available from: http://www.nhm.ac.uk/research- curation/research/projects/chalcidoids/index.html.

Noyes, J.S., 2015. Universal Chalcidoidea database. Available from: http://www.nhm.ac.uk/research- curation/research/projects/chalcidoids/index.html.

Noyes, J.S., Valentine, E.W., 1989. Chalcidoidea (Insecta: Hymenoptera) – introduction, and review of genera in smaller families. *Fauna of New Zealand*, 18.

Nyman, T., Vikberg, V., Smith, D.R., Boevé, J.L., 2010. How common is ecological speciation in plantfeeding insects? A 'Higher' Nematinae perspective. *BMC Evolutionary Biology*, 10:266.

Okiwelu, S.N., Noutcha1, M.A.E., 2014. The Evolution of Integrative Insect Systematics. *Annual Research & Review in Biology*, 4, 2302–2317.

Padial, J.M., Miralles, A., De la Riva, I., Vences, M., 2010. The integrative future of Taxonomy. *Frontiers in Zoology*, 7, 2–14.

Patwardhan, A., Ray, S., Roy, A., 2014. Molecular markers in phylogenetic studies-a review. *Journal of Phylogenetics & Evolutionary Biology*, 2:131.

Pauls, S.U., Blahnik, R.J., Zhou, X., Wardwell, C.T., Holzenthal, R.W., 2010. DNA barcode data confirm new species and reveal cryptic diversity in Chilean *Smicridea* (*Smicridea*) (Trichoptera: Hydropsychidae). *Journal of the North American Benthological Society*, 29, 1058–1074.

Quacchia, A., Ferracini, C., Nicholis, J.A. *et al.,* 2013. Chalcid parasitoid community associated with the invading pest *Dryocosmus kuriphilus* in north-western Italy. *Insect Conservation and Diversity*, 6, 114–123.

Quicke, D.L.J., 1997. Parasitic wasps. UK, Cambridge University Press.

Quicke, D.L.J., Fitton, M.G., Harris, J., 1995. Ovipositor steering mechanisms in braconid wasps. *Journal of Hymenoptera Research*, 4, 110–120.

Rannala, B., Yang, Z., 2008. Phylogenetic inference using whole genomes. *Annual Review of Genomics and Human Genetics*, 9, 217–231.

Ravigné, V., 2010. La spéciation. In: Thomas, F., Lefevre, T., Raymond, M. Biologie évolutive. 1st ed., De Boeck University, pp. 9–52.

Rokas, A., Nylander, J.A.A., Ronquist, F., Stone, G.N., 2002. A maximum-likelihood analysis of eight phylogenetic markers in gall wasps (Hymenoptera: Cynipidae): Implications for insect phylogenetic studies. *Molecular Phylogenetics and Evolution*, 22, 206–219.

Rosen, D., 1986. The role of taxonomy in effective biological control programs. *Agriculture Ecosystems and Environment*, 15, 121–129.

Rosen, D., Debach, P., 1973. Systematics, morphology and biological control. *Entomophaga*, 18, 215–222.

Rubinoff, D., Cameron, S., Will, K., 2006. A Genomic perspective on the shortcomings of mitochondrial DNA for ‘‘barcoding’’ identification. *Journal of Heredity*, 97, 581–594.

Rundle, H.D., Nosil, P., 2005. Ecological speciation. *Ecology Letters*, 8, 336–352.

Rzhetsky, A., Nei, M., 1992. Statistical properties of the ordinary lea squares, generalized least-squares and minimum-evolution methods of phylogenetic inference. *Journal of Molecular Evolution*, 35, 367–3.

Saitou, N., Nei, M., 1987. The Neighbor-joining method: a new method for reconstructing phylogenetic trees. *Molecular Biology and Evolution*, 4, 406**ï** 425.

Schlick-Steiner, B.C., Steiner, F.M., Seifert, B., Stauffer, C., Christian, E., Crozier, R.H., 2010. Integrative Taxonomy: A Multisource Approach to Exploring Biodiversity. *Annual Review of Entomology*, 55, 421–38.

Schluter, D., 2001. Ecology and the origine of species. *Trends in Ecology & Evolution*, 16, 372–380.

Schoonhoven, L.M., van Loon, J.J.A., Dicke, M., 2005. Insect-plant biology. 2nd ed., Oxford University Press.

Schuh, R.T., Brower, A.V.Z., 2009. Biological systematics: principles and applications. 2nd ed., Cornell university press.

Shoubridge, E.A., Wai, T., 2007. Mitochondrial DNA and the mammalian oocyte. *Current Topics in Developmental Biology*, 77, 87–111.

Sites, J.W., Marshall, J.C., 2004. Operational criteria for delimiting species. *Annual Review of Ecology, Evolution and Systematics*, 35, 199–227.

Smith, M.A., Wood, D.M., Janzen, D.H., Hallwachs, W., Hebert, P.D.N., 2007. DNA barcodes affirm that 16 species of apparently generalist tropical parasitoid flies (Diptera, Tachinidae) are not all generalists. *Proceedings of the Royal Society USA*, 104, 4967–4972.

Smith, M.A., Woodley, N.E., Janzen, D.H., Hallwachs, W., Hebert, P.D.N., 2006. DNA barcodes reveal cryptic host-specificity within the presumed polyphagous members of a genus of parasitoid flies (Diptera: Tachinidae). *Proceedings of the National Academy of Sciences of the United States of America*, 103, 3657–3662.

Sokal, R., Michener, C., 1958. *A statistical method for evaluating systematic relationships*. University of Kansas Science Bulletin.

Song, H., Buhay, J.E., Whiting, M.F., Keith, A., Crandall, K.A., 2008. Many species in one: DNA barcoding overestimates the number of species when nuclear mitochondrial pseudogenes are coamplified. *Proceedings of the National Academy of Sciences of the United States of America*, 105, 13486–13491.

Sriphirom, P., Sopaladawan, P.N., Wongpakam, K., Pramual, P., 2014. Molecular phylogeny of black flies in the *Simulium tuberosum* (Diptera: Simuliidae) species group in Thailand. *Genome*, 57, 45–55.

Stireman, J.O., Nason, J.D., Heard, S.B., Seehawer, J.M., 2006. Cascading host-associated genetic differentiation in parasitoids of phytophagous insects. *Proceedings of the Royal Society of London B*, 273, 523–530.

Stone, G.N., Schönrogge, K., Atkinson, R.J., Bellido, D., Pujade-Villar, J., 2002. The population biology of oak gall wasps (Hymenoptera: Cynipidae). *Annual Review of Entomology*, 47, 633–668.

Taekul, C., Valerio, A.A., Austin, A.D., Klompen, H., Johnson, N.F., 2014. Molecular phylogeny of telenomine egg parasitoids (Hymenoptera: Platygastridae s.l.: Telenominae): evolution of host shifts and implications for classification. *Systematic Entomology*, 39, 24–35.

Tahseen, Q., 2014. Taxonomy-the crucial yet misunderstood and disregarded tool for studying biodiversity. *Journal of Biodiversity and Endangered Species*, 2:128.

Talavera, G., 2012. Phylogenetic Inference at different taxonomic levels. 377 p. PHD Thesis: Universitat Autònoma de Barcelona.

Trizzino, M., Jäch, M.A., Audisio, P., Alonso, R., Ribera, I., 2013. A molecular phylogeny of the cosmopolitan hyperdiverse genus *Hydraena* Kugelann (Coleoptera, Hydraenidae). *Systematic Entomology*, 32, 192–208.

Vamosi, J.C., Armbruster, W.S., Renner, S.S., 2014. Evolutionary ecology of specialization: insights from phylogenetic analysis. *Proceedings of the Royal Society of London B*, 281, 20142004.

van Velzen1, R., Weitschek, E., Felici, G., Bakker, F.T., 2012. DNA Barcoding of Recently Diverged Species: Relative Performance of Matching Methods. *PLoS ONE*, 7, e30490.

Veijalainen, A., Broad, G.R., Wahlberg, N., Longino, J.T., Saaksjarvi, I.E., 2011. DNA barcoding and morphology reveal two common species in one: *Pimpla molesta* stat. rev. separated from *P. croceipes* (Hymenoptera, Ichneumonidae). *ZooKeys*, 124, 59–70.

Vet, L.E.M., Dicke, M., 1992. Ecology of infochemical by natural enemies in a tritrophic context. *Annual Review of Entomology*, 37, 141–72.

W. Coleman, A.W., 2003. ITS2 is a double-edged tool for eukaryote evolutionary comparisons. *TRENDS in Genetics*, 19, 370–375.

Wägele, J.W., 2005. Foundations of Phylogenetic Systematics. Germany, Verlag Dr. *Friedrich Pfeil. München*.

Wahlberg1, N., Braby, M.F., Brower, A.V.Z., de Jong, R., Lee, M-M., Nylin, S., Pierce, N.E., Sperling, F.A.H., Vila, R., Warren, A.D., Zakharov, E., 2005. Synergistic effects of

combining morphological and molecular data in resolving the phylogeny of butterflies and skippers. *Proceedings of the Royal Society B*, 272, 1577–1586.

Warlop, F., 2006. Limitation des populations de ravageurs de l'olivier par le recours à la lutte biologique par conservation. *Cahiers de l'Agriculture*, 15, 1–7.

Wiens, J.J., Servedio, M.R., 2000. Species delimitation in systematic: inferring diagnostic differences between species. *Proceedings of the Royal Society of London B*, 267, 631–636.

Wiley, E.O., Lieberman, B.S., 2011. Phylogenetics: Theory and practice of phylogenetic systematics. 2nd ed., Hoboken, New Jersey, John Wiley & Sons, Inc.

Will, K.W., Mishler, B.D., Wheeler, Q.D., 2005. The Perils of DNA Barcoding and the Need for Integrative Taxonomy. *Systematic Biology* 54, 844–851.

Wortley, A.H., Scotland, R.W., 2006. The effect of combining molecular and morphological data in published phylogenetic analyses. *Systematic Biology*, 55, 677–685.

Xiao, J.-H., Wang, N.-X., Li, Y.-W. *et al.*, 2010. Molecular approaches to identify cryptic species and polymorphic species within a complex community of fig wasps. *PLoS One*, 5, e15067.

Xing, J., 2006. Essential bioinformatics. UK, Cambridge University Press.

Yang, Z., 2006. Computational molecular Evolution. Oxford, Oxford University Press.

Yara, K., 2006. Identification of *Torymus sinensis* and *T. beneficus* (Hymenoptera: Torymidae), introduced and indigenous parasitoids of the chestnut gall wasp *Dryocosmus kuriphilus* (Hymenoptera: Cynipidae), using the ribosomal *ITS2* region. *Biological Control*, 36, 15–21.

Zhang, D.-X., Hewitt, G.M., 1996. Nuclear integrations: challenges for mitochondrial DNA markers. *Tree*, 11, 247–251.